SUMMER FACULTY RESEARCH PROGRAM

LEVEL II

Research Reports

Volume I of II

UNCLASSIFIED

SECURITY CLASSIFICATION OF THIS PAGE (When Data Entered)

REPORT DOCUMENTATION PAGE		READ INSTRUCTIONS BEFORE COMPLETING FORM
1. REPORT NUMBER AFOSR-TR-79-0234	2. GOVT ACCESSION NO.	3. RECIPIENT'S CATALOG NUMBER
4. TITLE (and Subtitle) 1978 USAF-ASEE Summer Faculty Research Program. Volume 1.		5. TYPE OF REPORT & PERIOD COVERED Final report. 1 Jan 76 - 30 Sep 78,
		6. PERFORMING ORG. REPORT NUMBER
7. AUTHOR(s) Mr J. Fred O'Brien		8. CONTRACT OR GRANT NUMBER(s) F44620-75-C-0031
9. PERFORMING ORGANIZATION NAME AND ADDRESS Auburn University Auburn, Alabama		10. PROGRAM ELEMENT, PROJECT, TASK AREA & WORK UNIT NUMBERS 61102F, 2307/D1
11. CONTROLLING OFFICE NAME AND ADDRESS Air Force Office of Scientific Research/XOP Bldg. 410 Bolling AFB, Washington D.C. 20332		12. REPORT DATE Sep 1978
		13. NUMBER OF PAGES 278 549p
14. MONITORING AGENCY NAME & ADDRESS(if different from Controlling Office)		15. SECURITY CLASS. (of this report) UNCLASSIFIED
		15a. DECLASSIFICATION/DOWNGRADING SCHEDULE

16. DISTRIBUTION STATEMENT (of this Report)

Distribution unlimited; approved for public release.

17. DISTRIBUTION STATEMENT (of the abstract entered in Block 20, if different from Report)

18. SUPPLEMENTARY NOTES

19. KEY WORDS (Continue on reverse side if necessary and identify by block number)

20. ABSTRACT (Continue on reverse side if necessary and identify by block number)

The USAF-ASEE Summer Faculty Research Program was begun in 1975 with 22 members of engineering and science faculties from colleges and universities throughout the country. These professors were assigned to various USAF research laboratories at Wright-Patterson AFB and Eglin AFB for a ten-week period of concentrated research in their selected field and of mutual interest and benefit to the participant (and his university) and the USAF. In 1976, this program was expanded to a total of 53 faculty participants assigned to all Air Force Systems Command laboratories. In 1977, the number of participants

next page

DD FORM 1 JAN 73 1473 390 276 UNCLASSIFIED

SECURITY CLASSIFICATION OF THIS PAGE(When Data Entered)

cont. was expanded to seventy professors and continued at that level in 1978.

SECURITY CLASSIFICATION OF THIS PAGE(When Data Entered)

1978 USAF/ASEE SUMMER FACULTY RESEARCH PROGRAM (NON-WPAFB)

Conducted by

Auburn University

with Assistance from

Ohio State University

and

Other Installations

under

USAF Contract Number F 44620-75-C-0031

PARTICIPANTS' RESEARCH REPORTS

Volume I of II

Submitted to

Air Force Office of Scientific Research

Bolling Air Force Base

Washington, D.C.

by

J. Fred O'Brien, Jr., University Project Director
Associate Director, Engineering Extension Service
Auburn University
Sch of Eng

September 1978

PREFACE

The USAF-ASEE Summer Faculty Research Program was begun in 1975 with twenty-two members of engineering and science faculties from colleges and universities throughout the country. These professors were assigned to various USAF research laboratories at Wright-Patterson AFB and Eglin AFB for a ten-week period of concentrated research in their selected field and of mutual interest and benefit to the participant (and his university) and the USAF. In 1976, this program was expanded to a total of fifty-three faculty participants assigned to all Air Force Systems Command laboratories. In 1977, the number of participants was expanded to seventy professors and continued at that level in 1978.

The basic program objectives are:

(1) To provide scientific and technological benefits to the USAF while enhancing the research interested and capabilities of engineering educators.

(2) To stimulate continuing relations among participating faculty members and their professional peers at the AFSC laboratories.

(3) To form the basis for continuing research of interest to the Air Force at the participant's institution.

(4) To sponsor research in areas of mutual interest to the USAF, the faculty member, and his institution.

The program in conducted under contracts with Auburn University and Ohio State University. The American Society for Engineering Education is co-sponsor of the program.

This document is a compilation of the reports written by participants assigned to laboratories other than Wright-Patterson Air Force Base (Auburn University contract). Mr. J. Fred O'Brien, Jr., Project Director, has exercised certain administrative prerogatives to produce this report.

Similar documentation for the 1975, 1976 and 1977 research efforts are on file in the Defense Documentation Center in Washington, D.C. under the following numbers:

1975	Research Reports	ADA031017
1976	Research Reports	ADA033822
1977	Research Reports	ADA051624 (Volume I)
		ADA051514 (Volume II)

The appendix (In Volume II of this report) contains indexes of the previous programs.

1978 USAF/ASEE SUMMER FACULTY RESEARCH PROGRAM

LIST OF PARTICIPANTS

NAME/ADDRESS	DEGREE, SPECIALTY & LABORATORY ASSIGNMENT
Dr. S. Reza Ahsan Professor of Cartography & Remote Sensing Department of Geography & Geology Western Kentucky University Bowling Green, KY 42101 (502)745-4555 Ext. 7 [redacted]	Degree: Ph.D., Geography, 1963 Specialty: Cartography & Remote Sensing, Landuse & Env. Impact Assigned: CEEDO (Tyndall) [redacted]
Dr. Jon S. Bailey Associate Professor, Psychology Dept. Florida State University Tallahassee, FL 32306 (904)644-6443 [redacted]	Degree: Ph.D., Psychology, 1970 Specialty: Developmental Psychology & Behavior Analysis Assigned: AFHRL (Williams) [redacted]
Professor Nicola Berardi Electrical Engineering Technology Dept. MGL Building Purdue University West Lafayette, IN 47907 (317) 493-2593 [redacted]	Degree: M.S., Electrical Engineering, 1974 Specialty: Control Systems & Digital Design Assigned: RADC (Griffiss) [redacted]
Dr. Theodore S. Boilis Assistant Professor of Mathematics Dept. of Mathematical Sciences SUNY College at Oneonta Oneonta, NY 13820 (607)431-3384 [redacted]	Degree: Ph.D., Mathematics, 1971 Specialty: Analysis, Algebra, Statistics Assigned: RADC (Griffiss) [redacted]
Dr. R. Leonard Brown, Jr. Assistant Professor Applied Math/Computer Science Thornton Hall University of Virginia Charlottesville, VA 22903 (804)924-7201 [redacted]	Degree: Ph.D., Computer Science, 1975 Specialty: Numerical Methods for Digital Computers Assigned: AEDC (Arnold) [redacted]
Dr. Roger K. Bunting Associate Professor, Chemistry Dept. Illinois State University Normal, IL 61761 (309)438-7659 [redacted]	Degree: Ph.D., Chemistry, 1965 Specialty: Inorganic Chemistry Assigned: FJSRL (AF Academy) [redacted]
Dr. Paul R. Caron Professor of Electrical Engineering Southern Massachusetts University North Dartmouth, MA 02747 (617)997-9321 Ext. 355 [redacted]	Degree: Ph.D., Engineering, 1963 Specialty: Antennas, Plasmas Assigned: RADC (Hanscom) [redacted]

NAME/ADDRESS	DEGREE, SPECIALTY & LABORATORY ASSIGNMENT
Dr. Robert L. Carroll Assistant Professor Dept. of Electrical & Computer Engineering University of South Carolina Columbia, SC 29208 (803)777-4195 [redacted]	Degree: Ph.D., Electrical Engineering, 1973 Specialty: Systems Theory Control & Identification Assigned: AFATL (Eglin) [redacted]
Dr. Shyhming Chang Associate Professor of Mechanical Eng. School of Engineering California State University - Fresno Fresno, CA 93740 (209)487-2566 [redacted]	Degree: Ph.D., Solid Mechanics, 1972 Specialty: Composite Material Analysis, Structural Dynamics Assigned: AFRPL (Edwards) [redacted]
Dr. Irvin M. Citron Professor of Chemistry Fairleigh Dickinson University Rutherford, NJ 07070 (201)933-5000 Ext. 255 [redacted]	Degree: Ph.D., Chemical Education, 1969 Specialty: Analytical Chemistry (Instrumental Analysis) Assigned: AFRPL (Edwards) [redacted]
Dr. Henry D'Angelo Professor, Dept. of Mathematical Sciences Memphis State University Memphis, TN 38152 (901)454-2762 [redacted]	Degree: Ph.D., Electrical Engineering, 1964 Specialty: Modeling, Systems Theory, Microcomputer Structures Assigned: EDS (Hanscom) [redacted]
Dr. Louis A. DeAcetis Professor of Physics Bronx Community College/CUNY 181st St. & University Ave. Bronx, NY 10453 (212)367-7300 Ext. 433 [redacted]	Degree: Ph.D., Physics, 1969 Specialty: Electromagnetic Diffraction & Microwave Optics Assigned: AFATL (Eglin) [redacted]
Dr. Alan A. Desrochers Assistant Professor Dept. of Systems & Computer Engineering Boston University 110 Cummington St. Boston, MA 02215 (617)353-2808 [redacted]	Degree: Ph.D., Electrical Engineering, 1977 Specialty: Automatic Control Assigned: AFATL (Eglin) [redacted]
Dr. Richard Dobrin Professor of Physics Sarah Lawrence College Bronxville, NY 10708	Degree: Ph.D., Physics, 1971 Specialty: Radiological, Atomic, & Solid State Physics Assigned: RADC (Hanscom) [redacted]

NAME/ADDRESS	DEGREE, SPECIALTY & LABORATORY ASSIGNMENT
Dr. Philip J. Feinsilver Assistant Professor Department of Mathematics Southern Illinois University Carbondale, Il 62901 (618)453-5302	Degree: Ph.D., Mathematics, 1975 Specialty: Probability Assigned: AFRPL (Edwards) [redacted]
Dr. Robert H. Foulkes, Jr. Associate Professor Electrical Engineering Youngstown State University Youngstown, OH 44555 (216)746-1851 Ext. 423 [redacted]	Degree: Ph. D., Systems Engineering, 1970 Specialty: Control, Communication & General Systems Theories Assigned: RADC (Griffiss) [redacted]
Dr. Albert J. Frasca Associate Professor of Physics Wittenberg University Springfield, OH 45501 (513)327-7827 [redacted]	Degree: Ph.D., Nuclear Physics, 1966 Specialty: Applied Nuclear Physics/Accelerators & Dosimetry Assigned: AFWL (Kirtland) [redacted]
Dr. Robert B. Green Assistant Professor, Dept. of Chemistry West Virginia University Morgantown, WV 26506 (304)293-5220 [redacted]	Degree: Ph.D., Chemistry, 1974 Specialty: Analytical Chemistry, Spectroscopy Assigned: AFWL (Kirtland) [redacted]
Dr. Robert L. Gutmann Assistant Professor Electrical & Computer Engineering Dept. University of Massachusetts Amherst, MA 01003 (413)545-0714 [redacted]	Degree: Ph.D., Electrical Engineering, 1976 Specialty: Control Systems Assigned: AFWL (Kirtland) [redacted]
Dr. Michael Hankamer Assistant Professor Department of Electrical Engineering Texas A & I University Kingsville, TX 78363 (512)595-2001	Degree: Ph.D., Electrical Engineering, 1978 Specialty: Information Theory & Coding; Communication Systems Assigned: SAM (Brooks) [redacted]
Dr. Donald C. Haueisen Assistant Professor of Physics Pacific Lutheran University Tacoma, WA 98447 (206)531-6900 Ext. 281 [redacted]	Degree: Ph.D., Experimental Physics, 1972 Specialty: Laser Systems, Nonlinear Optics Assigned: AFWL (Kirtland) [redacted]

NAME/ADDRESS	DEGREE, SPECIALTY & LABORATORY ASSIGNMENT
Dr. William A. Hornfeck Assistant Professor of Electrical Eng. Gannon College Perry Square Erie, PA 16501 (814)456-7523 [redacted]	Degree: Ph.D., Electrical Eng. Digital Systems, 1971 Specialty: Computer Architecture/ Digital Simulation/Microprocessors Assigned: AFATL (Eglin) [redacted]
Dr. James W. Jeter, Jr. Associate Professor, Mechanical Eng. Virginia Military Institute Lexington, VA 24450 (703)463-6308 [redacted]	Degree: Ph.D., Applied Mechanics, 1972 Specialty: Dynamic Loads, Finite Elements, Structural Analysis Assigned: AFWL (Kirtland) [redacted]
Dr. Robert A. Kadlec Assistant Professor Aerospace Engineering Sciences Engineering Center, ECOT 6-16 University of Colorado Boulder, CO 80302 (303)492-7880 [redacted]	Degree: Ph.D., Aeronautics & Astronautics, 1973 Specialty: Fluid Mechanics & Plasma Physics Assigned: FJSRL (Af Academy) [redacted]
Dr. James C. Lauffenberger Associate Professor of Physics Canisius College 2001 Main Street Buffalo, NY 14208 (716)883-7000 [redacted]	Degree: Ph.D., Solid State (Surface Physics), 1965 Specialty: Optics, X-Ray Diffraction Assigned: AFRPL (Edwards) [redacted]
Dr. June K. Lee Assistant Professor Dept. of Engineering Mechanics Ohio State University 155 West Woodruff Columbus, OH 43210 (614)422-7371 [redacted]	Degree: Ph.D., Engineering Mechanics, 1976 Specialty: Continuum Mechanics, Finite Element Methods Assigned: AFATL (Eglin) [redacted]
Dr. Gordon A. Lewandowski Assistant Professor Dept. of Chemical Engineering New Jersey Institute of Technology 323 High Street Newark, NJ 07102 (201)645-5402 [redacted]	Degree: D. Eng. Sci., Chemical Engineering, 1970 Specialty: Air Pollution Control Assigned: CEEDO (Tyndall) [redacted]
Dr. James A. Liburdy Assistant Professor of Mechanical Eng. Memphis State University Memphis, TN 38152 (901) 454-2173 [redacted]	Degree: Ph.D., Mechanical Engineering, 1976 Specialty: Turbulence, Fluid Mechanics, Heat Transfer Assigned: AEDC (Arnold) [redacted]

NAME/ADDRESS	DEGREE, SPECIALTY & LABORATORY ASSIGNMENT
Dr. Robert E. Lovell Associate Professor of Engineering Industrial & Management Systems Engineering Arizona State University Tempe, AZ 85281 (602)965-2700 [redacted]	Degree: Ph.D., Systems Engineering, 1975 Specialty: Systems Engineering (Simulation by Computer) Assigned: ESD (Hanscom) [redacted]
Dr. James D. Lowther Professor, Dept. of Mechanical Engineering Louisiana Tech University Box 4875 Ruston, LA 71272 (318)256-4436 [redacted]	Degree: Ph.D., Mechanical Engineering, 1968 Specialty: Thermodynamics, Mechanical Reliability Assigned: CEEDO (Tyndall) [redacted]
Dr. John L. Lowther Associate Professor of Computer Science Dept. of Mathematics & Computer Science Michigan Technological University Houghton, MI 49931 (906)487-2183 [redacted]	Degree: Ph.D., Computer Science, 1975 Specialty: Computer Science, Mathematics, Physics Assigned: CEEDO (Tyndall) [redacted]
Dr. Robert W. McLaren Associate Professor Dept. of Electrical Engineering University of Missouri Columbia, MO 65201 (314)882-3553 [redacted]	Degree: Ph.D., Electrical Engineering, 1966 Specialty: Artificial Intelligence; Computer Engineering Assigned: RADC (Griffiss) [redacted]
Dr. Owen W. Miller Associate Professor, Industrial Eng. Room 111 University of Missouri Columbia, MO 65201 (314)882-2691 [redacted]	Degree: D.Sc., Industrial Engineering, 1966 Specialty: IE Apps., Human Factors Engr., Productivity Assigned: AFHRL (Luke) [redacted]
Professor Dean E. Nold Chairman, Dept. of Electrical Eng. Tech. Purdue University 2101 Coliseum Blvd., East Fort Wayne, IN 46805 (219)482-5738 [redacted]	Degree: M.S., Electrical Engineering, 1963 Specialty: Aviation & Fuze Systems Assigned: AFHRL (Luke) [redacted]
Dr. Russell E. Petersen Professor, Aerospace & Mechanical Eng. Aero. Bldg. 16 University of Arizona Tucson, AZ 85721 (602)884-1265 [redacted]	Degree: Ph.D., Eng. Science & Applied Physics, 1958 Specialty: Combustion/Propulsion Assigned: AFRPL (Edwards) [redacted]

NAME/ADDRESS	DEGREE, SPECIALTY & LABORATORY ASSIGNMENT
Dr. Robert Premus Associate Professor of Economics Wright State University Dayton, OH 45435 (513)873-3165 [redacted]	Degree: Ph.D., Economics, 1974 Specialty: Economic Theory, Quantitative Meth. & Reg'l Econ. Assigned: AFCEC (Tyndall) [redacted]
Dr. John E. Reissner Assistant Professor, Physical Sciences Pembroke State University Pembroke, NC 28372 (919)·521-4214 Ext. 247 [redacted]	Degree: Ph.D., Chemistry, 1972 Specialty: Physical Chemistry Assigned: AEDC (Arnold) [redacted]
Dr. Charles W. Sanders Assistant Professor, Electrical Eng. University of Houston Cullen Blvd. Houston, TX 77004 (713)749-2782 [redacted]	Degree: Ph.D., Electrical Engineering, 1973 Specialty: Parameter & State Est., Optimal & Stochastic Control Assigned: ADTC (Eglin) [redacted]
Dr. Jay R. Sculley Associate Professor, Dept. of Civil Eng. Virginia Military Institute Lexington, VA 24450 (703)463-6331 [redacted]	Degree: Ph.D., Env. Engr. & Oper. Research Specialty: Operations Research, Computer Sci., Env. Engr. Assigned: AFCEC (Tyndall) [redacted]
Dr. Marvin S. Seppanen Assistant Professor, Industrial Eng. University of Alabama P. O. Box 6316 University, AL 35486 (205)348-7160 [redacted]	Degree: Ph.D., Operations Research, 1975 Specialty: Industrial Engr., Oper. Research, Computer Sci. Assigned: FJSRL (AF Academy) [redacted]
Dr. Wesley W. Shelton, Jr. Assistant Professor, Dept. Electrical Eng. Florida Institute of Technology Melbourne, FL 32901 (305)723-3201 Ext. 215 [redacted]	Degree: Ph.D., Electrical Engineering, 1974 Specialty: Electrical/Biomedical Eng. & Biophysics Assigned: SAM (Brooks) [redacted]
Dr. Rex D. Stith Associate Professor Dept. of Physiology & Biophysics Health Sciences Center University of Oklahoma P. O. Box 26901 Oklahoma City, OK 73190 (405)271-2243 [redacted]	Degree: Ph.D., Physiology, 1971 Specialty: Endocrinology, Neuroendocrinology Assigned: SAM (Brooks) [redacted]

NAME/ADDRESS	DEGREE, SPECIALTY & LABORATORY ASSIGNMENT
Dr. Timothy F. Thomas Associate Professor, Dept. of Chemistry University of Missouri-Kansas City Kansas City, MO 64110 (816)276-1555 [redacted]	Degree: Ph.D., Chemistry, 1964 Specialty: Physical Chemistry (Photochemistry & Chem. Kinetics) Assigned: AFGL (Hanscom) [redacted]
Dr. Kenneth W. Wegner Associate Professor, Education 305 McGuinn Hall Boston College Chestnut Hill, MA 01267 (617)969-0100 Ext. 4079 [redacted]	Degree: Ed.D., Counseling Psych. (Educ. Psych.), 1961 Specialty: Psychological Testing, Behavioral Analysis, Training Assigned: AFISC (Norton) [redacted]
Dr. Thomas A. Williamson Assistant Professor College of Engineering & Technology Northern Arizona University Flagstaff, AZ 86011 (602)523-3589 [redacted]	Degree: Ph.D., Electrical Eng. & Computer Science Specialty: Nuclear Electronics Assigned: AFWL (Kirtland) [redacted]

PARTICIPANT LABORATORY ASSIGNMENT

1978 USAF/ASEE SUMMER FACULTY RESERACH PROGRAM

AFCEC — AIR FORCE CIVIL ENGINEERING CENTER (TYNDALL AIR FORCE BASE)
1. Dr. Robert Premus - Wright State University
2. Dr. Jay Raymond Sculley - Virginia Military Institute

CEEDO — DET 1 (CIVIL & ENVIRONMENTAL ENGINEERING DEV. OFFICE), HQ ADTC(AFSC) (TYNDALL AIR FORCE BASE)
1. Dr. S. Reza Ahsan - Western Kentucky University
2. Dr. Gordon Lewandowski - New Jersey Institute of Technology
3. Dr. James David Lowther - Louisiana Tech University
4. Dr. John L. Lowther - Michigan Technological University

ADTC — AIR FORCE ARMAMENT LABORATORY (ELGIN AIR FORCE BASE)
1. Dr. Robert L. Carroll - University of South Carolina
2. Dr. Louis Anthony DeAcetis - Bronx Community College/Cuny
3. Dr. Alan Alfred Desrochers - Boston University
4. Dr. William Alfred Hornfeck - Gannon College
5. Dr. June K. Lee - Ohio State University
6. Dr. Charles Woodford Sanders - University of Houston

RADC/ET — ROME AIR DEVELOPMENT LABORATORY (HANSCOM AIR FORCE BASE)
1. Dr. Paul R. Caron - Southern Massachusetts University
2. Dr. Richard Dobrin - Long Island University

ESD — ELECTRONICS SYSTEMS DIVISION (HANSCOM AIR FORCE BASE)
1. Dr. Henry D'Angelo - Memphis State University
2. Dr. Robert E. Lovell - Arizona State University

AFGL — AIR FORCE GEOPHYSICS LABORATORY (HANSCOM AIR FORCE BASE)
1. Dr. Timothy F. Thomas - University of Missouri-Kansas City

FJSRL — FRANK J. SEILER RESEARCH LABORATORY (AIR FORCE ACADEMY)
1. Dr. Robert A. Kadlec - University of Colorado
2. Dr. Roger K. Bunting - Illinois State University
3. Dr. Marvin S. Seppanen - University of Alabama

AEDC — ARNOLD ENGINEERING DEVELOPMENT CENTER (ARNOLD AIR FORCE BASE)
1. Dr. R. Leonard Brown, Jr. - University of Virginia
2. Dr. James A. Liburdy - Memphis State University
3. Dr. John Eric Reissner - Pembroke State University

AFRPL — AIR FORCE ROCKET PROPULSION LABORATORY (EDWARDS AIR FORCE BASE)
1. Dr. Philip J. Feinsilver - University of Utah
2. Dr. James C. Lauffenburger - Canisius College
3. Dr. Irvin M. Citron - Fairleigh Dickinson University
4. Dr. Shyhming Chang - California State University
5. Dr. Russell E. Petersen - University of Arizona

PARTICIPANT LABORATORY ASSIGNMENT Continued

RADC ROME AIR DEVELOPMENT CENTER (GRIFFISS AIR FORCE BASE)

1. Robert H. Foulkes, Jr. - Youngstown State University
2. Dr. Theodore S. Bolis - Syny College at Oneonta
3. Dr. Robert W. McLaren - University of Missouri
4. Nicola Berardi - Purdue University

SAM SCHOOL OF AEROSPACE MEDICINE (BROOKS AIR FORCE BASE)

1. Dr. Michael Hankamer - New Mexico State University
2. Dr. Wesley W. Shelton - Florida Institute of Technology
3. Dr. Rex D. Stith - University of Oklahoma

AFHRL-FT AIR FORCE HUMAN RESOURCES LABORATORY (WILLIAMS AIR FORCE BASE)

1. Jon S. Bailey - Florida State University

AFHRL-FT AIR FORCE HUMAN RESOURCES LABORATORY (LUKE AIR FORCE BASE)

1. Dr. Owen W. Miller - University of Missouri
2. Dean E. Nold - Purdue University

AFWL AIR FORCE WEAPONS LABORATORY (KIRTLAND AIR FORCE BASE)

1. Dr. Albert J. Frasca - Wittenberg University
2. Dr. Robert B. Green - West Virginia University
3. Dr. Robert L. Gutmann - University of Massachusetts
4. Dr. Donald C. Haueisen - Pacific Lutheran University
5. Dr. James W. Jeter, Jr. - Virginia Military Institute
6. Dr. Thomas A. Williamson - Northern Arizona University

AFISC HQ,USAF INSPECTION AND SAFETY CENTER (NORTON AIR FORCE BASE)

1. Dr. Kenneth W. Wegner - Boston College

RESEARCH REPORTS

1978 USAF/ASEE SUMMER FACULTY RESEARCH PROGRAM

VOLUME I

Report No.	Title	Research Associates
1	Environmental Remote Sensing for Air Force Resource Management	Dr. S. Reza Ahsan
2	Control of JP-4 Emissions from Underground Storage Tanks	Dr. Gordon A. Lewandowski
3	Forestry Lands Allocated for Managing Energy (Flame) Feasibility Study	Dr. James D. Lowther
4	Sensitivity Analysis of Air Quality Assessment Model Predictions for Air Force Operations	Dr. John L. Lowther
5	A Comprehensive Socioeconomic Impace Assessment Model	Dr. Robert Premus
6	The Environmental Technical Information System for Air Force Use	Dr. Jay R. Sculley
7	Adaptively-predictive Linear Optimal Guidance: Target Seeking	Dr. Robert L. Carroll
8	Wide-Band Radome Research in Refractive Error Correction	Dr. Louis A. DeAcetis
9	Analysis of a Zoom Chain Optical System	Dr. Alan A. Desrochers
10	Data System Architectures for Stores Management Systems	Dr. William A. Hornfeck
11	A Three-dimensional Elastic-Plastic Analysis of High Velocity Impace Problems By a Finite Element Method	Dr. June K. Lee
12	On-Line Spectral Estimation Via Maximum Entropy Processing	Dr. Charles W. Sanders
13	Advanced Acquisition/Strike System Guidance Techniques	Robert H. Foulkes, Jr.
14	Application of Bayesian Techniques to Reliability Demonstration Estimation and Updating of the Prior Distribution	Dr. Theodore S. Bolis

RESEARCH REPORTS (Continued)

Report No.	Title	Research Associates
15	Digital Image Processing: Design Considerations for Future Systems	Dr. Robert W. McLaren
16	Clutter Suppression Through Radar Polarization Processing	Nicola Berardi
17	Measuremnet of Photodissociation Cross Sections of Water Cluster Ions	Dr. Timothy F. Thomas
18	A Quantitative Approach to Aggregation in the Modeling of Tactical Command and Control Systems	Dr. Henry D'Angelo
19	Specialized Stimulation Concepts for Command-Control-Communications-Intelligence (C^3I) Systems	Dr. Robert E. Lovell
20	Overlapped Sub-Array Techniques for Use in a Space Radar	Dr. Paul R. Caron
21	Design of an Imaging System to Conduct Human Thermal Signature Analysis with a 256 Element Schottky Barrier IRCCD Detector	Dr. Richard Dobrin
VOLUME II		
22	Investigation of the Computational Aspects of the Numerical Solution of Flow on a Core	Dr. R. Leonard Brown
23	Numerical Investigations of Natural Convection Inside of a Finite Horizontal Cylinder	Dr. James A. Liburdy
24	Gas Sampling Probe Computer Program	Dr. John Eric Reissner
25	The Application of Laser Doppler Velocimetry to the Study of Vortex Formation and Propagation in Unsteady Separated Flows	Dr. Robert A. Kadlec
26	Physical Properties of Molten Chloroaluminate Salt Systems	Dr. Roger K. Bunting
27	Technical Planning for the USAF Standard Base Supply System (SBSS); Rimstop and Beyond	Dr. Marvin S. Seppanen
28	Engineering Equations Verification Study: X-Ray Deposition Analysis	Dr. Philip Feinsilver
29	Target Materials for Low Energy X-Ray Sources	Dr. James C. Lauffenburge

RESEARCH REPORTS (Continued)

Report No.	Title	Research Associates
30	The Quantitative Determination of Trace Levels of Titanium in Hydrazine	Dr. Irvin M. Citron
31	Evaluation of Current Research in Fracture and Failure Behavior of Solid Propellant	Dr. Shyhming Chang
32	An Investigation of Critical Erosion Analysis Deficiencies	Dr. Russell E. Petersen
33	Adaptive/Predictive Data Compression for Electrocardiagrams	Dr. Michael Hankamer
34	In Vitro Study of Microwave Effects on Calcium Efflux in Rat Brain Tissue	Dr. Wesley W. Shelton, Jr.
35	Effect of Microwave Exposure on Certain Neuro-endocrine Parameters in Various Regions of the Rat Brain	Dr. Rex D. Stith
36	Applied Behavior Analysis in Flying Training Research	Dr. Jon S. Bailey
37	A Proposed Model System: Production Planning and Control for a Research and Development Function	Dr. Owen W. Miller
38	Using Fourier Coefficients as a Proposed Indicator of ACM Pilot Tracking Skills (Terminal Phase) for the Simulator for Air-to-Air Combat (SAAC)	Dean E. Nold
39	Neutron Production from Collective Ion Acceleration and Plasma Heating Experimentation Using a 6MeV 150 Kiloampere Field Emission Generator	Dr. Albert J. Frasca
40	Laser-Induced Fluorescence Studies of SnO and PbF	Dr. Robert B. Green
41	Adaptive Identification and Control of a Gimbaled Laser Pointing and Tracking System	Dr. Robert L. Gutmann
42	Nonlinear Adaptive Optics	Dr. Donald C. Haueisen
43	Inelastic Dynamic Response of Reinforced Concrete	Dr. James W. Jeter
44	Optimized Procedures for Radiation Testing of LSI Circuit Technology	Dr. Thomas A. Williamson
45	Relationship of Fighter Pilot-Operator Age and Flying Experience to Selected Unsafe Acts and Psychophysiological and Environmental Variables in Major/Class A Mishaps	Dr. Kenneth W. Wegner

1978 SUMMER FACULTY RESEARCH PROGRAM

Sponsored by

THE AIR FORCE OFFICE OF SCIENTIFIC RESEARCH

Conducted by

AUBURN UNIVERSITY AND OHIO STATE UNIVERSITY

PARTICIPANT'S FINAL REPORT

ENVIRONMENTAL REMOTE SENSING FOR AIR FORCE RESOURCE MANAGEMENT

Prepared by:	Dr S. Reza Ahsan
Academic Rank:	Professor of Cartography and Remote Sensing
Department and University:	Department of Geography and Geology Western Kentucky University Bowling Green, KY 42101
Assignment:	Det 1 ADTC/ECA (CEEDO) Tyndall AFB FL 32403
USAF Research Colleague:	Capt Richard Padgett

Date:	18 August 1978
Contract:	No. F44620-75-C-0031

ENVIRONMENTAL REMOTE SENSING FOR AIR FORCE RESOURCE MANAGEMENT

by

S. Reza Ahsan

ABSTRACT

The study was undertaken to assist the Air Force in evaluating remote sensing for resource management. Air Force environmental resource management needs were evaluated for possible remote sensing applications. Areas identified for remote sensing application include: (a) inventory of DOD range resources, (b) land use classification, change and monitoring, (c) environmental assessment and planning, (d) archeological and historical site location, (e) endangered species habitat identification, (f) conservation and recreation area location and (g) mineral deposit and energy resources identification, (h) preparation of environmental baseline data summaries.

The remote sensing techniques evaluated for Air Force resource management needs were: (a) aerial photos, (b) Skylab S190A and SB, (c) Landsat CCT, (d) Radar SLAR, (e) UV, and (f) Multispectral thermal IR. Four case studies cite the utility of using CIR (Color Infrared) in resource management. It was found that NASA aircraft high altitude CIR gives the best advantages for use in Air Force resource management. Recommendations were made for establishment of (a) remote sensing lab, (b) training of personnel, (c) use of CIR in Air Force resource management, (d) preparation of a CIR manual, (e) use of Landsat and Skylab S190B in Air Force and DOD range planning on an experimental basis, (f) routine use of high altitude CIR to prepare environmental data bases and evaluate AICUZ zones, (g) evaluation of an automated computer/remote sensing system for resource management (similar to those used by USGS and several other federal and state agencies), and lastly (h) the establishment of a remote sensing center for resource management and to coordinate activities in the field.

The results showed that Air Force can use remote sensing in environmental resource management. Color infrared should be used for resource management, with suitable minimal training of personnel. An important conclusion of the study is that CIR remote sensing could be used by base (range) Civil Engineers in their comprehensive planning programs.

ACKNOWLEDGMENTS

The study was made possible by a USAF/ASEE Summer Faculty Research Associateship at Civil Engineering and Environmental Development Office (CEEDO) at Tyndall AFB, Panama City, Florida. Fred O'Brien admirably coordinated the program for Auburn University. He deserves the author's gratitude. Many persons provided assistance. Captain Richard E. Padgett, Environmental Scientist, suggested this project, served as technical advisor, and helped in many other ways to facilitate this study. A1C Dennis Strutz, CEEDO, Tyndall AFB, was highly valuable in providing essential logistical support and expediting the paperwork. Major Peter Daley, Major J. D. Thompson and Major Brad Grems were very helpful in giving direction, background information and technical editing. They always made their valuable time available and provided social occasions for continuing these discussions for which I owe a debt of gratitude. The following colleagues in CEEDO and Civil Engineering Center also contributed valuable background information: Captain D. A. Armstrong, Captain G. Plummer and Capt Hawkins as well as Lt J. Tarquinio, Lt J. Kent, Ms Joan Scott, and Ms G. Armstrong (Librarian).

The author is indebted to Col J. Pizzuto, Major P. Crowley, Maj Emil Frein and others of the Environics Directorate for providing a cordial and helpful work environment. It has been a pleasure to work with these capable people.

I am also grateful to Dr Clark I. Cross, Professor of Remote Sensing and Chairman, Geography Department, University of Florida for consultation on aspects of remote sensing, and to Dr Wayne Hoffman, Professor of Regional Planning and head of the Department of Geography and Geology, Western Kentucky University on aspects of planning and resource management.

For various secretarial assistance, the author is indebted to Mrs. L. Evans, and Mrs. L. Nichols.

NOMENCLATURE

Band: A wavelength interval in the electromagnetic spectrum. For example, in Landsat the bands designate specific wavelength intervals where images are acquired.

BW: Black and White.

BWIR: Black and White Infrared.

CCT: Computer Compatible Tape. A reconstruction of data in magnetic tape form suitable for computer analysis. Landsat data for computer analysis is available from EROS data center.

CIR: Color Infrared.

EROS: Earth Resource Observation System, a branch of USGS located in Sioux Falls, SD, for dissemination of NASA space and aircraft data.

FCC: False Color Composite. A false color reconstruction of multiband photography created from two or more filtered photographic bands. In the case of Landsat, generally band 4, 5, and 7 are used to make an FCC.

Image-100: General Electric Company computer for use with Landsat CCT.

Landsat: NASA satellite for earth resource monitoring from 570 miles in space.

MDAS: Bendix computer system for use with Landsat CCT.

Mosaic: A number of overlapping air photos whose edges have been matched to form a continuous photographic representation of a given area.

Near Infrared: Electromagnetic wavelength from 0.7 to 2.0 micrometer where the range of solar radiation still reflects. Photographic BW and CIR works in this region.

Remote Sensing: The collection of information about an object without being in physical contact with that object. Remote Sensing is restricted to methods that record the electromagnetic radiation reflected or radiated from an object.

SAR: Synthetic Aperture Radar. SLAR system in which high resolution is achieved by utilizing Doppler principle to give the effect of a very long antenna.

Skylab S190A and S190B: Besides other sensors, Skylab Earth Resource Experiment Package (EREP) contained S190A and S190B multispectral cameras. S190A provided 2.2" photos simultaneously on six bands. S190B is referred as "earth terrain camera" and has 4.5" photos on two bands - Color and CIR.

SLAR: Side-Looking Airborne Radar, a general term.

Thematic Maps: Map showing theme like spatial resource location.

Thermal IR: The portion of the infrared region from approximate 2 to 14 micrometer that corresponds to heat radiation.

USGS: United States Geological Survey.

UV: The ultraviolet region consisting of wavelengths from 0.01 to 0.4 micrometer.

INTRODUCTION

Remote Sensing from aircraft and spacecraft is an extremely cost-effective means of collecting data, and during the last two decades many new sensors and techniques for collection of data have been developed. The availability of new remote-sensing instruments and their ability to collect data have in many respects outstripped the capability of the scientific and resource management community to utilize such data effectively. This handicap has been offset to a large extent by the fact that there are in the Air Force literally thousands of persons who, with a small amount of training, and knowledge of availability, could effectively use such data in their studies or in resource management decisions.

Growing populations near Air Force bases, coupled with a widening horizon of demands being made on land resources, have brought about an expanding array of pressures on limited available resources. These pressures have brought about encroachments on Air Force land and air space which in many instances are mission limiting. Some examples of obvious conflicts include: agricultural production in conflict with real estate development and resulting urbanization; environmental protection against energy production demands; recreational development versus the use of the land for forestry, grazing, and extractive uses; conservation of coastal areas for recreational uses in the face of needs for more port facilities and shoreline industrial sites; and preservation of wetlands for natural wildlife and fisheries habitat in the face of new demands for development of such wetlands for urban uses, agricultural production, and recreational uses.

Air Force range planning programs are presently addressing natural resource issues related to range land and air space requirements and other land uses. Recent environmental legislation, changing terms and conditions for the continued withdrawal of lands from the public domain, and public inquiries about alternative or multiple uses of Air Force bases make it imperative that sound scientific information be developed concerning the natural resources contained in these lands. For this purpose the ecological, cultural and natural resource inventories and land use classification and terrain information data are critically valuable to Air Force resource managers. This information can be provided from the products of remote sensing technology.

OBJECTIVES

This study was undertaken to assist the Air Force in evaluating remote sensing, specifically aircraft and satellite imaging techniques, for resource management purposes. The Air Force is responsible for thousands of acres of land spread over hundreds of bases and supporting installations. Effective management of these resources requires the develment of techniques and tools which will aid in the evaluation, classifcation, and monitoring of large tracts of land. Remote sensing has great potential for effective natural resource management. The goal of the study was to evaluate different remote sensing techniques based on (a) effectiveness, (b) availability and accessibility of data (c) cost, (d) and training required for users. Only those techniques which were found suited to the Air Force environmental resource management needs were considered in detail.

EVALUATION OF AIR FORCE ENVIRONMENTAL RESOURCE MANAGEMENT

The application of remote sensing to Air Force environmental resource management requires an evaluation of needs. Air Force resource managers are required to conduct studies that fulfill obligations under a number of laws passed during the last decade. Some of these laws are:

(a) National Environmental Policy Act of 1969

(b) The Federal Land Policy and Management Act of 1976

(c) Sikes Act-Conservation and Recreational Uses of DOD Lands

(d) Clean Air Act as Amended

(e) Historic Preservation Acts

(f) Endangered Species Act of 1973

These laws require managers to assemble resource inventory, land use classification, soil and vegetation data. The Air Force Civil Engineering and Environmental Development Office, Civil Engineering Center and Headquarters Air Force have made efforts to fulfill these requirements by various systematic evaluation programs. One such effort is the preparation of TAB A-1 environmental narratives for Air Force bases.

The TAB A-1 is a compilation of baseline data containing the natural, social, and economic environs of the region influenced by an Air Force installation. The primary purpose of the TAB A-1 is to provide Air Force base personnel with an up-to-date data base to support the environmental impact analysis process or other studies required by law. Another use of TAB A-1 is for planning activities.

The TAB A-1 is not always complete. One recurring deficiency is the lack of current land use, natural resource location (thematic maps), and environmental monitoring data. Remote sensed data could materially improve the quality and quantity of the TAB A-1 data. Table I indicates areas of the TAB A-1 that are potential candidates for application of remote sensing data.

TABLE I. POTENTIAL REMOTE SENSING METHODS APPLICABLE TO TAB A-1 PREPARATION

TAB A-1 AF Environmental Reference No.	Subject	Remote Sensing Method
1.4	Geographic Location	High Altitude CIR, Landsat or Skylab
3.1.1	Physiography	Air Photo Color or CIR
3.1.2	Geology	High Altitude CIR, Color or Landsat
3.1.3	Soils	Air Photo Color
3.2.1	Hydrology	CIR
3.2.3.1	Sewerage Pollution	Thermal IR
3.4.1	Plants	CIR or BWIR
3.4.2.5	Threatened and Endangered Species (Animals)	Medium Altitude BW
3.7	Natural Hazards - Flood, Landslide, Rock-slide Prone areas, Tidal Zones, Fault lines	CIR and Landsat
4.1.1	Population (Distribution) and change	High Altitude CIR Skylab S190B
4.2.5.4	On-Base Housing (Energy Leakage)	Thermal IR
4.4.1.1	Transportation General	High Altitude CIR
4.4.3.1	Existing Land Use	Medium/Low Altitude CIR
4.4.3.2	Land Ownership and Value	Medium Altitude BW
4.4.3.5	Summary of on-base land and facilities	Remote Sensing based digital information/ inventory system used by various agencies like USGS
4.4.3.7	Historical/Archeological Sites	Medium/Low Altitude COLOR or CIR
4.4.3.8	Air Installation Compatible Use Zone (AICUZ)	High Altitude CIR

Environmental Impact Statement (EIS) data are generally extracted from TAB A-1 reports. The EIS could be assembled more cost effectively through the use of remote sensing data. In addition, studies of endangered species habitat, historical/archeological sites and recreational activities located on Air Force bases could use remotely sensed data.

Remote sensing techniques could play a critical role in work carried out under the following topics:

(a) Inventory of Range Resources (Thematic Maps and Computer Data Base)

(b) Land Use Classification, Change, and Monitoring

(c) Environmental Assessment and Planning

(d) Archeological and Historical Sites Location

(e) Endangered Species (Habitat) Identification

(f) Conservation and Recreation Areas Location

(g) Mineral Deposits and Energy Resources

Remote sensing is successfully being used by various state and federal agencies to provide information for most of the above mentioned topics. Numerous publications are available indicating such uses. However, the techniques used by the agencies are designed to suit their individual needs.

<u>REMOTE SENSORS:</u>

Remote sensors suitable for Air Force environmental needs are (In decreasing importance):

A. Aerial Photos: CIR, COLOR and Black/White

B. Skylab S190B and S190A

C. Landsat imageries and CCT based computer enhanced products

D. RADAR - SLAR (SAR)

E. UV

F. Multispectral Thermal IR

A. Aerial photos have been used in TVA mapping and resource management since its inception in the middle 1930s. Adoption of color and infrared films subsequently for aerial photography have made it still more useful. In the enthusiasm for satellite imagery and new forms of airborne remote sensing, such as thermal IR and RADAR, the advantages of conventional aerial photography should not be overlooked. Generally, the following four types of films are used in aerial photography: black and white (BW) film called Panchromatic, black and white Infrared, (BWIR) color and color Infrared, (CIR). Each of these have several variants.

Panchromatic Films: Panchromatic film having approximately the same range of light sensitivity as the human eye is the standard film for aerial photography. Images on panchromatic film are rendered in varying shades of gray, with each tone comparable to the density of an object's color as seen by the human eye. Pan films distinguish objects of truly different colors. These films have been used by resource managers in many useful ways.

Infrared Film: Infrared black and white film is primarily sensitive to blue, green, red and near infrared light radiations. It is sometimes exposed through a red filter for near infrared radiation imprints. Gray tones on infrared result from reflections from the surface of the objects. Broadleaf vegetation is highly reflective whereas coniferous or needleleaf vegetation are less reflective. Bodies of water absorb infrared wave lengths. Therefore, this film has been used in forestry for tree species delineations and to distinguish or map water land contact points.

Color film: Photo interpreters who wish to identify natural resources, such as vegetation, terrain, and soil types and above all, quality of water, have used color films successfully. Some counties have been mapped in color for State Highway Departments. Most available coverage has been black and white, however, more color aerial photos have become available. High altitude color aerial photos are available from EROS, Data Center. Color film is specially valuable for soils identification, water quality and industrial stockpiles.

Infrared Color: Infrared color is a false-color film. Three emulsion layers are sensitized to green, red and infrared radiation. In spring and summer, healthy deciduous trees photograph magenta or red and healthy conifers photograph reddish to bluish-purple. Dead or dying foliage registers as a bright green. Healthy foliage whose leaves have simply turned red or yellow in autumn photograph yellow and white respectively. Waterbodies are dark blue to black, and built up areas show up as gray to blue. This film in recent years is proving itself to be the most useful for resource management planning and environmental mapping.

Scale: The use of aerial photography for problem solving requires some understanding of scale. An aerial photo generally is available in a format of 9" x 9" square. They cover large or small areas based on their scale. The resolution also varies with scale.

The following table roughly shows the guidelines for resource management surveys based on aerial photos.

ENVIRONMENTAL RESOURCE MANAGEMENT GUIDELINES
FOR PHOTO SCALE SELECTION

Description of Topic	Film Type	Scale
a. Inventory of Range Resources	CIR	1:30,000 to 1:125,000
b. Environmental Assessment and Planning	CIR and Color	1:4,000 to 1:12,000
c. Land Use	CIR, Color, and BW	1:12,000 to 1:125,000
d. Archeological and Historical Sites Location	CIR and Color	1:4,000 to 1:12,000
e. Critical Habitat Identification	CIR and Color	1:12,000 to 1:24,000
f. Endangered Species Habitat Identification	CIR and Color	1:12,000 to 1:24,000
g. Conservation and Recreation areas Location	CIR and Color	1:24,000 to 1:125,000
h. Mineral Deposit	Color and BW	1:12,000 to 1:24,000
i. Population Studies	CIR	1:12,000 to 1:60,000

B. Skylab S190B and S190A have been used successfully as resource management inputs. The Skylab EREP (Earth Resource Experiment Package) contained various remote sensors. Of these, especially S190B and S190A are of interest. The S190B terrain mapping camera provided color and color infrared photographic products for most parts of the United States. The S190A multispectral camera provided color, CIR, and four black and white photos representing four bands in the visible spectrum. Aldrich (in Pacific Southwest Forest and Range Experiment Station Paper PSW-113) has come to the following conclusion:

> The Skylab photographic data was found useful at two resource-oriented sites for broad classification. Land use classes, such as forest and nonforest, and range vegetation classes at the Region level (Deciduous, Coniferous, and Grassland) were distinguished with acceptaaccuracy when checked against ground truth. Enlarged Skylab S190B photographs (1:125,000) can be used for coniferous and Grassland classes mapping with an accuracy of 90 percent. Paved and gravel roads, utility corridors, large mining excavations and clusters of buildings can also be mapped.

Skylab S190B photos in some cases can be used for Air Force environmental management needs where scales of 1:125,000 are applicable. The photo enlargements can be ordered for fifty dollars per each color print of size 36" x 36" covering an area fifty to one hundred percent larger than Edwards AFB. (Approximately 300 square miles)

C. Landsat satellites move in an almost perfectly circular orbit at an altitude of 570 miles inclined at an 81 degree relative to a plane passing through the earth's equator. Two imaging sensor systems operate on the Landsat. One is a television camera system called Return Beam Vidicon (RBV). The second is a Multispectral Scanner (MSS), which produces a continuous image strip built up from successive scan lines extended perpendicular to the forward direction of the satellite's orbital motion. The four bands of the multispectral scanners are:

MSS Band No.	Wave Length (Micrometer)	Spectral Region
4	0.5 to 0.6	Green
5	0.6 to 0.7	Red
6	0.7 to 0.8	Near Infrared
7	0.8 to 1.1	Near Infrared

(RBV bands are numbered 1, 2, and 3).

Various features found on the surface of the earth reflect differing amounts of light at different wavelengths and therefore, they can be identified by their own characteristic reflectance pattern. The digital video data are reformated into Computer Compatible Tapes (CCT) and analyzed by users through a variety of computer based programs. Each of the four black and white images represents a particular band. The gray tones associated with individual features vary from one band image to the next in proportion to the amount of light reflected from each small surface area. Color images are made from combination of individual black and white images by projecting each given band through a particular filter. The usual combination consists of band 4 (green) projected through a blue filter, band 5 (red) projected through a green filter, and band 7 (infrared) projected through a red filter. In this rendition called False Color Composite (FCC), growing vegetation appears in shades of red, rock and soil normally show colors ranging from blue through yellows and browns, water stands out as blue to black depending on depth and amount of suspended sediment, and cultural features (towns and roads) usually are recognized by bluish-black tones arranged in characteristic patterns.

The photographic product and the FCC, give a display of the location, but probably cannot be used to fulfill Air Force resource management needs. The CCT, however, have been used effectively on MDAS (Bendix) and Image-100 (GE) computers to generate maps as large as 1:24,000 showing land use, water quality in Michigan lakes, etc. For small or medium sized Air Force installations, the cost may be a limiting factor. It should be pointed out that the cost of these maps has been dropping. Still, a large base like Nellis AFB could effectively use Landsat data for resource inventory.

Many experiments using Landsat data have been published. Commercial corporations like Bendix and General Electric carry out resource management studies using Landsat imageries. NASA, USGS and many other federal agencies

have carried out experiments successfully using Landsat for land use and environmental resource inventories. Ellefsen and associates have demonstrated the use of Landsat CCT for land use studies. Universities, have also used Landsat data on a cost effective basis.

D. RADAR specially developed for reconnaissance and continuous mapping purposes by the Air Force is called SLAR (the Side-Looking Airborne Radar). Synthetic Aperture Radar (SAR), an off shoot of SLAR, has proved itself useful in mapping resource in Brazil and Venezuela. Two commercial corporations are foremost in the RADAR mapping field. They are:

1. Aero Service-Goodyear Aerospace

2. Motorola Aerial Remote Sensing Inc

A SLAR K band or L band have all weather capabilities with maximum penetration of clouds, fog and rain. With an imaging range of more than 50 km and a recording width of 37 km, large area surveys become economical. The result is a continuous mosaic with low distortion, which especially highlights the terrain. RADAR is a useful tool but may not be applicable to Air Force environmental management needs.

E. UV (Ultraviolet) photography and scanning imagery have been used for monitoring oil films. UV photography may be acquired with suitable film and filter combinations, but optical-mechanical scanners using UV filter and detector produce better images. Because of scattering of UV energy at high altitudes, low altitude photography (less than 3,000 feet) has been recommended. Air Force resource management use of UV photography could become important in the future.

F. Multispectral Thermal IR is highly useful for monitoring environmental conditions, thermal plumes, oil films on water, and underground mine coal fires. Building heat loss surveys is another use. Thermal IR images are produced by airborne scanner systems. Multispectral systems are costly and there is no ready source of existing imageries. Equipment and contractors have to be tasked to do specific jobs. The importance of thermal IR in archeological or historical site studies, however, should not be discounted. The Air Force resource management need of Multispectral Thermal IR will probably be minimal, but may be useful for specific applications in the future.

APPLICATIONS:

Evaluation of different types of remote sensing techniques and remote sensors that could be of use in Air Force environmental resouce management indicates that existing high altitude (scale 1:31,250 to 1:130,000) NASA aircraft color Infrared (CIR) aerial photos are of highest value. These photos are available from EROS Data Center (USGS) Sioux Falls, SD for over 60 percent of the continental United States. Private companies like Mark Hurd Aerial Photos also have high altitude aerial photos available from their files. It is recommended to use these existing CIR aerial photos because of their low cost and ready availability.

Many studies have shown that color-infrared aerial photography is superior to other types of photography for interpretation of environmental resources.

CIR lends itself especially to land and water surveys because of its ability to distinguish man-made from natural surface materials such as built up areas, vegetation, bare soil and water, and its ability to penetrate haze and air pollution.

Case Studies:

i. A remote sensing survey of land use and water quality relationship, Wisconsin Shore, Lake Michigan, was conducted by Haugen and others of US Army Corps of Engineers (CRREL) for NASA. The primary focus of this report was to examine the feasibility of using remote sensing methods to rapidly and economically assess, on a regional scale, the effect of land use as it influences sediment loading of streams. A test area consisting of several major watersheds in Eastern Wisconsin was selected for the development and evaluation of techniques to achieve this objective. A variety of aerial remote sensors were applied to the test area for evaluating and developing data. The most useful imagery product was found to be NASA color infrared photography acquired at 60,000 feet with 9 inch format using R. C. 8 and Zeiss cameras.

ii. A Practical Method for the Collection and Analysis of Housing and Urban Environmental Data: An Application for Color Infrared Photography by Robert Joyce, Director of Los Angeles Community Analysis Bureau. This study was presented at an Eastman Kodak Seminar on "Aerial Photography as a Planning Tool" (Kodak Publication M128). This study for using CIR in Los Angeles City/County Planning suggests that remote sensing offers an attractive alternative to current urban data gathering techniques, especially when using color infrared film. The ability of color infrared film to resolve small objects and to differentiate by color hue makes it possible to derive a wide range of information from aerial photographs. Several properties of CIR film make it almost an ideal sensor in the urban environment: (1) vegetation is enhanced and can be correlated with socioeconomic factors, (2) haze penetration is possible, (3) small objects can be examined, (4) more directly observable information is contained on a CIR image than on any other sensor image, (5) interpretation is quite easy because of CIR's close relationship to normal photographic systems with which most people are familiar, (6) A minimum of interpretation equipment is needed if the imagery is examined visually, and (7) the imagery is inexpensive relative to more exotic sensor types. The city/county was expected to obtain CIR at a scale of 1:5,000 and develop a data bank to store the planning data from CIR.

iii. Study in Remote Sensing for Land Use by Richard D. Shinn and Frank V. Westerlund. This unpublished study was conducted under contract to Det 1, ADTC, Tyndall AFB FL. This study has evaluated three remote sensing techniques:

1. Photo Interpretation of High Altitude Aircraft CIR

2. Equidensitometric Processing of Aircraft or Landsat Imagery

3. Statistical Analysis of Landsat Digital Data.

The conclusion of this study was that high altitude aircraft CIR photo interpretation was the most cost effective method of preparing land use maps of Fairchild AFB, Washington and McChord AFB, Washington.

iv. USGS, Landuse Maps (1:250,000 and 1:24,000). USGS has used high altitude aerial CIR photos for preparing a series of maps which include up to level II land use (Anderson and others) on a scale of 1:250,000 and level III and some IV on urban area maps on a scale of 1:24,000. Anderson's classification, Land Use and Land System for Use with Remote Sensor Data, attempts to meet the need for current overview of land use/land cover on a basis that is uniform in categorization at the generalized first and second levels. It is intentionally left open-ended so that independent agencies may have flexibility in developing more detailed land use classification. cover and use. Anderson land use classification is based on four digits and is similar to Air Force environmental numbering system. The first digit 99 class) of level I land use. Second, third, and fourth digit represents II, III, and IV levels of land use intensity subclasses.

Interpretation and Effectiveness:

Possible applications of CIR for Air Force needs are: AICUZ, Environmental narrative (base line), EIS, Range Planning, Population Distribution and APZ. The high altitude 9 inch format could be enlarged to 36 inch format. One 9 x 9 comprises approximately 17 x 17 miles = 300± square miles in area at a scale of 1:125,000. When enlarged to 36" x 36" format, the scale would be 1:31,250. Further enlargements could be done as needed for spatial location. However, it costs less to order fewer large scale CIR (1:5,000 or larger) photographs from private companies as needed. Topographic maps with 2 to 4 feet contour intervals can be prepared using these CIR. Small contour interval maps have very important applications in engineering projects dealing with site improvements, drainage and waterline routing.

Air Force bases and ranges vary greatly in area, location, climate, terrain, and degree of isolation. CIR remote sensing could be effectively utilized by base (range) Civil Engineers in their comprehensive planning programs. Specific applications could deal with locating and planning in the following areas: (a) transportation and parking, (b) residential, office and commercial facilities, (c) water supplies and drainage, (d) agricultural and forestry land use, (e) sports and recreations, (f) zoning recommendations, (g) archeological and historical sites, (i) endangered species critical habitat identification and (j) environmental assessment.

Interpretation Equipment needed:

		No.	Cost
a.	B&L Magnifyer (Tube type) 5X	2	$50
b.	Pocket Stereoscope (Abram or CF6),	2	50
c.	Mirror Stereoscope with Binocular and Height Finder (F71)	1	550
d.	Dot Grid (acre grids)	3	10
e.	Polar Planimeter K&E	1	200
f.	Zoom Transferscope ZTS4 (Bausch and Lomb)	1	6000
g.	Portable Imagery Light Table, K&E	1	400
h.	Drafting Table and Light Table	1	800
i.	Mapograph (with suitable accessories)	1	4000
j.	Stereotope	1	1800
	TOTAL		$13,860

Most of these are available through Forestry Supply Company (Appendix A)

Source of CIR:

NASA has used RB-57 or U-2 high altitude aircraft to obtain medium and high altitude CIR. These are available from EROS Data Center (See Appendix B) at scales varying between 1:31,250 to 1:130,000. High and medium altitude CIR are also available from Mark Hurd Aerial (Appendix A). But to gather range USGS also has land use data base built up primarily on high altitude CIR, which are available to users.

Cost:

i Imagery and Photo

		Cost
a.	CIR Photo on paper 9 inch format	$7
b.	CIR Photo on paper 36 inch format	50
c.	CIR film positive 9 inch format	15
d.	Skylab and Landsat products (See Appendix B)	

ii A modest remote sensing lab for CIR photo interpretation will cost $24 to 30 thousand dollars without a film processing capability.

iii A Remote Sensing Graphic Terminal with digitizer system (without computer) will cost $40 to 60 thousand dollars.

Training Requirement for User:

As a minimum two to four people will be required to use CIR for Air Force environmental resource management needs. Some experience in photo interpretation would be an asset. This training could be provided in a series of short courses, in photo interpretation. Basic mensuration, CIR interpretation, and data extraction from CIR are primary objectives for such training. Professional seminars and symposiums would be of some value. Department of Highways and Transportation, and the Defense Mapping Agency (DMA), either at St Louis, Louisville, or San Antonio should be visited for demonstration of manipulations and specialized uses of aerial photos.

Alternate Techniques:

Skylab S190B photo enlargements could be used as an alternative to high altitude CIR. In large area studies, Skylab S190B photos would be highly valuable for study of population, land use, transportation routes, and vegetation. Skylab S190B product can be obtained from EROS (See Appendix B).

Landsat CCT can greatly enhance environmental assessment for large areas like Nellis AFB and adjacent ranges on a cost effective basis. In the range planning study proposed for Nellis AFB, either Image-100 (GE) or MDAS (Bendix) and CCT, could be used to complete an en array of environmental resource inventory parameters .

Color and BW (high altitude) aerial photos could be used for gaps where CIR is not available. In case of shallow water areas, Color will be superior to other photos.

<u>RECOMMENDATIONS:</u>

a. Establishment of Remote Sensing Lab

Remote sensing is going to play an increasingly important role in natural resource management and planning, as the quality increases and the costs decrease. In order to utilize this remote sensing capability, Air Force should establish a remote sensing lab as a focal point for Air Force resource assessment and management.

b. Training of Personnel

At least two persons would be required full time to fulfill the needs of remote sensing in resource management. The training of researchers and managers should be arranged through short courses (two or three days) and demonstration visits for application and other training.

c. High Altitude CIR be used for resource management.

High altitude CIR from NASA aircraft should be primarily used for Air Force resource management and environmental needs

d. Manual of CIR (high altitude) Use.

For the use of CIR in the Air Force environmental resource management needs, a manual of CIR (high altitude) applications should be prepared.

e. Landsat CCT enhanced products be used for large area Air Force range planning, such as Nellis AFB and its range complex. Skylab S190B and high altitude CIR be used for inventorying and extracting data for smaller bases on an experimental basis, such as Edwards AFB Precision Impact Range (PIRA).

f. Environmental baseline documents and AICUZ could use high altitude CIR for general location maps and Compatible Use District identification on a regular basis.

g. Automated Resource Management Systems based on aerial photography or space data (like USGS, Cornell, NY, BLM, US Dept of Interior, and various states like Florida, Minnesota, and South Carolina) should be evaluated as possible future systems for US Air Force Resource Management.

h. Air Force should establish a remote sensing center to coordinate its own activities in the field.

BIBLIOGRAPHY

Anderson, J. R., (1976) Introduction (to) Chapter 4. Application to Land-use Mapping and Planning; in U.S. Geol. Survey Prof. Paper 929, ERTS-1, A New Window on Our Planet, pp. 223-224.

Anderson, J. R., Hardy, E. E., Roach, J. T., and Witmer, R. E. (1976) A Land-use and Land Cover Classification System for Use With Remote Sensor Data: U.S. Geol. Survey Prof. Paper 964, 28 pp.

Austin, Alan and Adams, Robert (1978), Aerial Color and Color Infrared Survey of Marine Plant Resources; Photogramm. Engg. and Remote Sensing Vol. XLIV No 4, pp. 469-480

Avery, T. E., (1977) Interpretation of Aerial Photographs (3rd ed.): Minneapolis, Burgess Pub. Co., 392 pp.

Avery, T. Eugene, (1970), Photo-interpretation for Land Managers (Kodak Publication M-76), Eastman Kodak Company, Rochester, NY

Buzzanell, P. J., Potential Usefulness of CARETS data for Environmental Impact Assessment: NASA (GSFC) and U. S. Geol. Survey, 72pp. NTIS E77-10021

Eastman Kodak Company: (1974) Proceedings of Kodak Seminar: Aerial Photography as a Planning Tool (Kodak Publication M-128) Eastman Kodak Company, Rochester, NY.

Ellefsen, Richard, Gaydos, Leonard, Swain, Phillip, and Wray, James R, (1974), New Techniques in Mapping Urban Land-use and Monitoring Change for Selected U. S. Metropolitan Areas - An Experiment Employing Computer-assisted Analysis of ERTS-1 MSS Data: Intl. Society of Photogramm., Comm. VII, Symposium on Remote Sensing and Photo Interpretation, Banff, Canada, Oct 7-11, 1974, Proc., Vol. 1, p. 51-63

Ellefsen, Richard, Gaydos, Leonard and Wray, J. R., (1976), Computer-aided Mapping of Land Use: in U.S. Geol. Survey Prof. Paper 929, ERT-1 A New Window on Our Planet, pp. 234-242.

Environmental Systems Research Institute, (1977), DIMECNV-A System for Converting Scanner-digitized Mapping data Tapes to Polygon Format: Environmental Systems Research Inst. and U. S. Geol. Survey, 9 pp. 1976 Appendices NTIS PB266-438.

Estes, John E., (1966), Some Applications of Aerial Infrared Imagery, Annals of the Association of American Geography, pp. 673-682

Fitzpatrick, K. A., (1977), Cost Accuracy and Consistency Comparisons of Land Use Maps Made from High-altitude Aircraft Photography and ERTS Imagery: NASA(GSFC) and U. S. Geol. Survey p. 61 NTIS E77-10017

Haugen, R. K., McKim, H. L., and Marlar, T. L., (1976), Remote Sensing of Land Use and Water Quality Relationships - Wisconsin Shore, Lake Michigan, NASA and Corps of Engineers, U. S. Army Cold Region Research and Engg. Lab., Hanover, NH NTIS ADA 030746.

Joyce, Robert (1974): A Practical Method for the Collection and Analysis of Housing and Urban Environment Data: An Application of Color Infrared Photography, Kodak Publication M-128, Eastman Kodak Company, Rochester, NY pp. 15-20.

Klooster, S. A. and Scherz, J. P., (1974), Water Quality by Photographic Analysis, Photogrammetric Engineering, Vol. 15 No. 8, pp. 927-935.

Link, Lewis E. Jr., (1974), The Use of Remote Sensing Systems for Acquiring Data for Environmental Management Purposes; Report 1, A Procedure for Predicting Image Contrasts in Photographic Remote Sensor Systems, U. S. Army Engineer Waterways Experiment Station, Vicksburg, Mississippi, NTIS AD-A-002070.

Link, L. E., (1973) The Use of Remote Sensing Technique for Detecting and Identification of Pollutant Discharges, Army Engineering Waterways Experiment Station, Vicksburg, Mississippi Misc. Paper NTIS AD-A 017727.

Lins, H. F. Jr., (1976) Land Use Mapping from Skylab S190B Photography; Photogramm. Engg. and Remote Sensing V. 42 No. 3 pp. 301-307.

Marshal, J. R., and Meyer, M. P., (1978), Field Evaluation of Small Scale Forest Resource Aerial Photography, Photogramm. Engg. and Remote Sensing, Vol. XLIV No. 11 pp. 37-42.

Mitchell, W. B., Guptil, S. C., Anderson, E. A., Fegeas, R. G., and Hallam, C. A., (1977), GIRAS - A Geographic Information Retrieval and Analysis System for Handling Land Use and Land Cover Data: U. S. Geol. Survey Prof. Paper 1059 16 pp.

NASA Earth Resource Survey Symposium, (1975) at Houston, TX, X-58168, U. S. Government Printing Office, Washington DC.

NASA: Mission to Earth: Landsat Views the World, (1976) NASA SP-360, National Aeronautics and Space Administration, Washington DC.

Olson, Charles E., Jr., (1967), Accuracy of Land-use Interpretation from Infrared Imagery in the 4.5 to 5.5 Micron Band, Annals of the Association of Geographers, pp. 382-388.

Pacific Southwest Forest and Range Experiment Station, (1976), Evaluation of Skylab (EREP) Data for Forest and Rangeland Surveys (USDA Forest Service Research Paper (PSW-113), Pacific Southwest Forest and Range Experiment Station, Berkeley, California 94701.

Proceedings of the International Workshop on Earth Resources Survey Systems, (May 1971), Vol. 1 and 11, U. S. Government Printing Office, Washington DC.

Reeves, R. G., (1975), ed. Manual of Remote Sensing, Vol 1 and 11: Am. Soc. Photogrammetry, Falls Church, VA..

Remote Sensing of the Electro-Magnetic Spectrum; (1977), Land Use and Land Cover Maps and Statistics from Remotely Sensed Data (Special edition, edited by James R. Anderson), RSEMS, Dept of Geog-Geology, The University of Nebraska, at Omaha, Nebraska, Vol. 4, No. 4, (Oct 1977).

Sabins, Floyd F. Jr., (1978), Remote Sensing: Principles and Interpretation; W. H. Freeman and Company, San Francisco.

Simpson, Robert B., (1966), Radar, Geographic Tool; Annals of the Association of the American Geographers, pp. 80-96.

Smith, John, T., Edit. in Chief: (1968), Manual of Color Aerial Photography, American Society of Photogrammetry, Falls Church, VA 22046.

U. S. Air Force AICUZ, (1975) Environmental Planning Bulletin 1-1X, USAF/PREV Environmental Planning, Washington DC 20330.

U. S. Air Force Headquarters: ((1975), TAB A-1, Environmental Narrative - Phase II (The Comprehensive Plan), USAF/PREV Environmental Planning, Washington, DC 20330.

U. S. Geological Survey, (April 1977), Warning and Preparedness for Geologic-Related Hazards: Federal Register, V. 42 No. 70.

APPENDIX A

Names of Important Commercial Groups
in Remote Sensing/Resource Management

	Agency	Services/Equipment
1.	Aero Service Goodyear Aerospace 8100 Westpark Drive P. O. Box 1939 Houston, Texas 77001 Telephone: 713-784-5800	SLAR (SAR), Aerial Photo Utilities and Urban Planning
2.	General Electric, Space Division ATTN: Mr Howard L. Heydt 5030 Herzel Place Beltsville, Maryland 20705 Telephone: 301-937-3500	Landsat, CCT and Skylab leased Environmental and Land Use Mapping Using Image-100 System
3.	Bendix Research Labs Bendix Center ATTN: Dr Roger Southfield, Michigan 48076 Telephone: 313-352-7846	Landsat CCT based Color enhanced digitized maps of land use and environmental resources
4.	Motorola Aerial Remote Sensing Inc 4350 E. Camelback Road Phoenix, Arizona 85018	RADAR Mapping Aerial Photos
5.	Mark Hurd Aerial Surveys Inc 345 Pennsylvania Ave S. Minneapolis, Minnesota 55426 Telephone: 612-545-2583	Aerial CIR
6.	Forestry Supply Company Jackson, Mississippi	Remote Sensing Lab Equipment

HOW TO REQUEST A GEOGRAPHIC SEARCH

This form is used to request a computer search for imagery over a point or area of interest.

Data from this inquiry sheet will be used to initiate a computer Geosearch. The results will be returned on a computer listing along with a decoding sheet, from which imagery can be selected and ordered.

Complete the form as follows:

A. Enter your NAME, ADDRESS, and ZIP CODE clearly. If you have had previous contact with that facility, include your ACCOUNT number. Enter a PHONE number where you can be reached during business hours.

B. Complete the required information for either the POINT SEARCH, or AREA RECTANGLE inquiry, which includes the geographic LATITUDE and LONGITUDE coordinates. If coordinates are not available, please supply the GEOGRAPHIC NAME AND LOCATION or a map with the area of interest identified. It is beneficial that you minimize your area of interest, thereby allowing for a faster and more critical retrieval of information.

C. Complete all other information.

D. Complete the APPLICATION AND INTENDED USE portion of the inquiry. e.g. Will it be used for identifying buildings or will it be framed and placed on a wall. This information will assist our technicians in determining whether the products available will satisfy your requirements.

E. Return completed form to the FACILITY NEAREST YOU.

NOTE: If an inquiry is made for Landsat Data, and the Worldwide Reference of PATH and ROW numbers are available, please insert them in the appropriate locations. Otherwise, geographic coordinates will suffice.

☆ U.S. Government Printing Office: 1977—766-396/54 Region No. 6

INQUIRY FORM

GEOGRAPHIC COMPUTER SEARCH

U.S. DEPARTMENT OF THE INTERIOR
GEOLOGICAL SURVEY

Return completed form to the facility nearest you.

DATE ____________

NAME MR / MS ____________ (FIRST) ____________ (INITIAL) ____________ (LAST) ACCOUNT NO (IF KNOWN) ____________

COMPANY ____________ (IF BUSINESS ASSOCIATED) PHONE (Bus) ____________

ADDRESS ____________ PHONE (Home) ____________

CITY ____________ Your Ref No ____________ (P.O. GOV'T ACCT OR OTHER)

TO INITIATE AN INQUIRY AND COMPUTER GEOSEARCH COMPLETE THE FOLLOWING

POINT SEARCH

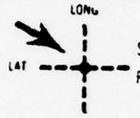

Imagery with any coverage over the selected point will be included.

	POINT #1	POINT #2	POINT #3
Latitude	____ ° ____ ' N or S	____ ° ____ ' N or S	____ ° ____ ' N or S
Longitude	____ ° ____ ' E or W	____ ° ____ ' E or W	____ ° ____ ' E or W

Landsat Only (Worldwide Reference System)

Path ____	Path ____	Path ____	Path ____	Path ____
Row ____	Row ____	Row ____	Row ____	Row ____

AREA RECTANGLE

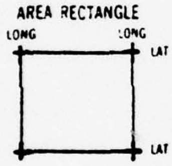

Imagery with any coverage over the selected area will be included

	AREA #1	AREA #2	AREA #3
Lat.	____ ° ____ ' N or S to	____ ° ____ ' N or S to	____ ° ____ ' N or S to
Lat.	____ ° ____ ' N or S	____ ° ____ ' N or S	____ ° ____ ' N or S
Long	____ ° ____ ' E or W to	____ ° ____ ' E or W to	____ ° ____ ' E or W to
Long	____ ° ____ ' E or W	____ ° ____ ' E or W	____ ° ____ ' E or W

If the above geographic coordinates cannot be supplied please specify area by GEOGRAPHIC NAME AND LOCATION (include a map if possible.)

PREFERRED TYPE OF COVERAGE

	Black & White	Color or Color Infrared
☐ Landsat	☐	☐
☐ Skylab	☐	☐
☐ Nasa-Aircraft	☐	☐
☐ Aerial Mapping Photography (Minimum color available)		

PREFERRED TIME OF YEAR

Check maximum of three

☐ JAN-MAR
☐ APR-JUNE
☐ JULY-SEPT
☐ OCT-DEC

☐ All coverage
☐ Latest coverage
☐ SPECIFIC DATES ____________

NOTE. Seasonal coverage normally applies only to Landsat coverage.

MINIMUM QUALITY RATING ACCEPTABLE

☐ 0-2 (VERY POOR) ☐ 3-4 (POOR) ☐ 5-6 (FAIR) ☐ 7-9 (GOOD)

MAXIMUM CLOUD COVER ACCEPTABLE

☐ 10% ☐ 30% ☐ 50% ☐ 80% ☐ 100%

NOTE Classification of percent of cloud cover is subjective and is relative to the amount of clouds appearing on the imagery and not to their location

APPLICATION AND INTENDED USE ____________

FORM 9-1936
(Jan 1977)

NCIC HEADQUARTERS
U.S. Geological Survey
507 National Center
Reston, VA 22092
FTS: 928-6045
COMM: 703-860-6045

EROS APPLICATIONS FACILITY
NSTL
U.S. Geological Survey
Bay St. Louis, MS 39520
FTS: 494-3541
COMM: 688-3472

NCIC MID-CONTINENT
U.S. Geological Survey
1400 Independence Rd.
Rolla, MO 65401
FTS: 276-9107
COMM: 314-364-3680

EROS DATA CENTER
U.S. Geological Survey
Sioux Falls, SD 57198
FTS: 784-7151
COMM: 605-594-6511

NCIC ROCKY MOUNTAIN
U.S. Geological Survey
Stop 510, Box 25046
Denver Federal Ctr.
Denver, CO 80225
FTS: 234-2326
COMM: 303-234-2326

NCIC WESTERN
U.S. Geological Survey
345 Middlefield Rd.
Menlo Park, CA 94025
FTS: 467-2427
COMM: 415-323-8111

PRICE LIST

STANDARD REMOTE SENSING DATA

U. S. DEPARTMENT OF THE INTERIOR
GEOLOGICAL SURVEY

JANUARY 1, 1977

SATELLITE DATA

STANDARD LANDSAT

IMAGE SIZE	NOMINAL SCALE	PRODUCT FORMAT	BLACK and WHITE UNIT PRICE	BLACK and WHITE PRODUCT CODE	COLOR UNIT PRICE	COLOR PRODUCT CODE
55.8mm (2.2 in.)	1:3369000	Film Positive	$ 8.00	11		
55.8mm (2.2 in.)	1:3369000	Film Negative	10.00	01		
18.5cm (7.3 in.)	1:1000000	Paper	8.00	23	$12.00	63
18.5cm (7.3 in.)	1:1000000	Film Positive	10.00	13	15.00	53
18.5cm (7.3 in.)	1:1000000	Film Negative	10.00	03		
37.1cm (14.6 in.)	1:500000	Paper	12.00	24	25.00	64
74.2cm (29.2 in.)	1:250000	Paper	20.00	26	50.00	66

COLOR COMPOSITE GENERATION	BLACK and WHITE UNIT PRICE	BLACK and WHITE PRODUCT CODE	COLOR UNIT PRICE	COLOR PRODUCT CODE
			$50.00	59

NOTE: 1) Portrayed in false color (infrared) and not true color
2) Cost of product from this composite must be added to total cost

COMPUTER COMPATIBLE TAPES (CCT)

TRACKS	b.p.i.	FORMAT	SET PRICE	PRODUCT CODE
7	800	Tape Set	$ 200.00	82
9	800	Tape Set	200.00	83
9	1600	Tape Set	200.00	84

SELECTED COVERAGE

IMAGE SIZE	FORMAT	BAND(S)	BLACK and WHITE UNIT PRICE	BLACK and WHITE PRODUCT CODE	COLOR UNIT PRICE	COLOR PRODUCT CODE
18.5cm (7.3 in.)	Paper	5	$ 8.00	41	$12.00	46
18.5cm (7.3 in.)	Paper	4, 5, 6, 7	32.00	45		
37.1cm (14.6 in.)	Paper	5	12.00	42	25.00	47
74.2cm (29.2 in.)	Paper	5	20.00	43	50.00	48

MANNED SPACECRAFT DATA

SKYLAB S190A

IMAGE SIZE	NOMINAL SCALE	PRODUCT FORMAT	BLACK and WHITE UNIT PRICE	BLACK and WHITE PRODUCT CODE	COLOR UNIT PRICE	COLOR PRODUCT CODE
55.8mm (2.2 in.)	1:2850000	Film Positive	$ 8.00	11	$10.00	51
55.8mm (2.2 in.)	1:2850000	Film Negative	10.00	01		
16.3cm (6.4 in.)	1:1000000	Paper	8.00	23	12.00	63
32.5cm (12.8 in.)	1:500000	Paper	12.00	24	25.00	64
65.0cm (25.6 in.)	1:250000	Paper	20.00	26	50.00	66

SKYLAB S190B

IMAGE SIZE	NOMINAL SCALE	PRODUCT FORMAT	BLACK and WHITE UNIT PRICE	BLACK and WHITE PRODUCT CODE	COLOR UNIT PRICE	COLOR PRODUCT CODE
11.4cm (4.5 in.)	1:950000	Paper	$ 6.00	22	$ 8.00	62
11.4cm (4.5 in.)	1:950000	Film Positive	8.00	12	12.00	52
11.4cm (4.5 in.)	1:950000	Film Negative	10.00	02		
21.8cm (8.6 in.)	1:500000	Paper	8.00	23	12.00	63
43.4cm (17.1 in.)	1:250000	Paper	12.00	24	25.00	64
86.9cm (34.2 in.)	1:125000	Paper	20.00	26	50.00	66

APOLLO/GEMINI

IMAGE SIZE	NOMINAL SCALE	PRODUCT FORMAT	BLACK and WHITE UNIT PRICE	BLACK and WHITE PRODUCT CODE	COLOR UNIT PRICE	COLOR PRODUCT CODE
55.8mm (2.2 in.)	Variable	Film Positive	$ 8.00	11	$10.00	51
55.8mm (2.2 in.)	Variable	Film Negative	10.00	01		
22.6cm (8.9 in.)	Variable	Paper	8.00	23	12.00	63
45.5cm (17.9 in.)	Variable	Paper	12.00	24	25.00	64

AIRCRAFT DATA

AERIAL MAPPING

IMAGE SIZE	PRODUCT FORMAT	BLACK and WHITE UNIT PRICE	BLACK and WHITE PRODUCT CODE	COLOR UNIT PRICE	COLOR PRODUCT CODE
22.9cm (9.0 in.)	Paper	$ 3.00	23	$ 7.00	63
22.9cm (9.0 in.)	Film Positive	5.00	13	15.00	53
22.9cm (9.0 in.)	Film Negative	6.00	03		
45.7cm (18.0 in.)	Paper	10.00	24	25.00	64
68.6cm (27.0 in.)	Paper	15.00	25	30.00	65
91.4cm (36.0 in.)	Paper	20.00	26	50.00	66

PHOTO INDEXES

IMAGE SIZE	PRODUCT FORMAT	BLACK and WHITE UNIT PRICE	BLACK and WHITE PRODUCT CODE	FILM SOURCE
25.4x30.5cm (10x12 in.)	Paper	$ 5.00	36	B & W – Size A
OTHER	Paper	5.00	37	B & W – Size B

NASA RESEARCH

IMAGE SIZE	PRODUCT FORMAT	BLACK and WHITE UNIT PRICE	BLACK and WHITE PRODUCT CODE	COLOR UNIT PRICE	COLOR PRODUCT CODE
55.8mm (2.2 in.)	Film Positive	$ 3.00	11	$10.00	51
55.8mm (2.2 in.)	Film Negative	4.00	01		
11.4cm (4.5 in.)	Paper	3.00	22	7.00	62
11.4cm (4.5 in.)	Film Positive	4.00	12	12.00	52
11.4cm (4.5 in.)	Film Negative	5.00	02		
22.9cm (9.0 in.)	Paper	3.00	23	7.00	63
22.9cm (9.0 in.)	Film Positive	5.00	13	15.00	53
22.9cm (9.0 in.)	Film Negative	6.00	03		
22.9x45.7cm (9x18 in.)	Paper	6.00	31	20.00	69
22.9x45.7cm (9x18 in.)	Film Positive	10.00	14	30.00	56
22.9x45.7cm (9x18 in.)	Film Negative	12.00	04		
45.7cm (18.0 in.)	Paper	10.00	24	25.00	64
68.6cm (27.0 in.)	Paper	15.00	25	30.00	65
91.4cm (36.0 in.)	Paper	20.00	26	50.00	66

MISCELLANEOUS

MICROFILM

FORMAT	BLACK and WHITE ROLL PRICE	BLACK and WHITE PRODUCT CODE	COLOR ROLL PRICE	COLOR PRODUCT CODE
16mm (30.5m/100 ft.)	$15.00	72	$40.00	73
35mm (30.5m/100 ft.)	20.00	72	45.00	73

KELSH PLATES

FORMAT	BLACK and WHITE UNIT PRICE	BLACK and WHITE PRODUCT CODE
Contact Prints on Glass Specify thickness (0.25 or 0.06 inch) and method of printing (emulsion to emulsion or through film base).	$12.00	70

TRANSFORMED PRINTS

FORMAT	BLACK and WHITE UNIT PRICE	BLACK and WHITE PRODUCT CODE
From convergent or transverse low oblique photographs	$ 8.00	71

VIEWING SLIDES

FORMAT	COLOR UNIT PRICE	COLOR PRODUCT CODE
35mm mounted duplicate of available printing master	$ 1.00	50

NOTE: 35mm original will require additional $5.00, not to include cost of mounted duplicate.

Complete roll reproduction delivered in roll format carries a 50% reduction in frame pricing.
Custom processing of non-standard products is available at three times the standard product price. If a non-standard size is desired, the cost is three times the next larger standard product price.
Priority service with guaranteed five working days shipment is offered for standard products only, at three times the standard product price.
Extra care should be taken to insure that monies and related order forms are forwarded to the same facility.

☆ U.S. G.P.O. 1977-766-398/61 REG.#6

1978 USAF-ASEE SUMMER FACULTY RESEARCH PROGRAM
sponsored by
THE AIR FORCE OFFICE OF SCIENTIFIC RESEARCH
conducted by
AUBURN UNIVERSITY AND OHIO STATE UNIVERSITY

PARTICIPANT'S FINAL REPORT

CONTROL OF JP-4 EMISSIONS FROM UNDERGROUND STORAGE TANKS

Prepared by:	Dr Gordon A. Lewandowski
Academic Rank:	Assistant Professor
Department and University:	Department of Chemical Engineering and Chemistry New Jersey Institute of Technology 323 High St Newark, NJ 07102

Assignment:	Det 1 (CEEDO) ADTC/ECC (AFSC) Tyndall AFB, Florida 32403
USAF Research Colleague:	Mr Thomas B. Stauffer
Date:	August 18, 1978
Contract No.:	F44620-75-C-0031

CONTROL OF JP-4 EMISSIONS FROM UNDERGROUND STORAGE TANKS

BY

Dr Gordon A. Lewandowski

ABSTRACT

The South Coast Air Quality Management District, in southern California, is presently requiring controls on underground JP-4 tanks at March, Norton, George, and Edwards AFB. It is expected that such controls may eventually be required at other Air Force installations. Therefore, an engineering study was undertaken to: (1) review the problem for Southern California and make recommendations where appropriate, and (2) determine the extent of the problem for the USAF as a whole.

This report covers the first of these objectives. After visiting the above mentioned Air Force bases, and completing an engineering assessment of potential control strategies, low temperature refrigeration and recovery of condensed JP-4 vapors is recommended as the best control method.

ACKNOWLEDGMENT

The author is indebted to the members of the Environmental Sciences Division, Environics Directorate, of the Civil and Environmental Engineering Development Office (Tyndall AFB), for their help in preparing this report. Special thanks go to my Air Force Research Colleague, Mr Thomas B. Stauffer, for his suggestions and assistance regarding Air Force procedures.

Congratulations are also due to Mr J. Fred O'Brien for smoothing the paper work, and helping to make this an enjoyable summer.

TABLE OF CONTENTS

I. INTRODUCTION

JP-4 underground storage tanks are used primarily to supply fuel hydrants along the operational apron at many USAF bases, although at some locations they are also used to fill tank trucks (notably at Edwards AFB). This means that they must be located adjacent to, or on the operational apron, which places additional constraints on the methods available for vapor control (see Alternative Systems below).

The underground tanks are normally 50,000 gallon horizontal cylinders, about 12 ft in diameter by 60 ft long, with a vent pipe and submerged pump at one end, and various inspection hatches. They are filled, either by pump or gravity, from large bulk storage facilities where the fuel is initially brought on base. The bulk storage tanks generally have internal floating roofs, and are often far from the operational apron, which makes vapor balance impractical ("vapor balance" is where the vapors from the underground tanks would be returned to the vapor space above the bulk storage tanks, during filling operations).

II. OBJECTIVES

The objective of the summer program was to recommend a control method for JP-4 emissions from underground storage tanks.

The result was a recommendation for low temperature vapor condensation (See Section V.B).

III. AIR QUALITY REGULATIONS

Using Southern California as an example, any tanks larger than 40,000 gallons, containing volatile organics with a true vapor pressure of 1.5 psia or higher, must either: (a) install a floating roof, or (b) provide a vapor recovery system capable of achieving a 95 percent reduction in emissions (for the Mojave Desert, this has been modified to 90 percent). Underground JP-4 storage tanks at March, Norton, George and Edwards AFB fall under this regulation when the fuel temperature rises above 66°F (See Figure 1). Because the tanks are horizontal cylinders, floating roofs cannot be installed, and vapor recovery must be resorted to.

At the present time, both March and Edwards AFB have condensation systems for vapor control. However, the system at March AFB only achieves a 20 percent reduction in vapor emissions (see below, Section V.B, Low Temperature Condensation, for a discussion of these two units).

IV. JP-4 VAPOR COMPOSITIONS

Based on data from Petroleum Analytical Research (PAR) [1], laboratory data taken by Capt Harvey J. Clewell [2], and data taken at March AFB by the University of California at Riverside, the liquid composition of JP-4 was approximated, and the saturated vapor composition calculated at various temperatures. (See Appendix A).

These calculations are largely confirmed by actual data (See Table I and Figure 1).

It should be noted that JP-4 is not an exact mixture of hydrocarbons. Its composition varies to some extent, and this is allowed for in the military specification.

Still uncertain is the extent to which the vapor space, or "ullage", above the liquid level in the tanks is saturated with hydrocarbons during actual filling operations. Some data indicate a close approach to saturation (e.g. the University of California data at March AFB), while others indicate that saturation is not achieved (EPA data at March AFB[3]). This will be a strong function of the filling method and schedule.

Considerations of the extent of saturation of the ullage may be important from a safety standpoint, since the upper flammable limit of JP-4 vapors may be more closely approached for an unsaturated condition. (See Table II). This will become a factor in considering alternative designs.

V. REFRIGERATION SYSTEMS

Two types of refrigeration systems were investigated:

A. Compression and condensation of vapors

B. Low temperature condensation of vapors at atmospheric pressure on the surface of refrigeration coils.

A. Compression and Condensation of Vapors

This type of system could present serious safety problems, because it necessitates the compression of JP-4 vapors, whose concentration may lie within the flammable region. Such a system is shown schematically in Figure 2.

In order to minimize the safety hazard, a precompression spray chamber is needed to insure saturation of the vapors with JP-4. However, at fuel temperatures below about 50°F, no amount of saturation can bring the vapor composition above the flammable limit. In such cases, a detonation would occur in the compressor.

B. Low Temperature Condensation

This involves passing the JP-4 vapors over a cold refrigeration coil, and condensing out the hydrocarbons. The natural pressure of the vapor being forced out of the tank is sufficient to drive it across the coils and out the vent (maximum pressure drop is about 2" W.C.). Therefore, no blowers or compressors are needed to motivate the vapor, and consequently, there is no ignition source in the vapor path.

This type of refrigeration system is diagrammed in Figure 3. It is compact, and relatively easy to operate. The only utility requirement is electricity, and the condensed JP-4 can be directly returned to a storage tank. Data from March and Edwards AFB, where condensation systems are already installed (see below), indicate that fuel quality remains unchanged by reintroduction of condensed vapors into the underground storage tanks.

Because the JP-4 vapors are not compressed, the refrigeration coil temperature must be very low. For 90-95 percent vapor recovery, the coil temperature will have to be about -100°F, or lower (See Appendix B for calculations). This temperature is supported by USAF data[4], and is necessitated by the dilution of the hydrocarbons with air (only 12 to 26 percent of the vent vapors is JP-4). In addition, -100°F is in the typical range for 90 percent condensation of gasoline vapors, to which JP-4 is similar, and for which present-day commercial equipment is readily available (See Appendix C, Edwards Engineering brochure). In fact, Edwards Engineering has 88 such units presently operating in the United States, and its model VC500, installed at the Southern Pacific Pipe Lines Terminal (in Sacramento, California), has been verified by the California Air Resources Board as achieving 97 percent vapor recovery at a gasoline loading rate of 305,000 gallons per day[7].

It should be noted that March AFB currently has a refrigeration unit (designed by the US Army Corps of Engineers) operating at about +40°F, and recovering only 20 percent of the JP-4 vapors[3]. At +40°F, 20 percent recovery checks approximately with the calculation method used above (See Appendix B). However, Edwards AFB has a design nearly identical to that at March, with the same coil temperature, but claiming a recovery of 96 percent [8]. This contradiction has yet to be resolved.

At a temperature of -100°F, water vapor will freeze on the refrigeration coil as the hydrocarbons condense. Periodically, a defrost cycle (lasting approximately 1/2 hour) will melt the ice, which is then collected and processed separately. Although the condensed hydrocarbons may carry over a trace of water into the JP-4 tanks, this moisture should easily be removed by the existing oil/water separators.

The coil temperature is maintained at all times at -100°F, and therefore, the unit is always ready to receive vapors. A temperature sensor turns on the refrigeration compressor when the coil temperature rises, and shuts it off again when the temperature drops down to a preset value. Therefore, no actuator (such as a fuel flow indicator) is needed to turn on the unit. During standby, when no vapors are being emitted, the heat load on the coil is very small, and the compressor should only kick-on for about 5 or 10 minutes per hour. The reasons why the heat load is so small during standby are: (1) the unit is well-insulated, and (2) the air circulation is very poor, since it has to rely on natural convection down a narrow vent pipe. However, proper sizing of the unit is critical, so that when vapors are generated there will be sufficient refrigeration capacity to maintain a -100°F coil.

In order to proceed with sizing a refrigeration unit, or indeed any control device, the system capacity must be determined. That is, how many cubic feet per minute of vapor will be vented? This in turn will depend on the method of refilling the underground storage tanks.

Assuming only one tank is filled at a time, at a fill rate of 600 gpm, the vent rate to the refrigeration system will be 80 acfm (See calculations in Appendix D). Such a flow rate will require about 4 tons of refrigerant (48,000 BTU/hr), with a 10 hp compressor. This translates to an electrical cost of about 30¢/hr of operation. However, 80 acfm of vent gas will contain about 100#/hr of JP-4 (for a fuel temperature of 70°F). At a price of 44¢/gal, this translates to a recovered value of $8.46/hr of operation. Therefore, the value of the recovered JP-4 will exceed electrical cost for running the refrigeration compressor by $8.16/hr of operation.

VI. ALTERNATIVE SYSTEMS

A. Incineration

Incineration could theoretically provide a viable alternative to refrigeration/condensation systems. This would involve burning JP-4 vapors at temperatures ranging from about 600°F (for catalytic oxidation) to about 1400°F (for standard combustion). However, because of the proximity of the underground JP-4 tanks to the operational apron, a combustion source may be highly undesirable.

Instead, the vapors could be collected and piped far enough away from the apron to satisfy safety requirements, and the incinerator located at that distance. However, again because of proximity to the operational apron, underground vent lines may be required in many situations, which entails a high capital investment. For those locations where the underground tanks are in the middle of the apron (such as at March AFB), the runway would have to be ripped up to install such lines.

As a further safety consideration, the JP-4 vapors may have to be compressed, in order to force them through the combustion burners. However, because of uncertainty regarding the degree of saturation of the vapors (as mentioned above), they will have to be passed through a spray chamber prior to compression. Again, even presaturation will not be sufficient for fuel temperatures below about 50°F., when a detonation is likely to occur in the compressor.

Finally, since the JP-4 vapors are burned, there is no recovery value as with refrigeration. Although the vapors should be able to support combustion without auxiliary fuel (See Appendix E), an ignition source is always required, and possibly the combustion chamber will have to be maintained hot during periods when vapors are not being vented. Therefore, operating costs will be high compared to a refrigeration system.

B. Mono-Layer Vapor Suppression

A relatively new method of vapor suppression, still in the developmental stage, is to cover the surface of a volatile liquid (such as gasoline) with a monomolecular layer of high boiling point, low density, immiscible organic liquid. This has the effect of coating the gasoline surface, and suppressing its vapor pressure.

The major obstacle to utilization of this technique is the method of application of the mono-layer: i.e., getting an even coating. For JP-4 tanks, which have a submerged discharge pump, this would involve a surface application each time the tank was emptied, and would be prohibitive from both an operational and cost standpoint.

Furthermore, the mono-layer compound could contaminate the JP-4 unless tailored specifically for this application.

C. Carbon Adsorption

A third alternative would be to adsorb the vented hydrocarbons on activated carbon. Conceivably, this would take the form of a 55 gallon drum, supplied by the carbon manufacturer, and attached to the end of the vent pipe. As the drum became saturated with adsorbed hydrocarbons, the manufacturer would replace it with a fresh drum.

However, as with incineration, this method prevents the recovery of any JP-4. Furthermore, using a "typical" loading for low molecular weight hydrocarbons of 0.1#/# of activated carbon [9], the carbon usage would amount to about 1000#/hr of operation. This is far too excessive.

VII. RECOMMENDATIONS AND FUTURE DEVELOPMENT

1. A test refrigeration unit using low temperature condensation should be installed at March AFB. This is the most likely location, since they have an existing vapor collection system and a high fuel turnover rate (March is a SAC base, fueling B-52s).

2. In order to size a refrigeration unit for March AFB, the vent rate, and therefore the schedule for refilling the JP-4 underground tanks, must be pinned down and adhered to. The more tanks that are filled simultaneously at a given fill rate, the higher will be the capital cost.

3. After installation, the unit should be tested from winter through summer seasons, to insure operation over a wide fuel temperature range. Also, the capacity limits of the unit should be tested.

4. If it tests favorably, similar units should be specified for Norton, George, and (possibly) Edwards AFB. In this regard, the vapor recovery of the existing refrigeration unit at Edwards AFB must be confirmed,and the contradiction resolved with the measured recovery presently observed at March AFB (see Section V.B above).

REFERENCES

1. Letter from: Paul Hayes, Jr., Fuels Branch, Fuels and Lubrication Division, Air Force Aero Propulsion Laboratory, Wright-Patterson Air Force Base; To: OLAA/AFCEC (Lt Ricco), Kirtland AFB (12/13/75); Subject: JP-4 Component Analysis.

2. Personal communication from Capt Harvey J. Clewell, Det 1 (CEEDO) ADTC (AFSC), Tyndall AFB FL.

3. Letter from: Howard W. Lange, Acting Air Pollution Control Officer, Southern California Air Pollution Control District, Riverside Zone; To: Colonel N. A. Corrao, Base Civil Engineer, March AFB (7/22/76).

4. "Analysis of Aeration Effluents of Fuel Tank Purging Fluids", pg 1, Aerospace Fuels Laboratory, Wright-Patterson AFB (January 1973).

5. Information from Tyndall AFB Fire Dept.

6. R. H. Perry and C. H. Chilton, Chemical Engineers' Handbook, 5th ED, (1973).

7. "Source Test Report, Southern Pacific Pipe Lines' Vapor Recovery System for Gasoline Terminals", by the State of California Air Resources Board, Report No. C7-034 (July 1977).

8. "Report on Performance Test of Vapor Emission Control System for Edwards AFB Civil Engineering Office", by Pacific Environmental Services, Inc (October 26, 1977).

9. "Control Characteristics of Carbon Beds for Gasoline Vapor Emissions", by M. J. Manos, et al, US EPA Publication No. EPA/600/2-77/057 (February, 1977).

TABLE 1

COMPOUNDS	JP-4 LIQUID MOLE FRACTIONS			VAPOR MOLE FRACTIONS							
	REF. (1)	%	REF. (2)	@110^{O}F	%	@70^{O}F	%	REF. (2)	@59^{O}F	%	U of CA Data at March AFB
C2P	.000025*	.0025	-	.0010	.4	.0007	.6	.5%	.0006		.0009
C3P	.0016*	.16	-	.0208	8.1	.0128	10.4	11.7	.0110		.0037
C4P	.0160*	1.6	1.6%	.0800	31.3	.0432	35.3	31.2	.0352		.0371
n-C5P	.0100			.0130		.0062			.0048		.0095
i-C5P	.0300*	4.0	4.0	.0446	22.5	.0218	22.9	27.8	.0171		.0103
n-C6P	.0269			.0124		.0051			.0038		.0046
i-C6P	.0599	11.3	12.1	.0359	21.7	.0150	18.8	17.0	.0102		.0071
C6C	.0226			.0063		.0025			.0018		.0036
C6A	.0033			.0009		.0004			.0003		-
n-C7P	.0452			.0072		.0027			.0019		.0018
i-C7P	.0548	18.3	20.2	.0115	11.7	.0042	9.1	8.3	.0029		.0075
C7C	.0756			.0106		.0040			.0029		.0027
C7A	.0078			.0007		.0002			.0002		.0010
n-C8P	.0460			.0028		.0009			.0006		.0006
i-C8P	.0620	20.4	22.6	.0043	4.2	.0016	3.0	2.9	.0010		.0020
C8C	.0786			.0031		.0010			.0008		.0012
C8A	.0169			.0005		.0002			.0001		.0006
	.5572	55.7%	60.5%	.2556^{+}	99.9%$^{++}$	.1225^{+}	100.1%$^{++}$	99.4%$^{++}$	.0952^{+}		.0942^{+}
C9	.155**										
C10	.120**	Assumed to have a Negligible Vapor Contribution									
C11	.110**										
C12	.042**										
C13+	.015**										
	1.0000										

* Assumed (Compounds were not represented in PAR Data).
** Modified PAR data, to account for light-ends representation.
\+ Total hydrocarbon mole fraction in vapor space.
++ Percent breakdown of hydrocarbons.

TABLE II

Source	Temperature	Volume Percent Hydrocarbon in Vapor Space	Flammability Limits (Volume % HC)
Calculated At Saturation	70°F	12.3	
			1.3 - 8.0[5]
EPA Measurements at March AFB[3]	76°F	8.9	

Figure 1

FUELS
True Vapor Pressure vs Temperature

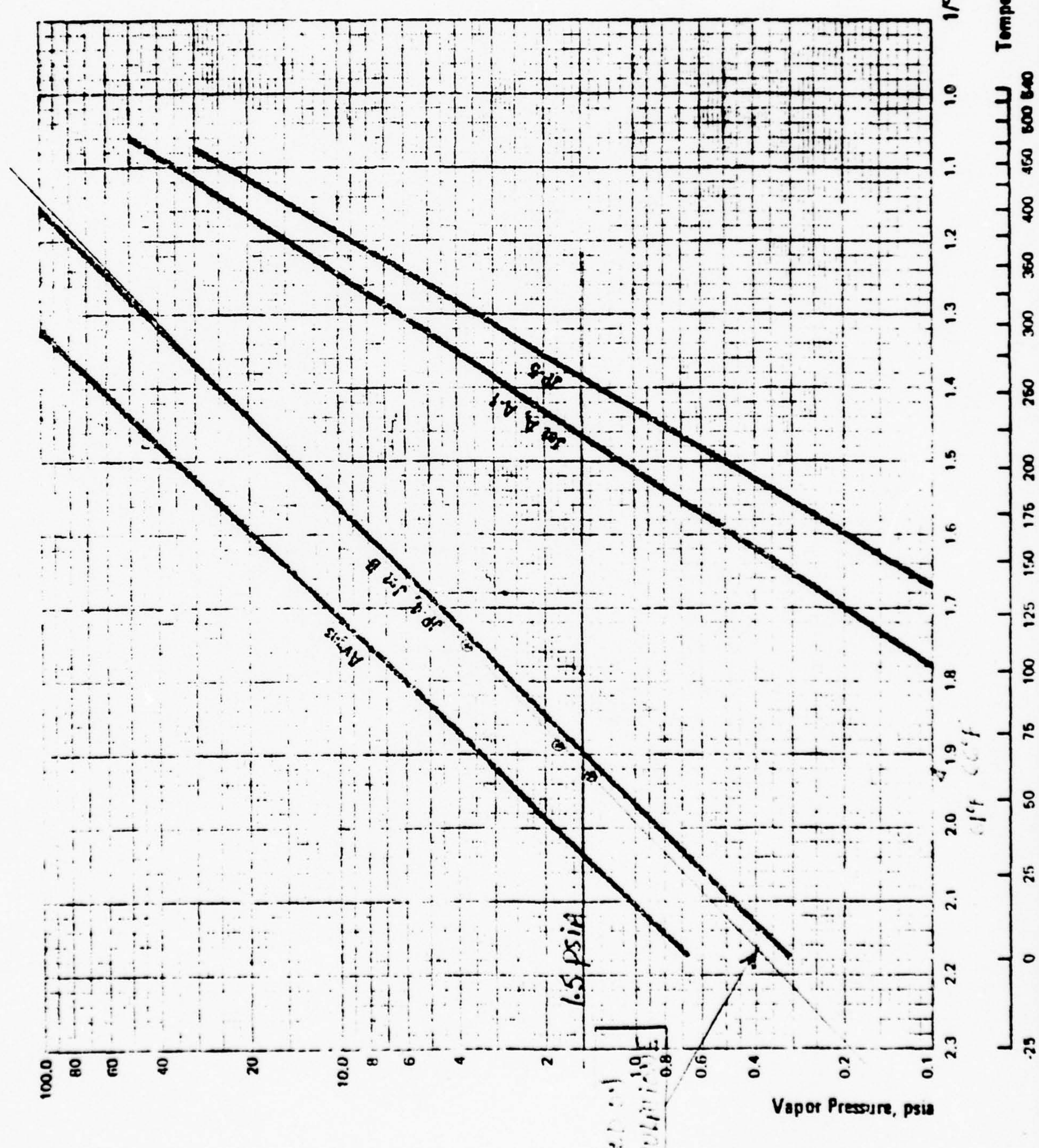

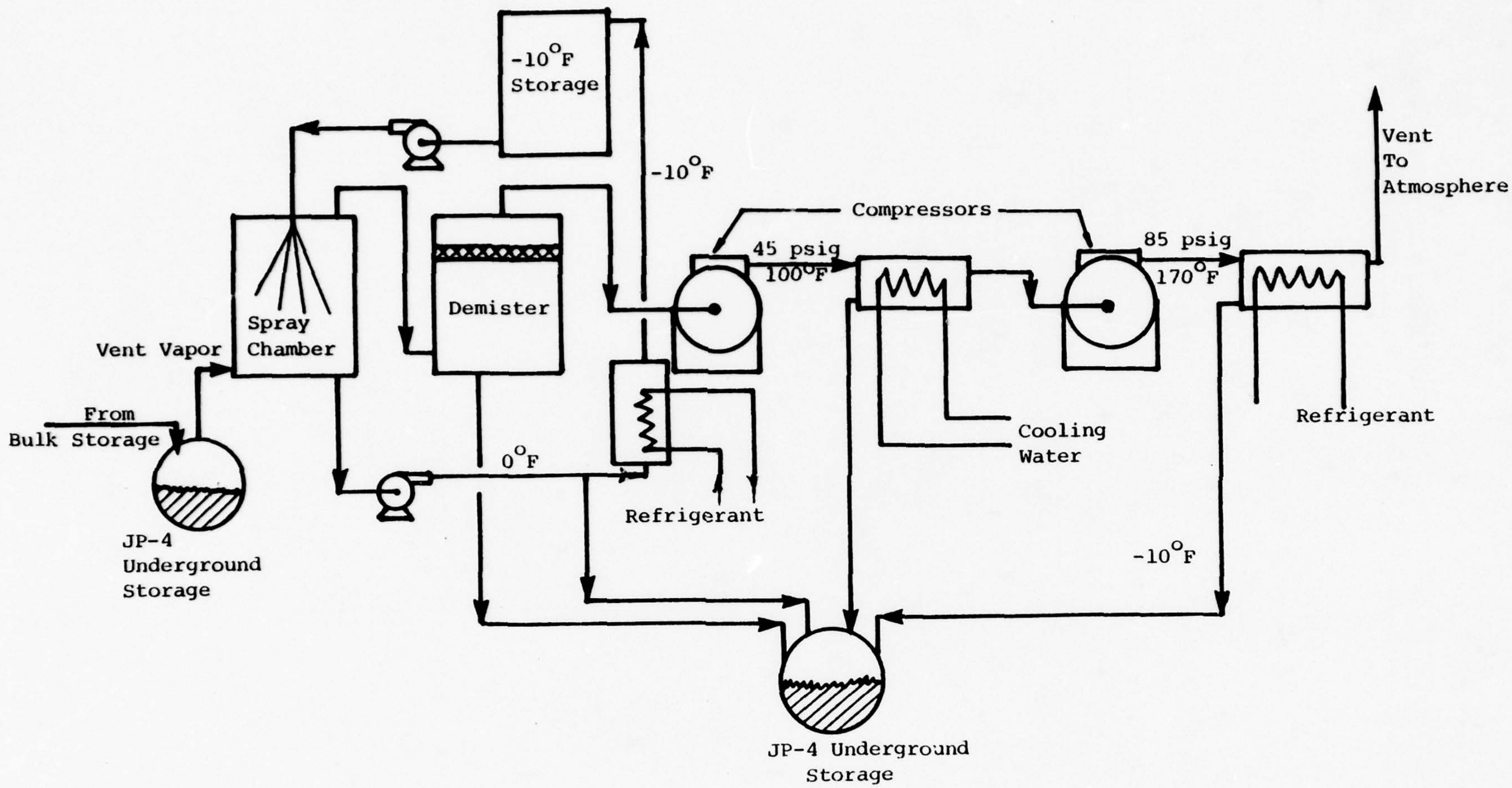

Figure 2. Compression/Condensation System

APPENDIX A

CALCULATED JP-4 VAPOR COMPOSITIONS

The calculated vapor compositions were based on the following equation:

$$Y_i = K_i X_i$$

where Y_i = mole fraction of component i in the vapor

X_i = mole fraction of component i in the liquid

K_i = distribution coefficient, or "K factor", determined empirically, and a function of temperature.

The K factors for paraffins up to C9 were obtained from a DePriester nomograph. For all other hydrocarbons, the K factors were approximated using Raoult's Law:

$$K_i = \frac{P_i^o}{\pi}$$

where P_i^o = vapor pressure of component i at temperature T [6]
π = total system pressure

This approximation can often result in serious errors: however, in the present case, these do not seem to be major, since good agreement was obtained with experimental values.

Neglecting the vapor contribution of C9+ (which will be negligible), mole fractions were calculated for each component in the vapor phase, and summed:

ΣY_i = total mole fraction of hydrocarbon in the vapor

$1 - \Sigma Y_i$ = mole fraction of air

(NOTE: Mole fraction is equivalent to volume fraction)

$\pi\Sigma Y_i$ = Total vapor pressure of JP-4

T	$\pi\Sigma Y_i$	
59°F	1.40 psia	These are plotted in Figure 1 along with actual JP-4 vapor pressure data.
70	1.80	
110	3.76	

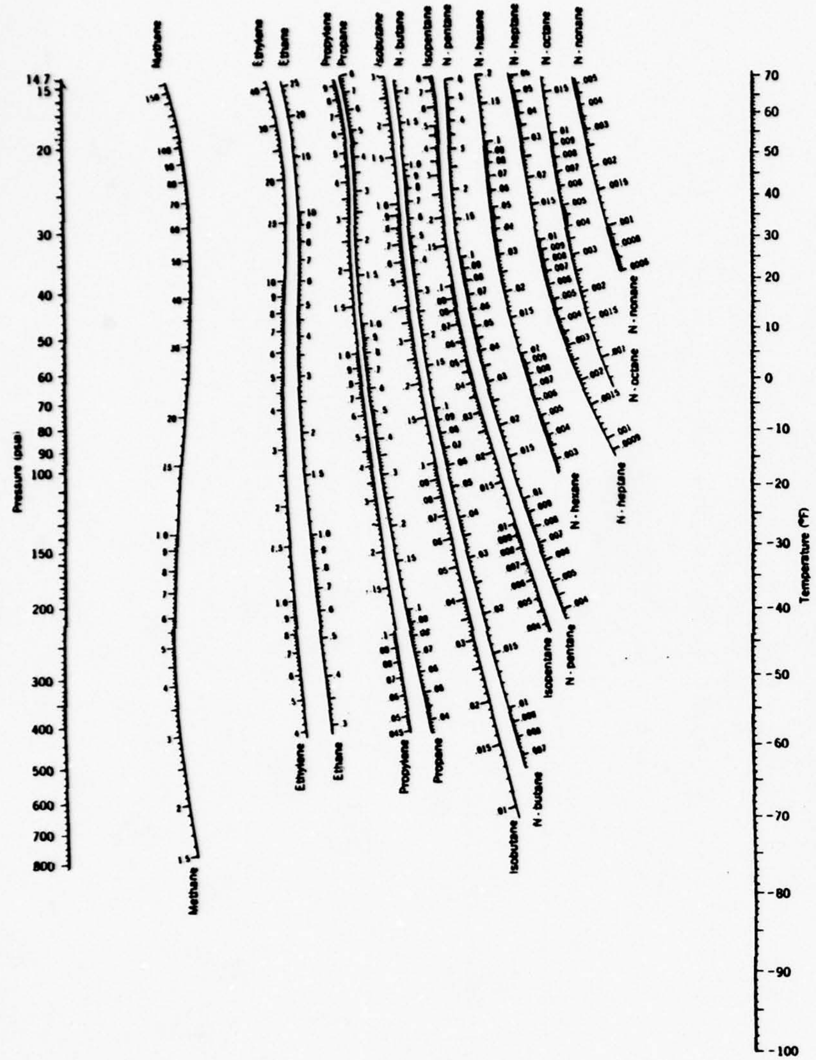

Fig. 8-18 *Equilibrium constants in light-hydrocarbon systems. Low-temperature range.* [Reproduced by permission from C. L. DePriester, *Chem. Eng. Progr., Symposium Ser.* 7:49 (1953).]

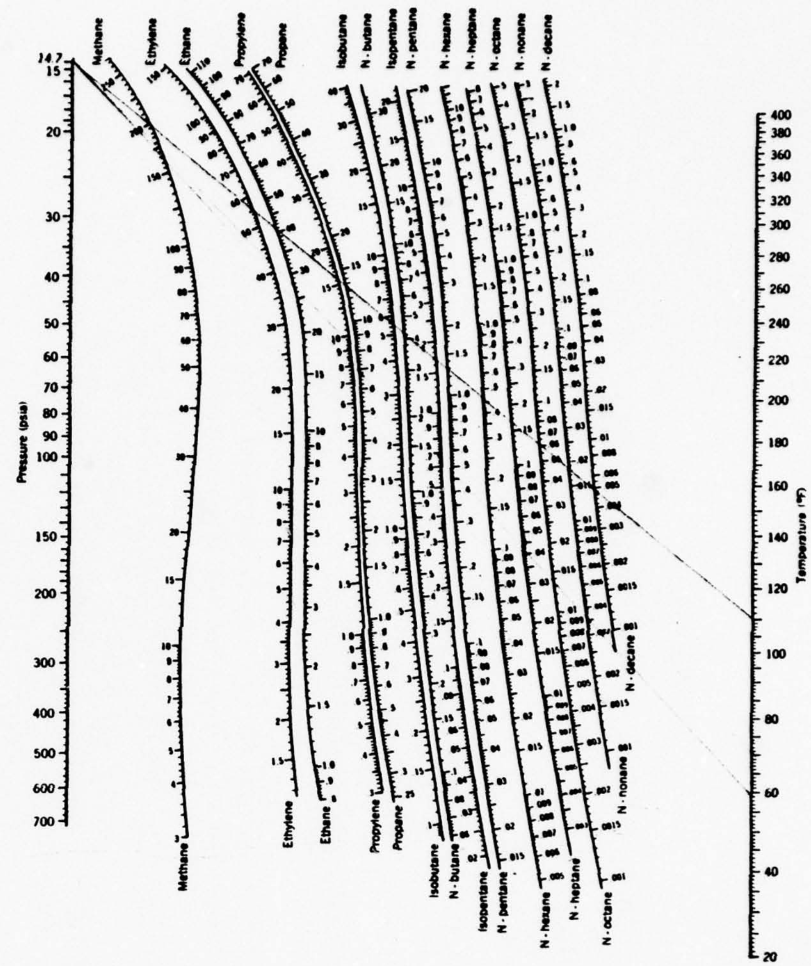

Fig. 8-19 *Equilibrium constants in light-hydrocarbon systems. High-temperature range.* [Reproduced by permission from C. L. De Priester, *Chem. Eng. Progr., Symposium Ser.* 7:49 (1953).]

APPENDIX B

CALCULATED CONDENSATION TEMPERATURES FOR JP-4 VAPOR
(at atmospheric pressure)

The following equations were used to determine the condensation temperature required for 90 percent removal of JP-4 vapors:

$VY_i + LX_i = WZ_i$ material balance around component i

$V + L = W$ overall material balance

where Z_i = initial mole fraction of i in the vapor

Y_i = equilibrium mole fraction of i in the vapor

X_i = equilibrium mole fraction of i in the liquid

W = initial total amount of vapor

V = final amount of vapor

L = final amount of liquid

Dividing by W:

$$f_v Y_i + f_l X_i = Z_i$$

where f_v = vapor fraction = V/W

f_l = liquid fraction = L/W

$f_v + f_l = 1.0$

*NOTE: f_l = fraction of initial amount of vapor which condenses. Since most of the initial vapor is non-condensible, f_l will never be > .25

Also, as in Appendix A:

$$Y_i = K_i X_i$$

$$f_v K_i X_i + (1 - f_v) X_i = Z_i$$

$$\left[f_v(K_i - 1) + 1\right] X_i = Z_i \qquad (1)$$

Z_i = vapor mole fractions given in Table I (a function of temperature)

Since all of the condensate is hydrocarbon (water has been ignored in this analysis),

$$\Sigma X_i = 1.0$$

Method of Solution

a. Pick T (find K factors)

b. Pick f_v

c. Use equation (1) to find X_i

d. See if $\Sigma X_i = 1.0$

If not, return to (b), until correct f_v is calculated for a given temperature.

e. When f_v is found, calculate $Y_i = K_i X_i$

f. Calculate average molecular weight of equilibrium vapor ($\overline{MW}$).

g. $$\left[\frac{\Sigma Y_i}{1 - \Sigma Y_i}\right]\left[\frac{\overline{MW}}{29}\right] = \frac{\text{\# hydrocarbon in vapor}}{\text{\# air}}$$

h. Initially:

$$\left[\frac{\Sigma Z_i}{1 - \Sigma Z_i}\right]\left[\frac{70}{29}\right] = \frac{\text{\# hydrocarbon in vapor}}{\text{\# air}}$$

i. $\therefore$ Wt. percent of hydrocarbon condensed =

$$\frac{\left[\frac{\Sigma Z_i}{1 - \Sigma Z_i}\right]\left[\frac{70}{29}\right] - \left[\frac{\Sigma Y_i}{1 - \Sigma Y_i}\right]\left[\frac{\overline{MW}}{29}\right]}{\left[\frac{\Sigma Z_i}{1 - \Sigma Z_i}\right]\left[\frac{70}{29}\right]} = 1 - \left[\frac{\Sigma Y_i}{\Sigma Z_i}\right]\left[\frac{1 - \Sigma Z_i}{1 - \Sigma Y_i}\right]\left[\frac{\overline{MW}}{70}\right]$$

The following pages show example calculations. The calculated wt. percent condensation at $40^{o}F$ checks approximately with the measured EPA results at March AFB [3], and the final result is consistent with data taken by the Aerospace Fuels Laboratory at Wright-Patterson AFB [4].

NOTE: The calculation method is not accurate enough to distinguish between 90 percent and 95 percent recovery. Ninety five percent should only require about $10^{o}F$ lower temperature.

RESULT: T = $-90^{o}F$ (vapor temperature)

To maintain a reasonable driving force for condensation, a $-90^{o}F$ vapor will require a $-100^{o}F$ coil.

@ $40^{o}F$

Compound	K_i	X_i			Y_i	(Initially, Vapor @ $70^{o}F$) Z_i	Wt. Percent of Hydrocarbon Condensed
		f_v = .9	.975	.99			
C2P	19.5	.00004	.00004	.00004	.00078	.0007	
C3P	5.1	.00273	.00256	.00253	.01290	.0128	
C4P	1.55	.02890	.02812	.02797	.04335	.0432	
n-C5P	.31	.01636	.01895	.01956	.00606	.0062	
i-C5P	.42	.04561	.05017	.05120	.02150	.0218	
n-C6P	.09	.02818	.04523	.05146	.00463	.0051	10 Percent Calculated
i-C6P	.106	.07677	.11687	.13050	.01383	.0150	20 Percent Measured
C6C	.048	.01746	.03482	.04346	.00209	.0025	by EPA at March AFB(3)
C6A	.044	.00287	.00589	.00747	.00033	.0004	
n-C7P	.025	.02204	.05468	.07770	.00194	.0027	
i-C7P	.029	.03331	.07884	.10850	.00315	.0042	
C7C	.015	.03524	.10095	.16097	.00241	.0040	
C7A	.012	.00181	.00545	.00914	.00011	.0002	
n-C8P	.0076	.00842	.02777	.05136	.00039	.0009	
i-C8P	.0082	.01490	.04849	.08831	.00072	.0016	
C8C	.0055	.00953	.03294	.06475	.00036	.0010	
C8A	.0037	.00194	.00699	.01464	.00005	.0002	
		.34611	.65876	.90956*	.1146	.1225	

$\overline{MW}$ = 68

*Approximate solution, since C9+ compounds will contribute somewhat to the liquid mole fraction even though their values of Z_i are very small.

@ -90°F

Compound	K_i	X_i			Y_i	(Initially, Vapor @ 70°F) Z_i	Wt. % of Condensed Hydro-carbon
		$f_v = .9$	$f_v = .88$	$f_v = .89$			
C2P	2.8	.00027	.00027	.00027	.00076	.0007	
C3P	.25	.03938	.03765	.03850	.00963	.0128	
C4P	.029	.34259	.29687	.31809	.00922	.0432	
n-C5P	-	.062	.05167	.05636	-	.0062	90 Percent
i-C5P	-	.218	.18167	.19818	-	.0218	
n-C6P	-	.051	.04250	.04636	-	.0051	
i-C6P	-	.150	.12500	.13636	-	.0150	
C6C	-	.025	.02083	.02273	-	.0025	
C6A	-	.004	.00333	.00364	-	.0004	
n-C7P	-	.027	.02250	.02455	-	.0027	
i-C7P	-	.042	.03500	.03818	-	.0042	
C7C	-	.040	.03333	.03636	-	.0040	
C7A	-	.002	.00167	.00182	-	.0002	
n-C8P	-	.009	.00750	.00818	-	.0009	
i-C8P	-	.016	.01333	.01455	-	.0016	
C8C	-	.010	.00833	.00909	-	.0010	
C8A	-	.002	.00167	.00182	-	.0002	
		1.04024	.88312	.95504*	.01961	.1225	

$\overline{MW} = 50$

Where data do not exist, K_i assumed to be 0 in equation (1).

* Approximate solution, allowing for the condensation of some higher boiling components.

APPENDIX C

EDWARDS ENGINEERING BROCHURE ON LOW TEMPERATURE CONDENSATION

Edwards (DE) Series

Hydrocarbon Vapor Recovery Unit

DESIGNED TO MEET REQUIREMENTS OF LOCAL AIR POLLUTION AUTHORITIES, THE NEW EDWARDS DE UNITS OFFER:

1. Continuous performance monitoring as required by the authorities. All new units are equipped with three analyzing, metering and recording devices:
   (a) Hydrocarbon vapor analyzer for determining periodic mol percentage of Hydrocarbon Vapor entering and leaving the unit.
   (b) 24-hour or weekly chart available indicating recovery condenser temperature.
   (c) Meter giving recovered Hydrocarbon in liquid gallons.

   With these instruments the unit recovery performance and terminal recovery performance can be determined in a few minutes. This equipment meets new local Environmental Protection Authorities requirements that Environmental Protection Authority personnel can easily and quickly determine performance of unit or of complete terminal at anytime.
2. Lowest electrical operating costs in industry.
3. Requires no replacement or reactivation of solid adsorbents or use of liquid absorbents. Meets new local Environmental Protection Authority Requirements.

Under discussion in various localities is the requirement that permits for installation will not be approved unless the equipment contains constant performance monitoring capability.

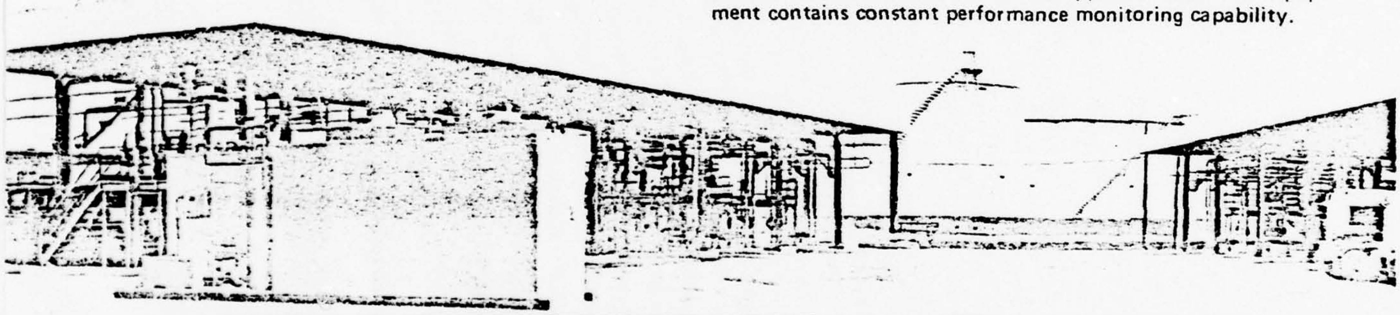

for Gasoline Truck Loading Terminals and Bulk Plants
Tank Farms
Tanker and Barge Loading
Flare Gas Recovery in Refinery Facilities

Edwards offers the petroleum industry an automatically controlled direct condensing unit for the recovery of hydrocarbon vapors. The operation of the unit is based on the direct condensation of the hydrocarbon vapor at atmospheric pressure on cold refrigerated surfaces. The DE-series equipment is carefully designed so that the percent hydrocarbon vapor recovery is approximately constant (90 or greater over a wide range of entering hydrocarbon vapor in air concentration (10 to 35) and over a range of gasoline Reid Vapor Pressures (10 to 14

The value of the recovered hydrocarbon vapors is more than sufficient to pay for the direct operating cost of the equipment. In most cases the value of the recovered hydrocarbon is sufficiently high to recover the cost of the capital investment in reasonable period of time. The capital cost is rapidly recoverable where the equipment is in almost continuous operation.

Patent No. 4 027 495 [illegible]

Edwards ENGINEERING CORP.
101 ALEXANDER AVE., POMPTON PLAINS, NEW JERSEY 07444
ph.(201) 835 2808 TELEX: 130131

Edwards HYDROCARBON VAPOR RECO

The features of the Edwards DE series direct single stage condensing unit are:

- No time lost for frost or hydrate removal
- Constant rate of vapor recovery
- Vapor compression or storage not required
- Simple fully automatic operation
- Low operating cost
- Low maintenance cost
- Long equipment life
- Fully factory packaged to your specifications
- No cold brine required
- Recovered liquid hydrocarbons contain no water
- Direct meter record of hydrocarbon recovery in gallons
- Recovered liquid hydrocarbons can be pumped to any location within the terminal
- All components weather-proof or enclosed
- Wiring meets explosion-proof codes as ordered.

OUTSTANDING FEATURES

• No time lost for frost or hydrate removal

Since the DE-unit is equipped with a precooler coil, the quantity of hydrate formed is minimal. Since the unit is in normal operation only 10% of the time in a typical terminal, the unit can be quickly defrosted during periods of little activity (1 to 4 a.m.). If the equipment is to be run continuously, the unit can be equipped with a double set of heat recovery and low temperature coils thru which the hydrocarbons vapors can be passed alternately. While one set of coils is being used for condensation of hydrocarbons and water vapor, *the alternate* set of coils is being defrosted. By this technique, the operation of the unit is continuous and no time is lost for the removal of moisture and hydrates.

• Direct meter record of hydrocarbon recovery in gallons

Direct reading indicator provides the user and operator with a cumulative record of the recovered condensate vapor in gallons. No additional equipment or gages are required. Hydrocarbon vapor recovery is excellent and is well in excess of 90% depending upon the setting of the controls.

• Constant rate of vapor recovery

In cool temperatures, the refrigeration capacity of the equipment increases which in turn compensates for the usual lowering of the Reid Vapor Pressure *during cold seasons.* In effect, the DE-series of vapor recovery machines has been designed to achieve a constant rate of recovery for either an increase or decrease in hydrocarbon percentage in the vapor-air entering, as well as for a change in Reid Vapor Pressure.

• Simple fully automatic operation

Operation of the complete unit is fully controlled from the single panel within the enclosure. All functions are automatic. However, remote operation with safety controls are available at the option of the purchaser.

The Edwards Vapor Recovery Units are furnished with automatic controls which *provide* operation without full-time attendance.

• Low operating cost

The electrically operated vapor recovery package has a particularly modest energy consumption per gallon of liquid hydrocarbon recovered.

• Low maintenance cost

Recovery of condensable vapors is accomplished by passing vapor-air mixtures over cold heat transfer surfaces, resulting in the direct condensation of hydrocarbon vapors at atmospheric pressure. No preliminary or intermediate compression of vapors is required, thus simplifying the equipment required and reducing maintenance. The maintenance costs are reasonable.

• Fully factory packaged to your specifications

Factory packaged units are available with various custom modifications to meet on-site specifications. The standard enclosure is designed to be mounted on a concrete pad and does not include a flooring. If the unit is to be mounted on elevated supports, a flooring can be provided. All operating components are mounted on a steel i-beam base ready to place on site. The refrigeration machinery, except for the vapor condenser and defrost brine storage reservoir, is located within a weather-proof fire resistant enclosure. Pick-up lugs are provided for the unit for ease in rigging.

• Hydrocarbon vapor compression not required

The elimination of a preliminary or intermediate vapor compressor unit simplifies the total operating mechanism and reduces the power consumption. In addition, maintenance costs are reduced and equipment safety is improved.

• Recovered liquid hydrocarbon can be pumped to any location

Simple piping can be used to automatically return the condensed liquid hydrocarbons from the insulated condenser package directly to any convenient location. Condensed water vapor is separated from the condensed hydrocarbons and can be piped to the terminal waste water disposal facilities.

• Quality of the effluent vapor

The partial vapor pressure of the hydrocarbons in the effluent gas and air mixture will be from 0.1 to 0.5 p.s.i. depending upon the finned surface temperature and chemical quality of the vapor input to the unit.

• All components weather-proof or enclosed

All working components and electrical controls are either of weather-proof construction or are housed in a weather-proof enclosure constructed of fire-proof building panels with an *exterior* of painted aluminum panels. This enclosure provides full room for attending personnel to enter for routine maintenance and service.

• Wiring meets explosion-proof codes

The Edwards Hydrocarbon Recovery Unit is constructed as ordered by the customer to meet any local code requirements. All wiring is complete and may include, if ordered and requested by the customer, a main disconnect switch mounted within the enclosure.

• Long equipment life

The cascade refrigeration system follows conventional circuit design with an almost indefinite life.

.RY UNIT . . . for Gasoline Bulk Stations

SCHEMATIC DIAGRAM

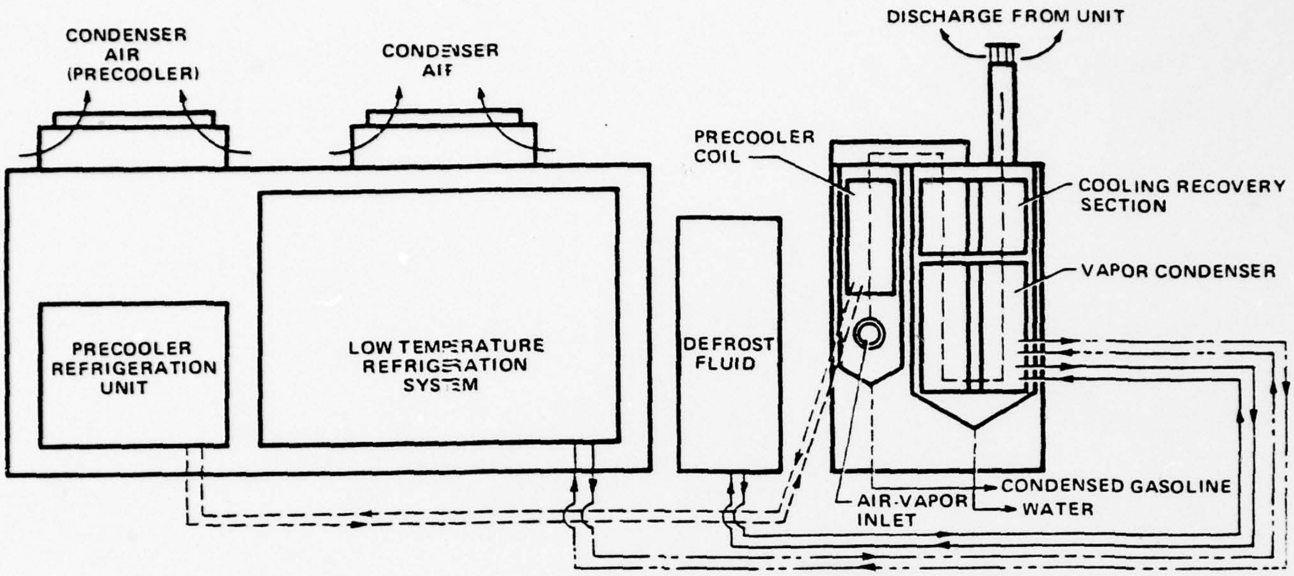

HOW THE EDWARDS HYDROCARBON VAPOR RECOVERY UNIT WORKS

A conventional Edwards refrigeration chiller provides glycol and water at 34ºF for precooling the vapors to remove as much water vapor as possible without the formation of hydrates. The effluent vapors leave the precooler at a standardized water vapor dew-point condition of approximately 34ºF and 34ºF dry bulb.

The vapors after leaving the precooler pass through a cooling recovery section which can remove up to 25% of the cooling effect of the low temperature refrigeration system. After passing through the cooling recovery interchanger, the vapors pass through the low temperature refrigeration vapor condenser which may operate between −80ºF to −115ºF. In this section the hydrocarbon vapors are condensed to a liquid form or to a hydrocarbon hydrate. Entrained moisture in the entering vapor-air mixture condenses and collects as frost on the cold plate fins. Condensed liquid hydrocarbon is collected at the bottom of the vapor condenser.

At periodic intervals, defrosting of the finned surfaces is accomplished by circulation of warm brine stored in a separate reservoir. The temperature of the warm defrost brine is maintained by heat reclamation from the refrigeration equipment.

Minimal shut-down time is required to accomplish defrosting in the standard DE–unit, since the unit is equipped with a precooler as previously described. The precooler acts to remove most of the water vapor in the entering hydrocarbon vapor-air mixture, thereby reducing the time required for defrost. Defrosting is completed in 30 to 60 minutes depending upon the amount of frost collected on the finned coil.

CONDENSATION and RECOVERY OF FLARE VAPORS.

These vapor recovery units can be used for the recovery of hydrocarbon vapors in flare gases. Since the daily 24 hour capacity of this unit is in many cases 8 to 10 times greater than the typical total daily loading of the refinery truck terminal, the unit can be simultaneously used for the recovery of valuable hydrocarbons that are present in flare gases. The condenser construction should be specified for such application. Product recovered from the flare gas could amply contribute toward the recovery of costs. This type of application is particularly ideal where the unit is to be installed in conjunction with a refinery. The products recovered from the flare gas would be butanes and heavier hydrocarbons with some absorbed propane. A by-pass leading to the vapor condenser is installed around a relief damper located in the flare gas vapor line. The purpose of the relief damper is to permit the vapors to go directly to the flare if for any reason the vapor condenser cannot handle the quantity of the flare gas.

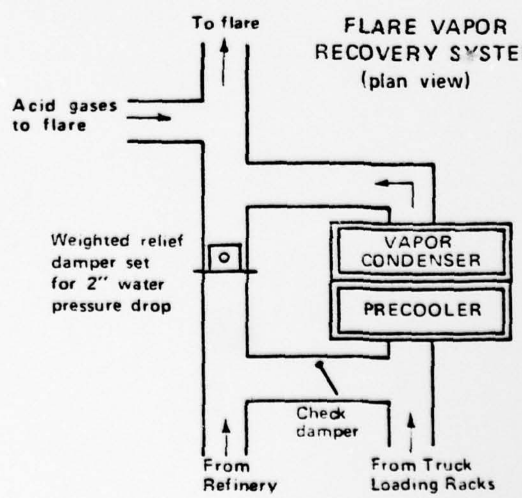

SPECIFICATIONS of VAPOR RECOVERY UNITS

Model ratings are based on 35% by volume of hydrocarbon vapor in air mixture entering condenser with 90% recovery rate for Reid Vapor Pressure of 12 RVP. All data presented is for preliminary estimating and is not to be used for final construction and installation without consulting the factory. Data presented is based on belt-driving open compressors at speeds ranging from 1100 to 1300 rpm. Compressors are capable of running at 1750 rpm. It is suggested that units be purchased with motors of sufficient horsepower capacity to operate the compressors at 1750 rpm if added capacity is required. It is recommended that the capacity of the electrical lines to the compressors be sufficient to run the compressors at 1750 rpm in the event that the added capacity is required.

MODEL	TRUCK LOADING RATE or GAS PROCESSING RATE					AVERAGE DAILY CAPACITY and POWER USAGE at 60° ambient temperature, based on 10% of maximum daily through-put			AVERAGE OPERATING POWER at 60° ambient temperature	
	GAL. per MIN. CONTINUOUS	GAL. per MIN. INSTANTANEOUS for alternating 2½ min. intervals	GAL. per HR. CONTINUOUS	GAL. per DAY MAXIMUM for 24 Hr. operation	CU. FT. per DAY	GAL. per DAY	AVER. POWER USAGE per HR.			
							HP	KW	HP	KW
DE500	500	1000	30,000	720,000	96,000	72,000	2.8	2.5	14	13
DE700	700	1400	42,000	1,000,000	133,000	100,000	3.8	3.4	19	17
DE1000	1000	2000	60,000	1,440,000	192,000	144,000	5.6	5.0	28	25
DE1400	1400	2800	84,000	2,020,000	269,000	202,000	7.6	6.8	38	34
DE2000	2000	4000	120,000	2,880,000	384,000	288,000	11.0	9.9	55	49
DE2400	2400	4800	144,000	3,450,000	460,000	345,000	13.2	11.9	66	59
DE3000	3000	6000	180,000	4,320,000	576,000	432,000	16.4	14.8	82	74
DE3400	3400	6800	204,000	4,890,000	652,000	489,000	18.6	16.7	93	84
DE4000	4000	8000	240,000	5,760,000	768,000	576,000	22.0	19.8	110	99
DE4800	4800	9600	288,000	6,910,000	920,000	691,000	26.4	23.8	132	119
DE6000	6000	12000	360,000	8,640,000	1,150,000	864,000	33.0	29.7	165	149
DE7000	7000	14000	420,000	10,100,000	1,350,000	1,010,000	38.4	34.5	192	173
DE8000	8000	16000	480,000	11,500,000	1,530,000	1,150,000	44.0	39.6	220	198
DE9600	9600	19200	576,000	13,800,000	1,840,000	1,380,000	52.8	47.5	264	238
DE12000	12000	24000	720,000	17,300,000	2,300,000	1,730,000	66.0	59.4	330	297

APPROXIMATE SHIPPING DIMENSIONS															
MODEL DE–	500	700	1000	1400	2000	2400	3000	3400	4000	4800	6000	7000	8000	9600	12000
Width	7'0"	7'0"	9'6"	9'6"	10'0"	10'0"	10'0"	10'0"	11'10"	11'10"	11'10"	11'10"	11'10"	11'10"	11'10"
Length	22'0"	24'0"	26'0"	30'0"	30'0"	33'0"	34'0"	34'0"	41'0"	43'0"	44'0"	52'0"	52'0"	56'0"	56'0"
Height	9'6"	9'6"	9'6"	9'6"	9'6"	9'6"	9'6"	9'6"	9'6"	9'6"	9'6"	9'6"	9'6"	9'6"	9'6"

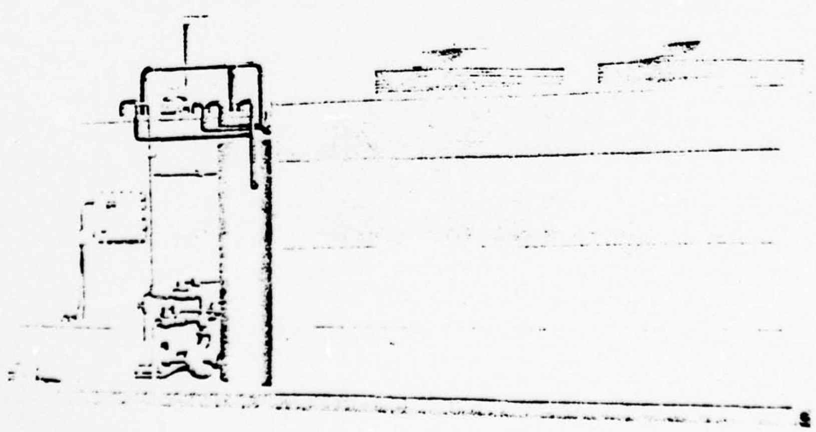

Vapor Recovery starts at...

Edwards
ENGINEERING CORP.
POMPTON PLAINS, NEW JERSEY 07444
ph.(201) 835-2808 TELEX: 130-131

FORM EVR-DE-3
[illegible] EVR-DE-2
[illegible] 1978

APPENDIX D

CALCULATION OF REQUIRED REFRIGERATION CAPACITY AND ELECTRICAL COST

At a fill rate of 600 gpm:

$$\text{Vent rate} = \text{fill rate} = \frac{600\ \frac{\text{gal}}{\text{min}}}{7.48\ \frac{\text{gal}}{\text{ft}^3}} = 80\ \text{acfm}$$

For vapors at 70°F, pounds of hydrocarbon emitted per hour is:

$$\frac{\left[.1225\ \frac{\#\ \text{moles HC}}{\#\ \text{mole vapor}}\right]\left[80\ \frac{\text{ft}^3\ \text{vapor}}{\text{min}}\right]\left[\frac{60\ \text{min}}{\text{hr}}\right]\left[70\ \frac{\#\ \text{HC}}{\#\ \text{mole HC}}\right]}{\left[359\ \frac{\text{ft}^3\ \text{vapor}}{\#\ \text{mole vapor}}\right]\left[\frac{530^0\text{R}}{492^\text{o}\text{R}}\right]} = 106\ \frac{\#\ \text{HC}}{\text{hr}}$$

The EPA measured 94 #/hr at March AFB [3] for vapors at 76°F, and a vent rate of 93 cfm.

Heat capacities for paraffins average about 0.55 $\frac{\text{BTU}}{\#^\text{o}\text{F}}$ [6].

Assuming an average value of 0.40 $\frac{\text{BTU}}{\#^\text{o}\text{F}}$ for the other hydrocarbons, the average heat capacity of JP-4 vapors is:

$$\left[0.55\ \frac{\text{BTU}}{\#^\text{o}\text{F}}\right](0.932) + \left[0.40\ \frac{\text{BTU}}{\#^\text{o}\text{F}}\right](0.068) = 0.54\ \frac{\text{BTU}}{\#^\text{o}\text{F}}$$

$$\left[0.54\ \frac{\text{BTU}}{\#^\text{o}\text{F}}\right]\left[\frac{70\#}{\#\ \text{mole}}\right] = 38\ \frac{\text{BTU}}{\#\ \text{mole}\ ^\text{o}\text{F}}$$

$$\text{Heat capacity of air} = \left[0.25\ \frac{\text{BTU}}{\#^\text{o}\text{F}}\right]\left[29\ \frac{\#}{\#\ \text{mole}}\right] = 7.25\ \frac{\text{BTU}}{\#\ \text{mole}\ ^\text{o}\text{F}}$$

Therefore, molar weighted average heat capacity of JP-4 vapors is:

$$(0.1225)\left[38\ \frac{\text{BTU}}{\#\ \text{mole}\ ^\text{o}\text{F}}\right] + (0.8775)\left[7.25\ \frac{\text{BTU}}{\#\ \text{mole}\ ^\text{o}\text{F}}\right] = 11\ \frac{\text{BTU}}{\#\ \text{mole}\ ^\text{o}\text{F}}$$

For a refrigeration temperature of -90°F, the rate of sensible heat removal for a single storage tank is:

$$\frac{\left[80\ \frac{ft^3}{min}\right]\left[60\ \frac{min}{hr}\right]\left[70^\circ F-\left(-90^\circ F\right)\right]\left[11\ \frac{BTU}{\#mole\ ^\circ F}\right]}{\left[359\ \frac{ft^3}{\#\ mole}\right]\left[\frac{530\ ^\circ R}{492\ ^\circ R}\right]} = 21845\ \frac{BTU}{hr}$$

In addition, there is latent heat removal of:

$$(106\ \#/hr)\ \left(162\ \frac{BTU}{\#}\right) = 17172\ BTU/hr$$

(where 162 BTU/# is the approximate latent heat of the paraffinic hydrocarbons (6) in JP-4 vapors).

$\therefore$ Total heat removal required = $39017\ \frac{BTU}{hr}$

Allowing for 20 percent heat leak, the required refrigeration capacity =

$$39017\ \frac{BTU}{hr} \times 1.2 = 46820\ \frac{BTU}{hr}$$

This corresponds to a 4 ton (48000 BTU/hr) refrigeration unit, for a single storage tank being filled at 600 gpm.

From Reference 6 (p.12-31), it would appear that Freon 13 (monochlorotrifluoromethane) would be a good refrigerant for this application, requiring a theoretical horsepower of about 1.2/ton of refrigerant.

$\therefore$ Total theoretical hp = (1.2)4 = 4.8

which, with the compressor and motor inefficiency, will probably mean an effective power consumption of about 10 hp, or 7.5 KW. At an electrical cost of 4¢/KW·hr, this becomes 30¢/hr of operation.

APPENDIX E

HEAT OF COMBUSTION OF JP-4 VAPORS

Heats of combustion of paraffins are all about 19500 $\frac{BTU}{\#HC}$ [6], and the vapors are all richer than the lower flammable limit. Therefore, theoretically, all that is required is an ignition source. However, the incinerator may have to be maintained hot even on standby, which will require auxiliary fuel.

Heat requirement:

$$\frac{\left[11\ \frac{BTU}{\#\ mole\ ^{o}F}\right](600^{o}F-70^{o}F)}{\left[.1225\ \frac{\#\ mole\ HC}{\#\ mole\ vapor}\right]\left[70\ \frac{\#\ HC}{\#\ mole}\right]} = 680\ \frac{BTU}{\#HC}$$ (for catalytic oxidation at $600^{o}F$)

OR, $1706\ \frac{BTU}{\#HC}$ (for standard combustion @ $1400^{o}F$)

Therefore, the heat content of the vapors is more than sufficient to maintain combustion temperatures.

1978 USAF-ASEE SUMMER FACULTY RESEARCH PROGRAM
sponsored by
THE AIR FORCE OFFICE OF SCIENTIFIC RESEARCH
conducted by
AUBURN UNIVERSITY AND OHIO STATE UNIVERSITY

PARTICIPANT'S FINAL REPORT

FORESTRY LANDS ALLOCATED FOR

MANAGING ENERGY (FLAME)

FEASIBILITY STUDY

Prepared by:	James D. Lowther Ph D
Academic Rank:	Professor
Department and University:	Department of Mechanical Engineering Louisiana Tech University
Assignment:	
(Air Force Base)	Tyndall AFB
(Laboratory)	Civil Engineering and Environmental Development Office
(Division)	Environics
(Branch)	Energy Research
USAF Research Colleague:	Capt William Tolbert
Date:	August 11, 1978
Contract No.:	F44620-75-C-0031

FORESTRY LANDS ALLOCATED FOR
MANAGING ENERGY (FLAME)
FEASIBILITY STUDY

by
James D. Lowther

ABSTRACT

This study evaluated the feasibility of using wood grown on USAF installations as fuel to supply the heating energy requirements of the installations, replacing conventional fossil fuels currently being used. Arnold Engineering Development Center, Tennessee; Barksdale AFB, Louisiana; Eglin AFB, Florida; and Tyndall AFB, Florida have the potential for supplying significant portions of their heating energy requirements with non-merchantable timber grown on the installations. Avon Park Air Force Range, Florida has the potential to supply its own small heating energy requirements plus those of MacDill AFB, which is 75 miles away.

Arnold Engineering Development Center presently has a central plant heating system. The system can be converted to a wood-burning system by altering existing boilers or replacing them with boilers having wood-firing capability. The remaining installations do not have central plant heating systems, but use small natural gas and oil-fired heating units in individual buildings. Conversion of these installations to burn wood would require construction of a wood-fired central system or systems. An alternate method of converting these installations is through the use of a pyrolysis unit to convert wood to fuel gas and fuel oil which can be burned in existing heating units. The latter alternative cannot be implemented until a large scale, continuously operated pyrolysis unit is developed.

ACKNOWLEDGEMENTS

The author is sincerely grateful to the Air Force Office of Scientific Research for support of this summer research. Thanks are due also to ASEE and to Auburn University. The thorough and efficient manner in which the program was administered by Mr. Fred O'Brien, Major Harold Hock and Major James K. Morrow has helped to make the summer both productive and enjoyable.

The author is indebted to the staff of the Energy Research Branch and the entire Environics Division of the Civil Engineering and Environmental Development Office for providing a very professional environment in which to work. Special thanks are due to the author's research colleague, Captain William Tolbert for his excellent administrative guidance and help.

LIST OF TABLES

INTRODUCTION

Shortages, curtailments, and increasing costs of natural gas and fuel oil used to supply energy for comfort heating and heating of industrial and test facilities at USAF installations are well known. Predictions indicate that these conditions will become even more critical in the future as national energy requirements increase and fossil fuel supplies are depleted. In addition, the risks associated with dependence on foreign oil supplies are apparent. In order to prevent jeopardizing the missions at these USAF installations, alternate fuels to replace natural gas and fuel oil must be developed.

Some USAF installations have large forested areas. For these installations, wood can be considered as an alternate to natural gas and fuel oil presently being used as heating fuel. In addition to the obvious advantage of availability in close proximity to the point of use, the wood represents a dependable supply that is not subject to the curtailments and shortages associated with oil and gas. Equally as important, wood represents a renewable energy resource rather than a depletable energy resource. Wood is clean burning with low sulfur content and low ash content compared to coal. In fact, wood can be burned in combination with high sulfur coal in order to reduce emissions to an acceptable level. In some cases the cost of wood fuel is lower than that of other fuels.

Wood fuel is not without its disadvantages, however. Wood is bulky and requires complex handling and storage facilities compared to oil and gas. The handling and storage facilities required for wood are very similar to those required for coal. Wood has a low heating value compared to fossil fuels. The burning efficiency of wood is lower than that of conventional fossil fuels, primarily due to the high moisture content of most wood fuel. The cost of wood as a fuel is influenced by the fact that there are competing uses for wood. Poles, posts, sawtimber, pulpwood and stumpwood represent high value wood products presently harvested from USAF forest lands. Finally, conversion of existing heating systems from natural gas and fuel oil to wood can require large capital investments.

OBJECTIVE

The objective of this study is to evaluate the feasibility of using trees grown on USAF installations as fuel to supply heating energy for the installations in the event of a severe shortage or cutback of oil and gas fuels. The study will include an evaluation of the modifications to installation heating plants that are necessary to allow for a change to wood fuel.

WOOD RESOURCES

A survey of USAF installations indicates that 31 installations have a total of approximately 581,980 acres of timber lands managed under forestry management programs as shown in Appendix 1(1)*. Of these 581,980 acres, 94 percent of the forest lands is on six installations as

* Numbers in parentheses refer to entries in the List of References.

shown in Table 1. The remaining 25 installations have forested areas ranging from 60 to 6000 acres. Since these installations contain almost all the USAF forest resources, the remainder of this report will be confined to an examination of these six installations. Note that five of the six bases are located in the southeastern United States.

TABLE 1

SIX LARGEST USAF FOREST AREAS

Base and State	Approximate Forest Acreage
Eglin AFB, Florida (EAFB)	400,000
Avon Park Range, Florida (APAFR)	60,000
Arnold Engineering Dev Center, Tennessee (AEDC)	31,000
Tyndall AFB, Florida (TAFB)	26,000
Barksdale AFB, Louisiana (BAFB)	17,000
U.S. Air Force Academy, Colorado (USAFA)	14,000
	548,000
All Other	33,980
Total	581,980

AVAILABLE FORMS

For the purpose of this study, the available forms of wood fuel can be classified as merchantable, non-merchantable, and fuel trees.

Merchantable

Forest products currently being harvested and sold from the six bases are poles, posts, sawtimber (for manufacture of lumber), pulpwood, stumpwood (for distillate wood) and firewood.

The Air Force Forestry Management Program operates under the Reimbursable Forestry Program as set forth in Public Law 86-601, Section 511 of 1960 (see AFM 126-1). This law provides that annual operating costs for forestry management operations such as reforestation, fire protection, and timber stand improvement for the entire USAF program cannot exceed the total annual receipts from forest sales from USAF lands.

Non-Merchantable

One form of non-merchantable timber is the residue from the harvesting of merchantable timber. This residue consists of tops, branches, foliage, stumps, and roots. Tops and branches are sometimes chipped up and sold. Some residue must be left in the woods to maintain soil quality and wildlife habitat. However, excess residue left on USAF forest lands is currently being burned as a forestry management practice to reduce the danger of

forest fires. Another form of non-merchantable timber consists of trees killed by natural causes and trees of poor form or of a specie that is undesirable commercially (culls). An example of a cull specie is a hardwood in a southern pine forest. Barksdale AFB is currently paying $30.00 per acre to have cull species in their pine forests killed as a part of their timber stand improvement program. A third category of non-merchantable timber consists of saplings, seedlings and understory vegetation which must be cleared out periodically for timber stand improvement, fire protection and wildlife management purposes. Prescribed burning is frequently employed to clear out this type of vegetation.

Manufacturing wastes such as bark, sawdust, shavings, end trims, slabs and edgings represent another non-merchantable source of wood fuel. The wood manufacturing industry has used their wood wastes as fuel for decades and is moving toward energy self-sufficiency through the use of their wood wastes (2,3). For this reason, manufacturing wastes will not be available as a fuel source outside the industry in future years. Urban wood wastes are best considered as a component of potential fuel derived from solid wastes.

Fuel Trees

Fuel trees are fast growing species grown on "biomass farms" or "energy plantations" specifically for the purpose of providing fuel. Research indicates that fuel tree farms may be feasible (4,5), but not as economical as using non-merchantable wood that results from the managed production of merchantable forest products (2,3).

HEATING ENERGY AVAILABLE

Anticipated average annual sales of merchantable timber from the six installations are shown in Table 2. Under present economic conditions these products are much more valuable as materials than they would be as fuel. The production and manufacture of products from wood is much less energy-intensive than the production and manufacture of alternate products from other materials (3). This means that this merchantable wood sold from USAF bases contributes much more to the national economy and energy supply in the form of raw material for wood products than as fuel. Decreasing supplies and increasing costs of fossil fuels in the future will cause the growing of merchantable timber to continue to be a high-priority objective of USAF forest management plans. This fact, coupled with the dwindling supply of manufacturing wood wastes available outside the industry and the lower economic incentive for growing fuel trees, leads to the conclusion that the best source of wood fuel on the six installations is harvesting residues, culls, saplings and seedlings from forest lands managed to optimize the production of merchantable timber. The use of the harvesting residues, culls, saplings and seedlings for fuel is compatible with good forest management practices for timber stand improvement, fire prevention, wildlife protection and environmental protection.

Table 3 shows the heating energy estimated to be available on a continuous basis from wood grown on each of the six installations. The

timber sold by the Air Force Academy is pine firewood cut primarily for insect, disease and parasitic plant control. The base forester recommends leaving the residue on the ground to aid in regeneration of the forest. Thus, the only fuel wood assumed to be available at the Air Force Academy is that presently sold for firewood.

For the five installations other than the Air Force Academy the heating energy available from harvesting residue was calculated based on the anticipated annual timber sales shown in Table 2. The harvesting residue includes tops, branches, foliage, stumps, roots and all bark except the main stem bark. The mass of residue resulting from the harvest of a certain mass of merchantable timber (main stem) was estimated using information contained in Reference 6.

Heating energy available annually from culls, saplings, and seedings was more difficult to estimate because information on the growth rates of this type of wood is not available. Historically, forest inventories have included only merchantable timber. However, inventories of cull hardwoods in representative southern pine forests were made in 1968 and 1977 (8,14). The inventories show an increase of 25 billion cubic feet of cull hardwoods on 80 million acres of southern pine forests over the nine-year period or an average growth rate of 35 cubic feet per acre per year. This volume represents main stem wood only and excludes branches, tops, foliage, stumps and roots. This estimate of the growth rate of cull hardwoods will, therefore, be very conservative. Use of such a conservative estimate will compensate for such factors as unfavorable climate, poor soil fertility and terrain poorly suited for harvesting at some locations. If the dry weight of the wood is taken to be 32.8 pounds per cubic foot (6), then the average southern pine forest produces approximately 1140 pounds of dry wood per acre per year. It is interesting to note that an independent estimate of cull hardwood growth in the pine forest at Barksdale AFB, made by the base forester, is 0.5 cords per acre per year. This quantity is equivalent to 1250 pounds per acre per year if the green wood weighs 5000 pounds per cord and has a 50 percent moisture content.

Based on a higher heating value of 8600 BTU per pound of dry wood and a boiler efficiency of 67 percent, cull hardwoods in southern pine forests are conservatively estimated to produce 6.6 million BTU of heating energy per acre per year. The values shown in Table 3 are based on 6.6 million BTU per acre per year.

ENERGY REQUIREMENTS

Consumption of fossil fuel for heating purposes on each of the six installations was determined for FY77 and is shown in detail in Appendix 2. It should be noted that all bases having fuel oil standby capability burned fuel oil rather than natural gas during January, February and March of 1977 in order to help alleviate a severe national natural gas shortage. Because Avon Park Air Force Range has limited heating energy requirements, the heating energy requirements of MacDill AFB, which is 75 miles away, were included with those of Avon Park.

TABLE 2

ANTICIPATED ANNUAL TIMBER SALES

Installation	Quantity	Products
AEDC	[illegible]4,500 Tons	Pine and Hardwood Pulpwood Hardwood Sawtimber
APAFR	25,000 Tons	Pine Pulpwood
EAFB	10^6 Board Feet (International)	Pine Sawtimber
EAFB	100,500 Tons	Pine Posts, Poles, Pilings Sawtimber, Pulpwood
	10,000 Tons	Pine Stumps
TAFB	1[illegible],500 Tons	Pine Pulpwood
USAFA	24[illegible] Cords	Pine Firewood

Source: Base Foresters

TABLE 3

HEATING ENERGY AVAILABLE FROM WOOD
EFFICIENCY CORRECTED[1]

Billions of BTU per Year

Installation	Merchantable Timber	Harvesting Residue[2]	Culls, Saplings, Etc[3]	Total
AEDC		123	185	308
APAFR			205	205
BAFB		30	112	142
EAFB		282	2,640	2,922
TAFB		42	172	214
USAFA	0.4			0.4

1 Based on:
- 50% moisture content, green-basis (3)
- 5000 lb/cord density, green (7)
- 67% boiler efficiency (7)
- 8600 BTU/lb higher heating value, oven-dry wood (6)

2 Tops, branches, foliage and bark on tops, branches and foliage is considered to be 35.5% of main stem mass (excluding bark) for softwoods and 47.5% for hardwoods. Stumps, roots, and bark on stumps and roots are considered to be 23% of the main stem mass (excluding bark) for both hardwoods and softwoods (6).

3 Based on average southern area growth rate of 1140 pounds of dry wood per acre per year (main stem only).

Table 4 shows a comparison of the annual heating energy available from wood with FY77 heating energy requirements. The quantities in Table 4 reflect the typical burning efficiencies of the wood, natural gas, fuel oil and propane. Table 4 shows that all of the six bases except the Air Force Academy have the potential to supply a significant portion of their heating energy requirements with wood grown on the installation. It should be noted that the quantities shown in Table 4 represent wood burning potential only. The wood energy availability must be verified by in-depth studies of cull growth rates, etc. In addition, the economic feasibility of harvesting and transporting the fuel wood and converting existing heating systems to burn wood must be considered.

TABLE 4

COMPARISON OF ANNUAL HEATING ENERGY AVAILABLE FROM WOOD WITH FY77 HEATING ENERGY REQUIREMENTS (EFFICIENCY CORRECTED)

Installation	Wood Energy Available[1] Billions of BTU	Heating Energy Requirements[2] Billions of BTU	Percentage of Requirements Available From Wood
AEDC	308	621	50
APAFR + MAFB	205	167	123
BAFB	142	332	43
EAFB	2,922	607	481
TAFB	214	178	120
USAFA	0.4	822	0.05

[1] See Table 3.

[2] Based on consumption listed in Appendix 2 and the following burning efficiencies (7):

Natural Gas	77.8%
Fuel Oil	82.5%
Propane	78.7%

EXISTING HEATING SYSTEMS

Descriptions of the heating systems at the six bases were obtained from the TAB A-1 Environmental Narrative, Phase II for each base and through conversations with base Civil Engineering personnel. A brief description of the heating system at each base follows.

ARNOLD ENGINEERING DEVELOPMENT CENTER

Arnold Engineering Development Center has a central heating plant that supplies steam for comfort heating plus steam for some of the test facility heaters. In addition, natural gas and propane are burned directly in some of the test facility heaters. Plant A consists of three boilers with a capacity of 60,000 lb/hr each of 200 psig saturated steam and one boiler that supplies 20,000 lb/hr of 200 psig saturated steam. Input capacity of these boilers are 70 million BTUH each and 23.5 million BTUH, respectively. Plant A, installed in 1951, was coal fired until 1971 when the boilers were converted to natural gas and fuel oil. The larger boilers were pulverized coal fired and the smaller boiler was stoker fed. Much of the coal and ash handling equipment is still installed, however, the pulverizer units are not in salvageable condition.

Plant B, installed in 1965, supplies 42,000 lb/hr of 725 psig saturated steam for the test facilities and runs only when needed. This boiler is a natural gas and fuel oil-fired package boiler with a 65.6 million BTUH heat input. In addition to the steam system, direct-fired natural gas and propane heaters with a total input capacity of 800 million BTU are used as needed in the test facility. Family housing is heated by individual electric resistance heaters. A FY79 MCP proposes adding to Plant A a new boiler supplying 80,000 lb/hr of 200 psig saturated steam and fired by coal and refuse-derived fuel (9). The estimated total cost in FY79 dollars is $3.04 million. Clearly, wood should be one of the fuels burned by this new boiler.

AVON PARK AIR FORCE RANGE

No TAB A-1 is available for Avon Park Air Force Range. Discussions with the Base Civil Engineer indicate that there is no central heating plant at Avon Park. Older buildings are heated by propane-fired space heaters. Two buildings utilize oil-fired hot water-type heating systems. The newer buildings are heated electrically. The small size of the facilities coupled with the mild winter climate make heating energy requirements at Avon Park quite small.

MACDILL AFB

MacDill AFB is located 75 miles west of Avon Park and has primary responsibility for operation of the range. MacDill AFB is the closest USAF installation to Avon Park and, therefore, the installation that could best make use of wood fuel grown at Avon Park.

MacDill AFB has no central heating plant. The base hospital is heated with three oil-fired boilers having a total input capacity of 18 million

BTUH. Sixty-five natural gas-fired boilers ranging in size from 195,000 to 8,375,000 BTUH supply individual buildings with steam or hot water. Thirty-three oil-fired heating systems, ranging in size from 190,000 to 980,000 BTUH supply steam or hot water for individual buildings. Family housing units are heated by 706 individual natural gas-fired furnaces of 80,000 BTUH each.

BARKSDALE AFB

Barksdale AFB has no central heating plant. One small central system provides heating for four buildings. All other buildings are heated with individual gas-fired units. The EPA Air Pollution Emissions Report contained in the Barksdale AFB TAB A-1 lists 2460 individual combustion sources on the base.

EGLIN AFB

No TAB A-1 is available for Eglin AFB. Eglin AFB has no central heating plant. Most buildings utilize individual natural gas-fired heating systems. Some buildings use fuel oil and LPG-fired units. In order to provide a short-term solution to the problem of natural gas curtailments, heating units in 17 buildings have been converted to burn fuel oil as well as natural gas. All of these units have a capacity greater than 100 boiler horsepower. Units in an additional 35 buildings are scheduled for conversion to natural gas/fuel oil firing.

As a long-term solution to natural gas shortages, plans are being made to install six central plants to supply steam and hot water for heating and absorption cooling. One plant would be fueled with refuse and wood, three with wood and two with coal. Estimated annual consumptions of wood and coal are 61,500 tons and 116,600 respectively. The 2,922 billion BTU of wood energy potentially available annually as shown in Table 3 represents approximately 254,000 dry tons of wood. Eglin AFB has the potential to supply much more of its heating and cooling energy needs from wood fuel than is currently planned.

TYNDALL AFB

Tyndall AFB has no central heating plant. Buildings are heated with individual natural gas-fired units. Three of the larger buildings have fuel oil standby firing capability.

U. S. AIR FORCE ACADEMY

The Air Force Academy has two natural gas/fuel oil-fired central heating plants that provide the bulk of the heating energy for the installation. Family housing and some outlying buildings are heated with individual gas-fired units. A FY80 MCP proposes to convert the two existing central plants to a single coal-fired central plant.

UTILIZATION OF WOOD FUEL

In a typical harvesting operation, residue from merchantable timber, cull trees, etc., would be chipped in the woods with a mechanical chipper and blown into a chip van. The chip van would then be transported by road to the central heating plant where the chips would be unloaded into storage silos, bins, or a storage pad, either covered or uncovered.

The wood may be burned directly in a central plant to produce steam or hot water for heating or converted to alternate forms of fuel such as fuel gas, fuel oil and charcoal in a process such as pyrolysis. Direct burning is adaptable to an installation having an existing central heating plant by converting the boiler to wood-firing or replacing the boiler with a wood-fired boiler. Existing distribution and return lines, and heat exchangers in buildings served by the existing central plant could be used without alteration. The conversion of an installation having an existing central heating plant is, therefore, attractive from the standpoint of the low capital investment required for conversion.

Conversion of an installation not having an existing central heat plant would require either constructing a wood-fired central heating system or systems to serve the heating needs of the installation or constructing a plant such as a pyrolysis plant to convert the wood to fuel gas and/or fuel oil that could be used to fire existing heating systems. A pyrolysis unit would require minimum changes to existing heating units on an installation having small natural gas or fuel oil-fired heating units in individual buildings. Converting such an installation to a wood-fired central plant system would require not only the construction of a central wood-fired boiler but the construction of steam or hot water distribution and condensate return lines from the central plant to individual buildings, and the replacement of the existing furnaces and small boilers in individual buildings with heat exchangers that could utilize the steam or hot water from the central plant.

DIRECT FIRING

Wood-fired boilers may be of the spreader-stoker type, cyclone type or fluidized bed type. Spreader-stoker type boilers require the least fuel preparation while cyclone type boilers require elaborate fuel preparation facilities. More than 200 wood-fired boilers have been constructed in the United States during the last decade (10). Installation of wood-fired boilers would require no technology not already available. For those installations where all of the heating energy requirements cannot be supplied with wood, consideration should be given to burning wood in combination with coal, refuse-derived fuel and sewage sludge. A mixture of high sulfur coal and wood provides a fuel that can meet EPA requirements for sulfur dioxide emissions.

PYROLYSIS

A number of processes have been developed that use pyrolysis to convert wood to fuels such as gas, oil and charcoal (11). The advantage of such a conversion process is that the fuel gas and fuel oil could

replace natural gas and fuel oil used to fuel existing heating systems. Since the four installations that do not have central heating plants have a large number of small natural gas-fired heating units and a number of small oil-fired heating units, a pyrolytic conversion unit is an extremely attractive possibility for utilizing wood as a fuel without the high capital costs required to construct a wood-fired central plant. The major disadvantage of the pyrolytic fuel gas is its low higher heating value - typically 200 BTU/cu. ft. compared to 1000 BTU/cu. ft. for natural gas. The higher heating value of pyrolytic fuel oil is approximately 66 percent that of No. 2 Fuel Oil. Some of the pyrolytic fuel oil is highly corrosive to mild steel, a characteristic that could pose problems in using the oil in existing systems.

A commerical prototype pyrolysis plant designed to process 50 dry tons/day of lumber mill wastes was installed in a small lumber mill in Cordele, Georgia in 1973 (12,13). The Cordele plant was operated on a 24-hours-per-day basis for a period of eighteen months, producing gas, oil and charcoal. Technology for the pyrolytic process has not yet reached the state that would allow the construction of a large scale, continuously operating pyrolytic conversion unit for use at a USAF installation.

COMPARATIVE FUEL COSTS

Table 5 shows average unit fuel prices paid by the five installations in FY77. Also shown in Table 5 are the equivalent costs of wood (50 percent moisture content, green basis) and bituminous coal. For example, at AEDC the average cost of fuel oil in FY77 was $.39/gal. Fuel oil at $.39/gal, wood at $19.36/ton and bituminous coal at $77.42/ton all have the same cost per BTU of heat added to heating steam, water or heated air. Wood at less than $19.36/ton or coal at less than $77.42/ton would be more economical than fuel oil at $.39/gal.

TABLE 5

FY 77 FUEL PRICES AND EQUIVALENT COST OF WOOD AND COAL

Installation	Natural Gas $/MCF	No. 2 Fuel Oil $/gal	Propane $/gal
AEDC	1.75 (12.91) [51.62]	.39 (19.36) [77.42]	.33 (26.87) [107.47]
BAFB	1.15 (8.48) [33.92]		
EAFB	1.55 (11.43) [45.72]	.35 (17.37) [69.48]	.32 (26.05) [104.21]
TAFB	1.55 (11.43) [45.72]	.40 (19.86) [79.41]	
APAFR & MAFB	1.62 (11.95) [47.79]	.37 (18.37) [73.45]	

( ) = Equivalent Cost of Wood, $/ton (50 percent moisture content, green basis)

[ ] = Equivalent Cost of Bituminous Coal, $/ton

A 1976 test by Weyerhauser Company on hardwoods in pine forests in North Carolina showed that the average cost of harvesting, chipping and delivering hardwood chips was $11.00 to $12.50 per ton (50 percent moisture content, green basis) for trees 5 - 8 inches DBH (diameter breast height) and $9.50 - $10.00/ton for trees 9 - 24+ inches DBH (2). Weyerhauser projected that improvements in harvesting technology would reduce these costs to $9.00/ton for trees 5 - 24+ inches DBH by 1978 and $8.00/ton for trees 0 - 24 inches DBH by 1981. These costs do not include any costs associated with converting heating plants to wood fuel or operating chip storage and handling facilities at the heating plant.

Reference to Table 5 shows that wood fuel would be competitive in cost to the fuel oil burned at the five installations. Most of the fuel oil is burned during periods of natural gas curtailment. As natural gas prices rise wood fuel harvesting and delivery prices are expected to be competitive with natural gas prices.

CONCLUSIONS

Preliminary information indicates that Arnold Engineering Development Center, Barksdale AFB, Eglin AFB, and Tyndall AFB have the potential for supplying a significant portion of their heating energy needs from non-merchantable wood grown on the installation. Avon Park Air Force Range has the potential for supplying all of its own heating energy needs plus those of MacDill AFB. The harvesting of wood for fuel would be consistent with forestry management practices designed to optimize the production of merchantable timber, improve wildlife habitats and protect the environment.

Of the above installations, only Arnold Engineering Development Center has an existing central plant heating system which could be adapted to burn wood fuel by installing a boiler with wood-firing capability. The installations not having central heating systems can be converted to burn wood by either installing a central heating plant system using wood-fired boilers or by installing a pyrolysis system to convert wood to fuel gas and fuel oil that can be burned in existing heating systems. Further research is required to establish the technical feasibility of the pyrolysis system.

Although waste wood from wood products industries near USAF installations is currently available, the supply of manufacturing wastes available for purchase will decrease as the wood products industry supplies more and more of their energy needs by burning their own waste wood. For this reason, USAF installations cannot depend on manufacturing wastes as a source of wood energy. Cull trees from non-USAF forest lands near USAF installations may be a source of wood fuel for these installations.

RECOMMENDATIONS

It is recommended that the USAF take steps to implement the burning of wood to supply heating energy at Arnold Engineering Development Center, Barksdale AFB, Eglin AFB, Tyndall AFB, and MacDill AFB. Specific recommendations are as follows:

1. Detailed studies should be made at Arnold Engineering Development Center, Avon Park Air Force Range, Barksdale AFB, Eglin AFB and Tyndall AFB in order to define more exactly the quantities of wood fuel that can be harvested annually on a continuous basis under the specific conditions of climate, soil characteristics, terrain, road systems, existing timber stands and mission requirements on each installation.

2. A study should be made of the technical and economic feasibility of a large scale pyrolysis plant capable of continuous operation and production of fuel gas or fuel gas and fuel oil from wood.

3. A study should be made to determine what modifications, if any, are needed to burn pyrolytic fuel gas and pyrolytic fuel oil in existing small natural gas and fuel oil-fired heating units.

4. At Eglin AFB, where plans are underway to build central heating plants burning wood, coal and refuse-derived fuel, forested lands can probably supply more wood than the initial system designs specify. The system should be designed to make as much use of wood fuel as is consistent with current mission requirements.

5. At Arnold Engineering Development Center, where plans are underway to convert the central heating plant to burn coal and refuse-derived fuel, plans should be altered to include wood burning capability.

6. For installations not having an existing central heating plant, a study should be performed to determine whether conversion to a wood-fired central plant system or a system using a pyrolysis plant and existing heating units is more cost effective. Absorption air conditioning and cogeneration should be examined for possible inclusion in any conversion to a central plant system.

7. A study should be made to formulate the forestry management plans necessary to implement a program for supplying wood fuel for heating on the five USAF installations.

In addition to the above recommendations, a study should be made to determine if wood fuel is available on non-USAF owned lands near USAF installations. National Forest lands as well as private lands should be considered.

REFERENCES

1. Kornman, William M., Staff Forester, HQ USAF/PREV, Personal Communication, June 13, 1978.

2. Jamison, Robert L., "Trees as a Renewable Energy Resource," Symposium Papers: Clean Fuels From Biomass and Wastes, January 25-28, 1977 at Orlando, Florida, Sponsored by the Institute of Gas Technology.

3. Saeman, Jerome F., "Energy and Materials from the Forest Biomass," Symposium Papers: Clean Fuels From Biomass and Wastes, January 25-28, 1977 at Orlando, Florida, Sponsored by the Institute of Gas Technology.

4. Mitre Corporation, "Silvicultural Biomass Farms," Mitre Technical Report No. 7347, the Mitre Corporation, Metrek Division, McLean, Virginia, 1977.

5. Szego, G. C., "Feasibility of Meeting the Energy Needs of Army Bases with Self-Generated Fuels Derived From Solar Energy Plantations," Intertechnology Corporation, Warrington, Va., AD-A031 163, July, 1976.

6. Curtis, A. B., "Forest Residues for Energy in the South," Symposium on Energy in Forestry-Production and Use, Florida Chapter, Society of American Foresters, May 30-31, 1978.

7. U. S. Forest Service, Southeastern Area State and Private Forestry, Fuel Value Calculator, Publication Number 76-19.

8. The Southern Forest Resource Analysis Committee, "The South's Third Forest," 1969.

9. Arnold Engineering Development Center, "Engineering Report for Project 821-116 Coal/Solid Refuse Boiler Addition to Steam Plant," April 1977.

10. Beardsley, William H., "Forests as a Source of Electric Power," Symposium Papers: Clean Fuels From Biomass, Sewage, Urban Refuse and Agricultural Wastes, January 27-30, 1976 at Orlando, Florida, Sponsored by the Institute of Gas Technology.

11. Coyne, James K. III. "Pyrolysis of Solid Wastes for Production of Gaseous Fuels and Chemical Feedstocks," Symposium Papers. Clean Fuels From Biomass and Wastes, January 25-28, 1977 at Orlando, Florida, Sponsored by the Institute of Gas Technology.

12. Bowen, M. D., et al, "A Vertical Bed Pyrolysis System," Engineering Experiment Station, Georgia Institute of Technology.

13. Tatom, J. W., et al, "Clean Fuels From Agricultural and Forestry Wastes," Engineering Experiment Station, Georgia Institute of Technology, Report Number EPA-600/12-76-090, April 1976.

14. Brown, Clair A., and Grelen, Harold R., "Identifying Hardwoods Growing on Pine Sites," Southern Forest Experiment Station, Louisiana State University, 1978.

APPENDIX 1

U. S. Air Force Installations with Forestry Management Programs (1)

Base and State	Approximate Forest Acreage
Arnold Engrg Development Ctr, TN	31,000
Avon Park Air Force Range, FL	60,000
Barksdale AFB, LA	17,000
Charleston AFB, SC	300
Columbus AFB, MS	1,000
Dobbins AFB, GA	900
Eglin AFB, FL	400,000
England AFB, LA (Claiborne Range)	780
Griffiss AFB, NY	600
K. I. Sawyer AFB, MI	2,000
Langley AFB, VA	100
Little Rock AFB, AR	3,000
Loring AFB, ME	6,000
McChord AFB, WA	1,000
MacDill AFB, FL	800
McEntire ANGB, SC	1,200
Moody AFB, GA	600
Myrtle Beach AFB, SC	1,800
New Hampshire Satellite Tracking Sta., NH	2,800
Pease AFB, NH	2,400
Plattsburgh AFB, NY	780
Robins AFB, GA	2,300
Rickenbacker AFB, OH	60
Scott AFB, IL	600
Shaw AFB, SC	1,700
Tyndall AFB, FL	26,000
U.S. Air Force Academy, CO	14,000
Vandenberg AFB, CA	2,500
Wright-Patterson AFB, OH	300
Wurtsmith AFB, MI	200
Youngstown Municipal Airport, OH	260

APPENDIX 2

FOSSIL FUEL CONSUMPTION FOR HEATING
FY 77

Installation	Use	Fuel[1]	Quantity	Energy Content, MMBTU[2]	Cost $
AEDC	Central Heating Plants	NG	371,406 MCF[3]	382,548	649,960
	Central Heating Plants	FO	1,875,513 gal	253,194	731,450
	Test Facility Fired Heaters	NG	139,170 MCF	143,345	243,548
	Test Facility Fired Heaters	LPG	40,911 gal	3,743	13,484
				782,830	1,638,422
APAFR + MAFB		NG	119,361 MCF	122,942	193,678
		FO	617,845 gal	85,689	228,140
		LPG	3,942 gal	367	1,258
				208,998	423,076
BAFB		NG	407,929 MCF	427,102	467,629
EAFB	Family Housing	NG	221,000 MCF	221,000	
		NG	475,750 MCF	475,750	
			696,750	696,750	1,079,519
		FO	513,714 gal	71,920	187,779
		LPG	70,860 gal	6,590	22,616
				775,260	1,280,914

(continued)

APPENDIX 2

FOSSIL FUEL CONSUMPTION FOR HEATING (continued)
FY 77

Installation	Use	Fuel[1]	Quantity	Energy Content, MMBTU[2]	Cost $
TAFB	Family Housing	NG	55,605 MCF	57,940	90,109
		NG	159,200 MCF	165,886	242,781
		FO	35,346 gal	4,902	14,290
				228,728	347,180
USAFA	Central Heating Plants	NG	646,578 MCF	662,655	889,045
	Central Heating Plants	FO	1,028,000 gal	153,840	362,335
	Family Housing, Misc. Bldgs.	NG	281,033 MCF	270,635	424,641
				1,047,130	1,676,021

1 Fuel: NG = Natural Gas, FO = Fuel Oil, LPG = Propane

2 *Energy content based on higher heating value of fuel:*
MMBTU = millions of BTU

3 MCF = thousands of cubic feet

1978 USAF-ASEE SUMMER FACULTY RESEARCH PROGRAM

sponsored by

THE AIR FORCE OFFICE OF SCIENTIFIC RESEARCH

conducted by

AUBURN UNIVERSITY AND OHIO STATE UNIVERSITY

PARTICIPANT'S FINAL REPORT

SENSITIVITY ANALYSIS OF AIR QUALITY ASSESSMENT MODEL PREDICTIONS FOR AIR FORCE OPERATIONS

Prepared by: John L. Lowther, Ph.D.

Academic Rank: Associate Professor of Computer Science

Department and University: Department of Mathematical and Computer Sciences, Michigan Technological University

Assignment:

(Air Force Base) Tyndall AFB FL
(Office) Civil and Environmental Engineering Development Office
(Directorate) Environics Directorate
(Division) Environmental Assessment Research
(Branch) Environmental Modelling

USAF Research Collegue: Lt Harold Scott

Date: August 11, 1978

Contract Number: F44620-75-C-0031

SENSITIVITY ANALYSIS OF AIR QUALITY ASSESSMENT MODEL PREDICTIONS FOR AIR FORCE OPERATIONS

by

John L. Lowther

ABSTRACT

The Air Quality Assessment Model (AQAM) was developed for the Air Force by Argonne National Laboratory. The model was designed to serve as a multi-source, generalized air quality model that can be used to assess the impact of Air Force operations on the environment.

In order to develop an improved streamlined version of AQAM, a sensitivity analysis and parametric studies were performed to evaluate the effects of input parameters and changes in input parameters on AQAM predictions. As a result of this work, an improved, streamlined version of AQAM was developed that allows simplification of the data collection process with the minimum loss in output quality.

LIST OF FIGURES

LIST OF TABLES

INTRODUCTION

The Air Quality Assessment Model (AQAM) was developed for the Air Force by Argonne National Laboratory[1,2,3,4]. The model has been used by the Air Force[9] and the Navy[10] to assess the impact of airbase operations on the air environment.

In order to make the model simpler and cheaper to apply on a routine basis it is desirable to streamline the data collection process. This can be accomplished by performing a sensitivity analysis of the influence of changes to input data on output and eliminating these data inputs that add little to the output quality.

The objective of sensitivity analysis is to identify the model's critical input parameters in order to:

(1) indicate data collection priorities and accuracy requirements;

(2) streamline the data collection process;

and (3) aid in the design of validation studies by indicating optimum receptor locations (i.e., sampling stations) in order to minimize the cost in equipment and manpower to operate sampling stations, and insure the accuracy and usefulness of the model.

The improved model may be used to assess air environmental impact of airbases quickly and efficiently without using expensive sampling stations.

Netzer[6] has completed sensitivity analysis of AQAM predictions for Naval Air Operations to meteorological and dispersion model parameters. Netzer investigated changes in wind speed, wind direction, temperature, Turner stability class, lid height, average emission height, initial horizontal dispersion, and initial vertical dispersion. These meteorological and dispersion parameters are interrelated in the Gaussian dispersion formula. Netzer found that with the exception of the Turner stability

class and wind speed, the effects of variations in these meteorological and dispersion parameters were negligible. The Navy's sensitivity study was conducted for operations at Miramar NAS, California, to precede a validation study at that base.

This report briefly describes AQAM software, the sensitivity analysis techniques employed, the effects of sensitivity tests, and changes incorporated in AQAM software in order to produce a streamlined version of AQAM that allows simplification of the data collection process with a minimum loss in output quality.

OBJECTIVES

This investigation was conducted to determine the sensitivity of various geographical, meteorological, and dispersion parameters of AQAM to Air Force operations. On the basis of sensitivity analysis and problems inherent in the data collection process, a streamlined version of AQAM was to be designed and implemented.

MODEL DESCRIPTION

AQAM is a large scale, multi-source, generalized air quality model consisting of three submodels: source emission inventory, short-term dispersion, and long-term dispersion.

The source emission inventory submodel has input parameters for aircraft, airbase, and environ sources. Some of the required data are difficult or time consuming to collect and have a great deal of inherent error. The number of parameters contributes to a lengthy and expensive data collection period (as much as three man-months are required). The output of the source emission inventory submodel is a complete audit of emissions (carbon monoxide-CO, hydrocarbons-HC, oxides of nitrogen-NO_x, particulate matter-PT, and sulfur dioxide-SO_2), a complete audit of sources and meteorological conditions, and a list of aircraft and engine characteristics.

The short-term dispersion and long-term dispersion submodels are Gaussian plume models which calculate hourly and annually averaged pollutant concentrations, respectively, at points on a receptor grid. The long-term submodel uses an existing AF meteorological tape of the airbase as part of its data source.

SENSITIVITY ANALYSIS

Sensitivity analysis is used to identify critical model input parameters in order to indicate data collection priorities and accuracy requirements. Usually sensitivity analysis precedes validation or calibration studies.

Model sensitivity can be determined by observing changes in calculated concentrations caused by changes in input parameters. For instance, if a small change in a specific input causes a large change in a pollutant's concentration, then the model is sensitive to that input, and this input is necessary and needs to be accurately collected. Conversely, if a large change in a specific input causes little or no change in a pollutant's concentration, then the model is not sensitive to that input, and little or no effort needs to be expended to achieve high accuracy for that input.

Note that sensitivity is not likely to remain constant over the whole range of values that input parameters can assume. It is possible that for certain combinations of input parameters values, the model's output will be independent of the changes in one or more inputs.

In this research, a sensitivity test consisted of the following steps:

(1) modification of prototype base's data,

(2) execution of source inventory submodel using prototype base's data, and

(3) execution of the short-term dispersion model using the output from the source inventory submodel.

The receptor locations were placed, for the short-term dispersion submodel, to include the base in a 2 by 2 grid and supplemented by 16 other special receptors downwind from the base (see Table 3 and Figure 1). To measure incremental changes induced input parameters variations, the receptor with maximum concentration was selected in each sensitivity test. For a given sensitivity test the receptor with the maximum concentration change may be different for different pollutants.

LUKE AFB – 2x2 GRID – 16 SPECIAL RECEPTORS

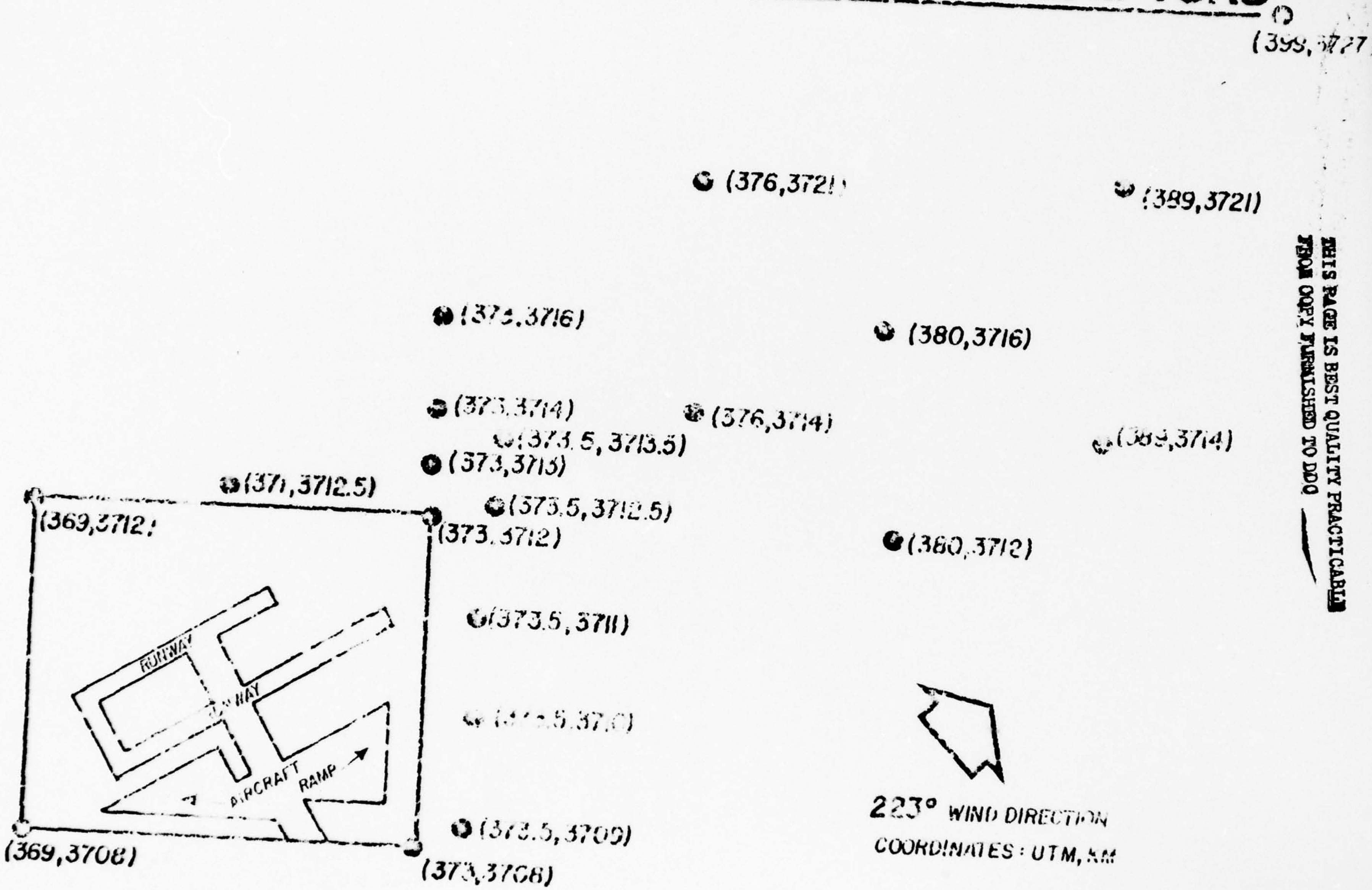

FIGURE 1

RESULTS AND DISCUSSION

Multiple source models such as AQAM have a variety of input parameters: meteorological, dispersion, geographical, and operational. It is this variety and number of input parameters that make it impossible to perform sensitivity studies on each individual input parameter. An alternative is to perform sensitivity studies on either groups of inputs, i.e., a parameter that occurs in many data sets. (See Menicucci[4] for a complete description of all data sets).

All of the sensitivity tests were performed using worst case, one hour periods in order for the output to be compared with Federal Primary and California Air Quality Standards, Table 1.

Additionally, many sensitivity tests were designed as a result of comments from those who have collected AQAM data. These tests were designed to verify that changes in AQAM could be made to simplify data collection, thereby reducing data collection time.

Finally, some sensitivity tests were operational or parametric in nature. These tests indicate possible changes in base operations or procedures that may effect emissions or concentration levels of pollutants.

RECEPTOR LOCATIONS

Receptor Locations, Table 3, were chosen to encompass most of the base in a 2 by 2 grid and to lie downwind from the base. Environ emission sources were absent allowing the receptors to measure concentrations which typify the base as a source of pollution. Using this receptor arrangement, effects due to near source locations were minimized.

Maximum concentrations of all pollutants generally occurred at receptor 12 (see Tables 3 and 5).

EFFECT OF METEOROLOGICAL PARAMETERS

Netzer(6), Ludwig and Dabberdt(7), and Freas and Lee(8) verify for multiple and single source air pollution dispersion models that the effect in individual meteorological parameters, with the exception of Turner stability classes and wind speed, result in small or negligible output changes. Sensitivity tests, Tables 4 and 5, confirmed Netzer's observation that an ambient temperature change of 10°F has little effect on predicted concentrations. Netzer also discusses lid height, stability class, wind speed, and wind direction.

EFFECT OF DISPERSION MODEL PARAMETERS

Sensitivity tests 4, 5, 6, 7, and 8 involving the horizontal and vertical dispersion parameters of groups of airbase point sources showed no change occurred at receptor location 12. Even changes as large as 200 percent had negligible effect on all receptors.

Tests 13, 14, and 15 involving emission heights, line widths, and initial vertical dispersion parameters of specific groups of airbase line sources produced a 1 percent or less change at maximum concentration receptor location 12.

Netzer (6) universally increased the initial vertical dispersion parameter of all point, line, and area sources, irrespective of data set, by 150 percent. This increase "had negligible effect on predicted concentration except at near source, special receptors. Even at the latter locations predicted variations were less than 20 percent."

PARAMETRIC OR OPERATIONAL PARAMETERS

Parameters of petroleum storage tanks such as paint, diameter, seal, and rivet factors, vapor space height, throughput factors, fuel temperature and temperature variation of vapor space (see sensitivity tests 9, 10, and 11), should probably all be defaulted since they cause no change in the concentration at any receptor location.

Setting hydrocarbon breathing losses due to petroleum tank truck parking to zero caused a 2 percent drop in hydrocarbon concentration at the maximum receptor location. Hence, for quick surveys of a base, this data set need not be included.

Changes in the height of airbase line sources from 0 to 5 meters caused negligible change in maximum concentration. CO and PT increased and decreased by 3 percent, respectively.

CO and PT increased and decreased by 3 percent respectively, when both military and civilian vehicles follow EPA distributions.

Worst case aircraft engine venting caused approximately a 200 percent increase in hydrocarbons. By strictly controlling venting, which is a function of aircraft type, hydrocarbon concentrations may be reduced.

Sensitivity test 21 demonstrated the effect of replacing an industrial natural gas power plant having low sulfur and ash emissions by an industrial large scale coal burning plant having high sulfur and ash emissions. CO, HC, and NO_x concentrations at maximum receptor location remained the same. However, due to the location of the power plant, maximum PT and SO_2 receptor moved to location 17 with a 35 percent increase in PT and a 5 percent increase in SO_2.

EFFECT OF GEOGRAPHICAL PARAMETERS

Geographical parameters; such as, taxiway segments, taxiway paths, runway geometry, parking squares and areas; can be simplified in order to aid data collection. However, this simplification may in some cases cause significant changes in output concentrations. For example, sensitivity test 2 shows the effect of converting a taxiway path consisting of many taxiway segments into a taxiway path consisting of one taxiway segment (from parking area to runway.) Since the distances over which aircraft taxied was shortened, there was significant reductions in pollutant concentrations.

MODIFICATIONS OF AQAM SOFTWARE

Various types of modifications have been incorporated into a streamlined version of AQAM software. These modifications are listed as follows:

(1) Optimization -- Code that was isolated or never executed was eliminated. Some control structures were simplified.

(2) Data Collection Simplification -- Six out of 37 data sets were eliminated either because they contributed little to output quality or because they were seldom used in data collection. These were data sets 13, 19, 33, 34, 35, and 36. The format of some data sets was simplified.

(3) Corrections -- Various errors were found and corrected.

(4) Default parameters -- Some default parameters were permanently set based on results of sensitivity tests.

(5) Dispersion submodel modifications -- Terrain heights of receptors may now vary; multiple reflection for coupling coefficients added; sigmas calculated differently.

Altogether, about 40 changes and rewrites have been made in the AQAM software. (A technical note is available which summarizes these modifications.)

CONCLUSIONS AND RECOMMENDATIONS

As a result of this investigation, a streamlined version of AQAM software has been designed and implemented. Further redesign and streamlining is possible. However, before more work is done, AQAM software needs more source code documentation. A complete, modular rewrite in FORTRAN 77, the new official ANSI standard, would improve readability, modifiability, and perhaps the efficiency of AQAM.

Argonne is currently defining the accuracy of AQAM. Accuracy could further be defined by turning AQAM into a single source model and compare the resulting output with an EPA or some other single source model that has been extensively used.

Software could be designed to interactively aid in the preparation of data for the source inventory model. Additional interactive software could interrogate the data base built up by the source inventory model in order to give selective displays of airbase emissions, aircraft emission data, and characteristics of emission sources.

Based on data collection practices and further sensitivity tests, revisions of AQAM software are possible and should be pursued in order to have cost effective air pollution control.

REFERENCES

1. D. M. Rote and L. E. Wangen, "A Generalized Air Quality Assessment Model for Air Force Operations," Air Force Weapons Laboratory, Kirtland AFB, NM, Tech Report No. 74-304, March 1975.

2. D. J. Bingaman and L. E. Wangen, "Air Quality Assessment Model for Air Force Operations - Source Emissions Inventory Computer Code Documentation," Argonne National Laboratory, Report No. CEEDO-TR-76-33 (NTIS ADA 046-229), April 1977.

3. D. J. Bingaman, "Air Quality Assessment Model for Air Force Operations - Short-Term Emission/Dispersion Computer Code Documentation," Argonne National Laboratory, Report No. CEEDO-TR-76-34 (NTIS ADA 046-348), April 1977.

4. D. Menicucci, "Air Quality Assessment Model (AQAM) Data Reduction and Operations Guide," Air Force Weapons Laboratory, Kirtland AFB, NM, Tech Report No. 75-307 (NTIS ADA 033-001), October 1976.

5. G. R. Thompson and D. W. Netzer, "An Ambient Air Quality Model for Assessment of US Naval Aviation Emittants," Naval Postgraduate School, Monterey, CA, Tech Report NPS-57Nt 76091, September 1976.

6. D. W. Netzer, "Sensitivity of AQAM Predictions for Naval Air Operations to Meteorological and Dispersion Model Parameters," Naval Postgraduate School, Monterey, CA, Tech Report NPS-67Nt 78051, May 1978.

7. F. L. Ludwig, et.al., "A Practical, Multi-Purpose Urban Diffusion Model for Carbon Monoxide," Stanford Research Institute, Menlo Park, CA, PB-196 003, September 1970.

8. W. P. Freas and R. F. Lee, "Sensitivity Analysis of the Single Source (CRSTER) Model," US Environmental Protection Agency, Appendix E of "User's Manual for Single-Source (CRSTER) Model, EPA-450/2-77-013, July 1977.

9. D. Naugle, B. Grems, and P. Daley, "Air Quality Impact of Aircraft at Ten US Air Force Bases," J. Air Pollution Control Association, Volume 28, No. 4, pp. 370-373, April 1978.

10. K. Weal, G. Thompson, and D. Netzer, "Modifications of an Ambient Air Quality Model for Assessment of US Naval Aviation Emittants," J. Air Pollution Control Association, Volume 28, No. 3, pp. 247-248, March 1978.

TABLE 1

FEDERAL PRIMARY AND CALIFORNIA POLLUTANT STANDARDS

Pollutant	Standards $\mu g/m^3$ California	Standards $\mu g/m^3$ Federal Primary
CO	46,000[1]	40,000[1]
NO_x	470[1]	100[4]
HC	None	160[2]
PT	100[3]	260[3]
SO_2	1,310[1]	365[3]

(1) 1-hour concentration not to be exceeded more than once per year.

(2) 3-hour concentration not to be exceeded more than once per year.

(3) 24-hour concentration not to be exceeded more than once per year.

(4) annual arithmetic mean.

TABLE 2

SUMMARY OF SOURCES AT PROTOTYPE BASE

I. Air Base Sources		
a. Point Sources		
	Test Cells	3
	Run-Up Stands	6
	Power Plants	2
	Storage Tanks	11
b. Area Sources		
	Filling	6
	Tank Truck Parking	1
	Vehicle Parking	14
	Space Heating	5
II. Aircraft Sources		
a. Aircraft Types		8
	C-97, C-9A, C-130, F4-C/F, O-1, F-104A, F-15, F-5	
b. Parking Areas		5
c. Taxiway Line Segments		19
d. Runways		4

TABLE 3

RECEPTOR LOCATIONS

Receptor Number	Receptor Location (kilometer) x	y
1	369.0	3708.0
2	369.0	3712.0
3	373.0	3708.0
4	373.0	3712.0
5	371.0	3712.5
6	373.0	3713.0
7	373.0	3714.0
8	373.0	3716.0
9	373.5	3709.0
10	373.5	3710.0
11	373.5	3711.0
12	373.5	3712.5
13	373.5	3713.5
14	376.0	3714.0
15	376.0	3721.0
16	380.0	3712.0
17	380.0	3716.0
18	389.0	3714.0
19	389.0	3721.0
20	399.0	3727.0

TABLE 4

COMPUTER TEST FOR SENSITIVITY STUDY

Test Number	Description
1	Control run: Modified Luke AFB data. Data sets 13, 17, 22, 25, 27, 33, 34, 35, 36, and 37 empty.
2	Geographical: taxiway paths set equal to taxiway segments.
3	Meteorological: 10°change in ambient temperature.
4	Dispersion: 25 percent change in initial horizontal disperion parameter (12.5 in) for test cells
5	Dispersion: 25 percent change in initial vertical and horizontal dispersion parameters (12.5) for test cells.
6	Dispersion: 25 percent change in initial horizontal dispersion parameter (6.25 in) for run-up stands.
7	Dispersion: 200 percent change in vertical dispersion parameter (10.0 in) for run-up stands.
8	Dispersion: Initial vertical dispersion parameter set to be four times the diameter of the stack of a power plant; intital horizontal dispersion parameter, two times the diameter.
9	Parametric: Fuel temperature and temperature variation of vapor space of petroleum storage tanks defaulted.
10	Parametric: Defaulted vapor space height, throughput factors, paint, rivet, and seal factors.
11	Parametric: Combined tests 9 and 10.
12	Parametric: HC breathing losses due to petroleum tank truck parking set to zero.
13	Dispersion: Emission height (16m), width of line (30m), and initial vertical dispersion (12 in) for aircraft taxiway path segments.
14	Dispersion: Emission height (16m), width of line (30m), and initial vertical dispersion (12m) for aircraft runways.

TABLE 4 (Continued)

Test Number	Description	
15	Dispersion:	Combined tests 13 and 14.
16	Parametric:	33 percent increase in average speed of civilian motor vehicles.
17	Parametric:	Average height of emissions (5m) for airbase line sources.
18	Parametric:	Average height of emission (0m) for airbase line sources.
19	Parametric:	Military and civilian EPA vehicle distributions.
20	Parametric:	Worst case venting (5 gal/vent) for each aircraft.
21	Parametric:	Industrial natural gas powerplant replace by industrial large scale coal burning plant.
22	Parametric:	All defaultable parameters, defaulted.
23	Parametric:	Deletion of data set 24 - military and civilian vehicle HC breathing loss.

TABLE 5

MAXIMUM RECEPTOR CONCENTRATIONS FROM TOTAL SOURCES

Test Number	Grid Location Concentration, $\mu gm/m^3$ CO	HC	NO_x	PT	SO_2
1	12 710.9	12 684.2	12 71.03	12 17.49	12 19.97
2	11 702.1	12 661.5	12 65.41	12 16.66	12 17.92
3	12 711.2	12 685.6	12 69.88	12 17.51	12 20.04
4	12 710.9	12 684.2	12 71.03	12 17.49	12 19.97
5	12 710.9	12 684.2	12 71.03	12 17.49	12 19.97
6	12 710.9	12 684.2	12 71.03	12 17.49	12 19.97
7,8,9,10,11	12 710.9	12 684.2	12 71.03	12 17.49	12 19.97
12	12 710.9	12 684.2	12 71.03	12 17.49	12 19.97
13	12 699.8	12 682.0	12 70.52	12 17.42	12 19.78
14	12 709.7	12 684.0	12 70.76	12 17.47	12 19.92
15	12 698.7	12 681.9	12 70.25	12 17.39	12 19.74
16	12 709.1	12 684.0	12 71.11	12 17.49	12 19.97
17	12 710.5	12 684.1	12 70.97	12 17.49	12 19.97
18	12 710.9	12 684.2	12 71.03	12 17.49	12 19.97

TABLE 5. (Continued)

Test Number	CO	HC	NO_x	PT	SO_2
19	12 688.7	12 681.4	12 70.41	12 16.97	12 19.44
20	12 710.9	12 1260.0	12 71.03	12 17.49	12 19.97
21	12 710.9	12 684.2	12 71.03	17 23.55	17 20.9
22	12 619.4	12 492.1	12 82.1	12 18.24	12 21.85
23	12 710.9	12 670.3	12 71.03	12 17.49	12 19.97

1978 USAF-ASEE SUMMER FACULTY RESEARCH PROGRAM
sponsored by
THE AIR FORCE OFFICE SCIENTIFIC RESEARCH
conducted by
AUBURN UNIVERSITY AND OHIO STATE UNIVERSITY

PARTICIPANT'S FINAL REPORT

A COMPREHENSIVE SOCIOECONOMIC IMPACT ASSESSMENT MODEL

Prepared by:	Robert Premus, Ph D
Academic Rank:	Associate Professor
Department and University	Department of Economics Wright State University
Assignment:	Tyndall Air Force Base Civil Engineering Center Environmental Protection Planning
USAF Research Colleagues:	John E. Palmer W. Allen Nixon
Date:	August 11, 1978
Contract No.:	F44620-75-C-0031

A COMPREHENSIVE SOCIOECONOMIC IMPACT ASSESSMENT MODEL

by

Robert Premus

ABSTRACT

A model for predicting the economic consequences of military actions (base closures and realignments) at the regional and community levels is presented. The model contains equations and algorithms for measuring changes in gross regional output, total income, employment, unemployment by race, population, per capita income and school enrollments. Both the absolute amount and rate of change of these attributes are predicted.

A suggested comprehensive framework for analyzing and measuring the magnitude of socioeconomic impacts associated with base closures, expansions and realignments is presented in this report. An economic base approach was adopted for this purpose because (1) it is the most extensively used methodology for undertaking impact analysis that currently exists; (2) it provides a measure of short-run impacts, removing the difficulties of predicting structural changes in the regional economy (3) it is readily applied to area specific primary and secondary data; and (4) it is a relatively cost effective approach to regional impact modeling. Of course, its neglect of interregional trade relations and long-run structural changes in the region of influence are major deficiencies, but, overall, its extensive use in regional economic theory and econometric applications suggests that the benefits of using the economic base framework to analyze short-run socioeconomic impacts outweigh its costs.

A model can be described by the attributes (or "key indicators") that it measures and predicts. The key attributes of the suggested comprehensive socioeconomic impact assessment model (CSIAM) are: total output, total employment, unemployment by race, population, total personal income and per capita income. Both the magnitude and rate of change in each of the attributes is predicted by the model. In addition, a set of mathematical procedures (algorithms) are included which allocate changes in the model's attribute to the communities in the region of influence (ROI). The inclusion of community (or area) impacts clearly distinguishes CSIA from the OESAS, SIFS, RIMS and the Battelle I/O models. Finally, algorithms are presented which relate changes in the models attributes to key institutions within the ROI. Specifically, impacts on local governments, special districts (e.g., schools and parks), financial institutions, public utilities and infrastructure facilities (e.g., roads, sewers, and water) are measured.

The report is divided into three sections reflecting the analytical, spatial and institutional dimensions of the CSIA. The theoretical, or analytical, structure of the aggregate model is presented in Section I. Section II presents an allocation model capable of measuring socioeconomic impacts at the community level. Finally, Section III contains a summary and comments on the feasibility of constructing algorithms for relating aggregate and community impacts to key institutions within the ROI.

SECTION I

THE AGGREGATE MODEL

The aggregate model component of the CSIA measures changes in key attributes at the ROI level with no initial concern for the implications of these changes at the community (or micro) level. The key attributes in the order in which they are presented are: gross regional product, employment, unemployment, population, personal income and per capita income.

PRODUCT MARKET IMPACTS

(1) $\Delta GRP_t = m\Delta Y_{ig} + m\Delta Y_{pg} + m(1-\nu)\gamma\sigma\tau\Delta Y_{kg} + m\nu\Delta Y_{kg} + \Delta Y_{kg}$

where:

GRP_t = change in gross regional product (expenditures)

ΔY_{ig} = direct change in local consumption expenditures due to the military action.

ΔY_{pg} = direct change in local military procurement expenditures due to the military action.

ΔY_{kg} = direct change in military construction expenditures due to action

and

$(1-\nu)\gamma\sigma\tau\Delta Y_{kg}$ = direct change in local spending due to base construction activity.

$\nu\Delta Y_{kg}$ = direct change in local spending due to increased purchases of materials during base construction period.

where:

m = regional multiplier

$1-\nu$ = fraction of construction expenditures other than for purchases of materials from local economy.

v = fraction of construction expenditures for materials purchased locally.

γ = fraction of construction expenditures that accrues to labor.

σ = income tax rate.

τ = local saving rate, i.e., fraction of income after taxes that is saved.

Solve for ΔY_{ig}

$$\Delta Y_{ig} = \Delta Y_c + \Delta Y_{mt} + \Delta Y_{mp}$$

where:

$$\Delta Y_c = W_c w_c \tau\sigma$$

$$\Delta Y_{mt} = W_{mt} w_{mt} \tau\sigma$$

$$\Delta Y_{mp} = W_{mp} w_{mp} \tau\sigma$$

and

W_c = total wages of civilian personnel affected by action.

w_c = fraction of civilian wages spent in ROI

W_{mt} = total wages of military trainees affected by action.

w_{mt} = fraction of military trainees wages spend in ROI

W_{mp} = total wages of military permanent affected by action.

w_{mp} = fraction of military permanent wages spent in ROI.

or

$W_c = R\alpha_c w_c$

$W_{mt} = R\alpha_{mt} w_{mt}$

$W_{mp} = R\alpha_{mp} w_{mp}$

and

R = total number of new positions being transferred to ROI.

α_c = fraction of new positions to be filled by civilians.

W_c = average wage of civilians affected by action.

α_{mt} = fraction of new positions filled by military trainees.

w_{mt} = average wage of military trainees.

α_{mp} = fraction of new positions to be filled by military permanent.

w_{mp} = average wage of military permanent.

solve for ΔY_{pg}

$$Y_{pg} = \frac{Y_{pi} - Y_q)}{L}$$

where:

Y_{pi} = total amount of procurement expenditures in ROI.

Y_q = total amount of procurement expenditures in ROI for commissary and BX goods purchased by retirees.

L = total number of persons employed by and assigned to to the base.

ΔY_{pg} = change in procurement expenditures in ROI as a result of the action.

R = number of new positions being transferred to ROI.

let

$X_1 = \Delta Y_{ig}$

$X_2 = \Delta Y_{pg}$ (see equation (1))

$X_3 = (1-\nu)\gamma\sigma\tau\Delta Y_{kg}$

$X_4 = v\Delta Y_{kg}$

$X_5 = \Delta Y_{kg}$

then:

$$\Delta GRP_t = mX_1 + mX_2 + mX_3 + mX_4 + X_5$$

and

$$(1') \quad GRP_i = [GRP_t - (X_1 + X_2 + X_3 + X_4 + X_5)]$$

where:

GRP_i = induced (or indirect) change in gross regional product (total expenditures) due to the action.

LABOR MARKET IMPACTS

$$\text{(2)} \qquad \Delta E_t = \frac{m(X_1)}{p_{rs}} + \frac{m(X_2)}{p_{ws}} + \frac{m(X_3)}{p_{rs}} + \frac{m(X_4)}{p_v} + \frac{X_5}{p_{ks}}$$

where:

ΔE_t = total expansion of employment opportunities in ROI due to the military action.

p_{rs} = sales per employee in retail and personal services sector of ROI (productivity in retail of personal services).

p_{ws} = labor productivity in wholesale and service sector in ROI.

p_{ks} = labor productivity in construction sector of ROI.

p_v = labor productivity in sectors that supply construction sector.

let

X_1' = X_1/p_{rs} (number of jobs in retail and service sectors directly related to the military action through payrolls).

X_2' = X_2/p_{rs} (number of jobs in wholesale and service sectors directly related to the military action through payrolls).

X_3' = X_3/p_{rs} (number of jobs in retail and service sectors directly related to the military action through construction expenditures).

X_4' $= X_4'/p_v$ (number of jobs in materials sector directly related to construction expenditures).

X_5' $= X_5/p_{ks}$ (number of construction jobs in ROI directly related to construction expenditures).

then

$$\Delta E_t = mX_1' + mX_2' + mX_3' + mX_4'$$

and

$$(2') \quad \Delta E_i = [\Delta E_t - (X_i + X_2' + X_3' + X_4' + X_5')]$$

where

ΔE_i = induced, or secondary, employment change in ROI due to the military action.

$$(2'') \quad \dot{E}_t = \frac{E_t}{E_t}$$

where

$\dot{E}_t$ = rate of change of total employment in nonmilitary sector of economy in ROI as a result of the military action.

Solve for:

$$P_{rs} = \frac{Y_{rst} + Y_{sst}}{E_{rst} + E_{sst}}$$

where:

Y_{rst} = total regional output (a sales) for retail sector in period t (constant dollars).

Y_{sst} = total regional output (a sales) for services sector in period t (constant dollars)

E_{rst} = total regional employment in retail sector in period t.

E_{sst} = total regional employment in services sector in period t.

t = most recent year for which USAF wage and procurement information is available.

$$P_{ws} = \frac{Y_{wst} + Y_{sst}}{E_{wst} + E_{sst}}$$

where:

Y_{wst} = total regional output (or sales) for wholesale sector in period t (constant dollars).

E_{wst} = total regional employment in wholesale sector in period t (constant dollars).

$$P_{ks} = \frac{Y_{kst}}{E_{kst}}$$

where

Y_{kst} = total state output for construction sector in period t (constant dollars).

E_{kst} = total state employment in construction sector in period t.

UNEMPLOYMENT:

(3) $$\Delta V^{di} = \Delta L_S^{di} - \Delta L_D^{di}$$

where:

ΔV = direct and induced change in number of unemployed persons in civilian labor force market as a result of direct and induced changes in labor supply and demand because of the military action.

ΔL_S^{di} = direct and induced changes in labor force size as a result of the military action.

ΔL_D^{di} = direct and induced changes in labor force demand as a result of the military action.

Solve for ΔL_S^{di}

ΔL_S^{d} = direct change in labor force size as a result of the military action.

ΔL_S^{i} = induced change in labor force size due to net migration change resulting from the military action.

Solve for ΔL_S^{d}

$$L_S^d = E_{wd} + E_{sj}$$

where:

E_{wd} = number of dependents of USAF personnel who will seek civilian employment.*

E_{sj} = number of USAF personnel who will seek a second job.*

* Method of calculation involves a weighted average of military permanent, military trainees, civilian transfers and civilians hired from outside ROI, weighted by the number of dependents in each of these groups who will seek a job, as well as the fraction of all military personnel who will seek second jobs.

Solve for ΔL_S^i

$$\Delta L_S^i = \zeta_m \times \Delta E_t$$

where:

ΔE_t = total employment expansion in ROI (see equation (1)) as a result of the military action.

ζ_m = fraction of new jobs (ΔE_t) which will be filled by civilians who migrate to the ROI.

where:

$$\zeta_m = \frac{m^{t-k}}{p^{t-k}}$$

and

Δm^{t-k} = amount of net migration during (t-k)-t period for ROI (e.g., 1960-1970 where t = 1970 and k = 10).

p^{t-k} = amount of population change in ROI during (t-k)-t period (e.g., 1960-1970 where t = 1970 and k = 10).

Solve for ΔL_D^{di}

$$\Delta L_D^{di} = \Delta L_D^{d} + \Delta L_D^{i}$$

where:

ΔL_D^{d} = direct change in demand for labor in ROI as a result of military action.

ΔL_D^{i} = total induced change in labor demand in ROI as a result of the military action.

and

$$\Delta L_D^{d} = \alpha_{hl} R$$

where:

α_{hl} = fraction of new positions to be filled by civilians hired from within ROI.

R = total number of new positions being transferred to ROI.

and

$$\Delta L_D^{i} = \Delta E_t$$

where:

ΔE_t = total employment expansion in ROI as a result of the military action.

(3') $$\dot{V} = \frac{\Delta V^{di}}{V_{t_1}}$$

where: $\dot{V}$ = percentage change in number of unemployed persons in ROI as a result of the military action over period t_1 to t_2.

ΔV^{di} = absolute change in unemployed persons (see equation (3) from t_1 to t_2.

V_{t_1} = number of unemployed persons in period t_2.

(3a'') $$V_r^{t_2} = \frac{V_{t_1} + \Delta V^{di}}{L_{t_1} + \Delta L_S^{di}}$$

where: L_{t_1} = size of labor force in period t_1 in ROI.

$V_r^{t_2}$ = unemployment rate in ROI in period t_2 (after military action is complete).

(3a''') $$\Delta V_r^{di} = V_r^{t_2} - V_r^{t_1}$$

where: ΔV_r^{di} = direct and indirect change in ROI unemployment rate.

$V_r^{t_1}$ = unemployment rate in ROI at period t_1.

(3b'') $$V_{rb}^{t_2} = V_r^{t_2} \cdot \theta$$

where:

$V_{rb}^{t_2}$ = black unemployment rate in period t_2.

θ = ratio of black to total unemployment rate in period t_1.

(3b''') $$\Delta V_{rb}^{di} = V_{rb}^{t_2} - V_{rb}^{t_1}$$

where:

ΔV_{rb}^{di} = direct and induced change in black unemployment rate as a result of the military action.

POPULATION IMPACTS

(4) $$\Delta P = \Delta P_d + \Delta P_i$$

where:

ΔP = total change in population in ROI.

ΔP_d = direct population change in ROI related to military action.

ΔP_i = induced population change in ROI as a result of military action induced secondary employment expansion.

Solve for ΔP_d

$$\Delta P_d = R \times f_{hb}$$

where:

R = change in military employment opportunity due to the military action.

f_{hb} = average size of families of military personnel.

and

$$f_{hl} = \alpha_t f_t + \alpha_{hl} f_{hl} + \alpha_{mt} f_{mt} + \alpha_{mp} f_{mp}$$

where:

α_t α_{hl} α_{mp} and α_{mp} represent fraction of new positions (R) that will be filled by civilian transferees, civilians hired from outside ROI, military trainees and military permanent, whereas the f_i represent the fraction of the new positions to be filled by these respective subgroups.

Solve for ΔP_i

$$\Delta P_i = \frac{1}{\pi} \times \frac{1}{1-V_1^{t_1}} + \Delta E_t$$

where:

π = labor force participation rate in ROI.

$V_r^{t_1}$ = total unemployment rate in period t_1

and

π = E_{tt_1}/P_{tt_1}, i.e., total civilian employment/ total population ratio in period t_1.

or

$$\Delta P_i^* = \Delta\lambda L_{si}$$

where:

λ = median family size of net migrant stock entering ROI.

ΔL_{st} = induced expansion in size of labor force in ROI due to net migration (see equation (3)).

NOTE: ΔP_i^* should be close to ΔP_i and is presented only as a check on the internal accuracy of the projected employment, unemployment and population level impacts.

(4?) $$\dot{P} = \frac{\Delta P}{P}$$

where:

$\dot{P}$ = population growth rate due to the military action.

REGIONAL INCOME IMPACT

(5) $$Y_t = mw_{rs}X_1' + mw_{ws}X_2' + mw_{rs}X_3' + mw_v X_4' + \gamma X_5$$

where:

m = regional multiplier.

w_{rs} = average wage in retail and service sectors in period t.

w_{ws} = average wage in wholesale and service sectors in period t.

w_v = average wage in nation for all industries.

γ = fraction of output from new construction that goes to wages and income.

Y_t = total change in personal income in ROI due to the military action (constant dollars).

Let

$$X_1'' = w_{rs} X_1'$$

$$X_2'' = w_{vs} X_2'$$

$$X_3'' = w_{rs} X_3'$$

$$X_4'' = w_v X_4'$$

$$X_5'' = X_5'$$

then

$$Y_t = mX_1'' + mX_2'' + mX_3'' + mX_4'' + X_5''$$

(5') $$Y_i = Y_t - (X_1'' + X_2'' + X_3'' + X_4'' + X_5'')$$

where:

Y_i = induced change in total nonmilitary personal income as a result of the action.

*NOTE: Y_t and Y_i exclude total wages paid to military personnel as a result of the action.

(5'') $$\dot{Y}_t = \frac{\Delta Y_t}{Y_t}$$

where:

$\dot{Y}_t$ = rate of change in total personal income within ROI as a result of the military action.

<u>Calculations</u>

w_{rs} w_{rs} and w_v are in real terms; i.e., corrected for price changes over period difference inherent in using data sources available in different time periods.

PER CAPITA INCOME IMPACTS

(6) $$yt_2 = \frac{Y_t^{t_1} + \Delta Y_t^{t_1}}{P_t^{t_1} + \Delta P_t^{t_2}}$$

where:

Y_t = total regional personal income

$\Delta Y_t^{t_2}$ = change in total regional personal income over period t_1 to t_2.

$P_t^{t_1}$ = total regional population in period t_1

$\Delta P_t^{t_2}$ = change in regional population over periods t_1 to t_2.

yt_2 = per capita regional income in period t_2

(6') $$\Delta y = y^{t_2} - y^{t_1}$$

where:

y^{t_1} = regional per capita personal income in period t_1.

(6'') $$\dot{y} = \frac{\Delta y}{y^{t_1}}$$

where:

$\dot{y}$ = rate of change in regional/personal income as a result of the military action.

SECTION II

COMMUNITY IMPACT ASSESSMENT

Normally, the ROI will consist of a number of political subdivisions (counties, cities, villages and townships) as well as special districts (e.g., schools). The purpose of the subcomponent of SIAM is to relate impacts at the ROI level to the attributes of the various communities within the ROI. Population, school enrollments, total personal income and per capita changes are the "key indicators" of community (or micro) impacts in the model. The availability of land and local government growth policies are constraining forces in the analysis.

POPULATION

<u>No Constraints to Growth</u>:

(7) $$\Delta P_{tj} = \Delta P_{ij} + \Delta P_{dj}$$

where:

ΔP_{tj} = total change in population of the j^{th} community as a result of the military action.

ΔP_{ij} = induced population change in the j^{th} community as a result of the military action.

ΔP_{dj} = direct population change in the j^{th} community as a result of the military action.

Solve for ΔP_{ij}

$$\Delta P_{ij} = c_j \Delta P_i$$

where:

$c_j = P_j / P_t$

and

c_j = proportion of ROI population residing in j^{th} community in period t_1.

P_j = population level of community j in period t_1.

P_t = population level of ROI in period t_1.

Identities:

Σc_j = 1, over n communities in ROI.

$\Delta P_i = \Sigma P_{ij}$, over n communities in ROI.

where:

ΔP_i = induced population change in ROI as a result of the action.

Solve for ΔP_{dj}

$$\Delta P_{dj} = z_j \, \Delta P_d$$

where:

z_j = proportion of j^{th} community population directly associated with the military establishment residing in community j.

ΔP_d = direct change in population in ROI as a result of the military action.

and

$z_j = P_{mj}/P_t$

where:

P_{mj} = number of persons in community j who are directly related to employees of military establishment in ROI.

P_t = total military related population in ROI at period t_1.

and

$$P_{mj} = R_j \times f^j_{hb}$$

where:

R_j = number of military personnel residing in j^{th} community.

f^j_{hb} = average family size of military families residing in j^{th} community.

and

$$P_t = R \times f_{hb}$$

where:

R = number of positions at military establishment in ROI.

f_{hb} = average family size of military families.

<u>Constraints to growth</u>:

(7') Let $P^*_{t_2}$ = maximum obtainable population level for j^{th} community because of physical (e.g., level area) or political (e.g., local growth policies) constraints to growth.

If $P_{tj} + \Delta P_{tj} < P^*_{tj}$, then community j can absorb the projected population change associated with the action.

If $P_{tj} + \Delta P_{tj} > P_{tj}$, solve for

$$\Delta P'_{tj} = \Delta P_{tj} - (P^*_{tj} - P_{tj})$$

Next, allocate $\Delta P'_{ti}$ among the other n-k communities in a manner similar to the procedures presented in equation (7)*.

NOTE: * Changes in population at the community level cannot be mechanically projected as equations (7) and (7') may imply. The analyst should consult with local builders and planners to get a better understanding of development patterns within the ROI. When local, perceived development patterns significantly diverge from the projected patterns, ad hoc adjustments to the projected patterns may be in order.

SCHOOL ENROLLMENTS

The following analysis assumes that school district and community boundaries are coterminous. In cases where school districts encompass more than one community, the appropriate adjustments must be made.

(8) $$\Delta S = n\Delta P_{dj} + r\Delta P_{ij}$$

where:

ΔS = total change in school enrollments in community j.

n = proportion of population in community j directly related to the military action of school age.

r = proportion of induced population change in community j of school age.

(8') $$\Delta S_e = b\Delta S$$

where:

ΔS_e = change in elementary school enrollment.

b = fraction of school age children entering j^{th} community who will enroll in elementary school.

(8'') $$\Delta S_h = \Delta S - \Delta S_e$$

where:

ΔS_h = change in high school and junior high school enrollments.

(10')
$$\Delta y_j = y_{jt_2} - y_{jt_1}$$

(10'')
$$\dot{y}_j = \Delta y_j / y_{jt_1}$$

where:

Δy_j = absolute change in per capita income in community j as a result of the action.

$\dot{y}_j$ = rate of changes in per capita income in community j resulting from the action.

SECTION III

SUMMARY AND CONCLUSIONS

A model for predicting the impact of changes in the level of military activities (base closures and realignments) was presented. The model provided equations for predicting changes in output, employment, income, population and per capita income at the ROI level. It also contained algorithms which disaggregate changes in population and income at the ROI level to the various communities within the ROI. These allocations are influenced by local constraints to growth, such as the availability of land and community attitudes toward growth. Changes in school enrollments and per capita income are also predicted at the local level.

The model outlined in the preceding pages has a number of deficiencies, notably the absence of algorithms for measuring derived impacts on key institutions within the ROI, such as local governments and financial institutions. Also, questions concerning the choice of procedures to estimate the multiplier and threshold values were not addressed, and the procedures for estimating the parameters in the model are too simplistic. Parameterizing a model is a complex process which must be done on a case by case basis. Finally, the equations set forth in the paper are only guidelines for measuring community impacts; they are not ironclad rules which must be applied irrespective of the circumstances.

1978 USAF-ASEE SUMMMER FACULTY RESEARCH PROGRAM

Sponsored by

THE AIR FORCE OFFICE OF SCIENTIFIC RESEARCH

Conducted by

AUBURN UNIVERSITY AND OHIO STATE UNIVERSITY

PARTICIPANT'S FINAL REPORT

DEVELOPMENT AND IMPLEMENTATION OF THE ENVIRONMENTAL TECHNICAL INFORMATION SYSTEM FOR AIR FORCE USE

Prepared by:	Jay R. Sculley Ph.D., P.E.
Academic Rank:	Associate Professor
Department and University:	Department of Civil Engineering Virginia Military Institute
Assignment:	Tyndall AFB Air Force Civil Engineering Center Environmental Protection Planning
USAF Research Colleague:	John E. Palmer
Date:	11 August 1978
Contract No. :	F44620-75-C-0031

DEVELOPMENT AND IMPLEMENTATION OF
THE ENVIRONMENTAL TECHNICAL INFORMATION SYSTEM
FOR AIR FORCE USE

by

J. R. Sculley

ABSTRACT

The Environmental Technical Information System (ETIS) was developed to assist the Department of the Army (DA) in complying with NEPA and AR 200-1. The entire system has been in development for approximately five years with three subsystems currently ready for field implementation. The Air Force has been investigating and supporting the modification of ETIS to suit Air Force specific requirements through the expenditure of R&D funds. Pilot testing has been concluded with the recommendation that ETIS be implemented as an Air Force-wide tool for environmental analysis. Its use is required by AFR 19-2. ETIS has been undergoing pilot usage for approximately two years on the R&D machine upon which they were developed. This machine supports the UNIX operating system and C language. The current version of ETIS represented is an optimal application of recent minicomputer technology to the solution of complex data analysis and management problems.

ACKNOWLEDGMENT

The author is grateful to the Air Force Systems Command for support of this summer research. Thanks are due Mr. J. Fred O'Brien of Auburn University for his enthusiastic and excellent administrative support.

The author is indebted to the Environmental Protection Planning Division of the Air Force Civil Engineering Center for providing a most pleasant work environment. The professionalism exhibited by these extremely capable people is gratifying and reassuring. Special thanks are due Lt Col Sterling E. Schultz, Mr John E. Palmer, Captain Ron Hawkins and Mr W. Allen Nixon for their guidance, encouragement and assistance.

I also wish to express my thanks to Mr Ron Webster and Ms Brenda Griffin of the US Army Construction Engineering Research Laboratory for their invaluable assistance in the preparation of the Data Automation Requirement.

INTRODUCTION:

Section 102(2)(C) of the National Environmental Policy Act (NEPA) forms the legislative basis for preparing environmental impact assessments (EIA) and statements (EIS) for federal actions expected to have significant impact on the quality of the environment and for those actions whose impacts are likely to be controversial.

The assessment and statement differ in purpose and use. The EIA is to provide a basis for intra-agency review of an actions impacts and in turn provide necessary information as to whether an EIS should be prepared.

The CEQ has periodically issued guidelines to assist federal agencies in the preparation of environmental impact statements[1,2]. In addition, executive orders, Department of Defense directives, and Air Force regulations have further delineated guidelines for EIS preparation[3,4,5,6,7]. These documents stress policies and procedures but give little assistance how to carry out that analysis.

Since 1969, many methodologies have been developed to assist the preparer of environmental impact assessments/statements fully respond to Council on Environmental Quality (CEQ) guidelines for EIA/EIS content. A review and analysis of these methodologies has been prepared by the Construction Engineering Research Laboratory (CERL)[8]. A listing and summary of evaluations can be found in appendix A.

Since 1971 the United States Army Construction Engineering Research Laboratory has spent approximately 3.5 million dollars on the development of ETIS. In addition the Air Force has invested $225 thousand to tailor ETIS for its use. Air Force use to date has been almost exclusively in the Environmental Impact Analysis Process. Currently ETIS consists of three major interactive computer programs: CELDS, Computer-aided Environmental Legislative Data System; EICS, Environmental Impact Computer System; and EIFS, Economic Impact Forecast System. The component subsystems of ETIS are briefly described in appendix B.

In the professional opinion of the author, the Environmental Technical Information System (ETIS) is the best system developed to date to provide Air Force users with the capability of meeting the objectives of the Environmental Impact Analysis Process (EIAP). This process is clearly defined in the Handbook for Environmental Impact Analysis: Interim Environmental Planning Bulletin 11, Department of the Air Force, Washington, D.C. (June 1976).

Of primary concern to the Air Force is to keep ETIS "on-line." Currently, ETIS is maintained for CERL by the Center for Advanced Computer Studies at the University of Illinois-Urbana on a Digital Equipment Corporation PDP 11/50 and run under the UNIX system. The Center for Advanced Computer Studies is scheduled to be dissolved during early CY79. Not only will the hardware be unavailable after that time, the major portion of programming support given CERL by University of Illinois graduate students will be no longer available.

Further complicating the situation are directives to CERL from the office of the Chief of Engineers, US Army stating that CERL will concentrate its efforts in the area of research and not in development and operations.

In view of these circumstances, the Air Force must take action to assure itself that ETIS remains operable. The initial step is to prepare a Data Automation Requirement (DAR) in accordance with AFR 300-12. DARs for AFCEC are submitted through AFESC to HQ USAF/ACD.

OBJECTIVES:

The major thrust of this research has been to provide the Air Force with the documented justification required to obtain the necessary hardware to support ETIS. The justification has been developed and incorporated in a DAR.[9] The following is a detailed summary from the DAR.

The previous methodology for the preparation of environmental analyses was ad hoc in nature, depending upon a combination of contractor support, conjecture, and "best guess" analysis. No methodology existed which insured consistent, uniform, and reliable analyses. The Environmental Technical Information System (ETIS) was developed to insure such a process utilizing recent computer methodologies to supply data, models, and analyses to DOD environmental planners. Without ETIS, environmental analyses would suffer from several deficiencies:

a. No "institutional learning" aspect would be available to new analysts.

b. All studies would be ad hoc with no uniform approach or scoping mechanism.

c. Costs of analyses would be considerably higher, as data acquisition would also be ad hoc.

The ETIS concept revolves around the storage and retrieval of environmental planning data from a centralized computer system interactively servicing USAF users via acoustically-coupled portable terminals using a combination of types of phone lines (toll free, foreign exchange, commercial, and FTS). The subject information includes biophysical and socioeconomic baseline data, abstracts of laws and regulations, model analyses and other environmentally related data.

The objective of ETIS is to provide appropriate data and analyses to the environmental planner through immediate interactive requests by the user. The basic assumption having bearing upon these analyses is that the need for adequate analyses will increase as CEQ and subsequent Air Force regulations become more stringent. The resources available for these required analyses, particularly permanent manpower allocations, will remain critically short, allowing little time for analyses, even with systematic aids. In addition, it should be remembered, that for ETIS to be effective it must possess the attributes of simplicity of use, quick response, thoroughness, easy access, and be inexpensive.

ALTERNATIVES:

The alternatives considered for ETIS implementation are as follows:

(1) Commercial large mainframe

(2) Commercial minicomputer

(3) Commercial minicomputer in C

(4) Government large mainframe

(5) Government minicomputer

(6) Government minicomputer in C

(7) Augmented Air Force hardware in C

Due to the peculiar mixture of computational requirements with large data base manipulations, the use of a non-standard high level language designed specifically for problems such as the ETIS system is considered.

The current R&D version of ETIS is programmed in C language using the UNIX operating system. Appendix C lists many characteristics and advantages of UNIX. The system has proven to be an extremely cost effective and responsive system for the developmental system and pilot testing. It will be used for the evaluation of alternatives 3 and 6.

An additional alternative involves the implementation of ETIS on Air Force hardware using UNIX. Augmentation of an existing system (communications, a larger processor, and additional disk) is analyzed as alternative 7.

COSTS:

Costs for the various alternatives have been aggregated into four major categories: (1) conversion, (2) contract and administration, (3) communications, and (4) operation and maintenance.

The major factor affecting conversion costs is the language. Estimates provided by the Center for Advanced Computation, University of Illinois-Urbana indicate that the conversion from C to FORTRAN would cost $120,000 and to COBOL nearly twice that amount. Conversion to FORTRAN costs are used in the analysis. Contract and administration costs not only include the writing and award of contracts but reporting, materials and supplies.

Communications are anticipated to be a mixture of user supported communication and special FEX and WATS requirements. Hardware at the site should be approximately $10,000 per year to cover maintenance and upkeep of modems, etc. Additionally, 3 FEX lines at $500 per month each and 2 incoming band-5 WATS lines at $850 per month each would be required. This represents a communication cost of $38,400 per year. This will be considered essentially the same for all alternatives. It should be noted that whereas CERL experience with FTS has been satisfactory, experience with AUTOVON has been unsatisfactory.

Operation and Maintenance costs calculations (Table 1) differ between commerical alternatives (alternatives 1, 2, and 3) and government alternatives (alternatives 4, 5, 6 and 7). In the commercial alternatives, operation and maintenance costs are primarily a function of connect time (usage) and storage (data base size). The estimates provided by CERL reflect current usage, anticipated ETIS development and, projected use. Similarly calculations for alternative 4, government large mainframe are based on charges by NSDRC as a function of storage and connect time.

Government minicomputer maintenance costs for alternatives 5, 6 and 7 are based on CERL estimates of $13,500/year. Operational costs for alternatives 5 and 6 were calculated using Table 2 and amortizing the initial investment of $211,452 in five years. For alternative 7 an initial cost of $100,000 was estimated to upgrade an existing 11/35 to an 11/70.

Table 3 summarizes the estimated costs for the seven alternatives. It is clear from the analysis that the least cost alternative is alternative 7, augmentation of existing Air Force hardware. In the event that suitable hardware is not available for augmentation, then the next best alternative is alternative 6, government purchase of the PDP 11/70 configuration listed in Table 2.

Table 1
OPERATION AND MAINTENANCE COSTS
FOR SELECTED ALTERNATIVES

Yr	Connect Time (Hrs)	Disk (mb)	Alternative 1 Commercial Large Mainframe [1]				Alternative 2 & 3 Commercial Mini[2]	Alternative 4 Government Large Mainframe NSRDC[3]
			ADP	Litton	GE	UCS		
1	2100	50	40,500	38,793	73,401	99,588	42,000	55,968
2	3737	100	76,833	64,322	195,731	195,280	74,740	110,772
3	5375	150	97,267	94,526	290,139	290,985	107,500	165,582
4	7012	200	149,508	124,721	384,532	386,680	140,240	220,390
5	8650	250	185,850	154,926	478,941	482,385	173,000	275,200
6	8650	250	185,850	154,926	478,941	482,385	173,000	275,200

1 Based upon GSA published rates applied to the projected system loading

2 Based upon UNIX and adding additional overhead (figured at $20 per connect hour)

3 Based upon previous ETIS use of Naval Ship Research and Development Center Computer

Table 2
11/70 CONFIGURATION

11/70 VA CPU with 64 KWA Core	$60,000
FP-70-CU Floating Point Processor	6,800
MJ11-BE Additional 64KW Core	11,000
2RWPO4AA 88 MB Disk and Controller @ 35,000	70,000
RJ11JAA 2.4 MB Disk and Controller	9,900
3 RK05J-AAs 3 additional 2.4 MB Disks	15,300
TMB 11-EA Tape Drive and Controller	12,075
TU10W-EE Tape Drive	8,400
DH11-AD 16 Line Asynch Multiplexor	6,000
BC-5D-25 Cables	1,920
LP11-WA 230 lpm Printer	13,375
Disk Packs	
	216,470
8% disc on all except RWP04	-11,718
	204,752
UNIX License	6,700
	$211,452
	or $42,290/yr.

Table 3
ETIS COSTS IN $(000)/YR

ALTERNATIVE	CONVERSION * TOTAL	CONVERSION * ANNUAL	ANNUAL CONTRACT * ADMINISTRATION	ANNUAL COMMUNICATION	MEAN ANNUAL O&M	ANNUAL TOTAL
1 Commercial Large Mainframe (Litton)	120	[illegible]	6	38	95	163
2 Commercial Minicomputer	120	24	6	38	107	175
3 Commercial Minicomputer in C	10	2	10	38	107	157
4 Government Large Mainframe	120	24	4	33	[illegible]	231
5 Government Minicomputer	120	24	10	38	58	130
6 Government Minicomputer in C	10	2	10	38	58	108
7 Augmented Air Force Hardware in C	10	[illegible]	4	38	34	76

* Estimates by Center for Advanced Computation
University of Illinois - Urbana

CONCLUSIONS AND RECOMMENDATIONS:

ETIS represents the best technology available for Air Force use in the Environmental Impact Analysis Process. The Air Force should continue to require its use. With the loss of current hardware support scheduled for FY79 and U.S. Army intentions unclear, the Air Force should take immediate steps to assure that ETIS will remain "on-line" without interruption.

The evaluation of implementation alternatives shows that implementation of ETIS on an Air Force minicomputer under the UNIX system is the cost effective choice.

Suggested steps and target dates for implementation on an Air Force minicomputer are as follows:

(1) Coordinate draft DAR within AFCEC by 18 Aug 78.

(2) Send DAR to AFDSDC for comments by 25 Aug 78.

(3) Brief Commander AFCEC by 1 Sept 78.

(4) Submit DAR to HQ USAF/ACD by 15 Sept 78.

It is further recommended that the ADP program single manager for AFESC maintain close communications with HQ USAF/ACD with follow-up actions as required to prevent unnecessary delays in gaining approval. AFDSDC has indicated hardware delivery times ranging from 90 to 130 days. With June 79 the target date for implementation it is imperative that the recommended schedule be closely followed.

ETIS development and expansion should continue during implementation and beyond. The major thrust should be in the preparation base-line data bases for use in comprehensive planning and resource allocation. Continued cooperation with CERL and additional cooperation with universities and other government agencies is recommended for model development and data source identification.

Additionally it is recommended that AFCEC obtain the services of a computer scientist/systems analyst and two (2) programmers for ETIS development.

REFERENCES

1 "Preparation of Environmental Impact Statements: Guidelines," Federal Register, Vol 38, No. 147, Part II (August 1, 1973), pp 20550 - 20562.

2 Council on Environmental Quality Memorandum dated 10 February, 1976.

3 Executive Order 11752, "Prevention, Control, and Abatement of Air and Water Pollution at Federal Facilities," 17 December 1973.

4 Executive Order 11514, "Protection and Enhancement of Environmental Quality," 5 March 1970.

5 Department of Defense Directive 6050.1, "Environmental Considerations in DOD Actions," 19 March 1974.

6 Air Force Regulation (AFR) 19-1, "Pollution Abatement and Environmental Quality," 20 February 1974.

7 Air Force Regulation (AFR) 19-2, "Environmental Assessments and Statements," 22 November 1974.

8 Jain, R.K. and L.V. Urban, A Review and Analysis of Environmental Impact Assessment Methodologies, Technical Report E-69 (Construction Engineering Research Laboratory (CERL), June 1975

9 "Justification For Using Minicomputer Facilities for the Environmental Technical Information System," Data Automation Requirement (DRAFT), Air Force Civil Engineering Center, Tyndall AFB, FL, August 1978.

APPENDIX A: ENVIRONMENTAL IMPACT ASSESSMENT METHODOLOGIES

Adkins, William G. and Burke Dock, Jr., Interim Report; Social, Economic, and Environmental Factors in Highway Decision Making. Research conducted for the Texas Highway Department in cooperation with the U.S. Department of Transportaion, Federal Highway Administration (Texas Transportation Institute, Texas A & M University, October 1971).

Dee, Norbert, et al, Environmental Evaluation System for Water Resources Planning, report to the U. S. Bureau of Reclamation (Battelle Memorial Institute, January 1972).

Dee, Norbert, et al, Planning Methodology for Water Quality Management: Environmental Evaluation System (Battelle Memorial Insitiute, July 1973).

The Environmental Assessment Notebook Series prepared for the U. S. Department of Transportation, (National Technical Information Service, Springfield, Va., 1975.)

Environmental Resources Management, prepared for the Department of Housing and Urban Development (Central New York Regional Planning and Development Board, October 1972).

Jain, R. K., et al, Environmental Impact Assessment Study for Army Military Programs, Interim Report D-13/AD771062 (U. S. Army Construction Engineering Research Laboratory (CERL), December 1973.

Jain, R. K., et al, Handbook for Environmental Impact Analysis, Technical Report E-59/ADA006241 (CERL, September 1974).

Jain, R. K. et al, A Review and Analysis of Environmental Impact Assessment Methodologies, Technical Report E-69 (CERL, June 1975).

Krauskopf, Thomas M. and Dennis C. Bunde, Evaluation of Environmental Impact Through a Computer Modelling Process, Environmental Impact Analysis: Philosophy and Methods, Robert Ditton and Thomas Goodale, eds. (University of Wisconsin Sea Grant Program, 1972), pp 107 - 125.

Transportation and Environment: Synthesis for Action: Impact of National Environmental Policy Act of 1969 on the Department of Transportation, Vol 3, prepared for Office of the Secretary, Department of Transportation (Arthur D. Little, Inc., July 1971).

Urban, L. V., et al, User Manual - Computer-Aided Environmental Impact Analysis for Construction Activities, Technical Report E-50 (CERL, March 1975).

Walton, L. Ellis, Jr. and James E. Lewis, A Manual for Conducting Environmental Impact Studies (Virginia Highway Research Council, January 1971).

Warner, M. L. and E. H. Preston, A Review of Environmental Protection Impact Assessment Methodologies (U. S. Environmental Protection Agency, April 1974).

APPENDIX B: ETIS SUBYSTEMS

The Environmental Impact Computer System (EICS) is a matrix approach relating Air Force activities to potential impacts on environmental attributes or characteristics. The user is provided a tailored matrix depending upon inputs interactively provided in answer to specific filter questions.

The Computer-aided Environmental Legislative Data System (CELDS) provides abstracts of state and federal legislation and regulations depending upon multiple keyword criteria interactively provided by the user.

The Economic Impact Forecast System (EIFS) provides baseline data and socioeconomic predictions for any multicounty region in the US as defined by the user.

The Clearinghouse Information System (CHIS) provides points of contact for local governmental coordination as directed by OMB Cir A-95 subject to user provision of geographic designation.

The Baseline Information System (BLIS) is still under development and is intended to provide points of contact for environmental data for assistance in analyzing potential impacts as defined by EICS.

The Interagency Intergovernmental Coordination of Environmental Programs System (IICEPS) identifies pertinent state agencies with which coordination in certain major environmental categories is required by Air Force direction.

The Land Use Compendium (LUC) identifies points of contact at agencies having designated categorical land use control responsibilities at a state level.

Several systems and models are envisioned for future ETIS inclusion. These other systems will be similar in orientation, directly related to base and MAJCOM environmental planning. Some will be in direct response to new regulations requiring scoping processes which are being implemented by the President's Council on Environmental Quality (CEQ).

APPENDIX C: CHARACTERISTICS AND ADVANTAGES OF UNIX AND C-LANUGAGE

- UNIX allows multiple interactive users all utilizing the same data concurrently.

- The interactive system supports initiation and access of data files by the user program, without the use of control commands external to the user program, and the typical response time for trivial requests is less than 5 seconds.

- UNIX allows single disk file up to 15 megabytes.

- UNIX has the ability to execute system commands from inside user programs.

- UNIX permits parallel processes. A program may have other processes working for it simultaneously.

- UNIX supports hierarchical directory/file structure. Data may be grouped and organized into directories with an arbitrary number of subdirectories. This is automatic, free, requiring no programming or knowledge of the system. No frustration.

- UNIX files themselves contain no structure whatsoever. Each file is simply an ordered set of characters. (A "new line" is *simply another character*, just like any other, it merely happens to print "funny.") This means that there are no restrictions on the size or the contents of files. This concept makes data bases with variable length records throughout easy to handle.

- Shell files (i.e., command files) may be created and executed. There is complete transparency between shell files or executable code. This means that there is no disruption switching back and forth between interpreted and compiled code.

- UNIX provides simple input and output switching as well as pipes and filters. This means that any process (be it a command file, or executable code) may serve as a filter for some other process and may "pipe" the output to another process or even to many processes simultaneously.

- All peripherals are treated as files, so diverting output to and from peripherals is simple. Also, this means that adding a peripheral is trivial, amounting to no more that writing a driver for it.

- UNIX has a powerful text editor and many tools for manipulating lines of text. With the use of these tools and the editor, many applications of data management require absolutely no programming whatsoever.

- UNIX has excellent inter-terminal communications. Again,

since terminals look like files to UNIX, writing to them, allowing users to communicate with each other, is a trivial matter. Also, UNIX provides an excellent "mail" facility for users not logged in or permanent records. Each user has a "mailbox" file which is checked in at log-in time (or whenever the user pleases).

- The UNIX environment encourages "software tool building." Any procedures written can be strung together with other procedures easily, or used as filters, to produce new procedures.

- UNIX has an excellent document formatter (text-processing) and phototypesetter.

In short, UNIX is the kind of environment to provide the flexibility necessary in a research organization. Some of the features are unmatched elsewhere, let alone on a single system. Modifications to software or hardware can be made with a minimum hassle. New areas and application are continually being made available. Currently, at least two smaller versions of UNIX have been implemented on microprocessors. For a more descriptive discussion of UNIX features and advantages, the following references are offered.

Ivie, I. L., The Programmers Workbench - A Machine for Software Development, Communications of the Association for Computing Machinery, Vol. 20, No. 10, October 1977.

Kernighan, B. W., A Tutorial Introduction to the UNIX Text Editor, Internal Memorandum, Bell Laboratories, Murray Hill, N.J.

________________, Programming in C - A Tutorial, Internal Memorandum, Bell Laboratories, Murray Hill, N.J.

Madden, J. G., C: A Language for Microprocessors? BYTES, Date Unknown.

Ritchie, D. M. and Ken Thompson, The UNIX Timesharing System, Communications of the Association for Computing Machinery, Vol. 17, No. 7 July 1974.

______________ UNIX Programmers' Manual Bell Laboratories, Murray Hill, N.J.

Stiefel, M.L., UNIX, Mini Micro Systems, April 1978.

1978 USAF-ASEE Summer Faculty Research Program
sponsored by
The Air Force Office of Scientific Research
conducted by
Auburn University and Ohio State University

Participant's Final Report

Adaptively-predictive Linear Optimal Guidance:
Target Seeking

Prepared by:	Robert L. Carroll, Ph.D.
Academic Rank	Associate Professor
Dept. and University	Electrical & Computer Engineering University of South Carolina Columbia, S.C. 29208
Assignment:	Eglin Air Force Base Armament Lab - DLMA
USAF Research Colleague:	Lieutenant Tom L. Riggs, Jr.

Date:	July 29, 1978
Contract No.:	F44620-75-C-0031

ADAPTIVELY-PREDICTIVE LINEAR OPTIMAL GUIDANCE

TARGET SEEKING

BY

ROBERT L. CARROLL

Research into guidance laws of target seeking devices (e.g. air-to-air missiles) is undertaken in this report. The objective is to find a linear-quadratic-martingale control law which takes into account the target maneuvering and the longitudinal thrust constraint of the system. A proof indicating improved performance is given. Simulation results in two dimensions is exhibited.

ACKNOWLEDGEMENT

The author is grateful to the Air Force for support of this summer research. The ASEE and its summer program administrator, Mr. Fred O'Brien, deserve especial thanks for their efforts.

It has been a pleasure working in the Air Force Armament Laboratory at Eglin Air Force Base. I wish to express thanks to Dr. O. Charles Williams, Mr. Jesse M. Gonzalez and, in particular, my research colleagues, Lieutenant Tom Riggs and Major Jim Anderson, for providing a cordial environment and helpful suggestion during the period of this research.

The excellent typing by Ms Georgia Carter is appreciated.

Introduction

Control of target seeking devices (e.g., air-to-air missiles) has traditionally been accomplished by guidance laws synthesized by optimal control formulations subjected to restrictive assumptions. Such assumptions have been imposed mainly to cause the resulting guidance law to be computationally brief. For example, the model of the target chase is chosen linear (ignoring aerodynamics of the missile and target), the target is assumed to have constant velocity (non-maneuvering), the missile is assumed completely controllable, and the target and missile are assumed to be in a fixed relative orientation. To some extent, non-linearity in the target seeking device is accounted for by introduction of another, independently-designed, control system known as an adaptive autopilot.

Dissatisfaction with traditional control systems is that the closest launch distance to the target required to achieve an interception is perceived to be excessive.

Investigation is presently being conducted by the Guided Weapons Division, Systems Analysis & Simulation Branch, Air Force Armament Laboratory to achieve a more satisfactory control system, including alternative guidance laws and estimation algorithms. At issues are the assumptions made in the formation of control and estimation algorithms, alternative approaches to synthesis of control and estimation algorithms, and the heuristic sectioning of the control systems design into independent tasks, or loops.

Two limitations of previous control formulations were considered for improvement during the 10-week research term of the author. These are the lack of knowledge of a maneuvering target and the lack of complete controllability of the missile. An attempt was made to include knowledge of target maneuvering into the control law, and to formulate the control law so that control commands exist only in the controllable subspace of the system. Since the design assumed a noisy environment, theoretical analysis was made to examine the quality of the performance (by means of the Kolmogorov equation and invariant-imbedding), and computer simulation was made to determine the closest launch distance permitted, depending upon the initial missile-target orientation, for the control laws synthesized. These topics are expanded upon in the next sections of this report.

Formulation of Target-seeking Model

Consider a point-mass target and seeker in fixed axes (shown in two dimensions in Fig. 1). The vector $\underline{S}$ represents the separation between the missile and target, while $\underline{a}^t$ and $\underline{a}^m$ represent vectors of acceleration for target and for missile. The vectors $\underline{S}$, $\underline{a}^t$, and $\underline{a}^m$ are assumed to have representation according to mutually orthonormal bases having a known origin ($\underline{X}_1$ and $\underline{X}_2$ shown in Fig. 1).

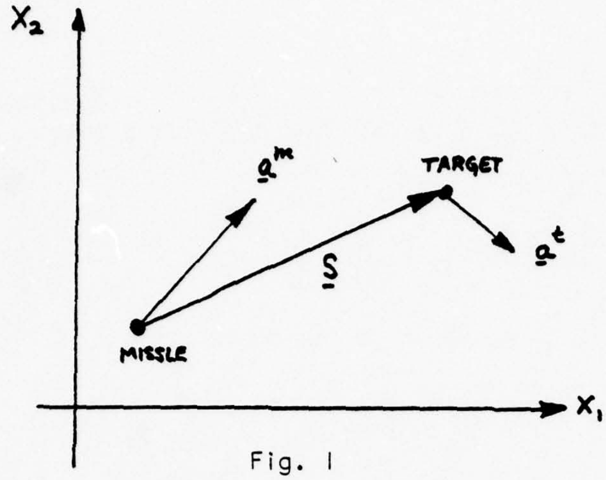

Fig. 1

The target-seeker dynamic model may be written

$$\frac{d}{dt}\begin{bmatrix}\underline{S}\\ \dot{\underline{S}}\end{bmatrix} = \begin{bmatrix}0 & I\\ 0 & 0\end{bmatrix}\begin{bmatrix}\underline{S}\\ \dot{\underline{S}}\end{bmatrix} + \begin{bmatrix}0\\ I\end{bmatrix}(\underline{a}^{t} - \underline{a}^{m}) \qquad (1)$$

wherein $\dot{\underline{S}} = \frac{d}{dt}\underline{S}$. The model whose behavior is described by (1) is a particularly simple, yet desirable, formulation from a conceptual viewpoint, since it is linear and time invariant; it is well-known that such problems are readily ameniable to feedback control. The more obvious limitations of (1) are the difficulty in measuring $\underline{S}$ and $\dot{\underline{S}}$ from a missile, the lack of a description of aerodynamic effects, and the uncertainty of the representation of all vectors in inertial coordinate axes. Of particular distress is the presence of the term $\underline{a}^{t}$, the target acceleration vector, since it is not directly accessible either before or during system operation.

Previous attempts at controlling a missile-target system have generally utilized the model or (1) by assuming that $\underline{a}^{t} = 0$ (or, in more advanced efforts, that $E[\underline{a}^{t}] = 0$) and that $\underline{S}$, $\dot{\underline{S}}$ are adequately approximated by measureable quantities (perhaps by an optimal observer).

Another limitation is that the missile acceleration $\underline{a}^{m}$, which is to be controlled, cannot be oriented at will due to the lack of a throttle control (i.e., the acceleration directed along the missile velocity vector is specified, subject to aerodynamic forces, solely by the engine thrust). The control law should, therefore, produce an acceleration command at all times perpendicular to the missile velocity vector, which is a controlled vector.

For purpose of this study, the following model is chosen

$$\dot{x} = \begin{bmatrix}0 & I & 0\\ 0 & 0 & 0\\ 0 & 0 & 0\end{bmatrix} x + \begin{bmatrix}0\\ -I\\ I\end{bmatrix} u + \begin{bmatrix}0\\ I\\ 0\end{bmatrix} v + \begin{bmatrix}0\\ -I\\ I\end{bmatrix} w \qquad (2)$$

where $x = [\underline{S}^T, \dot{\underline{S}}^T, v^{mT}]^T$, $v = \underline{a}^T$, u = control, and w = thrust acceleration of the missile. The controlled quantity is the response vector

$$r = Hx + Du = \begin{bmatrix} I & 0 & 0 \\ 0 & 0 & I \\ 0 & 0 & 0 \end{bmatrix} x + \begin{bmatrix} 0 \\ 0 \\ I \end{bmatrix} u = \begin{bmatrix} \underline{S} \\ \underline{v}^m \\ \underline{u} \end{bmatrix} \qquad (3)$$

Control of the response vector is achieved by minimizing the scalar quantity

$$J = \frac{1}{2} x^T S x \Big|_{t=t_f} + \frac{1}{2} \int_0^{tf} r^T Q r \, dt \qquad (4)$$

where $$x^T S x = x^T \begin{bmatrix} S_1 & 0 & 0 \\ 0 & 0 & 0 \\ 0 & 0 & 0 \end{bmatrix} x = \underline{S}^T S_1 \underline{S}.$$

and $$r^T Q r = r^T \begin{bmatrix} 0 & 0 & 0 \\ 0 & 0 & Q_6 \\ 0 & Q_6^T & Q_7 \end{bmatrix} r = 2 v_m^T Q_6 u + u^T Q_7 u$$

The rationale for choice of (4) is that the term $v_m^T u$ is the projection of commanded acceleration onto the missile velocity vector; this quantity must be zero. It was hoped at the beginning of this research that by choosing $Q_6 = q_6 I$ so that $q_6 \to \infty$, the control law u which minimizes (4) would have zero component along v_m, as required. This was subsequently found not to occur, so that a more conventional technique was eventually implemented. Nevertheless, the ~~term~~ $v_m^T u$ is retained in the control law.

The control law is derived as follows from the calculus of variation [1].

$$J = \tfrac{1}{2} x^T S x \Big|_{t=t_f} + \frac{1}{2} \int_0^{t_f} [u^T D^T Q D + 2u^T D^T Q H + x^T H^T Q H x + 2\lambda^T (Ax+Bu+Cy-\dot{x})] \, dt$$

$$= \frac{1}{2} (x^T S x - 2\lambda^T x) \Big|_{t=t_f} + \lambda^T x \Big|_{t=0} + \frac{1}{2} \int_0^{tf} [u^T D^T Q D u + 2u^T D^T Q H x + x^T H^T Q H x + 2\lambda^T (Ax+Bu+Cy) + 2\dot{\lambda}^T x] dt$$

Applying the Euler-Lagrange equation,

$$u = -(D^T Q D)^{-1} D^T Q H x - (D^T Q D) B^T \lambda$$
$$\dot{x} = [A - B(D^T Q D)^{-1} D^T Q H] x - B(D^T Q D)^{-1} B^T \lambda + Cy \qquad (5)$$
$$\dot{\lambda} = [H^T Q D (D^T Q D)^{-1} D^T Q H - H^T Q H] x - [A^T - H^T Q D (D^T Q D)^{-1} B^T] \lambda$$

Let $\hat{A} \equiv A - B(D^TQD)^{-1}(D^TQH)$

$\hat{B} \equiv B(D^TQD)^{-1}B^T$

$\hat{D} \equiv H^TQD(D^TQD)^{-1}D^TQH - H^TQH$

Then (5) becomes

$$\dot{x} = \hat{A}x - \hat{B}\lambda + Cy \qquad x(t_0) = x^0$$

$$\dot{\lambda} = \hat{D}x - \hat{A}^T\lambda \qquad \lambda(t_f) = Sx(t_f) \qquad (6)$$

Assuming $\lambda = Px + \eta$, then (6) is solved by $u = -(D^TQD)^{-1}(D^TQH + B^TP)x - (D^TQD)^{-1}B^T\eta$

where $\dot{P} = -P\hat{A} - \hat{A}^TP + \hat{D} + P\hat{B}P \qquad P(t_f) = S$

$\dot{\eta} = -(\hat{A} - \hat{B}P)^T\eta - PCy \qquad \eta(t_f) = 0$

The use of (7) is illustrated in Fig. 2

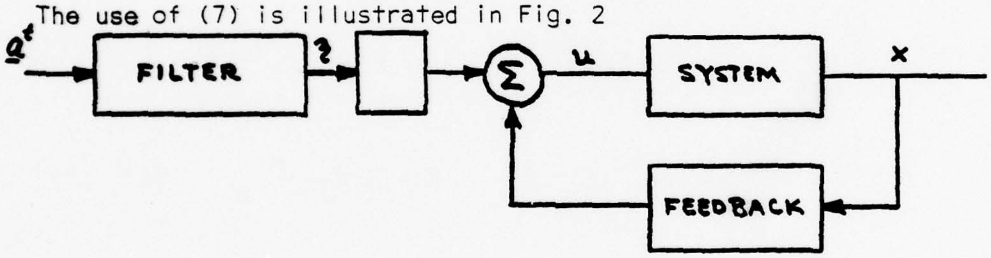

The target acceleration must be estimated, then low-pass filtered, to become part of the command acceleration. The feedback offers additional control.

The boundary condition placed upon the filter equation necessitates the estimation on the target acceleration for beginning until the end of the flight trajectory. It is assumed that, by observation of the target behavior from the initial time to the present time, an estimate can be produced from the present time until the terminal time. No work was undertaken to determine the properties of such an estimator. The estimate may be updated as often as desired, to allow a more accurate computation of η to be produced. The final time estimate is produced at any prior time by

$$t_f = \frac{|\underline{S}|}{|\dot{S}|} \qquad (8)$$

The advantage of choosing the linear model of the target-missile system is that the matrix Ricatti equation may be analytically solved. The equation

$$\dot{P} + P\hat{A} + \hat{A}^T P - \hat{D} - P\hat{B}P = 0 \,, \quad P(t_f) = S \tag{7a}$$

with

$$\hat{A} = \begin{bmatrix} 0 & I & 0 \\ 0 & 0 & \frac{q_6}{q_7} I \\ 0 & 0 & -\frac{q_6}{q_7} I \end{bmatrix} , \quad \hat{B} = \frac{1}{q_7} \begin{bmatrix} 0 & 0 & 0 \\ 0 & I & -I \\ 0 & -I & I \end{bmatrix}$$

$$\hat{D} = \begin{bmatrix} 0 & 0 & 0 \\ 0 & 0 & 0 \\ 0 & 0 & \frac{q_6^2}{q_7} I \end{bmatrix} , \quad Q_7 = q_7 I \,, \; Q_6 = q_6 I \,, \; S_1 = sI$$

has the solution

$$P(t) = \frac{1}{\epsilon} \begin{bmatrix} s q_7 (q_7 + q_6 t_{go}) I & q_7 s (q_7 + q_6 t_{go}) t_{go} I & \frac{s}{2} q_6 q_7 t_{go}^2 I \\ s q_7 (q_7 + q_6 t_{go}) t_{go} I & s q_7 t_{go}^2 (q_7 + q_6 t_{go}) I & \frac{s}{2} q_6 q_7 t_{go}^3 I \\ \frac{s}{2} q_6 q_7 t_{go}^2 I & \frac{s}{2} q_6 q_7 t_{go}^3 I & -q_6^2 t_{go} (q_7 + \frac{s}{12} t_{go}^3) I \end{bmatrix}$$

where

$$\epsilon = q_7^2 + q_7 q_6 t_{go} + \frac{s}{3} q_7 t_{go}^3 + \frac{s}{12} q_6 t_{go}^4$$

and

$$t_{go} = t_f - t$$

Computation of feedback controls leads to the following

$$u = \left[\frac{s t_{go} (q_7 + \frac{1}{2} q_6 t_{go})}{\epsilon} I \,, \; \frac{s t_{go}^2 (q_7 + \frac{1}{2} q_6 t_{go})}{\epsilon} I \,, \; \frac{\frac{s}{6} q_6 t_{go}^3 - q_6 q_7}{\epsilon} \right] x$$

$$- \frac{1}{q_7} \left[0 \quad -I \quad I \right] \eta$$

Examination of Feedback Gains

Consider two cases where in $q_6 = 0$ and $q_6 = \infty$. This corresponds to the case where no constraint is placed upon the control acceleration and the case where the term

$$\int_{t_0}^{t_f} \underline{v}^{m^T} u \, dt = 0$$

Table I and Table 2 summarizes the comparison.

	K_1	K_2	K_3
$q_6 = 0$	$\dfrac{s t_{go}}{q_7 + \frac{s}{3} t_{go}^3}$	$\dfrac{s t_{go}^2}{q_7 + \frac{s}{3} t_{go}^3}$	0
$q_6 = \infty$	$\dfrac{s t_{go}}{2q_7 + \frac{s}{6} t_{go}^3}$	$\dfrac{s t_{go}^2}{2q_7 + \frac{s}{6} t_{go}^3}$	$\dfrac{2s t_{go}^3 - 12 q_7}{t_{go}(s t_{go}^3 + 12 q_7)}$

Table I

	TIME FOR MAX K1 t_{go}	K_1 MAX	TIME FOR MAX K_2 t_{go}	K_2 MAX	K_3 MAX
$q_6=0$	$\sqrt[3]{\frac{3}{2}\frac{q_7}{s}}$	$\frac{2s}{3q_7} t_{go}^{MAX}$	$\sqrt[3]{\frac{6q_7}{s}}$	$\dfrac{s t_{go}^2}{3q_7}$	—
$q_6=\infty$	$\sqrt[3]{\frac{6q_7}{s}}$	$\frac{s}{3q_7} t_{go}^{MAX}$	$\sqrt[3]{\frac{24q_7}{s}}$	$\dfrac{s t_{go}^2}{6 q_7}$	∞ $t_{go}=0$

Table 2

Let the caret denote the case for which $q_6 = \infty$. Then as seen from tables I and 2,

$$\frac{\hat{t}_{go}}{t_{go}} = \sqrt[3]{4} = 1.5874 \text{ for } K_1$$

$$\frac{\hat{K}_1^{MAX}}{K_1^{MAX}} = \frac{1}{2}\sqrt[3]{4} = 0.7937$$

$$\frac{\hat{t}_{go}^{MAX}}{t_{go}} = \sqrt[3]{4} = 1.5874 \text{ for } K_2$$

$$\frac{\hat{K}_2^{MAX}}{K_2^{MAX}} = \frac{1}{2}\sqrt[3]{4} = 0.7937$$

It is therefore seen that the ratios of times at which the maximum magnitude occur, and the ratios of values themselves, are independent of the design parameters q_6 and s, with the peak in $\hat{K}$ occurring shortly before that of K_1 and the magnitudes of $\hat{K}$ less than that of K. This situation is illustrated in Figure 2.

Variation in cost due to estimation error

As explained earlier in the report, the target acceleration $\underline{a}^T$ is inaccessible for direct measurement. Under the assumption that observation of past performance of the target provides information concerning the future behavior of the target, an estimate $\underline{a}^T$ may be obtained for target acceleration for future time. This estimate may be used in the filter equation (7) for computing the variable ξ. An analysis was made by the author in order to determine the effect of error in the estimate. A deterministic case will be considered first.

Let

$$\dot{x} = Ax + Bu + Cy \tag{10}$$

$$J = \frac{1}{2} x^T(t_f) S x(t_f) + \frac{1}{2} \int_{t_0}^{t_f} u^T R u \, d\tau \tag{11}$$

As previously derived, the function J is minimized by

$$u = -R^{-1}B^T P x + R^{-1}B^T \xi \tag{12}$$

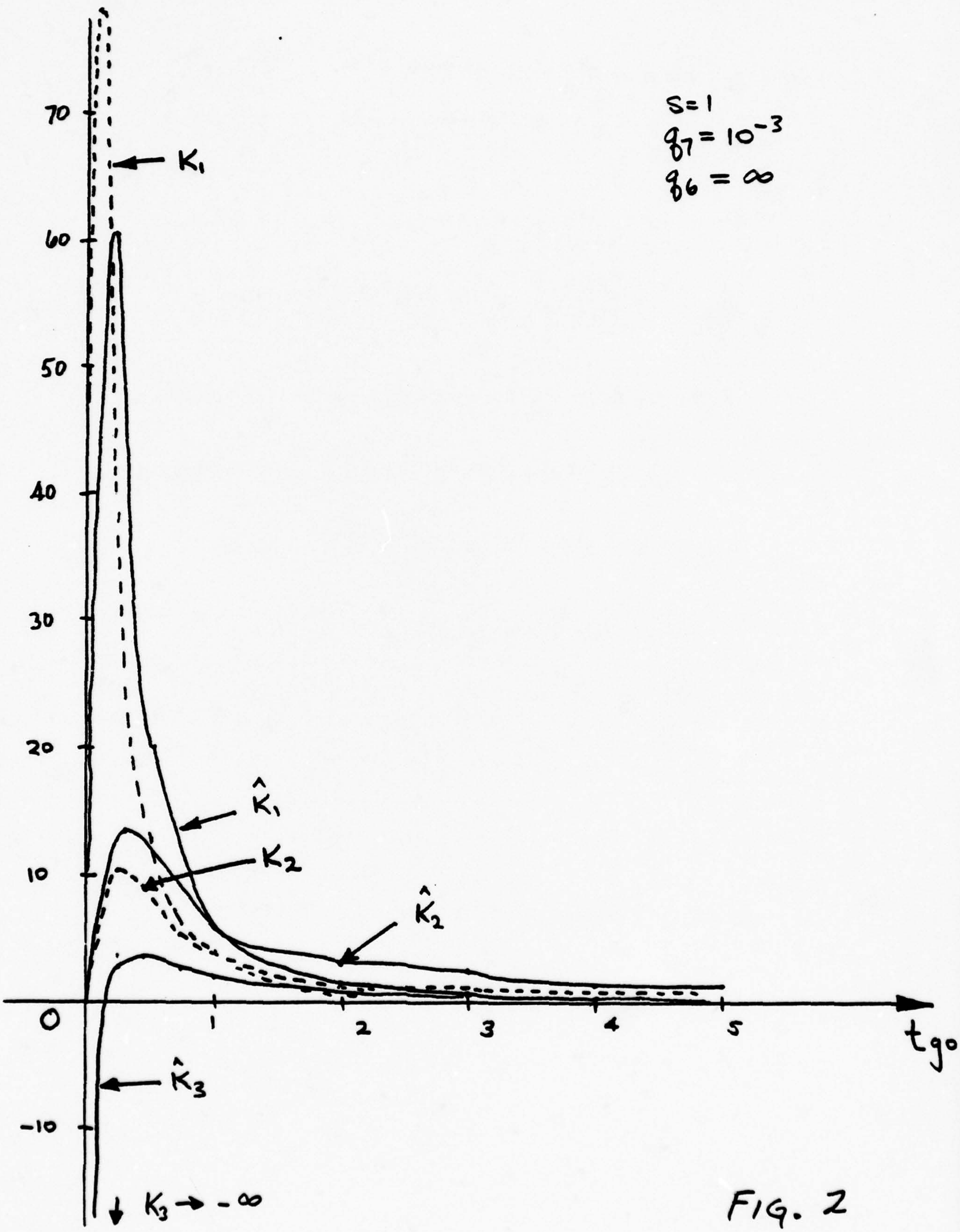

FIG. 2

where
$$\begin{aligned} \dot{P} &= -A^TP - PA + PBR^{-1}B^TP \,, \quad P(t_f) = S \\ \dot{\zeta} &= -[A - BR^{-1}B^TP]^T\zeta + PCy \,, \quad \zeta(t_f) = 0 \end{aligned} \tag{13}$$

The total cost, as a function of t_f, t_o, may be found by solving the Hamilton-Jacobi equation

$$\min_{u} \left\{ \frac{\partial V}{\partial t} + \left(\frac{\partial V}{\partial x}\right)^T \frac{dx}{dt} + \frac{1}{2} u^T R u \right\} = 0 \tag{14}$$

where $V[x_o, t_o, t_f]$ is the optimal cost. Eq (14) becomes

$$\frac{\partial V}{\partial t} + \left(\frac{\partial V}{\partial x}\right)^T \left[(A - BR^{-1}B^TP)x + BR^{-1}B^T\zeta + Cy\right] + \frac{1}{2}\zeta^T B^T R^{-1} B^T \zeta$$
$$- 2\zeta^T BR^{-1}B^TPx + x^TPBR^{-1}B^TPx = 0$$

choose
$$V = \frac{1}{2}x^TPx - \zeta^Tx + \alpha$$
$$\frac{\partial V}{\partial x} = Px - \zeta$$
$$\frac{\partial V}{\partial t} = \frac{1}{2}x^T\dot{P}x - \zeta^Tx + \dot{\alpha}$$

Substituting into Hamilton-Jacobi equation,

$$\dot{\alpha} = \frac{1}{2}\zeta^T BR^{-1}B^T\zeta + \zeta^T Cy \,, \quad \alpha(t_f) = 0 \tag{16}$$

Since $V[x_o, t_f, t_f] = \frac{1}{2}x^T(t_f)\, S\, x(t_f)$, therefore

$\zeta(t_f) = 0$, $P(t_f) = S$ and $\alpha(t_f) = 0$, so that

$$V = \frac{1}{2}x^T P x - z^T x + \alpha$$
$$= \frac{1}{2}(x - P^{-1}z)^T P (x - P^{-1}z) + \alpha - \frac{1}{2}z^T P^{-1} z \qquad (17)$$

Equation (16) and (17) represents the cost of the target acceleration in the optimal control, assuming that the target acceleration, y, is known completely. It is seen from the right side of (17) that z reduces the total cost, since $z^T P^{-1} z$ is a positive semi-definite quantity.

The results in Eqs. (16) and (17) are well known [2]; the following result is believed to be original. The system is given by

$$\dot{x} = Ax + Bu^* + Cy$$
$$u^* = -R^{-1}B^T P x + R^{-1}B^T z$$
$$\dot{z} = -[A - BR^{-1}B^T P]^T z + PC\hat{y} \qquad (18)$$

It is assumed that $\hat{y}$ is an estimate of the correct target acceleration y, but may contain an error in estimation, e. It is desired to determine the deterioration in performance when $\hat{y}$ is substituted for y in the preceeding scheme. The last equation of (18) can, by the linearity property, be written as

$$z = z_1 + z_2$$
$$\dot{z}_1 = -[A - BR^{-1}B^T P]^T z_1 + PCy$$
$$\dot{z}_2 = -[A - BR^{-1}B^T P]^T z_2 + PCe \qquad (19)$$
$$e = \hat{y} - y$$

The cost to be considered is

$$J = \frac{1}{2}x(t_f)^T S x(t_f) + \frac{1}{2}\int_{t_0}^{t_f} u^{*T} R u^* \, d\tau \qquad (20)$$

Let $\hat{V} = J[x_0, t_0, t_f, u^*]$. Then

$$J = \frac{1}{2} x(t_f)^T S x(t_f) + \frac{1}{2}\int_{t_0+\Delta t}^{t_f} u^T R u \, d\tau + \frac{1}{2}\int_{t_0}^{t_0+\Delta t} u^T R u \, d\tau \Bigg|_{u=u^*}$$

$$= \hat{V}[x_0+\Delta x, t_0+\Delta t, t_f, u^*] + \frac{1}{2} u^{*T} R u^* \Delta t + O(\Delta t^2)$$

$$= \hat{V}[x_0, t_0, t_f, u^*] + \left(\frac{\partial \hat{V}}{\partial x_0}\right)^T \Delta x_0 + \frac{\partial \hat{V}}{\partial t_0} \Delta t + \frac{1}{2} u^{*T} R u^* \Delta t$$

Therefore

$$\left(\frac{\partial \hat{V}}{\partial x}\right)^T \Delta x + \frac{\partial \hat{V}}{\partial t} \Delta t + \frac{1}{2} u^{*T} R u^* \Delta t = 0 \tag{21}$$

Substituting (18) and (19) leads to

$$\left(\frac{\partial \hat{V}}{\partial x}\right)^T \left[(A - BR^{-1}B^TP)x + BR^{-1}B^T z + Cy\right] + \frac{\partial \hat{V}}{\partial t} + \frac{1}{2}\left[z^T BR^{-1}B^T z - 2z^T BR^{-1}B^T Px + x^T PBR^{-1}B^T Px\right] = 0$$

Let $\rho \equiv \hat{V} - V$. After some algebraic manipulation and substituting $\frac{\partial \hat{V}}{\partial x} = \frac{\partial \rho}{\partial x} + Px - z$, the result is

$$\left(\frac{\partial \rho}{\partial x}\right)^T \left[(A - BR^{-1}B^TP)x + BR^{-1}B^T(z_1 + z_2) + Cy\right] + \frac{\partial \rho}{\partial t} + \frac{1}{2} z_2^T BR^{-1}B^T z_2 = 0 \tag{22}$$

Equation (22) is a partial differential equation representing the change in cost from using the estimated quantity $\hat{y}$ in the control law instead of the true quantity y. The equation will now be solved. Assume for a solution

$$\rho = \frac{1}{2} x^T Q x - m^T x + \beta \tag{23}$$

By direct substitution, it can be shown that the solution is

$$\dot{Q} = -Q(A-BR^{-1}B^TP) + (A-BR^{-1}B^TP)^TQ, \quad Q(t_f)=0$$

$$\dot{m} = -(A-BR^{-1}B^TP)^Tm + Q[BR^{-1}B^Tz + Cy], \quad m(t_f)=0 \qquad (24)$$

$$\dot{\beta} = -\tfrac{1}{2} z_2^T BR^{-1}B^T z_2 + m^T[BR^{-1}B^T(z_1+z_2) + Cy], \quad \beta(t_f)=0$$

It is easily seen that $Q(t) = 0$ and $m(t) = 0$ for all t. Therefore

$$\dot{\beta} = -\tfrac{1}{2} z_2^T BR^{-1}B^T z_2, \quad \beta(t_f)=0$$

or

$$\rho = \beta(t) = \frac{1}{2}\int_t^{t_f} z_2^T BR^{-1}B^T z_2 \, d\tau \qquad (25)$$

where $\dot{z}_2 = -[A-BR^{-1}B^TP]^T z_2 + PCe, \quad z(t_f)=0$

Consequently, the error in cost is proportional to the integral of the square of the error in measurement. Eq. (25) gives a means whereby R may be chosen as a time-varying matrix in order to reduce the final cost of performance. This was not pursued in this study.

By use of equations (25), an estimate of the improvement in behavior can be obtained when the target acceleration is included in the control law over the control law in which the target acceleration is ignored. In order to ignore target acceleration, $\hat{y} \equiv 0$. Then $y = -e$ so that $z_1 = -z_2$, or that

$$\beta = \frac{1}{2}\int_t^{t_f} z_1^T BR^{-1}B^T z_1 \, d\tau \qquad (26)$$

and

$$\dot{\alpha} = \tfrac{1}{2} z_1^T BR^{-1}B^T z_1 + z_1^T Cy, \quad \alpha(t_f)=0$$

Equivalently,

$$\alpha = -\frac{1}{2}\int_t^{t_f} [z_1^T BR^{-1}B^T z_1 + z_1^T Cy] \, d\tau \qquad (27)$$

Substitution of (27) and (23) into (17) yields for the altered cost

$$\hat{V} = \frac{1}{2}(x-P^{-1}z_1)^T P (x-P^{-1}z_1) + \int_t^{t_f} z_1^T C y \, d\tau - \frac{1}{2} z_1^T P^{-1} z_1 \tag{28}$$

Eq. (29) is the "optimal" cost of using no target acceleration in the control law. Comparing the two,

$$\frac{\hat{V}}{V} = \frac{\frac{1}{2}(x-P^{-1}z_1)^T P (x-P^{-1}z_1) + \int_t^{t_f} z_1^T C y \, d\tau - \frac{1}{2} z_1^T P^{-1} z_1}{\frac{1}{2}(x-P^{-1}z_1)^T P (x-P^{-1}z_1) + \int_t^{t_f} z_1^T C y \, d\tau - \frac{1}{2}\int_t^{t_f} z_1^T B R^{-1} B^T z_1 - \frac{1}{2} z_1^T P^{-1} z_1} \tag{29}$$

$$= \frac{\gamma}{\gamma - \delta}$$

where (30)

$$\delta = \frac{1}{2} \int_t^{t_f} z_1^T B R^{-1} B^T z_1 \, d\tau$$

Since δ is a positive semi-definite term, performance is degraded by not including the target acceleration. (It is uncertain whether there exists a target acceleration such that δ = 0; i.e.,

$$z_1^T B R^{-1} B^T z_1 \quad = \text{for all } t \in [t, t_f] \text{ .)}$$

The importance of (29-30) is that an analytical proof is given that performance is improved - certainly never degraded - by including the target acceleration in the control law; and that the amount of improvement is related to the output signal from the prefilter.

The stochastic version

Analogous to the preceeding action, the stochastic version of the target-seeking system may be analyzed by the Kolmogorov equation.

The system is $\dot{x} = Ax + Bu + Cy$

$$\dot{y} = Fy + Gw$$

w - white noise

$$E[w] = \alpha(t) \tag{31}$$

$$E[ww^T] = Q(t)$$

a more precise description of eq. (37) is

$$dx = Ax\,dt + Bu\,dt + C\,dy$$
$$dy = Fy\,dt + G\,dw \tag{32}$$

It is intended to minimize

$$J = E\left\{ \frac{1}{2} x^T(t_f) S x(t_f) + \frac{1}{2}\int_{t_0}^{t_f} u^T R u \, dt \right\} \tag{33}$$

The Kolmogorov equation is [3]

$$0 = \min_u \left\{ \frac{1}{2} E[u^T R u] + \frac{\partial V}{\partial t} + E\left[\frac{\partial V}{\partial x}^T \frac{dx}{dt}\right] + \frac{1}{2} \operatorname{Tr} Q \frac{\partial^2 V}{\partial x^2} \right\} \tag{34}$$

The minimizing u is

$$u = -R^{-1} B^T \frac{\partial V}{\partial x} \tag{35}$$

Substituting (35) into (34) yields

$$0 = \frac{1}{2}\left(\frac{\partial V}{\partial x}\right)^T B R^{-1} B^T \frac{\partial V}{\partial x} + \frac{\partial V}{\partial t} + \frac{1}{2}\left(\frac{\partial V}{\partial x}\right)^T [Ax + CF\tilde{y} + G\alpha]$$
$$+ \frac{1}{2}[Ax + CF\tilde{y} + G\alpha]^T \frac{\partial V}{\partial x} + \frac{1}{2} \operatorname{Tr} Q \frac{\partial^2 V}{\partial x^2} - \left(\frac{\partial V}{\partial x}\right)^T B R^{-1} B^T \frac{\partial V}{\partial x} \tag{36}$$

Eq. (36) is the partial differential equation for which the optimal cost may be determined.

Let

$$V = \frac{1}{2} x^T P x - z^T x + \beta \tag{37}$$

as a solution. Substitution of (37) into (36) yields

$$\begin{aligned}
\dot{P} &= -PA - A^T P + PBR^{-1}B^T P \qquad P(t_f) = S \\
\dot{z} &= -(A - BR^{-1}B^T P)^T z + PC(F\bar{y} + G\alpha) \,, \quad z(t_f) = 0 \\
\dot{\beta} &= \tfrac{1}{2} z^T B R^{-1} B^T z + z^T C(F\bar{y} + G\alpha) - \tfrac{1}{2} \mathrm{Tr}\, QP \,, \quad \beta(t_f) = 0
\end{aligned} \tag{38}$$

so that

$$V = \tfrac{1}{2}(x - P^{-1}z)^T P (x - P^{-1}z) + \beta - \tfrac{1}{2} z^T P^{-1} z \tag{39}$$

Eq. (39) is analogous to (17).

Simulation Results

A simulation was performed to evaluate the target-seeking algorithm previously mentioned. This simulation was in 2-dimensional space. It was found that the constraint on missile acceleration did not fully eliminate acceleration in the direction of the missile velocity vector. Consequently, to insure a realistic simulation, residual acceleration was discarded. Furthermore, maximum acceleration commanded was limited to 100 g. The target acceleration was made perfectly available to the control algorithm, and represented a target having 8g acceleration normal to the flight path and 2g acceleration tangential to the flight path (this results in an outward spiral of the target). The missile thrust lasted for 2.6 seconds, with initial acceleration of 28.55g and acceleration of 40.96 g at t = 2.6 seconds. For t greater than 2.6, thrust was zero. S = 20 and q = 10^{-4}.

Various initial conditions were tried in order to determine the closest range (magnitude of $\underline{S}$) from which the missile intercepted the moving target. Table 3 lists the closest range required to intercept (termed the inner launch boundary) for several initial missile-target configurations. An interception was considered to have accurred whenever the missile approached the target with a distance not exceeding 10 feet. In order to interpret Table 3, Figure 3 defines Θ_B, the bore angle and Θ_A, the aspect angle.

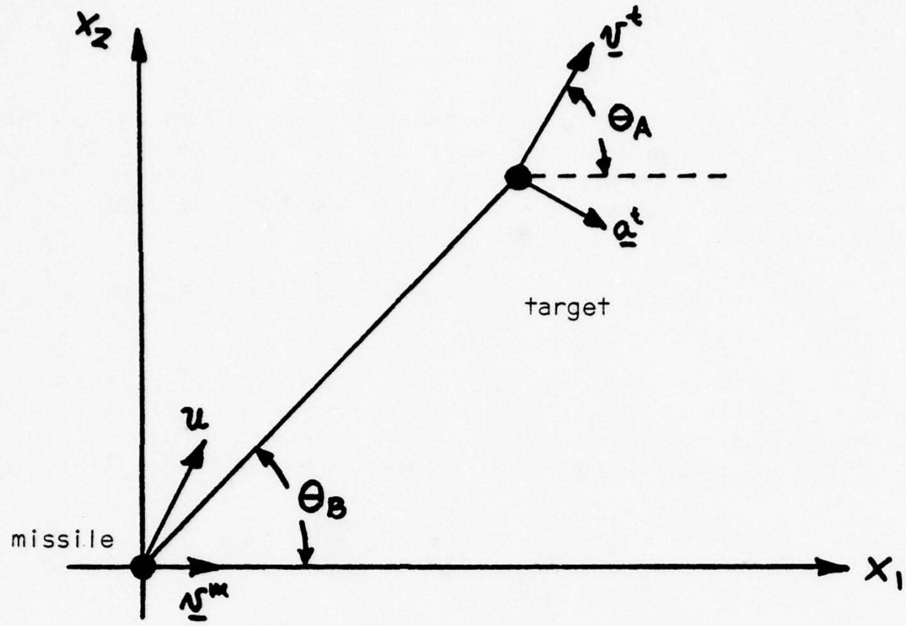

Note that $\underline{v}^m$ is always directed along the X_1 axis in this simulation. The magnitudes of $\underline{v}^m$ and $\underline{v}^t$ were both chosen to be 970 f/s.

0_B degrees	0_A degrees	Inner Launch Boundaries
0	0	$d < 200$
0	45	1500
0	90	1970
0	135	$d < 200$
0	180	1970
40	0	$9000 < d < 10000$
40	45	1930
40	90	$500 < d < 700$
40	135	5000
40	180	$9000 < d < 100000$

Table 3

It is noted that some distances are quite good while others are somewhat poor. An examination of the control acceleration in the poor cases indicate that, over a significant part of the flight trajectory, the commanded control was limited by the 100g maximum available from the missile.

Figure 4 plots the results shown in Table 3 for the θ° bore angle.

Figure 5-14 shows the data obtained for the boundary conditions given in Table 3. These figures were chosen to represent a configuration near the launch boundary; further from the launch boundary, the miss distance was improved, typically less than 1 foot.

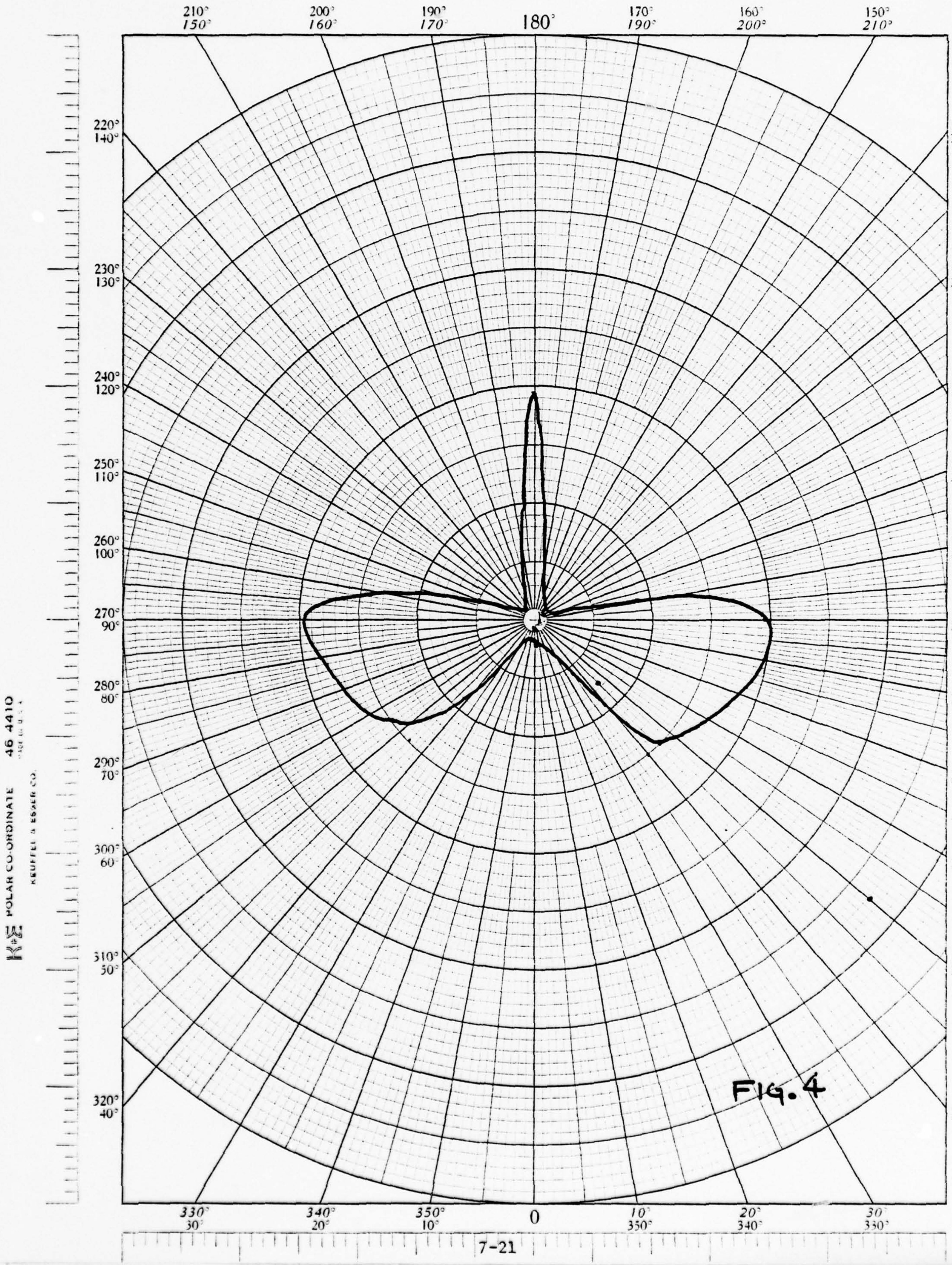
180°
0
210° 150°
200° 160°
190° 170°
170° 190°
160° 200°
150° 210°
330° 30°
340° 20°
350° 10°
10° 350°
20° 340°
30° 330°
K&E POLAR CO-ORDINATE 46 4410
KEUFFEL & ESSER CO.

FIG. 4

"H=" .005 "TUPDATE=" .1 "G=" 20. "Q7=" .0001
"WHAT IS THE INITIAL RANGE IN FT/SEC?"
2.498 OF SECONDS COMPILATION TIME750

"WHAT IS THE INITIAL BORE ANGLE, ALSO THE INITIAL TARGET VELOCITY ANGLE,
40 90

"WHAT IS THE TARGET VELOCITY AND THE MISSLE VELOCITY?"970 970

"STORE(N)=" -500.2035462392 558.8348703595 -1404.631407645 867.1767636925
970. 0.

TIME	VELOCITY 1	VELOCITY 2	ACCEL 1	ACCEL 2	POSITION 1	POSITION 2
0.00	-434.631	867.177	-259.149	-57.850	-500.204	558.835

TIME	RELATIVE DIST-X1	RELATIVE DIST-X2	RELATIVE VELOC-X1	RELATIVE VELOC-X2	ABSOLUTE VELOC-X1	ABSOLUTE VELOC-X2	FINTIM
.10	-644.851	628.786	-1471.399	529.447	1010.933	331.603	.45
.20	-791.228	664.740	-1440.722	191.926	954.590	662.316	.68
.30	-930.133	667.998	-1324.305	-121.043	812.696	967.808	[illegible]
.40	-1053.734	641.923	-1137.288	-392.458	600.405	1231.085	[illegible]
.50	-1155.775	591.254	-895.763	-611.618	333.825	1441.455	1.43
.60	-1231.589	521.535	-615.244	-772.852	28.485	1593.260	1.70
.70	-1277.995	438.679	-309.811	-874.302	-301.520	1684.643	1.95
.80	-1293.131	348.640	8.285	-916.850	-643.926	1716.515	2.16
.90	-1276.262	257.182	328.729	-903.251	-988.402	1691.625	2.26
1.00	-1227.590	169.730	643.073	-837.459	-1326.487	1613.944	2.25
1.10	-1148.077	91.276	944.575	-724.118	-1651.427	1488.126	2.17
1.20	-1039.279	26.326	1227.996	-568.186	-1957.970	1319.141	2.07
1.30	-903.213	-21.109	1489.387	-374.679	-2242.155	1112.916	1.97
1.40	-742.248	-47.564	1723.948	-154.024	-2499.170	877.191	1.89
1.50	-559.437	-51.791	1920.996	43.302	-2718.321	665.152	1.83
1.60	-358.668	-39.548	2085.170	162.187	-2904.238	531.026	1.79
1.70	-142.296	-18.454	2235.829	218.919	-3076.266	458.534	1.77

"DISTANCE" 9633.471616678 "TIME" 1.71999999999
"DISTANCE" 7514.603842519 "TIME" 1.72499999999
"DISTANCE" 5651.857524296 "TIME" 1.72999999999
"DISTANCE" 4048.722935849 "TIME" 1.73499999999
"DISTANCE" 2708.324662592 "TIME" 1.73999999999
"DISTANCE" 1623.541062764 "TIME" 1.74499999999
"DISTANCE" 827.088011594 "TIME" 1.74999999999
"DISTANCE" 291.573242588 "TIME" 1.75499999999
"DISTANCE" 29.52693346421 "TIME" 1.75999999999

TIME	CONTROL MAGNITUDE
.10	3220.000
.20	3220.000
.30	3220.000
.40	3220.000
.50	3220.000
.60	3220.000
.70	3220.000
.80	3220.000
.90	3220.000
1.00	3220.000
1.10	3220.000
1.20	3220.000
1.30	3220.000
1.40	2732.981
1.50	1644.622
1.60	667.705
1.70	123.965

"AT TIME" 1.75999999999 "THE MISS-DISTANCE WAS" [illegible]
STOP
9.500 OF SECONDS EXECUTION TIME

FIGURE 5

```
      2.500 CP SECONDS COMPILATION TIME
"H=" .005 "TUPDATE=" .1 "S=" 20. "Q7=" .0001
"WHAT IS THE INITIAL RANGE IN FT/SEC?"200

"WHAT IS THE INITIAL BORE ANGLE, ALSO THE INITIAL TARGET VELOCITY ANGLE, ]
0 135

"WHAT IS THE TARGET VELOCITY AND THE MISSLE VELOCITY?"970 970

"STORE(N)=" 200. 0. -1936.205200087 85.71762552088 970. 0.

 TIME VELOCITY 1 VELOCITY 2     ACCEL 1     ACCEL 2  POSITION 1 POSITION 2
 0.00   -966.205     85.718     -86.912    -250.901     200.000      0.000
  .40   -995.627    -16.287     -60.178    -258.619    -192.723     13.989
  .80  -1014.354   -120.787     -33.489    -263.408    -595.075    -13.362
 1.20  -1022.462   -226.644      -7.126    -265.432   -1002.790    -82.821
 1.60  -1020.131   -332.788      18.666    -264.871   -1411.652   -194.715
 2.00  -1007.633   -438.221      43.679    -261.911   -1817.538   -348.956
 2.40   -985.316   -542.022      67.734    -256.744   -2216.449   -545.074
 2.80   -953.593   -643.348      90.683    -249.563   -2604.537   -782.244
 3.20   -912.933   -741.430     112.407    -240.561   -2978.131  -1059.319
 3.60   -863.844   -835.579     132.808    -229.929   -3333.759  -1374.863
 4.00   -806.873   -925.180     151.811    -217.849   -3668.156  -1727.176
 4.40   -742.589  -1009.690     169.363    -204.502   -3978.282  -2114.328
 4.80   -671.581  -1088.636     185.426    -190.058   -4261.330  -2534.185
 5.20   -594.449  -1161.612     199.979    -174.681   -4514.730  -2984.440
 5.60   -511.800  -1228.277     213.013    -158.526   -4736.153  -3462.633
 6.00   -424.240  -1288.348     224.534    -141.738   -4923.515  -3966.182
 6.40   -332.373  -1341.601     234.554    -124.456   -5074.971  -4492.402
 6.80   -236.793  -1387.864     243.099    -106.808   -5188.918  -5038.531
 7.20   -138.086  -1427.015     250.200     -88.912   -5263.989  -5601.745
 7.60    -36.821  -1458.975     255.893     -70.879   -5299.046  -6179.184
 8.00     66.447  -1483.713     260.223     -52.811   -5293.179  -6767.962
 8.40    171.182  -1501.232     263.238     -34.801   -5245.693  -7365.192
 8.80    276.868  -1511.573     264.987     -16.935   -5156.107  -7967.991
 9.20    383.010  -1514.809     265.527        .710   -5024.138  -8573.502
 9.60    489.136  -1511.043     264.913      18.064   -4849.701  -9178.904
10.00    594.795  -1500.405     263.203      35.064   -4632.898  -9781.481

 TIME  RELATIVE  RELATIVE  RELATIVE  RELATIVE  ABSOLUTE  ABSOLUTE
        DIST-X1   DIST-X2  VELOC-X1  VELOC-X2  VELOC-X1  VELOC-X2 FINTIM
"DISTANCE" 8514.766393016 "TIME" .055
"DISTANCE" 6789.308944973 "TIME" .06
"DISTANCE" 5258.888420115 "TIME" .065
"DISTANCE" 3924.607376704 "TIME" .07
"DISTANCE" 2787.517066589 "TIME" .075
"DISTANCE" 1848.617661117 "TIME" .08
"DISTANCE" 1108.85849225 "TIME" .085
"DISTANCE" 569.1383083293 "TIME" .09
"DISTANCE" 230.305543974 "TIME" .095
  .10      3.065    -9.152 -1985.496  -271.087  1010.938   331.603    .10
"DISTANCE" 93.15860358839 "TIME" .1

   TIME          CONTROL MAGNITUDE
    .10                3220.000
"AT TIME" .1 "THE MISS-DISTANCE WAS" 9.65187047097
     STOP
      4.345 CP SECONDS EXECUTION TIME
```

THIS PAGE IS BEST QUALITY PRACTICABLE
FROM COPY FURNISHED TO DDQ

FIGURE 6

```
  2.502 CP SECONDS COMPILATION TIME
"H=" .005 "TUPDATE=" .1 "S=" 20. "Q7=" .0001
"WHAT IS THE INITIAL RANGE IN FT/SEC?"9000

"WHAT IS THE INITIAL BORE ANGLE, ALSO THE INITIAL TARGET VELOCITY ANGLE, I
40  180

"WHAT IS THE TARGET VELOCITY AND THE MISSLE VELOCITY?"970  970

"STORE(N)=" -6002.44255487 6706.018444314 -1550.506266986 -777.1180566618
970. 0.
```

TIME	VELOCITY 1	VELOCITY 2	ACCEL 1	ACCEL 2	POSITION 1	POSITION 2
0.00	-580.506	-777.118	167.836	-205.758	-6002.443	6706.018

TIME	RELATIVE DIST-X1	RELATIVE DIST-X2	RELATIVE VELOC-X1	RELATIVE VELOC-X2	ABSOLUTE VELOC-X1	ABSOLUTE VELOC-X2	FINTIM
.10	-6161.294	6625.840	-1626.953	-827.637	1063.501	30.168	5.19
.20	-6327.898	6539.993	-1705.387	-890.971	1159.520	73.608	5.06
.30	-6502.380	6446.933	-1784.227	-972.559	1256.461	135.769	4.93
.40	-6684.651	6344.554	-1860.671	-1078.203	1351.505	222.465	4.81
.50	-6874.248	6230.090	-1929.830	-1215.312	1439.748	341.113	4.69
.60	-7070.055	6099.953	-1983.327	-1392.897	1512.797	500.734	4.57
.70	-7269.852	5949.591	-2007.091	-1621.003	1556.565	711.380	4.45
.80	-7469.604	5773.489	-1978.423	-1908.258	1548.338	981.689	4.34
.90	-7662.537	5565.671	-1868.496	-2250.302	1459.274	1307.308	4.23
1.00	-7841.530	5323.892	-1703.382	-2581.864	1315.426	1622.972	4.14
1.10	-8001.716	5050.069	-1493.350	-2890.367	1127.051	1916.113	4.06
1.20	-8138.901	4746.727	-1244.340	-3171.657	900.071	2182.579	4.01
1.30	-8249.476	4416.742	-962.087	-3422.853	640.205	2419.500	3.97
1.40	-8330.390	4063.222	-651.985	-3642.116	352.834	2625.038	3.93
1.50	-8379.112	3689.418	-319.020	-3828.434	42.925	2798.188	3.90
1.60	-8393.584	3298.646	32.274	-3981.452	-285.001	2938.598	3.88
1.70	-8372.182	2894.233	397.817	-4101.319	-626.880	3046.422	3.87
1.80	-8313.667	2479.469	773.974	-4188.567	-979.092	3122.195	3.85
1.90	-8217.141	2057.579	1157.528	-4244.014	-1338.436	3166.738	3.84
2.00	-8082.009	1631.693	1545.659	-4268.679	-1702.106	3181.073	3.83
2.10	-7907.939	1204.831	1935.902	-4263.723	-2067.654	3166.364	3.82
2.20	-7694.830	779.894	2326.122	-4230.396	-2432.957	3133.861	3.81
2.30	-7442.778	359.654	2714.473	-4169.997	-2796.186	3054.867	3.80
2.40	-7152.051	-53.247	3099.372	-4083.845	-3155.772	2960.700	3.80
2.50	-6823.064	-456.300	3479.469	-3973.256	-3510.378	2842.678	3.80
2.60	-6456.355	-847.127	3853.616	-3839.523	-3858.872	2702.095	3.79
2.70	-6060.640	-1218.097	4056.299	-3576.860	-4035.752	2433.165	3.80
2.80	-5645.719	-1562.101	4238.944	-3301.323	-4192.461	2151.942	3.84
2.90	-5213.500	-1878.008	4402.144	-3015.160	-4329.604	1860.677	3.89
3.00	-4765.960	-2164.824	4545.245	-2719.732	-4446.540	1560.728	3.94
3.10	-4305.140	-2421.692	4667.687	-2416.440	-4542.724	1253.494	3.99
3.20	-3833.127	-2647.897	4769.008	-2106.71%A			

```
HUNG IN AUTOMATIC RECALL
  DROPPED IN INTGRL  NEAR LINE 27
```

FIGURE 7

THIS PAGE IS BEST QUALITY PRACTICABLE
FROM COPY FURNISHED TO DDO

```
2.500 CP SECONDS COMPILATION TIME
"H=" .005 "TUPDATE=" .1 "S=" 20. "DT=" .0001
"WHAT IS THE INITIAL RANGE IN FT/SEC?"10000

"WHAT IS THE INITIAL BORE ANGLE, ALSO THE INITIAL TARGET VELOCITY ANGLE, I
40  180

"WHAT IS THE TARGET VELOCITY AND THE MISSLE VELOCITY?"970  970

"STORE(N)=" -6669.380616523 7451.131604793 -1550.506266986 -777.118056661S
970. 0.
```

TIME	VELOCITY 1	VELOCITY 2	ACCEL 1	ACCEL 2	POSITION 1	POSITION 2
0.00	-580.506	-777.118	167.836	-205.758	-6669.381	7451.132

TIME	RELATIVE DIST-X1	RELATIVE DIST-X2	RELATIVE VELOC-X1	RELATIVE VELOC-X2	ABSOLUTE VELOC-X1	ABSOLUTE VELOC-X2	FINTIM
.10	-6826.474	7355.933	-1574.385	-1129.072	1010.933	331.603	5.77
.20	-6986.121	7236.225	-1616.660	-1268.258	1070.794	450.895	5.28
.30	-7149.023	7100.969	-1637.994	-1440.547	1110.227	603.757	5.10
.40	-7312.449	6946.632	-1625.053	-1650.002	1115.886	794.264	4.92
.50	-7472.098	6769.459	-1559.727	-1896.496	1069.645	1022.297	4.76
.60	-7621.679	6566.106	-1420.843	-2171.302	950.313	1279.133	4.61
.70	-7752.886	6334.727	-1191.900	-2452.128	741.375	1542.505	4.48
.80	-7858.439	6076.990	-912.457	-2695.292	482.373	1768.723	4.37
.90	-7934.201	5797.182	-597.700	-2893.126	188.477	1950.131	4.29
1.00	-7977.109	5499.936	-256.826	-3043.884	-131.130	2084.992	4.23
1.10	-7984.971	5189.982	101.949	-3147.380	-468.248	2173.125	4.17
1.20	-7956.364	4872.005	471.440	-3204.568	-815.710	2215.490	4.12
1.30	-7890.532	4550.554	845.480	-3217.198	-1167.362	2213.845	4.08
1.40	-7787.291	4229.974	1218.849	-3187.559	-1518.001	2170.481	4.04
1.50	-7646.931	3914.364	1587.196	-3118.271	-1863.291	2088.024	4.00
1.60	-7470.139	3607.549	1946.941	-3012.130	-2199.666	1969.276	3.96
1.70	-7257.927	3313.071	2295.182	-2871.998	-2524.245	1817.101	3.91
1.80	-7011.564	3034.187	2629.602	-2700.718	-2834.720	1634.346	3.87
1.90	-6732.528	2773.873	2948.387	-2501.056	-3129.296	1423.788	3.83
2.00	-6422.462	2534.813	3249.360	-2277.929	-3405.808	1190.323	3.78
2.10	-6083.630	2317.664	3522.183	-2071.943	-3653.935	974.594	3.74
2.20	-5718.789	2119.204	3771.549	-1903.981	-3878.385	797.446	3.69
2.30	-5329.802	1935.493	4006.527	-1776.311	-4088.240	661.181	3.64
2.40	-4917.769	1762.424	4233.493	-1690.121	-4289.893	566.976	3.59
2.50	-4483.262	1595.821	4456.666	-1645.597	-4487.575	515.020	3.55
2.60	-4026.523	1431.554	4678.551	-1641.575	-4683.807	504.148	3.50
2.70	-3557.253	1266.731	4705.313	-1654.139	-4684.766	510.444	3.46
2.80	-3085.474	1100.583	4730.353	-1667.980	-4683.870	518.600	3.46
2.90	-2611.194	933.010	4755.371	-1682.390	-4682.830	527.907	3.45
3.00	-2134.414	763.972	4780.389	-1696.983	-4681.684	537.978	3.45
3.10	-1655.134	593.464	4805.432	-1711.396	-4680.469	548.450	3.45
3.20	-1173.351	421.503	4830.506	-1725.444	-4679.204	559.137	3.44
3.30	-689.065	248.108	4855.611	-1739.011	-4677.903	569.921	3.44
3.40	-202.285	73.251	4880.702	-1752.345	-4676.534	581.046	3.44

```
"DISTANCE" 7287.791280724 "TIME" 3.42499999998
"DISTANCE" 3527.076790249 "TIME" 3.42999999998
"DISTANCE" 1115.748084801 "TIME" 3.43499999998
"DISTANCE" 54.92906307008 "TIME" 3.43999999998
```

FIGURE 8

```
 TIME          CONTROL MAGNITUDE
  .10                  3220.000
  .20                   979.741
  .30                  1302.581
  .40                  1709.281
  .50                  2202.767
  .60                  2762.702
  .70                  3220.000
  .80                  3220.000
  .90                  3220.000
 1.00                  3220.000
 1.10                  3220.000
 1.20                  3220.000
 1.30                  3220.000
 1.40                  3220.000
 1.50                  3220.000
 1.60                  3220.000
 1.70                  3220.000
 1.80                  3220.000
 1.90                  3220.000
 2.00                  3044.836
 2.10                  2488.886
 2.20                  1975.685
 2.30                  1497.094
 2.40                  1049.490
 2.50                   635.607
 2.60                   265.019
 2.70                    47.942
 2.80                    61.328
 2.90                    66.203
 3.00                    66.039
 3.10                    60.534
 3.20                    49.249
 3.30                    30.000
 3.40                     5.203
"AT TIME" 3.43999999998 "THE MISS-DISTANCE WAS" 7.411414377167
    STOP
    23.518 CP SECONDS EXECUTION TIME
..RUN;FTN
```

FIGURE 8 (CONT'D)

THIS PAGE IS BEST QUALITY PRACTICABLE
FROM COPY FURNISHED TO DDC

```
   2.475 CP SECONDS COMPILATION TIME
"H=" .005 "TUPDATE=" .1 "S=" 20. "Q7=" .0001
"WHAT IS THE INITIAL RANGE IN FT/SEC?"5000

"WHAT IS THE INITIAL BORE ANGLE, ALSO THE INITIAL TARGET VELOCITY ANGLE, IN
40  135

"WHAT IS THE TARGET VELOCITY AND THE MISSLE VELOCITY?"970  970

"STORE(N)=" -3334.690308261 3725.565802397 -1936.205200087 85.71762552088
970. 0.
```

TIME	VELOCITY 1	VELOCITY 2	ACCEL 1	ACCEL 2	POSITION 1	POSITION 2
0.00	-966.205	85.718	-86.912	-250.901	-3334.690	3725.566

TIME	RELATIVE DIST-X1	RELATIVE DIST-X2	RELATIVE VELOC-X1	RELATIVE VELOC-X2	ABSOLUTE VELOC-X1	ABSOLUTE VELOC-X2	FINTIM
.10	-3531.734	3717.033	-1987.726	-264.210	1013.163	324.725	2.58
.20	-3728.962	3672.674	-1941.322	-620.712	959.069	655.814	2.66
.30	-3917.115	3593.714	-1808.529	-952.768	819.254	962.263	2.77
.40	-4088.288	3483.512	-1604.384	-1243.263	608.757	1226.976	2.90
.50	-4236.148	3346.813	-1344.923	-1481.377	343.613	1439.153	3.05
.60	-4355.947	3189.180	-1045.636	-1661.327	39.311	1593.029	3.20
.70	-4444.419	3016.555	-720.607	-1781.150	-290.065	1686.659	3.35
.80	-4499.621	2834.930	-382.108	-1841.638	-632.246	1720.851	3.50
.90	-4520.739	2650.117	-40.488	-1845.470	-976.883	1698.303	3.63
1.00	-4507.900	2467.596	295.763	-1796.536	-1315.489	1622.921	3.74
1.10	-4461.993	2292.416	619.854	-1699.426	-1641.276	1499.314	3.82
1.20	-4384.694	2128.901	919.536	-1569.188	-1941.998	1342.544	3.87
1.30	-4279.391	1978.521	1190.965	-1439.383	-2203.814	1186.190	3.88
1.40	-4149.371	1840.893	1415.238	-1315.277	-2437.824	1035.533	3.83
1.50	-3996.959	1715.217	1629.941	-1201.049	-2651.620	894.788	3.75
1.60	-3823.831	1600.268	1830.514	-1101.139	-2850.645	758.381	3.65
1.70	-3631.180	1494.360	2021.225	-1020.385	-3039.172	661.135	3.54
1.80	-3419.809	1395.341	2205.599	-963.245	-3220.732	577.593	3.43
1.90	-3190.204	1300.629	2386.444	-933.811	-3398.137	521.230	3.33
2.00	-2942.609	1207.285	2565.810	-935.112	-3573.443	496.891	3.24
2.10	-2677.106	1112.127	2744.909	-968.877	-3747.868	504.519	3.15
2.20	-2393.694	1011.888	2924.202	-1035.036	-3921.880	544.656	3.10
2.30	-2092.360	903.406	3103.612	-1131.506	-4095.406	615.234	3.04
2.40	-1773.111	783.826	3282.890	-1254.106	-4268.205	712.084	2.99
2.50	-1435.976	650.798	3462.034	-1396.746	-4440.283	829.129	2.95
2.60	-1080.962	502.618	3641.562	-1552.292	-4612.164	959.248	2.92
2.70	-717.489	340.307	3631.120	-1670.590	-4593.501	1052.299	2.90
2.80	-354.369	170.152	3633.724	-1722.287	-4587.317	1078.940	2.90

```
"DISTANCE" 8252.259104323 "TIME" 2.874999999998
"DISTANCE" 4991.418723727 "TIME" 2.879999999998
"DISTANCE" 2545.52928414 "TIME" 2.884999999998
"DISTANCE" 915.1770007667 "TIME" 2.889999999998
"DISTANCE" 100.9449288236 "TIME" 2.894999999998
```

2.90	9.256	-4.212	3640.852	-1756.526	-4585.099	1088.326	2.90

FIGURE 9

THIS PAGE IS BEST QUALITY PRACTICABLE
FROM COPY FURNISHED TO DDC

TIME	CONTROL MAGNITUDE
.10	3220.000
.20	3220.000
.30	3220.000
.40	3220.000
.50	3220.000
.60	3220.000
.70	3220.000
.80	3220.000
.90	3220.000
1.00	3220.000
1.10	3220.000
1.20	2902.581
1.30	2510.267
1.40	2194.057
1.50	1908.988
1.60	1630.204
1.70	1343.966
1.80	1046.360
1.90	739.296
2.00	431.467
2.10	135.327
2.20	131.837
2.30	350.800
2.40	501.813
2.50	566.920
2.60	533.425
2.70	370.757
2.80	46.025
2.90	622.459

"AT TIME" 2.894999999998 "THE MISS-DISTANCE WAS" 10.0471353541
STOP
17.822 CP SECONDS EXECUTION TIME

FIGURE 9 (CONT'D)

"H=" .005 "TUPDATE=" .1 "S=" 20. "Q7=" .0001
"WHAT IS THE INITIAL RANGE IN FT/SEC?"
2.527 CP SECONDS COMPILATION TIME 10000

"WHAT IS THE INITIAL BORE ANGLE, ALSO THE INITIAL TARGET VELOCITY ANGLE, I
90 0

"WHAT IS THE TARGET VELOCITY AND THE MISSLE VELOCITY?"970 970

"STORE(N)=" -6669.380616523 7451.131604793 0. 0. 970. 0.

TIME	VELOCITY 1	VELOCITY 2	ACCEL 1	ACCEL 2	POSITION 1	POSITION 2
0.00	970.000	0.000	64.400	257.600	-6669.381	7451.132

TIME	RELATIVE DIST-X1	RELATIVE DIST-X2	RELATIVE VELOC-X1	RELATIVE VELOC-X2	ABSOLUTE VELOC-X1	ABSOLUTE VELOC-X2	FINTIM
.10	-6673.536	7446.913	-81.884	-86.488	1057.982	112.331	10.00
.20	-6685.499	7433.445	-156.022	-184.637	1137.535	236.474	10.00
.30	-6704.469	7409.662	-222.013	-292.500	1208.257	370.464	10.00
.40	-6729.630	7374.679	-279.875	-408.368	1270.167	512.573	10.00
.50	-6760.183	7327.769	-329.908	-530.817	1323.569	661.359	10.00
.60	-6795.366	7268.334	-372.581	-658.706	1368.934	815.664	10.00
.70	-6834.472	7195.876	-408.446	-791.158	1406.815	974.591	10.00
.80	-6876.848	7109.973	-438.075	-927.516	1437.787	1137.468	10.00
.90	-6921.898	7010.259	-462.020	-1067.309	1462.406	1303.283	10.00
1.00	-6968.760	6896.076	-474.247	-1216.756	1474.642	1479.803	9.37
1.10	-7015.955	6766.271	-468.506	-1379.533	1468.249	1669.124	8.51
1.20	-7061.502	6619.534	-441.133	-1555.100	1439.566	1871.211	7.79
1.30	-7103.029	6454.635	-387.944	-1742.411	1384.417	2085.001	7.19
1.40	-7137.715	6270.482	-304.231	-1939.721	1298.096	2308.736	6.68
1.50	-7162.256	6066.207	-184.990	-2144.249	1175.606	2539.616	6.24
1.60	-7172.832	5841.284	-25.076	-2351.962	1011.808	2773.595	5.86
1.70	-7165.130	5595.667	180.241	-2557.280	801.977	3005.079	5.53
1.80	-7134.402	5329.952	434.802	-2753.015	542.279	3226.865	5.25
1.90	-7076.356	5045.613	729.181	-2929.661	242.148	3429.438	5.00
2.00	-6988.002	4744.848	1040.496	-3081.483	-75.531	3607.033	4.78
2.10	-6867.783	4430.146	1366.046	-3208.423	-408.046	3759.595	4.60
2.20	-6714.400	4103.987	1703.380	-3310.645	-752.940	3887.270	4.44
2.30	-6526.788	3768.829	2050.283	-3388.495	-1107.991	3990.391	4.31
2.40	-6304.091	3427.085	2404.767	-3442.450	-1471.294	4068.483	4.20
2.50	-6045.642	3081.116	2765.052	-3473.090	-1840.789	4114.932	4.11
2.60	-5750.941	2733.223	3129.549	-3481.067	-2215.151	4137.561	4.03
2.70	-5424.394	2394.086	3398.685	-3297.086	-2494.707	3998.003	3.96
2.80	-5071.610	2074.419	3654.863	-3093.247	-2761.852	3818.345	3.95
2.90	-4693.869	1776.023	3897.613	-2871.839	-3016.108	3620.867	3.94
3.00	-4292.574	1500.606	4125.757	-2633.795	-3256.288	3406.490	3.94
3.10	-3869.242	1249.785	4338.182	-2380.124	-3481.270	3176.215	3.93
3.20	-3425.497	1025.066	4533.847	-2111.913	-3690.006	2931.117	3.92
3.30	-2963.064	827.848	4711.789	-1830.314	-3881.519	2672.339	3.91
3.40	-2483.883	659.204	4862.195	-1551.554	-4045.992	2416.099	3.91
3.50	-1993.395	513.778	4934.084	-1378.325	-4132.432	2265.081	3.90
3.60	-1498.756	380.699	4952.300	-1294.702	-4165.674	2203.345	3.90
3.70	-1003.779	253.293	4945.080	-1257.426	-4173.947	2187.637	3.90
3.80	-510.155	128.443	4927.824	-1238.690	-4172.639	2190.131	3.90

"DISTANCE" 9040.094791055 "TIME" 3.884999999997
"DISTANCE" 4868.779972713 "TIME" 3.889999999997
"DISTANCE" 1978.415628753 "TIME" 3.894999999997

3.90	-18.537	4.958	4907.101	-1226.031	-4168.310	2198.358	3.90

"DISTANCE" 368.1984470557 "TIME" 3.899999999997
"DISTANCE" 37.31881408849 "TIME" 3.904999999997

FIGURE 10

```
    TIME          CONTROL MAGNITUDE
     .10                 1090.619
     .20                 1113.705
     .30                 1128.073
     .40                 1135.286
     .50                 1136.818
     .60                 1133.985
     .70                 1127.918
     .80                 1119.564
     .90                 1109.694
    1.00                 1186.871
    1.10                 1329.691
    1.20                 1490.590
    1.30                 1672.231
    1.40                 1877.361
    1.50                 2106.454
    1.60                 2359.696
    1.70                 2633.593
    1.80                 2923.010
    1.90                 3220.000
    2.00                 3220.000
    2.10                 3220.000
    2.20                 3220.000
    2.30                 3220.000
    2.40                 3220.000
    2.50                 3220.000
    2.60                 3220.000
    2.70                 3220.000
    2.80                 3220.000
    2.90                 3220.000
    3.00                 3220.000
    3.10                 3220.000
    3.20                 3220.000
    3.30                 3220.000
    3.40                 2385.244
    3.50                 1064.747
    3.60                  362.950
    3.70                   67.456
    3.80                    4.923
    3.90                     .298
"AT TIME" 3.904999999997 "THE MISS-DISTANCE WAS" 6.10891267645
     STOP
     42.943 CP SECONDS EXECUTION TIME
..RUN:FTN
```


FIGURE 10 (CONT'D)

2.494 CP SECONDS COMPILATION TIME

"H=" .005 "TUPDATE=" .1 "S=" 20. "Q7=" .0001
"WHAT IS THE INITIAL RANGE IN FT/SEC?" 2000

"WHAT IS THE INITIAL BORE ANGLE, ALSO THE INITIAL TARGET VELOCITY ANGLE:
0 180

"WHAT IS THE TARGET VELOCITY AND THE MISSLE VELOCITY?"970 970

"STORE(N)=" 2000. 0. -1550.506266986 -777.1180566618 970. 0.

TIME	VELOCITY 1	VELOCITY 2	ACCEL 1	ACCEL 2	POSITION 1	POSITION 2
0.00	-580.506	-777.118	167.836	-205.758	2000.000	0.000
.40	-509.166	-855.738	188.447	-187.064	1781.791	-326.821
.80	-430.084	-926.569	206.542	-166.870	1590.699	-683.551
1.20	-344.269	-989.077	222.114	-145.501	1438.621	-1066.966
1.60	-252.727	-1042.854	235.186	-123.259	1319.047	-1473.648
2.00	-156.448	-1087.605	245.806	-100.421	1237.071	-1900.045
2.40	-56.399	-1123.145	254.046	-77.238	1194.392	-2342.504
2.80	46.483	-1149.380	259.992	-53.938	1192.329	-2797.320
3.20	151.302	-1166.307	263.744	-30.725	1231.836	-3260.767
3.60	257.201	-1173.996	265.414	-7.780	1313.514	-3729.134
4.00	363.371	-1172.588	265.119	14.736	1437.633	-4198.751
4.40	469.050	-1162.284	262.982	36.682	1604.146	-4666.018
4.80	573.528	-1143.335	259.130	57.938	1812.713	-5127.485
5.20	676.143	-1116.039	253.690	78.399	2062.719	-5579.572
5.60	776.285	-1080.733	246.791	97.977	2353.297	-6019.188
6.00	873.397	-1037.785	238.558	116.598	2683.343	-6443.140
6.40	966.971	-987.590	229.117	134.204	3051.543	-6848.449
6.80	1056.546	-930.564	218.588	150.746	3456.386	-7232.301
7.20	1141.712	-867.140	207.091	166.189	3896.191	-7592.047
7.60	1222.104	-797.763	194.737	180.506	4369.119	-7925.219
8.00	1297.402	-722.887	181.638	193.682	4873.195	-8229.525
8.40	1367.329	-642.971	167.897	205.708	5406.325	-8502.857
8.80	1431.648	-558.474	153.614	216.583	5966.311	-8743.291
9.20	1490.160	-469.858	138.883	226.311	6550.869	-8949.087
9.60	1542.706	-377.577	123.794	234.905	7157.643	-9118.688
10.00	1589.159	-282.083	108.430	242.380	7784.221	-9250.720

FIGURE 11

```
 TIME  RELATIVE   RELATIVE   RELATIVE   RELATIVE   ABSOLUTE   ABSOLUTE
        DIST-X1    DIST-X2    VELOC-X1   VELOC-X2   VELOC-X1   VELOC-X2 FINTIM
  .10  1842.906    -62.269 -1574.546   -466.360   1011.094   -331.109    1.15
  .20  1686.258    -97.152 -1560.789   -251.820   1014.922   -565.543    1.15
  .30  1529.851   -115.523 -1572.192   -125.240   1044.425   -711.550    1.15
  .40  1370.967   -123.533 -1608.938    -39.307   1099.772   -816.431    1.15
  .50  1207.505   -123.981 -1662.397     28.525   1172.314   -902.724    1.15
  .60  1038.137   -118.081 -1726.227     88.914   1255.697   -981.077    1.15
  .70   862.076   -106.222 -1795.932    148.128   1345.407  -1057.751    1.15
  .80   678.835    -88.389 -1869.758    208.510   1439.673  -1135.080    1.15
  .90   488.022    -64.435 -1947.347    270.556   1538.125  -1213.551    1.15
 1.00   288.757    -34.836 -2036.601    324.211   1648.645  -1283.103    1.15
"DISTANCE" 9798.052147574 "TIME" 1.09
"DISTANCE" 7755.254608648 "TIME" 1.095
 1.10    77.006     -4.306 -2174.329    319.097   1808.030  -1293.252    1.14
"DISTANCE" 5948.536692186 "TIME" 1.1
"DISTANCE" 4376.740831691 "TIME" 1.105
"DISTANCE" 3040.303876652 "TIME" 1.11
"DISTANCE" 1943.320175991 "TIME" 1.115
"DISTANCE" 1089.8953458 "TIME" 1.12
"DISTANCE" 484.1461461131 "TIME" 1.125
"DISTANCE" 130.2012368641 "TIME" 1.13
"DISTANCE" 32.42778975269 "TIME" 1.135

   TIME          CONTROL MAGNITUDE
    .10                   3063.482
    .20                   1497.936
    .30                    747.450
    .40                    359.814
    .50                    164.900
    .60                     68.707
    .70                     27.238
    .80                      6.255
    .90                      9.447
   1.00                     60.688
   1.10                     74.485
"AT TIME" 1.135 "THE MISS-DISTANCE WAS" 5.69454034604l
     STOP
      5.667 CP SECONDS EXECUTION TIME
..RUN;FTN
```

FIGURE 11 (CONT'D)

```
     2.479 CP SECONDS COMPILATION TIME
"H=" .005 "TUPDATE=" .1 "S=" 20. "D7=" .0001
"WHAT IS THE INITIAL RANGE IN FT/SEC?" 1500

"WHAT IS THE INITIAL BORE ANGLE, ALSO THE INITIAL TARGET VELOCITY ANGLE.
0,45

"WHAT IS THE TARGET VELOCITY AND THE MISSLE VELOCITY?" 450,970

"STORE(N)=" 1500. 0. -460.437670846 [illegible]
```

TIME	VELOCITY 1	VELOCITY 2	ACCEL 1	ACCEL 2	POSITION 1	POSITION 2
0.00	509.562	825.376	-185.[illegible]	190.121	1500.000	0.000
.40	431.554	897.385	-204.[illegible]	165.679	1688.475	344.[illegible]
.80	346.522	960.95[illegible]	-220.[illegible]	147.965	1844.307	[illegible].781
1.20	255.519	1015.631	-234.[illegible]	125.304	1964.897	1112.402
1.60	159.582	1061.1[illegible]	-245.158	101.[illegible]	2048.064	1588.058
2.00	59.725	1097.1[illegible]	-253.[illegible]	78.307	2092.040	1960.001
2.40	-43.072	1123.[illegible]	[illegible]	54.488	2095.483	2404.530
2.80	-147.871	[illegible]	-26[illegible]	30.752	2057.316	2857.74[illegible]
3.20	-253.775	1148.374	-265.428	7.298	1977.009	3315.892
3.60	-359.929	1146.675	-265.063	-15.705	1854.2[illegible]	3777.10[illegible]
4.00	-465.569	1135.[illegible]	-262.779	-38.106	[illegible]	[illegible]
4.40	-569.925	1116.287	-258.712	-59.778	1481.97[illegible]	[illegible]
4.80	-672.319	1088.180	-252.996	-80.611	123[illegible]	[illegible]
5.20	-772.120	1051.923	-245.770	-100.511	[illegible].487	[illegible]
5.60	-868.751	1007.906	-237.167	-119.402	616.178	[illegible]
6.00	-961.688	956.544	-227.321	-137.[illegible]	249.958	[illegible]
6.40	-1050.460	898.276	-216.361	-153.[illegible]	-152.61[illegible]	6780.734
6.80	-1134.645	833.558	-204.412	-169.[illegible]	-589.7[illegible]	7075.308
7.20	-1213.874	762.856	-191.594	-183.839	-1059.672	7394.782
7.60	-1287.821	686.646	-178.024	-197.009	-1560.192	7684.858
8.00	-1356.207	605.409	-163.812	-208.976	-2089.187	7943.429
8.40	-1418.798	519.626	-149.062	-219.740	-2644.385	8168.580
8.80	-1475.398	429.777	-133.874	-229.310	-3223.427	8358.588
9.20	-1525.851	336.336	-118.341	-237.699	-3823.884	8511.922
9.60	-1570.037	239.773	-102.551	-244.925	-4443.272	8627.240
10.00	-1607.869	140.548	-86.587	-251.013	-5079.066	8703.386

FIGURE 12

THIS PAGE IS BEST QUALITY PRACTICABLE
FROM COPY FURNISHED TO DDC

TIME	RELATIVE DIST-X1	RELATIVE DIST-X2	RELATIVE VELOC-X1	RELATIVE VELOC-X2	ABSOLUTE VELOC-X1	ABSOLUTE VELOC-X2	FINTIM
.10	1449.965	67.642	-528.719	539.882	1019.496	304.259	1.59
.20	1394.903	111.710	-570.593	348.649	1042.095	513.754	2.02
.30	1335.941	138.573	-608.489	192.397	1060.244	687.757	2.29
.40	1273.168	150.765	-647.531	53.802	1079.085	843.583	2.40
.50	1206.206	149.805	-692.680	-71.465	1103.593	985.552	2.37
.60	1134.049	137.109	-751.709	-181.561	1141.559	1111.814	2.25
.70	1054.737	114.504	-835.591	-270.433	1203.972	1216.310	2.08
.80	965.068	84.666	-957.790	-327.396	1304.312	1288.346	1.91
.90	860.429	51.703	-1132.016	-335.145	1456.306	1310.613	1.76
1.00	736.443	20.224	-1340.450	-301.980	1642.152	1291.403	1.63
1.10	590.190	-5.557	-1571.674	-229.087	1850.447	1231.900	1.54
1.20	419.818	-21.415	-1815.146	-118.444	2070.665	1134.075	1.47
1.30	224.879	-24.033	-2058.605	19.326	2290.562	1008.547	1.43

```
"DISTANCE" 9613.185504973 "TIME" 1.36
"DISTANCE" 7555.875388323 "TIME" 1.365
"DISTANCE" 5737.091605386 "TIME" 1.37
"DISTANCE" 4161.760945142 "TIME" 1.375
"DISTANCE" 2834.835725761 "TIME" 1.379999999999
"DISTANCE" 1761.29365868 "TIME" 1.384999999999
"DISTANCE" 946.3377675426 "TIME" 1.389999999999
"DISTANCE" 395.33890414 "TIME" 1.394999999999
 1.40     5.239    -9.254 -2325.134   266.215  2533.237   778.320   1.41
"DISTANCE" 113.0822954004 "TIME" 1.399999999999
"DISTANCE" 103.6466255692 "TIME" 1.404999999999
```

TIME	CONTROL MAGNITUDE
.10	2412.485
.20	1611.839
.30	1268.990
.40	1047.280
.50	842.979
.60	596.271
.70	267.089
.80	171.687
.90	726.803
1.00	1008.920
1.10	1102.229
1.20	960.236
1.30	525.309
1.40	1146.232

```
"AT TIME" 1.404999999999 "THE MISS-DISTANCE WAS" 10.1806986 7785
     STOP
      7.433 CP SECONDS EXECUTION TIME
..RUN,FTN
%A
%A
```

FIGURE 12 (CONT'D)

```
2000 0 90 970 970

"H=" .005 "TUPDATE=" .1 "S=" 20. "07=" .0001
"WHAT IS THE INITIAL RANGE IN FT/SEC?"
      2.486 CP SECONDS COMPILATION TIME
"WHAT IS THE INITIAL BORE ANGLE, ALSO THE INITIAL TARGET VELOCITY ANGLE, ]
0 90

"WHAT IS THE TARGET VELOCITY AND THE MISSLE VELOCITY?"970,970

"STORE(N)=" 2000. 0. -1404.631407645 867.1767636925 970. 0.
```

TIME	VELOCITY 1	VELOCITY 2	ACCEL 1	ACCEL 2	POSITION 1	POSITION 2
0.00	-434.631	867.177	-259.149	-57.850	2000.000	0.000
.40	-536.883	838.627	-251.673	-84.652	1805.597	341.518
.80	-635.640	799.665	-241.727	-109.878	1570.960	669.513
1.20	-729.974	750.955	-229.601	-133.374	1297.675	979.950
1.60	-819.068	693.212	-215.574	-155.026	987.680	1269.072
2.00	-902.216	627.191	-199.915	-174.754	643.215	1533.416
2.40	-978.817	553.672	-182.882	-192.508	266.781	1769.825
2.80	-1048.370	473.451	-164.716	-208.264	-138.899	1975.460
3.20	-1110.469	387.328	-145.645	-222.020	-570.921	2147.800
3.60	-1164.794	296.100	-125.880	-233.793	-1026.237	2284.642
4.00	-1211.107	200.553	-105.619	-243.618	-1501.687	2384.104
4.40	-1249.247	101.459	-85.041	-251.541	-1994.032	2444.612
4.80	-1279.120	-.434	-64.313	-257.622	-2499.982	2464.898
5.20	-1300.697	-104.402	-43.583	-261.927	-3016.222	2443.988
5.60	-1314.005	-209.749	-22.989	-264.531	-3539.437	2381.193
6.00	-1319.123	-315.810	-2.653	-265.515	-4066.333	2276.094
6.40	-1316.176	-421.956	17.316	-264.963	-4593.659	2128.534
6.80	-1305.331	-527.587	36.823	-262.962	-5118.221	1938.598
7.20	-1286.791	-632.144	55.780	-259.603	-5636.898	1706.607
7.60	-1260.790	-735.101	74.115	-254.975	-6146.659	1433.097
8.00	-1227.591	-835.967	91.764	-249.168	-6644.571	1118.806
8.40	-1187.478	-934.289	108.672	-242.271	-7127.810	764.663
8.80	-1140.758	-1029.651	124.794	-234.375	-7593.672	371.769
9.20	-1087.753	-1121.668	140.092	-225.565	-8039.578	-58.612
9.60	-1028.798	-1209.992	154.535	-215.926	-8463.081	-525.072
10.00	-964.241	-1294.309	168.102	-205.540	-8861.870	-1026.071

FIGURE 13

```
TIME  RELATIVE  RELATIVE  RELATIVE  RELATIVE  ABSOLUTE  ABSOLUTE
       DIST-X1   DIST-X2   VELOC-X1  VELOC-X2  VELOC-X1  VELOC-X2 FINTIM
 .10  1855.316    70.078 -1474.518   539.110  1014.051   321.939   1.21
 .20  1706.478   110.762 -1500.763   288.179  1014.632   566.063   1.28
 .30  1555.142   129.562 -1528.038    95.765  1016.429   750.999   1.32
 .40  1400.328   131.151 -1571.069   -59.436  1034.186   898.062   1.32
 .50  1239.857   118.934 -1640.692  -182.843  1078.754  1012.680   1.29
 .60  1070.425    96.299 -1748.402  -270.406  1161.643  1090.813   1.25
 .70   887.754    67.292 -1901.435  -314.194  1290.103  1124.540   1.21
 .80   687.376    36.723 -2096.097  -308.546  1460.456  1108.211   1.16
 .90   465.300    10.422 -2324.835  -243.986  1665.162  1032.361   1.12
1.00   219.299    -5.826 -2568.479  -124.022  1885.065   900.507   1.10
"DISTANCE" 7727.748783127 "TIME" 1.05
"DISTANCE" 5541.136151146 "TIME" 1.055
"DISTANCE" 3713.138362398 "TIME" 1.06
"DISTANCE" 2249.178098009 "TIME" 1.065
"DISTANCE" 1154.679181964 "TIME" 1.07
"DISTANCE" 435.0663044989 "TIME" 1.075
"DISTANCE" 95.76474872228 "TIME" 1.08

   TIME          CONTROL MAGNITUDE
    .10                 2709.948
    .20                 1800.151
    .30                 1256.564
    .40                  841.864
    .50                  441.204
    .60                    1.692
    .70                  436.643
    .80                  759.030
    .90                  879.522
   1.00                  666.376
"AT TIME" 1.08 "THE MISS-DISTANCE WAS" 9.785946490876
      STOP
       5.803 CP SECONDS EXECUTION TIME
..RUN;FTN
```

FIGURE 13 (CONT'D)

Items for Further Study

(1) It is believed that inclusion of target acceleration is desirable in target-seeking control laws. This necessitates a predictive estimator for supplying estimates of the future target trajectory. Such estimates should be model-independent.

(2) It is believed that the constraint upon missile thrust is essential in design of a control law. This has been included on an ad-hoc basis only prior to this report. The constraint in this report proved to be inadequate, however. This implies that a non-linear model must be adopted. Further study is required to select a suitable non-linear model and a control synthesis technique which permits a computationally feasible control law to be implemented on-board a missile. It is presently unknown how to include the cost of computation in a design cost function.

(3) Since a control law based upon non-linear design must be used with an estimator, study should be directed toward optimization of the estimation and control laws simultaneously. The separation property of linear-quadratic design probably does not hold for the non-linear model.

(4) A serious limitation on optimal control schemes is that time-to-go is not readily available. The simulation studies conducted herein indicate that the present algorithm is very sensitive to the time-to-go estimate. A comprehensive theory is needed accounting for the stability and the optimality of the time-to-go estimate.

(5) A theory of sensitivity of cost to initial conditions is needed. Included in this broad category is the important question of finding a way to reflect the desired payoff - the inner launch boundary - in the cost function.

References

(1) Sage and White, Optimum System Control, 2nd ed., Prentice Hall, 1977.

(2) Schultz, Peter, "An Optimal Control Problem with State Vector Measurement Errors", Advances in Control Systems, Vol. I, Academic Press, 1964.

(3) Fleming, Wendell, and Raymond Rishel, Deterministic and Stochastic Optimal Control, Springer-Verlag, 1975.

1978 UASF-ASEE SUMMER FACULTY RESEARCH PROGRAM
Sponsored by
THE AIR FORCE OFFICE OF SCIENTIFIC RESEARCH
conducted by
AUBURN UNIVERSITY AND OHIO STATE UNIVERSITY

PARTICIPANTS FINAL REPORT

WIDE-BAND RADOME RESEARCH IN REFRACTIVE ERROR CORRECTION

Prepared by:	Louis A. DeAcetis, Ph.D.
Academic Rank:	Professor of Physics
Department and University:	Department of Physics City University of New York Bronx Community College
Assignment:	Eglin Air Force Base Air Force Armament Laboratory Guided Weapons Division Air-to Air Missiles Branch
USAF Research Colleague:	Fred E. Howard and Joseph B. Oliphint

Date:	28 July, 1978
Contract No:	F44620-75-C-0031

CONTENTS

ABSTRACT

A study was made of the relevant design factors for radomes on air-to-air missiles travelling at hypersonic speeds. Textbooks, journal articles, and government reports were reviewed, and a bibliography of some of the more relevant sources is included. Methods to calculate the "boresight error" introduced by a radome are considered, including ray-tracing and a recently programmed electromagnetic field calculation. It is concluded that a two-dimensional major-plane-only ray tracing formulation is inadequate to determine either the absolute error or the trend in the error as the physical parameters of the radome are varied. Since the possibility of a "lensed" radome with a layer or layers of ablative material is currently under serious consideration, a library search to determine the effects of ablative materials and ablation on the radome was also made, but its results were inconclusive. Finally, several programs were written utilizing the Tektronix 4014-1 graphics terminal in order to visually display and compare some of the radome shapes and ray-tracing techniques.

ACKNOWLEDGEMENTS

In most texts, reports, articles, etc., where an "acknowledgement" appears, it is usually rivaled only by the "bibliography" for its dryness. Most readers are not concerned with its contents which are usually directed and meaningful to only the small number of people mentioned. It is for these reasons that I will name no names nor express individual thanks. I will say only that I have been fortunate to have spent ten weeks in a most enjoyable and rewarding setting, working with colleagues who created an atmosphere conducive to research, in a program that is efficiently and professionally run, in an office with competent and courteous secretarial staffing. Those people responsible will recognize who they are (Right Fred, Joe, Fred, and Karen?), and to all of them I say thanks.

I. INTRODUCTION

The problem of the distortion of radar frequency (RF) radiation passing through a radar dome (radome) has existed since the advent of airborne radar during World War II.[1] As is well known, the best shape electrically would be a hemispherical shell of uniform thickness with a detector at the center of curvature (the thickness would depend upon the incident frequency). Unfortunately, such a shape is too blunt from an aerodynamic point of view, especially for high speed flight. It was the objective of this ten week project under the USAF/ASEE Summer Faculty Associate Program to investigate past work done on the design of radomes for hypersonic flight, to evaluate some of the current work in radome distortion calculation, and to explore other approaches that might prove fruitful.

II. RADOME SHAPES

In general, four basic shapes have been used for radomes: cone, ogive, VonKarman, and power series (Fig. 1).[2] Current analytical work and experimental results indicate that a half-power radome (i.e., the surface of revolution generated by the curve $Y = (D/2)(X/L)^{1/2}$) may have the best aerodynamic characteristics for hypersonic flight.[3] Given this outer shape of the radome, perhaps uniformly coated with ablative material(s) to protect it against rain and intensive heating, the question then arises as to what distortions are introduced by such a shape. Next, can these distortions be eliminated (or minimized) by varying some of the material parameters, including the shape of the innermost wall of the radome?

Before attempting to answer the above questions, a clearer definition of the "distortion" is needed. When radiation passes through a radome, it is refracted as it passes through the radome material and its amplitude distribution is changed (Fig. 2). From a practical point of view, these factors manifest themselves as an apparent shift in the direction of the radiation from what it would be were the radome not there (Free-space condition). This shift is called the "boresight error" and it is a nonlinear function of the "look angle". In addition, the change in the boresight error per unit angle ("boresight error slope") is an important parameter in missile guidance stability. Thus, calculation, evaluation, and minimization of boresight error is a significant aspect of radome design.

RADOME PROFILES

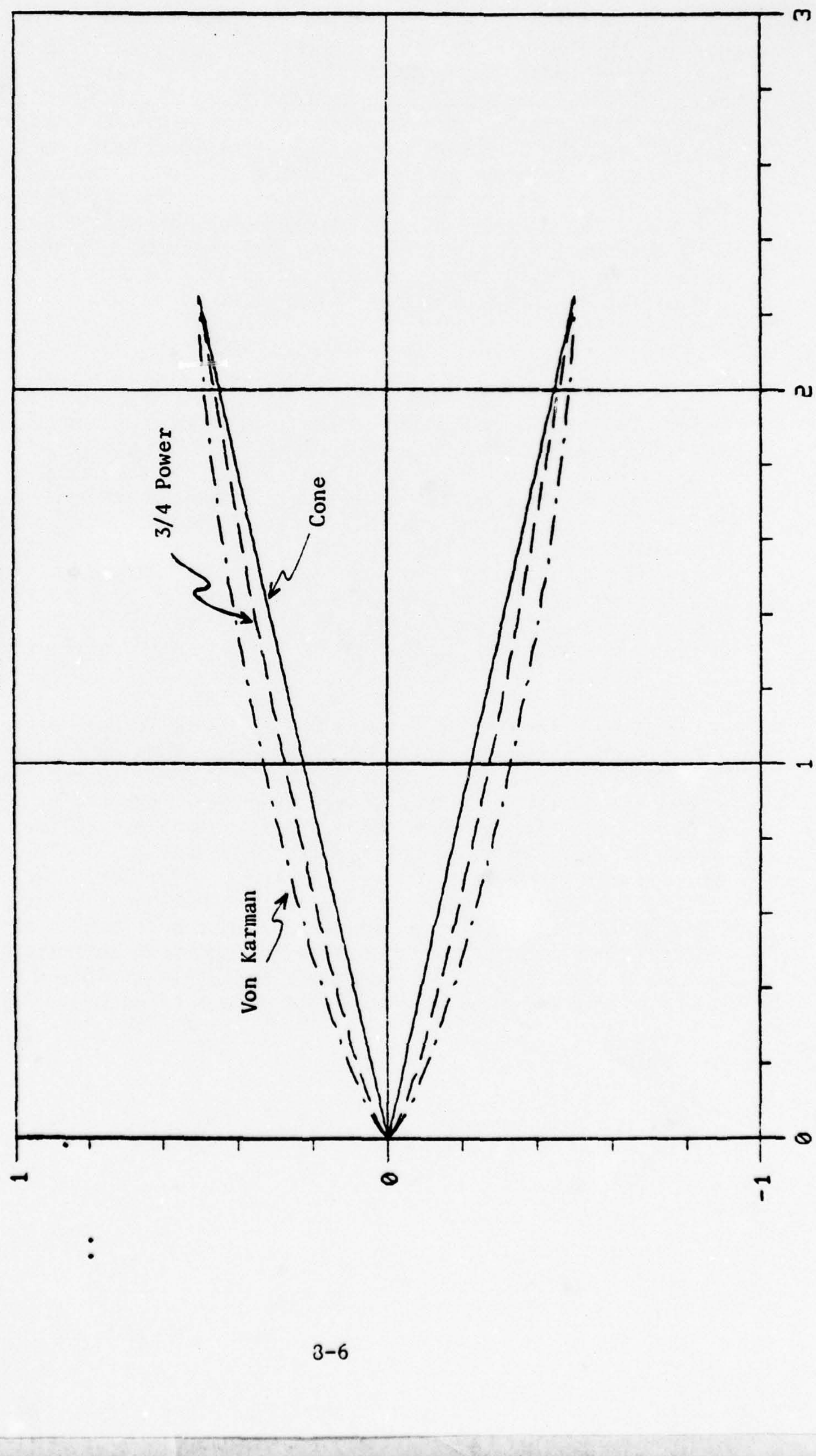

Fig. 1

III. THEORETICAL BORESIGHT ERROR ANALYSIS

Since radome construction and testing are costly endeavors, analytical approaches to both the aerodynamic and electrical properties of a radome have been used, especially since the advent of high speed computers. Several recent reports have considered a two-dimensional analysis of boresight error using ray-tracing techniques[4], which follow incident rays as they are refracted by the radome structure. Figures 3 - 6 are examples of such ray-tracing techniques. These results were generated on the Tektronix 4014 at Eglin AFB, using a program written by the author. Phase or wave-fronts can be represented (as in Fig. 2) by measuring equal optical path lengths along each of the rays, and connecting these points. Figures 5 and 6 are "lensed" radomes where the inner surface is not designed to be parallel to the outer one.

In Figures 3 - 6, the radiation is seen passing through the major plane of the radome, i.e., a plane which cuts the radome in half. It was hoped that such a major-plane-only simulation might lead to an adequate indication of boresight error, or at least allow meaningful comparisons to be made between various radome shapes and antenna locations.[5] Groutage and Smith apparently have proceeded in their earlier work precisely on this assumption. Crowe[6], however, convincingly shows that the contributions from radiation passing through other parts of the radome can have a significant effect on the boresight error, and he concludes that "a major-plane-only simulation cannot, in general, be expected to adequately represent the electrical performance of a radome."[7]

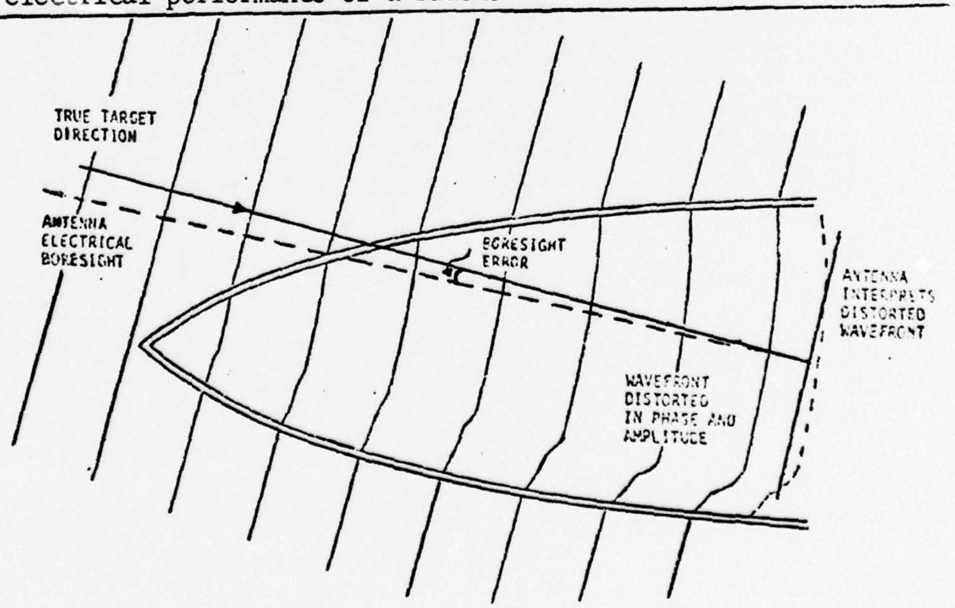

Fig. 1. From Crowe, P. 2-2.

INDICES OF REFRACTION XN1,XN2:

1.,1.5

SLOPE OF INCIDENT RADIATION (XM1):

-1.

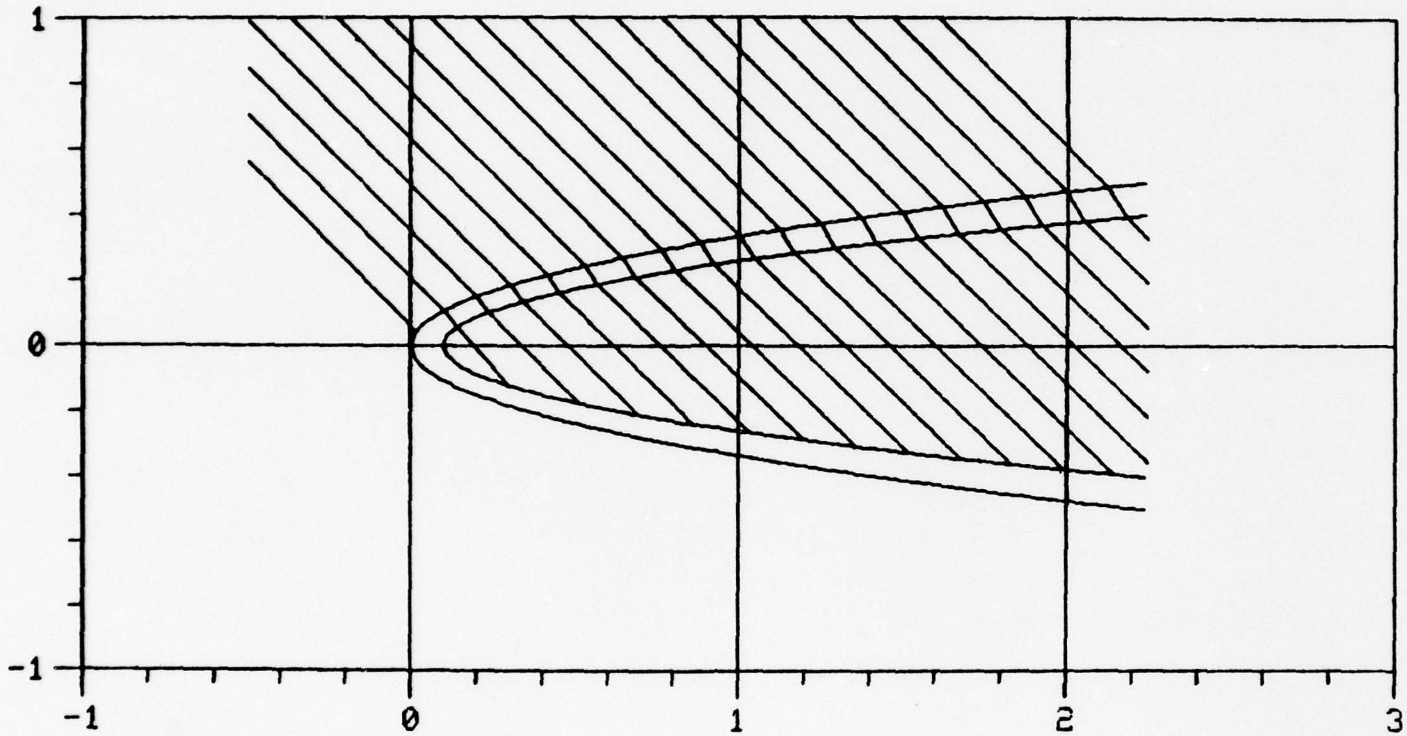

Fig. 3

INDICES OF REFRACTION XN1,XN2:

1.,1.5

SLOPE OF INCIDENT RADIATION (XM1):

-.1

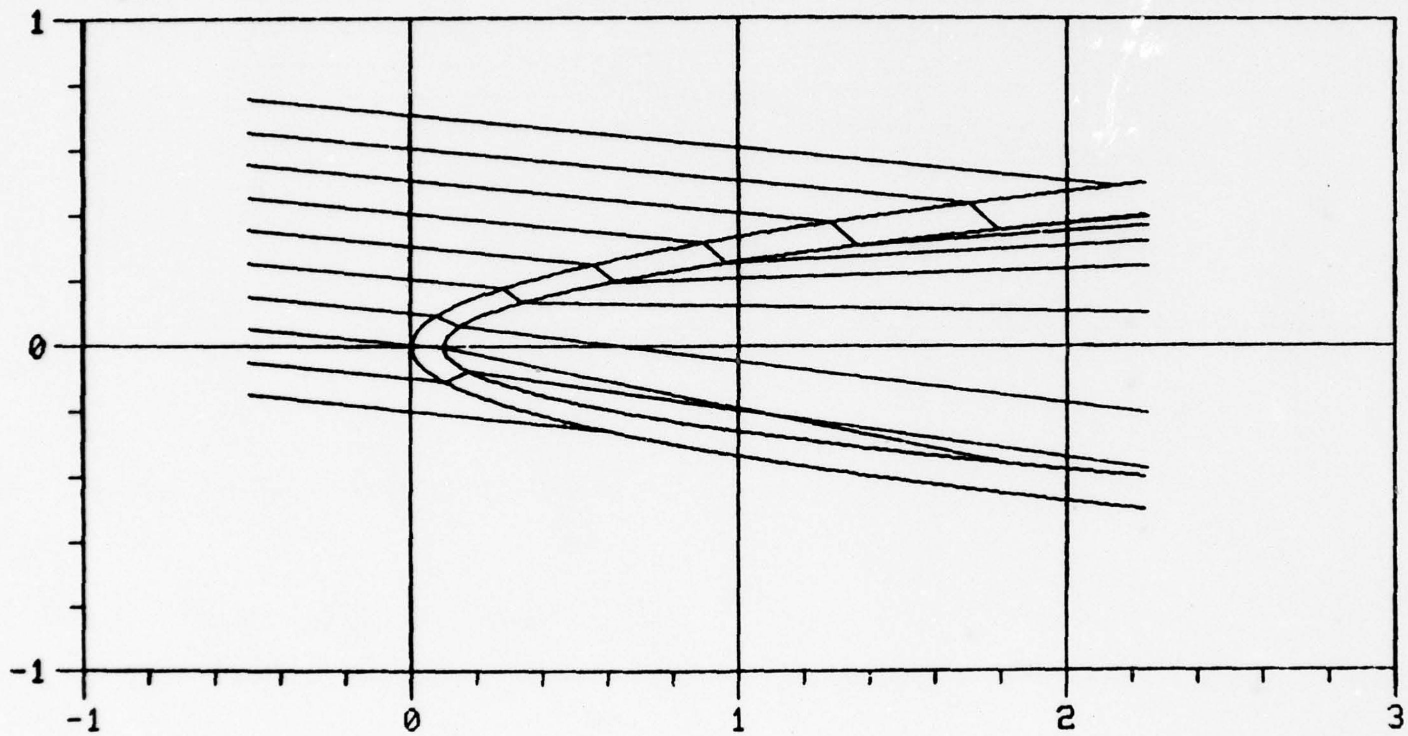

Fig. 4

INDICES OF REFRACTION XN1,XN2:

1.,1.5

SLOPE OF INCIDENT RADIATION (XM1):

.00001

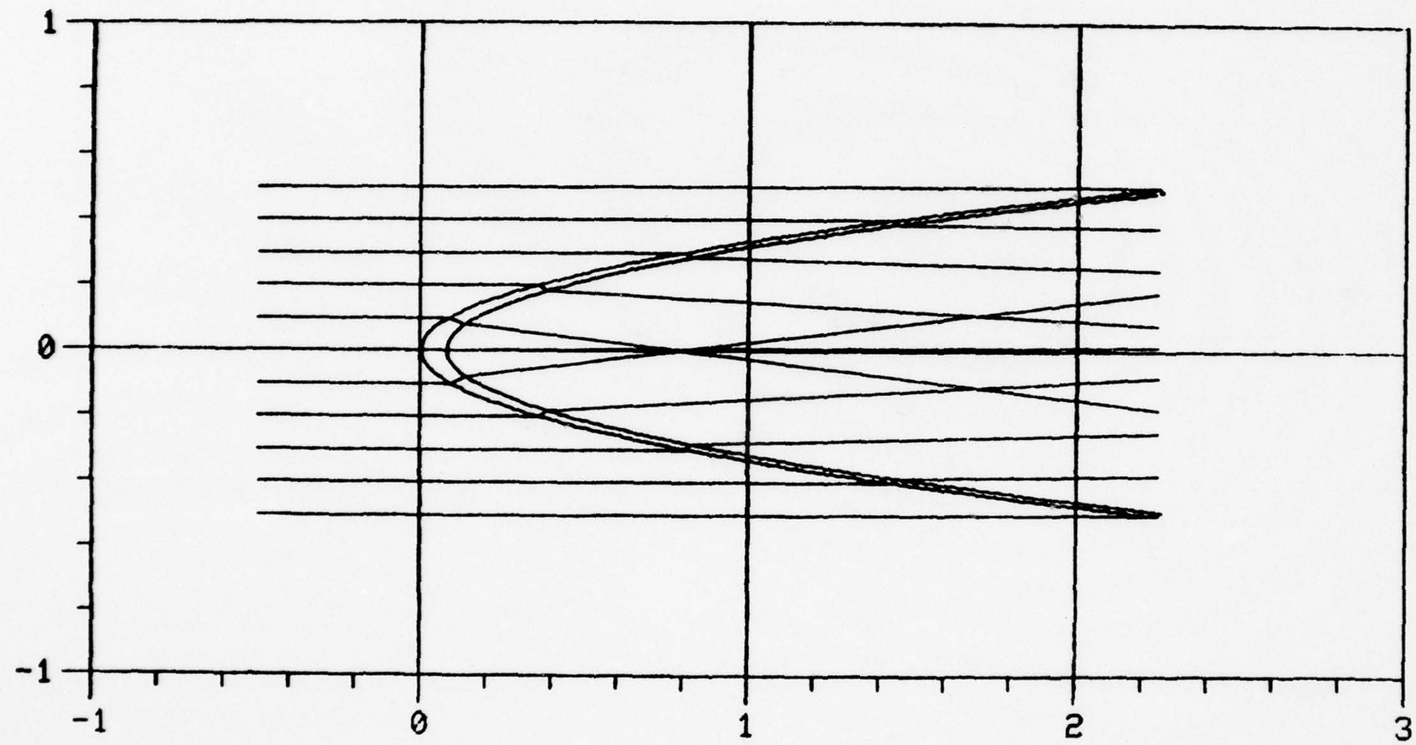

Fig. 5

INDICES OF REFRACTION XN1,XN2:

1.,1.732

SLOPE OF INCIDENT RADIATION (XM1):

-.1

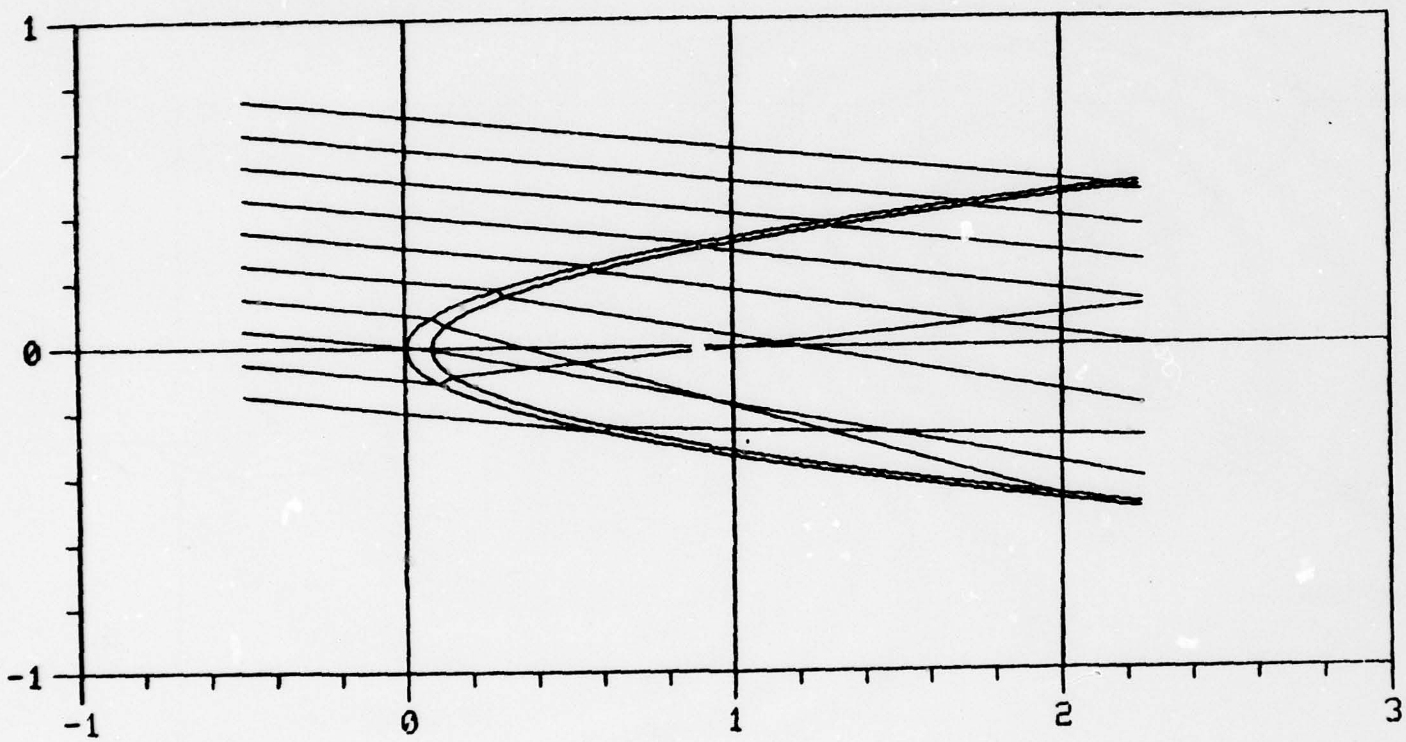

Fig. 6

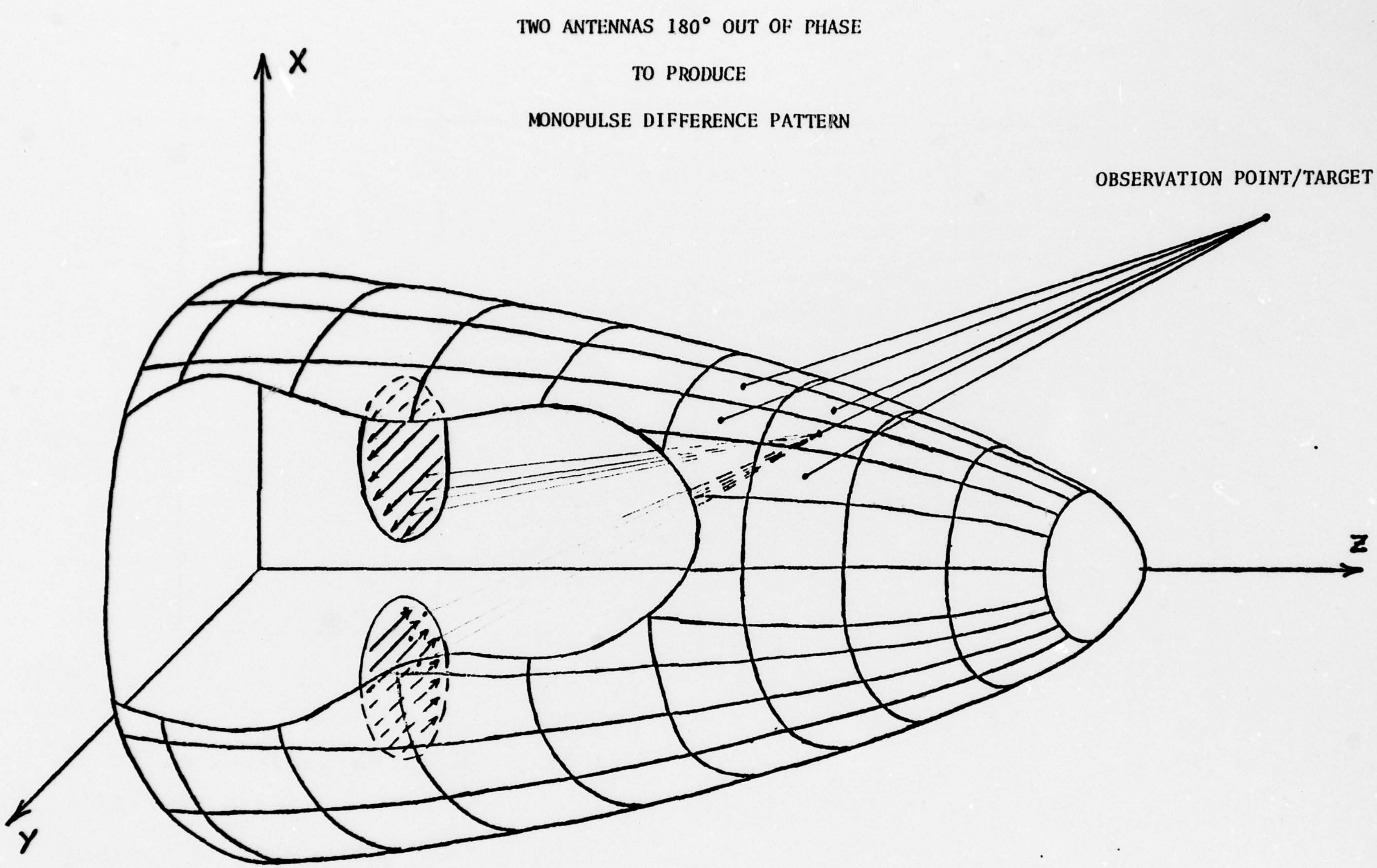

Fig. 7. From Groutage and Smith.

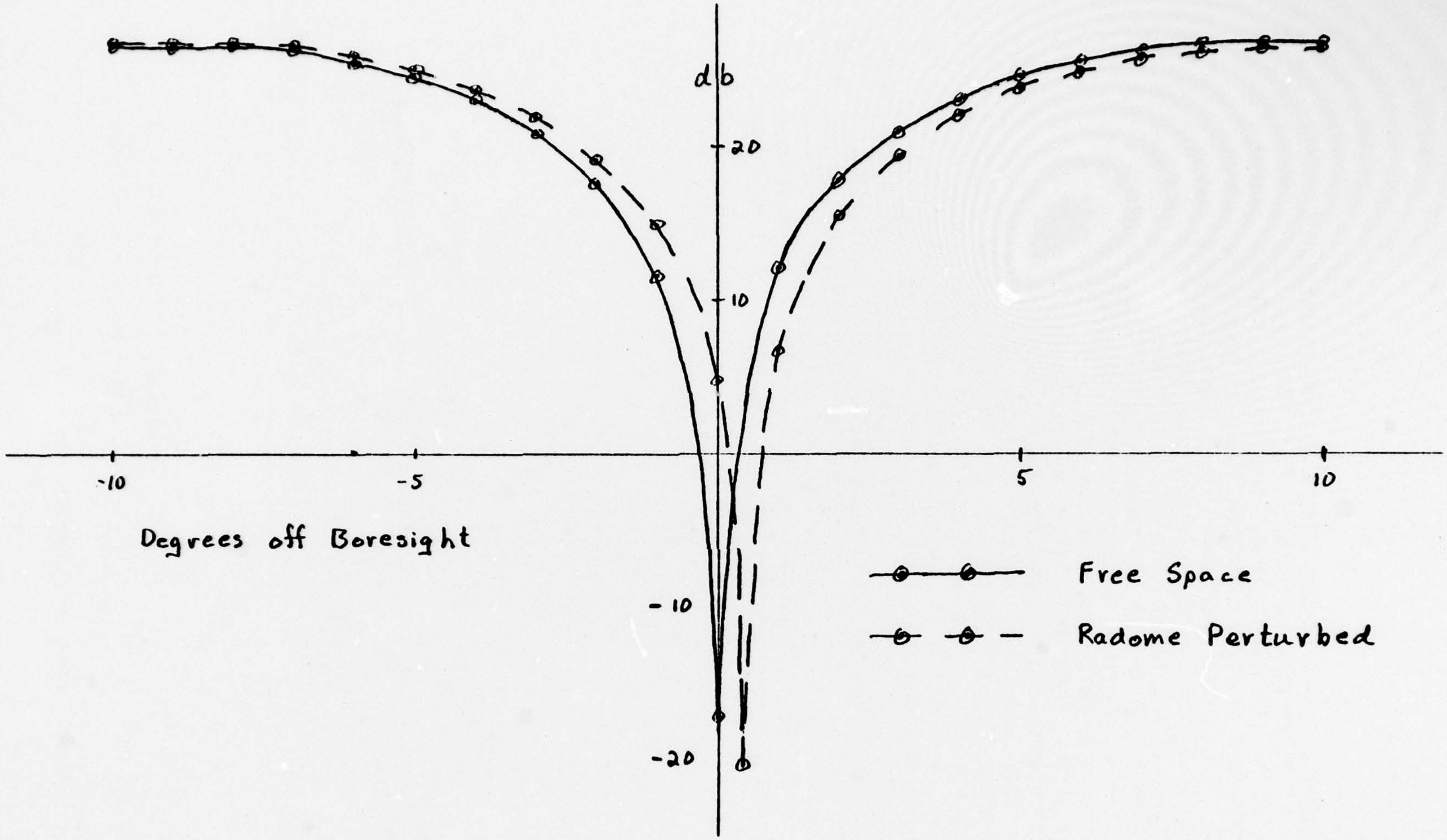

Far Field Difference Pattern

Fig. 8. From Groutage and Smith.

With the need for a three-dimensional analysis established, Crowe extended his ray-trace work to a "multi-plane simulation."[8] Groutage and Smith[9] have also recently programmed a 3-D model based upon the "plane-wave spectrum technique"[10] and transmission through layered media. This latter calculation uses numerical integration techniques to first find the transmitted fields that impinge upon the inner surface of the radome, and then a series of matrix products which take these fields through the radome surface(s) to the outer surface, and then a numerical integration over the outer surface to find the far-field radiation patterns (See Fig. 7). If the source is a circular mirror, then the shift in the angular position of the maximum of the transmitted pattern from where it would have been without the radome (free-space position), defines the boresight error. If a monopulse array is used in the "difference Mode", then the shift in the angular position of the minimum would define the boresight error (See Fig. 8).[11] Approximations used in this calculation include the assumption that the field passing through the radome can be treated as if it is locally passing through a flat sheet or sheets, and only fields in the forward half-space of the antenna are considered with all multiple scattering and surface waves ignored. Figure 9 presents results obtained by Groutage and Smith for a two-dimensional ray-tracing analysis and the three-dimensional "plane-wave spectrum" calculation. The disparity between these results is obvious.

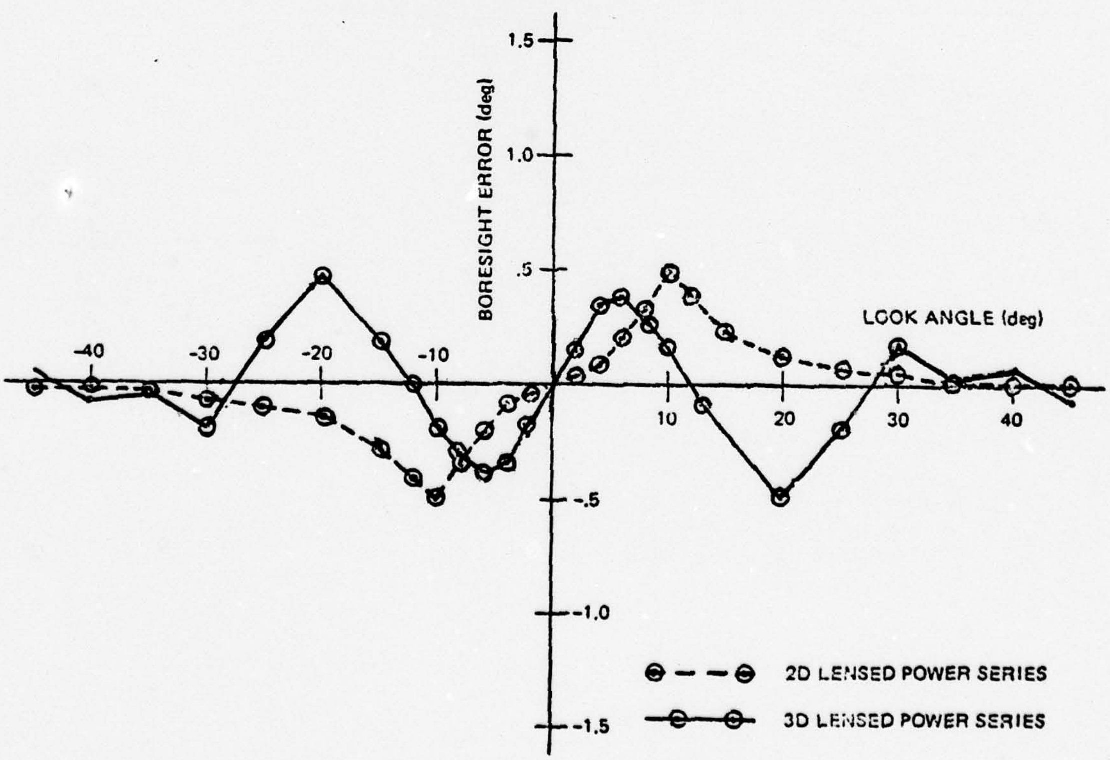

Fig. 9. From Groutage and Smith, P. 12.

DLMI at Eglin has expressed interest in a cooperative effort in radome design with Groutage (who is at Naval Ocean Systems Command). As currently envisioned, the radome will consist of two outer coats of ablative material and an inner, "lensed" body. The design procedure will be essentially "trial-and-error", with the parameters of dielectric constant, thickness, and shape of the inner surface varied until the boresight error and BSE slopes are within acceptable levels (to be determined).

IV. ABLATIVE COATING

Because of the high speeds of future air-to-air missiles, the use of ablative materials to protect the missile from rain and/or excessive heat has been contemplated. A preliminary search of standard sources did not produce much information on this topic, with the exception of one disturbing statement by L.B. Weckesser:[12] "Use of an ablative coating over the window portion of the radome has the obvious disadvantage of affecting the electrical performance. For this reason, an ablator is only used for the early portion of a flight when and if the radar is not needed at that time." Since there was no analytical or experimental substantiation of this statement, a further search of both unclassified and classified work during the past ten years was conducted through the Defense Documentation Center. Nothing that would clarify the above statement was found. Fortunately, DLMI/ADTC decided that it might be worthwhile if I attended the "Fourteenth Symposium on Electronmagnetic Windows," held 21-23 June 1978 at the Georgia Institute of Technology, Atlanta GA 30332. Mr Weckesser and many other radome specialists attended this meeting and the effects of ablative coatings came up both in the presentations and during the questions and discussions afterwards. A copy of the "Trip Report" for this meeting is attached in Appendix I, where the most relevant aspects of the meeting are summarized, including discussions I had with Weckesser regarding the matter above. A reading of that report will indicate that, as yet, there is conflicting opinion and data on the consequences of ablation. Apparently a system-by-system analysis may be the only way of determining the impact of radome boresight error.

V. ADDITIONAL AND FUTURE WORK

In an attempt to understand the ray-tracing techniques discussed above, this author wrote several computer programs for graphic display (cf. Figs. 1, 3-6). In addition, an initial calculation was made to calculate the shape that the inner surface of the radome must have in order that plane-wave radiation incident upon the radome parallel to its axis will be refracted so as to emerge as plane radiation within the radome. The calculation (See Appendix II) is in two dimensions only, but because of the axial symmetry, this would represent the correct cross-section for the three-dimensional radome surface for this case.

Figures 10 and 11 are sample outputs from this program, where the wave fronts are constructed from a "Huygens wavelet" construction. As can be seen, the wavefronts are in fact flat. The next extension of these results would include generalizing to arbitrary angle of incidence, still in two-dimensions, and then extending this to three-dimensions if the results appear fruitful.

One other area of possible investigation is the approximation used in the 3-D electromagnetic theory analysis discussed above, where it is assumed that the transmission of the fields from the inner surface of the radome to the outer surface can be treated locally as transmission through flat slabs. At the Symposium at Georgia Tech, this assumption was questioned several times, with no satisfactory response. An investigation of the limits of validity of this assumption would seem to be in order.

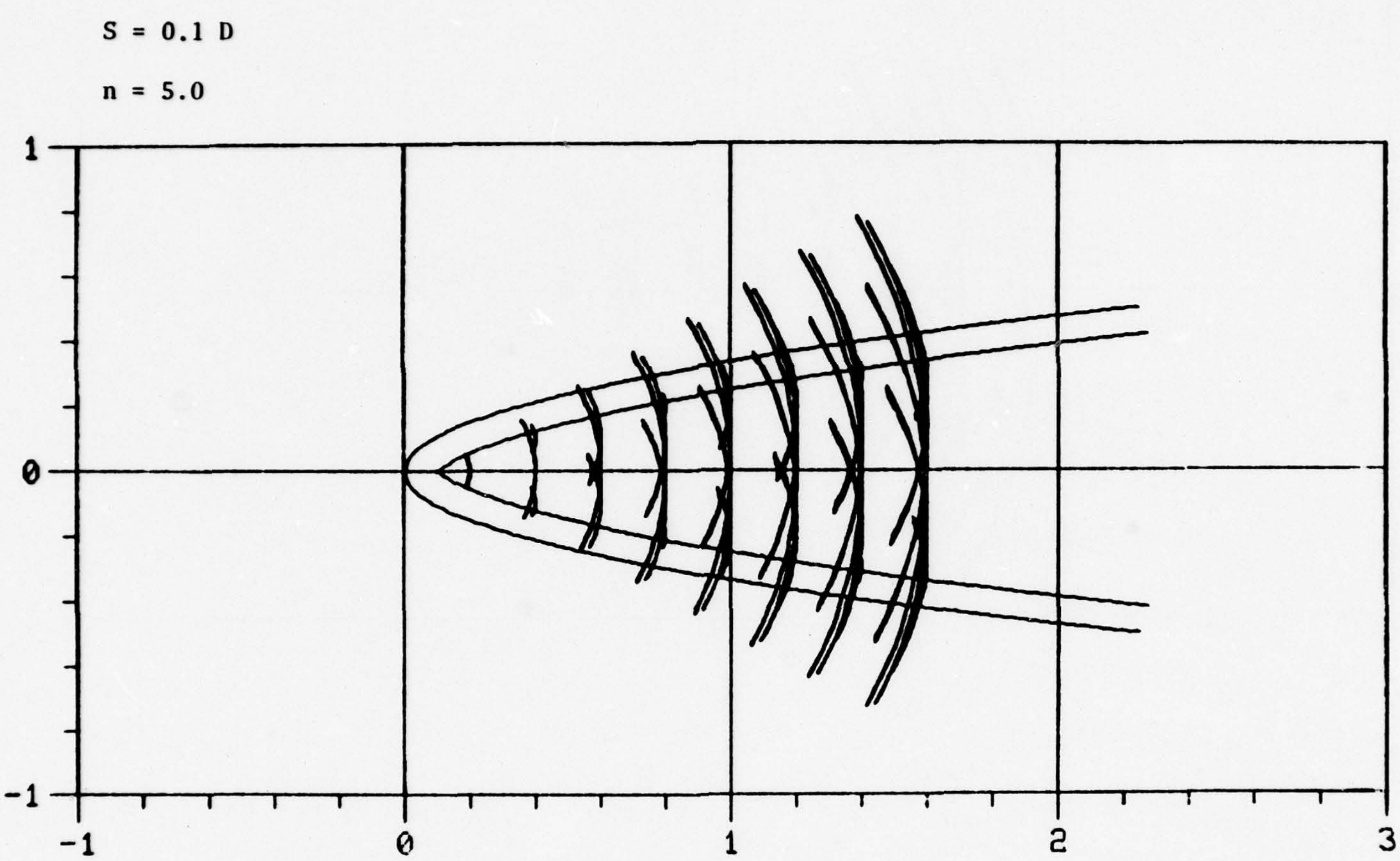

Fig. 10

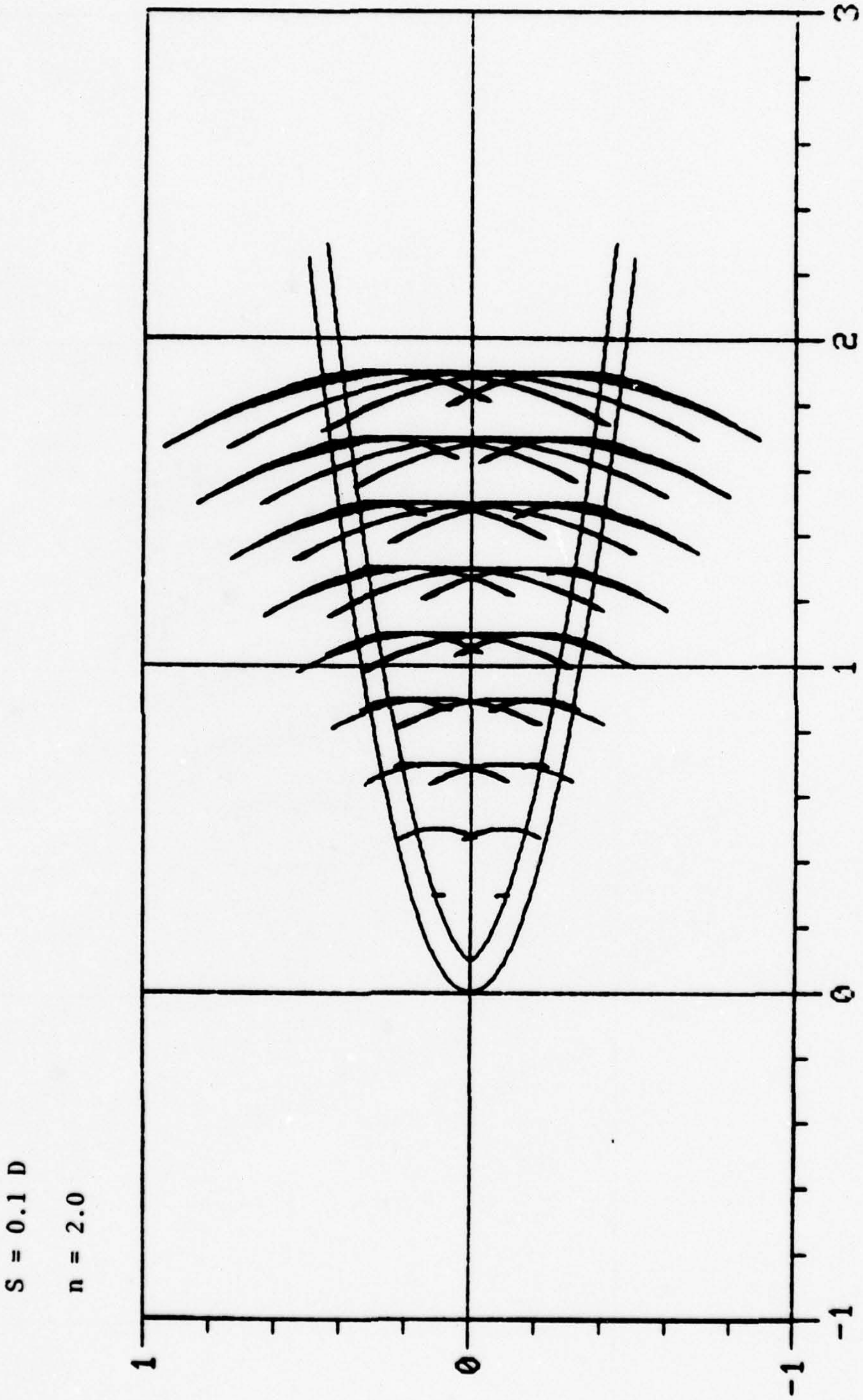

Fig. 11

FOOTNOTES

1. A comprehensive review of all aspects of radomes, including their history of development, can be found in Walton, II.

2. The cone and "ogive" shapes were historically easiest to manufacture; the VonKarman shape yields the maximum volume-to-drag ratio for a given length-to-base ratio; the power series using the 3/4 power approximates the minimum drag shape for a given length-to-base ratio as predicted by the "Newtonian Approximation" in aerodynamics.

3. Air Force Academy Wind Tunnel Tests for Pave Brazo, November 1976; L = length of the radome, D = diameter of the base. The ratio of L to D is called the "fineness ratio".

4. Groutage; Crowe

5. See Crowe, P. 2-23; the major reason for this hope was the simplicity and low computer costs of such a simulation.

6. Ibid., P. 2-23ff

7. Ibid., P. 2-28

8. Ibid., P. 2-28ff

9. Groutage and Smith

10. Wu and Rudduck, I and II

11. Groutage and Smith; Figures 7 and 8 are pre-publication figures made available to this author.

12. Walton, II. P.84

BIBLIOGRAPHY

1. Basset, H.L., "High Temperature RF Transmission Tests on EM Windows Conducted at the French Solar Furnace," IEEE Trans. Ant. Prop. AP-22, 129(1974).

2. Born, M. and E. Wolf, Principles of Optics, Pergamon Press, New York, 1965

3. Burleson, W.G., "Comparison of Calculated Aerothermal Ablation With Empirical Aerodynamic Heating and Rain Effects for Avcoat - 8027 Epoxy and Teflon on Sled Tests at Mach 5," Redstone Arsenal, Alabama 35809, 28 April 1976, ADB012798.

4. Cornbleet, S., Microwave Optics, Academic Press, New York, 1976.

5. Cox, R.N. and L.F. Crabtree, Elements of Hypersonic Aerodynamics, Academic Press, New York, 1965.

6. Crowe, B.J., "Air Launched Tactical Missile Radome Study," Flight Systems, Inc., NASC Contract #N00017-C-76-0232, January 1977.

7. Fradin, A.Z., Microwave Antennas, Pergamon Press, New York, 1961.

8. Groutage, F.D., "Radome Development For a Broadband RF Missile Sensor", NELC TR 2023, 25 January 1977.

9. Groutage, F.D. and D.E. Smith, "Multi-Layered Power Series Radome With Integrated Lens," Paper delivered at the Fourteenth Symposium on Electromagnetic Windows, Georgia Institute of Technology, Atlanta, Georgia 30332, June 1978.

10. Hardy, A.C. and F.H. Perrin, The Principles of Optics, McGraw-Hill Book Co., Inc., New York, 1932

11. Hutchins, G.J. and R.F. Sullivan, "Transient Microwave Insertion Loss Tests in an Arc-Heated Wind Tunnel," Harry Diamond Laboratories, Washington, D.C., July 1973, AD#769588.

12. Jenkins, F.A., and H.E. White, Fundamentals of Optics, 3rd Ed., McGraw-Hill Book Co., Inc., New York, 1957.

13. Jones, D.S., The Theory of Electromagnetism, Pergamon Press, New York, 1964.

14. Krasnov, N.F., Aerodynamics of Bodies of Revolution, RAND-R-445-PR, American Elsevier Publishing Co., New York, 1970.

15. Mathis, H.F., "Transmission Characteristics of Sandwiches," IRE Trans, Microwave Th. and Tech., 57(Oct 1955).

16. Mayhan, "Composite Material Radomes in K_a-band. Effect of Random Phase Errors Due to Radome," IEEE Trans. Ant. Prop., AP-24, 356(1976).

17. Miller, F.H., Analytic Geometry and Calculus, John Wiley and Sons, Inc., New York, 1955.

18. Moorefield, S.A., J.B. Styron, and L.C. Hoots, "Manufacturing Methods for Advanced Radome Production," Final Report AFML-TR-77-182, November 1977.

19. Morse, O.M., and H. Feshbach, Methods of Theoretical Physics, Parts I and II, McGraw-Hill Book Company, Inc., New York, 1953.

20. Pelton & Munk, "A streamlined Metallic Radome," IEEE Trans. Ant. Prop., AP-22, 790(1974).

21. Rudduck, R.C., D.C.F. Wu and M.R. Intihar, "Near-Field Analysis by the Plane-Wave Spectrum Approach," IEEE Trans. Ant. Prop., AP-21, 231-234(1973).

22. Scala, "A Study of Hypersonic Ablation," AD#226989, 1959.

23. Tice, T.E., ed., "Techniques for Airborne Radome Design," Vol. I, RTD-AL-TR-66-391(I), Dec. 1966, AD#811355.

24. Vennard, J.K., Elementary Fluid Mechanics, 4th Edition, John Wiley and Sons, Inc., New York, 1961.

25. Walton, Jr., J.D., I. "Techniques for Airborne Radome Design, Vol. II, ed., RTD-AL-TR-66-391(II), Dec. 1966, AD#811356.

II. Radome Engineering Handbook, Marcel Dekker, Inc., New York, 1970.

26. Wu, D.C.F., and R.C. Rudduck, I. Final Technical Report 2696-4, Electroscience Laboratory, Ohio State University, Contract #N00019-70-C-0252, March 1971, AD#722634.

II. "Plane Wave Spectrum-Surface Integration Technique for Radome Analysis," IEEE Trans. Ant. Prop, AP-22, 497-500(1954).

27. Yost, D.J., L.B. Weckesser, and R.C. Mallalieu, Radome/Seeker Boresight Error Technology Program for Homing Missiles, APL/JHU, Johns Hopkins Road, Laurel, Maryland 20810.

Appendix I

DEPARTMENT OF THE AIR FORCE
AIR FORCE ARMAMENT LABORATORY (AFSC)
EGLIN AIR FORCE BASE, FLORIDA 32542

REPLY TO
ATTN OF: DLMI (Dr. DeAcctis/2-2960)

SUBJECT: Trip Report - Attendance at Fourteenth Symposium on Electromagnetic Windows

TO: DLMI
DLM
IN TURN

1. The Fourteenth Symposium on Electromagnetic Windows was held 21-23 June 1978 at the Georgia Institute of Technology, Atlanta, GA 30332 (See attached "Final Program"). This meeting dealt extensively with radome analysis, materials, and testing including a paper by F. Dale Groutage of Naval Ocean Systems Command with whom members of DLMI and I have had extensive discussions. Many of the papers dealt with areas of radome performance that I have been researching during the past nine weeks. This report will briefly summarize those sessions and presentations which would be of particular significance for the related work at Eglin AFB,FL.

a. Session I - EM Window Analysis and Design:

Of the papers presented, perhaps one of the most important was presented by Weckesser et. al., "Aerodynamic Heating Effects on Radome Boresignt Errors". Its main thrust was that the here-to-fore unanalyzed effects of thermal expansion and temperature variation of dielectric constant of the radome material(s) may lead to problems of stability, especially for high speed missiles with stringent boresight error (BSE) requirements. The conclusion was that "most likely, new radome correction procedures will have to be developed to account for changes in BSE in flight [Proceedings, P.49]". However, a later paper by Kuehne and Yost ("When are Boresight Error Slopes Excessive?") yielded some evidence contrary to that above -- "missile instability due to these large [BSE] slopes may not necessarily result in significant performance degradation if the large slopes are confined to small regions of the radome [Proceedings, P.62]". (It should be pointed out that Kuehne and Yost were among the authors of the first paper mentioned, being part of the group from APL/JHU). It thus appears that it is not clear as to what radome tolerances are necessary for a given level of missile performance. Apparently each missile system (including radome, guidance, size and propulsion) must be analyzed individually for such a determination. More investigation is obviously needed in the area of system requirements.

A paper which may be of interest to those in DLMI who are interested in multi-mode detection systems was presented by Tanzilli et. al., "Potential for Chemically Vapor Depositied Silicon Nitride as a Multimode Electromagnetic Window (Vis, IR, RF)." The material discussed is transparent to em radiation over a wide region, including the visible.

b. Session II - Environmental Considerations
Session III - Materials and Coatings

Most of the papers in these sessions dealt with tests conducted on radome materials, including both body, and protective or ablative coatings. There is apparently some interest in a relatively new material, Sialon, which may have some potential on the basis of preliminary tests. Of especial significance to DLMI, however, were two papers dealing with erosion and ablation. Balageas et. al., "Aerothermal and Electrical Effects of Rain Erosion for a Slip-cast Fused Silica Radome", reported that in sled tests at approximately Mach 4 conditions and 15° angle of attack, rain erosion of the outer surface "destroyed the electrical symmetry of the radome and strongly degraded its electrical performance [Proceedings, P.99]." These measured effects on BSE were confirmed analytically, using actual erosion values as input to the program. Again, however, balancing information was given by Markarian and Patton during the question-and-answer period following their paper, "Aerothermal Evaluation of Quartz Reinforced Missile Radomes." The speaker (I believe it was Markarian) indicated that NWC intends to conduct tests on the aerothermal and electrical performance of ablative coatings, and that some preliminary simulation analyses indicate that up to 30 mils of a surface can be eroded or ablated without significantly changing the miss-distance performance of some missiles. This analysis only considered change in thickness due to erosion or ablation -- no thermal expansion or change in dielectric constant was taken into account.

c. Session V - Measurements

This group of papers dealt with descriptions of test facilities, and one considered the fabrication of a resonant metallic radome surface. Dowling et. al., from Raytheon described on "Automated Radome Test Facility" which consists of a mini-computer driven data collecting facility capable of collecting data from upwards of 115,000 observation points in the vicinity of a radome. This information is interpreted in terms of BSE, thereby obtaining a map of the errors for a particular radome. Such a system is used by Raytheon as a designing tool (data not available - I asked), but it would be the precursor of a microprocessor based compensation system which would use the error mapping as a databank to correct incoming information.

A second paper, "Solar Testing at the Advanced Components Test Facility" by Altman suggested a method of testing a radome as its temperature changes. The facility described a prototype solar energy facility at Georgia Tech. By placing a radome with transmitter at the focus of the collecting - mirror field, transmission as a function of temperature could be measured.

2. Summary:

a. It is clear that much work is going on in the area of radome materials, although no new and dramatic breakthroughs were announced or contemplated.

b. Much analysis of boresight error and BSE slope is also underway, with most work having advanced to three-dimensional and surface-integration type techniques (mostly based upon the "plane-wave spectrum representation" of Wu and Rudduck, Final Report 2969-4, AD#722634, March 1971).

c. There is apparently fundamental disagreement and conflicting evidence about boreisght error requirements of radomes. I approached L.B. Weckesser during one of the "coffee breaks" regarding a statement he made in an earlier article: "Use of an ablative coating over the window portion of the radome has the obvious disadvantage of affecting the electrical performance (Radome Engineering Handbook, J.D. Walton, Ed., Marcel Dekker, Inc., New York, 1970, P.84)." He indicated that his concern was (and is) the change in thickness of what was otherwise a very accurately machined surface. Yet his own colleagues presented contrary information (see Item 1a above).

d. A perusal of the thirty - five papers presented indicated that over 60% (22) were either U.S. Government supported, supported by a foreign ally government, or conducted in government supported facilities. It would thus appear that attendance at such a meeting would be an important (and convenient) way to determine the type of work being done elsewhere with government support. It also is a convenient medium for industry to communicate its state-of-the-art work to its biggest customer. Since the scope of this type of meeting is so small, one can be relatively sure that a large fraction of the papers would be of interest to anyone working in such an area (the latter is generally not true at meetings of scientific or professional associations which are broader in scope). I am sure that other members of DLMI could have benefited from attendance at this meeting, and I urge such attendance in the future, even if a paper is not presented.

LOUIS A. DeACETIS
USAF/ASEE Summer Faculty Associate
at DLMI

Louis A. DeAcetis

Appendix II

Calculation of the Inner Surface of a Radome

Assumptions:

a) The outer surface of the radome has a half-power shape of the form:

$$y = a\,(x^{1/2}).$$

b) The incident radiation is travelling parallel to the x-axis which is the axis of the radome.

Consider two rays incident upon the front surface of the radome, one passing through the center and the other at some height y_p above the center. Let:

n = index of refraction of the radome material

S = axial thickness of the radome.

For the radiation within the radome to be plane parallel, the optical path ABC must equal the optical path $A_oB_oC_o$ (Fig. A1).

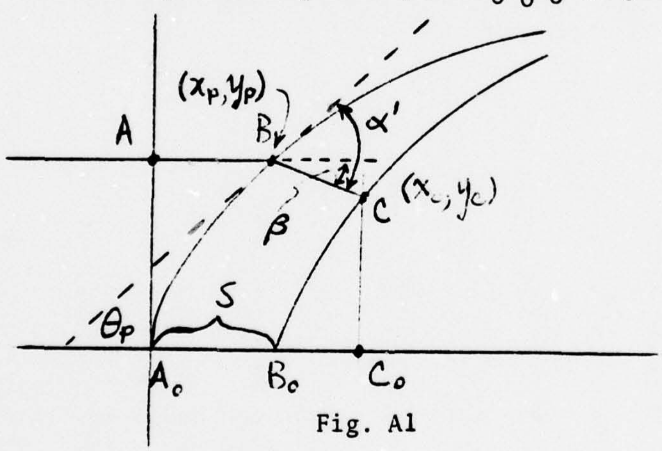

Fig. A1

Thus,

$$(AB) + n(BC) = n(A_oB_o) + (B_oC_o) \tag{1}$$

Since the front surface passes through the origin, then

$$x_p + n(BC) = n\,S + x_c - S = S\,(n-1) + x_c. \tag{2}$$

Now, $(BC) = (x_c - x_p)/\cos(\beta)$. Thus,

$$x_p + n(x_c - x_p)/\cos(\beta) = S(n-1) + x_c.$$

Solving for x_c yields:

$$x_c = \frac{S + N\,x_p}{N} \tag{3}$$

where,

$$N = \frac{n - \cos(\beta)}{(n-1)\cos(\beta)}. \tag{4}$$

The equation of the ray from B to C is given by

$$y = \tan(\beta)\,x + y_p - \tan(\beta)\,x_p. \tag{5}$$

If we let g(x) represent the equation of the inner surface, then ray BC intersects this curve when g(x) = y from equation (5). Let (x_c, y_c) be the point of intersection. Then,

$$K\,x_c + L = g(x_c), \text{ with} \tag{6a}$$

$$K = \tan(\beta), \text{ and} \tag{6b}$$

$$L = y_p - K\,x_p. \tag{6c}$$

(6)

Choose the form of g(x) to be:

$$g(x) = r\sqrt{x - S}. \tag{7}$$

Then, combining Eq. 6a and Eq. 7, we ge can solve for r to get:

$$r = \frac{K\,x_c + L}{\sqrt{x_c - S}} \tag{8}$$

Substituting for x_c from equation 3, we get:

$$r = \frac{K\,S + N\,a\sqrt{x_p}}{\sqrt{N\,S + N^2\,(x_p - S)}}. \tag{9}$$

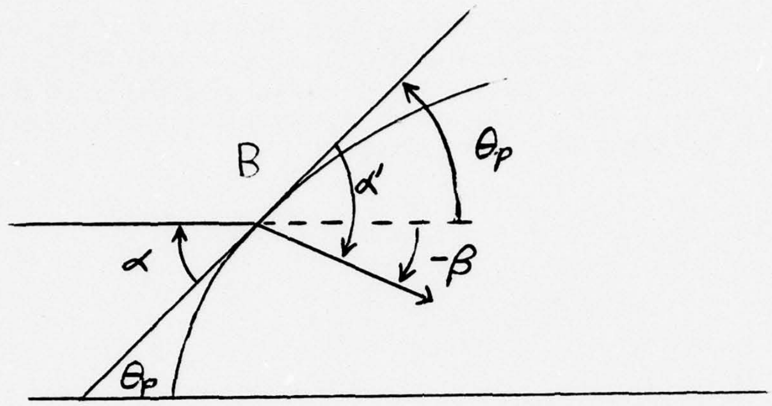

Fig. A2

The slope of the outer surface at point (x_p, y_p) is given by the derivative of the function $y = a\sqrt{x}$, which is:

$$y' = \frac{a}{2\sqrt{x}} . \tag{10}$$

Then angle $\theta_p = \arc\tan\left(\frac{a}{2\sqrt{x_p}}\right)$.

Applying Snell's law to the refraction that takes place at this surface, we can find angle α' (see Fig. A2) from:

$$\cos(\alpha') = \frac{\cos(\alpha)}{n} = \frac{\cos(\theta_p)}{n} = \frac{2\sqrt{x_p}}{n\sqrt{a^2 + 4x_p}} \tag{11}$$

Then, using $\beta = \theta_p - \alpha'$, we get:

$$\beta = \arc\tan\left(\frac{a}{2\sqrt{x_p}}\right) - \arc\cos\left(\frac{2\sqrt{x_p}}{n\sqrt{a^2 + 4x_p}}\right). \tag{12}$$

In summary, given values for n, S, a, and values of x_p, we can use equations 12, 4, 6b, with equation 3 and $y_c = r\sqrt{x_c - S}$ to calculate values for (x_c, y_c), i.e., points on the curve g(x) which is the inner surface. Figures 10 and 11 are sample outputs from this procedure, where the value of the constant "a" is given by

$$a = \frac{D}{2\sqrt{L}}, \text{ with } D = 1, \text{ and } L = 2.25 .$$

1978 USAF-ASEE SUMMER FACULTY RESEARCH PROGRAM
Sponsored by
THE AIR FORCE OFFICE OF SCIENTIFIC RESEARCH
conducted by
AUBURN UNIVERSITY AND OHIO STATE UNIVERSITY

PARTICIPANTS FINAL REPORT

ANALYSIS OF A ZOOM CHAIN OPTICAL SYSTEM

Prepared by:	Alan A Desrochers, Ph.D.
Academic Rank:	Assistant Professor
Department and University:	Department of Systems and Computer Engineering Boston University
Assignment:	Eglin Air Force Base Air Force Armament Laboratory Guided Weapons Division Air-to-Air Missiles Branch
USAF Research Colleague:	Mr James Long

Date:	28 July 1978
Contract No:	F44620-75-C-0031

ANALYSIS OF A ZOOM OPTICAL CHAIN SYSTEM

Dr. Alan A Desrochers

ABSTRACT

The Zoom Chain Optical System is designed to simulate range closure between a missile and a target. The main objective of this work is to determine the feasibility of this system. No other systems are commercially available and none have been designed with this magnification ability. Consequently, the equations of motion for this mirror system are developed and analyzed. Maximum velocities of the mirrors are calculated and the sensitivity of these maximum velocities to the simulated variables and the optical system parameters is also computed. Present results indicate that the proposed mirror system is quite feasible using existing hardware.

I. INTRODUCTION

The purpose of this work is to determine and analyze the equations of motion for the Zoom Chain Optical System shown in Figure 1. This system of mirrors is intended to simulate the range closure of a missile flying at a constant velocity as it approaches a target. The quantities of particular interest here are the maximum velocity of each table and the sensitivity of these maximum velocities to variations in the simulated variables as well as to variations in the optical system parameters. In addition, a set of specifications, based on the above analysis, is required for the stepper motors which drive the tables. Throughout the analysis, paraxial rays are assumed and the effects of lens aberrations are neglected.

II. EQUATIONS OF MOTION

The Zoom Optical System is required to simulate the range closure of a missile flying at a constant velocity, V, as it approaches a target of height H. The target is located at an initial distance R_0, measured from the missile to the target. In the zoom optical system, the target is simulated by the fixed image formed by mirror 1 (fixed in size and location). The object distance of this image to mirror 2, $S_2(t)$, corresponds to the distance between the missile and the target, R(t). Since the missile approaches the target at the constant velocity, V, the motion of mirror 2 is constrained by

$$\frac{dS_2(t)}{dt} = kV \ , \quad S_2(0) = S_{20} \tag{1}$$

where k is a positive constant, and the initial object distance S_{20}, is determined by the desired zoom ratio of the entire optical chain. The zoom ratio is defined as the height of the final image formed by mirror 5 to the height of the initial image produced by mirror 5. Thus, the desired zoom ratio, Z_D, can be expressed as

$$Z_D = \prod_{i=2}^{5} \frac{m_i(t_f)}{m_i(0)}$$

where $m_i(\cdot)$ is the magnification of the ith mirror and t_f is the time at which the blind range is reached. The blind range is the distance from the target at which further control action will be ineffective and is due to sampling rates and guidance and flight control computation time.

In order to maintain a uniform zoom rate, the motion of the mirrors should cause the magnification of each mirror to change identically and synchronously. This requirement translates into

$$\frac{dm_i(t)}{dt} = \frac{dm_{i+1}(t)}{dt} \qquad i = 2,3,4 \qquad (2)$$

The solution to equation (1) specifies the motion of mirrors 2 and 4. The constraint in (2) will be used along with the lens formula [1] to specify the motion of mirrors 3 and 5 which will be a function of mirrors 2 and 4.

Assuming that all distances measured outward from the lens are positive, the appropriate lens formula becomes

$$\frac{1}{S_i'(t)} + \frac{1}{S_i(t)} = \frac{1}{f} \qquad (3)$$

Where $S_i'(t)$, is the image distance from the ith mirror, $S_i(t)$ is the object distance and f is the focal length, assumed to be the same for each mirror. This equation will now be used to obtain a differential equation for the motion of mirrors 3 and 5. Solving (3) for the image distance of mirror 3

$$S_3'(t) = f\,(1 + m_3(t)) \qquad (4)$$

where the magnification $m_3(t)$ is defined as

$$m_3(t) = \frac{S_3'(t)}{S_3(t)} \qquad (5)$$

Then differentiating (4) gives

$$\frac{dS_3'(t)}{dt} = f\,\frac{dm_3(t)}{dt} \qquad (6)$$

using the constraint imposed by (2)

$$\frac{dS_3'(t)}{dt} = f\,\frac{dm_2(t)}{dt} \qquad (7)$$

This couples the motion of mirrors 3 and 5 to mirrors 2 and 4. To simplify (7), apply the lens formula again to obtain

$$m_2(t) = \frac{f}{S_2(t) - f} \tag{8}$$

and then differentiating for use in (7) gives

$$\frac{dm_2(t)}{dt} = \frac{-f}{(S_2(t) - f)^2} \frac{dS_2(t)}{dt} \tag{9}$$

Now (7) can be solved from a knowledge of $S_2(t)$ found from the solution of (1) to be

$$S_2(t) = S_{20} + kVt \tag{10}$$

Substituting (10) into (9) and the result into (7) gives a differential equation to describe the motion of Mirror 3,

$$\frac{dS_3'(t)}{dt} = \frac{-f^2 kV}{(S_{20} + kVt - f)^2} \tag{11}$$

This equation can be solved by separating the variables and integrating,

$$\int_0^t dS_3'(\tau) = \int_0^t -f^2 kV \, (S_{20} + kV\tau - f)^{-2} \, d\tau \tag{12}$$

to obtain

$$S_3'(t) = S_3'(0) + f^2 \left(\frac{1}{S_{20} - f} - \frac{1}{S_{20} + kVt - f} \right) \tag{13}$$

Equations (1) and (10) reveal that Table 1, the table containing mirrors 2 and 4, moves toward the stationary image formed by mirror 1 (V is less than zero). To understand the motion of Table 2, first consider an expression for the image distance of mirror 2,

$$\frac{dS_2'(t)}{dt} = f \frac{dm_2(t)}{dt} \tag{14}$$

Using (9),

$$\frac{dS'_2(t)}{dt} = \frac{-f^2}{(S_2(t) - f)^2} \frac{dS_2(t)}{dt} \qquad (15)$$

Which indicates that $S'_2(t)$ is increasing. To see what happens to $S_3(t)$ apply the lens formula again to obtain

$$S_3(t) = f\left(1 + \frac{1}{m_3(t)}\right) \qquad (16)$$

and then differentiating

$$\frac{dS_3(t)}{dt} = \frac{-f}{m_3^2(t)} \frac{dm_3(t)}{dt} \qquad (17)$$

$$= \frac{-f}{m_3^2(t)} \frac{dm_2(t)}{dt} \qquad (18)$$

because of (2). Then

$$\frac{dS_3(t)}{dt} = \frac{f^2}{m_3^2(t) \; (S_2(t) - f)^2} \frac{dS_2(t)}{dt}$$

If $m_3(t)$ is chosen to be less than 1 for all time, then $S_3(t)$ is decreasing at a faster rate than $S'_3(t)$ is increasing which implies that Table 2 must move in the same direction as Table 1. An alternate argument can be used to reach the same conclusion. In order to obtain a useful, stationary output from the optical system, it is desired to have the image formed by mirror 3 (and mirror 5) fixed. This requirement, and the fact that $dS'_3(t)/dt > 0$, says that Table 2 moves in the same direction as Table 1. Examination of initial and final positions will also lead to this conclusion.

SLIDE AXIS MOTION

The equations of motion, (10) and (13), refer to changes in the object and image distance along the axis. In actual operation, the motion of the tables is restricted to the slide axis. Let the location of the image formed by Mirror 1 be the origin of a rectangular coordinate system with the z axis parallel to the slide axis. Then at any time t,

$$\bar{z}_2(t) = (S_2^2(t) - d^2)^{1/2} \bar{z} \quad (20)$$

where $\bar{z}_2(t)$ is a vector from the origin to Table 1 along the z axis, d is the constant distance from the center of mirror 2 to the z axis, and $\bar{z}$ is a unit vector in the direction of the positive z axis. Simularly, let $\bar{z}_3(t)$ be the vector from the origin to Table 2 in the z direction and then

$$\bar{z}_3(t) = -S_3'(t) \cos\alpha \; \bar{z} \quad (21)$$

$$\bar{z}_3(t) = \frac{-S_3'(t)}{S_2(t)} \bar{z}_2(t) \quad (22)$$

from geometrical considerations and the law of reflection.

INITIAL AND FINAL TABLE POSITIONS

The initial positions for (10) and (13) can be established from the lens formula. Specifically,

$$S_{20} = f \left(1 + \frac{1}{m_2(0)}\right) \quad (23)$$

and

$$S'_{20} = f (1 + m_2(0)) \quad (24)$$

and

$$S_{30} = f \left(1 + \frac{1}{m_3(0)}\right) \quad (25)$$

and

$$S'_{30} = f (1 + m_3(0)) \quad (26)$$

and the initial magnification of each mirror is given by

$$m_i(0) = Z_D^{-1/n} \quad (27)$$

where n is the number of mirrors in the zoom system; n = 4 in Figure 1. The final magnification, $m_i(t_f)$ is then implied to be 1. Since (27) states that $m_2(0) = m_3(0)$, then

$$S_{20} = S_{30} \quad (28)$$

and

$$S'_{20} = S'_{30} \quad (29)$$

which leads to

$$S'_{30} = m_3(0) S_{30} = m_2(0) S_{20} \quad (30)$$

Note that equations (28) and (29) also imply that the image formed by mirror 3 is also located along the line z = 0.

Now examine the final position of each table in order to compute the total travel distance of each table. At the final time, t_f, $m_i(t_f) = 1$. From the lens formulae,

$$S_2(t_f) = 2f = S'_2(t_f) = S_3(t_f) = S'_3(t_f) \tag{31}$$

and the total travel distance of each table is

$$S_i(t_f) - S_i(0) = f\left(1 - \frac{1}{m_i(0)}\right)$$

III. SIMULATION RESULTS

This section discusses the implementation of the motion equations. From equation (10),

$$S_2(t) = S_{20} + kVt \tag{32}$$

the final table position is used to evaluate k,

$$k = \frac{S_2(t_f) - S_{20}}{Vt_f} \tag{33}$$

The final time, t_f, is determined from the time it takes the missile to fly at a constant velocity V from R_o to a distance away from the target equal to the flind range, R_B. Thus,

$$t_f = \frac{R_B - R_o}{V} \tag{34}$$

Now the maximum change in the object distance with respect to time is of particular interest here. Since

$$\max \frac{dS_2(t)}{dt} = kV = \frac{S_2(t_f) - S_{20}}{t_f} \tag{35}$$

using (34)

$$\max \frac{dS_2(t)}{dt} = \frac{(S_2(t_f) - S_{20})\, V}{R_B - R_o} \tag{36}$$

From the knowledge of the initial and final table positions

$$\max \frac{dS_2(t)}{dt} = \frac{f\,(1 - Z_D^{1/n})\,V}{R_B - R_o} \tag{37}$$

Note that (37) is a constant. This equation was plotted for various simulation tasks and is shown in Figure 2. Here, the focal length was 1.25 feet, the desired zoom ratio was 30, and the blind range was 1000 feet. Presently, the maximum velocity of the tables is limited to .25 feet per second and consequently only the case for R_o = 20000 feet can be implemented.

The maximum change in the image distance $S_2(t)$ with respect to time is equal to the maximum time rate of change in $S_3'(t)$. This can be shown after manipulating (11) with the help of (23) and (37). Furthermore, each maximum speed occurs at t_f. Thus, the instant at which the blind range is encountered, the tables are moving with the same speed. Consequently, no further change in magnification occurs as the simulation stop time is approached.

Figures 3 through 6 are graphs of velocity and position versus time for a specific case. This case was chosen because it represents the most realistic situation which can be simulated using the existing hardware. Note that in Figure 3, the magnitude of the velocity decreases as a function of time, instead of remaining constant. This is due to the effect of the cos α in Figure 1.

IV. SENSITIVITY ANALYSIS

In this section, the sensitivity of equation (37) to several variables is considered. Let

$$S_2^m = \max \frac{dS_2(t)}{dt}$$

and then the sensitivity of S_2^m to a variable x is defined as

$$S_2^{mx} = \frac{\partial S_2^m}{\partial x} \frac{x}{S_2^m} \tag{38}$$

Table I summarizes the pertinent equations and sensitivities.

TABLE I

OPERATING POINT:	$Z_D = 30$	$R_o = 20000$	$R_B = 1000$

$$S_2^{mf} = 1$$

$$S_2^{mV} = 1$$

$$S_2^{mR_B} = \frac{-R_B}{R_B - R_o} = .0526$$

$$S_2^{mZ_D} = \frac{-.25Z_D^{1/4}}{1 - Z_D^{1/4}} = .4365$$

$$S_2^{mR_o} = \frac{R_o}{R_B - R_o} = -1.0526$$

This table indicates the dependency of the motion of Table 1 on simulated variables and optical system parameters. Thus, if the zoom ratio were increased by 50%, one could expect a 21.82% increase in the final velocity of Table 1. On the other hand, the blind range has very little effect on the maximum velocity about the chosen operating point and a change in the focal length, missile approach velocity, or initial target distance essentially causes an identically proportional change in S_2^m. These dependencies are illustrated graphically in Figures 7 through 12.

In Figures 7 and 8, it is seen that the maximum speed of each table can be reduced by decreasing the focal length. However, a shorter focal length will place the tables closer together and the effects of lens aberrations could be severe. Also note that the graphs are identical and this is because each table has the same maximum velocity occurring at, t_f, as previously discussed. These graphs were generated for a zoom ratio of 30 and the maximum velocities are along the z axis.

Figures 9 and 10 illustrate the dependency of the maximum velocity of each table on the blind range. As the blind range increases, the maximum speed increases, which is contrary to intuition. This effect is caused by the angle, α, in Figure 1. As the blind range decreases, cos α, decreases, thus causing a decrease in the maximum speed of each table.

Figures 11 and 12 show the dependency of maximum table velocities on the zoom ratio. Here the blind range was 1000 feet.

CONCLUSIONS AND RECOMMENDATIONS

Using the existing hardware, the present mirror system can adequately simulate most desired missile range closures. If higher velocities of the tables are required, then cable or chain driven slides will be needed. This is also true for shorter range simulations.

In this work it was assumed that the missile approaches the target with a constant velocity. In actual operation, this is not true. The system can still handle this case with certain modification to the derived equation. Equation (1) will no longer be a simple linear differential equation. It will probably have to be solved on line, numerically. The motion of Table 2 will then be a non-linear differential equation also requiring a numerical solution.

The analysis also assumed a final magnification of one for each mirror. Removing this assumption will lead to different maximum velocities for the tables.

At this point, it seems most appropriate to construct the system, evaluate the image quality, and correct for lens aberrations if necessary.

REFERENCES

1. Jenkins and White, Fundamentals of Optics, McGraw Hill, 1957

Figure 1.

ZOOM CHAIN OPTICAL SYSTEM

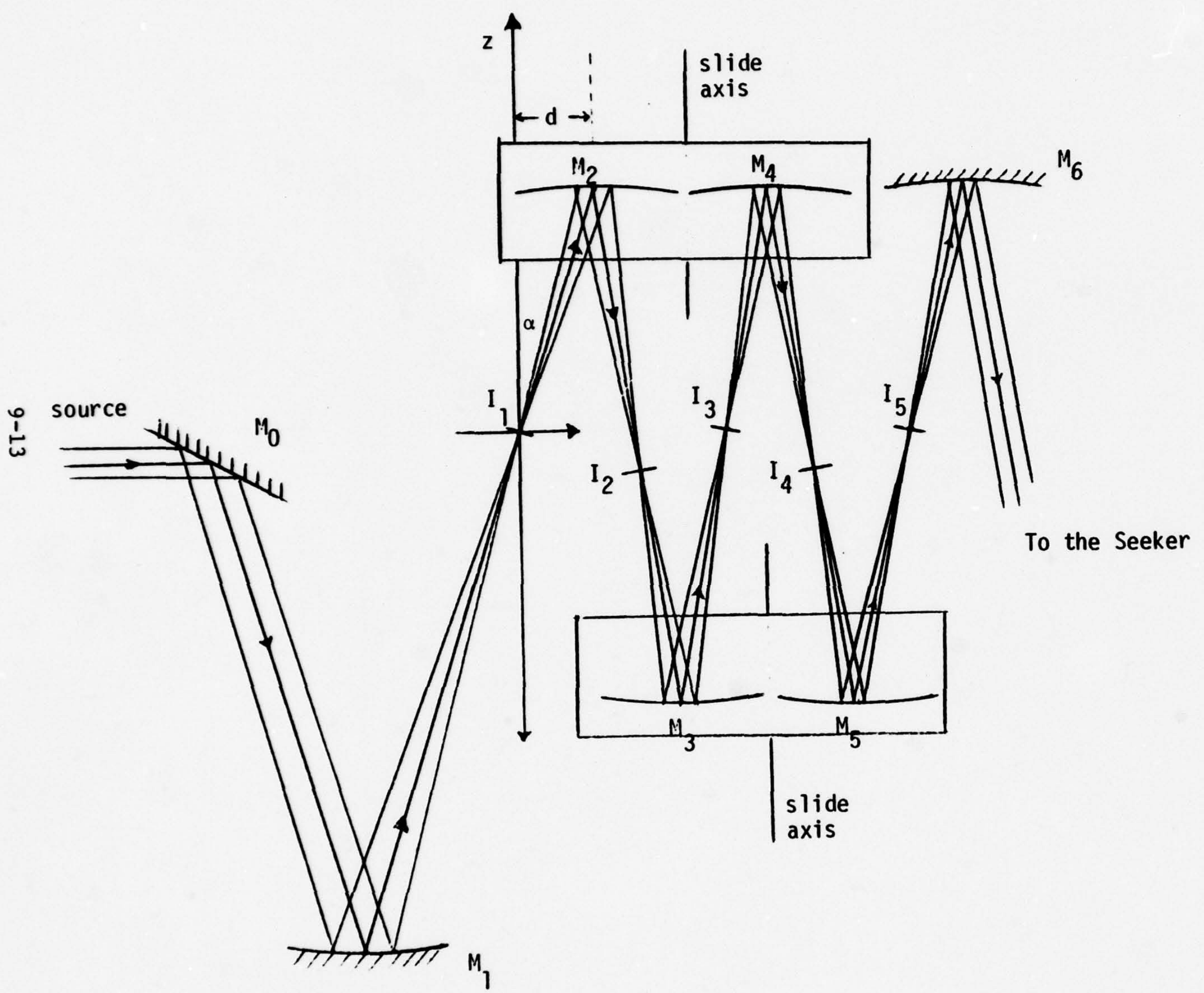

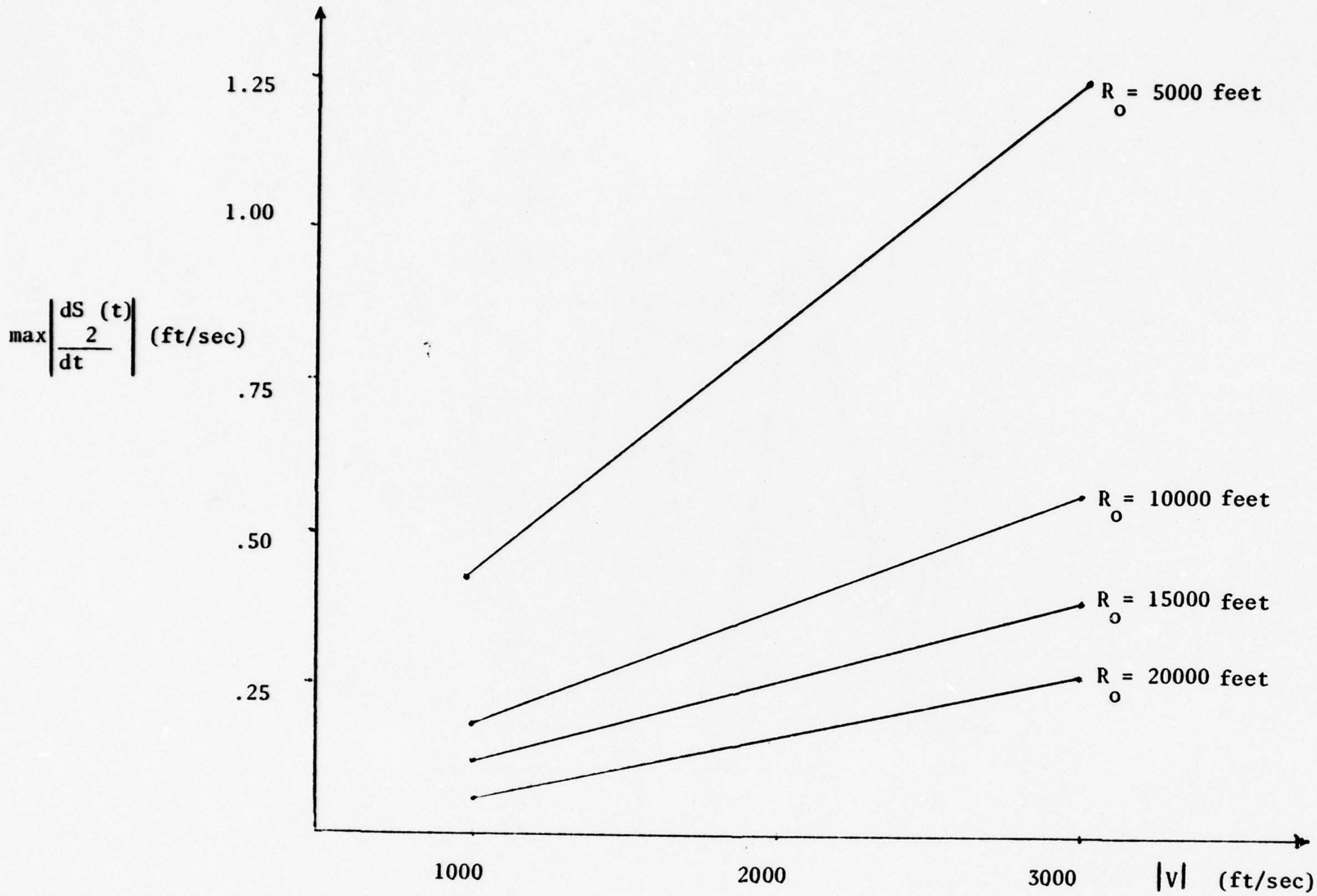

Figure 2. Maximum Change in the Object Distance vrs. $|V|$

Figure 3. Table 1 Velocity vrs. Time

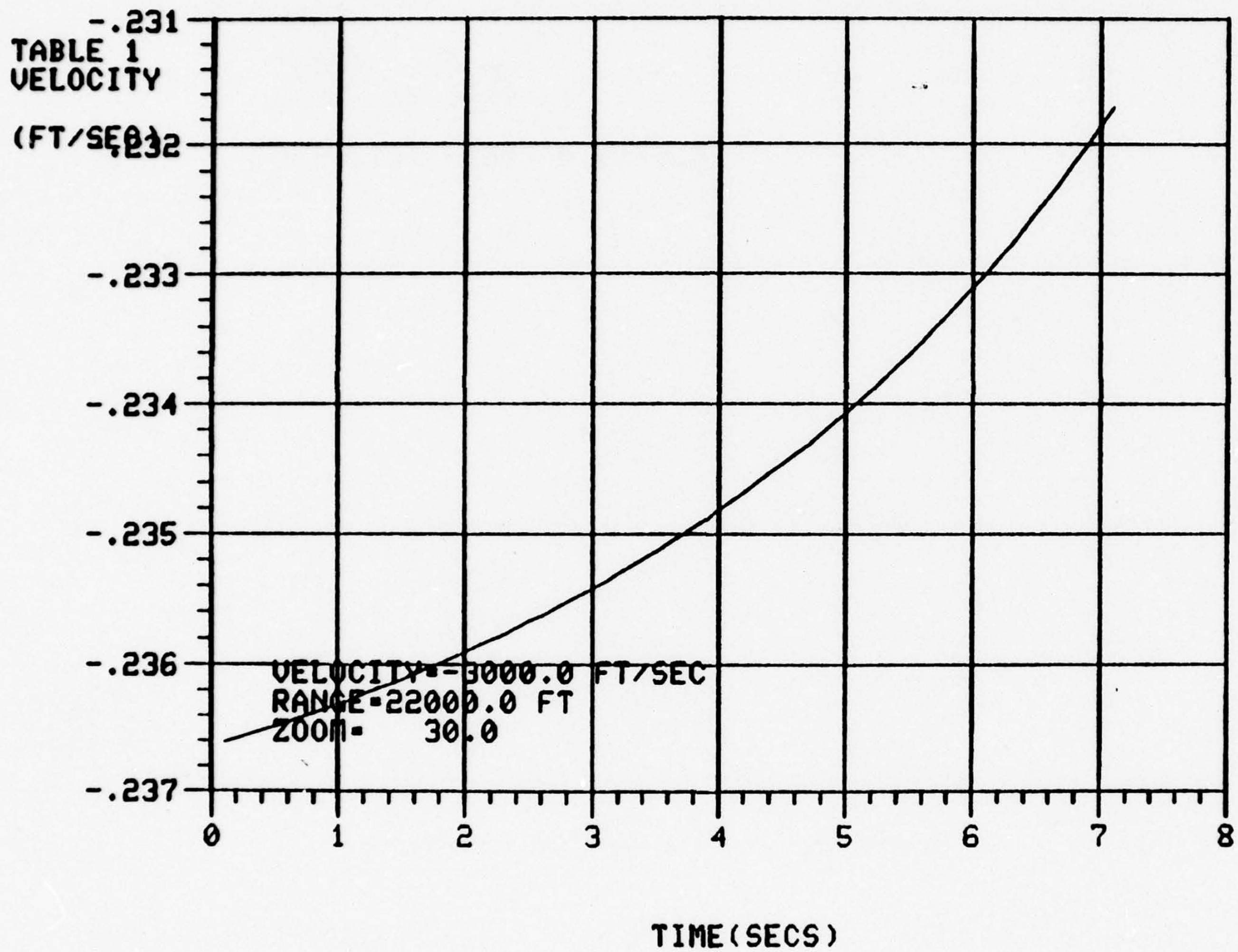

Figure 4. Table 2 Velocity vrs. Time

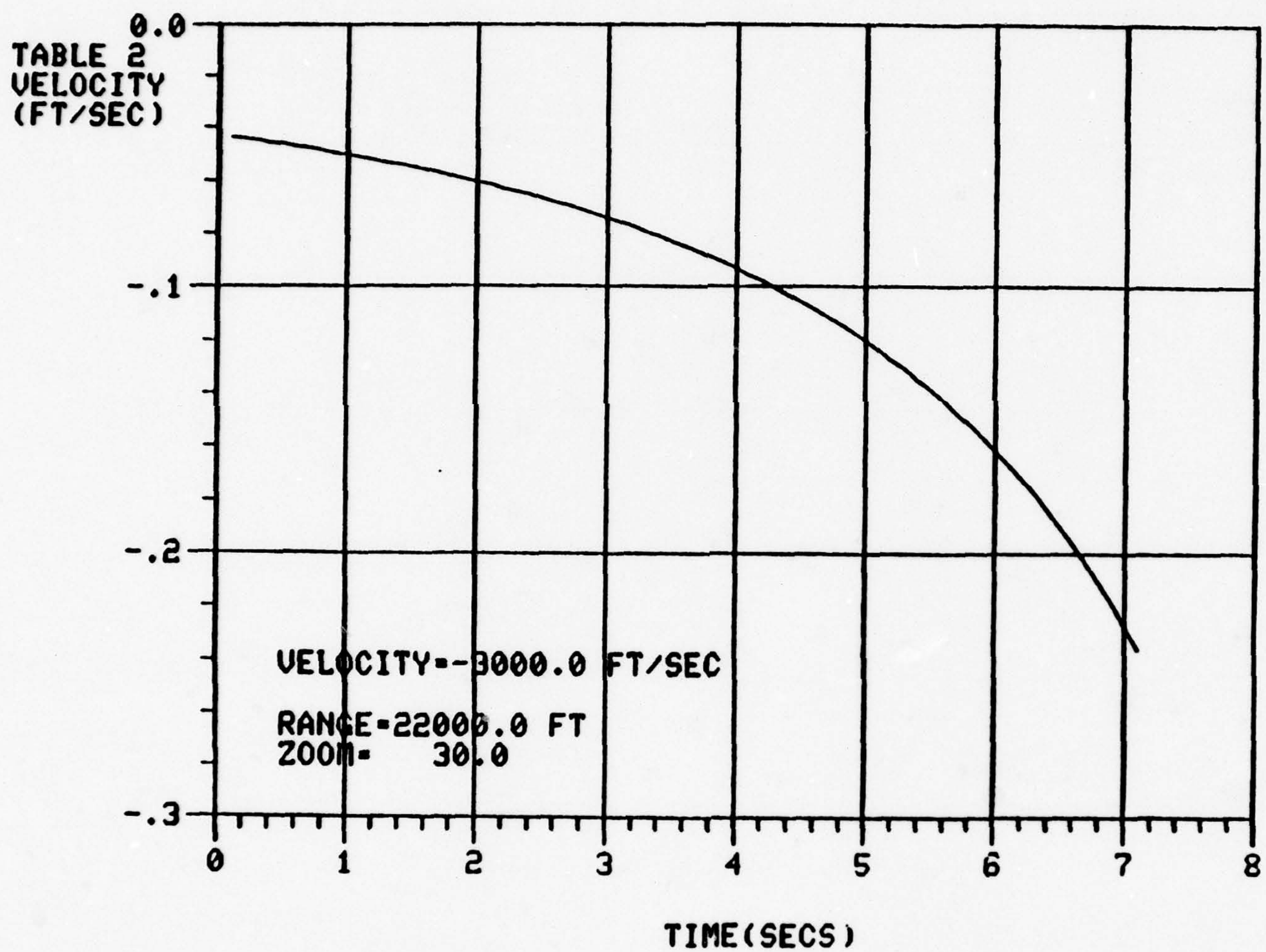

Figure 5. Table 1 Position vrs. Time

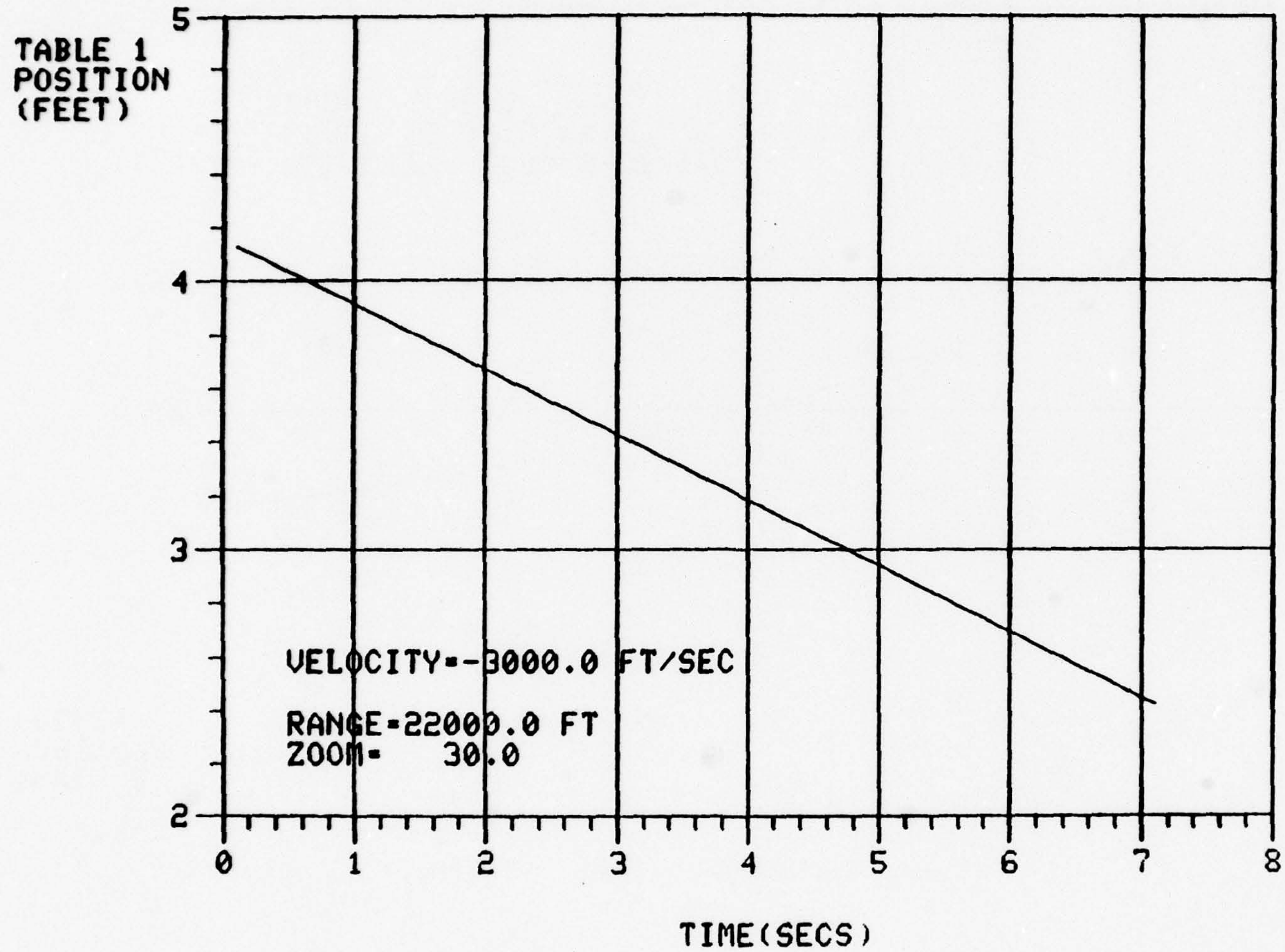

Figure 6. Table 2 Position vrs. Time

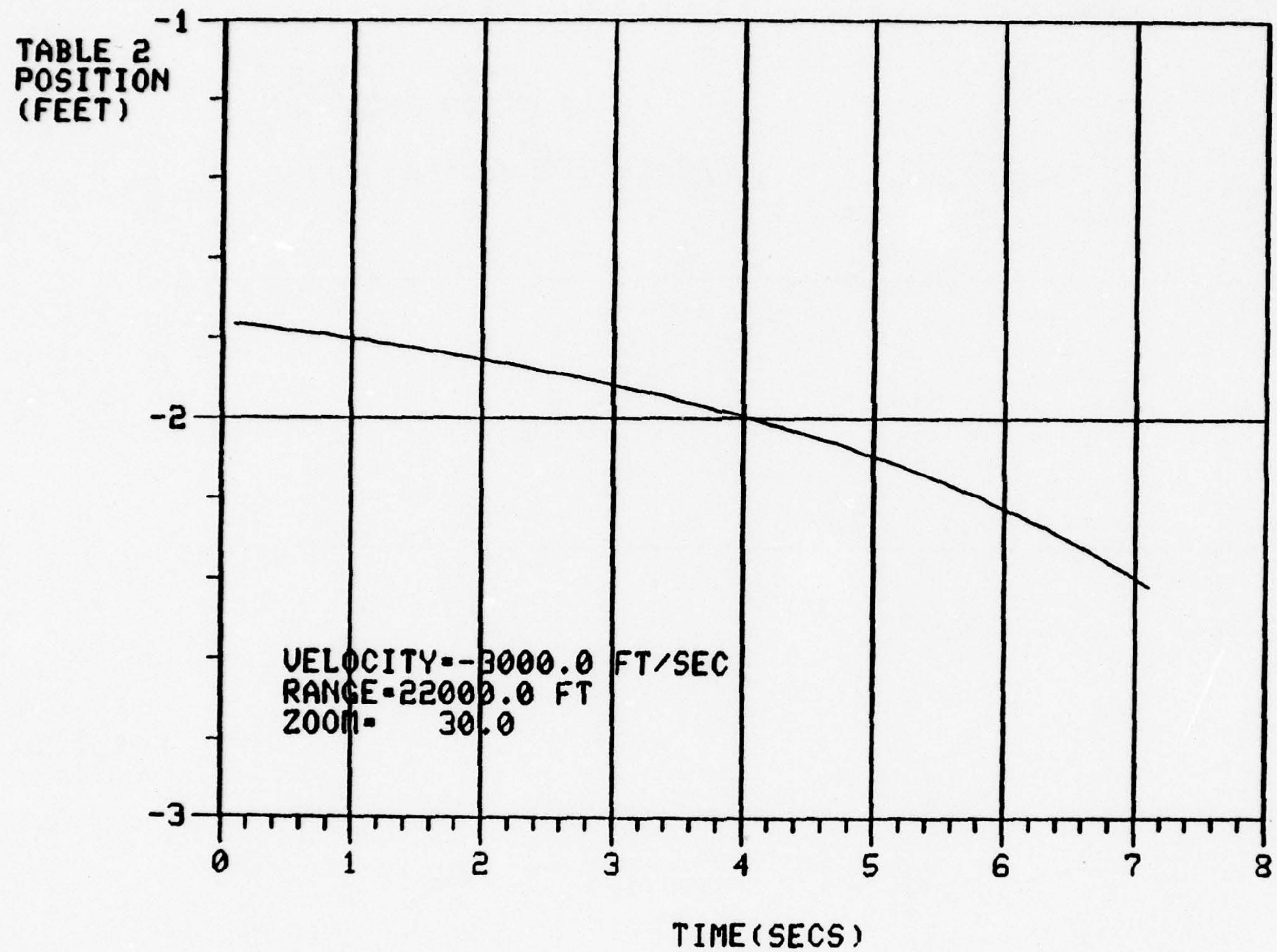

Figure 7. Table 1 Maximum Velocity vrs. Focal Length

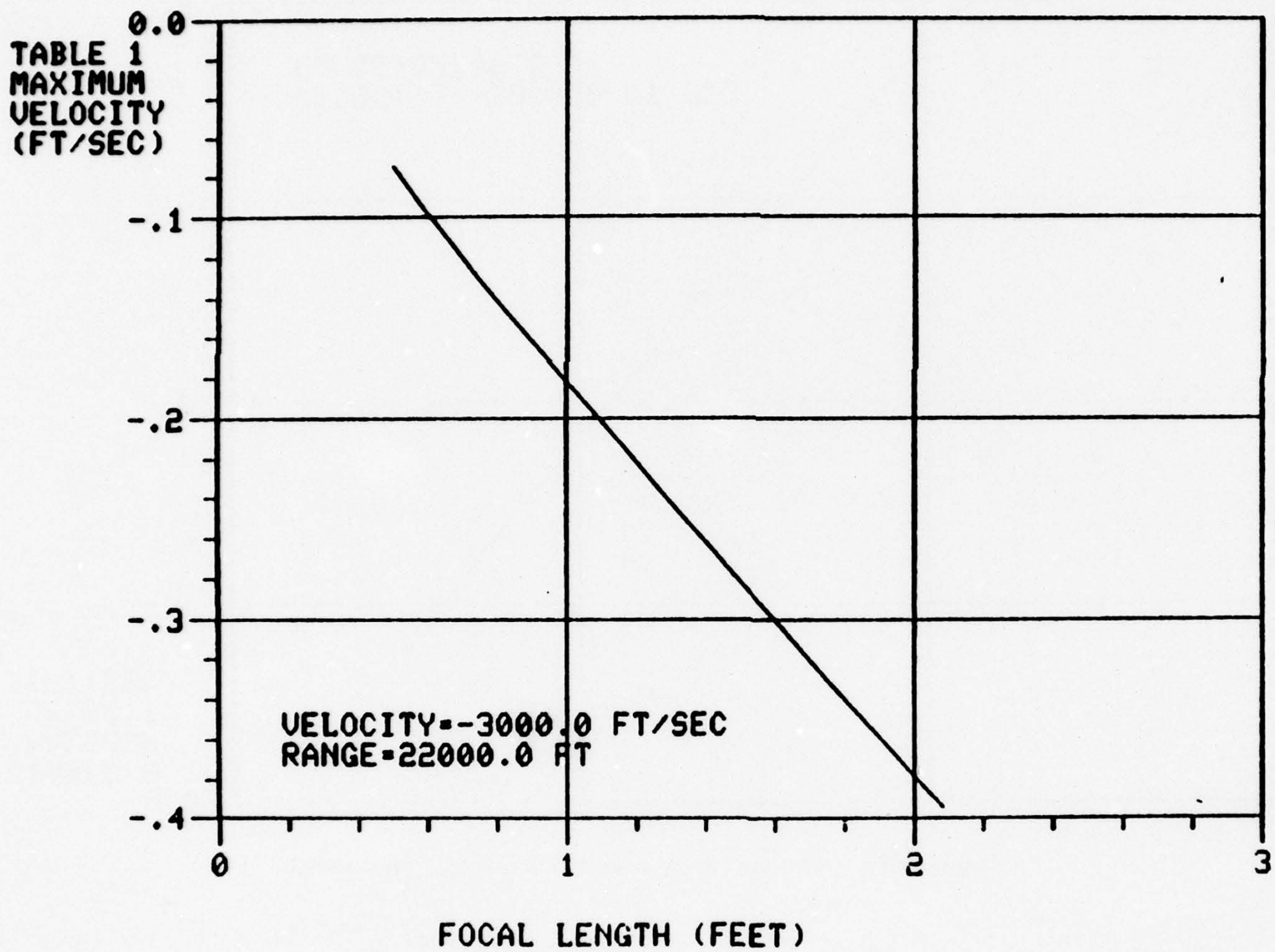

Figure 8. Table 2 Maximum Velocity vrs. Focal Length

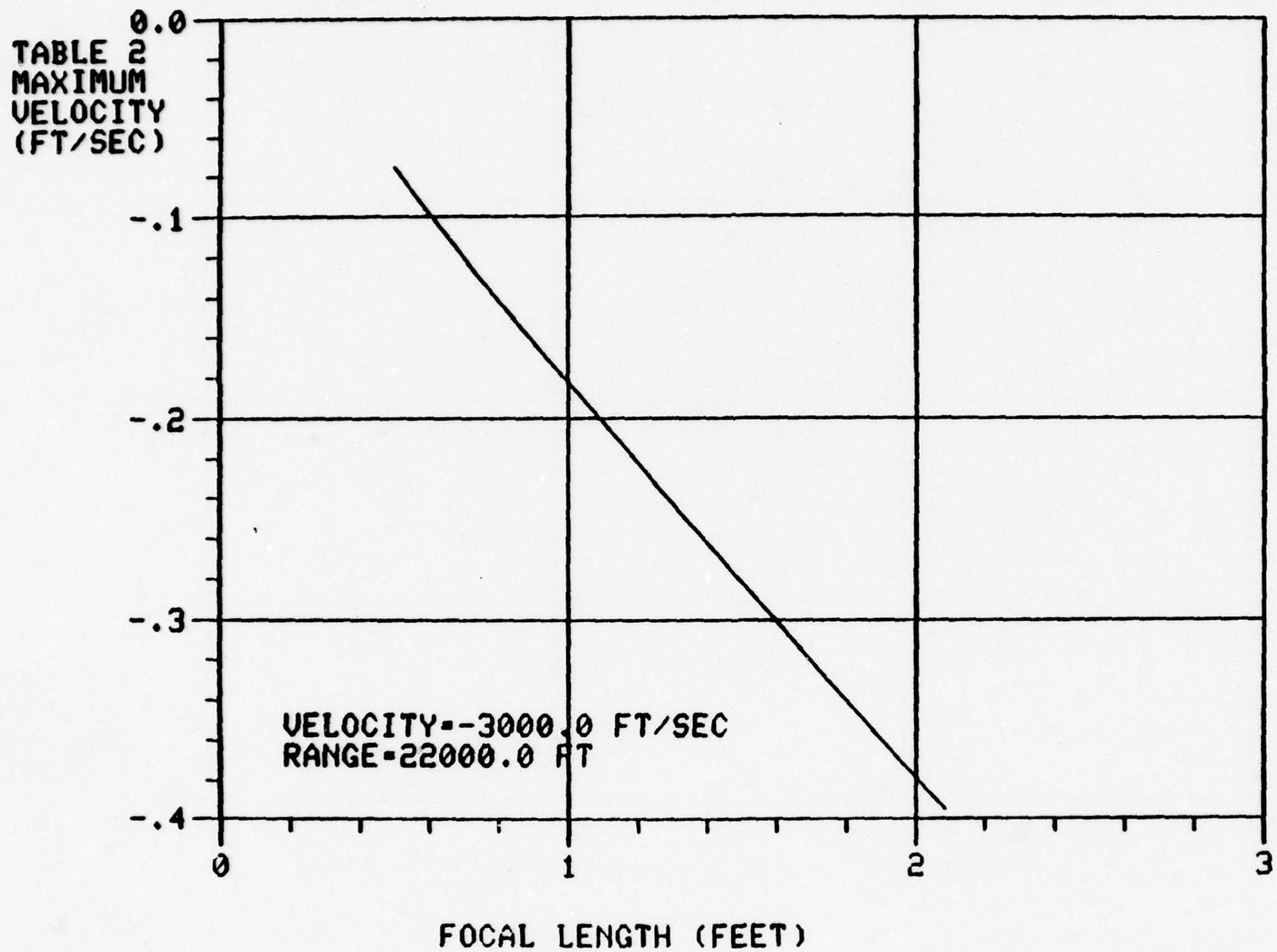

Figure 9. Table 1 Maximum Velocity vrs. Blind Range

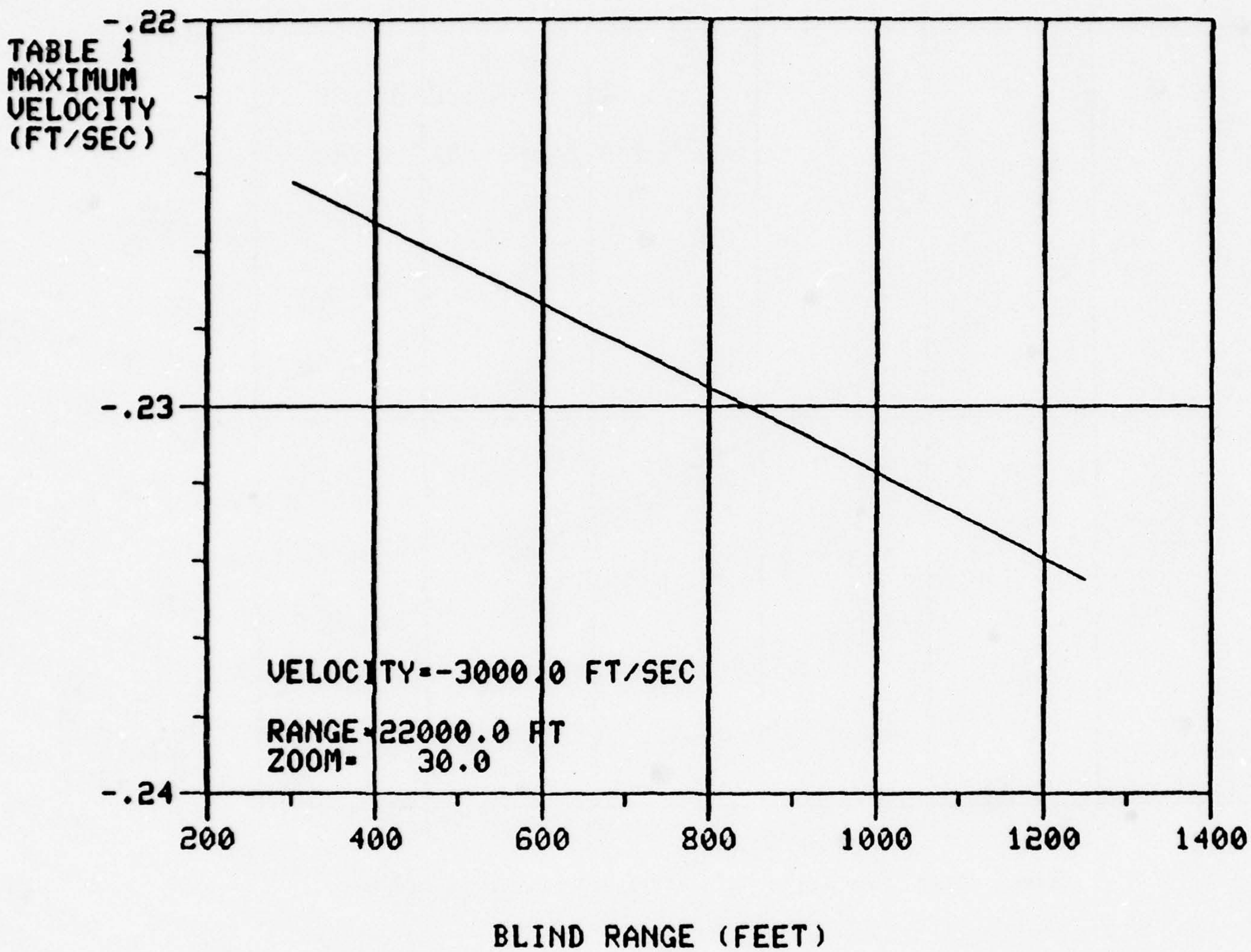

Figure 10. Table 2 Maximum Velocity vrs. Blind Range

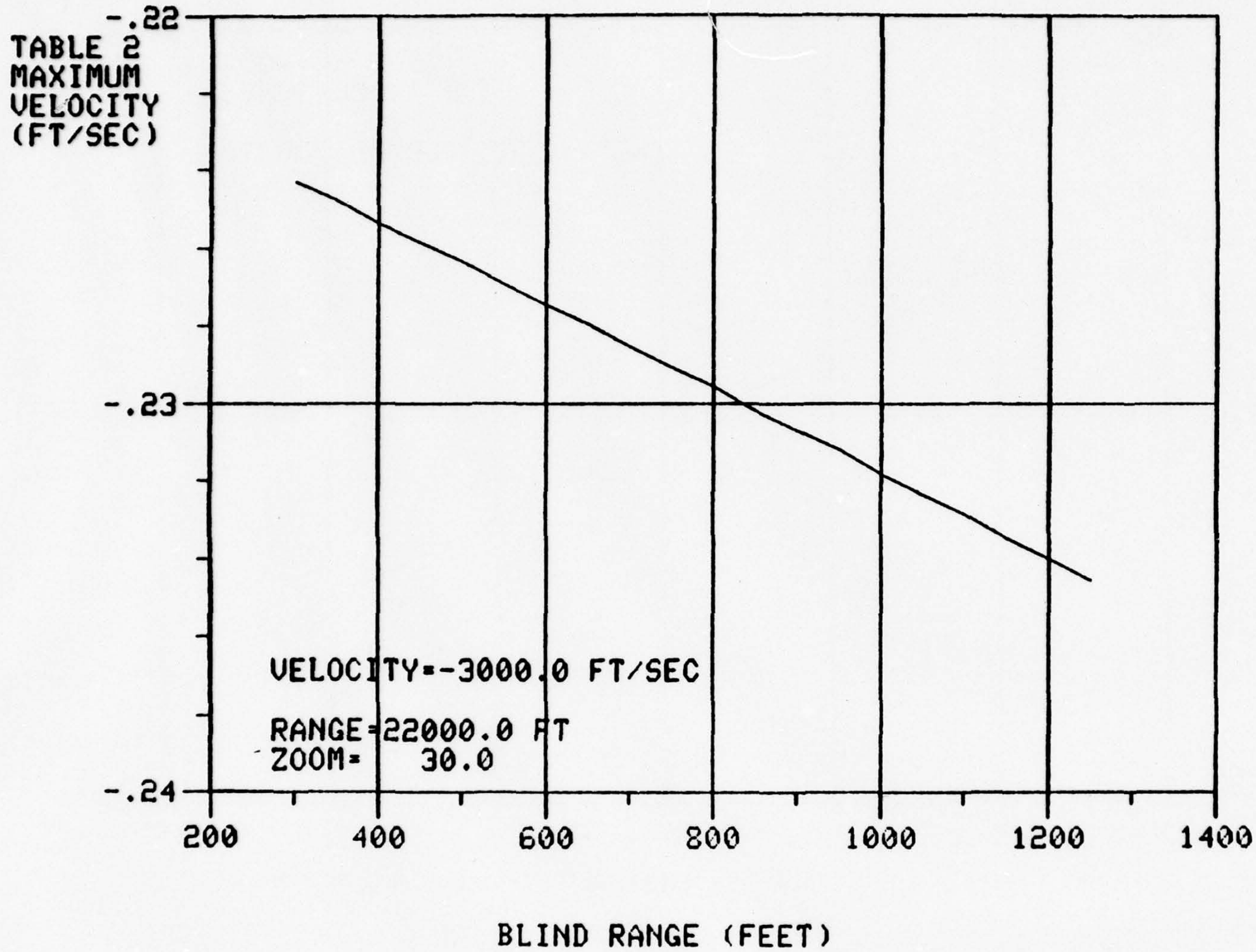

Figure 11. Table 1 Maximum Velocity vrs. Zoom

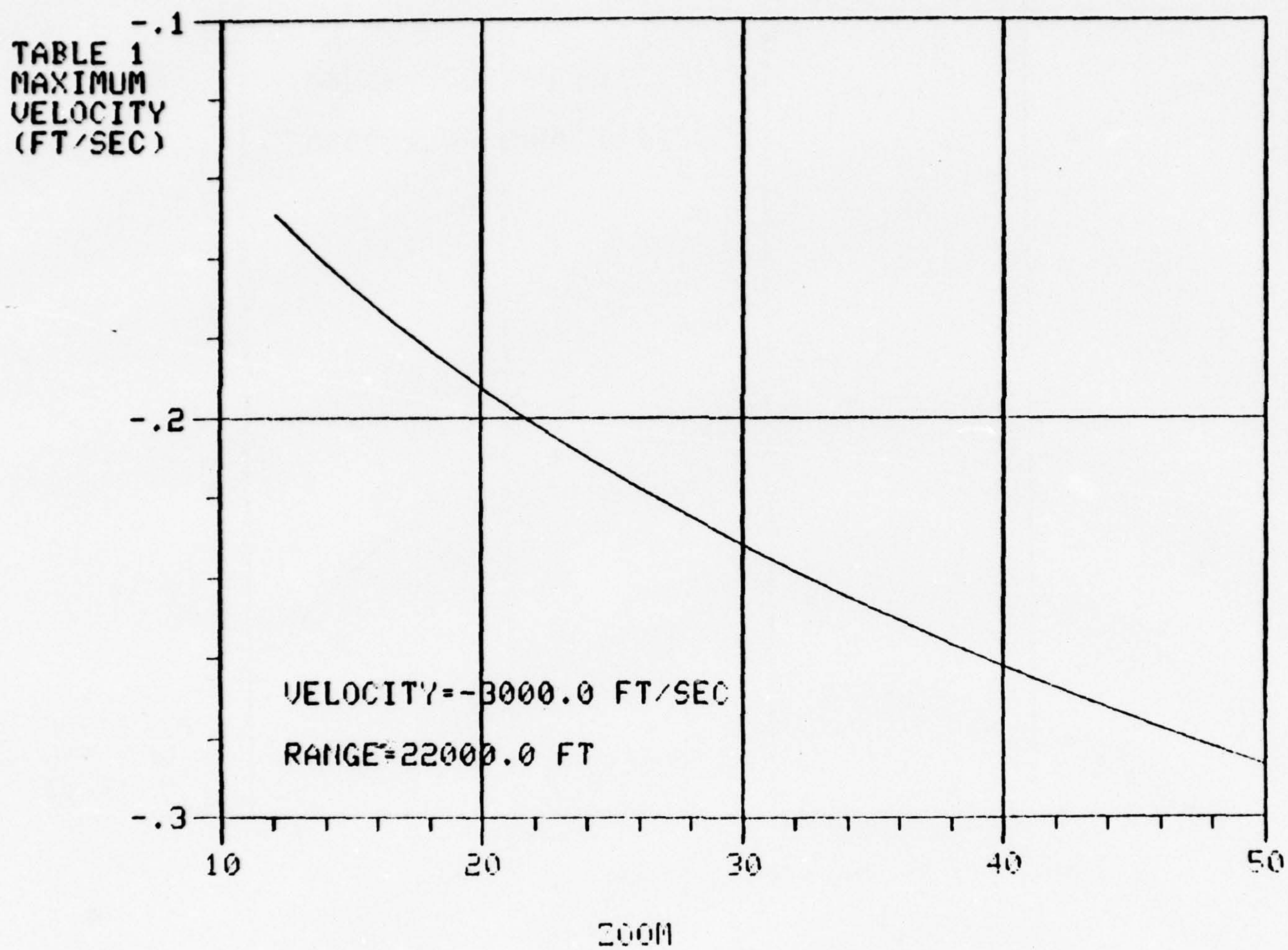

Figure 12. Table 2 Maximum Velocity vrs. Zoom

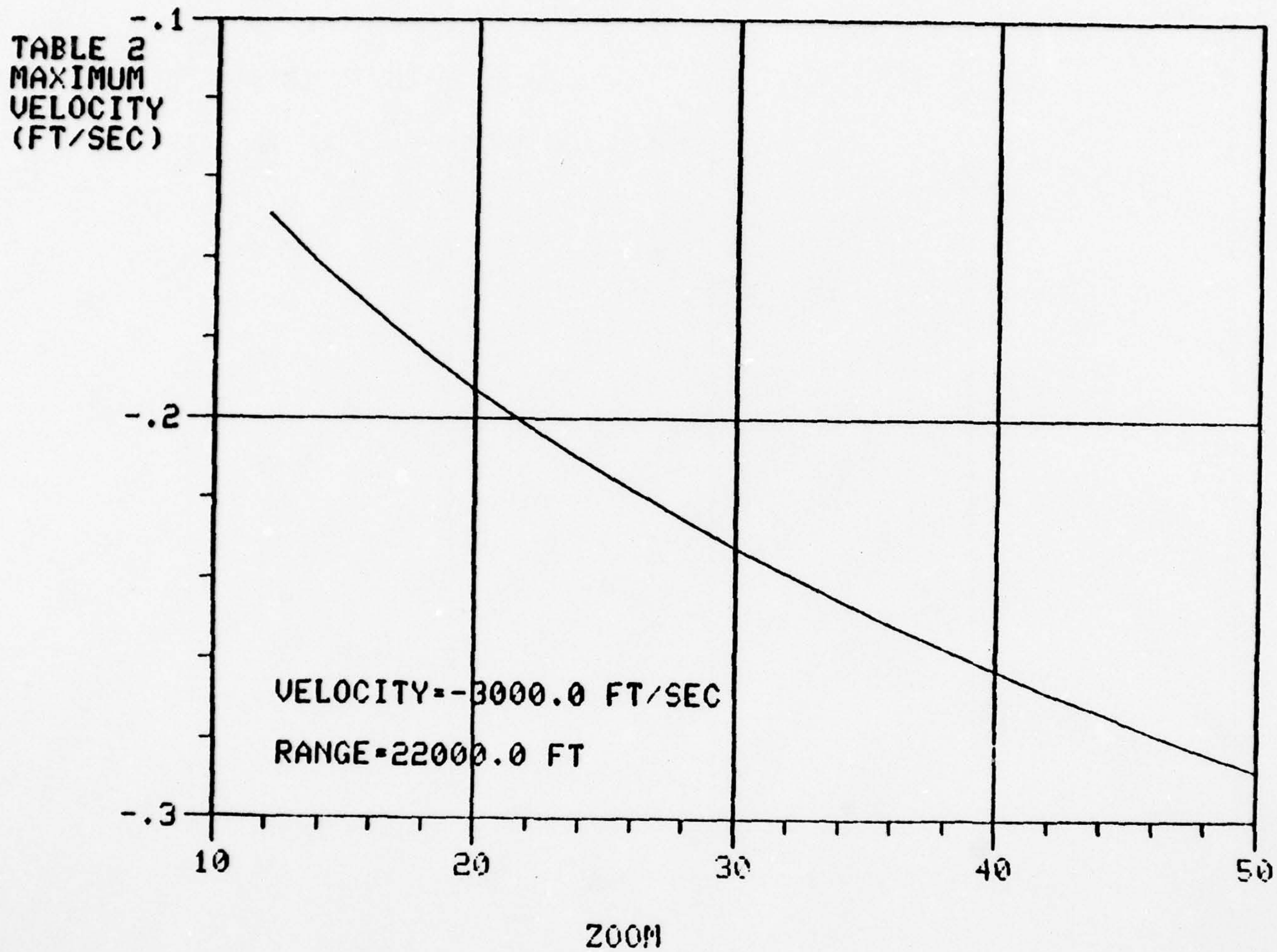

1978 USAF-ASEE SUMMER FACULTY RESEARCH PROGRAM
sponsored by
THE AIR FORCE OFFICE OF SCIENTIFIC RESEARCH
and conducted by
AUBURN UNIVERSITY AND OHIO STATE UNIVERSITY

PARTICIPANT'S FINAL REPORT

DATA SYSTEM ARCHITECTURES FOR STORES MANAGEMENT SYSTEMS

Prepared by:	William A. Hornfeck, Ph.D.
Academic Rank:	Assistant Professor
Department and University:	Department of Engineering Gannon College
Assignment:	Eglin Air Force Base Armament Laboratory Munitions Division Munition/Aircraft Interface Branch
USAF Research Colleagues:	Mr. John Cavin/Mr. Ron Boulet

Date:	August 18, 1978
Contract No:	F44620-75-C-0031

DATA SYSTEM ARCHITECTURES
FOR
STORES MANAGEMENT SYSTEMS

by

W. A. Hornfeck

ABSTRACT

Current approaches to aircraft design have identified stores management as a distinct functional entity. In general, aircraft stores are defined as the complement of weapons and suspension devices which are intended as line replaceable. The management of aircraft stores involves the control and communications system necessary in providing the pilot efficient interaction with the aircraft stores which are present.

Recent technology advances have provided the impetus to optimize the design and integration of Stores Management Systems (SMS) with two principal goals in mind: (1) reducing the complexity of the hardware required without sacrificing the capability and reliability of stores management features; and (2) increasing the range of applications of stores management systems in order to reduce the number of custom aircraft/stores configurations. Both of these goals, if achievable, could yield a drastic reduction in the overall life cycle costs associated with the weapon systems under consideration.

This report examines current trends in Stores Management Systems and the changes to future systems which are anticipated due to advances in electronics and communications technology. Systems aspects of SMS design--architecture, communication, hardware, software, operations--are discussed and an approach to an integrated/adaptive SMS is proposed. An important part of this report's conclusions deals with recommended areas of research and development to be pursued by the Air Force. The rationale for such recommendations being based on the opportunity for future SMS configurations to capitalize on current and anticipated breakthroughs in related technologies.

ACKNOWLEDGEMENT

The author wishes to express his appreciation to the Air Force Systems Command for support of the research project described herein. First, to Mr. Fred O'Brien of Auburn University and Mr. Walt Dittrich of the Air Force Armament Laboratory for their attention to the administration of the project.

The author would like to acknowledge the help and encouragement provided by the entire Munition/Aircraft Interface Branch. In particular, Mr. John Cavin, for many hours of fruitful discussions and cogent suggestions; Lt Col J.D. McEwen and Mr. Ron Boulet for their attention and guidance in the project; and Captain Dave Cooper, Mr. Phil Cunningham, and Captain Jim Dyer for the lending of their professional support and opinions.

Finally, special thanks are due to Col. James R. Tedeschi and Mr. Tom Maney of the Air Force Armament Laboratory for the interest and consideration given to this project.

LIST OF FIGURES

I. INTRODUCTION

PROGRAM BACKGROUND

This report will document the results of a research effort which has been performed in support of the Air Force Armament Laboratory at Eglin Air Force Base. The research has specifically involved problems related to aircraft Stores* Management Systems (SMS) and associated technologies.

The issues being addressed by the Air Force in the area of stores management include functional concepts such as:

- centralization of stores management functions,
- functional partitioning of stores management functions, and
- transparency of pilot-to-store and store-to-pilot interface;

as well as system concepts such as:

- enhancement of reliability and confidence levels,
- aircraft/stores interoperability, and
- minimization of pilot recognition/reaction time.

Perhaps the pre-eminent issue involving aircraft/stores interface is one of rising life-cycle costs associated with growing set of aircraft and stores having limited interoperability characteristics. This situation has evolved primarily because interface standards have been nonexistent and stores have traditionally been designed for specific aircraft/application.

A solution to the interoperability problems will involve a well-conceived set of standards and some radical departures from established design strategies for Stores Management Systems. In addition, a careful assessment of technology trends must be undertaken to pinpoint those technologies which should be further encouraged by the Air Force, and where technology breakthroughs should be anticipated. An SMS to address the needs of aircraft for the 1980's, 1990's, and beyond will need to be flexible as well as efficient (goals which are usually incompatible) and must take advantage of the most current systems and hardware technology.

OBJECTIVES AND APPROACH

The initial objective of the research task undertaken in conjunction with the Munition/Aircraft Interface Branch was an assessment of directions being taken by Stores Management Systems architects and trends observed within

---

* In general, aircraft stores are defined as the complement of weapons and suspension devices which are intended as line replaceable.

relevant technologies. Trends would also be assessed in related areas such as interoperability requirements, military standards, and life-cycle cost factors.

From these studies, a second objective was the establishment of an overall aircraft/stores development picture which places the Stores Management function into a more meaningful perspective. The final objective is the formulation of cogent suggestions which will aid the Air Force in establishing research and development directions to be pursued. The basis for such recommendations being the likelihood of future SMS configurations benefiting from current and anticipated progress in related technologies.

The approach taken in this research was as follows:

(1) Familiarization with Stores Management concepts;

(2) a. Investigation of current digital multiplex communications/processing system;

b. Assessment of current and anticipated technology trends which relate to the Stores Management function;

(3) Formulation of observations/conclusions regarding desirable evolution of Stores Management Systems;

(4) Identification of research areas which are vital to timely development of next-generation Stores Management Systems.

This report is organized to include background material, system considerations, and concepts related to an adaptive Stores Management scheme for future aircraft/stores operational systems. Section II reviews background and rationale establishing the basis for this Stores Management Systems study. Section III discusses the key technical aspects--architecture, communication, hardware, software, operations and support--of the overall Stores Management System. Section IV considers the high-level aspects of a Stores Management System which takes maximum advantage of anticipated technological improvements and aircraft/stores operational evolution.

Recommendations and conclusions are included in the final section of the report. An important part of this section deals with recommended areas of research and development to be pursued by the Air Force. These recommendations are based on: (1) trends observed in aircraft/stores interface design; (2) Stores Management Systems evolution; and (3) technology advances.

II. BACKGROUND AND RATIONALE

An aircraft Stores Management System must provide a suitable interface between the pilot and the full complement of aircraft stores and associated suspension equipment which is onboard. This interface must be capable of providing the pilot with the communications, control, and display functions necessary for efficient management of onboard stores during all phases of a particular mission. Figure 1 illustrates the conceptual problem associated with providing this interface.

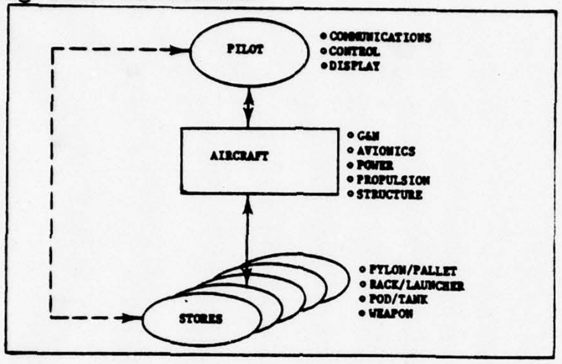

Figure 1. Virtual and Actual Pilot-Stores Interface.

The solid connecting lines indicate the hardware interfaces which are present and necessary for the integration of pilot/aircraft/stores functions and operations. The dashed connector shows a "virtual" interface which reflects direct pilot interaction with onboard stores. An efficient Stores Management System will provide the appearance of virtually direct control but will utilize all appropriate aircraft subsystems and interfaces in performing the Stores Management functions.

If one begins with the attributes which are characteristics of an overall Stores Management System, the following list includes the principal items which must be addressed:

- effective centralization of the functions associated with stores management;
- continuous pilot appraisal of the complete inventory of stores onboard;
- a flexible but efficient means for control of any of the available stores' operational modes;
- maximum interoperability of available aircraft and stores;
- transparency of pilot-to-store and store-to-pilot interface;
- minimum pilot recognition/reaction time;
- enhancement of system reliability and confidence levels.

To a fairly high degree, the attributes listed above are achievable with the exception of the fourth item--interoperability of aircraft and stores. Unfortunately, it is the interoperability attribute which has the most drastic effect on the operational costs of an aircraft/stores suite. These operational costs can be considered to include penalties which are not strictly dollar costs, such as: a limited set of aircraft on which stores can be flown; the time associated with flight-time operations in fitting aircraft/stores configurations; and logistics and repair delays associated with custom aircraft/stores configurations.

To form an appreciation of the interoperability problem, Figure 2 shows the proliferation of aircraft and stores which has accompanied advances in weapons requirements and new technologies.

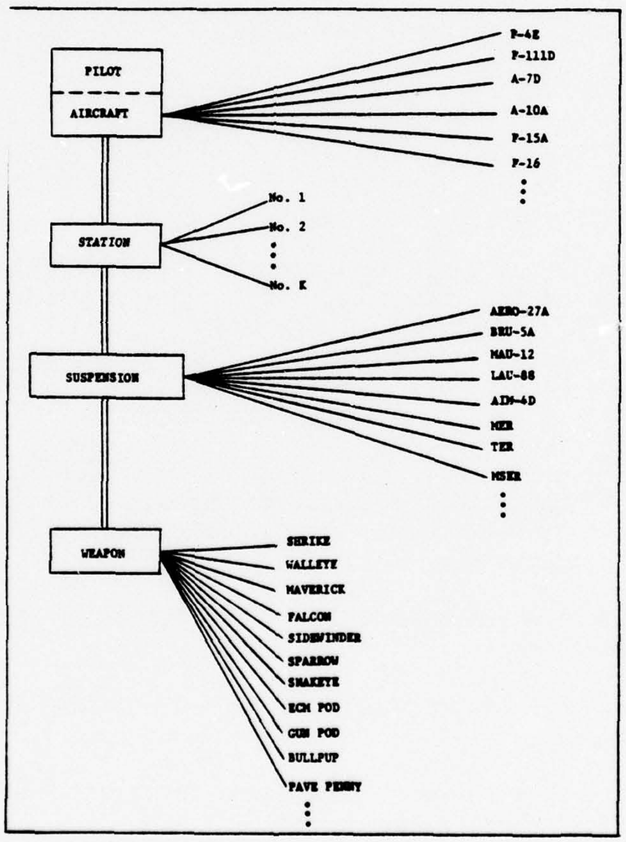

Figure 2. Proliferation of Available Aircraft and Stores.

The reader can easily appreciate the number of unique configurations which may (or may not) be flown. Nevertheless, certain comments are appropriate:

- the aircraft shown includes only principal Air Force attack and fighter aircraft;

- the number of stations may vary from eight to eleven for the aircraft listed;
- the lists of suspensions and weapons are simply meant to be a sample--a complete list of unique suspension devices could number over 100 and weapons could number over 200.

A typical calculation on the F-4E aircraft which has nine weapons stations, 17 compatible suspension devices, and 62 possible stores, would show the number of unique configurations to be greater than 2,000. Only a fraction of these configurations is possible due to interoperability problems between weapons, suspensions and stations. Much more severe restrictions on interoperability are encountered when different aircraft are considered.

The rapid development of advanced weapons has been spurred by breakthroughs in related technology areas and designs have been influenced by predominant trends in aircraft technology. These trends are principally:

- increased number of types and sophistication of aircraft/subsystems/weapons;
- continuing use, improvements and confidence in digital techniques for a signal processing, communications, and data handling;
- increased use of microelectronic devices;
- advances in software development technology and methodology;
- improvements in communications systems technology;
- operational distributed processing systems and increased use of digital multiplex data bus techniques;
- hardware functions increasingly displaced by firmware and software implementations; and
- military standards to promote interoperability.

The interoperability and technology considerations discussed above have a profound effect on the development and design of an efficient and cost-effective Stores Management System. The most tenuous problem which must be addressed is the development of Stores Management Systems satisfying a significant interoperability requirement in the face of changing technologies and a dynamic aircraft/stores suite.

Despite the difficulties inherent in the development of a Stores Management System which will have application across a wide range of aircraft and stores, progress in related areas in making this objective feasible. There are two specific design trends which are influencing the evolution of Stores Management Systems:

(1) Increased use of digital techniques and microelectronics devices. This trend places added emphasis on distribution of signal and data processing, digital multiplex data bus communication, and highly modular hardware systems.

(2) The use of increasingly information-intensive system. This results in the realization of a greater proportion of functions via software and closer attention to the application of engineering principles to all aspects of the software life cycle.

There are a number of current digital multiplex communications/processing systems in various stages of development which reflect the trends outlined above. The systems which have been investigated in conjunction with this study include:

° F-15 Avionics Data Bus	operational
° F-16 Stores Management Set ° F-18 Redundant Multiplex Data Bus ° B-1 Data Multiplex Buses ° Space Shuttle Multiplex Data Bus System ° Navy Shipboard Data Multiplex System (SDMS)	Developmental
° Eglin F-4E SMS Flight Test Program ° AFAL DAIS Multiplex System ° Integrated Digital Avionics for Medium STOL Aircraft (IDAMST) ° Advanced Remotely Piloted Vehicle (ARPV)	Investigative

This list represents a group of bellwether systems from which valuable lessons can be learned regarding systems design for advanced military aircraft. By no means is this group inclusive of all systems which offer data points useful in determining directions for evolving Stores Management Systems. Other sources include industrial systems, telecommunications systems, programming systems, and so on. The critical consideration which should be given to advanced SMS development is to avoid a reliance on serendipity for the evolution of improved systems. Rather, careful attention should be given to the areas of research and development which should be encouraged for future applications.

III. SYSTEM STUDIES

SMS ARCHITECTURE

Data communications/processing architectures have undergone considerable changes during recent years. These changes have resulted from the increased capability of hardware and better understanding of communications techniques. Figure 3 illustrates the classical approaches to computer communications networks. For many years, the advantages of distributed architectures were apparent; however, the realization of effective distributed systems had to await the arrival of mini-computer systems, micro-processor technologies, and a better understanding of computer networking strategies. This now being the case, not only effective distributed systems, but also federated or embedded* architectures are somewhat commonplace.

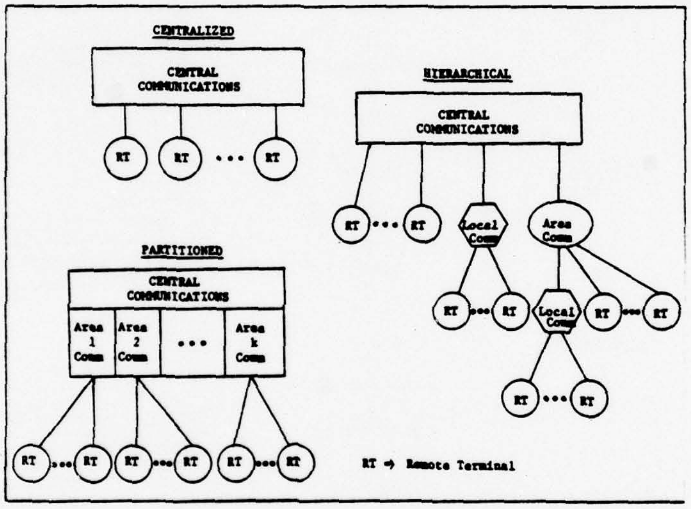

Figure 3. Classical Computer/Communications Networks.

The system designer's problem has changed from one of adapting a solution to an available architecture to one of selecting the appropriate architecture for a problem solution. Not only are the classical architectural concepts being used, "hybrid" architectures using aspects of more than a single type are being implemented, as well as "custom" architectures devised for a particular application.

This freedom of architectural form allows the development of a Stores Management System concept which is tailored to functions and constraints of the aircraft/stores environment. A principal consideration is the MIL-STD-1553B multiplex data bus. This standard is an effective compromise between

---

* A federated architecture is generally considered to be one which employs identical computing elements, whereas an embedded architecture employs subsystem-unique computing elements.

the sophistication required for efficient communications links and the simplicity required for modularization and interoperability. In this report, it will be assumed that a MIL-STD-1553B multiplex digital data bus will be used for all communications; however, the topology of the computer/communications network will be tailored to the SMS function.

A second set of assumptions which will influence an SMS architecture involves the physical characteristics of the aircraft/stores configurations to be considered. Figure 4 shows the three basic configurations which will be assumed as representative of virtually all aircraft/stores which are of interest. Several points should be noted concerning the nature of these

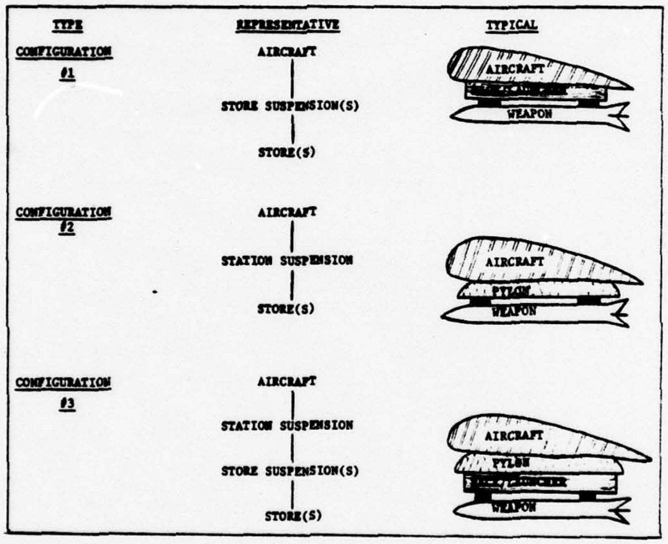

Figure 4. Basic Aircraft/Store Configurations.

configurations:

- aircraft stations may be wing stations, wingtip stations, or fuselage stations;
- a station suspension may be a pylon, conformal pallet, or other aircraft-unique device; and may carry single or multiplex stores or store suspension devices;
- a suspension device may be a rack, launcher, or other store-unique device;
- store suspension devices may carry single or multiple stores;
- stores are considered to be missiles, munitions, guns, pods, fuel tanks, etc.

- stores and store suspensions can be released or jettisoned without adversely affecting SMS operation;

- all elements of the assumed configurations are potentially "smart" devices, i.e., have data-handling or data-processing capabilities.

A final set of assumptions considers the communications paths which are required to accomplish the Stores Management function. First, it will be assumed that avionics data will be required by the SMS and therefore data transfer (two-way) between the avionics bus and SMS bus must be possible. (This also assumes a bus structure for the avionics subsystem.) Secondly, all independent buses will require a bus controller. Third, all digital data interfaces are MIL-STD-1553B compatible. All units connected to a single bus must appear as remote terminals and any SMS remote terminal may communicate with any other SMS remote terminal.

The simplest architectural concept for SMS consideration would be a single SMS multiplex bus with all related subsystems appearing as remote terminals. This structure is shown in Figure 5 and can be viewed as a "horizontal" bus structure. An assessment of this architecture in relation

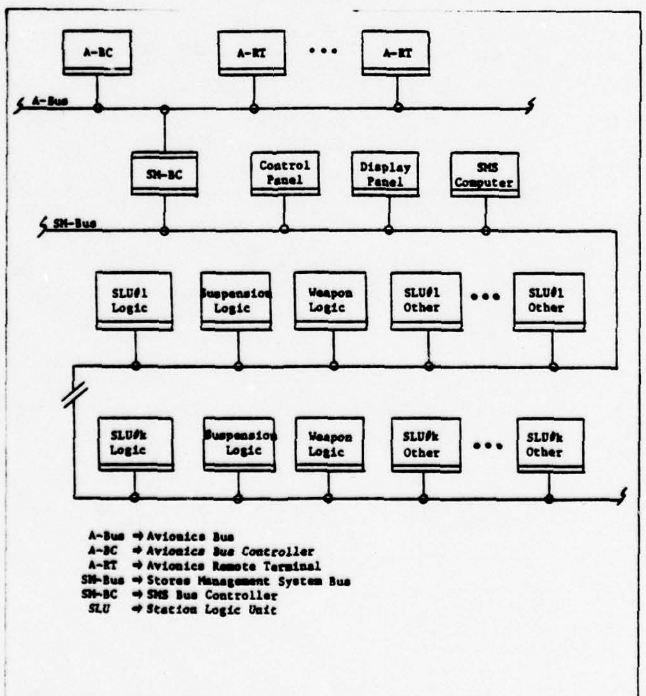

Figure 5. Universal (Horizontal) Bus Structure for SMS.

to the overall SMS functions yields the following list of advantages and disadvantages:

ADVANTAGES	DISADVANTAGES
uncomplicated structure	single-point-failure possibilities
inherent modularity would promote software simplicity	possibility of excessive SM-BC traffic
communications and control algorithms could be straightforward.	exclusively serial data/communications transmissions
	bus length
	restricted communications protocol
	sensitivity of bus traffic to subsystem changes.

It is important to note that the above list, by simply considering the number of items in each column, would promote a negative reaction. However, the "weight" or importance, which should be assigned to each item has not been considered. Quantitative measures would be difficult, and in the conceptual stages of a study such as presented here, can only be estimated.

Figure 6 shows an SMS architecture which could be considered as a "vertical" bus structure. This architecture allows independent communication

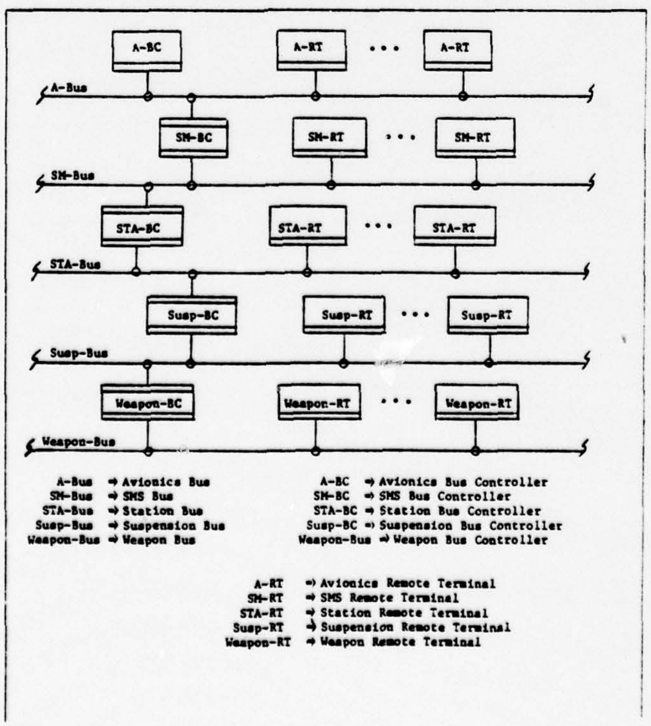

Figure 6. Nested (Vertical) Bus Structure for SMS.

on three separate, but interconnected, SMS buses plus an interface to the aircraft avionics bus and any weapon buses. A list of advantages and disadvantages associated with this architecture follows:

ADVANTAGES	DISADVANTAGES
bus lengths	speed
isolation of subsystem changes	restricted communications protocol
opportunity for independent subsystem optimization	bus controller overhead
parallel communications and data transfer	possibility of excessive SM-BC traffic
failure isolation	
immunity to functional or technological changes	
physical compatibility with aircraft/stores structure	

In addition to the strictly horizontal or vertical structures, there are a large number of "diagonal" bus structure possibilities. In general, such a diagonal structure would increase communications speed at the expense of hardware and software complexity. One possible diagonal structure is shown in Figure 7 and employs a special controller in order to reduce the communications overhead associated with the multiplicity of bus levels in

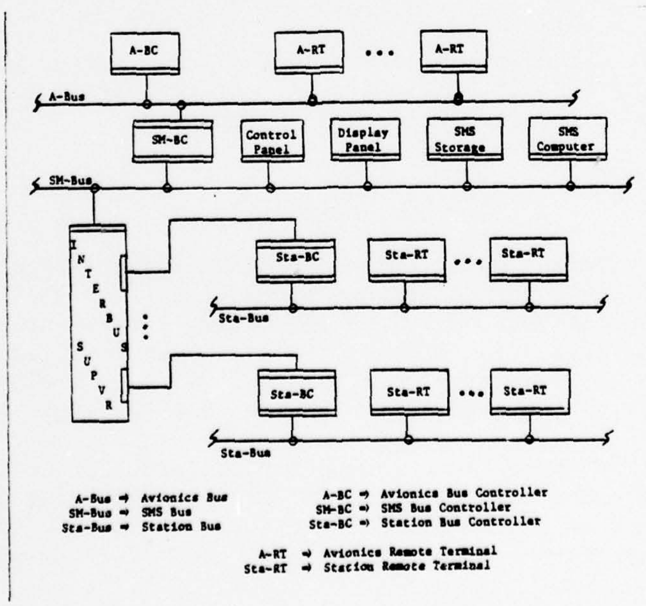

Figure 7. Interbus (Diagonal) Bus Structure for SMS.

a vertical arrangement. This type of architecture would have the following advantages and disadvantages:

ADVANTAGES	DISADVANTAGES
moderate bus controller overhead	single-point-failure possibility
balanced controller workloads	unique interbus supervisor
speed/complexity tradeoff	complicated protocol
failure isolation	software complexity
some immunity from functional or technological changes	
optimization at the station level	

An assessment of the candidate architectures which have been discussed must involve not only the listed advantages/disadvantages, but, as mentioned earlier, their relative importance. In addition, all relevant technical aspects of an overall SMS must be considered. These include:

- communications
- hardware
- software
- operations and support

Before a proposal is put forth concerning a suggested architecture, the next section will discuss the four technical areas mentioned above, as they relate to the Stores Management function.

SMS COMMUNICATIONS

Directly related to the selection of an SMS architecture is the specification of the data communications procedures which shall be used. The problem is somewhat bounded by the assumption concerning use of the MIL-STD-1553B multiplex data bus. However, this standard still allows considerable flexibility in the communications protocol which is employed, especially with the addition of a broadcast option in the 1553B version.

Choice of an appropriate communications protocol is generally a compromise between (1) the time required for transmission of a complete message from one communications terminal to another and (2) the complexity of a network which minimizes message transmission times for all possible communications paths.

There are three basic communications structures which have received considerable attention in applications involving distributed terminals having certain characteristic data communications requirements. The three structures can be described as central, partitioned, and hierarchical, and are shown in Figure 8. These communications structures strongly reflect the architectural nature of a particular system configuration. The centralized structure is particularly appropriate for a universal (horizontal)

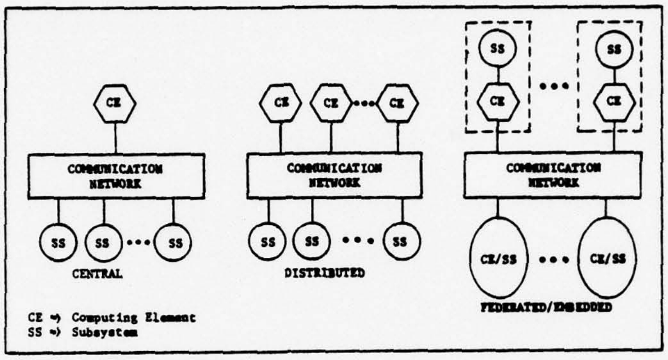

Figure 8. Communications Structures.

architecture as shown previously in Figure 5. A partitioned structure would suit the interbus (diagonal) architecture of Figure 7, and the hierarchical structure is most appropriate for the nested (Vertical) architecture of Figure 6. The final choice of a communications structure, however, will depend not only on the system architecture, but on such considerations as:

- number of remote terminals
- functional relationship of remote terminals
- communications protocol
- required communications rates
- data rates
- physical constraints
- modularity and flexibility requirements

The actual communications protocol to be followed imposes rules upon central, area, or local communication nodes with the objectives being an orderly and reasonably efficient flow of network messages. If a time-division-multiplex data bus is assumed, three principal types of communication protocol would merit investigation. These protocols are described in the following paragraphs and the principal attributes of each are listed:

(1) Round-Robin Protocol - is a dynamic control protocol where any remote terminal connected to the data bus may operate as a controller terminal. In this method, each terminal is given control of the bus in turn; however, only one terminal may transmit at a time. The order in which control is offered may or may not be fixed. If a terminal has data to be transmitted, this is accomplished during the time period allotted; otherwise, control immediately passes to the next terminal in sequence. This arrangement has the following attributes:

- difficult to extend to multiple communication (bus) levels;
- inefficiency in resource utilization;
- timing is not deterministic;
- simplex control structure;
- difficult to achieve configuration flexibility;
- moderate speed.

(2) Polling Protocol - is a synchronous command-response protocol where all remote terminals are queried in a sequential fashion to determine if a message action is required. If a particular remote terminal is queried and desires to initiate a message transmission, the data bus is made available for the required time and the next terminal in the sequence is queried. If a terminal requires no message action, control is simply offered to the next terminal. The following attributes are inherent in this arrangement:

- allows nesting of of communications (bus) levels;
- graceful degradation features;
- flexible control structures are possible;
- timing is predictable;
- moderate inefficiency in resource utilization;
- moderate speed.

(3) Interrupt Protocol - is an asynchronous, interrupt-processing protocol where any remote terminal may request use of the data bus at any time. All requests are either handled immediately or, in the case of multiple active interrupts, are stacked for eventual handling in an appropriate fashion (LIFO, FIFO, priority, etc.). The attributes are as follows:

- complex control structure is required;
- graceful degradation features;
- nesting dramatically complicates control;
- fast;
- very efficient resource utilization;
- timing and validation extremely difficult.

It is possible, for a particular communications network, to adopt one of the above protocols exclusively. In addition, a communications structure may employ a combination of the three possibilities. The selection is dependent upon the characteristics desired in a particular application.

For Stores Management System applications, a command-response polling protocol would be compatible with MIL-STD-1553B and would provide a reasonably simple control structure. In addition, testing and validation are simplified due to the synchronous nature of communication. Message transmission speeds are critical constraints. On the other hand, an interrupt protocol would provide a speed advantage but an additional interrupt bus would be required. Also, an interrupt system is asynchronous in nature and testing/validation procedures would require considerable effort. Finally, it should be mentioned here that a round-robin protocol provides advantages of synchronous operation but this protocol is not well suited to the configuration changes associated with the SMS environment.

SMS-RELATED TECHNICAL AREAS

There are a large number of technology considerations which will influence the evolution of advanced Stores Management Systems. The preceding two sections have discussed the conceptual aspects of an SMS architecture and communications structure. Figure 9 shows the general technology areas which will affect their evolution.

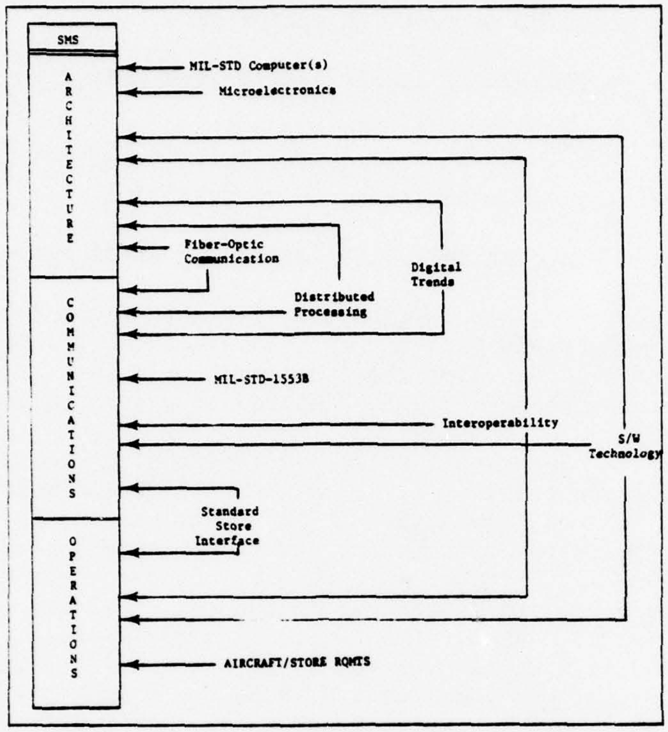

Figure 9. Principal Technology Considerations.

The chart shown in Figure 9 also considers the operational aspects of a Stores Management System. These include the operations necessary for the development, test and validation, integration, flight procedures, and maintenance of the system. These are recurring costs and drastically affect the overall life-cycle-costs associated with the system.

The following paragraphs will highlight the specific technologies which are implied by items shown in Figure 9.

Digital Trends - Whenever possible, it is becoming increasingly advantageous to represent information in digital form. This trend is accelerated by the widespread use of LSI processors and the greater number of subsystems which are capable of data processing functions. Representation in digital form allows data manipulation and has the added advantage of inherent standardization.

Microelectronics - This single area of technology has done more to revolutionize the system design process than any other related technology. Specific devices which provide the system designer with very powerful tools and which are currently available or soon to be in a production stage include:

- Linear IC devices
- Digital IC devices
- LSI processors
- LSI memory devices
- Programmable interface devices
- Mass memory micro-devices

The effect of microelectronics advances on the design process cannot be overstated; it remains for the military users to exploit these advances and promote further research in areas which promise cost or operational benefits.

Fiber-Optic Communications - The increasing use of multiplex data bus techniques for handling of information as well as the growing volume of information to be processed aboard an aircraft will ultimately require more sophisticated communications links. Fiber-optic technology shows a high probability as a solution in this area, and will soon become an available hardware technology. Fiber-optic cables have the potential to provide wide bandwidth (up to 100 MHZ), high noise immunity communication links with the added advantage of allowing alternative multiplexing techniques.

Distributed Processing - The techniques and technologies required to support distributed processing systems are reaching maturity. Current system configurations make liberal use of distributed, federated and embedded architectures, as well as combinations of these basic architectures. This allows data system configurations to be better tailored to the physical and functional characteristics of any particular application.

Software Technology - Recent advances in the software area have centered around the effective management of software projects and enhancement of programming techniques. Management efforts are attracting more emphasis as it is recognized that costs associated with integration, test and validation, and maintenance are the overriding software cost factors. Improved programming techniques are a direct result of the recognition of this fact. The Software Engineering area has developed to the point of being an identifiable scientific discipline.

Military Standards - The promulgation of a well-conceived set of military standards benefits the systems architect in promoting more cost-effective designs and usually more efficient systems. In particular, the following standards will affect SMS development:

- MIL-STD-1553B - Multiplex Data Bus
- MIL-STD-483/490 - Software Documentation

- Proposed MIL-STD - Computers

- Proposed MIL-STD - Store Interface

Interoperability - The importance of aircraft/stores physical interoperability was discussed in Section II. Just as important is the requirement for hardware interoperability on a functional level in order to promote subsystem designs which can proceed concurrently and face minimum integration problems at system test time. This allows all phases of aircraft/weapons design to enjoy a maximum amount of development time and also permits subsystem modifications without prohibitive integration or retrofit costs.

Aircraft/Stores Requirements - The added technological sophistication of both aircraft and stores is requiring much greater efficiency in a Stores Management System which must have a powerful, yet uncomplicated, weapons management facility for the pilot.

IV. STORES MANAGEMENT SYSTEM DEVELOPMENT APPROACH

The preceding section discussed the various technical aspects of the Stores Management function and related technologies. This section will explore an approach to an advanced SMS which addresses the interoperability problem and takes maximum advantage of developing technologies.

A characterization of the results of current methods in SMS development is shown by the state diagram of Figure 10(a). The present inventory of aircraft and stores carries with it an unwieldy number of custom SMS designs tailored to specific aircraft and specific stores. This situation remains

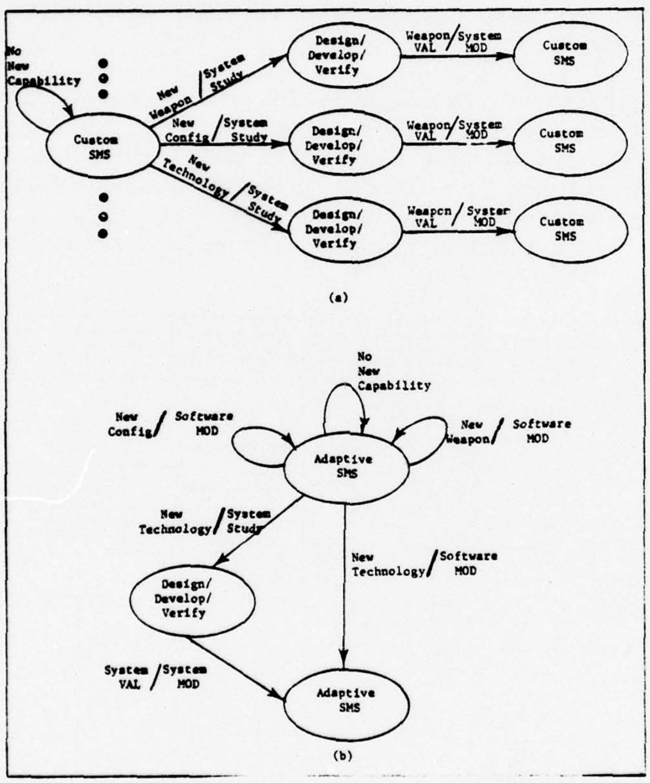

Figure 10(a). Present SMS Evolution. (b) Adaptive SMS Methods.

stable, although inefficient, if current capabilities remain fixed. However, when any new weapon, new configuration, or new technology is proposed, a transition is precipitated involving system studies and leading to a design/development/verification "state" or cycle. Once validation of any new capability is complete and a system modification implemented, the result is generally another custom SMS. The implications of this cycle are readily foreseeable from the diagram and reflect the current state-of-affairs in aircraft/stores interoperability.

Figure 10(b) depicts a more desirable situation. This state diagram reflects a Stores Management System which has minimum sensitivity to weapon,

configuration, or technology changes. The implication here is the capability of an advanced SMS to adapt, through purely software, or programming, means to changes in program or mission requirements. In addition, technology changes would have a minimum effect on an adaptive SMS. It is recognized that changes must be accounted for which would require a design/development/verification cycle; however, once implemented, the forerunner SMS would be replaced by the more current version.

The feasibility of an adaptive SMS and the extent to which it would be universal between aircraft and stores is certainly open to debate. On the other hand, the cost effectiveness is self-evident. The remainder of this section will discuss the key features of a Stores Management System which has maximum potential for interoperability and adaptability to configuration/weapon/technology changes.

Effective development of an adaptive SMS would necessarily be in the context of anticipated aircraft technology evolution. The diagram shown in Figure 11 is a graphic description of the technical trends affecting the Stores Management function. The blocks which are shaded represent technology driving functions and were discussed in the previous section. The overall diagram illustrates the evolution toward integrated aircraft/avionics/weapons systems.

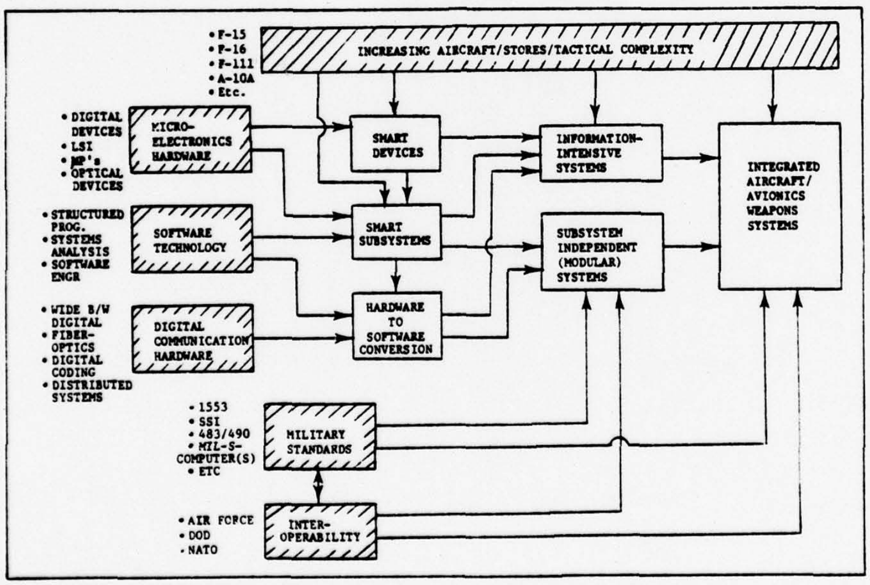

Figure 11. Aircraft Technology Trends Toward Integrated Systems.

A Stores Management System architecture which is best suited to highly integrated aircraft design with a maximum degree of modularity would be based on the nested architecture described in Section III and shown in Figure 6. Reviewing the list of advantages and disadvantages for this architecture reveals that the list of advantages allows considerable optimism. In addition, of the four disadvantages listed, only two present problems of the "make-or-break" variety. That is, (1) speed, and (2) bus controller overhead are

disadvantages which must be overcome in order for the architecture to have any degree of viability. Fortunately, the two are related and a solution for either would probably have an effect in both areas.

Figure 12 shows the nested architecture of Figure 6 in greater detail. From this figure, correspondence with the physical aspects of an aircraft/stores interface is observable and the inherent modularity can also be seen.

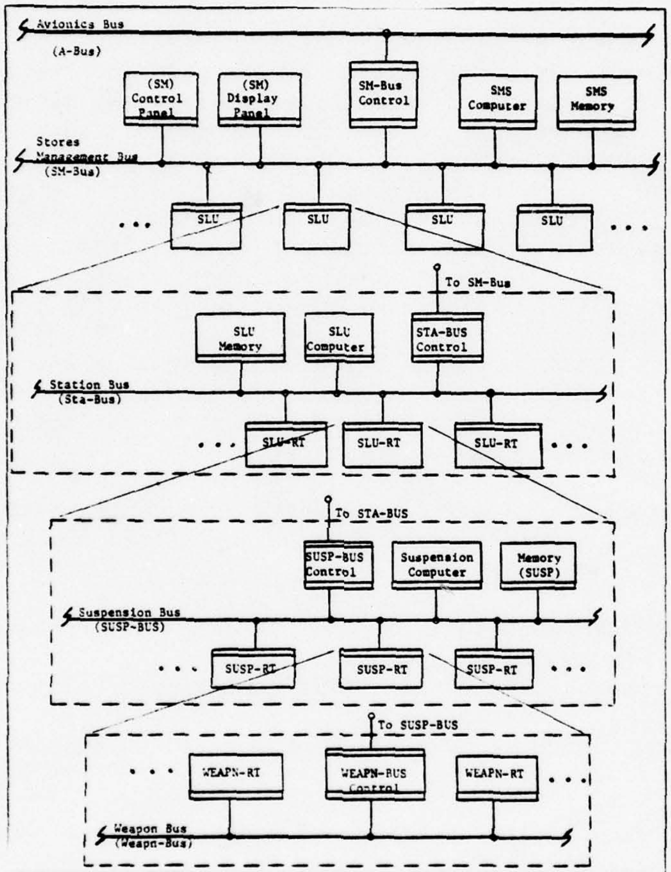

Figure 12. Nested Bus Architecture for Avionics/SMS/Stores Communication.

The unique feature of the architecture is in the capability of local communication so that parallel data transfer operations can take place at very high rates, taking full advantage of distributed processing capabilities.

The core of the Stores Management System would include the SM-BUS with associated terminals and the STA-BUS with its associated terminals. In a development sense, the store suspension architecture as well as weapon architecture would be the responsibility of the appropriate development programs. Central to the interoperability features would be a standard

multiplex data bus interface, communications protocol, and software structure. These concepts are presently being employed at the avionics bus level and the proposed architecture would require similar communications in a nested arrangement. The communications rate problem is encountered when data transfers are required across a number of bus levels. In this situation, the efficiency provided by the bus controller units in transferring information becomes critical. Bus controller capacity is also the issue when considering the overhead associated with data transfer between any two bus levels.

There are a number of technological and operational considerations which tend to support the investigation of a nested architecture. First, the nature of stores management communications is such that the necessity for transferring large volumes of data at high rates across several bus levels does not presently exist. In the event that future requirements dictate such a need, a low-risk posture is afforded by the potential benefits of technological advances in fiber-optics links, component speeds, memory capacities, and processor throughput capabilities.

Efficient control of overall SMS communications will be a formidable problem. This control will reside principally in SM-BUS level components but will be distributed to a large extent among station level components as well as lower-level processing systems. Ultimately, the effectiveness of the control schemes will depend in large part on the software structure adopted during the conceptual design stages.

The role played by the software aspects of advanced systems is increasing in both volume and importance. This is emphasized by an observation of current trends, such as:

- increased application of digital processing techniques;
- greater proportions of processing functions realized via software;
- microelectronics devices allowing greater volumes of software to be onboard;
- greater flexibility/intelligence required within systems, subsystems and devices;
- systems are increasingly information-intensive;
- evolution of software implementation techniques toward a scientific/engineering discipline.

The greater proportion of overall system design which involves aspects of software technology has demanded more emphasis on software development techniques. An advanced SMS having considerable software and firmware requirements will place added importance on the definition of SMS functional requirements and the functional partitioning of the requirements. These are early-design-stage tasks which have a great influence on the final hardware/software architecture and implementation. Reference 12 contains some detailed analyses of this concept.

The tendency to replace more and more hardware functions by software and firmware functions has significant advantages in flexibility and the increased capability associated with added intelligence embedded in the software. As is always the case, however, it is not a situation where one gets "something for nothing." The problems introduced by the added reliance on software functions involve the management of software systems and testability of software items. These problems are particularly acute for software systems which are meant to be flexible, adaptive, or generic in some framework.

Figure 13 illustrates an operational scenario which is implied by a Stores Management System which, in the interest of interoperability, incorporates a high degree of flexibility. The nucleus of such an operational system would be the software base to support a limited number of SMS designs, each of which is generic to a maximum extent.

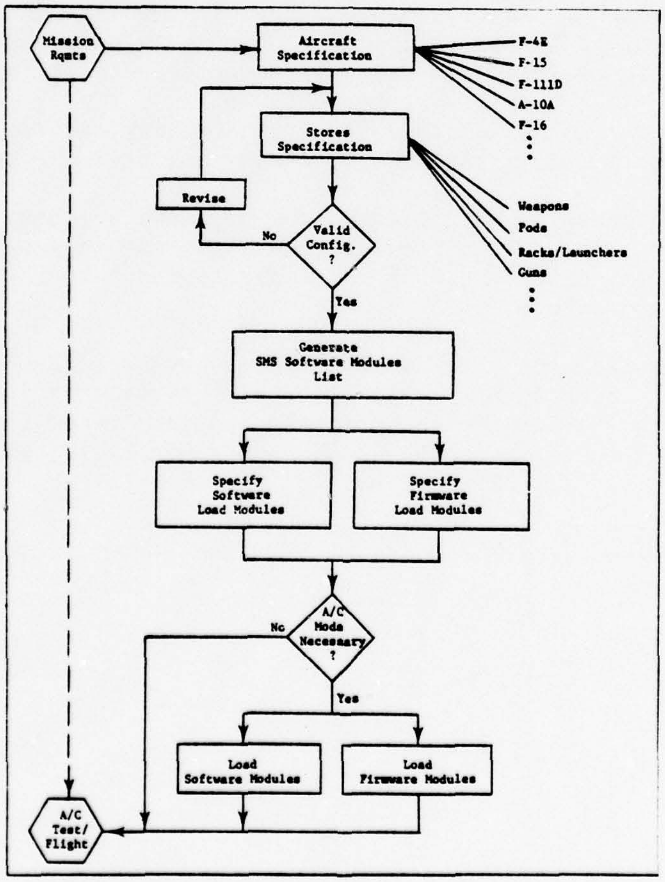

Figure 13. Mission Requirements-to-Aircraft Test/Flight Operations with Adaptive SMS Features.

There are three phases of operations implied by the flow diagram of Figure 13. First, specification of the aircraft/stores configuration would be proposed in response to stated mission requirements. The allowable configurations would depend upon the interoperability which has been achieved. That cross-section of aircraft and stores which are truly interoperable will depend not only on the flexibility of a Stores Management System, but also on careful planning in this direction for other subsystems, interfaces, and functions.

The second phase, generation and specification of software/firmware modules would depend upon an extensive support software base. This software support facility would be required to have the capability to either (1) retrieve the necessary load software from an extensive data base or (2) generate the necessary software module lists so that appropriate modules could be combined to form the complete load software. Any combination software modules would be previously validated for the specific aircraft/stores configuration.

The third operational phase would be part of the actual aircraft flight preparation procedures. Any software or firmware modifications which are necessary are accomplished at this point. During this phase, the advantages in ease of software modification relative to hardware modification is realized.

There are two critical areas which would require careful attention in the development of an advanced SMS of the nature just described:

(1) An exhaustive investigation of the applicable concepts and technologies. Both would require a level of maturity sufficient to support the development of a generic approach to the Stores Management function.

(2) The establishment of an SMS software development/support facility. Figure 14 shows the operational elements which would be required to assure (i) coordinated software development--main support facility, (ii) local autonomy--local support facility, and (iii) overall control and management--standards and coordination.

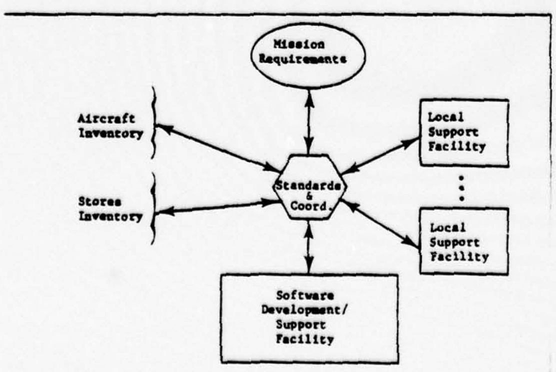

Figure 14. Operational Elements of an Advanced/Adaptive SMS.

V. CONCLUSIONS AND RECOMMENDATIONS

The development of a wide variety of aircraft and stores to fulfill the Air Force mission has created the need for solutions to problems involving interoperability. These problems concern not only the Air Force, but the entire Department of Defense and the NATO nations.

This report has described the technical aspects of a Stores Management System for advanced applications which treats the interoperability issue as a design focal point. In doing so, several critical technical aspects are exposed for consideration. The computer/communications network which would be best suited for the Stores Management function is one. A nested architecture has been described which has an inherent physical compatibility with the aircraft/stores structure and is considered to be the most suitable scheme for immediate investigation.

The selection of an architecture is not independent of the optimum communications protocol for a Stores Management System. It is pointed out that both synchronous and asynchronous communications schemes bear consideration. The speed advantages of an asynchronous (e.g., interrupt-driven) system must be compared with the greater simplicity of a synchronous (e.g., command-response) system. Other tradeoffs include consideration of additional hardware, testability, compatibility with 1553 multiplex standard, and so on.

The selection of an SMS communications protocol, in turn, will have a great effect on the complexity of the required software. The adaptive SMS which is suggested in the previous section would rely heavily on the effective management of software development and maintenance efforts. A sufficiently complex software structure would pose a threat to the basic feasibility of such an attempt to enhance aircraft/stores interoperability features.

An objective of this report has been to establish a frame of reference for the pursuit of an effective Stores Management System which would provide, to some degree, a solution to the interoperability problem. Keeping this objective in mind and considering the state of the art in relevant technologies, the following research and development areas appear as vital to well-coordinated advances in Stores Management Systems.

R & D Areas of Immediate Interest:

Coordination of the Stores Management functions and an effective functional partitioning which will optimize control, data processing, and management schemes of an operational system.

Development and proper influence in military standards preparation.

Development of the pilot interface aspects of SMS, including standard I/O, display technologies, and human factors.

Investigation of wide-bandwidth digital fiber-optic communications, with different evolutionary phases considered: all-optical systems, electrical-optical systems, and transition systems.

Investigation of the all-digital aircraft concept in which all information, signal processing, and control functions are digitized and all switching functions are electronically implemented.

R & D Areas of Short-Range Interest:

Development of an analysis and simulation capability for performance measurement of alternative communications/processing networks.

Investigation of the feasibility of an adaptive SMS concept and the manageability of all operational aspects.

Development of software technologies associated with management, development, implementation, maintenance, testability, and documentation of software systems.

Development of interrupt-driven communications/processing systems with reasonable levels of testability.

R & D Areas of Long-Range Interest:

Definition of standard communications/processing systems: universal components, universal interconnections, universal communications modules, and so on.

Investigation of basic relationships between functional definitions, process representations, programming languages, and software functions.

Investigation of basic relationships between network architectures and software structures.

Finite-State Models for representation of communications networks and processing functions.

Stores Management Systems higher-order language and implied architectures.

Investigation of modular communications networks which are dynamically adaptable to changing communications traffic and processing functions.

Investigation of Time-Division-Multiplex/Frequency-Division-Multiplex communication systems which could optimize the inherent advantages of wide-bandwidth/optical technologies.

VI. REFERENCES:

1. Aaronson, G., et. al., A Study of Application of Optics to C^3 Systems, Volume I, RADC Technical Report 77-393(I), GTE Sylvania, Inc., Needham, MA, November 1977.

2. AGARD Conference Proceedings No. 219, Optical Fibres, Integrated Optics and Their Military Applications, edited by Dr. H. Hodara, October 1977.

3. Barnes, B., et. al., Analysis of Hardwired Versus Multiplexed Stores Management Systems, AFATL Technical Report 76-73, Volume I, Harris Electronic Systems Div., Melbourne, FL, July 1976.

4. Barnes, B., et. al., Analysis of Hardwired Versus Multiplexed Stores Management Systems, AFATL Technical Report 76-73, Volume II, Harris Electronic Systems Div., Melbourne, FL, June 1976.

5. Cunningham, P.M., et. al., Advanced Fiber Optics System Architecture Study, Naval Air Systems Command Report No. 2-37100/7R-3425, Vought Corp., Dallas, TX, October 1977.

6. Drgon, J.A. and Pivar, L., Digital Guided Weapons Technology, Volume III, AFATL Technical Report 76-132, Hughes Aircraft Co., Canoga Park, CA, November 1976.

7. Fowler, V.J. and Harris, J.H., A Study of Application of Optics to C^3 Systems, Volume II, RADC Technical Report 77-393(II), GTE Sylvania, Inc., Needham, MA, November 1977.

8. Hardy, F.W., et. al., Digital Guided Weapons Technology (DGWT), Volume I, AFATL Technical Report 76-132, Hughes Aircraft Co., Canoga Park, CA, November 1976.

9. Mennie, D., Communications and Microwave Technology, IEEE Spectrum, January 1978.

10. Military Standard, Aircraft Internal Time Division Command/Response Multiplex Data Bus, draft MIL-STD-1553B superseding MIL-STD-1553A, June 1978.

11. Military Standard, Aircraft/Stores Electrical Interface Requirements, proposed MIL-STD-XXX, January 1978.

12. Natha, N., et. al., Digital Processing Analysis/Partitioning (DRAP), Final Report, AFATL Report No. R-1121, The Charles Stark Draper Laboratory, Inc., Cambridge, MA, November 1977.

13. Proceedings of the Multiplex Data Bus Conference, sponsored by Air Force Systems Command, Aeronautical Systems Div., Dayton, OH, November 1976.

14. Proceedings of the 3rd International Conference on Software Engineering, IEEE Catalog No. 78CH1317-7C, Atlanta, GA, May 1978.

15. Putnam, L.H. and Wolverton, R.W., Quantitative Management:Software Cost Estimating. COMPSAC '77 Tutorial, IEEE Catalog No. EHO 129-7, November 1977.

16. Severance, J.D., et. al., Study of Aircraft Stores Interface Standardization, AFATL Technical Report 78-14, Booz,Allen Applied Research Div., Fort Walton Beach, FL, January 1978.

17. Station Logic Unit, Prepared by General Motors Corp., Delco Electronic Div., for U.S. Air Force Armament Laboratory, AFATL Technical Report 77-104, August 1977.

18. Type A Specification for the Stores Management System, Second Edition, Booz, Allen Applied Research Div., Fort Walton Beach, FL, June 1978.

19. Type B Specification for the Stores Management System Software, Volumes I and II, Booz, Allen Applied Research Div., Fort Walton Beach, FL, November 1977.

20. Type C Specification for the Stores Management System Software (Preliminary), Volumes I, II, and III, Booz, Allen Applied Research Div., Fort Walton Beach, FL, June 1978.

21. Woolley, R. L., et. al., Digital Guided Weapons Technology (DGWT), Volume II, AFATL Technical Report 76-132, Hughes Aircraft Co., Canoga Park, CA, November 1976.

1978 USAF-ASEE SUMMER FACULTY RESEARCH PROGRAM
sponsored by
THE AIR FORCE OFFICE OF SCIENTIFIC RESEARCH
conducted by
AUBURN UNIVERSITY AND OHIO STATE UNIVERSITY

PARTICIPANT'S FINAL REPORT

A THREE-DIMENSIONAL ELASTIC-PLASTIC ANALYSIS OF HIGH VELOCITY IMPACT PROBLEMS BY A FINITE ELEMENT METHOD

Prepared by:	June K. Lee, Ph.D.
Academic Rank:	Assistant Professor
Department and University:	Department of Engineering Mechanics Ohio State University
Assignment:	Eglin AFB Air Force Armament Laboratory Munitions Division Bombs & Warheads Branch
USAF Research Colleague:	Daniel A. Matuska, Major, USAF
Date:	August 23, 1978
Contract Number:	F44620-75-C-0031

A THREE-DIMENSIONAL ELASTIC-PLASTIC ANALYSIS OF HIGH VELOCITY IMPACT PROBLEMS BY A FINITE ELEMENT METHOD

by

June K. Lee

ABSTRACT

This report outlines a development of a set of consistant governing equations based on an explicite Lagrangian finite element formulation. The tetrahedron finite element is adopted because of its simplicity and its better behavior under a relatively severe distortion. The Von-Mises yield criterion is employed to account for plasticity effect. The fracture is characterized by equivalent strain. The Mie-Grüneisen equation of state, known to be applicable to a wide range of materials, is used. Derived equations are implemented by modifying the existing EPIC-3 code (*).

(*) G. R. Johnson, D. D. Colby, and D. J. Vavrick, "Further Development of the EPIC-3 Computer Program for Three Dimensional Analysis of Intense Impulsive Loading," Final Report to USAF Systems Command, ADTC, Eglin Air Force Base, Florida, Contract Number F08635-77-C-0121.

LIST OF FIGURES

ACKNOWLEDGMENT

The author is sincerely grateful to the Air Force Office of Scientific Research for support of this summer research. A deep appreciation is due to ASEE and Auburn University and in particular Mr. Fred O'Brien and Lieutenant Colonel R. H. Kauffman for their excellent administrative support.

The author is indebted to the active members of the "hydrocode group" in DLJW branch of the Armament Laboratory for providing a cordial and helpful work environment. It has been a professionally gratifying experience to work with these very capable people. In particular, thanks are due to Lt Col J. Osborn, Maj D. A. Matuska, Mr W. H. Cook, and Ms C. Westmoreland. Lastly, but not least, secretarial assistance provided by Mrs M. J. Stribling, is deeply appreciated.

INTRODUCTION

High velocity impact problems have been a subject of intensive research for the last three decades. In recent years, more attentions have been diverted to computational investigations largely due to the advent of modern high speed computers and advances in numerical methods. The correlation between the theory and experiment justifies the current trend in almost every aspect of mechanics. Furthermore, the use of theory in studying the high velocity impact of deformable bodies has given insights into some of the basic phenomena that are unobservable by currently available experimental techniques.

Most of the high velocity impact calculations in the past have been two-dimensional analysis based on the finite difference method (see, for example,[1] and [2]), some of which have been applied quite successfully within a certain limit. However, a reliable and economical technique for three-dimensional analyses of oblique impact problems is still in demand.

Recent reports by Reddy [3] and Gordon [4] on three-dimensional finite element analyses of high velocity impacts certainly look promising although they both need further refinements and developments. The finite element method, which has been proven to be one of the most powerful tool in general structural mechanics area, is now recognized as a general method of approximation of partial differential equations (see, for example, [5] and [6]), and should provide a plausible alternative to the finite difference method.

In this report, a set of consistant governing equations, using the tetrahedron element and the Lagrangian description of motion, is developed. The resulting equations of motion are explicit Lagrangian form and are integrated directly rather than through the traditional stiffness matrix approach as advocated in [4]. This approach of direct integration certainly saves a considerable amount of computing time and seems to provide reasonable accuracies according to numerical examples given in [4]. The tetrahedron element is selected among others because of the following reasons:

° It simplifies the equations of motion because each element is in the state of constant stress.

° It is well suited to represent complicated geometrical shape.

° It behaves better than other types of elements under a relatively severe distortion.

° It does not contain any spurious element mechanism such as unrealistic zero energy mode.

An element is assumed to be failed either plastically if the Von-Mises yield criterion is met or in fracture if the equivalent strain exceeds a specified limit. A failed element is treated as an inviscid compressible fluid and the hydrostatic pressure is computed via the Mie-Grüneisen equation of state.

Derived equations are implemented in a computer code by modifying the EPIC-3 code described in [4] and numerical experiments are underway. Computational results and detailed modification of the code will be reported in a separate report due to the shortage of time allowed in the summer research program.

REVIEW OF GOVERNING EQUATIONS

The basic equations of a continuum in the Lagrangian description are (Cf.[7]):

° Continuity equation: The law of conservation of mass leads to the simple relationship between the original and the current material density or volume

$$\rho = \rho_0 / J \quad \text{or} \quad dV = J\, dV_0 \tag{1}$$

where J is the determinant of the deformation gradient

$$F_{ij} = \partial x_i / \partial X_j \tag{2}$$

in which x_i and X_j are spatial and referential coordinates of the same material point. Throughout the report, lower character indices will vary 1 ~ 3 and the Einstein summation convention is implied on repeated indices unless stated otherwise.

° Equations of Motion: The law of balance of linear momentum leads to the celebrated Cauchy's equation of motion

$$\partial \sigma_{ij} / \partial x_j + \rho f_i = \rho\, dv_i / dt \tag{3}$$

Here f_i is the body force per unit mass, v_i are components of velocity vector and σ_{ij} is the Cauchy stress tensor. Recall that the Cauchy stress is defined on the current surface referring to the spatial coordinates .

° Energy equation: The law of conservation of energy (the first law of thermodynamics) leads to

$$\rho\, de/dt = \sigma_{ij} \dot{\varepsilon}_{ij} + (\rho r - \partial q_i / \partial x_i) \tag{4}$$

where e is specific internal energy per unit mass, and

$$\dot{\varepsilon}_{ij} = \frac{1}{2} (\partial v_i / \partial x_j + \partial v_j / \partial x_i) \tag{5}$$

is the rate of deformation (strain rate) tensor, and r and q_i are internal heat generation and heat flux, respectively.

° Equation of state: The pressure P is related to the internal energy e and the density ρ through an equation of state

$$P = P(e, \rho) \tag{6}$$

Here, the Mie-Grüneisen equation is adopted

$$P = P_v + \Gamma e \rho_0 (1 + \mu) \tag{7}$$

where

$$P_v = (K_1 \mu + K_2 \mu^2 + K_3 \mu^3)(1 - \Gamma \mu / 2) \tag{8}$$

in which $\mu = V_0/V - 1 = \rho/\rho_0 - 1 = 1/J - 1$, K_i are material constants and Γ is the Gruneisen number.

Additional relations will be introduced later as needed.

MECHANICS OF A TETRAHEDRON ELEMENT

Consider the motion of a tetrahedron shown in Fig. 1.

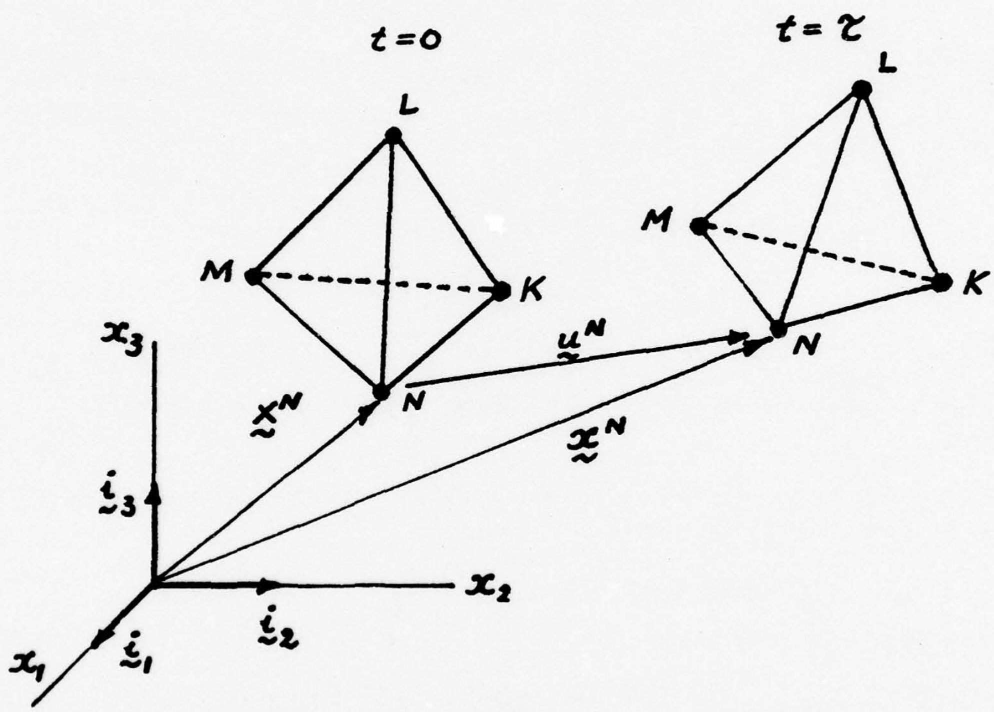

Fig. 1 Motion of a Tetrahedron Element

Displacement and velocity (*) within an element are given as linear function of the original coordinates

$$u_m(\underset{\sim}{X}, t) = \beta_m^o(t) + \beta_{mi}(t) X_i \qquad (9)$$
$$v_m(\underset{\sim}{X}, t) = \alpha_m^o(t) + \alpha_{mi}(t) X_i$$

(*) We continue to use the same symbols for approximations to avoid complicated notation.

so that $\alpha_m^o = \dot{\beta}_m^o$, $\alpha_{mi} = \dot{\beta}_{mi}$, and the Lagrangian description of motion is

$$x_m(\underset{\sim}{X}, t) = X_m + u_m(\underset{\sim}{X}, t) \tag{10}$$

In equation (9), for $m = 1 \sim 3$,

$$\begin{aligned} \beta_m^o &= a_o^N u_m^N / 6V_o , \quad \beta_{m1} = b_o^N u_m^N / 6V_o \\ \beta_{m2} &= c_o^N u_m^N / 6V_o , \quad \beta_{m3} = d_o^N u_m^N / 6V_o \end{aligned} \tag{11}$$

and α's are defined similarly with u_m^N replaced by the nodal velocity vector v_m^N in which N=1~4 is the element node number, u_m^N is the component of displacement at node N,

$$a_o^1 = \begin{vmatrix} X_1^2 & X_2^2 & X_3^2 \\ X_1^3 & X_2^3 & X_3^3 \\ X_1^4 & X_2^4 & X_3^4 \end{vmatrix}, \qquad b_o^1 = - \begin{vmatrix} 1 & X_2^2 & X_3^2 \\ 1 & X_2^3 & X_3^3 \\ 1 & X_2^4 & X_3^4 \end{vmatrix}$$

$$c_o^1 = \begin{vmatrix} 1 & X_1^2 & X_3^2 \\ 1 & X_1^3 & X_3^3 \\ 1 & X_1^4 & X_3^4 \end{vmatrix}, \qquad d_o^1 = - \begin{vmatrix} 1 & X_1^2 & X_2^2 \\ 1 & X_1^3 & X_2^3 \\ 1 & X_1^4 & X_2^4 \end{vmatrix}$$

other values can be obtained by permuting superscripts and

$$V_o = \frac{1}{6} \begin{vmatrix} 1 & X_1^1 & X_2^1 & X_3^1 \\ 1 & X_1^2 & X_2^2 & X_3^2 \\ 1 & X_1^3 & X_2^3 & X_3^3 \\ 1 & X_1^4 & X_2^4 & X_3^4 \end{vmatrix}$$

In view of (9) and (10), the relation (2) can be written as

$$F_{mi} = \delta_{mi} + \beta_{mi} \tag{13}$$

and the strain rate (5) can be found, by using the chain rule, as

$$\dot{\varepsilon}_{ij} = \frac{1}{2}(\alpha_{ik} F^{jk} + \alpha_{jk} F^{ik}) \tag{14}$$

where $F^{ik} = (F_{ik})^{-1}$.

Component of the resultant force acting on the face opposite to N^{th} node can be found to be (see Fig. 2)

$$\begin{aligned} f_i^{(N)} &= \sigma_{ij} n_j^{(N)} S^{(N)} \\ &= -\frac{1}{2}(\sigma_{i1} b^N + \sigma_{i2} c^N + \sigma_{i3} d^N) \end{aligned} \tag{15}$$

where the geometric constants b^n, c^n, and d^n are similarly defines as in (12) except that the original nodal positions $\underset{\sim}{X}^M$ are replaced by the current nodal coordinates $\underset{\approx}{x}^M$. Once element stresses are computed, the resultant nodal forces can be obtained with the aid of (15). The equivalent resultant nodal force in (15) will be equally distributed over the corner nodes K, M, and L (see Fig. 2) of the surface $S^{(n)}$. Forces on other faces are computed in the similar manner

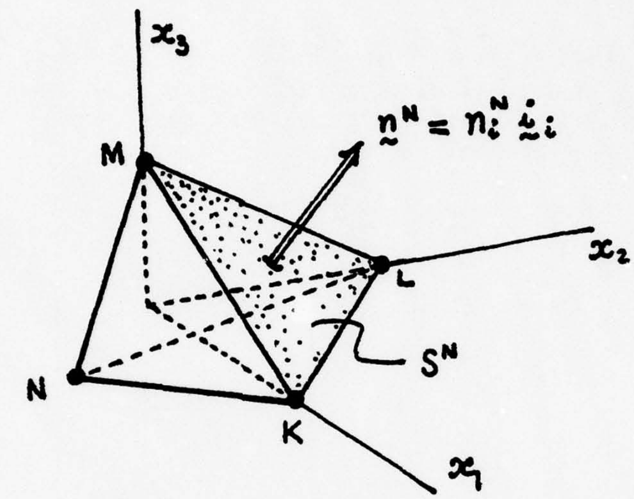

Fig. 2 Portion of an element as the Cauchy-Tetrahedron

When basic mechanics of an element are laid out, the rest follows from the governing equations stated in (1) (8).

ALGORITHM

It is often convenient to express the stress and strain rate in normal and deviatoric components, viz,

$$\sigma_{ij} = S_{ij} - (P+Q)\delta_{ij} \tag{16}$$

$$\dot{\varepsilon}_{ij} = \dot{e}_{ij} + \frac{1}{3}\dot{\varepsilon}_v \delta_{ij} \tag{17}$$

where P is the hydrostatic pressure, Q is the artificial viscosity which can be computed by

$$Q = \begin{cases} C_L \rho C_s h |\dot{\varepsilon}_v| + C_Q \rho h^2 (\dot{\varepsilon}_v)^2 & \text{if } \dot{\varepsilon}_v < 0 \\ 0 & \text{if } \dot{\varepsilon}_v \geq 0 \end{cases} \tag{18}$$

and $\dot{\varepsilon}_v = \dot{\varepsilon}_{11} + \dot{\varepsilon}_{22} + \dot{\varepsilon}_{33}$ is the volumetric strain rate, and δ_{ij} is the Kronecher delta. In (18), C_L and C_Q are material constant, h is the minimum altitude of the tetrahedron and C_s is the sound speed which can be computed by

$$C_s^2 = \frac{1}{\rho_o}\left[K_1(1-\Gamma\mu) + K_2(2\mu-1.5\Gamma\mu^2) + K_3(3\mu^2-2\Gamma\mu^3) + \Gamma/(1+\mu)\cdot P_v \right] + \Gamma(1+\Gamma)e \tag{19}$$

which can be obtained by taking a derivative of (7) with respect to the current density ρ .

Through the time step trial stresses are approximated by

$$S_{ij}^{t+\Delta t} = \eta(S_{ij}^{t} + 2G\,\dot{e}_{ij}\Delta t) \tag{20}$$

where G is the shear modulus and

$$\eta = \begin{cases} 1 & \text{if } \bar{S} > \bar{\sigma} \\ \bar{S}/\bar{\sigma} & \text{if } \bar{S} < \bar{\sigma} \end{cases} \tag{21}$$

In (21), $\bar{S}$ is the tensile strength of the material and $\bar{\sigma}$ is the equivalent equivalent stress defined by

$$\bar{\sigma} = \left(\frac{3}{2} S_{ij} S_{ij}\right)^{1/2} \tag{22}$$

Relations (20) (22) stem from the Von-Mises yield criterion.

The energy equation (4) can be put into the central difference form

$$e^{t+\Delta t}(2+\Gamma\dot{\varepsilon}_v\Delta t) = \frac{\Delta t}{\rho_o V_o}\Big[(V S_{ij}\dot{e}_{ij} - V P_v\dot{\varepsilon}_v)^{t+\Delta t} + (V S_{ij}\dot{e}_{ij} - V P_v\dot{\varepsilon}_v - QV\dot{\varepsilon}_v - \Gamma\rho_o V_o e\,\dot{\varepsilon}_v)^{t} - Q^t(V\dot{\varepsilon}_v)^{t+\Delta t}\Big] + 2e^t \tag{23}$$

with the aids of (1), (16) and (17). The difference form (23) can be linearized if we assume that V, ρ and $\dot{e}_{ij}$ are constant within the time step Δt, viz,

$$e^{t+\Delta t}(2+\Gamma\dot{\varepsilon}_v\Delta t)$$
$$=\frac{\Delta t}{\rho_0}J\left[\dot{e}^{t}_{ij}(S^{t+\Delta t}_{ij}+S^{t}_{ij})-\dot{\varepsilon}_v\left(2P_v+2Q+\frac{\Gamma\rho_0}{J}e\right)^{t}\right]$$
$$+\ 2e^{t} \tag{24}$$

which is readily solvable.

The rest of algorithms remains the same as in [4] including the determination of the next time step t and mechanism of sliding surfaces. A brief calculational loop is shown in Fig. 3.

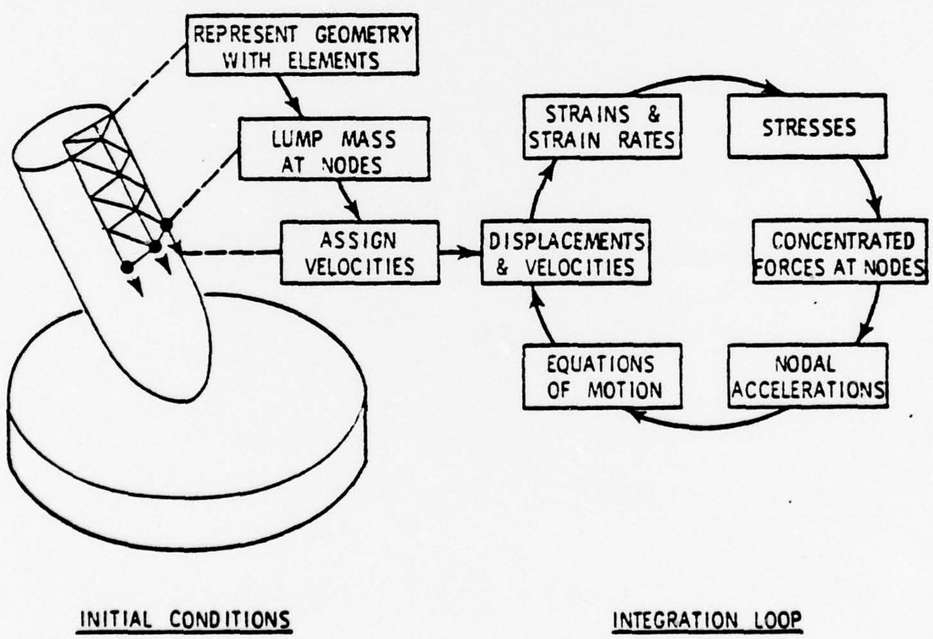

Fig. 3 Calculation loop (after Johnson [4])

The final form of the equations of motions are expressed at a node N for i^{th} component,

$$(\ddot{u}_i^N)^t = F_i^{(N)} / M_i^{(N)} \tag{25}$$

where $F_i^{(N)}$ is the equivalent force at node N computed by using (15) and $M_i^{(N)}$ is the lumped mass at N in i -direction.

CONCLUDING REMARKS

The equations developed herein are consistent with the theory of continuum mechanics and finite element method. Thereby, they should improve the results of EPIC-3 code. It is regrettable that no computational comparisons can be made in this report due to the lack of time. It is hoped that a detailed separate report including computational results would be made in the near future to the AFATL/DLJW.

Some of the important issues such as more realistic failure mechanism of an element and more rigorous treatment of sliding surfaces are not touched upon during the ten-weeks of research program, which should be challenging and important areas of future research. An economical rezoning capability is also in order.

REFERENCES

1. M. L. Wilkins, "Calculation of Elastic-Plastic Flow," Methods in Computational Physics, Vol. 3, Ed. by B. Alder, et al, Academic Press, New York (1964).

2. W. Herrmann, L. D. Bertholf, and S. L. Thompson, "Computational Methods for Stress Wave Propagation in Nonlinear Solid Mechanics," Lecture Notes in Mathematics, #461 Computational Mechanics, proceeding of the First International Conference on Computational Methods in Non-linear Mechanichs, Austin, Texas, 1974, Ed. by J. T. Oden, Springer-Verlag, New York (1975).

3. J. N. Reddy, "Finite Element Analysis of the Initial Stages of Hypervelocity Impact," Computer Method in Applied Mechanics and Engineering, Vol. 9, pp 47-63, 1976.

4. G. R. Johnson, D. D. Colby, and D. J. Vavrick, "Further Development of the EPIC-3 Computer Program for Three Dimensional Analysis of Intense Impulsive Loading," Final Report to USAF Systems Command, ADTC, Eglin Air Force Base, Florida, Contract Number F08635-77-C-0121.

5. O. C. Zienkiewicz, The Finite Element Method in Engineering Science, McGraw-Hill, New York (1971).

6. J. T. Oden, Finite Element of Nonlinear Continua, McGraw-Hill, New York (1972).

7. C. Truesdell and R. Toupin, "The Classical Field Theories," Encyclopedia of Physics, Vol. III/1, Springer-Verlag, New York (1960).

1978 USAF-ASEE SUMMER FACULTY RESEARCH PROGRAM

Sponsored by

THE AIR FORCE OFFICE OF SCIENTIFIC RESEARCH

Conducted by

AUBURN UNIVERSITY AND OHIO STATE UNIVERSITY

PARTICIPANT'S FINAL REPORT

ON-LINE SPECTRAL ESTIMATION VIA MAXIMUM ENTROPY PROCESSING

Prepared by:	Charles W. Sanders, PhD.
Academic Rank:	Assistant Professor
Department and University	Department of Electrical Engineering University of Houston
Assignment:	Eglin Air Force Base, Florida Armament Development and Test Center Deputy for Development Plans System Concepts
USAF Research Colleague:	Doyle R. Dingus, PhD.
Date:	July 28, 1978
Contract No:	F44620-75-C-0031

ON-LINE SPECTRAL ESTIMATION VIA

MAXIMUM ENTROPY PROCESSING

by

C. W. Sanders

ABSTRACT

A careful integration of continuing developments in the separate technology areas of analog and digital hardware should, in the near future, provide the capability for on-line implementation of a number of appropriately structured signal processing algorithms. This report and a more detailed supplement [8] suggests a hybrid structure for implementing an on-line spectral estimator based on the maximum entropy algorithm. After a brief introduction to this method it is noted that although the algorithm presents a considerable computational requirement, its structure should admit an implementation via hybrid special-purpose hardware wherein charge-coupled devices are organized around a microprocessor host. Suggestions for further research in this area are also given.

ACKNOWLEDGEMENT

The author would like to thank the Air Force Systems Command, Air Force Office of Scientific Research, and the American Society of Engineering Education for providing him the opportunity to spend a most worthwhile and interesting summer at Eglin Air Force Base. Special acknowledgement is also due to the Engineering Extension Division of Auburn University and especially Mr. J. Fred O'Brien for a well-organized program and for many informative discussions.

Finally, he would like to thank Mr. Heyward Strong and Dr. Doyle Dingus of the Directorate of System Concepts for numerous helpful discussions and guidance and for providing a working atmosphere which enabled the author to expand his horizons considerably in the area of advanced concepts for Air Force systems.

I. INTRODUCTION:

The problem addressed in this project is motivated by two aspects of Air Force command/control systems: (1) the signalling environments in which significant numbers of these systems must function are increasingly cluttered with numerous sources of interference, both intentional and otherwise, and (2) sensor performance, while adequate for the case of single isolated target sources, is often considerably degraded by the presence of multiple target sources. More specifically, since pulsed radar-like sources can be effectively discriminated via their pulse-repetition frequencies (PRF), the motivation for this project centers primarily around the problem of discriminating between continuous-wave (CW) sources wherein no PRF information exists.

Terminal guidance of air-to-ground missiles via bearing signals obtained from interferometer (phase comparison monopulse) based estimation procedures provides an excellent example of such problems. In this situation multiple-emitters within the relatively wide field-of-view (FOV) of the sensor will provide a phase null bearing estimate which lies at an appropriately defined centroid of the emitter placement geometry with the location of this centroid depending on the relative emitter signal strengths and phases. Furthermore, wandering of this centroid and consequent hunting of the terminal guidance control system can be caused by very slight differences in the emitter frequencies and/or by intentional emitter "blinking" at blink rates which are low enough to be followed by the control system.

Typically, in the phase comparison monopulse, bearing estimates are obtained from quadrature and in-phase components of the incoming signals.

Considering only the case of azimuth information these components form a four-channel process each component of which contains a downshifted version of each emitter frequency. As indicated in the previous paragraph, the straightforward processing of this four-channel data will lead to estimation errors and possible control system oscillation. This project is motivated by the idea of utilizing the small frequency differences between the emitters to effectively separate these sources into those which are within the reachable set of the missile and those which are outside of this set. Thus, it is envisioned that if such an on-line spectral estimation capability can be developed then it should be possible to utilize emitter signatures to achieve the capability of tracking designated targets even in the presence of multiple sources of emission.

It should be noted that some technology has already been developed to perform spectral analysis of noise corrupted signals of known structure - e.g., matched filtering and spread spectrum techniques using charge-coupled device (CCD) correlators.[1] In addition, some spectral estimation algorithms have been recently developed which are capable of providing very high resolution spectra but for which completely digital implementations require large-scale computational resources.[2-7]

The proposed signal discrimination process which is studied in this project is based on the maximum entropy method (MEM) introduced by Burg[2-3] for spectral analysis of geophysical signals. Briefly, this method estimates optimal autoregressive model parameters for the signal process from on-line process measurements. Data windowing

problems which tend to degrade the spectral resolution are minimized in MEM processing by optimizing only over the available data and by being maximally noncommittal, in the information-theoretic entropy sense, regarding the non-available data. While this method was originally restricted to single channel processes it has very recently been extended to the multi-channel case by several workers.[4-7]

Although MEM is a highly structured algorithm it requires many convolution-like computations and thus many multiplications. It is therefore somewhat doubtful that this algorithm could be implemented with sufficient computational speed and bandwidth for an on-board weapon delivery system via microprocessors with a strictly digital approach. However, preliminary investigation indicates that it should be possible to organize the relevant MEM computational requirements (i.e., Levinson-Durbin recursions, and correlations) around CCD based shift registers which are under the control of a microprocessor control unit. Such an organizational structure utilizes the analog and digital units in the roles for which they are best suited; analog parallel multiplication and summation via the CCD's and sequence control and some small-scale computations via the microprocessor.

II. OBJECTIVES:

The objectives of this project were:

(1) To survey and categorize the research literature in the area of maximum entropy spectral estimation and its applications.

(2) To develop a unified review/tutorial description of the maximum entropy algorithm for use by division personnel in objectively assessing and monitoring research in this area.

(3) To ascertain the computational requirements of the MEM to determine its applicability to on-board air-to-ground missile weapon delivery systems.

(4) To determine whether there exist special-purpose hybrid implementations of the MEM algorithm which could be used in air-to-ground applications.

Due to space limitations, this report focuses exclusively on the latter two objectives while work on the first two objectives is being furnished as a separate report.[8]

III. PHASE COMPARISON MONOPULSE:

One of several potential application areas for high-resolution spectral estimates is illustrated by the effect of multiple-emitters on the performance of a phase comparison monopulse. This technique is a well-known method for using the phase information contained in two time-displaced versions of a CW signal to estimate the direction to an emitter. Consider, for example, the single emitter geometry shown in Figure 1.

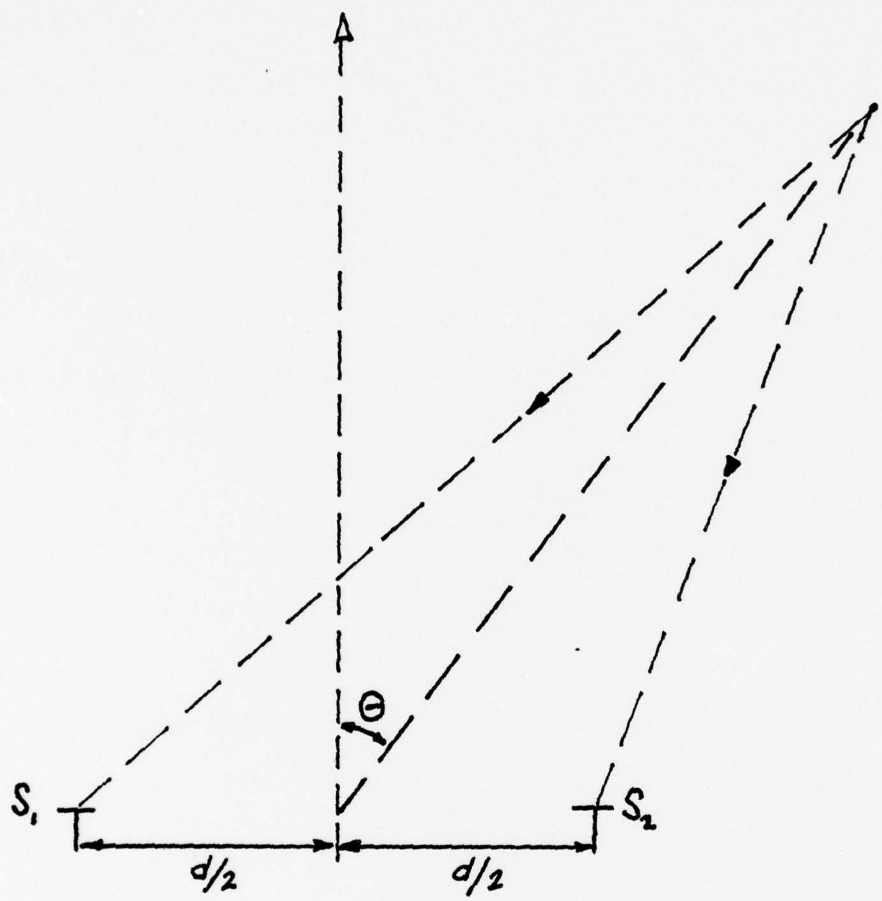

FIGURE 1 - PHASE COMPARISON MONOPULSE GEOMETRY

The phase difference between signals S_1 and S_2 is easily shown to be

$$\Delta \phi = \frac{2\pi d}{\lambda} \sin \theta \qquad (1)$$

from which it follows that

$$\theta = \sin^{-1}\left(\frac{\lambda \Delta \phi}{2\pi d}\right) \qquad (2)$$

wherein λ is the wavelength of the emitted signal and d is the separation between the receiving elements.

From the above results, it follows that if $\Delta\phi$ can be estimated then an estimate of the direction, θ , can be formed from (2). One system for estimating $\Delta\phi$ from S_1 and S_2 creates in-phase and quadrature components of S_1 and S_2 and then computes $\Delta\phi$ as shown in Figure 2.

Since $\Delta\phi = 0$ implies $\theta = 0$,

the signal $\hat{\theta}$ computed from (2) with $\Delta\phi$ replaced by its estimate, $\widehat{\Delta\phi}$, can be used to drive a control loop to steer the antenna toward the emitter. Thus, the control law looks for a phase null where $\hat{\theta} = 0$.

While the method described above works adequately for the case of a single emitter, there are some potential problems when multiple emitters are in the field-of-view of the antenna. For example, for the multiple-emitter geometry shown in Figure 3 and the phase detector of Figure 2 it is easily shown that the phase null condition is given by

$$G_1 \sin(\Delta\phi_1) + G_2 \sin(\Delta\phi_2) + A_1 A_2\, g(t) = 0 \qquad (3)$$

wherein

$$G_1 = 2A_1^2 + A_1A_2$$

$$G_2 = 2A_2^2 + A_1A_2$$

$$\Delta\phi_i = K_i \sin\theta_i$$

$g(t)$ contains frequency components $\pm (f_2 - f_1)$, $\pm 2\,(f_2 - f_1)$, $2f_0 - (f_1 + f_2)$, $2\,(f_1 - f_0)$, and $2\,(f_2 - f_0)$, and is also a function of the RF phases α_1, α_2. The above result indicates the potential problems of phase null bias (in case $f_1 = f_2$) and phase null "hunting"

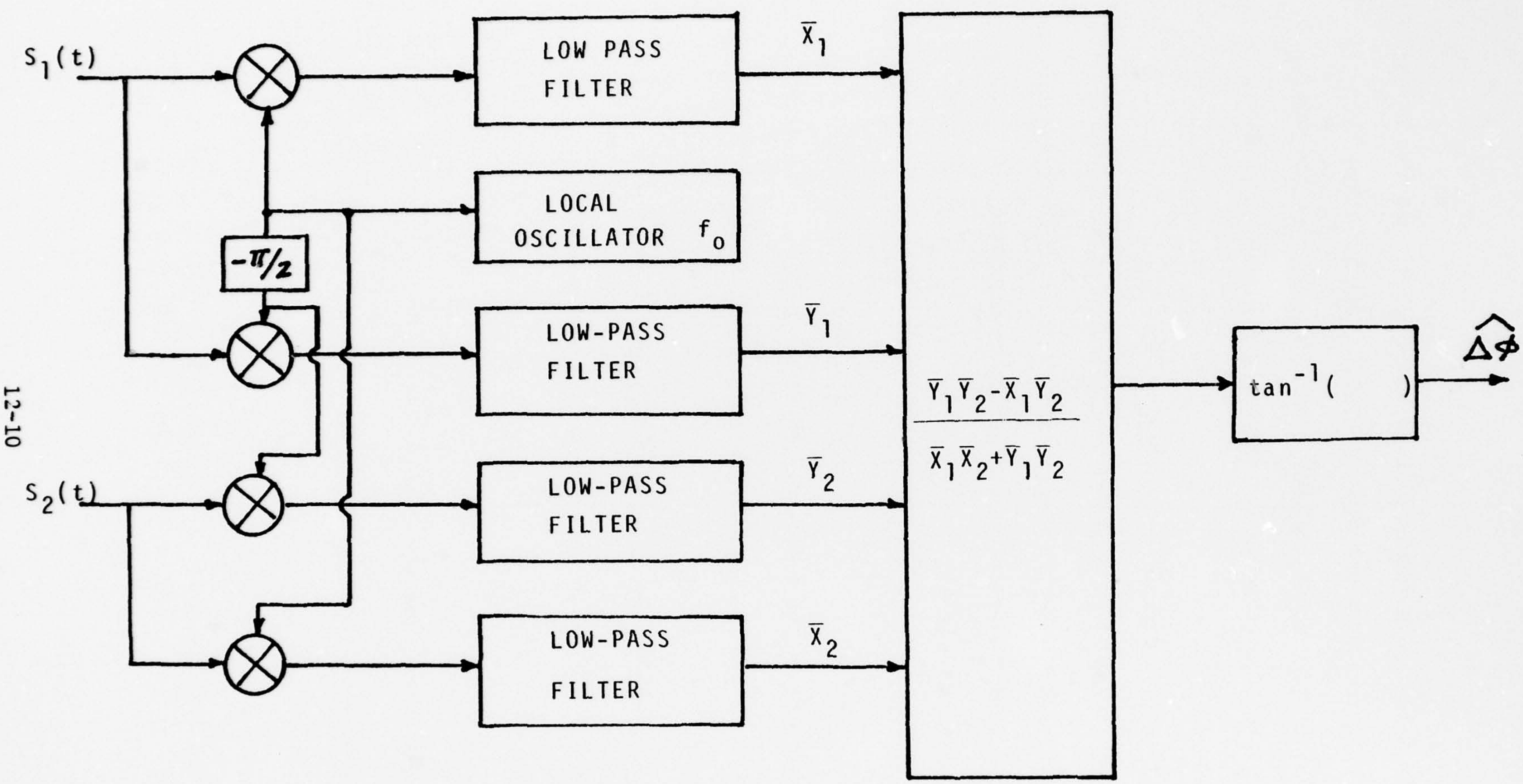

FIGURE 2 - PHASE DETECTOR

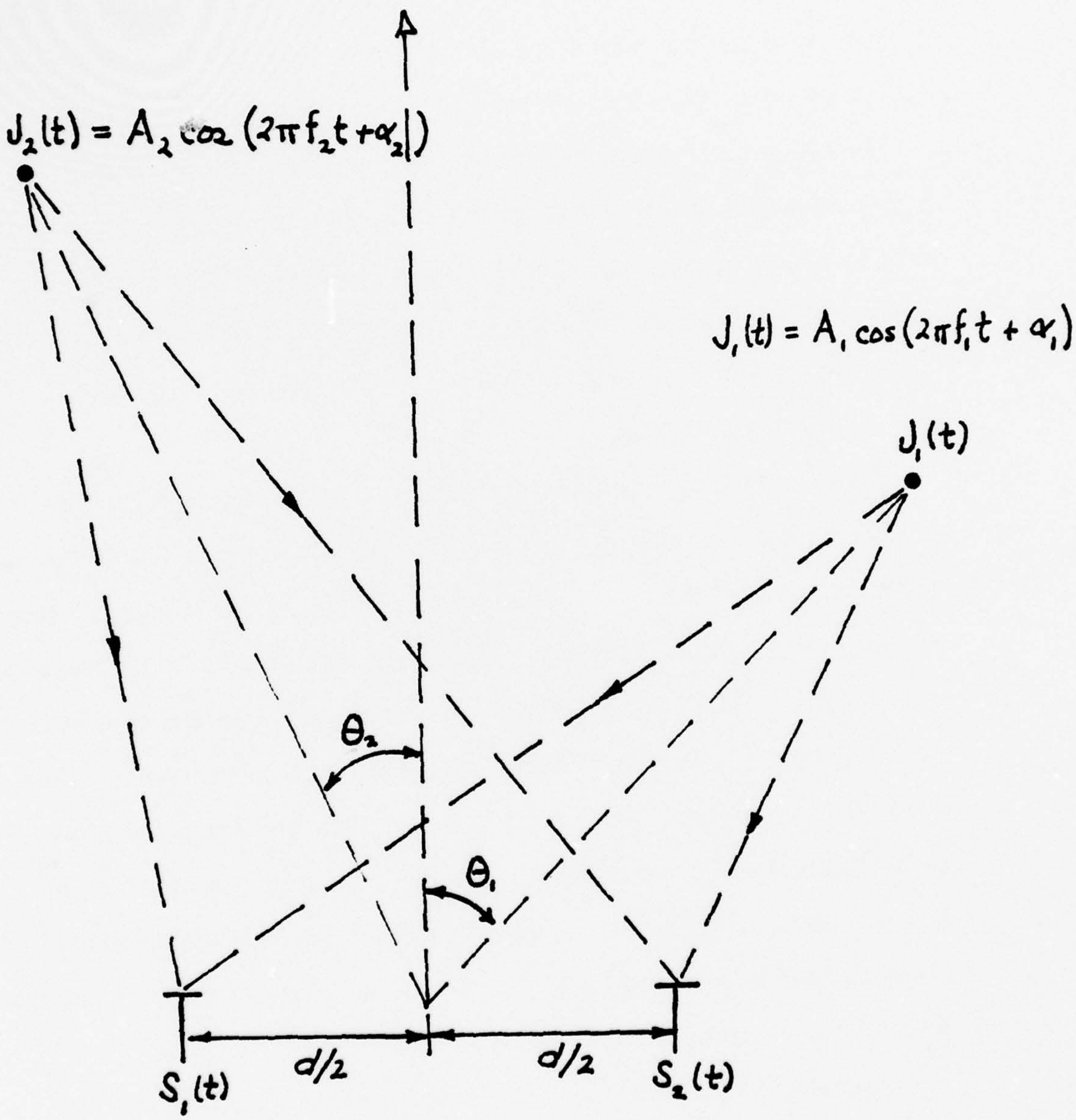

FIGURE 3 - MULTIPLE EMITTER GEOMETRY

in case the frequencies in g(t) are low enough to be followed by the control loop and associated system dynamics. Another significant source of phase null hunting may be caused by blinking wherein over certain time periods which are sufficiently long in relation to the system dynamics the emitters are cycled on and off.

In the situation described above an on-board near real-time high-resolution spectral estimation capability could play an important role by allowing the detection of two or more nearly equal spectral lines. The integration of this capability with some appropriate logic* might then allow a missile to track a single designated emitter.

IV. SPECTRAL ESTIMATORS

Some general considerations which must be addressed regardless of the particular processing algorithm via which a spectral estimator is to be implemented are: (1) sampling rate ($^1/T_s$), (2) number of samples available (M), and, if the processing is done digitally, (c) computer word length. Specific considerations which are algorithm dependent are, for example: (1) how the nonavailable data is to be treated--classical windowing techniques allow the data to be smoothly truncated whereas techniques based on the discrete Fourier transform assume that the data is periodic, (2) if the algorithm involves on-line modelling of the data then a decision as to the number of model parameters and how they are to be computed must be made.

Regarding the general considerations suppose that it is desired to generate spectral estimates over the frequency range $\left[f_{min}, f_{max}\right]$.

---

* It should be noted that the creation of decision algorithms which utilize this spectral information forms another important area of basic research.

In order to avoid aliasing problems it is necessary to sample with * $f_s = {}^1/T_s \gg 2 f_{max}$. In addition, in order to reduce the sensitivity of the spectral estimates to the phase of the signal, it is necessary to have a record length which is at least several (2 or 3) cycles long (e.g., see [8]). From the above two considerations it follows that the storage factor M must satisfy $M \gg CP\ (f_{max}/f_{min})$ wherein $f_s = Cf_{max}$ $(C \gg 2)$ and the record length $MT_s = P/f_{min}$ $(P \gg 2)$.

Classical Fourier spectral analysis usually extends the data beyond the window by truncation. Although considerable emphasis is placed on different window functions which allow the data to be truncated "gracefully," these assumptions about the non-available data can degrade the resolution by spreading each spectral line into a band of frequencies.

Burg and Parzen[9] have suggested the use of autoregressive process models as a means of minimizing the loss in resolution due to finite data records. In this technique the process to be analyzed is modeled via an autoregressive process of the form

$$z(t) = \sum_{k=1}^{N} a_k\, z(t-k) \tag{4}$$

wherein N is the <u>order</u> of the model and the a_k are the <u>model parameters</u>. From this model the spectrum is estimated via

$$\hat{S}(f) = \frac{K}{|1 + \sum a_k \exp(j 2\pi f T_s k)|^2} \tag{5}$$

In the maximum entropy method one computes the model parameters by determining the model of a given order that best fits the available data in the least squares sense. It can be shown[10] that (assuming a Gaussian process) this procedure is equivalent to extrapolating the autocorrelation function of the process from given values in such

*the frequency f_{max} is the maximum deviation of emitter frequency from f_o and similarly for f_{min}.

a way that the entropy of the random vector representing the process is maximized. In this sense the method is maximally non-committal regarding the nonavailable data.

The primary contribution of Burg and probably the most important aspect of the MEM is that the parameters α_k can be estimated directly using only the available data and without the conventional intermediate step of estimating the autocorrelation function of the process. Furthermore, although the method is computationally rather lengthy it can be conveniently structured around a recursive procedure based on refinements[11, 12] of early work of Levinson[13] in Weiner filtering. In fact, the computations involved have a convolution or inner product type of structure and in addition allow one to determine the optimal AR model of order N+1 from the one of order N. Although there are some anomalies[14] (especially for short data records), one typically obtains better models (improved resolution) as the order is increased until (if the process is truly autoregressive) all of the correlation information has been removed leaving only a noise process as remainder.

V. RECOMMENDATIONS:

The maximum entropy method is capable of producing high resolution spectral estimates but requires a considerable computational capability involving many convolution-like operations. It is unlikely that a strictly digital approach will allow its implementation as an on-board element in guided weapons. However, given the fact that the MEM algorithm is highly structured with convolution-like operations and the fact that CCD's have been successfully utilized to implement the discrete Fourier

transform method of spectral analysis, it would appear that the use of CCD's as basic building blocks for MEM spectral processors is a promising area for research. In addition to the question of processor organization some basic questions for this research would include: The effects of transfer inefficiencies, tap weight errors, shot and surface noise and of nonlinearities on the performance of the MEM algorithm.

REFERENCES

1. M. H. White and W. R. Webb, "Study of the Use of Charge-Coupled Devices in Analog Signal Processing Systems," Westinghouse Defense and Electronic System Center, Final Report Contract N00014-74-C-0069, DDC No. AD783-703, May, 1974.

2. J. P. Burg, "Maximum Entropy Spectral Analysis," presented at the Society of Exploration Geophysicists, Oklahoma City, Oklahoma, 1967.

3. J. P. Burg, "A New Analysis Technique for Time Series Data," presented at the NATO Advanced Study Institute on Signal Processing with Emphasis on Underwater Acoustics, Enschede, Netherlands, August, 1968.

4. R. H. Jones, "Multivariate Maximum Entropy Spectral Analysis," presented at the Applied Time Series Analysis Symposium, Tulsa, OK, May, 1976.

5. A. H. Nuttall, "Positive Definite Spectral Estimate and Stable Correlation Recursion for Multivariate Linear Predictive Spectral Analysis," Naval Underwater System Center, NUSC Tech. Doc. 5729, New London, CT, Nov., 1976.

6. O. N. Strand, "Multichannel Complex Maximum Entropy (Autoregressive) Spectral Analysis," IEEE Trans. Automatic Control, AC-22. No. 4, pp. 634-640, August, 1977.

7. M. Morf, A. Vieira, D. T. L. Lee, T. Kailath, "Recursive Multichannel Maximum Entropy Spectral Estimation," IEEE Trans. on Geoscience Electronics, Vol GE-16, No. 2, pp. 85-94, April, 1978.

8. C. W. Sanders, "The Maximum Entropy Method of Spectral Analysis: A Tutorial Review and Literature Survey," Technical Report to System Concepts Directorate, Deputy for Development Plans, Armament Development and Test Center, Eglin AFB, Ft Walton Beach, FL.

9. E. Parzen, "Multiple Time Series Modeling," in Multivariate Analysis II, P. R. Krishnaiah (ed), Academic Press, New York, 1969.

10. A. Van den Bos, "Alternative Interpretation of Maximum Entropy Spectral Analysis," IEEE Trans. Information Theory, IT-17, pp. 493-494, July, 1971.

11. J. Durbin, "The Fitting of Time-Series Models" Rev. Inst. Int. Statistics, Vol. 28, No. 3, pp. 233-243, 1960.

12. R. A. Wiggins and E. A. Robinson, "Recursive Solution to the Multichannel Filtering Problem," J. Geophysical Research, Vol. 70, pp. 1885-1891.

13. N. Levinson, "The Wiener RMS (root mean square) Error Criterion in Filter Design and Prediction," Appendix B of N. Wiener, Extrapolation, and Smoothing of Stationary Time Series, MIT Press, Cambridge, Mass., 1949.

14. W. Y. Chen and G. R. Stegen, "Experiments with Maximum Entropy Power Spectra of Sinusoids," Journal of Geophysical Research, 79, No. 20, pp. 3019-3022, July 10, 1974.

1978 USAF-ASEE SUMMER FACULTY RESEARCH PROGRAM
sponsored by
THE AIR FORCE OFFICE OF SCIENTIFIC RESEARCH
conducted by
AUBURN UNIVERSITY AND OHIO STATE UNIVERSITY

PARTICIPANT's FINAL REPORT

ADVANCED ACQUISITION/STRIKE SYSTEM GUIDANCE TECHNIQUES

Prepared by:	Robert H. Foulkes, Jr.
Academic Rank:	Associate Professor
Department and University:	Electrical Engineering Youngstown State University

Assignment:

(Air Force Base)	Griffiss AFB
(Laboratory)	Rome Air Development Center
(Division)	Communications and Control
(Branch)	Location & Control
(Section)	Active Location & Control
USAF Research Colleague:	Henry J. Mancini
Date:	August 23, 1978
Contract No.:	F44620-75-C-0031

ADVANCED ACQUISITION/STRIKE SYSTEM
GUIDANCE TECHNIQUES

ABSTRACT

by

Robert H. Foulkes, Jr.

This report contains a discussion of an application of stochastic control theory to the control of a weapon vehicle containing munitions to be deployed against an enemy target.

An overall system model containing a vehicle model, a disturbance model, and a measurement model is developed and converted to an equivalent discrete-time model. A control system containing a one-step Kalman predictor and a set of control gains is proposed. The control system structure is discussed and algorithms for calculation of the control and filter gains are given.

ACKNOWLEDGMENTS

The author is grateful to the Air Force Systems Command for providing the support for this research opportunity. Gratitude is also due to ASEE and Auburn University and especially to Mr. J. Fred O'Brien and Mr. John Huss for efficient administration of the program.

The author would like to express his appreciation to the people of the Location and Control Branch and especially to those in the Active Location and Control Section for providing a friendly and helpful environment. A special thanks goes to Ms. Barbara Silfer for her help during the ten weeks and for the typing of this report.

INTRODUCTION AND OBJECTIVES

The research effort described here is carried out within the Air Force MTI Radar Surveillance Strike System (MRS^3) program. The objective of the MRS^3 program is to demonstrate the feasibility of automatic detection, tracking, and striking of moving ground targets in real time. This objective requires the development of radar and radar signal processing for both weapon and target tracking, weapon system navigation/guidance control laws, data links, jam resistance and low probability of intercept features, and necessary data processing.

The overall acquisition/track/strike system would include target tracking, guidance of a launch vehicle to a launch position, and post-launch tracking and control of the weapon until strike. Various system configurations are under consideration, involving different tracking schemes and different weapon systems. Tracking of both weapon and target using range measurements from two airborne radar platforms and tracking using range/angle measurements from a single platform are being evaluated. Also being evaluated are weapon vehicles that fly basically different trajectories, including high altitude approach with pitchover to a near-vertical final approach and a glideslope approach from launch to target.

This research effort involves an application of stochastic control theory to the design of a control system for a weapon vehicle flying a glideslope from a launch point to a strike point. The control problem is posed as a regulator problem and the control system is designed to keep the vehicle near the glideslope.

The control system design requires the development of an overall system model, including a vehicle model, a disturbance model, and a measurement model. The modeling section of this report consists of a brief summary of the development of these models.

The section on control system development deals with the design of a digital compensator based on an application of stochastic optimal control theory. The compensator is made up of a discrete one-step Kalman predictor, used to obtain estimates of the vehicle and disturbance states, and a set of control gains, used with the above estimates to obtain actuator commands.

The report concludes with a description of current activity and recommendations for continued work.

MODEL DEVELOPMENT

In this section, vehicle, disturband, and measurement models are developed.

The Vehicle Model

The vehicle is modeled using a perturbation model about a desired glide-slope. The nonlinear equations of motion are written and linearized about the desired equilibrium. The details are outlined below. The notation used here follows Etkin [1]. It is assumed that the Earth is an inertial system and is locally flat.

Let $\bar{V}$ denote the mass center velocity with respect to the atmosphere and let $\bar{W} = \bar{W}_S + \bar{W}_g$ denote the wind velocity with respect to the Earth, where $\bar{W}_S$ and $\bar{W}_g$ are steady wind and gust terms, respectively. The $\bar{V}^E = \bar{V} + \bar{W}_S + \bar{W}_g$ is the inertial velocity of the mass center.

The force equation in the body axis reference frame is

$$\bar{f}_B = m\left(\frac{d}{dt}\bar{V}^E{}_B + \bar{\omega}^B{}_B \times \bar{V}^E{}_B\right)$$

where $\bar{f}$ is the external force, $\bar{\omega}^B$ is the body-axis angular velocity, and the subscript B refers to the body axes.

In order to use airspeed V, angle of attack α, and sideslip angle β as state variables, $\bar{V}_B$ is expressed as $L_{BW}\bar{V}_W$ and W_{SB} as $L_{BV}\bar{W}_{SV}$, where L_{BW} transforms wind-axis components into body-axis components and L_{BV} transforms vertical-axis components into body-axis components [1]. Then

$$\bar{f}_B = m\left(\frac{d}{dt}(L_{BW}\bar{V}_W) + \bar{\omega}^B{}_B \times L_{BW}\bar{V}_W + \frac{d}{dt}\bar{W}_{g_B} + \bar{\omega}^B{}_B \times \bar{W}_{g_B}\right) \tag{1}$$

The external force is expressed as $\overline{f}_B = \overline{A}_B + m\overline{g}_B$, where $\overline{A}_B$ is the aerodynamic force and $m\overline{g}_B$ the gravity force. $\overline{A}_B$ is given in terms of the lift L, sideforce Y, and drag D: $\overline{A}_B = L_{BW}\,[-D \;\; Y \;\; -L]'$.

Under suitable assumptions (see [1]), the moment equation in the body axes is $\overline{G}_B = \frac{d}{dt}\overline{h}_B + \overline{\omega}^B{}_B \times \overline{h}_B = I\frac{d}{dt}\overline{\omega}^B{}_B + \overline{\omega}^B{}_B \times I\,\overline{\omega}^B{}_B$ (2)

where $\overline{G}_B$ is the external moment and $\overline{h}_B = I\overline{\omega}^B{}_B$ is the angular momentum, with I denoting the body axes moments of inertia.

In addition to the six degrees of freedom described in (1) and (2), the basic nonlinear model consists of the kinematic constraints relating body axes Euler angle rates to $\overline{\omega}^B{}_B = [p\ q\ r]$:

$$\dot{\phi} = p + q\sin\phi\tan\theta + r\cos\phi\tan\theta \tag{3.1}$$

$$\dot{\theta} = q\cos\phi - r\sin\phi \tag{3.2}$$

$$\dot{\psi} = (q\sin\phi + r\cos\phi)\sec\theta \tag{3.3}$$

As indicated in the discussion of the measurement model, relative grid radar measurements will provide weapon vehicle position with respect to the target. Hence, the vehicle model should include velocity with respect to the target. To do this, target velocity with respect to the Earth is subtracted from vehicle velocity with respect to the Earth.

Let $\overline{T}^E{}_V$ denote target velocity. Then the vehicle velocity with respect to a reference frame translating with the target is $\overline{V}^T{}_V - \overline{T}^E{}_V$, where the subscript V denotes a vertical reference frame. Expressing $\overline{V}^E{}_V$ as airspeed plus wind speed,

$$\overline{V}^T{}_V = L_{VB}L_{BW}\overline{V}_W + \overline{W}_{SV} + L_{VB}\overline{W}_{g_B} - \overline{T}^E{}_V \tag{4}$$

The three components of $\overline{V}^T{}_V$ are downrange velocity $\dot{x}_r$, crossrange velocity $\dot{y}_r$, and vertical velocity $\dot{z}_E$.

In order to keep the project to a reasonable size, only the longitudinal control system was considered. Hence, the nonlinear model consisted of the drag and lift components of (1), the pitch rate component of (2), equation (3.2), and the downrange and vertical components of (4). The model can be represented as a single nonlinear vector equation $\dot{X} = f(X,U,D,\dot{D})$, where $X = [V \; \alpha \; q \; \theta \; X_r \; \xi_E]'$ is the state vector, $U = [\delta_e]$ (δ_e = elevator) is the control vector, and $D = [u_g \; w_g \; q_g \; W_{S_X} \; X_T]'$ is the disturbance vector, where u_g, w_g, and q_g are gust components, W_{S_X} is the X-direction steady wind, and X_T is the X-direction target position.

The perturbation model consists of the first-order terms in a Taylor series expansion of the nonlinear equation about the glideslope equilibrium. The equilibrium is determined under a zero disturbance condition. Using

$$x = [\delta V \; \delta\alpha \; \delta q \; \delta\theta \; \delta X_r \; \delta\xi_E]'$$

$$u = [\delta_e]$$

$$y_d = D = [u_g \; w_g \; q_g \; W_{S_X} \; X_T]'$$

as perturbation state, control, and disturbance vectors, respectively, the perturbation model in usual state-variable form is

$$\dot{x} = Ax + Bu + D_{01} y_d - D_{02} \qquad (5)$$

The Disturbance Model

As seen above, the disturbance vector Y_d consists of gust velocities, a steady-wind component, and the X-direction target position. The gust velocities are modeled using the Dryden spectra and are produced for simulation and filter design purposes by a linear system processing white noise. As an example of the linear system design, consider the gust velocity u_g, normalized by the equilibrium airspeed V_e. The power density spectrum of the normalized u_g is [2]

$$\Phi_{u_g}(\omega) = \frac{2L_u\sigma_u^2}{V_e^3}\,\frac{1}{1+\left(\frac{L_u}{V_e}\omega\right)^2}$$

where σ_u is the rms gust velocity in ft/sec, L_u is a turbulence scale factor in feet, and ω is the frequency variable in rad/sec.

Now, if a linear system with transfer function

$$H(j\omega) = \frac{1}{1+j\omega\frac{L_u}{V_e}}$$

is subjected to a white noise input with variance $\sigma^2 = 2L_u\sigma_u^2/V_e^3$, the output is a random process with the spectrum $\Phi_{u_g}(\omega)$ [3]. A system with the required transfer function is described in state-variable form by

$$\dot{d}_1 = -\frac{V_e}{L_u}d_1 + \frac{V_e}{L_u}\xi_1$$

$$y_{d_1} = d_1$$

where ξ_1 is a mean zero white noise process with variance $2L_u\sigma_u^2/V_e^3$, d_1 is a state variable, and y_{d_1} isthe output having the required spectrum. The remaining gust velocities are generated in a similar manner.

The steady-wind W_{s_x} is modeled as $\dot{d}_5 = \xi_3$ and $y_{d_4} = d_5$, where ξ_3 is normal, mean zero, with small variance.

Putting together the gust equations, the steady-wind equation, and the target motion equations yields a disturbance model of the form

$$
\begin{aligned}
\dot{d} &= A_d\, d + B_d\, \zeta \\
Y_d &= C_d\, d
\end{aligned}
\qquad (6)
$$

where d is the disturbance state vector, ζ is white noise, and Y_d is the disturbance vector used in the perturbation model (5).

The Measurement Model

For control purposes, it is assumed that several on-board sensor readings are available, as well as relative grid radar data. On-board sensors include airspeed indicator (V), angle-of-attack indicator (α), pitch and pitch rate gyros (θ, q), body-mounted accelerometers ($\ddot{x}_B$. $\ddot{z}_B$), and altimeter ($h_w = -z_E$). It is assumed that a single airborne radar platform provides range-to-weapon (R_W), range-to-target (R_T), and relative angle between the two (θ_{WT}).

The total measurements above are processed into incremental measurements to provide inputs for the Kalman filter. The filter input vector is

$$y = [\delta V \quad \delta\alpha \quad \delta q \quad \delta\theta \quad \delta\ddot{x}_B \quad \delta\ddot{y}_B \quad \delta h_w \quad \delta x_r]'$$

Essentially, the incremental measurements are computed by subtracting equilibrium values from the total measurements. For example, $y_1 = \delta V = V - V_e$, where V = airspeed indicator reading and V_e = equilibrium airspeed.

For purposes of the longitudinal control system design, X_r is treated as the ground distance between weapon and target. It is calculated from R_W, R_T, θ_{WT}, and H_w as follows:

$$X_r = \sqrt{R_W^2 + R_T^2 - 2 R_W R_T \cos\theta_{WT} - h_w^2}$$

In order to compute δh_w and δx_r, let h_0 and X_0 be initial altitude and downrange position, respectively. Then the equilibrium altitude at time t is $h_0 + (V_e \sin\gamma_e)t$ and the equilibrium downrange position is $X_0 + (V_e \cos\gamma_e)\,t$, where γ_e is the equilibrium flight path angle.

For filter design purposes, Y is expressed as a combination of the perturbation vehicle and disturbance state vectors:

$$y = C \begin{bmatrix} x \\ \hdashline d \end{bmatrix} + v \qquad (7)$$

ν is a normal, mean zero measurement noise vector whose covariance depends on the accuracies of the total measurements.

Control System Development

As indicated in the introduction, the control system consists of a Kalman one-step predictor and a set of control gains. This section contains an outline of the design approach.

From the previous section, equations (5), (6), and (7) give the overall system model:

$$\dot{x} = Ax + Bu + D_{01} y_d + D_{02} \dot{y}_d \tag{5}$$

$$\left.\begin{aligned} \dot{d} &= A_d d + B_d \xi \\ y_d &= C_d d \end{aligned}\right\} \tag{6}$$

$$y = C \begin{bmatrix} x \\ \hdashline d \end{bmatrix} + \nu \tag{7}$$

Eliminating Y_d and $\dot{Y}_d$ from the first equation gives

$$\dot{x} = Ax + Bu + D_0 d + D_1 \xi \tag{8.1}$$

$$\dot{d} = A_d d + B_d \xi \tag{8.2}$$

$$y = C \begin{bmatrix} x \\ \hdashline d \end{bmatrix} + \nu \tag{8.3}$$

where $D_0 = D_{01} C_d + D_{02} C_d A_d$ and $D_1 = D_{02} C_d B_d$.

A continuous-time regulator problem involves minimizing a cost function of the form

$$J = \frac{1}{2} E\left\{ \int_0^{t_f} (x'Qx + u'Ru)\,dt + x'(t_f)\, Q_f\, x(t_f) \right\} \tag{9}$$

For a discrete-time control system, equations (8) and (9) are transformed to equivalent discrete-time equations. The discrete-time equivalent of (8) is obtained by integrating (8) over each sample period. Assuming u is held constant over each sample period, equation (8) becomes [4]

$$\left.\begin{aligned} x_{k+1} &= \Phi\, x_k + \Gamma_1 u_k + \Gamma_2\, d_k + \xi_k \\ d_{k+1} &= \Phi_d\, d_k + \eta_k \\ y_k &= C \left[\begin{array}{c} x_k \\ \hdashline d_k \end{array}\right] + \nu_k \end{aligned}\right\} \qquad (10)$$

where

$$\left[\begin{array}{c:c} \Phi & \Gamma_2 \\ \hdashline 0 & \Phi_d \end{array}\right] = e^{\left[\begin{array}{c:c} A & D_0 \\ \hdashline 0 & A_d \end{array}\right] T}$$

$$\Gamma_1 = \left(\int_0^T e^{At} dt \right) B$$

and $\left[\begin{array}{c} \xi_k \\ \hdashline \eta_k \end{array}\right]$ is a white, gaussian noise sequence of mean zero and covariance

$$E\left\{ \left[\begin{array}{c} \xi_k \\ \hdashline \eta_k \end{array}\right] \left[\begin{array}{c} \xi_k \\ \hdashline \eta_k \end{array}\right]' \right\} = \int_0^T e^{\left[\begin{array}{c:c} A & D_0 \\ \hdashline 0 & A_d \end{array}\right] t} \left[\begin{array}{c} D_1 \\ \hdashline B_d \end{array}\right] E\{\rho\rho'\} \left[\begin{array}{c} D_1 \\ \hdashline B_d \end{array}\right]' e^{\left[\begin{array}{c:c} A & D_0 \\ \hdashline 0 & A_d \end{array}\right]' t}\, dt \,.$$

T is the sample period in seconds.

The discrete-time equivalent of (9) is obtained by writing the integral as a sum of integrals over each of the sample periods. Assuming Q and R are constants, J is given by [4]

$$J = \frac{1}{2} E\left\{ \sum_{k=0}^{N-1} \left(x_{k+1}' \hat{Q} x_{k+1} + 2 x_{k+1}' \hat{N} d_{k+1} + 2 x_k' \hat{M} u_k + u_k' \hat{R} u_k \right) \right\} \qquad (11)$$

where

$$\hat{Q} = \int_0^T e^{A't} Q\, e^{At} dt$$

$$\hat{M} = \int_0^T e^{A't} Q \left(\int_0^t e^{As} ds \right) dt \cdot B$$

$$\hat{R} = RT + B' \int_0^T \left(\int_0^t e^{As} ds \right)' Q \left(\int_0^t e^{As} ds \right) dt \cdot B$$

and

$$\hat{N} = \int_0^T e^{A't} Q \left(\int_0^t e^{A(t-s)} D_0\, e^{A_d s} ds \right) dt$$

The control that minimizes (11) subject to (10) is given by [4]

$$u_k = -H_k\, \hat{x}_k - H_{dk}\, \hat{d}_k \qquad (12)$$

where $\hat{X}_k$ and $\hat{d}_k$ are one-step predicted least-squares estimates of X_k and d_k, and where H_k and H_{dk} are calculated as follows:

$$H_k = -\tilde{R}_k^{-1} G_k \,, \qquad H_{dk} = \tilde{R}_k^{-1} G_{dk}$$

$$\tilde{R}_k = \hat{R} + \Gamma_1' P_k \Gamma_1$$

$$G_k = \Gamma_1' P_k \Phi + \hat{M}' \,, \qquad G_{dk} = \Gamma_1' (D_k \Phi_d + P_k \Gamma_2)$$

$$P_{k-1} = \Phi' P_k \Phi + \hat{Q} - G_k' H_k \,, \quad P_N = \hat{Q}$$

$$D_{k-1} = (\Phi - \Gamma_1 \tilde{R}_k^{-1} G_k)' (D_k \Phi_d + P_k \Gamma_2) \,, \quad D_N = \hat{N}$$

Since the system and cost function matrices are constant, a suboptimal design consisting of the steady-state gains can be used.

The estimates $\hat{X}_k$ and $\hat{d}_k$ are obtained by using a one-step Kalman predictor on the augmented system given in (10). Assuming the noise covariances are constant, a steady-state filter can be used. The filter equation is

$$\begin{bmatrix} \hat{x}_{k+1} \\ \hat{d}_{k+1} \end{bmatrix} = \begin{bmatrix} \Phi & \Gamma_2 \\ 0 & \Phi_d \end{bmatrix} \begin{bmatrix} \hat{x}_k \\ \hat{d}_k \end{bmatrix} + \begin{bmatrix} \Gamma_1 \\ 0 \end{bmatrix} u_k + L \left(Y_k - C \begin{bmatrix} \hat{x}_k \\ \hat{d}_k \end{bmatrix} \right) \qquad (13)$$

where the gain matrix is calculated from the following relations:

$$L = \begin{bmatrix} \Phi & \Gamma_2 \\ 0 & \Phi_d \end{bmatrix} \Sigma C' (C \Sigma C' + \Theta)^{-1}$$

where Σ satisfies

$$\Sigma = \Xi + \begin{bmatrix} \Phi & \Gamma_2 \\ 0 & \Phi_d \end{bmatrix} \left(\Sigma - \Sigma C' (C \Sigma C' + \Theta)^{-1} C \Sigma \right) \begin{bmatrix} \Phi & \Gamma_2 \\ 0 & \Phi_d \end{bmatrix}'$$

and

$$\Theta = E\left\{ \nu_k \nu_k' \right\} \quad \text{and} \quad \Xi = E\left\{ \begin{bmatrix} \xi_k \\ \hline \eta_k \end{bmatrix} \begin{bmatrix} \xi_k \\ \hline \eta_k \end{bmatrix}' \right\}$$

are the measurement and state noise covariance matrices, respectively. See [5] for details.

The control system, then, is implemented using equations (12) and (13).

CONCLUSIONS AND RECOMMENDATIONS

At the present time, the basic continuous-time model of equation (8) has been developed and changed into the discrete-time model of equation (10). Also, the discrete-time equivalent cost function given in (11) has been developed from (9).

Current activity centers on determination of the control gains needed in (12). An iterative approach to solving the gain equations has been programmed and is being debugged.

Following completion of the longitudinal control system, future work could include development of the lateral control system and of a six degree-of-freedom digital simulation including winds and target dynamics. The simulation would be used to time the control system design and to examine the effects of the radar data rates, the control update rate, and data link failure.

A comment on implementation is in order. Since the measurement information consists of basically two sets, viz., radar and altimeter in one set and on-board sensors except altimeter in the other, the control calculation can be broken into two parts. Part one is based on radar data and would be accomplished at a ground control station. Part two is based on on-board sensor data and could be accomplished using an on-board digital processor. In case of a data link failure, the on-board calculation could continue uninterrupted.

REFERENCES

[1] B. Etkin, Dynamics of Atmospheric Flight. New York: John Wiley and Sons, Inc., 1972.

[2] J. Roskam, Flight Dynamics of Rigid and Elastic Airplanes. Roskam Aviation and Engineering Corp., 519 Boulder, Lawrence, Kansas, 1972.

[3] A. Papoulis, Probability, Random Variables, and Stochastic Processes. New York: McGraw-Hill Book Company, 1965.

[4] N. Halyo and R. H. Foulkes, "On the Quadratic Sampled-Data Regulator With Unstable Random Disturbances," 1974 International Conference of IEEE Systems, Man, and Cybernetics Society, Dallas, Texas, 1974.

[5] J. S. Meditch, Stochastic Optimal Linear Estimation and Control. New York: McGraw-Hill Book Company, 1969.

1978 USAF-ASEE SUMMER FACULTY RESEARCH PROGRAM

sponsored by

THE AIR FORCE OFFICE OF SCIENTIFIC RESEARCH

conducted by

AUBURN UNIVERSITY AND OHIO STATE UNIVERSITY

PARTICIPANT'S FINAL REPORT

APPLICATION OF BAYESIAN TECHNIQUES TO RELIABILITY DEMONSTRATION ESTIMATION AND UPDATING OF THE PRIOR DISTRIBUTION

BY THEODORE S. BOLIS, Ph.D.

Assistant Professor of Mathematics

Department of Mathematical Sciences

State University College at Oneonta, New York

Assignment:	Griffiss Air Force Base
	Rome Air Development Center
	Reliability and Compatibility Division
	Reliability Branch
USAF Research Colleague:	Anthony Coppola, RADC/RBRT
Date:	August 18, 1978
Contract No.:	F44620-75-C-0031

APPLICATION OF BAYESIAN TECHNIQUES

TO RELIABILITY DEMONSTRATION

ESTIMATION AND UPDATING OF THE PRIOR DISTRIBUTION

by

T. S. Bolis

ABSTRACT

A method is presented for the estimation of the shape and scale parameters of an inverted gamma prior distribution of the mean-time-to-failure for equipment having exponential time-to-failure distribution. This method, akin to the Maximum Likelihood Method, allows the use of all sorts of existing failure data on the equipment in question, provided a certain sufficient condition is satisfied. Further, this method (we call it the Generalized Maximum Likelihood Method) is usable to update the prior distribution, when new failure data become available. In the long run, this updating process will give rise to a solid prior, which can confidently be used in Reliability Demonstration.

Various facets of the sufficient condition for the applicability of this estimation method are exposed, the variance-covariance matrix of the estimators is given under various randomness assumptions and some numerical considerations are discussed.

There is a brief discussion of alternate estimators in the case of a truncated test data.

ACKNOWLEDGEMENTS

The author wishes to express his thanks to the Air Force Systems Command for the support of this project. Thanks are also due to ASEE and the Auburn Research Foundation, particularly to Mr. Fred O'Brien, Jr. for the excellent administration of this program.

The author also wishes to express his thanks and indeptedness to the Rome Air Development Center for providing a cordial and stimulating work environment. In particular thanks are due to Mr. John Huss of the Plans Office, Mr. Anthony Coppola, Mr. Jerome Klion and Mr. Eugene Fiorentino of the Reliability Branch.

Finally thanks are expressed to Mrs. Patricia Parkhurst and Mrs. Johanna Leonard for providing clerical assistance to this project.

1. INTRODUCTION

1.1 We consider equipment with exponentially distributed time-to-failure, i.e. the probability density function of the time-to-failure is given by

(1.1.1) $$\varphi(t|\theta) = \theta^{-1}\exp(-t/\theta), \quad t>0; \ \theta>0,$$

where the parameter θ is the mean-time-to-failure (MTTF) of the equipment. We assume that θ itself has a prior distribution of the inverted gamma type, i.e. the prior probability density function of θ is given by

(1.1.2) $$g(\theta;\lambda,\gamma) = \frac{\gamma^{\lambda}}{\Gamma(\lambda)}\,\theta^{-(\lambda+1)}\exp(-\gamma/\theta), \quad \theta>0; \ \lambda>0, \gamma>0,$$

where λ is the shape parameter and γ is the scale parameter of the prior distribution.

1.2 Bayesian Reliability Test Plans based on the prior (1.1.2) have been developed by Schafer et al. [4] and Goel [1] under various combinations of risks. The implementation of these plans require the estimated values of λ and γ in (1.1.2). Since the true MTTF θ of an equipment is not observable, we cannot directly fit existing data to the inverted gamma distribution (1.1.2). To get around this difficulty, we consider the probability function of the number of failures r in a fixed time T, given θ. Because of the exponentiality assumption (1.1.1), this probability function is Poisson with parameter T/θ, i.e.

(1.2.1) $$P_T(r|\theta) = \frac{1}{r!}(T/\theta)^r\exp(-T/\theta), \quad r=0,1,2,\cdots; \ T>0$$

Thus, the unconditional probability function of the number of failures r in a fixed time T is

(1.2.2) $$P_T(r) = \int_0^{\infty} P_T(r|\theta)\,g(\theta;\lambda,\gamma)\,d\theta$$

By using (1.1.2) and (1.2.1) and performing the integration, we obtain

(1.2.3) $$P_T(r) = \binom{\lambda+r-1}{r}\left(\frac{\gamma}{T+\gamma}\right)^{\lambda}\left(\frac{T}{T+\gamma}\right)^{r}, \quad r=0,1,2,\cdots$$

which is a negative binomial distribution with parameters λ and $T/(T+\gamma)$.

If existing data on a type of equipment are of the form "number of failures

in a fixed common time T", then the parameters λ and γ can be estimated by using (1.2.3). Schafer et al. [3] used the method of moments for this purpose, whereas Goel and Joglekar [2] used the maximum likelihood method.

1.3 An extreme and rather hypothetical case results when we keep the number of failures r fixed and observe the time T until the rth failure. Since T is the sum of r exponential random variables, its probability density is gamma with parameters r and θ^{-1}

$$f_r(T|\theta) = \frac{\theta^{-r}}{(r-1)!} T^{r-1} \exp(-T/\theta), \quad T > 0. \tag{1.3.1}$$

Thus, the unconditional probability density function of T is

$$\begin{aligned} f_r(T) &= \int_0^\infty f_r(T|\theta)\, g(\theta;\lambda,\gamma)\, d\theta \\ &= \frac{r}{T} \binom{\lambda+r-1}{r} \left(\frac{\gamma}{T+\gamma}\right)^{\lambda} \left(\frac{T}{T+\gamma}\right)^{r}, \quad T > 0. \end{aligned} \tag{1.3.2}$$

This is just a scale transform of the inverted beta distribution written in this form to show its similarity with (1.2.3).

1.4 Existing failure data (especially field data) usually do not exhibit any of the two features discussed above. Usually the test or operational time varies from equipment to equipment of the same type. Thus the data will usually be of the form $(r_i\ T_i)$, $i=1, \ldots, n$, where r_i is the number of failures of the ith equipment in time T_i. In a test situation, it is feasible to control either r_i or T_i, but cost considerations recommend the control of T_i. Thus, it is desirable to estimate λ and γ in this more general situation, which encompasses the situations discussed in sections 1.2 and 1.3 as special cases. Schafer et al. [3] present a method of estimation akin to the method of moments. This method however is not applicable if a single equipment had no failures at all.

1.5 In this report we present a general estimation method which we call <u>The Generalized Maximum Likelihood Method</u>. A sufficient condition for the existence of the estimators is given. In the case of fixed time data,

it is shown that the condition is also necessary. The method has the advantage of being usable to <u>update the prior</u> when new data become available e.g. from reliability demonstration tests.

If the data used for the estimation of the prior distribution are generated by a planned test, the estimability condition dictates ways of choosing (controlling) either the test times T_i or the number of failures r_i in such a way that the resulting Generalized Maximum Likelihood Equations have a solution, i.e. the estimators exist.

In the case of fixed time data, if the estimability condition is violated, some alternate estimation methods are presented.

2. THE GENERALIZED MAXIMUM LIKELIHOOD ESTIMATION METHOD

2.1 We suppose that n identical equipments with exponential time-to-failure distribution are tested in the following way: the ith equipment is tested for T_i hours, $i = 1, \ldots, n$. Let r_i denote the number of failures of the ith equipment. We assume that the prior distribution of the MTTF θ is given by (1.1.2). Then, the unconditional probability function of r_i is given by (1.2.3), i.e.

$$(2.1.1)\qquad P_{T_i}(r_i) = \binom{\lambda+r_i-1}{r_i}\left(\frac{\gamma}{T_i+\gamma}\right)^{\lambda}\left(\frac{T_i}{T_i+\gamma}\right)^{r_i}.$$

The <u>Generalized</u> <u>Likelihood</u> <u>Function</u> of the sample (r_i, T_i), $i = 1, \ldots, n$ is defined to be

$$(2.1.2)\qquad L = \prod_{i=1}^{n}\binom{\lambda+r_i-1}{r_i}\left(\frac{\gamma}{T_i+\gamma}\right)^{\lambda}\left(\frac{T_i}{T_i+\gamma}\right)^{r_i}.$$

Just as in the classical Maximum Likelihood Estimation technique, the best explanation of the data (r_i, T_i), $i = 1, \ldots, n$ is provided by the values $(\hat{\lambda}, \hat{\gamma})$ of (λ, γ) at which the function L attains its maximum, if L has a maximum. As usual, in order to maximize L, it is enough to maximize its natural logarithm

$$(2.1.3)\qquad \ln L = \sum_{i=1}^{n}\ln\binom{\lambda+r_i-1}{r_i} + \lambda\sum_{i=1}^{n}\ln\frac{\gamma}{T_i+\gamma} + \sum_{i=1}^{n} r_i \ln\frac{T_i}{T_i+\gamma}.$$

In order to obtain the critical point of L, we have to solve simultaneously the <u>Generalized</u> <u>Likelihood</u> <u>Equations</u>

$$(2.1.4)\qquad \frac{\partial}{\partial\lambda}\ln L = 0, \quad \frac{\partial}{\partial\gamma}\ln L = 0$$

which in our case become

$$(2.1.5)\qquad \frac{\partial}{\partial\lambda}\ln L = \sum_{i=1}^{n}\left(\frac{1}{\lambda}+\cdots+\frac{1}{\lambda+r_i-1}\right) - \sum_{i=1}^{n}\ln\left(1+\frac{T_i}{\gamma}\right) = 0$$

$$(2.1.6)\qquad \frac{\partial}{\partial\gamma}\ln L = \frac{\lambda}{\gamma}\sum_{i=1}^{n}\frac{T_i}{T_i+\gamma} - \sum_{i=1}^{n}\frac{r_i}{T_i+\gamma} = 0.$$

If we set $\alpha_j = \sum_{r_i \geq j} 1$ the above equations are reduced to

$$(2.1.7)\qquad \sum_{j\geq 1}\frac{\alpha_j}{\lambda+j-1} = \sum_{i=1}^{n}\ln\left(1+\frac{T_i}{\gamma}\right)$$

$$\lambda = \gamma \sum_{i=1}^{n} \frac{r_i}{T_i+\gamma} \Big/ \sum_{i=1}^{n} \frac{T_i}{T_i+\gamma} \quad (2.1.8)$$

Since λ is given explicitly in terms of γ by (2.1.8), we can substitute in (2.1.7) to obtain an equation in γ alone. The resulting equation can be solved numerically (when a solution exists) to obtain the estimator $\hat{\gamma}$ and then, by means of (2.1.8) obtain the value $\hat{\lambda}$.

2.2 If we control the number of failures r_i and let T_i be random, the distribution of T_i is given by (1.3.2). It is immediate that the new Generalized Likelihood Function will be the same as the one given by (2.1.2) up to a factor

$$\prod_{i=1}^{n} r_i/T_i$$

which is independent of the parameters λ and γ. Therefore the resulting Generalized Likelihood Equations will be exactly the same as the ones given by (2.1.7) and (2.1.8). Thus, the Generalized Maximum Likelihood estimators will have the same form, irrespectively of whether we control the T_i's or the r_i's or any combination of them (e.g. controling r_i for $i = 1, \ldots, k$ and T_j for $j = k + 1, \ldots, n$).

3. A SUFFICIENT CONDITION FOR THE EXISTENCE OF THE GENERALIZED MAXIMUM LIKELIHOOD ESTIMATORS

3.1 The system of equations (2.1.7) and (2.1.8) does not always have a solution. Although we could produce examples of actual data for which the Generalized Maximum Likelihood estimators do not exist, for simplicity's sake we resort to the following rather contrived

EXAMPLE 3.1.1 Let $n = 3$, $r_i = 0$, $r_2 = 1$, $r_3 = 2$, $T_1 = T_2 = T_3 = T$.

Then the equations (2.1.7) and (2.1.8) are reduced to

$$\frac{2}{\lambda} + \frac{1}{\lambda+1} = 3\ln\left(1 + \frac{T}{\gamma}\right) \quad (3.1.1)$$

$$\lambda = \gamma/T \quad (3.1.2)$$

whose simultaneous solution calls for the zero of the function

$$\psi(\lambda) = \frac{2}{\lambda} + \frac{1}{\lambda+1} - 3\ln\left(1+\frac{1}{\lambda}\right), \quad \lambda > 0 .$$

We claim that actually $\psi(\lambda) > 0$ for all $\lambda > 0$. Indeed, $\lim_{\lambda \to 0+} \psi(\lambda) = +\infty$ and $\lim_{\lambda \to \infty} \psi(\lambda) = 0$ and thus it is enough to show that ψ is strictly decreasing. This is so since the derivative of ψ is negative

$$\psi'(\lambda) = -\frac{2}{\lambda^2} - \frac{1}{(\lambda+1)^2} + \frac{3}{\lambda(\lambda+1)} = -\frac{\lambda+2}{\lambda^2(\lambda+1)^2} < 0 .$$

3.2 We now give a sufficient condition for the solvability of the Generalized Likelihood Equations (2.1.7) and (2.1.8). We use the following notation:

$$\bar{r} = \frac{1}{n}\sum_{i=1}^{n} r_i , \quad s_r^2 = \frac{1}{n}\sum_{i=1}^{n} r_i^2 - \bar{r}^2 ,$$

$$\bar{T} = \frac{1}{n}\sum_{i=1}^{n} T_i , \quad s_T^2 = \frac{1}{n}\sum_{i=1}^{n} T_i^2 - \bar{T}^2 ,$$

$$\mathrm{cov}(r,T) = \frac{1}{n}\sum_{i=1}^{n} r_i T_i - \bar{r}\,\bar{T} .$$

We shall prove the following

THEOREM 3.2.1 If

(C) $$2\bar{r}\,\bar{T}\,\mathrm{cov}(r,T) < \bar{T}^2 (s_r^2 - \bar{r}) + \bar{r}^2 S_T^2 ,$$

then the Generalized Likelihood Equations (2.1.7) and (2.1.8) have a solution.

PROOF. It suffices to show that the function defined by

(3.2.1) $$W(\gamma) = \sum_{j\geq 1} \frac{\alpha_j}{\lambda(\gamma)+j-1} - \sum_{i=1}^{n} \ln\left(1+\frac{T_i}{\gamma}\right), \quad \gamma > 0$$

where $$\lambda(\gamma) = \gamma \sum_{i=1}^{n} \frac{r_i}{T_i+\gamma} \Big/ \sum_{i=1}^{n} \frac{T_i}{T_i+\gamma}$$

has a zero. We observe that $\alpha_1 \neq 0$, because, otherwise, all $\alpha_j = 0$ which implies that all $r_i = 0$ and the condition (C) violated (it is reduced to $0<0$). Since $\lambda(\gamma)$ tends to zero when γ tends to zero and since $\alpha_1 > 0$ we get

$$\lim_{\gamma \to 0+} W(\gamma) = +\infty .$$

Thus, it suffices to show that $W(\gamma)$ is negative for large γ. To this end we

observe that

$$(3.2.2)\quad \lambda(\gamma) = \gamma\left[\sum_{i=1}^{n} r_i - \sum_{i=1}^{n} r_i T_i \gamma^{-1} + o(\gamma^{-1})\right] \Big/ \left[\sum_{i=1}^{n} T_i - \sum_{i=1}^{n} T_i^2 \gamma^{-1} + o(\gamma^{-1})\right]$$

$$= \frac{\bar{r}}{\bar{T}}\gamma + \frac{\bar{r} s_T^2 - \bar{T}\,\mathrm{cov}(r,T)}{\bar{T}^2} + o(1) \quad \text{as} \quad \gamma \to +\infty .$$

Substituting (3.2.2) into (3.2.1) we obtain

$$(3.3.3)\quad W(\gamma) = \sum_{j\ge 1} \alpha_j \Big/ \left[\frac{\bar{r}}{\bar{T}}\gamma + \frac{\bar{r} s_T^2 - \bar{T}\,\mathrm{cov}(r,T)}{\bar{T}^2} + j - 1 + o(1)\right] - \sum_{i=1}^{n} \ln\left(1 + \frac{T_i}{\gamma}\right)$$

$$= \frac{\bar{T}}{\bar{r}}\gamma^{-1}\left[\sum_{j\ge 1}\alpha_j - \left[\frac{\bar{r} s_T^2 - \bar{T}\,\mathrm{cov}(r,T)}{\bar{r}\,\bar{T}}\sum_{j\ge 1}\alpha_j + \frac{\bar{T}}{\bar{r}}\sum_{j\ge 1}(j-1)\alpha_j\right]\gamma^{-1} + o(\gamma^{-1})\right] - \sum_{i=1}^{n} T_i\gamma^{-1} + \frac{1}{2}\sum_{i=1}^{n} T_i^2\gamma^{-2} + o(\gamma^{-2})$$

$$\text{as} \quad \gamma \to +\infty .$$

Since $\sum_{j\ge 1}\alpha_j = n\bar{r}$ and $\sum_{j\ge 1}(j-1)\alpha_j = \frac{1}{2}\left(s_r^2 + \bar{r}^2 - \bar{r}\right)$,
(3.3.3) is reduced to

$$W(\gamma) = -\frac{n}{2\bar{r}^2}\left[-2\bar{r}\,\bar{T}\,\mathrm{cov}(r,T) + \bar{T}^2(s_r^2 - \bar{r}) + \bar{r}^2 s_T^2\right]\gamma^{-2} + o(\gamma^{-2})$$

$$\text{as} \quad \gamma \to +\infty .$$

Because of the condition (C), $W(\gamma) < 0$ for large λ and the theorem is proved.

3.3 We observe that in case $T_i = T$ for all $i = 1, \ldots, n$, the condition (C) is reduced to

$$(C_1)\qquad \bar{r} < s_r^2$$

which is exactly the condition for the applicability of the method of moments to the estimation of the parameters of a negative binomial distribution. In the next section we will show that the condition (C_1) is also necessary for Maximum Likelihood estimability in the case of the negative binomial distribution.

If, on the other hand, $r_i = r$ for all $i = 1, \ldots, n$, then the condition (C) is reduced to

$$(C_2) \qquad \bar{T} < \sqrt{r}\, s_T$$

which is exactly the condition for the applicability of the method of mements to the estimation of the parameters of the *inverted beta distribution* (1.3.2). Of course, if the method of moments is applied to this situation, the value of $\hat{\lambda}$ will always be greater than 2, because this distribution does not have a second moment if $\lambda \leq 2$.

Another remark about the condition (C) is in order. Since the values ot T_i are usually large, both sides of the inequality become rather large. It is, therefore, convenient to write condition (C) in the following equivalent form

$$(3.3.1) \qquad \bar{r} < \frac{1}{n} \sum_{i=1}^{n} \left(r_i - \frac{\bar{r}}{\bar{T}} T_i\right)^2$$

3.4 *We now prove the following*

THEOREM 3.4.1 The Maximum Likelihood estimators of the parameters of the negative binomial distribution (1.2.3) exist if and only if $\bar{r} < s_r^2$.

The sufficient part of this theorem is contained in the Theorem 3.2.1. For the necessity part we need the following lemma

LEMMA 3.4.2 For all positive integers n and all positive λ we have

$$(3.4.1) \qquad \sum_{j=1}^{n} \frac{1}{(\lambda+j-1)^2} \geq \frac{n}{\lambda(\lambda+n-1)} .$$

The inequality is strict if $n > 1$.

The proof of the lemma is inductive. The inequality is obviously true for n = 1. Assuming it true for n, we shall prove it for n + 1. Indeed

$$\sum_{j=1}^{n+1} \frac{1}{(\lambda+j-1)^2} = \sum_{j=1}^{n} \frac{1}{(\lambda+j-1)^2} + \frac{1}{(\lambda+n)^2} \geq \frac{n}{\lambda(\lambda+n-1)} + \frac{1}{(\lambda+n)^2} =$$

$$= \frac{n+1}{\lambda(\lambda+n)} + \frac{n}{\lambda(\lambda+n-1)(\lambda+n)^2} > \frac{n+1}{\lambda(\lambda+n)} .$$

This completes the proof of the lemma.

PROOF OF THE THEOREM: We need only prove the necessity of the condition. Since $T_i = T$ for all $i = 1, \ldots, n$, the equations (2.1.5) and (2.1.6) are reduced to

(3.4.2) $$\sum_{i=1}^{n} \left(\frac{1}{\lambda} + \cdots + \frac{1}{\lambda + r_i - 1} \right) - n \ln \left(1 + \frac{T}{\gamma} \right) = 0$$

(3.4.3) $$T/\gamma = \bar{r}/\lambda \ .$$

Obviously, it is enough to prove that the function ψ defined by

$$\psi(\lambda) = \sum_{i=1}^{n} \left(\frac{1}{\lambda} + \cdots + \frac{1}{\lambda + r_i - 1} \right) - n \ln \left(1 + \frac{\bar{r}}{\lambda} \right), \quad \lambda > 0$$

has no zeros if $\bar{r} \geq s_r^2$. If all r_i are zero, then the function ψ is identically zero, the log-likelihood function (2.1.3) is reduced to

$$n \lambda \ln \frac{\gamma}{T + \gamma}$$

and it is obvious that this function has no maximum in the range of the parameters. Thus we may assume that at least one r_i is different than zero. Then

$$\lim_{\lambda \to 0+} \psi(\lambda) = +\infty \qquad \text{and} \qquad \lim_{\lambda \to +\infty} \psi(\lambda) = 0 .$$

Hence, in order to show that the function ψ has no zeros, it suffices to show that its derivative is nonpositive. By using the inequality (3.4.1) we get

(3.4.4) $$\begin{aligned} \psi'(\lambda) &= - \sum_{i=1}^{n} \left(\frac{1}{\lambda^2} + \cdots + \frac{1}{(\lambda + r_i - 1)^2} \right) + \frac{n\bar{r}}{\lambda(\lambda + \bar{r})} \\ &\leq - \sum_{i=1}^{n} \frac{r_i}{\lambda(\lambda + r_i - 1)} + \frac{n\bar{r}}{\lambda(\lambda + \bar{r})} . \end{aligned}$$

We now use the convexity of the function

$$\omega(x) = 1/(\lambda - 1 + x) , \qquad x \geq 1 \ ; \ \lambda > 0$$

with the r_i's in the numerator of the summand of the right hand side of the

inequality (3.4.4) used as weights and the r_i's in the demoninator as points in the domain of w. The so-called Jensen's inequality yields

$$\sum_{i=1}^{n} \frac{r_i}{\lambda + r_i - 1} \geq \frac{\Sigma r_i}{\lambda - 1 + \Sigma r_i^2 / \Sigma r_i} = \frac{n \bar{r}^2}{\lambda \bar{r} + s_r^2 + \bar{r}^2 - \bar{r}} .$$

Therefore, going back to (3.4.4), we get

$$\psi'(\lambda) \leq -\frac{1}{\lambda} \frac{n \bar{r}^2}{\lambda \bar{r} + s_r^2 + \bar{r}^2 - \bar{r}} + \frac{n \bar{r}}{\lambda(\lambda + \bar{r})}$$

$$= -\frac{n \bar{r}(\bar{r} - s_r^2)}{\lambda(\lambda + \bar{r})(\lambda \bar{r} + s_r^2 + \bar{r}^2 - \bar{r})} \leq 0 , \qquad \lambda > 0$$

since

$$\bar{r} \geq s_r^2 \quad , \quad s_r^2 + \bar{r}^2 - \bar{r} = \frac{2}{n} \sum_{j=1} (j-1) \alpha_j \geq 0 .$$

This completes the proof of the theorem.

4. CONTROLLING FOR ESTIMABILITY

4.1 If we let $n = 2m$, $T_i = T$ for $i = 1, \ldots, m$ and $T_i = kT$ for $i = m + 1, \ldots, 2m$, $k > 1$, then

(4.1.1) $$\bar{T} = \frac{k+1}{2} T, \quad s_T^2 = \left(\frac{k-1}{2}\right)^2 T^2, \quad \operatorname{cov}(r, T) = \frac{k-1}{2} T \left[\frac{1}{m} \sum_{i=m}^{2m} r_i - \bar{r}\right].$$

By substituting (4.1.1) into (C) we obtain

(4.1.2) $$\frac{2}{m} \bar{r} \sum_{i=m}^{2m} r_i < \frac{k+1}{k-1} (s_r^2 - \bar{r}) + \frac{3k+1}{k+1} \bar{r}^2,$$

a condition independent of T. This kind of test designing enhances the possibility of having $S_r^2 > \bar{r}$ and the condition (C) satisfied. In particular, if $k = 2$, the condition (4.1.2) is reduced to

(4.1.3) $$\frac{2}{m} \bar{r} \sum_{i=m}^{2m} r_i < 3(s_r^2 - \bar{r}) + \frac{7}{2} \bar{r}^2.$$

4.2 In the more expensive case of controlling the number of failures and letting the test time be random, we can always assure $\bar{r} < s_r^2$. We consider the the following design: $n = 2m$, $r_i = r$ for $i = 1, \ldots, m$ and $r_i = kr$ for $i = m + 1, \ldots, 2m$, $k > 1$. Then

(4.2.1) $$\bar{r} = \frac{k+1}{2} r, \quad s_r^2 = \left(\frac{k-1}{2}\right)^2 r^2, \quad \operatorname{cov}(r, T) = \frac{k-1}{2} r \left[\frac{1}{m} \sum_{i=m}^{2m} T_i - \bar{T}\right],$$

and the condition (C) is reduced to

(4.2.2) $$\frac{2}{m} \bar{T} \sum_{i=m}^{2m} T_i < \bar{T}^2 \left[\frac{k-1}{k+1} r + 2 \frac{k-2}{k-1}\right] + \frac{k-1}{k+1} S_T^2.$$

By choosing $k = 2$ and $r = 12$, or $k = 3$ and $r = 7$, or $k = 4$ and $r = 5$, or $k = 5$ and $r = 4$, <u>this condition is always satisfied</u>. Of course, one does not have to go to such extremes. For $k = 2$ and $r = 6$ for example, the condition will usually be satisfied.

5. VARIABILITY OF THE ESTIMATORS

5.1 The variance-covaniance matrix of the Genralized Maximum Likelihood estimators $\hat{\lambda}$ and $\hat{\gamma}$ is given by

(5.1.1)
$$\begin{pmatrix} \operatorname{var}(\hat{\lambda}) & \operatorname{cov}(\hat{\lambda},\hat{\gamma}) \\ \operatorname{cov}(\hat{\lambda},\hat{\gamma}) & \operatorname{var}(\hat{\gamma}) \end{pmatrix} = - \begin{pmatrix} E\frac{\partial^2}{\partial\lambda^2}\ln L & E\frac{\partial^2}{\partial\lambda\partial\gamma}\ln L \\ E\frac{\partial^2}{\partial\lambda\partial\gamma}\ln L & E\frac{\partial^2}{\partial\gamma^2}\ln L \end{pmatrix}^{-1}.$$

From (2.1.5) and (2.1.6) we obtain

(5.1.2)
$$\frac{\partial^2}{\partial\lambda^2}\ln L = -\sum_{i=1}^{n}\left(\frac{1}{\lambda^2}+\cdots+\frac{1}{(\lambda+r_i-1)^2}\right) = -\sum_{j\geq 1}\frac{\alpha_j}{(\lambda+j-1)^2}$$

(5.1.3)
$$\frac{\partial^2}{\partial\lambda\partial\gamma}\ln L = \frac{1}{\gamma}\sum_{i=1}^{n}\frac{T_i}{T_i+\gamma}$$

(5.1.4)
$$\frac{\partial^2}{\partial\gamma^2}\ln L = -\frac{\lambda}{\gamma^2}\sum_{i=1}^{n}\frac{T_i(2\gamma+T_i)}{(T_i+\gamma)^2} + \sum_{i=1}^{n}\frac{r_i}{(T_i+\gamma)^2}.$$

5.2 Assuming the T_i non-random and the r_i random, we obtain

(5.2.1)
$$E\frac{\partial^2}{\partial\lambda^2}\ln L = -\sum_{i=1}^{n}F\left(\frac{T_i}{T_i+\gamma};\lambda\right)$$

where

(5.2.2)
$$F(p;\lambda) = \sum_{j=1}^{\infty}p^j/j^2\binom{\lambda+j-1}{j} \quad ;$$

(5.2.3)
$$E\frac{\partial^2}{\partial\lambda\partial\gamma}\ln L = \frac{1}{\gamma}\sum_{i=1}^{n}\frac{T_i}{T_i+\gamma} \quad ;$$

(5.2.4)
$$E\frac{\partial^2}{\partial\gamma^2}\ln L = -\frac{\lambda}{\gamma^2}\sum_{i=1}^{n}\frac{T_i}{T_i+\gamma}.$$

By substituting (5.2.1), (5.2.3) and (5.2.4) in (5.1.1) we get

(5.2.5)
$$\operatorname{var}(\hat{\lambda}) = \lambda/\left[\lambda\sum_{i=1}^{n}F\left(\frac{T_i}{T_i+\gamma};\lambda\right) - \sum_{i=1}^{n}\frac{T_i}{T_i+\gamma}\right] ;$$

(5.2.6) $$\mathrm{var}(\hat{\gamma}) = \gamma^2 \sum_{i=1}^{n} F\left(\frac{T_i}{T_i+\gamma};\lambda\right) \Big/ \sum_{i=1}^{n} \frac{T_i}{T_i+\gamma}\cdot\left[\lambda \sum_{i=1}^{n} F\left(\frac{T_i}{T_i+\gamma};\lambda\right) - \sum_{i=1}^{n}\frac{T_i}{T_i+\gamma}\right];$$

(5.2.7) $$\mathrm{cov}(\hat{\lambda},\hat{\gamma}) = \gamma \Big/ \left[\lambda \sum_{i=1}^{n} F\left(\frac{T_i}{T_i+\gamma};\lambda\right) - \sum_{i=1}^{n}\frac{T_i}{T_i+\gamma}\right].$$

5.3 By assuming T_i random and r_i non-random, we obtain

(5.3.1) $$E\frac{\partial^2}{\partial\lambda^2}\ln L = -\sum_{j\geq 1}\frac{\alpha_j}{(\lambda+j-1)^2} \quad ;$$

(5.3.2) $$E\frac{\partial^2}{\partial\lambda\partial\gamma}\ln L = \frac{1}{\gamma}\sum_{i=1}^{n}\frac{r_i}{\lambda+r_i} \quad ;$$

(5.3.3) $$E\frac{\partial^2}{\partial\gamma^2}\ln L = -\frac{\lambda}{\gamma^2}\sum_{i=1}^{n}\frac{r_i}{\lambda+r_i+1} \quad .$$

Substituting into (5.1.1), we get

(5.3.4) $$\mathrm{var}(\hat{\lambda}) = \lambda\sum_{i=1}^{n}\frac{r_i}{\lambda+r_i+1}\Big/\Delta \quad ;$$

(5.3.5) $$\mathrm{var}(\hat{\gamma}) = \gamma^2\sum_{j\geq 1}\frac{\alpha_j}{(\lambda+j-1)^2}\Big/\Delta \quad ;$$

(5.3.6) $$\mathrm{cov}(\hat{\lambda},\hat{\gamma}) = \gamma\sum_{i=1}^{n}\frac{r_i}{\lambda+r_i}\Big/\Delta \quad ,$$

where

(5.3.7) $$\Delta = \lambda\sum_{j\geq 1}\frac{\alpha_j}{(\lambda+j-1)^2}\sum_{i=1}^{n}\frac{r_i}{\lambda+r_i+1} - \left(\sum_{i=1}^{n}\frac{r_i}{\lambda+r_i}\right)^2.$$

The case of mixed controls can be handled similarly. In order to estimate these variances and covariances, we substitute in the above formulas the estimated values $\hat{\lambda}$ and $\hat{\gamma}$ instead of λ and γ.

6. NUMERICAL CONSIDERATIONS

6.1 In writing up a computer program for the numerical solution of the Generalized Maximum Likelihood Equations (2.1.7) and (2.1.8) the following observations should be taken into account. The solution of these equations is reduced to finding the zero of the function W defined by (3.2.1). The shape of this function is given by figure 1.

If the Newton-Raphson iterative method is employed, care should be exercised in choosing the initial value. If the initial value is greater than the minimum m of the function W, the Newton-Raphson process will diverge to infinity (initial value γ_1, in Figure 1), whereas, if the initial value is less than m but near m, the first iteration will produce a negative value for γ (initial value γ_0 in Figure 1). Therefore, an initial value, at which W is positive, should be chosen, if the Newton-Raphson method is to be used. Because of the complexity of the derivative of W and since only nearest integer accuracy is required for γ, some slower converging interpolative method may be more suitable.

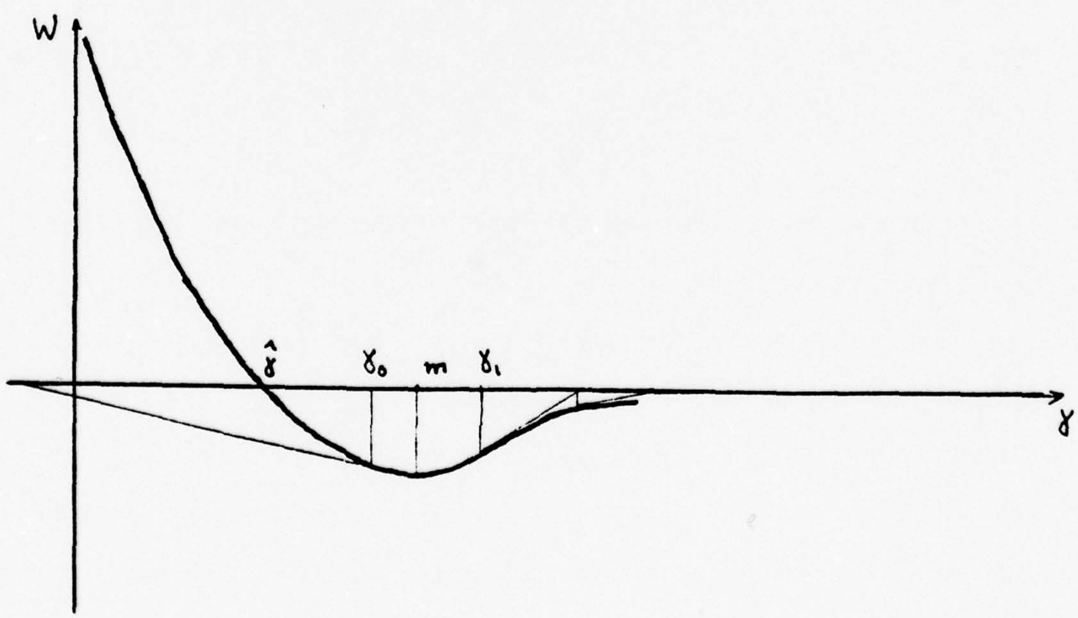

FIGURE 1

7. ALTERNATE ESTIMATORS (NEGATIVE BINOMIAL)

7.1 In the case of fixed time testing (i.e. $T_i = T$ for all $i = 1, \ldots, n$), we saw that the distribution of the number of failures is the negative binomial given by (1.2.3) and that the Maximum Likelihood estimators exist if and only if

(7.1.1) $$\bar{r} < s_r^2$$

by the theorem 3.4.1. Since the solution of the Likelihood Equations require numerical techniques, several alternate methods are often used. Among them, the method of moments is the most popular. It yields

(7.1.2) $$\hat{\lambda} = \bar{r}^2/(s_r^2 - \bar{r}) \quad , \quad \hat{\gamma} = \bar{r}\,T/(s_r^2 - \bar{r})$$

and it is highly efficient in a wide range of the parameters. Of course, this method is usable if and only if (7.1.1) is satisfied.

Other simple methods are:

(A) Matching first moments and first frequencies (the zero class of the sample with the expected number in the zero class). The resulting equations are

(7.1.3) $$\lambda T = \bar{r}\gamma \quad , \quad \frac{n_0}{n} = \left(\lambda/(\bar{r}+\lambda)\right)^{\lambda},$$

where n_0 is the zero class of the sample. It is not hard to prove that this method is usable if and only if

(7.1.4) $$\bar{r} > \ln(n/n_0).$$

(B) Matching first moments and the ratio of the first two frequencies. The resulting estimators are

(7.1.5) $$\hat{\lambda} = n_0\bar{r}/(n_1\bar{r} - n_0) \quad , \quad \hat{\gamma} = n_0 T/(n_1\bar{r} - n_0).$$

Obviously this method is usable if and only if

(7.1.6) $$\bar{r} > n_0/n_1 .$$

The efficiency of these two methods has been investigated by Katti and Gurland [5]. They found that there are ranges of the parameters, where these methods are superior to the method of moments.

7.2 Another estimation investigated by Katti and Gurland [5] is the minimum chi-squared method. It is a highly efficient and rather complicated method for which numerical techniques are required. We did not attempt to find necessary or sufficient conditions for the applicability of this method.

8. CONCLUSIONS AND RECOMMENDATIONS

In this report we presented a method for estimating the shape and scale parameters of an inverted gamma prior distribution of the mean-time-to-failure for equipment having exponential time-to-failure distribution. All sorts of existing failure data on the equipment in question are usable provided a certain sufficient condition is satisfied. Further, the method can be used to update the prior when new failure data become available. This periodic updating will give rise to a solid prior which can confidently be used in Reliability Demonstration.

It is recommended that a computer program be written to solve the Generalized Likelihood Equations that define these estimators and to compute their variance-covariance matrix. To this end, the recommendations put forward in Section 6 should be taken into account. The program can then be used for the periodic updating of the prior distribution.

REFERENCES

[1] A. L. Goel, "Design of Reliability Test Plans Based Upon Prior Distribution", Technical Report No. 78-12, Department of Industrial Engineering and Operations Research, Syracuse University, 1978

[2] A. L. Goel and A. M. Joglekar, "Reliability Acceptance Sampling Plans Based Upon Prior Distribution; Implications and Determination of the Prior Distribution", RADC-TR-76-294, Vol III (of five), 1976

[3] R. E. Schafer et al., "Bayesian Reliability Demonstration: Phase I - Data for the Prior Distribution", RADC-TR-69-389, 1969

[4] R. E. Schafer et al., "Bayesian Reliability Demonstration: Phase III - Development of Test Plans", RADC-TR-73-139, 1973

[5] S. K. Katti and John Gurland, "Efficiency of Certain Methods of Estimation for the Negative Binomial and the Neyman Type A Distributions", Biometrika, Vol. 49, 215-226, 1962

1978 USAF-ASEE SUMMER FACULTY RESEARCH PROGRAM

sponsored by

THE AIR FORCE OFFICE OF SCIENTIFIC RESEARCH

conducted by

AUBURN UNIVERSITY AND OHIO STATE UNIVERSITY

PARTICIPANT'S FINAL REPORT

DIGITAL IMAGE PROCESSING:
DESIGN CONSIDERATIONS FOR FUTURE SYSTEMS

Prepared by:	Robert W. McLaren, PH.D
Academic Rank:	Professor
Department and University:	Department of Electrical Engineering University of Missouri-Columbia
Assignment:	
(Air Force Base) (Laboratory) (Division) (Branch)	Griffiss AFB RADC Intelligence & Reconnaissance IRRE
USAF Research Colleague:	Ellsworth Hicks
Date:	August 18, 1978
Contract No:	F44620-75-C-0031

DIGITAL IMAGE PROCESSING:

DESIGN CONSIDERATIONS FOR FUTURE SYSTEMS

by

R. W. McLaren

ABSTRACT

The automated processing of imagery by computer is a significant factor in the development of an advanced computer image exploitation facility. The increasing capability of digital computers had led to the implementation of nearly all image processing functions by digital computer.

Advanced image processing techniques could be designed, developed, tested and evaluated on a Digital Image Processing (DIP) facility. The functional characteristics of a DIP facility have been partitioned into the following overlapping areas: 1) hardware and software, 2) data representation/input, 3) preprocessing, 4) information extraction, 5) information manipulation/feature generation, 6) decision processes, 7) user interaction/display, and 8) extended capability. In a highly interactive mode with the DIP facility, a human operator would be capable of applying a wide range of two-dimensional signal processing techniques and algorithms to an input digital image and giving a variety of output responses such as a modified image or an identification of specified areas in the image.

The objectives of this report are: 1) to present and discuss techniques and algorithms that should be included in a complete and flexible DIP facility, 2) to identify problem areas requiring further investigation, and 3) to recommend areas in which further work and investigation will potentially lead to the development of techniques that would extend the capabilities of current systems. The following problems or areas are proposed for further exploration: 1) special image processing hardware and software, 2) storage of high resolution digital images, 3) image data compression, 4) more operator interaction at the image preprocessing level, 5) extend capability of existing image processing procedures, 6) extend use of image context, 7) develop more effective texture measures, 8) evaluate syntactical image information processing, 9)incorporate sequential decision schemes, 10) increase operator interaction, 11) increase capability of display unit, and 12) extend capability of DIP facility to a predictive mode.

ACKNOWLEDGMENTS

The author wishes to express his gratitute to the Air Force Office of Scientific Research for the opportunity to participate in the 1978 USAF-ASEE Summer Faculty Research Program. He also expresses appreciation for the efficient administration of the program by the ASEE and Auburn University and in particular, Mr. J. Fred O'Brien. Their efforts have made the summer program more productive.

The author has been working the IRRE Branch at RADC. It has been a pleasure working with individuals at RADC. In particular, it has been a very rewarding experience working with Ellsworth Hicks and Don Bush in the IRRE Branch, both from a professional point of view and on a personal level.

LIST OF FIGURES

LIST OF TABLES

I. INTRODUCTION AND OBJECTIVES

Visual or image information represents probably the most important source or sensor of information for human beings. It allows man to evaluate on-going scenes and processes and render decisions crucial to short term and long-term planning as well as survival. A central goal here is to "identify" objects, situations and outcomes. Mechanisms which can preserve or store a record of visual or image information greatly enhances the value of visual information. The importance of visual information is underscored by its level of development in the brain (visual cortex) and associated activity as indicated for example, by EEG scans. Its role in learning behavior is very significant. The automated processing of image data is thus a crucial factor or adjunct in long-term planning and survival. The development and continuing improvement of digital computers has readily led to automated image processing by digital computer. This will be the central topic of this report. The availability of digital (computer) image processing hardware and software have yielded a great number of applications in a variety of fields, as for example, in medical diagnosis (for x-rays or computed tomography), aerial surveillance (agriculture, forestry, land-use planning, hydology) such as LANDSAT, military (navigation, target evaluation, mapping etc) and the like. It is noted that these applications represent different forms of images depending on the type of sensor used and whether, for example, it is active or passive. Examples are: passive "cameras" (monocular or stereo), x-ray sources (active), heat sensitive FLIR imagery or thermography (passive), and RADAR (active). Sensors are distinguished by various factors such as frequency response range from acoustical scanning (ultrasonic) to x-rays (in radiology), resolution, sensitivity, form of the output, and the like. Digital image processing hardware and software is being developed and used by the government, industry, and universities. A significant government application is found in the military, surveillance and defense mapping, for example. In industry, image processing is used for inspection and teleoperator systems, while universities use digital image processing for teaching and research. Another significant application not directly included in the above three categories is medical imagery for enhancement and diagnosis.

In image processing, the terminology is often confusing; image analysis and image processing are sometimes used interchangeably. Here, the phrase, digital image processing will refer to any process or procedure which is applied by a digital computer to an image in digital form (sampled and quantized), regardless of the source. These processes include the following: preprocessing, information extraction, and image decision making. Cost factors are not considered here. Such a basic system is illustrated in Fig. 1 below.

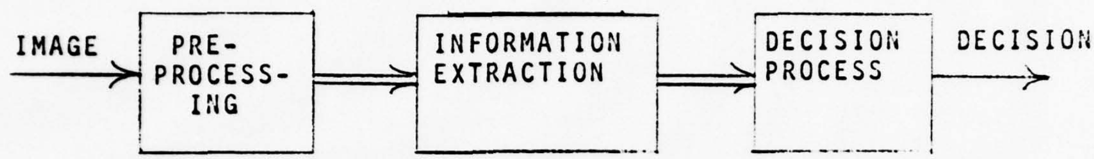

Fig. 1 Basic Image Processing System Configuration.

However, in an overall automated image processing system, there are additional factors crucial to its efficiency and usefulness. These factors include image storage and retrieval, image representation and display, image information manipulation, user interaction, and image generation. Figure 2 attempts to illustrate these additional factors. The particular configuration of such a system, including hardware, software, displays, information extraction, and the decision scheme or process used are application dependent. The algorithms or procedures which are applied to implement various image processing techniques depend on the application or objectives of the image processing system user.

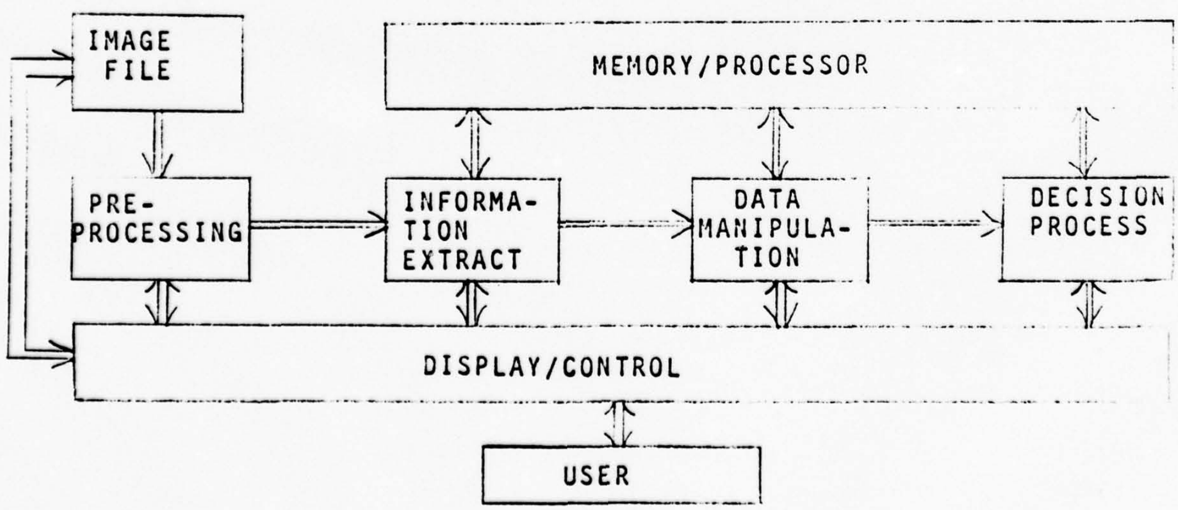

Fig 2. Illustration of a More Complete Image Processing System

The main thrust of this report is to present and discuss the techniques and processes relevant to digital image processing in terms of the aspects or processes as indicated in the previous paragraph, with emphasis on the perceived needs of RADC. The goals or objectives in this investigation have been: 1) present and discuss techniques and algorithms that should be included in a complete and flexible digital image processing system, 2) identifying problem areas requiring further investigation before effective implementation, and 3)make recommendations regarding techniques requiring further work or development to render them more effective in digital image processing, techniques requiring investigation as to their potential usefulness in this application, and new techniques or extensions to increase system capability. The overall objective is to increase the capability of image processing systems over that of current or near current systems; this would apply to the short term and in the long term. Short-term improvement refers to ideas, concepts or techniques which could be incorporated into existing or near existing digital image processing systems, while long term refers to systems based on: (1) using relatively well-developed techniques, (2) potential use of techniques requiring more work, and (3) considering concepts relevant to additional or extended capability to meet future requirements for such systems. Potential capabilities of (far) future systems can be based on extending the capabilities of current systems. These considerations of techniques, configurations, and processes will emphasize efficient user/machine interaction, automation of techniques, and their application on a developmental or demonstration digital image processing system to implement design, development, testing, and evaluation of image processing methods. Space and time limitations prohibit a discussion of all aspects of digital image processing. The purpose here is not to duplicate well-known methods or techniques but to consider various techniques and system configurations that could potentially improve the capability of digital image processing systems.

II. AN OVERVIEW OF THE MAJOR ASPECTS OF DIGITAL IMAGE PROCESSING SYSTEMS.

In consideration of various aspects or characteristics of digital image processing systems, one should try to retain in mind, the major objectives of such a system as a tool to: (1) relieve humans of repetitive tasks, (2) supplement human vision, (3) increase throughput, (4) aid in decision-making based on visual information, and the like. This section discusses eight major aspects or functions of a digital image processing system:

(1) hardware and software, (2) data representation/input, (3) preprocessing, (4) information extraction, (5) information manipulation/feature generation, (6) decision process, (7) user interaction/display, (8) extended capability. These aspects although distinct, are strongly interrelated in that a choice or constraint in one aspect strongly affects the selection of options in others. As an overview, a digital image processing (DIP) system can be described by hardware and software, whose designs are strongly interrelated. Hardware includes the main or host computer (cpu), memory, input/output devices, interfacing, image display units, additional user terminals, hardcopy output of results, and possibly image transmission equipment. Software considerations include form of image files, control of data transfers, general suitability for digital image processing, support of I/O functions, especially the image display unit, support of graphics, and ease of use for a non-expert programmer. Together, they should support design, development and evaluation of new software techniques (subroutines), flexibility in use, sufficient throughput, sufficient speed, precision, low error rate, and special software. Hardware/ software trade-offs must be carefully weighed in order to support these functions.

The next aspect is image (data) representation/input or source. This aspect includes how image data should be stored/ retrieved for later use and reference; this, of course, influences the memory requirements, image compression techniques for image storage/transmission, image coding, the form of the image data input, consideration of some form of optical data processing or representation, and the like.

One area or aspect of a DIP system which has received a great deal of attention is that of image preprocessing. This area considers techniques for improving the display of an image to a human observer, e.g., enhancement, which includes the use of transforms for filtering, restoration of images and image segmentation that precede further processing. Preprocessing can also include image normalization such as histogram modification, geometric corrections, control of scale and resolution, and image combining, such as subtraction or correlation, as well as techniques for noise surpression and data clustering.

Any decision process relevant to identifying objects, scenes, and the like, to be "logical" should be based on as much information as can be extracted from an image; thus the significance of the information to be extracted from an image A summary or set of measurements representing this information is called a feature set. The information extracted from an image would be used for the following: (1) eventual decision making, (2) generating a compressed image for later use, (3) providing information for direct viewing by the user (such as "manuscript" generation), and (4) providing cueing information. The basic elements of image information are the pixels: location and quantized gray-level, and color, if relevent (or spectral bands). Vectored data would be more meaningful for multi-spectral imagery for the same scene. Beyond this is the "putting together" or grouping of pixel data into structures, objects, and the like. This information includes gray-level information, contours, curves, and arcs, object edges, texture, and entropy. This information can be man or machine extracted. The purpose or intended use of information whether for decision-making or image representation (description) must be considered. If the information extracted from the image is for image description, especially for a user display, cueing, or the like, some thoroughmust be given to the relationship of the information extracted and how the human visual system can be helpful (with its capabilities) in developing future intelligent DIP systems.

Next, we consider information extracted for decision-making concerning the image-identifying objects, regions or situations. To accomplish this, the information extracted must be converted to a form useable by various decision schemes-features in the more commonly understood sense, or a vector of measurements. A feature or set of features is, in a sense, a summary of an image pattern;the emphasis here is in trying to generate features that are good for decision-making (discrimination), i.e., separating clusters or defined classes, ultimately for minimizing the number of classification errors or error rate (or weighted error, depending on the type of error). Features can be described in different ways; statistical (say, for clusters), structural, by membership functions (fuzzy sets), and context-sensitive. Feature selection is mainly based on effectiveness in recognition or classification, but computation time is also important. Feature selection is dependent on how the image classes are defined (detection is considered as a special problem). Feature selection for acceptable performance and rapid processing can be attacked indirectly by feature data analysis and reduction; feature analysis includes re-clustering, generating features for multi-imagery, and distribution of data in feature space, while the time constraints can be attacked by data reduction, method of principal components, and the like. Another factor is how such features can be used to define context information.

After features or feature vectors are generated for discrimination purposes, the system now applies a decision scheme to obtain a decision output. Factors here include fixed or sequential operation, form of the decision rule, required information to make it operate, purpose or final use of the decision, the structure of the decision mechanism, and the role of the user in the decision process.

A significant factor or part of the overall DIP system is the interaction of man and machine, especially in directly dealing with the image itself. The key element here is the display unit; potential characteristics here include the following: how "intelligent", hardware and software support, color and stereo capability, real-time function capability, graphics capability, and needs of the user/investigator. Problems related to this deal with how the user interacts with the display with respect to: (1) graphics and/or direct image management and (2) system control for image data transfers, call-up of programs and functions, and the like. Also, it is significant as to the extent that a user cannot only do image processing with a library of routines but use the machine to design, develop, and evaluate new software as to performance, and then have it in a "useful" form as a result. Also, the transportability of software could be considered.

The last of the eight aspects concerns extending the capability of most present DIP systems. One extension is the implementation of an active role for the DIP system instead of just a passive one. This means that the system would not just recognize patterns but could generate an action in the visual field, and then predict the result, again in the visual field. This extension could be expanded into a system that would project possible scenarios. Another extension is to expand the basic change-detection capability of the current systems. Another possibility is to attempt to incorporate some of the useful and powerful functions of the human visual system in this DIP system.

III. HARDWARE AND SOFTWARE

In general, the combination of hardware and software actually describe the complete digital image processing system. The design of hardware and software are intimately related and are difficult to separate. Hardware/software system design involves a number of trade-offs in regard to many factors. These factors include speed, precision, reliability, flexibility for expansion, modes of operation, ease of use, and interactive capabilities. The weights

and/or constraints imposed on these factors is strongly application dependent. The application of interest here is digital image processing, images being represented by an array of pixels, whose gray levels have been quantized. One constraint or guideline imposed on the system's operation was previously indicated - the system is to serve in a stand - alone mode for design, development, testing and evaluation of digital image processing algorithms and techniques. General digital image processing system requirements include consideration of the following: information handling capabilities, machine instruction (set), memory levels, size, and bandwidth, and processor functions required to implement "standard" DIP system capabilities. Various requirements exist for representing image information content; for example, a single frame of LANDAT imagery contains 30.10^6 bytes of information. This greatly increases memory size requirements over existing capacity (in general). For the storage of say, 1,000 such images, one needs some 3.10^{11} bits of storage. Such requirements need special attention. Memories can be arranged in a "hierarchical" or functional manner. To handle the I/O transfer of image data, a buffer memory of approximately 10^8 bytes, a temporary working space memory of 100 times this capacity (with DMA capability) with a bandwidth of 64 megabytes or more would be required. Additional, smaller memories, primarily associated with storing instructions (programs) would also be required, say, in the range of 25k - 512k bytes. In a multi-processor environment, each processor would be associated with a "local" memory unit. Instructions executable on the system must be compatible with digital image data processing, i.e., to implement particular functions and to handle I/O data transfers. In addition, because of the proposed emphasis on man/machine interactive image processing, the display unit (discussed in more detail in a later section) is to be an "intelligent" terminal with processors, memories, and graphic capability.

It is proposed to take advantage of current technology and any proposed system should include a limited capacity to incorporate future technology. This technology now includes the practical use of an array of microprocessor units; the structure of each unit would be based on MOS or bipolar technologies, and depending upon the unit, each would be capable of executing a fixed instruction set or would be micropogrammable (bit-slice architecture). Bipolar processors are generally faster. Micro-programmable units are faster than fixed instruction set units and are more flexible in matching the processor functions to the application; however for the microprogrammable units, required software (or "firmware") development is much more extensive. These processor units also provide the flexibility of an overall array processing architecture

because of bit-slicing. However, a shorter-term approach (less software) consists of using currently available micro-processor units(such as the Z-8000 and 68000) having defined instruction sets. As implied at this point and as is considered in more detail later, a multi-processor array configuration is proposed for implementing digital image processing functions. Because of the downward trend of prices for μ-processors and solid-state memories, this configuration can be considered to be cost effective; cost is not considered to be a major factor in the implementation of the proposed configuration. Because of advanced fabrication techniques and capabilities, one approach to the multi-processor array is a "ground-up" one-design a VLSI device to serve this purpose. Advantage can also be taken of solid-state memories; the main advantages are speed, random-access capability, and decreasing cost. For a 16k x 1 bit RAM unit, maximum access time is about 100ns and 50 ns for the write cycle. For non-volatile memory, solid-state devices (ROM's, PROM's) are available/ with comparable speeds and which can be used for firmware. Other memory devices of current interest include bubble memories and charge-coupled devices (CCD's), which are, at present, slower and less reliable; CCD's do have some advantages in display units. The display unit itself is expected to be a "smart" terminal, with some stand-alone capability.

In order to implement digital image processing techniques and satisfy reasonable goals relevant to throughput, manipulating images,and implementing various sophisticated algorithms in near real-time, along with the system goals, such as time-share, dedicated facility, and the like, it is recommended to utilize advanced computer architecture and organization - parallel processing - (associative) array processing - multi-processing. Computer architecture can be classified based on the properties of the data and instruction streams. This has led to 4 categories of computer architectures. These categories are summarized in Table 1 below.

	SD: SINGLE DATA STREAM	MD: MULTIPLE DATA STREAM
SI: SINGLE INSTRUCTION STREAM	UNIT PROCESSOR	PARALLEL PROCESSOR AND ASSOCIATIVE PROCESSOR
MI: MULTIPLE INSTRUCTION STREAM	PIPELINE PROCESSOR	MULTIPROCESSOR/ MULTICOMPUTER

TABLE 1 - A Classification of Generic Processor Architecture

Using this summary, one can consider the following architectures.

1) SISD - (single instruction stream/single data stream); uniprocessor; example: IBM 360.

2) MISD - (multiple instruction stream/single data stream); pipeline; example: CDC STAR 100.

3) SIMD - (single instruction stream/multiple data stream); parallel processor or array processor; example: ILLIAC IV or STARAN.

4) MIMD - (multiple instruction stream/multiple data stream); multiprocessor; example: Univac 1108.

5) SIMD and MIMD combined.

The architecture for a typical array or parallel processor is shown in Fig 3 below (SIMD).

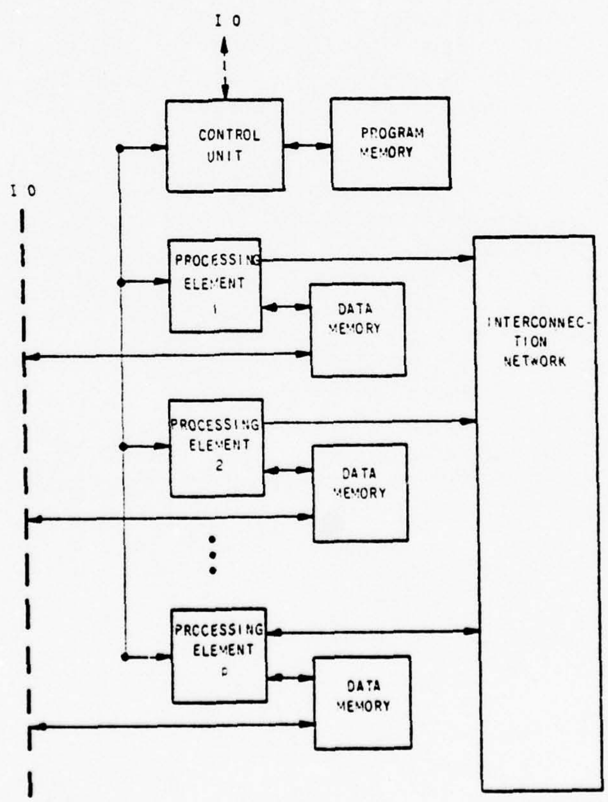

Fig 3 - Block Diagram of a Parallel Processor

Fig 4 shows a typical associative processor configuration (SIMD).

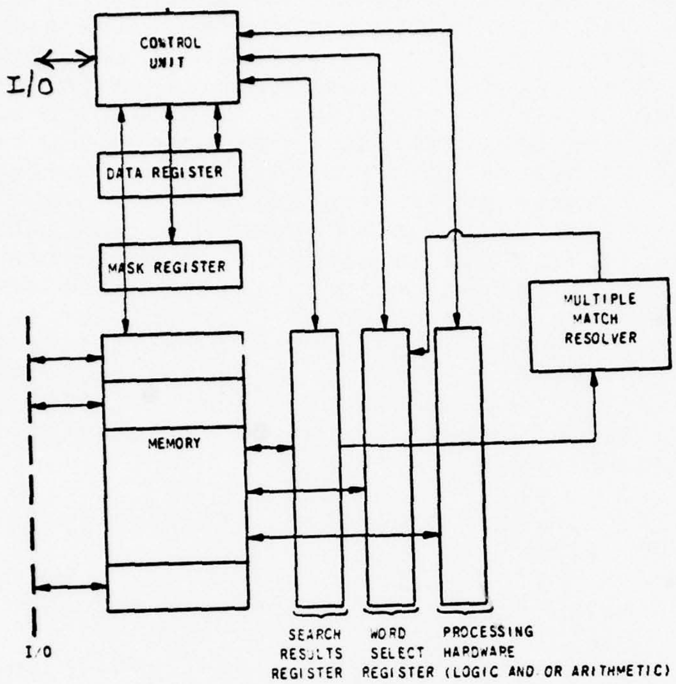

Fig 4 - Block Diagram of Associative Processor

Additional information on these categories and further details on examples for these categories can be found in the literature. Examples of SIMD machines include STARAN, OMEN, PEPE, and ILLIAC IV. These machines may be efficient for operating on fixed-length vectors but not efficient for mixed scalar and vector operations. The ILLIAC IV machine, although a powerful machine, is a "one-of-a-kind" facility which is considered not sufficiently flexible (for a machine using a similar structure) for the tasks of digital image processing. Most instructions on this machine are aimed toward 64 or 32 - bit floating point operations, while image processing often works on integer arrays of 8 or 12 - bit length, a mismatch. It is organized as a linear array rather than two-dimensional; all processors in its array execute the same command. The STARAN computer, an associative array or parallel processor, was not designed as a special purpose computer for digital image processing; however, it has been applied to some digital image processing tasks, but applications in this area have been limited thus far. Other examples of special machines for picture processing which are much faster than conventional machines are the CLIP series, PPM, and PICAP. The CDC Flexible Processor and the TOSPICS are two additional examples of more powerful machines, which are similar in their treatment of image processing tasks. A feature of some of these more powerful machines is having a special type of memory, CAM - content addressable memory.

Special purpose computer architecture for digital image processing can be partitioned into 2 broad classes, bit-plane processing and distributed processing. The bit-plane approach uses Boolean operators as processors on primarily binary images. The distributed computing approach appears to have more computational capability. Most of the existing machines designed for parallel and array processing have the disadvantage of not being "reconfigurable, whereas a variety of digital image processing tasks would greatly benefit from this feature. A multi-processor configuration should be considered; it may be useful to combine the capabilities of both parallelism and pipelining. Four principal areas where system performance can be improved for specific applications are: 1) devices and circuits, 2) system architecture, 3) system organization and 4) system software. Performance characteristics include throughput, flexibility, availability and reliability. The essential characteristics of a multi-processor are as follows:

1) contains two or more processors of approximately comparable capabilities.

2) all processors share access to common memory.

3) all processors share access to input/output channels, control units and devices.

4) entire system is controlled by one operating system providing interaction among processors and their programs at the job, task, step, and data set element levels.

A key to classifying such structures is the interconnection subsystem - its topology and operations. Three organizations of this subsystem are common: 1) time-shared or common bus, 2) cross-bar switch matrix and 3) multi-port memories. A cross-bar configuration must be capable of resolving conflict situations. Essential structure of a multi-processor system consists of a host computer such as a PDP 11/70 or 11/780, multiple-processors, shared memory, local memories, a mass-storage memory, interprocessor connections to link processors, memory, and I/O, and multi-port memories. A basic, but general multi-processor organization is illustrated in Fig 5.

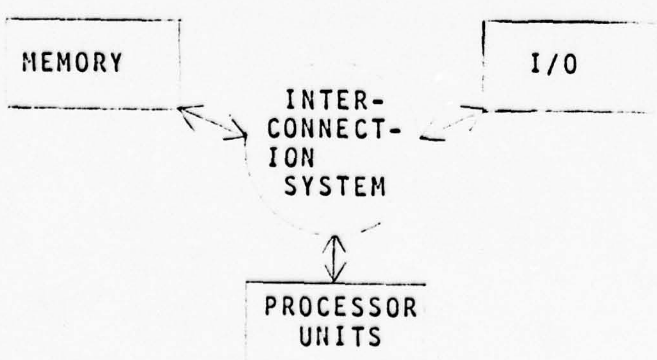

Fig 5. Basic Multiprocessor Organization

The RCA 215 is an example of a cross-bar multiprocessor, while the Univac 1108 is an example of a multi-port memory type multi-processor. The computational tasks relevant to a DIP system to be performed on such a machine can be summarized as follows. As indicated previously, one should take advantage of current technology in regard to the processors and memories. The overall system should include a certain amount of software support such as: an assembler (macro) an interactive source language edit and symbolic debugger, extended overlay linker, a text processing system, and the like. There are many operations, algorithm or techniques which a DIP system should be capable of performing. These can be divided into frequently-used ones, new ones to test and evaluate, and ones requiring more investigation to develop them.

It is suggested that the more frequently-used techniques be implemented through special-purpose hardware (firmware) so as to implement, say, image transforms; such firmware would be accessed through special commands or instructions. In order to be useful as a research/development tool, program development for new techniques or algorithms should be capable of being developed in a higher level language; the major purpose is make things easier for a non-expert programmer to design, develop, test, and evaluate applications software. An example of this is found with higher level extensions of FORTRAN IV, such as SYMBOLANG and TREETRAN. In addition, there is a desire to allow for software transportability; persons from outside the facility could bring-in software to run on the system for test and evaluation, and persons who have developed software on the DIP facility could also transport this software to run on another system. This convenience may require additional software, such as an appropriate cross-compiler. Of special consideration is the capability that the existing, special software and new software developed by users be accessible as sub-routines which can then be linked so that a complete program can be run which sequentially applies various techniques to an input image and outputs a modified image or a decision. The system should have a well-developed I/O handling capability for different terminals, including, perhaps modems for data transmission and for an image scanner. The power and flexibility of such a facility would invite more users; a time-share capability at multi-terminals would be needed, and a foreground/background mode would helpful-image processing in the foreground and program development in the background. A hardcopy unit would be useful for processed images and for alpha-numeric data such as statistics and decisions.

Suggested areas for additional AFES/Manuscript Generation System capability include 1) ability to link algorithms or techniques (software) as subroutines into a executable program, 2) ability to track program status as it is being applied to an input image to generate a processed image or statistics or the like, 3) more terminals operating in a multi-user environment, each with a foreground/background capability, 4) use of the most advanced display unit (such as Vector General 3400 series or ICI display, 5) increased graphics ability (see later section), and increased user interaction in selection of featureas as a part of a sequential decision process, for example.

A significant problem proposed for further study is to develop trade-offs and establish bounds for a digital image processing system assuming a multi-processor computer architecture; trade-offs would be developed in terms of hardware and software capabilities and limitations in implementing the increasing requirements for a DIP system.

IV. DATA PRESENTATION/INPUT

Useful imagery arises from many different sources - LANDSAT, RADAR, aerial, X-ray, FLIR, and the like. Pictorial information contains a great deal of information for possible extraction, processing and interpretation. The first problem is, of course, converting the image to a form that is amenable to digital computer processing. Equipment such as a camera or scan converter can be used for this purpose - yielding an array of pixels; A/D conversion from 8-12 bits can be accomplished in less than 20-30 msec for an entire image of 512 x 512 pixels. One problem is to define the size of the pixel array to "adequately" represent the original image. This would be matched by the memory file size and organization as well as display capabilities and needs. For current needs, 512 x 512 or 1024 x 1024 size images are adequate; a 2048 x 2048 pixel representation would probably be adequate for several years. The problem concerns potential information lost in the sampling process, i.e., spatial information versus sampling rate. For digital processing, a sampled image is represented as an n x n array of pixels. Each pixel, in turn, can be represented by 8-256 gray levels or 3-8 bits. A 4,000 x 4,000 pixel image represents 16.10^6 elements, but this is still only a fraction of the estimated 160 million picture elements in the human eye. Although not directly in the area of digital image data processing, optical data processing as a preprocessing step may be a useful adjunct, since it is a parallel operation.

This could be applied to improve the image signal-to-noise ratio before sampling; this can be important especially if the spatial sampling rate is low compared to noise frequencies, so that noise information would be aliased into the information spectrum and thus it would be more difficult to eliminate after sampling. Other functions of optical data preprocessing include correlation and detection, transformations, and compression. If the original image contains color information, then, of course, more bits will be required for representing the digital image. Color imagery or multi-spectral images could be stored in separate files. In the overall design of a DIP system, some thought must be given to the image chain-transmitters, transducers, signal conditioners, and processors, that is image chain analysis. For convenience of storage and retrieval of images, it is suggested that the main image file be digital, with "original" imagery as a back-up, that is, store all images after sampling and quantizing. Memory requirements (mass storage) might be as follows.

a 4,000 x 4,000 pixel x 8 bits/pixel image, gives almost 128 10^6 bits or roughly 10^8 bits/image. Then, for, say 1,000 images, one is considering about 10" bits, which exceeds the capacity range of most current mass storage facilities, at least, for near real-time access. To satisfy this need, one can consider the use of holographic information storage, a 4" x 6" card holds up to 2.10^8 bits. A LASER archival memory operated by IAC (Institute for Advanced Computation) at a California facility can store up to about one terabit; that facility, however, is a one of a kind. These requiremints for mass storage, auxiliary or temporary memories needed during processing, and for the processing and/or transmission of the images containing this much potential useful information leads to the possible need of image data compression - reduction of data without a significant reduction in "useful" information. There has been a great deal of work done in this area. One useful technique is transform compression, especially the discrete forms for the Kahunen-Loeve (K-L) and Fourier transforms. A major problem with the K-L transform is the computation time when this transform technique is applied to the entire image, that is, to generate the image eigenvectors. Instead, this transform is usually applied to a number of sub-images generated by a partition of the full image. This would provide a degree of optimal image representation and would allow a reduction of 8 bits/pixel to 1.5 - 2 bits/pixel. Further compression is possible through non-uniform quantization. Fourier transform and Hadamard transform compression have the advantage of fast generation and image reconstruction. Transformation is followed by

selected coefficient elimination (retaining only the larger ones), or eliminating only the higher (spatial) frequencies. Another class of compression techniques is represented by predictive compression; this technique is based on the correlation among pixels. This technique has shown acceptable results and further work is indicated. Other methods include image separation (high and low frequency information is separated), rate distortion techniques and adaptive compression, the latter two being worth additional work. The usefulness of compression for storage also carries over to image transmission. Compression techniques are closely related to image data coding techniques. As indicated previously, after digitalization, an image is represented by an array of real numbers (pixels) digitalization is really a sampling process, followed by quantization of the image gray values. Spatially band-limited imagery can be sampled with spacing to satisfy the sampling theorem with courser sampling,aliasing occurs and the reconstructed picture would have reduced resolution (perhaps "false" contours). Another way to sample (or resample) a picture is by orthonormal functions and then use the coefficients of the expansion as image samples. This approach could utilize further work because the processing techniques that would follow the sampling would have to be altered; the Fourier or Hadamord transforms are examples of orthonormal functions. Such a representation can also be effected by optical data processing of an image or resampling a digital image. Another sampling technique involves generating a sample value over each small sub-area of a picture. Quantization can be optimized through non-uniform quantization. For a fixed number of bits to represent an image, quantization and sampling must be traded-off to yield the "best" image for storage. For the representation and display of images (at least), a method which should receive some attention is the conversion, storage, etc of an image in the form of a half-tone transformation.

A central problem here which is in need of further development is image compression.

V. PREPROCESSING

The preprocessing stage of a DIP system is concerned with applying methods which will essentially have an image at the input and a modified "image" at the output. In general, the objectives of preprocessing can be divided into three parts or types: 1) to make the image look better, 2) "correct" or compensate for degradation, and 3) to prepare the image for information extraction. In

many references, type 3) above overlaps with certain types of information extraction. These three functions are commonly referred to as, respecitvely, enhancement, restoration, and segmentation. Methods or techniques which are applied to a digital image during preprocessing in implementing any of these techniques often overlap. All 3 functions utilize the image display unit and thus involve user interaction. The purpose of enhancement is, of course, to make the image look better to a viewer to ease the problem of process parameter tuning or to render subsequent user directed processing more effective. The idea is to improve image quality in some sense. A general approach to this is filtering; this is very general and includes smoothing (averaging), weighted or unweighted, emphasizing certain characteristics, reducing noise, and the like. A major factor in dealing with all 3 of these objectives is image transformation. There is a parallel here with one-dimensional, time-domain transforms (Laplace, Fourier), which are powerful analysis tools. For images, transforms include Fourier (FFT), Walsh, Hadamard, Hare, and the Karhunen-Loève (K-L); just as in one-dimensional digital signal processing, after image transformation, filtering can be applied-low-pass filtering for emphasizing contrast or high-pass filtering to emphasize edges, and the shape of the "window" becomes important. Noise can be treated in this manner also; after filtering, the transformed signal is retransformed back to an image domain for display or processing. Noise can also be reduced by spatial smoothing. Noise characteristics such as spatial dependence or independence makes a significant difference on the methods used. Quantization is unavoidable to an extent. Enhancement can be aided here along with restoration by perhaps resampling and applying adaptive quantization. Another approach to enhancement is gray-level modification which includes the following: 1) correction for non-uniform brightness on original image, 2) scale transformations involving contrast expansion gray-level reassignment, and the like, 3) gray-level conversions such as a log-function, 4) histogram modification and normalization, even over a portion of an image, and 5)color conversion (pseudo-color). A very important result here is very subjective, "sharpening" a blurred, edge, i.e., locating an edge in a blurred area. Due to noise or other unknown parameters, the actual position of the edge may not be known, but the human observer finds that an edge is a very useful reference. Such sharpening can be achieved through various techniques including: 1) applying the Laplacian or gradient techniques, 2) high-frequency emphasis filtering and 3) a log-function. In place of conventional image smoothing, smoothing could be varied spatially over the image, or the "average" over an area could be replaced by the media value over the same area. Other

Other techniques involve the reduction or elimination of special types of noise, breaking-up false contours, and generating binary images. Another enhancement method can treat multi-spectral images through using projections of ratio images. As indicated previously, certain techniques overlap the 3 objectives of preprocessing. One example is the use of interpolation for image enhancement and restoration.

Image restoration involves determining the original "object" distribution, f, given the recorded image g and knowledge about the point spread function, h. Image degradation can be categorized as point degradation, spatial degradation, temporal degradation, chromatic degradation, and combinations of these. Degradation can arise from several sources - the sensor itself, the scanning system, and the like. Here, in general, a knowledge of the degradation mechanism is required. Much restoration can be applied with a knowledge of the point - spread function which generated the input image. This can be estimated through measurements of the response of the input system to points and edges as inputs. With this information, degradations can be compensated for. With sufficient prior information motion effects can be minimized. With certain constraints imposed on the noise characteristics, image information can be "restored" through various filtering techniques, such as inverse filtering, Wiener filtering, constrainted deconvolution, recursive (feedback) filtering, maximum entropy, non-recursive filters based on using the transform domain, and the Bayesian method. In trying to evaluate the scanner, there are four performance factors: 1) signal-to-noise ratio measurements, 2) gray-level distribution, 3) scanner induced artifacts, and 4) the actual scanning operation. Another technique is based on interpolation of information between pixels based on the gray values of near-by pixels, using linear interpolation and the B-spline, for example.

Image segmentation is the process of partitioning the image into named areas or into large features. Segmenting produces an image which is suitable for information extraction by automated processes or by a human observer. One useful segmentation operation consists of using multiple threshold gray values to produce a new image, which can then be interpreted. Another approach is to interpret or describe an image in terms of a language, a syntactic picture language, especially for binary images. Segmentation results can be viewed as shown in Fig 6.

Fig 2. Segmentation of an Image

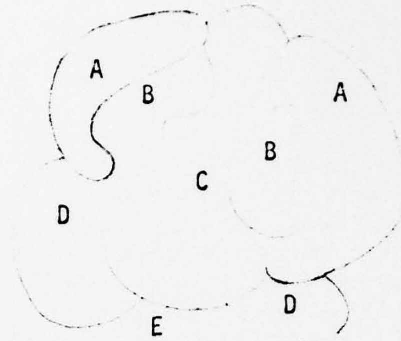

Each segment consists of a boundary, the connected region enclosed by the boundary, and a distinct label. Generating segment boundaries depends strongly on the original "object", the optical system, film, scanner and digitalization process. If segmentation is preceded by filtering or a gray-level transformation, such a preprocess can affect the segmentation and subsequent information extraction and use. Segmentation can be approached from a hierarchical point of view where the first step represents a rough analysis of the entire picture, such as the class of images, general characteristics of gray levels, and the like. Such global - level segmentation can, for example, consist of: 1) split and merge on thresholded gray levels for preliminary categorization of the image and 2) variable-span edge detection for a preliminary determination of the resolution needed for computing other characteristics of segments. Another technique is to detect "landmarks" to guide the process of boundary detection. An example of this is to use spatially dependent templates; templates, of course, can be used not only for segmentation but for pattern recognition. The description or label for a segment overlaps the subject of the next section - information extraction, such as edges, boundaries, curves, arcs, and the like. Effective segmentation can involve hierarchical procedures in which gray-level and spatial resolutions are optimized; this yields a variable resolution analysis allowing a refinement of resolution on portions of the image of greater interest. This can serve as a basis for generating minimum perimeter polygons to represent "blobs". A consideration of resolution has led to a possibility of increasing resolution (a restoration process) under certain conditions (spatially-bounded images and a minimum signal/noise ratio). This so-called super-resolution is based on "analytic continuation" or use of the "prolate spheroidal wave functions." A LASER scanner could achieve the required S/N ratio. An on-line technique for segment generation is region growing, a procedure which is initiated at a display point by a

user and then, as indicated by graphics a region around that point is grown, all pixels in that region having a predetermined variation and perhaps satisfying other constraints. A class of techniques which is involved in both image enhancement and restoration is geometric corrections; these include corrections for shading, barreling, and the like. Another example is the use of a de-warping procedure for correcting for a distorted image based on a coordinate transformation and interpolation. Some geometric correction can sometimes be implemented through combining two or more images. There have been significant past efforts devoted to a particular segmentation technique - clustering. Clustering is a method of grouping pixels together as a "clump" based on inter-spatial distances or other statistical-type properties and separates clusters with dissimilar properties.

Problems or areas which need further investigation include: 1) improved model for image degradation, 2) use of hierarchical preprocessing techniques, 3) image or context dependent methods, 4) develop or modify preprocessing techniques, 5) expand the capability of region-growing techniques, and 6) develop higher degree of user interaction in the segmentation process.

VI. INFORMATION EXTRACTION

This section and the one following both deal with the extraction or generation of features or characteristics of the image. This section considers the general characteristics, still having image connotation or relation - to be placed on a display for viewing or modification, a kind of reduced image. These characteristics can be used for image description or for pattern discrimination. The next section deals more directly with generating features for discrimination or recognition purposes, although there is certainly overlap in the subject areas and techniques discussed. Here, a distinction is made between "basic" characteristics and complete or constructed ones. The basic characteristics or elements include finding edges, curves, arcs, streaks, contours, and the like; associated with these features are their descriptions-straightness, slope, length, end points, convex or concave, etc. Edges, for example, can be found by gradiants, the Laplacian, transforms (Hueckel), image differences, and image matching (correlation). These properties depend upon local area characteristics of the image, rather than on point-to-point differences (depending on the window size). When this information is put together, one has segments or "blobs", which are useful for image description and discrimination later step). Thus, this process overlaps that of segmentation. This "putting together" process involves such procedures as edge

following, completing streaks, and the like. One approach to information extraction for segmentation or generating features is texture-complex visual patterns consisting of repeated entities or subpatterns and having characteristics such as brightness, color, and slope. Texture is a visual concept employed by humans to discriminate between "dissimilar" surfaces and to detect "similar" surfaces. To describe texture for automated digital image processing, there are basically two approaches to describing it: 1) local statistics and 2) a structural description. There has been much effort devoted to the development of useful texture measurements. Texture is as much a similarity measure as one for discrimination; that is, if two areas in an image seem to have the same visual texture, then the measurements that describe it should be the same (cluster), while, two different visual textures should yield two separated measurement vectors. Texture can be used for region growing as a part of a split and merge procedure, and for image edge detection. Texture has appeared to be highly effective on some imagery (e.g., medical images). The structural approach is based on 1) placement rules or a generative grammar and 2) use of Fourier harmonics or transform codes to represent texture. The statistical approach is based on 1) power spectrum (or autocorrelation), 2) gray-level statistics, local feature statistics of gray levels, and 3) local Markov properties. Some descriptions are very complex and require substantial computation time.

A technique of basic information extraction which could lead to segmentation is relaxation labeling, a technique of labeling or assigning a meaning (or object class) to nodes, edges, and boundary sections, and then generating segments based on iterating this method and relabeling. After segmentation, the next step or level is to group segments as to, for example, nearness, direction from one to another, and containment which represent a local context idea. This can also include grouping segments together to form more complex defined objects. Information extracted for pattern recognition purposes can be treated by using a syntactical description. In this approach, areas, or image segments are represented by "sentences" of a language and characterized by a grammar. Examples of picture languages includes webs, arrays, graphs, and trees (line drawings). There has been an increasing interest in the study of the properties and parsing algorithms for higher-dimensional languages. A language that can handle strings in a one-dimensional description may be extended to higher dimensions to treat trees.

This approach has been used for shape recognition. Geometric properties can contribute to an information base for the purpose of building-up "related" segments; these properties include shape, size and distance. Segmentation can assume the form of "skeletons". Picture subsets (segments) can be increased or decreased in size through the operationa of propagation and shrinking, methods which are amerable to parallel computation. Additional information which can be extracted from an image include directionality and slope of lines, "cross-section" information and the results of applying "thinning" operations.

One area proposed for further investigation is texture: 1) relate texture measurements to image scale, resolution and other factors, 2) develop texture measurements to more effectively discriminate "different" textures and cluster "similar" textures, and 3) develop an effective means to apply texture classification to an entire (non-segmented) image. Another area concerns providing a greater interaction between man and machine during the information extraction stage. A third area proposed for investigation would define the required information or measurements and associated limitations for identifying lineal features (roads, creeks, etc). Additional areas concern 1) greater use of global context for extended objectives, 2) dependence of the information extracted on the form and source of the imagery, 3) investigate the extraction of normalized information-information which tends to be insensitive to certain classes of image variations, 4) investigate the increased use of stereo and color imagery, 5) provide for more systematic extraction of information, and 6) explore the potential of utilizing knowledge about the human visual system for digital image processing.

VII. INFORMATION MANIPULATION/FEATURE GENERATION

This section deals with a further step in the image processing sequence leading toward image analysis. The input to this stage is image segments (computer or man extracted), or outputs from preprocessing (even from a transformed image or an equivalent form). The outputs from this stage are features or measurements that are, in a sense, a summary or "average" of image properties in a more abstract form. These features can be used as a summary of imagery for the final user, the particular

features depending on the nature of the classification (i.e., objects, land-use, or the like), the type of imagery, and the needs of the user. Such results would usually include classifications resulting from the decision process, the subject of the next section. The second major use of features is for pattern recognition-to discriminate between objects, area types, line characteristics or any other defined pattern classes. A set of measurements can be represented by a vector, $[X = x_1 \ldots x_n]'$. There have been numerous efforts devoted to pattern recognition, not only as it might apply to image patterns, but to various pattern recognition problems-speech, alpha-numeric characterics and medical diagnosis are examples. Here, the major topic of interest is the generation of "useful" features- features which can be used to effectively discriminate among image pattern classes. It is assumed that a set of meaningful classes or patterns has been defined; examples include soils, land-use, and military targets; this analysis may also include a "reject" class. Features must be defined or chosen not for the representation of defined pattern classes, but rather for the effective discrimination among defined pattern classes whether for the human decision maker or for computer-aided decision making. However, in general, the features used by these two decision makers will not be the same. Whatever form the decision maker or process may assume, the ultimate effectiveness or usefulness of features would be determined by the "hit-rate" (maximize) or "miss" rate (minimize). The problems involved in achieving this are non-trivial. The decision structure and the features selected as inputs to the decision process must be considered together. A significant concern is the form of the features-statistical, structural, transform coefficients, or even local pixel characteristics. In general, mixtures of these feature types are not used, but a hierarchical utilization of different feature types could be considered. The choice of a feature type depends on the type of imagery, the defined pattern classes, and on the final application. Use of features based on structure is represented by a syntactical approach, either using a "grammer" or a template to match the pattern through correlation. This approach is essentially non-numeric (at feature level). The use of statistical methods opens-up a very large set of data manipulation techniques which can be applied. The choice of such techniques depends on the computational speeds, nature of the data, size of the data base and prior knowledge and assumptions concerning the defined pattern classes.

As a source of information, texture can be defined by a structural description or by a set of statistics such as mean, variance, second-order statistics and the like. Data manipulation techniques include the following: generating first- and second-order statistics as well as higher-order statistics, reduction of dimensionality through various means, parameter estimation, clustering, and restructuring. Feature selection and ordering are important here; that is, from a large number of features, which features should be used first and in what order, if used one at a time. This sequential approach to feature selection and utilization is cost sensitive; it is assumed that it costs more in some sense to measure and utilize additional features for the decision process. The cost may be a function of the individual features chosen. In general, it must be assumed that the features are mutually statistically dependent, techniques for dealing with measurements of this type and with the corresponding data base involve multi-variable methods. Such features can be de-correlated but cannot be made statistically independent (in general). Such features contain, in some sense, redundant information but are useful to distinguish classes that are "close". More effective use of features for pattern classification can be obtained by combining the feature selection/ordering process and the decision process. Although the ultimate measure of feature effectiveness is the recognition performance, it is useful to approach the feature selection/ordering in an indirect manner, i.e., by evaluating measures of how well data from different pattern classes is separated and how close data is when it arises from the same pattern class. These measures include mean and variance, divergence, eigenvalues of the Wilkes-Bartlett matrix, and the like. Data representation is also important here; for example, in some situations, features are best represented by using a nomative scale (qualitative data), which cannot be ranked. This type of data requires special techniques for analysis and subsequent decision making such as contingency tables and the like. A common feature to use in imagery is shape; the descriptors used for shape include perimeter length, ' chain coding a boundary, end-points of lines, arcs, nodes, and "blobs". Additional descriptors include slope versus arc length, and the distribution of sizes and shapes of convex hulls. Feature effectiveness is measured by 1) intraclass invariance, 2) interclass sensitivity, 3) amount of storage, 4) cost of feature generation, and 5) reliability/precision. Some classes of features retain a meaning for the human observer in terms of the original image; this is reifereation. An example of this can be found in the use of chord statistics and slope density. On the other hand, syntactic descriptors provide descriptions of spatial relations among objects in an image and descriptors are highly dependent on the nature of the imagery and

hierarchical structure for feature selection and utilization to contribute a greater degree of interaction between human and computer. The basic syntactic descriptors are highly dependent on the nature of the imagery and the corresponding defined pattern classes.

Areas proposed for further investigation include the following: 1) explore feature selection techniques as they apply to syntactic features, 2) explore use of qualitative data for defining feature space, 3) investigate consequences of the multi-variate dependent feature situation, 4) how can the situation in 3) be treated, 5) develop more effective textures, and 6) explore the use of features defined by a human for effective pattern classification.

VIII. THE DECISION PROCESS

In a sense, the decision process represents the last step in the image analysis chain, its input is a set of features while its output is a decision (class). This output can represent a single decision or pattern class or a set of decisions. There is a substantial body of literature on decision processes, pattern recognition, and in particular image pattern recognition or classification. Decisions made on the basis of features extracted from images would (hopefully) lead to interpretations consistent with the original image (source). Decision schemes can be classified in different ways: parametric or non-parametric, fixed or sequential use of features (measurements), fixed structure or self-optimizing and qualitative measurements or quantitative measurements as input. Parametric schemes are based on using known or estimated parameters to determine decision boundaries; such boundaries may be linear or non-linear. A classic example of a parametric decision scheme is Bayes decision rule using given or estimated parameters. Non-parametric techniques do not use these statistics but rather, are based on metric properties of feature space; a well-known example of this is the nearest k-neighbor decision rule. Fixed or sequential use of measurements distinguishes between decision schemes which render a decision only after all features are presented at one time and schemes which utilize features, one at a time to sequentially eliminate unlikely decisions until a final decision is reached. Sequential schemes are much more powerful, efficient and flexible than fixed schemes. In addition, such sequential decision schemes make more efficient use of the information extracted from features and computational resources. Furthermore, a sequential

decision scheme can allow for the direct interaction of the human with the decision process as it is being applied. A classical example of this is the sequential Bayes decision scheme, the SPRT (sequential probability ratio test) and the GSPRT (generalized SPRT). The GSPRT is used to sequentially eliminate pattern classes from consideration while achieving a predetermined error rate when the final decision is made. Various extensions of this method include variable decision (reject) boundaries and the application of dynamic programming to optimize the feature selection/recognition error problem. This will lead to a tree-like decision structure. A more complex decision tree structure could be applied to the image pattern classification problem. This tree consists of several levels; at each level, there is a number of nodes, each representing a set of decisions (proper subsets of the set of all pattern classes). The single node at the highest level contains all pattern classes and is the starting point for the sequential decision scheme. Nodes are connected by directed branches, each branch corresponding to the use of a feature (value); branches are directed downwards in a decision structure. As feature information is received, the decision process moves downward in the tree. This tree structure has the following properties/advantages.

1) the structure allows for the trade-off of the size and composition of the decision set at the terminal node and the recognition error.

2) the human observor can not only observe the current decision set but can, as a consequence, select the next feature to be utilized in the decision process.

3) the decision can be terminated at any node; then, the corresponding decision node (set) would represent the final classification decisions.

4) the tree structure implements Bayes decision rule in sequential form; at the terminal node, a probability of recognition can be assigned to each of the decision classes in the terminal decision node.

Item 2) of this list is particularly useful when, in general, the features are statistically dependent and the joint distributions are not available. Such a decision structure is particularly amenable to qualitative features; a qualitative feature has values that occur as categories rather than as numbers; they are non-rankable. Then, each branch in the

sequential decision structure corresponds to one category. Discrete-valued measurements or analog measurements can easily be converted to qualitative form. Returning to the general discussion of decision schemes, a self-optimizing decision structure has the ability to change its own structure in seeking improved or optimal performance (in classification) as a result of receiving appropriate input information. This information consists of features or measurements and feedback information. The feedback information comes either from the observer who is interacting with the decision process or from the output of the decision process itself (decision-directed). The feedback information represents a measure of correct classification, that is, training information. With the features available, the decision scheme utilizes the feedback information to alter its decision parameters in such a way that recognition performance will be improved; a continual improvement in performance will lead to optimal conditions. Some self-optimizing decision schemes can perform these functions in an on-line mode. This structure is particularly applicable to situations in which there is little or limited prior information concerning the pattern classes. In addition, a decision scheme with settable decision parameters would allow the observer to intervene directly in the decision process to tune these parameters for optimal recognition accuracy and select the best features relative to recognition performance. Bayes decision rule is the only optimal decision scheme which can be applied to category-valued (qualitative) features because it is more fundamental than other schemes and in fact, serves as a lower limit on recognition error for other decision schemes. As indicated previously, a large number of dependent features presents a very difficult problem not only because the decision scheme is more complex but also because the estimation of joint probabilities for the decision process would require a very large data base. Other decision schemes would include the use of order-statistics to yield a distribution-free decision scheme and the use of fuzzy sets. There is a number of mathematical techniques that has not been fully exploited for their applications to feature selection and decision processes; these techniques include factor analysis, use of contingency tables and the like.

Areas proposed for further investigation and development are: 1) exploitation of sequential decision techniques in image pattern recognition, 2) develop an interactive mode for observer and DIP system to allow the observer to tune the decision parameters during a training mode and to

monitor and guide the sequential decision process as it operates, say choosing the sequence of measurements, 3) explore the value of using man-extracted measurements in a sequential decision mode, 4) investigate ways to treat features more than two at a time, 5) explore the possibility of using non-parametric decision schemes in the present DIP system configuration, 6) explore the expanded use of qualitative data to represent images, and 7) investigate the relationship of basic image data or information to the parameters of the decision process.

IX. USER INTERACTION/DISPLAY

A significant factor in the design and use of an image processing system is the interaction or interface between the system and user/observer. The modes of interaction between user/observer and the DIP system essentially depend on the objectives of the digital image processing facility; there are few standards to provide guidance in the design of this interface. It is assumed here that the facility is to be used for design, development, testing and evaluation of DIP techniques (mostly software) and limited hardware (modular) testing. Users of such a system could be classified as an end user (applies existing techniques to "new" imagery) and investigator/designers (design and evaluation of new techniques). In a general way, the functions or options that a user/investigator might like to have in an interactive DIP system include the following:

1) Monitoring the original input imagery.

2) Observation and manipulation of input images.

3) Monitoring of processed or generated images.

4) Multi-user environment using intelligent terminals.

5) Foreground/background capability; processing in the foreground and program development in the background.

6) Call-up a wide variety of digital image processing techniques.

7) Link-up processing routines as subroutines into a program to apply to imagery in a observer intervention mode; with status tracking.

8) Access to large image files, results files (memory) and terminal buffer memories.

9) Ability to modify existing image processing subroutines and store in temporary memory.

10) Interactive design of image processing techniques.

11) Interactive application of decision trees and feature selection.

12) Interactive graphics.

13) Use of black and white, color, and stereo imagery.

14) Control of scale and resolution.

15) Generate software in hardcopy form for transportability.

16) Availability of image processing functions in near real-time.

Other desirable characteristics for the overall DIP system include a hardcopy output of alphanumeric results and processed imagery, use of a high-level language for power and flexibility, provision for image transmission and reception to and from a remote site, and provision for a scanner input. The most important interface between man and machine in a DIP system is the image display unit. For such a unit, it is desired to have more flexibility, intelligence and responsiveness. Display functions should include the following:

1) Control, in near real-time, of the processing of data arrays (images) in a manner similar to that performed by function memories now.

2) Retain and process multiple copies of data arrays.

3) Ratio imaging and display.

4) Multiple simultaneous displays; stereo

5) Interactive real-time convolution

6) Handle large data arrays, 256 x 256 up to 4,000 x 4,000; high resolution .

7) Interactive zoom and roam.

8) Wide dynamic range; at least 8 bits/pixel.

9) Interactive graphics: joystick, trackball, light-pen, sonic tablet, and direct input (pointing).

10) Programmable display functions.

11) Variable displayed resolution.

12) Rapid traversing of data arrays larger than display area.

13) Dynamic image presentation

14) Stand-alone capability; refresh, storage (4 image planes, B&W, or 2 color), temporary image files, combining logic, special function logic, 16-bit cpu processor control, 4 graphic planes, ROM memory for rapid look-up.

15) Generate arbitrary boundary image mosaics from 2 or more images.

16) Multi-image overlays.

17) Multiple (color) interactive graphic overlays or replacement.

18) Access to host computer from same terminal.

19) Status tracking

In the design of such an interactive display system, one must consider the image chain and the display/user variables including visual acuity, visual field, viewing distance, magnification, scene contrast. luminance and color, object size, shape, orientation and position to which the observer is directed, background luminance, noise, observer characteristics, and eye and head movements.

Areas proposed for further investigation are 1) develop a set of requirements for a future digital image processing system, 2) investigate the corresponding hardware and software capabilities and trade-offs to meet the requirements of 1) and 3) explore the capabilities of displays other than the CRT.

X. EXTENTED CAPABILITIES

The objective of this section is to present some extensions of the functions that are commonly connected with a digital image processing or analysis system. The first one of thsse deals with expanding the capability of change detection, an ability to detect changes from one image to another of the same scene. To accomplish this more effectively, one needs a larger memory to store "past" and "present" imagery, an ability to change scale and warp an image, and register two or more images

accurately. This problem has overlap with another need-to-combine the intelligence from different image sensors in a reliable manner on the same scene. Related to this problem is that of utilizing not only direct imagery but the reliable use of auxiliary information from other sources and integrate all of the information into one "picture."

Usually for the feature extraction/decision process portion of a DIP system, the resulting decision class refers to objects, textures, and the like, a passive decision. Change detection over many images can lead to a predictive capability, i.e., what would the scene be at the next sensing? This should be investigated as a viable extension. A related extension is that, in addition to classifying or identifying objects, texture classes, etc., identify situations, such as a conflict situation, a battle situation, and the like. This would involve a much greater use of image context (and perhaps ancillary information) than in the past.

Another approach to the effective use of existing features is their use in prediction; by way of example, in the diagnosis of bone tumors, the radiologist employs a set of x-ray findings to not only make a diagnosis (decision), but a subset of these findings are used to predict the probability of 5-year survival, which is a prediction. Thus, a careful choice of features will allow a limited amount of predictive capability, this capability should be explored for the type of imagery discussed in this report.

The systems and techniques discussed in previous sections are essentially passive; an extension of this concerns active systems-the ability to generate a follow-up image, an almost continuous change in scale, and an ability to change the apparent viewing angle. Beyond this, an image could be imbedded into a game tree, in which as a result of image analysis, a scene or part of a scene is classified; as a result, an action is proposed (response); the system would respond by generating in an active mode a scenario to that action, or a set of possible scenarios, in terms of the expected imagery; this could be repeated in the framework of a natural sequential game.

XI. CONCLUSIONS AND RECOMMENDATIONS

The fundamental characteristics of a digital image processing facility have been partitioned into the following overlapping areas: 1) hardware and software, 2) data representation/input, 3) preprocessing, 4) information extraction, 5) information manipulation/feature generation, 6) decision processes, 7) user interaction/display, and 8) extended capability. For each area, a number of techniques or characteristics would contribute significantly to the development of an advanced digital image processing facility. Such a facility would provide for an increase in the level and extent of image exploitation.

A number of recommendations have been made concerning problems or areas requiring further study or development. These recommendations can be designated as short term (for current or near future systems) and long term (for "far" future systems). These recommendations are summarized below.

Short Term

1. Establish multi-user environment using intelligent terminals.

2. Allow for foreground/background operation.

3. Allow for transportability of software.

4. Utilize a higher-level language.

5. Utilize existing image processing software as sub-routines to build programs.

6. Increase the level of interaction of the operator during the test/evaluation phase.

7. Expand the capability of the region-growing method.

8. Expand the repertoire of image processing sub-routines.

9. Establish a hierarchical approach to image preprocessing.

10. Explore the more extensive use of stereo imagery and use of pseudo-color.

11. Develop an interactive training mode for feature extraction and decision-making.

12. Develop additional software to support graphics.

13. Add light-pen or sonic tablet capability.

14. Evaluate the use of syntactical image analysis.

Long Term

1. Develop hardware (firmware) to perform special image processing functions.

2. Explore use of a multiprocessor environment for digital image processing.

3. Explore the use of a special image processing software.

4. Extend present development in image data compression.

5. Develop better models for image degradation.

6. Exploit image context to a greater extent.

7. Develop hierarchical techniques for digital image processing.

8. Investigate technologies for mass storage of high resolution imagery.

9. Develop more effective measures of texture.

10. Explore techniques for image pattern recognition of lineal features.

11. Explore how the functions of the human visual system might be carried over to automated image processing.

12. Develop and test sequential decision procedures that are more flexible (and optimal).

13. Investigate the use of operator extracted features to be used for image pattern recognition.

14. Develop algorithms that allow for on-line training mode for the feature extraction and decision processes.

15. Explore use of qualitative image data for feature generation and decision making.

16. Develop procedures to be able to handle multi-dimensional dependent features.

17. Explore development of methods for extracting normalized image information (less sensitive to variations.).

18. Explore the use of digital image processing in a predictive mode.

12. Develop additional software to support graphics.

13. Add light-pen or sonic tablet capability.

14. Evaluate the use of syntactical image analysis.

<u>Long Term</u>

1. Develop hardware (firmware) to perform special image processing functions.

2. Explore use of a multiprocessor environment for digital image processing.

3. Explore the use of a special image processing software.

4. Extend present development in image data compression.

5. Develop better models for image degradation.

6. Exploit image context to a greater extent.

7. Develop hierarchical techniques for digital image processing.

8. Investigate technologies for mass storage of high resolution imagery.

9. Develop more effective measures of texture.

10. Explore techniques for image pattern recognition of lineal features.

11. Explore how the functions of the human visual system might be carried over to automated image processing.

12. Develop and test sequential decision procedures that are more flexible (and optimal).

13. Investigate the use of operator extracted features to be used for image pattern recognition.

14. Develop algorithms that allow for on-line training mode for the feature extraction and decision processes.

15. Explore use of qualitative image data for feature generation and decision making.

SELECTED REFERENCES

I. Hardware and Software

1. P. H. Enslow, "Multiprocessor Organization-A Survey," Computing Surveys, vol. 9, no. 1, March 1977.

2. N. V. Findler, et al, Four High-Level Extensions of FORTRAN IV:SLIP, AMPPL-II, TREETRAN, SYMBOLANG., Spartan Books, 1972.

3. K. S. Fu and K. Hwang, "PM^4: A Versatile Computer System for Pattern Recognition and Image Processing," republication paper from authors.

4. D. J. Kuck, "A Survey of Parallel Machine Organization and programming," Computing Surveys, vol. 9, no. 1, March 1977.

5. W. C. Meilander, "The Evolution of Parallel Processor Architecture for Image Processing," Proc. of 1977 COMPCON, IEEE Comp. Soc., Sept., 1977.

6. J. L. Potter, "The STARAN Architecture and Its Application to Image Processing and Pattern Recognition Algorithms," National Computer Conference Proc., 1978.

II. Data Representation/Input

1. T. Berger, Rate Distortion Theory, A Mathematical Basis for Data Compression, Prentice-Hall, 1971

2. K. S. Fu, editor, Syntactic Pattern Recognition Applications, Springer-Verlay, 1977.

3. D. J. Granrath and B. R. Hunt, "Signal Detection Trade-Off-Analysis of Optical Versus Digital Fourier Transform Computers," SPIE, vol. 118, Optical Signal and Image Processing, 1977.

4. B. R. Hunt, "An Optical Analogy to DPCM Digital Image Data Compression," SPIE, vol. 119, Application of Digital Image Processing, 1977.

5. J. D. Olsen and C. M. Heard, "A Comparison of the Visual Effects of Two Transform Domain Encoding Approaches," SPIE, vol. 119, Application of Digital Image Processing, 1977.

6. J. C. Stoffel, "Halftone Pictorial Encoding," SPIE, vol. 119, Application of Digital Image Processing, 1977.

III. Preprocessing

1. H. C. Andrews and B. R. Hunt, Digital Image Restoration, Prentice-Hall, 1977.

2. S. G. Carlton and O. R. Mitchell, "Image Segmentation Using Texture and Gray Level," Proc. 1977 IEEE Comp. Soc. Conf. on Pattern Recognition and Image Processing, June, 1977, pp. 387-391.

3. R. A. Hummel, "Histogram Modification Techniques," Univ of Maryland Computer Science Report TR-329, Sept., 1974.

4. D. L. Milgram, Et al, "Algorithms and Hardware Technology for Image Recognition," DARPA Report No. 3206 (U.S. Army Night Night Vision Lab), March 1978.

5. G. J. Vanderbrug and A. Rosenfeld, "Two-Stage Template Matching," IEEE Trans. on Comp., vol. C-26, no. 4, April, 1977. pp 384-393.

6. S. W. Zucker, "An Application of Relaxation Labeling to Line and Curve Enhancement," IEEE Trans. on Comp., vol. C-26, no. 4, April 1977, pp. 394-403.

IV. Information Extraction

1. R. W. Ehrich, "Detection of Global Edges in Textured Images," IEEE Trans. on Computers, vol. C-26, no. 6, June 1977, pp. 589-603.

2. W. Frei and C-C Chen, "Fast Boundary Detection : A Generalization and a New Algorithm," IEEE Trans. on Comp., vol. C-26, no. 10, Oct., 1977.

3. T. S. Huang and K. S. Fu, "Image Understanding and Information Extraction," RADC Report TR-77-102, March 1977.

4. R. Nevatia, "Locating Object Boundaries in Textured Environments," IEEE Trans. on Comp., vol. C-25, no. 11, Nov., 1976, pp. 1170-1175.

5. E. Personn and K. S. Fu, "Shape Discrimination Using Fourier Descriptors," IEEE Trans. on SMC, vol. SMC-7, no. 3, March 1977.

6. J. Sklansky, Image Segmentation and Feature Extraction," IEEE Trans. on SMC, vol. SMC-8, no. 4, April 1978, pp. 237-247.

V. Information Manipulation/Feature Generation

1. R. A. Eisenbeis and R. B. Avery, Discriminant Analysis and Classification Procedures, Lexington Books, 1972.

2. B. S. Everitt, The Analysis of Contingency Tables, Halsted Press, 1977.

3. R. Gnanadesikan, Methods for Statistical Data Analysis of Multivariate Observations, John Wiley, 1977.

4. J. A. Hartigan, Clustering Algorithms, John Wiley, 1975.

5. D. K. Hildebrand, et al, Prediction Analysis of Cross Classifications, John Wiley, 1977.

6. F. H. C. Marriott, The Interpretation of Multiple Observations, Academic, 1974.

VI. Texture Analysis

1. R. M. Haralick, et al, "Textural Features for Image Classification," IEEE Trans. on SMC, vol. SMC-3, no. 6, Nov., 1973, pp. 610-621.

2. S. Y. Hsu and E. Klimko, "Texture Tone Feature Extraction and Analysis," RADC Report TR-77-279, August 1977.

3. S. Y. Lu and K. S. Fu, "A Syntactic Approach to Texture Analysis," Computer Graphics and Image Processing, vol. 7, 1978.

4. O. R. Mitchell, et al, "A Max-Min Measure for Image Texture Analysis," IEEE Trans. on Comp., vol. C-26, no. 4, April 1977, pp. 408-414.

5. H. Tamura, et al, "Textural Features Corresponding to Visual Perception," IEEE Trans. on SMC, vol. SMC-8, no. 6, June 1978, pp. 460-472.

6. J. S. Weszka, et al, "A Comparative Study of Texture Measures for Terrain Classification," IEEE Trans. on SMC, vol. SMC-6, no. 4, April 1976.

VII. <u>Decision Processor</u>

1. R. O. Duda and P. R. Hart, <u>Pattern Classification and Scene Analysis</u>, John Wiley, 1973.

2. J. M. Mendel and K. S. Fu, <u>Adaptive, Learning, and Pattern Recognition Systems</u>, Academic Press, 1970.

3. E. A. Patrick, <u>Fundamentals of Pattern Recognition</u>, Prentice Hall, 1972.

4. J. L. Poage, "A Sequential Non-Parametric Pattern Classification Algorithm Based on the Wald SPRT," <u>IEEE Trans. on SMC</u>, vol. SMC-5, no. 1, Jan., 1975.

5. M. M. Tatsuoka, <u>Multivariate Analysis</u>, John Wiley, 1971.

VIII. <u>User Interaction/Display</u>

1. J. Adams and R. Wallis, "New Concepts in Display Technology," <u>Computer</u>, August, 1977.

2. W. Myers, "Interactive Computer Graphics: Poised for Takeoff," <u>Computer</u>, Jan., 1978, pp. 60-74.

3. J. N. Latta, "New Developments in Digital Image Processing Displays, "<u>SPIE</u>, vol. 119, Application of Digital Image Processing, 1977.

4. D. E. Sharp, <u>Handbook of Interactive Computer Terminals</u>, Reston, 1977.

5. L. E. Tannas and W. F. Goede, "Flat-Panel Displays: A Critique," <u>IEEE Spectrum</u>, July 1978, pp. 26-32.

IX. <u>General</u>

1. C. H. Chen, Editor, <u>Pattern Recognition and Artificial Intelligence</u>, Academic, 1976.

2. G. E. Forsen, et al, "Advanced Digital Exploitation Techniques (ADET)," RADC Report TR-77-145, April 1977.

3. K. S. Fu and A. Rosenfeld, "Pattern Recognition and Image Processing," <u>IEEE Trans. on Comp</u>., vol. C-25, no. 12, Dec., 1976.

4. J. C. Lietz, et al, "Applications of DICIFER," RADC Report TR-76-4, Jan., 1976.

5. A. Rosenfeld, and A. C. Kak, Digital Picture Processing, Academic Press, 1976.

6. Image Processing, SPIE, vol. 74, Feb., 1976.

1978 USAF-ASEE SUMMER FACULTY RESEARCH PROGRAM

sponsored by

THE AIR FORCE OFFICE OF SCIENTIFIC RESEARCH

conducted by

AUBURN UNIVERSITY AND OHIO STATE UNIVERSITY

PARTICIPANT'S FINAL REPORT

CLUTTER SUPPRESSION THROUGH RADAR POLARIZATION PROCESSING

Prepared by:	Nicola Berardi
Academic Rank:	Assistant Professor
Department and University:	EET Department Purdue University W. Lafayette, IN
Assignment:	
(Air Force Base) (Laboratory)	Griffiss AFB RADC
USAF Research Colleague:	Clarence Silfer

Data:	August 4, 1978
Contract No:	F44620-75-C-0031

ABSTRACT

This paper entails the study of methods and procedures for Multiple-Channel Radar Clutter Suppression, with emphasis on Radar Polarization Processes.

The choice of proper and applicable target-clutter models and their mathematical representation, play a very important role for the optimal filter design. The analytical manipulation of these models will, in fact, serve the purpose of derivation of their related optimum receive filter for a variety of transmit waveforms.

The case of elements of the transmit vectors would range from correlated to uncorrelated (disjoint). Additionally, the scattering matrix formulation is introduced in terms of directional vectors and directional transformation matrices. The field backscattered from a target for an arbitrarily polarized transmitted wave, is also specified using [S] complex scattering matrix formulations.

A noteworthy aspect of the scattering matrix formulation is the fact that the transmitted wave and the back-scattered wave are traveling in opposite directions. Thus, a three-dimensional problem is being characterized with only two dimensions.

The multiple-channel concepts are in direct relation to a single channel system; hence the compatibility of the chosen models can be ascertained through their evaluation with respect to conventional polarization processes.

In the case of our model, the choice of the transmit vector can be assumed to be an optimal waveform. This will partially ease the final formulation and solution of the optimal-filter equation.

I. INTRODUCTION

A backscatter radar environment is a stochastic phenomena having properties associated with Doppler, range and electromagnetic scattering (polarization scattering matrix). The environment consists of undesired (clutter) scatterers and desired (target) scatterers, each having its own characteristic Doppler, range and polarization properties. Clutter is defined as a conglomeration of unwanted radar echoes[6]. The name is descriptive of the fact that such echoes "clutter" the radar display and make difficult the recognition of wanted echo signals. To a radar searching for aircraft targets, clutter echoes include reflections from trees, vegetation, hills, man-made structures, and the surface of the sea.

Another clutter target is chaff, which consists of many small pieces of reflecting material, usually aluminum, deliberately released by a hostile aircraft to simulate a real aircraft target and confuse military radar defenses. Chaff is similar in some respects to other forms of clutter and their related model is a dipole. The model used in our case will satisfy all conditions of a dipole.

For a multiple-channel system the transmit waveform is a vector and the scattering function is a tensor of grade four. As indicated by several investigators [3,4], the parameters within the tensors are time averaged but Doppler and range spread correlations are not considered.

The application of the optimization[1] theory and its approaches, is used to analytically solve those sets of equations pertaining to the design of a radar system optimized over a set of radar environmental factors. The latter include the clutter scattering function on the transmit waveform, which is directly related to an autocovariance function of the noise resulting from the backscattered clutter with the transmitted incident waveform factored and deconvolved out[2].

It has been also shown[4] that some beneficial results can be derived by controlling the transmitted and receiving polarization waveforms, with respect to target discrimination, in order to take advantage of the degree of coherence of the signals in the receiving channels.

The general direction of this project is an extension of existing concepts and for the purpose of final solutions the following set of informations should be dwelled upon and used:

a. The statistical model for the doubly spread scatterer for a two-channel (polarization) radar.

b. An approach for optimal waveform design using this model.

c. The model for the ambiguity tensor function for a two-channel system.

d. Optimum receiver for a two-channel system.

e. System performance and evaluation.

It must be underlined that because a radar backscattering environment can be represented by a statistically time and range varying polarization scattering matrix, its model can therefore be safely used for the target as well as for the clutter.

A. SINGLE-CHANNEL PROCESSES

The understanding of the polarization process cases is based upon a brief review of the basic equations describing the signal received by a radar[1] in the single-channel system (Figure 1) for a slowly fluctuating point target in a clutter environment. i.e.:

$$\tilde{r}(t) = \tilde{b}\tilde{f}_d(t) + \tilde{n}_c(t) + \tilde{w}(t) \quad : H_1\text{-----target present} \quad (1)$$

$$\tilde{r}(t) = \tilde{n}_c(t) + \tilde{w}(t) \quad : H_0\text{-----target absent} \quad (2)$$

where:

$\tilde{f}_d(t)$ = complex random delayed Doppler shifted replica of the transmitted waveform f(t).

$\tilde{b}$ = complex random variable that represents the target backscatter, propagation losses and antenna responses.

$\tilde{n}_c(t)$ = received signal from the clutter and it is a complex random process.

$\tilde{w}(t)$ = additive white noise in the receiver.

The tilda ∿ designates the complex low pass equivalent.

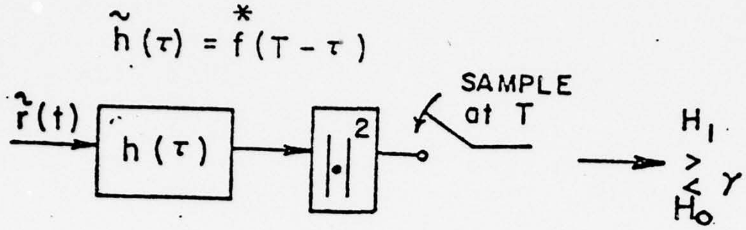

MATCHED FILTER RECEIVER

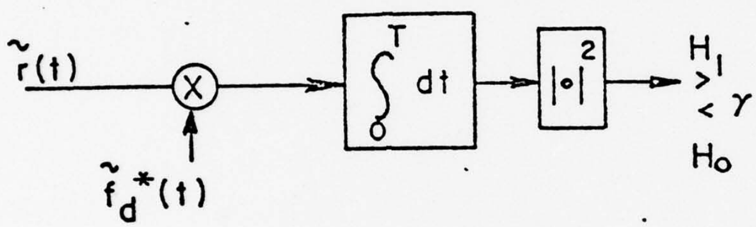

MODULATION RECEIVER

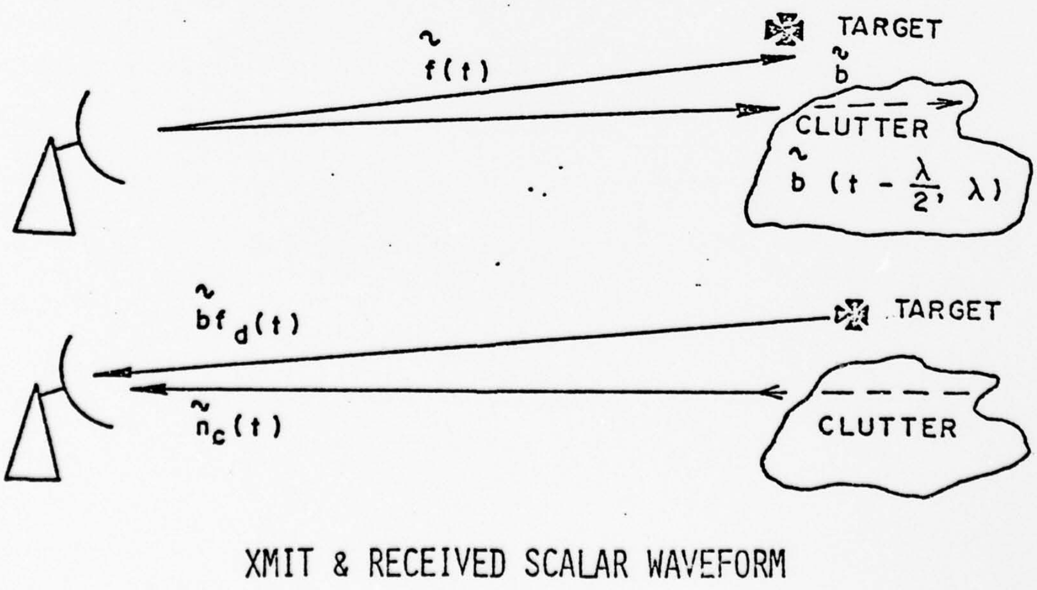

XMIT & RECEIVED SCALAR WAVEFORM

FIGURE 1

When modeling the clutter, it is taken into consideration that the received signal from the clutter is the convolution and the product of the clutter with the transmit waveform. The convolution itself is with respect to the range variable λ and the product is with respect to the time variable t.

i.e.:

$$\tilde{n}_c(t) = \sqrt{E_t} \int_{-\infty}^{\infty} \tilde{f}(t - \lambda)\, \tilde{b}\left(t - \frac{\lambda}{2}, \lambda\right) d\lambda \qquad (3)$$

This is a zero mean complex Gaussian random process with covariance[1] function $\tilde{K}_{\tilde{n}_c}(t, u)$. where:

$$\tilde{K}_{\tilde{n}_c}(t,u) = E_t \int_{-\infty}^{\infty} \tilde{f}(t-\lambda)\, \tilde{K}_{DR}\{t-u, \lambda\}\, \tilde{f}^*(u-\lambda)\, d\lambda \qquad (4)$$

or alternatively

$$\tilde{K}_{\tilde{n}_c}(t,u) = E_t \iint_{-\infty}^{\infty} \tilde{f}(t-u)\tilde{S}_{DR}\{f,\lambda\}\, \tilde{f}^*(u-\lambda) e^{j2\pi f(t-u)} df d\lambda \qquad (5)$$

where the correlation function, $\tilde{K}_{DR}(\tau,\lambda)$, is a two-variable function that depends on the reflective properties of the target and $\tilde{S}_{DR}(f, \lambda)$ represents the spectrum of the process $\tilde{b}(t,\lambda)$ and is called the scattering function of the clutter. The two functions $\tilde{K}_{DR}$ and $\tilde{S}_{DR}$ are a Fourier Transform pair.

The white noise $\tilde{w}(t)$ is likewise a complex Gaussian random process but with covariance function $\tilde{K}_{\tilde{w}}(t,u) = N_0\, \delta(t - u)$.

B. OPTIMAL WAVEFORM DESIGN:

The optimal waveform $\tilde{f}_o(t)$ must satisfy[1] the following integral equation

$$\int_{T_i}^{T_f} \tilde{h}_{ou}(t, u)\, \tilde{f}_o(u)\, du + \lambda_E\, \tilde{f}_o^*(t) - \lambda_B\, \tilde{f}_o(t) = 0 \qquad (6)$$

where

$\tilde{h}_{ou}$ (t, u) is the optimum unrealizable filter satisfying the equation

$$N_o\tilde{h}_{ou}(t,u) + \int_{T_i}^{T_f} \tilde{h}_{ou}(x,u)\tilde{\tilde{K}}_{nc}(t,x)\,dx = \tilde{\tilde{K}}_{nc}(t,u) \quad T_i \leq t,u \leq T_f \tag{7}$$

$\tilde{\tilde{K}}_{nc}$ (t,u) satisfies Equation (4) and (5)

where:

λ_E and λ_B are LaGrange multipliers with an energy and bandwidth constraint

$$\int_{T_i}^{T_f} |\tilde{f}(t)|^2 \, dt = 1 \tag{8}$$

$$\int_{T_i}^{T_f} \left| \frac{d\tilde{f}(t)}{dt} \right|^2 dt = B^2 \tag{9}$$

therefore $\tilde{f}_o(T_i) = \tilde{f}_o(T_f) = 0$ (10)

After having reviewed the optimum system for the single-channel case, let us extend these results to the two-channel case i.e., polarization diversity.

III. MULTIPLE-CHANNEL RECEIVER-POLARIZATION CASE

A. In the dual polarization case - when we transmit and receive over two channels - the received signals are given in the vector form, i.e.:

DUAL POLARIZATION CHANNELS

$$\underline{\tilde{W}}(T) = \begin{vmatrix} \tilde{W}_V(T) \\ \tilde{W}_H(T) \end{vmatrix} = \Big\{ \text{RECEIVER WHITE NOISE VECTOR}$$

$$\underline{\tilde{N}}_C(T) = \begin{vmatrix} \tilde{N}_{CV}(T) \\ \tilde{N}_{CH})T) \end{vmatrix} = \Big\{ \text{COLORED NOISE VECTOR DUE TO BACKSCATTER FROM CLUTTER}$$

WHERE $\underline{\tilde{N}}_C(T) = \sqrt{\bar{E}_T} \int_{-\infty}^{\infty} \underline{\tilde{B}}(T-\frac{\lambda}{2}, \lambda)\underline{\tilde{F}}(T - \lambda)D\lambda$

FOR T = TIME ; λ = RANGE $\Big\}$ EXPRESSED IN TIME

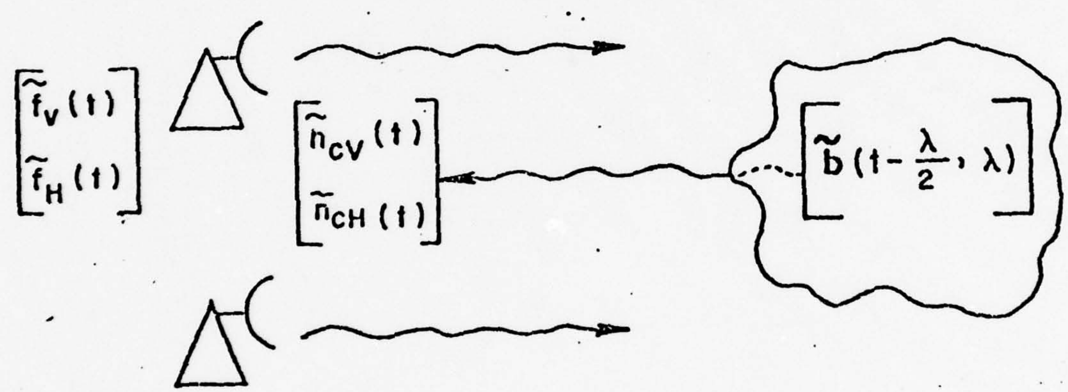

FIGURE 2

POLARIZATION MODULATION RECEIVER

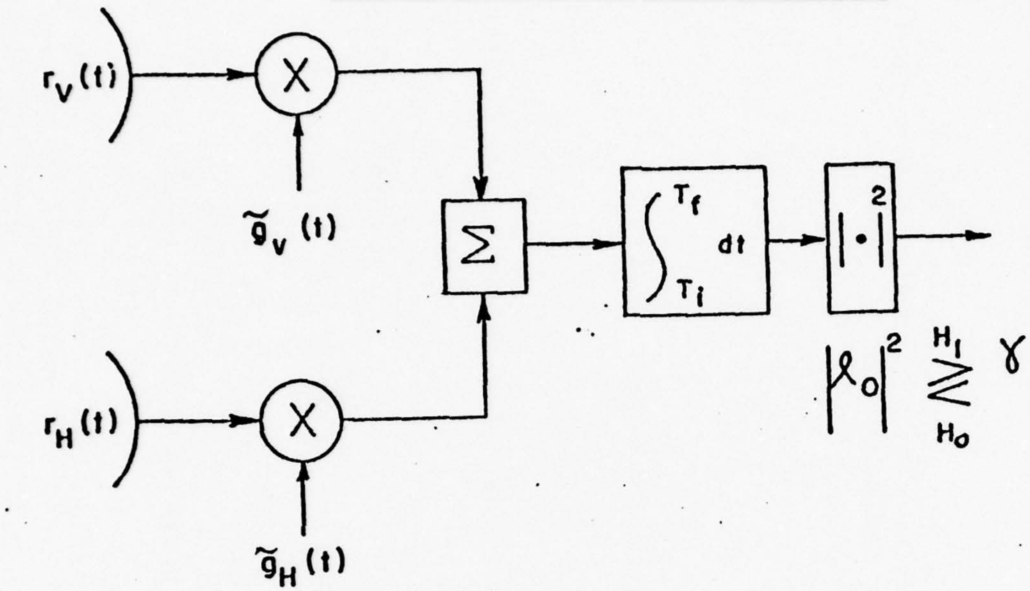

WHERE: ℓ_o = FINAL OUTPUT

γ = THRESHOLD (PREDETERMINED)

$$\underline{\tilde{G}}(T) = \begin{bmatrix} \tilde{G}_V(T) \\ \tilde{G}_H(T) \end{bmatrix} = \Big\{ \text{MUST SATISFY THE MATRIC EQUATION OF } \underline{\tilde{F}_D}(T)$$

$$\text{FOR } \underline{\tilde{F}_D}(T) = \int_{-\infty}^{\infty} \tilde{K}_{\tilde{N}C}(T,U)\tilde{G}(U)\, dU + N_0 \underline{\tilde{G}}(T)$$

FIGURE 3

$$\tilde{\mathbf{r}}(t) = \tilde{\mathbf{b}}\tilde{\mathbf{f}}_d(t) + \tilde{\mathbf{n}}_c(t) + \tilde{\mathbf{w}}(t) \quad : H_1\text{----target present} \quad (11)$$

$$\tilde{\mathbf{r}}(t) = \tilde{\mathbf{n}}_c(t) + \tilde{\mathbf{w}}(t) \quad : H_0\text{----target absent} \quad (12)$$

where boldface denotes vectors defined as follows:

$\tilde{\mathbf{r}}(t) \triangleq \begin{vmatrix} \tilde{\mathbf{r}}_V(t) \\ \tilde{\mathbf{r}}_H(t) \end{vmatrix}$ the received signal, a vector function having a vertical and horizontal component.

$\tilde{\mathbf{b}} \triangleq \begin{vmatrix} \tilde{b}_{VV} & \tilde{b}_{VH} \\ \tilde{b}_{HV} & \tilde{b}_{HV} \end{vmatrix}$ a scattering matrix for an assumed slowly fluctuating point target with zero mean complex Gaussian random elements.

$\tilde{\mathbf{f}}_d(t) \triangleq \sqrt{\bar{E}_t}\ \tilde{\mathbf{f}}(t - \tau_d)e^{j\omega_d t}$ time delayed, Doppler shifted replica of the transmit wave- form vector. (13)

$\bar{E}_t \triangleq$ the average energy in the transmit vector.

$\mathbf{w}(t) \triangleq \begin{vmatrix} \tilde{w}_V(t) \\ \tilde{w}_H(t) \end{vmatrix}$ the receiver noise vector assumed white.

$\tilde{\mathbf{n}}_c(t) \triangleq \begin{vmatrix} \tilde{n}_{cV}(t) \\ \tilde{n}_{cH}(t) \end{vmatrix} \triangleq \sqrt{\bar{E}_t} \int_{-\infty}^{\infty} \tilde{\mathbf{b}}(t-\frac{\lambda}{2},\lambda)\tilde{\mathbf{f}}(t-\lambda)d\lambda$ colored noise vector due to backscatter from clutter. (14)

where t is time and λ is range expressed in time.

The received vector, $\tilde{\mathbf{n}}_c(t)$, due to the clutter is obtained by convolving the Doppler-range variant scattering matrix of the clutter process, $\tilde{\mathbf{b}}(t-\frac{\lambda}{2}, \lambda)$ with the transmit waveform vector

$\tilde{\mathbf{f}}(t)$, with the scattering matrix $\tilde{\mathbf{b}}(t-\frac{\lambda}{2}, \lambda)$ a zero mean Gaussian random process.

The clutter vector covariance function is a matrix

$$\tilde{\tilde{K}}_{n_c}(t, u) \triangleq E\{\tilde{n}_c(t)\tilde{n}_c^{\dagger}(u)\} = \begin{bmatrix} \tilde{\tilde{K}}_{n_c VV}(t,u) & \tilde{\tilde{K}}_{n_c VH}(t,u) \\ \tilde{\tilde{K}}_{n_c HV}(t,u) & \tilde{\tilde{K}}_{n_c HH}(t,u) \end{bmatrix} \quad (15)$$

It has been shown that if it is assumed that the returns from different range intervals are statistically independent and that the return from each interval is a sample vector function of a stationary zero-mean Gaussian random process, then through matrix manipulations:

$$\tilde{K}_{n_c}(t,u) = E_t \int_{-\infty}^{\infty} \tilde{\mathbf{f}}^T(t-\lambda)\tilde{K}_{DR}\{t-u,\lambda\}\ \tilde{\mathbf{f}}^*(u-\lambda)\,d\lambda \quad (16)$$

or alternatively

$$\tilde{\tilde{K}}_{n_c}(t,u) = E_t \iint_{-\infty}^{\infty} \tilde{\mathbf{f}}^T(t-\lambda)\tilde{\mathbf{S}}_{DR}\{f,\lambda\}\tilde{\mathbf{f}}^*(u-\lambda)e^{j2\pi f(t-u)}\,df\,d\lambda \quad (17)$$

where $\tilde{\mathbf{K}}_{DR}$ and $\tilde{\mathbf{S}}_{DR}$ matrices are tensors of fourth grade.

The tensor correlation function $K_{DR}(\tau, \lambda)$ is a two-variable fourth-grade tensor that depends on the reflective properties of the target. It is obtained from the expectation terms of $\tilde{\mathbf{b}}$ (t, λ) elements as shown by V. C. Vannicola[2].

Because of the statistical independence of the range intervals and the stationarity of each interval, the $K_{DR}(\tau, \lambda)$ expression with some further matrix manipulation reduces to

$$\tilde{\mathbf{K}}_{DR}(\tau, \lambda) = \begin{bmatrix} \tilde{\mathbf{K}}_{DRVV}(\tau, \lambda) & \tilde{\mathbf{K}}_{DRVH}(\tau, \lambda) \\ \tilde{\mathbf{K}}_{DRHV}(\tau, \lambda) & \tilde{\mathbf{K}}_{DRHH}(\tau, \lambda) \end{bmatrix} \delta\ (\lambda - \lambda_1) \quad (18)$$

which can be written $[\tilde{\mathbf{K}}_{DR}(\tau, \lambda)] \;\; \delta(\lambda - \lambda_1)$

where $\tau = t - u$.

The subscripts DR denote that the clutter is doubly spread in Doppler and range. Through substitution and evaluation of this expression we obtain the result in (16).

The function $\tilde{\mathbf{S}}_{DR}(f, \lambda)$ is a two-variable fourth-rank tensor representing the spectrum of the process and is related to $K_{DR}(\cdot)$ by the Fourier Transform

$$\tilde{\mathbf{K}}_{DR}(\tau, \lambda) = \int_{-\infty}^{\infty} \tilde{\mathbf{S}}_{DR}(f, \lambda) e^{j2\pi f\tau} df \; ; \tag{19}$$

where $K_{DR}(\tau, \lambda)$ can be called the tensor scattering function of the process

$$\tilde{\mathbf{b}}(t, \lambda) \triangleq \begin{bmatrix} \tilde{\mathbf{b}}_{VV}(t, \lambda) & \tilde{\mathbf{b}}_{VH}(t, \lambda) \\ \tilde{\mathbf{b}}_{HV}(t, \lambda) & \tilde{\mathbf{b}}_{HH}(t, \lambda) \end{bmatrix} \tag{20}$$

Carrying out all the expectation[2] and omitting the variable τ and λ (to save space) we have:

$$\tilde{\mathbf{K}}_{DR}(\tau,\lambda) = E \begin{bmatrix} \begin{bmatrix} \tilde{b}_{VV}\tilde{b}_{VV}^* & \tilde{b}_{VV}\tilde{b}_{VH}^* \\ \tilde{b}_{VH}\tilde{b}_{VV}^* & \tilde{b}_{VH}\tilde{b}_{VH}^* \end{bmatrix} & \begin{bmatrix} \tilde{b}_{VV}\tilde{b}_{HV}^* & \tilde{b}_{VV}\tilde{b}_{HH}^* \\ \tilde{b}_{VH}\tilde{b}_{HV}^* & \tilde{b}_{VH}\tilde{b}_{HH}^* \end{bmatrix} \\ \begin{bmatrix} \tilde{b}_{HV}\tilde{b}_{VV}^* & \tilde{b}_{HV}\tilde{b}_{VH}^* \\ \tilde{b}_{HH}\tilde{b}_{VV}^* & \tilde{b}_{HH}\tilde{b}_{VH}^* \end{bmatrix} & \begin{bmatrix} \tilde{b}_{HV}\tilde{b}_{HV}^* & \tilde{b}_{HV}\tilde{b}_{HH}^* \\ \tilde{b}_{HH}\tilde{b}_{HV}^* & \tilde{b}_{HH}\tilde{b}_{HH}^* \end{bmatrix} \end{bmatrix}$$

$$= \begin{bmatrix} \begin{bmatrix} \tilde{K}_{VV,VV} & \tilde{K}_{VV,VH} \\ \tilde{K}_{VH,VV} & \tilde{K}_{VH,VH} \end{bmatrix} & \begin{bmatrix} \tilde{K}_{VV,HV} & \tilde{K}_{VV,HH} \\ \tilde{K}_{VH,HV} & \tilde{K}_{VH,HH} \end{bmatrix} \\ \begin{bmatrix} \tilde{K}_{HV,VV} & \tilde{K}_{HV,VH} \\ \tilde{K}_{HH,VV} & \tilde{K}_{HH,VH} \end{bmatrix} & \begin{bmatrix} \tilde{K}_{HV,HV} & \tilde{K}_{HV,HH} \\ \tilde{K}_{HH,HV} & \tilde{K}_{HH,HH} \end{bmatrix} \end{bmatrix} \tag{21}$$

Equation (21) provides 16 different elements (discriminants) - when one considers the statistical behavior of the polarization random process scattering matrix, - and completely describe the target and/or clutter irrespective of the transmit waveform and receiver design. They can be used in the waveform and receiver optimization as well as the performance equations in the same sense that the scalar correlation and scattering functions are used in the design equations of the single channel system.

B. OPTIMUM RECEIVER - UNIFORM DOPPLER-RANGE INVARIANT CLUTTER (Special Case):

Consider the special case when the clutter has a range invariant tensor correlation or scattering function

$$\tilde{\mathbf{K}}_{DR}(\tau, \lambda) \ , \quad \tilde{\mathbf{S}}_{DR}(f, \lambda)$$

and extends well beyond the range of a possible target. We can treat the clutter as if it were infinite in extent.

For the conventional receiver

$$\tilde{\ell} \triangleq \int_{-\infty}^{\infty} \tilde{\mathbf{r}}^T(t)\, \tilde{\mathbf{f}}^*(t - \tau_d)\, e^{-j\omega_d t}\, dt \tag{22}$$

where ℓ = final output

while for the optimum receiver

$$\tilde{\ell}_o \triangleq \int_{-\infty}^{\infty} \tilde{\mathbf{r}}^T(t)\, \tilde{\mathbf{g}}^*(t)\, dt. \tag{23}$$

Now by letting $\tilde{\mathbf{f}}(t) \longleftrightarrow \tilde{\mathbf{F}}\{\omega\}$ (24)

denote a Fourier Transform pair.

From Equation (13-126) of reference[1] we may find $\tilde{\mathbf{g}}(t)$

$$\tilde{\mathbf{g}}(t) \longleftrightarrow \tilde{G}(\omega) = [N_o\mathbf{I} + \tilde{\tilde{S}}_{n_c}(\omega)]^{-1}\tilde{\mathbf{F}}(\omega) \tag{25}$$

$$\text{where } \tilde{\tilde{S}}_{n_c}(\omega) = \int_{-\infty}^{\infty} \tilde{\mathbf{F}}^T(\alpha)\, \tilde{S}_{Du}(\omega - \alpha)\, \tilde{\mathbf{F}}^*(\alpha)\, d\alpha \tag{26}$$

The performance is obtained from (13 - 92)[1]

$$\rho_r = \frac{1}{N_o} \int_{-\infty}^{\infty} \tilde{\mathbf{F}}^T(\omega - \omega_d)\, \tilde{\tilde{S}}_{n_c}(\omega)\, \tilde{\mathbf{F}}^*(\omega - \omega_d)\, df \tag{27}$$

$$\Delta_{w_o} = \frac{\bar{E}_r/N_o}{1 + \rho_r} \tag{28}$$

For the optimum receiver:

$$\Delta_{w_o} = \bar{E}_r \int_{-\infty}^{\infty} \tilde{\mathbf{F}}^T(\omega-\omega_d)\, [N_o I + \tilde{S}_{n_c}(\omega)]^{-1} \tilde{F}^*(\omega-\omega_d)\, df \tag{29}$$

where Δ_{w_o} = Signal-to-Noise Ratio

C. OPTIMAL WAVEFORM DESIGN - POLARIZATION CASE:

The extension of the waveform design case to the polarization channels involves vectors, matrices and tensors in Equations (6) through (9). The optimum unrealizable filter $\tilde{h}_{ou}$ is a 2 X 2 matrix, the optimum waveform $\tilde{f}_o$ is a vector, the autocovariance function $\tilde{K}_{nc}$ is a matrix, and the multiplications indicated in (8) and (9) become vector dot products. It must be remembered that the autocovariance matrix contains factors of the waveform vectors as defined in Equation (16). Consequently, the filter must satisfy the equation

$$N_o\tilde{\mathbf{h}}_{ou}(t,u) = E_t \int_{T_i}^{T_f}\int_{-\infty}^{\infty} \tilde{\mathbf{f}}_o^T(t-\lambda)\tilde{K}_{DR}(t-x,\lambda)\tilde{\mathbf{f}}_o^*(x-\lambda)[\mathbf{I}\delta(x-u)-\mathbf{h}_{ou}(x,u)] \cdot d\lambda dx \tag{30}$$

and the optimal waveform vector must satisfy the integral equation

$$\int_{T_i}^{T_f} \tilde{\mathbf{h}}_{ou}(t,u)\, \tilde{\mathbf{f}}_o(u)\,du + \lambda_E\, \tilde{\mathbf{f}}_o(t) - \lambda_B \tilde{\mathbf{f}}_o(t) = 0 \tag{31}$$

The energy and bandwidth constraints become

$$\int_{T_i}^{T_f} \tilde{\mathbf{f}}^{\mathbf{T}}(t)\, \tilde{\mathbf{f}}^{*}(t)\, dt = 1 \tag{32}$$

and $$\int_{T_i}^{T_f} \tilde{\mathbf{f}}^{\mathbf{T}}(t)\, \tilde{\mathbf{f}}^{*}(t)\, dt = B^2 \tag{33}$$

IV. ANALYTICAL SOLUTION:

It has been previously shown that in order to solve for (a) optimum filter equation, (b) optimum waveform equation, (c) system performance etc. it will necessitate to find:

$$\tilde{\mathbf{K}}_{DR}\ (\tau,\ \lambda),\ \tilde{\mathbf{K}}_{n_c}\ (t,\ u),\ \tilde{\mathbf{n}}_c(t),\ \tilde{\mathbf{S}}_{DR}\ (\omega,\ \lambda),\ \tilde{\mathbf{g}}(t)\ \text{etc.}$$

The only data given and/or modeled are:

(a) Low pass equivalent Xmit waveform $\tilde{\mathbf{f}}(t)$

(b) Scattering matrix from chaff clutter $\tilde{\mathbf{b}}(t,\ \lambda)$

If it is assumed that the given $\tilde{\mathbf{f}}(t)$ is also the optimum waveform then it will be shown that the final solution can be derived if some statistical conditions of the clutter are taken into consideration.

A. XMIT WAVEFORM MODEL:

The assumed $\tilde{\mathbf{f}}(t)$ is a periodic, real,pulse train with real and sinusoidal carrier, and it can also be assumed to be the optimum waveform. The mathematical representation is as follows:

$$\tilde{\mathbf{f}}(t) = \begin{bmatrix} f_V(t) \\ f_H(t) \end{bmatrix} = \begin{bmatrix} \sum_{R=-\infty}^{\infty} \alpha(t-RT)\ \cos\omega_1\ (t-RT) \\ \sum_{R=-\infty}^{\infty} \alpha(t-RT)\ \cos\omega_2\ (t-RT) \end{bmatrix} = \tilde{\mathbf{f}}_o(t)\ \text{(optimum)} \quad (34)$$

for:

$\tau = 1\ \mu\text{sec}$

$T = 1\ \text{msec}$

$\omega_2 = \omega_1 + 2(\frac{2\pi}{\tau})$

$$\alpha(t) = \begin{cases} 1, & 0<t<\tau \\ 0, & \text{elsewhere} \end{cases}$$

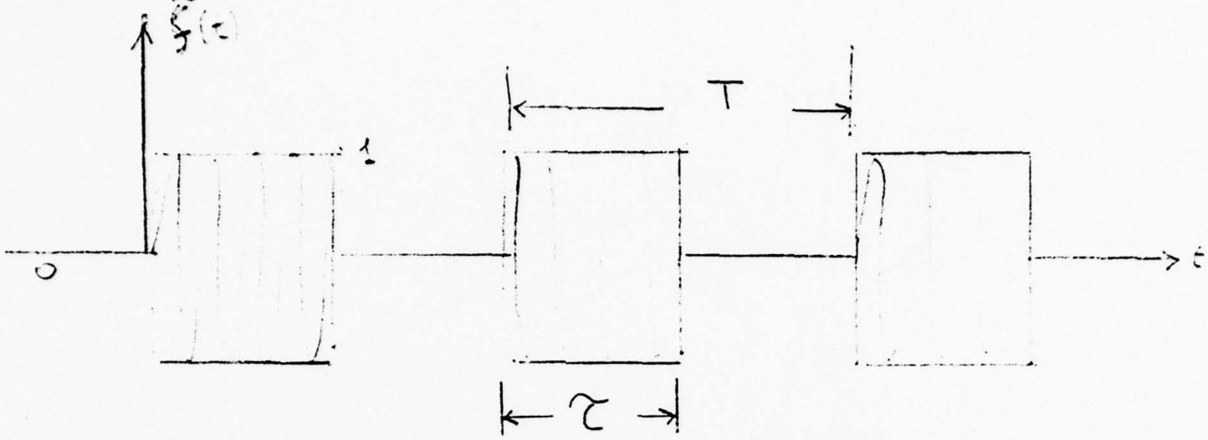

XMIT WAVEFORM

B. MODEL OF RANDOMLY ORIENTED DIPOLE:

A clutter formed by chaff can be treated as an ensemble of independent scatterers; the average scattering cross-section of a volume within the cloud is determined by the ensemble average for a single dipole.

Analytical representations for the radar cross-section of a dipole have often been discussed. The short dipole may be accurately described in terms of electric dipole scattering[7].

In view of the aforementioned, the following model has been chosen for the clutter scattering matrix $\tilde{\mathbf{b}}(t, \lambda)$.

FIGURE 4. CLUTTER AND TARGET MODEL

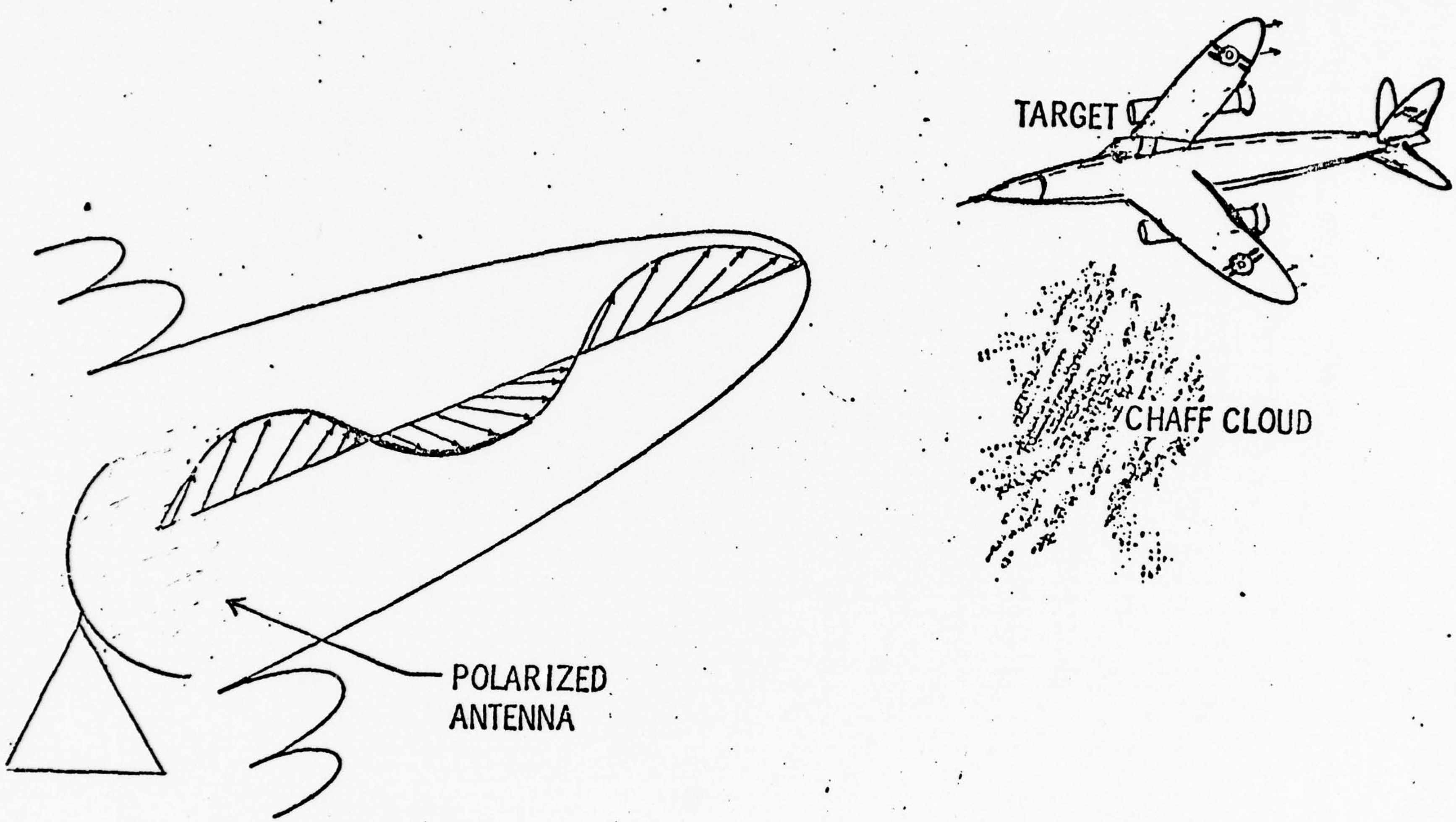

DIPOLE (CHAFF) MODEL

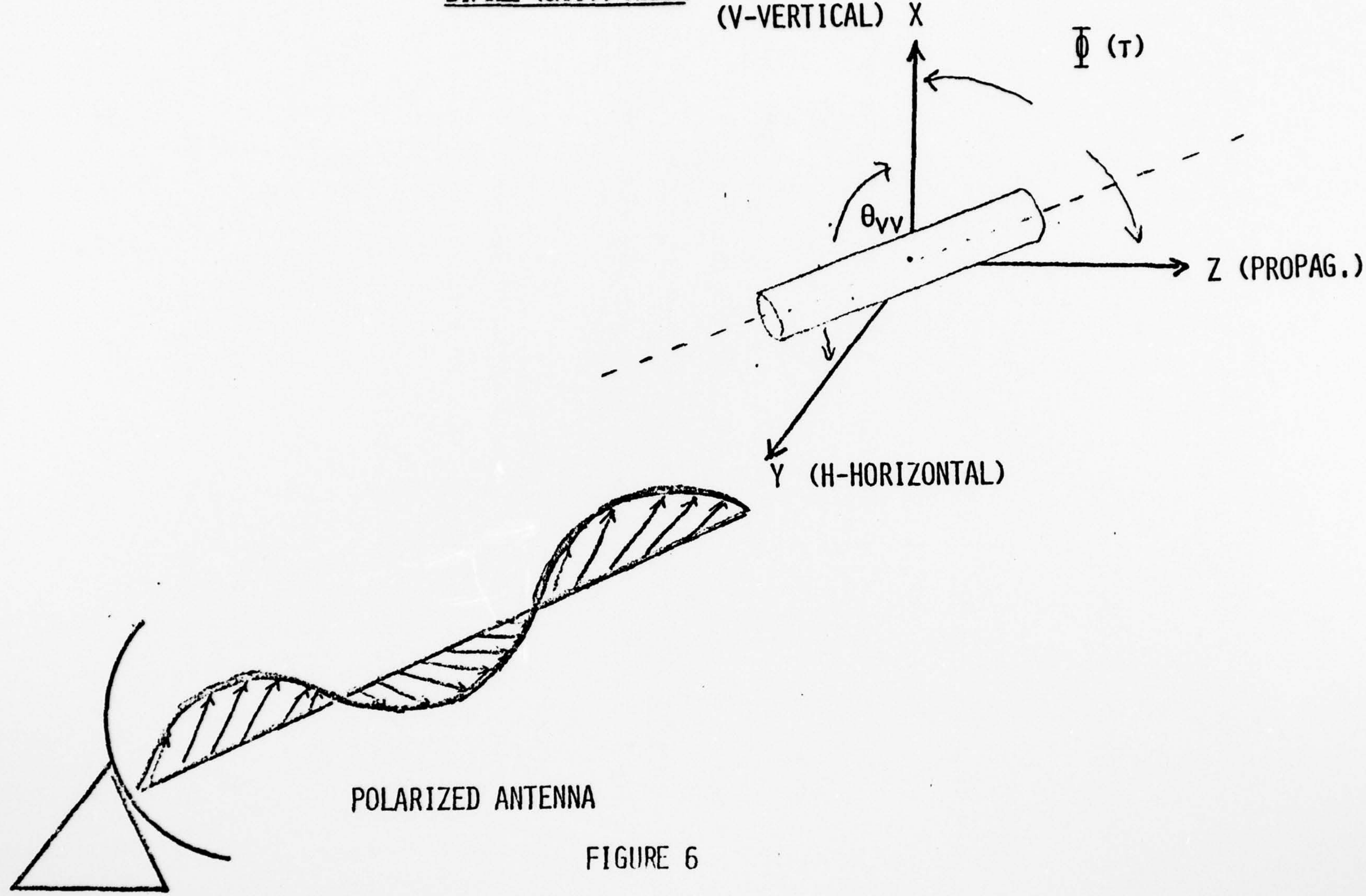

FIGURE 6

A statistical model is then computed according to the physical phenomena of a shifting, fluctuating free falling body, and its approximation is as follows:

$$\tilde{\mathbf{b}}(t, \lambda) = \alpha(t)\tilde{\mathbf{H}} = \alpha(t) \begin{bmatrix} \tilde{H}_{VV} & \tilde{H}_{VH} \\ \tilde{H}_{HV} & \tilde{H}_{HH} \end{bmatrix} \tag{35}$$

where:

$$\tilde{\mathbf{H}}_{VV} = \sigma_d \sin^2 [\, \phi(t) + \Theta_{RV} \,]$$

$$\tilde{\mathbf{H}}_{HH} = \sigma_d \cos^2 [\, \phi(t) + \Theta_{RV} \,]$$

$$\tilde{\mathbf{H}}_{VH} = \tilde{\mathbf{H}}_{HV} = \sigma_d \cos [\phi(t) + \Theta_{RV}] \sin [\phi(t) + \Theta_{RV}]$$

for $\Phi(t) = \frac{\Phi_o}{2} \sin \omega_a t$

with ω_a = rate of change of dipole fluctuation.

ϕ_o = constant angle assumed varying between 30° and 60°.

$\phi(t)$ = angle between the vertically polarized component of the field and the projection of the dipole axis on the wavefront.

Θ_{RV} = random angle made by the dipole axis rotating parallel to the axis of projection of the wavefront.

σ_d = radar cross-section of a single dipole.

An additional assumption would be:

$$\phi(t) = \frac{\phi_o}{2} \sin (\omega_a t + \gamma) \tag{36}$$

where γ is a random phase shift angle due to the pitch and roll of the free-falling dipole; it has been proven that the introduction of γ will not have any effect on the final solution.

The covariances of

$\alpha(t)$ and $\tilde{\mathbf{H}}$ are assumed statistically independent processes and are derived as statistical averages.

$\alpha(t)$ is a complex Gaussian random process with zero mean and autocorrelation

$$K_{\alpha}(\tau) = \sigma_0 e^{-\left|\frac{\tau}{Tc}\right|} \tag{37}$$

σ_o = $N\sigma_d$

T_c = 10 T

N = average total number of dipoles in a radar range cell.

The $\tilde{\mathbf{H}}$ directional scattering matrix has its randomness only in phase, but is truly an ergodic and deterministic process. This also implies that the covariance function of $\tilde{\mathbf{H}}$ can also be taken as time average; this assumption will ease computations.

C. $\tilde{\mathbf{K}}_{DR}(\tau)$ - SOLUTION:

All elements in the $\tilde{\mathbf{K}}_{DR}(\tau)$ tensor can be computed independently; however, considering that all elements in $\check{\mathbf{b}}(\tau, \lambda)$ are real, then it follows that there are only six (6) common terms to be solved. These are:

1. $\tilde{\mathbf{b}}_{VV}\,\tilde{\mathbf{b}}^*_{VV}$
2. $\tilde{\mathbf{b}}_{VH}\,\tilde{\mathbf{b}}^*_{VV} = \tilde{\mathbf{b}}_{HV}\,\tilde{\mathbf{b}}^*_{VV} = \tilde{\mathbf{b}}_{VV}\,\tilde{\mathbf{b}}^*_{VH} = \tilde{\mathbf{b}}_{VV}\,\tilde{\mathbf{b}}^*_{HV}$
3. $\tilde{\mathbf{b}}_{HH}\,\tilde{\mathbf{b}}^*_{VV} = \tilde{\mathbf{b}}_{VV}\,\tilde{\mathbf{b}}^*_{HH}$
4. $\tilde{\mathbf{b}}_{VH}\,\tilde{\mathbf{b}}^*_{VH} = \tilde{\mathbf{b}}_{HV}\,\tilde{\mathbf{b}}^*_{VH} = \tilde{\mathbf{b}}_{VH}\,\tilde{\mathbf{b}}^*_{HV} = \tilde{\mathbf{b}}_{HV}\,\tilde{\mathbf{b}}^*_{HV}$
5. $\tilde{\mathbf{b}}_{HH}\,\tilde{\mathbf{b}}^*_{VH} = \tilde{\mathbf{b}}_{HH}\,\tilde{\mathbf{b}}^*_{HV} = \tilde{\mathbf{b}}_{VH}\,\tilde{\mathbf{b}}^*_{HH} = \tilde{\mathbf{b}}_{HV}\,\tilde{\mathbf{b}}^*_{HH}$
6. $\tilde{\mathbf{b}}_{HH}\,\tilde{\mathbf{b}}^*_{HH}$

The expected value of all these elements will compute the $\tilde{K}_{DR}$ tensor.

hence: $E \left\{ [\alpha^*(t)\alpha(t+\tau)] [\tilde{H}_{ij}{}^*(t)\tilde{H}_{ji}(t+\tau)] \right\} =$

$E \left\{ \alpha^*(t)\ \alpha(t+\tau) \right\}$ $E \left\{ \tilde{H}_{ij}(t)\ \tilde{H}_{ji}(t+\tau) \right\}$ = statistically

independent processes but $E \left\{ \alpha^*(t)\ \alpha(t+\tau) \right\} = K_\alpha(\tau) = \sigma_o e^{-\left|\frac{\tau}{T_c}\right|}$

$$\therefore E \left\{ \tilde{b}_{ji}(t)\tilde{b}_{ij}(t+\tau) \right\} = K_\alpha(\tau)\ E \left\{ \tilde{H}^*_{ji}(t)\ \tilde{H}_{ij}(t+\tau) \right\} \qquad (38)$$

It follows that the computation of the expected value of the following elements shall suffice for the solution of all other elements within the tensor $\tilde{K}_{DR}$. These elements are

$\tilde{E}_{\alpha i}$; $i = 1, 2, \ldots\ldots, 6$

$$\text{where } \tilde{E}_{\alpha i} = K_\alpha(\tau)\ \tilde{E}_j \ ; \quad j = 1, 2, \ldots\ldots, 6 \qquad (39)$$

Therefore:

for $\phi(t) = \frac{\phi_o}{2} \sin \omega_a t$, let:

$$\tilde{E}_1 = E \left\{ \tilde{H}_{VV}\ \tilde{H}^*_{VV} \right\} = E \left\{ \sin^2[\phi(t+\tau)+\Theta_{RV}]\sin^2[\phi(t)+\Theta_{RV}] \right\}$$

$$= \lim_{T\to\infty} \frac{1}{2T} \int_{-T}^{T} \sin^2[\frac{\phi_o}{2} \sin\omega_a(t+\tau)+\Theta_{RV}]\sin^2 [\frac{\phi_o}{2} \sin\omega_a t+\Theta_{RV}]dt$$

$$= \frac{1}{8} [2 + J_o(2\phi_o \sin\frac{\omega_a\tau}{2}) + \cos 4\Theta_{RV} J_o(2\phi_o \cos\frac{\omega_a\tau}{2}) -$$

$$- 4 \cos 2\Theta_{RV} J_o(\phi_o)] \qquad (40)$$

where J_o = Bessel Operator

$$\tilde{E}_2 = E\,\{\tilde{H}_{VV}\tilde{H}^*_{VH}\} = E\{\sin[\phi(t+\tau)+\Theta_{RV}]\cos[\phi(t+\tau)+\Theta_{RV}]\cdot$$

$$\cdot\sin[\phi(t)+\Theta_{RV}]\cos[\phi(t)+\Theta_{RV}]\ \}$$

$$= \lim_{T\to\infty}\left\{\frac{1}{2T}\int_{-T}^{T}\sin[\frac{\phi_o}{2}\ \sin\omega_a(t+\tau)+\Theta_{RV}]\cos[\frac{\phi_o}{2}\ \sin\omega_a(t+\tau)+\Theta_{RV}]\cdot\right.$$

$$\left.\sin[\frac{\phi_o}{2}\ \sin\omega_a t+\Theta_{RV}]\cos[\frac{\phi_o}{2}\ \sin\omega_a t+\Theta_{RV}]dt\right\}$$

$$= \frac{1}{8}\,[\ J_o(2\phi_o\sin\ \frac{\omega_a\tau}{2}) - \cos\ 4\Theta_{RV}\ J_o(2\phi_o\cos\frac{\omega_a\tau}{2})\ ] \tag{41}$$

$$\tilde{E}_3 = E\,\{\tilde{H}_{VV}\tilde{H}^*_{HH}\} = E\,\{\sin^2[\phi(t+\tau)+\Theta_{RV}]\cos^2\ [\phi(t)+\Theta_{RV}]\ \}$$

$$= \lim_{T\to\infty}\ \frac{1}{2T}\int_{-T}^{T}\sin^2[\frac{\phi_o}{2}\ \sin\ \omega_a\ (t+\tau)+\Theta_{RV}]\cos^2[\frac{\phi_o}{2}\ \sin\ \omega_a t+\Theta_{RV}]dt$$

$$= \frac{1}{8}\,[2-J_o(2\phi_o\sin\ \frac{\omega_a\tau}{2})-\cos\ 4\Theta_{RV}J_o\ (2\phi_o\ \cos\ \frac{\omega_a\tau}{2}\ )\ ] \tag{42}$$

$$\tilde{E}_4 = E\,\{\tilde{H}_{VV}\ \tilde{H}^*_{HV}\} = E\,\{\sin^2[\phi(t+\tau)+\Theta_{RV}]\sin[\phi(t)+\Theta_{RV}]\cos[\phi(t)+\Theta_{RV}]\ \}$$

$$= \frac{1}{8}\,[2\sin 2\Theta_{RV}J_o(\phi_o)-\sin\ 4\Theta_{RV}J_o(2\phi_o\cos\ \frac{\omega_a\tau}{2}\ )] \tag{43}$$

$$\tilde{E}_5 = E\{\tilde{H}_{HH}\tilde{H}^*_{HV}\}=E\{\sin^2[\phi(t+\tau)+\Theta_{RV}]\sin[\phi(t)+\Theta_{RV}]\cos[\phi(t)+\Theta_{RV}]\ \}$$

$$= \frac{1}{8}\,[2\sin 2\Theta_{RV}J_o(\phi_o)\ +\ \sin\ 4\Theta_{RV}\ J_o\ (2\phi_o\cos\ \frac{\omega_a\tau}{2}\ )\ ] \tag{44}$$

$$\tilde{E}_6 = E\{\tilde{H}_{HH}\tilde{H}^*_{HH}\} = E\,\{\cos^2[\phi(t+\tau)+\Theta_{RV}]\cos^2[\phi(t)+\Theta_{RV}]\} \tag{45}$$

$$= \frac{1}{8}\,[2 + J_o(2\phi_o \sin \frac{\omega_a\tau}{2}) + \cos 4\Theta_{RV}\, J_o(2\phi_o \cos \frac{\omega_a\tau}{2}) + $$

$$+ 4 \cos 2\Theta_{RV}\, J_o(\phi_o)\,] \tag{46}$$

Thus for:

$$\tilde{E}_{\alpha 1} = E\,\{\tilde{H}_{VV}\,\tilde{H}^*_{VV}\}K_\alpha(\tau) \qquad \tilde{E}_{\alpha 3} = E\,\{\tilde{H}_{VV}\,\tilde{H}^*_{HH}\}K_\alpha(\tau)$$

$$\tilde{E}_{\alpha 2} = E\,\{\tilde{H}_{VV}\,\tilde{H}^*_{VH}\}K_\alpha(\tau) \qquad \tilde{E}_{\alpha 4} = E\,\{\tilde{H}_{VV}\,\tilde{H}^*_{HV}\}K_\alpha(\tau)$$

$$\tilde{E}_{\alpha 5} = E\,\{\tilde{H}_{HH}\,\tilde{H}^*_{HV}\}K_\alpha(\tau) \qquad \tilde{E}_{\alpha 6} = E\,\{\tilde{H}_{HH}\,\tilde{H}^*_{HH}\}K_\alpha(\tau)$$

$$\tilde{\mathbf{K}}_{DR}\,(\tau,\,\lambda) =$$

$$\begin{bmatrix} \begin{bmatrix} \tilde{E}_{\alpha 1} & \tilde{E}_{\alpha 4} \\ \tilde{E}_{\alpha 4} & \tilde{E}_{\alpha 2} \end{bmatrix} & \begin{bmatrix} \tilde{E}_{\alpha 4} & \tilde{E}_{\alpha 3} \\ \tilde{E}_{\alpha 2} & \tilde{E}_{\alpha 5} \end{bmatrix} \\ \begin{bmatrix} \tilde{E}_{\alpha 4} & \tilde{E}_{\alpha 2} \\ E_{\alpha 3} & E_{\alpha 5} \end{bmatrix} & \begin{bmatrix} \tilde{E}_{\alpha 2} & \tilde{E}_{\alpha 5} \\ E_{\alpha 5} & E_{\alpha 6} \end{bmatrix} \end{bmatrix} \tag{47}$$

This completes the computation of $\tilde{\mathbf{K}}_{DR}\,(\tau,\,\lambda)$.

D. OPTIMUM RECEIVER - UNIFORM DOPPLER RANGE INVARIANT CLUTTER

When solving for the special case of optimum receiver, if it is assumed that the clutter has a range invariant tensor correlation or scattering function and extends beyond the range of a possible target, then:

$$\tilde{\ell}_o \triangleq \int_{-\infty}^{\infty} \tilde{\mathbf{r}}^T(t)\ \tilde{\mathbf{g}}^*(t)\ dt$$

In order to compute $\tilde{\ell}_o$ it is necessary to solve for $\tilde{\mathbf{r}}(t)$ and $\tilde{\mathbf{g}}(t)$. The matrix of $\tilde{\mathbf{r}}(t)$ can be determined directly from (11) and (14). The matrix of $\tilde{\mathbf{g}}(t)$ is determined from (48), where the only unknown is $\mathbf{S}_{n_c}(\omega)$.

$$\tilde{\mathbf{g}}(t) \longleftrightarrow \tilde{\mathbf{G}}(\omega) = [N_o\ \mathbf{I} + \tilde{\mathbf{S}}_{n_c}(\omega)]^{-1} \tilde{\mathbf{F}}(\omega) \tag{48}$$

where $\tilde{\mathbf{g}}(t)$ = modulating function for multiple-channel systems.

N_o = thermal noise of receiver

$\tilde{\mathbf{F}}(\omega)$ = $\mathcal{F}\ \{\tilde{\mathbf{f}}(t)\}$

$$\tilde{\mathbf{S}}_{n_c}(\omega) = \int_{-\infty}^{\infty} \tilde{\mathbf{F}}^T(\alpha)\ \tilde{\mathbf{S}}_{du}(\omega - \alpha)\ \tilde{\mathbf{F}}^*(\alpha)\, d\alpha \tag{49}$$

$\tilde{\mathbf{S}}_{n_c}(\omega)$ is computed as follows:

$\tilde{\mathbf{K}}_{n_c}(t) \longleftrightarrow \tilde{\mathbf{S}}_{n_c}(\omega)$ = Fourier of clutter covariance function.

NOTE: For range and time invariant functions of $\tilde{\mathbf{K}}_{DR}(\tau, \lambda)$,

$$\tilde{\mathbf{K}}_{DR} = \tilde{\mathbf{K}}_{DU}$$

where $\tilde{\mathbf{S}}_{DU} = \tilde{\mathbf{S}}_{DR} = \mathcal{F}\ \{\tilde{\mathbf{K}}_{DR}\}$

Therefore:

$$\mathbf{S}_{DU}(\omega,\lambda) = \begin{bmatrix} \begin{bmatrix} \xi_{\alpha 1} & \xi_{\alpha 4} \\ \xi_{\alpha 4} & \xi_{\alpha 2} \end{bmatrix} & \begin{bmatrix} \xi_{\alpha 4} & \xi_{\alpha 3} \\ \xi_{\alpha 2} & \xi_{\alpha 5} \end{bmatrix} \\ \begin{bmatrix} \xi_{\alpha 4} & \xi_{\alpha 2} \\ \xi_{\alpha 3} & \xi_{\alpha 5} \end{bmatrix} & \begin{bmatrix} \xi_{\alpha 2} & \xi_{\alpha 5} \\ \xi_{\alpha 5} & \xi_{\alpha 6} \end{bmatrix} \end{bmatrix} \qquad (50)$$

for:

$$\xi_{\alpha 1} = \frac{N\sigma_d{}^2}{8}[F\{\xi_4\}+\cos 4\Theta_{RV}\, F\{\xi_2\}+ F\{\xi_1\}-4\cos 2\Theta_{RV}\, F\{\xi_3\}]$$

$$\xi_{\alpha 2} = \frac{N\sigma_d{}^2}{8}[F\{\xi_1\}-\cos 4\Theta_{RV}\, F\{\xi_2\}]$$

$$\xi_{\alpha 3} = \frac{N\sigma_d{}^2}{8}[F\{\xi_4\}-F\{\xi_1\}-\cos 4\Theta_{RV}\, F\{\xi_2\}]$$

$$\xi_{\alpha 4} = \frac{N\sigma_d{}^2}{8}[2\sin 2\Theta_{RV}\, F\{\xi_3\}-\sin 4\Theta_{RV}\, F\{\xi_2\}]$$

$$\xi_{\alpha 5} = \frac{N\sigma_d{}^2}{8}[2\sin 2\Theta_{RV}\, F\{\xi_3\}+\sin 4\Theta_{RV}\, F\{\xi_2\}]$$

$$\xi_{\alpha 6} = \frac{N\sigma_d{}^2}{8}[F\{\xi_4\}+F\{\xi_1\}+\cos 4\Theta_{RV}\, F\{\xi_2\}+4\cos 2\Theta_{RV}\, F\{\xi_3\}]$$

where:

$$F\{\xi_1\}=T_c\sum_{n=o}^{\infty}\frac{\phi_o^{2n}\,(-1)^n}{2^{2n-1}(n!)^2}\sum_{i=o}^{n}\binom{2n}{i}(-1)^i\,[A+B]\Big|_{\omega=\omega-\alpha}$$

NOTE: ! represents factorial notation

$$F\{\xi_2\}=T_c \sum_{n=o}^{\infty} \frac{\phi_o^{2n} (-1)^n}{2^{2n-1} (n!)^2} \sum_{i=o}^{n} \binom{2n}{i} [A+B] \Big|_{\omega = \omega - \alpha}$$

$$F\{\xi_3\}= \frac{2T_c}{1+T_c^2\omega^2} \sum_{n=o}^{\infty}(-1)^n \frac{\phi_o^{2n}}{2^{2n}(n!)^2} \Big|_{\omega = \omega - \alpha}$$

$$F\{\xi_4\}= \frac{4T_c}{1+T_c^2\omega^2} \Big|_{\omega = \omega - \alpha}$$

$$\text{for } [A+B]= \left[\frac{1}{1+T_c^2[\omega+(n-i)\omega_\alpha]^2} + \frac{1}{1+T_c^2[\omega-(n-i)\omega_\alpha]^2} \right]$$

Now let

$$F_V\{\beta\} = F\{\sum_{R=-\infty}^{\infty} \alpha (t-RT) \cos \omega_1 (t-RT)\}$$

$$F_H\{\beta\} = F\{\sum_{R=-\infty}^{\infty} \alpha (t-RT) \cos \omega_2 (t-RT)\}$$

$$\text{where } F_V\{\beta\}=\tau \sum_{R=-\infty}^{\infty} \left[\frac{\sin(\omega-\omega_1)\frac{\tau}{2}}{(\omega-\omega_1)\frac{\tau}{2}} + \frac{\sin(\omega+\omega_1)\frac{\tau}{2}}{(\omega+\omega_1)\frac{\tau}{2}} \right] \delta\left(\omega - \frac{2\pi R}{T}\right) \qquad (51)$$

$$\mathcal{F}_H\{\beta\}=\tau \sum_{R=-\infty}^{\infty} \left[\frac{\sin(\omega-\omega_2)\frac{\tau}{2}}{(\omega-\omega_2)\frac{\tau}{2}} + \frac{\sin(\ + \ _2)\frac{\tau}{2}}{(\omega+\omega_2)\frac{\tau}{2}} \right] \delta\left(\omega - \frac{2\pi R}{T}\right) \qquad (52)$$

Then for $\mathcal{F}_H\{\beta\}\Big|_{\omega=\alpha}$, $\mathcal{F}_V\{\beta\}\Big|_{\omega=\alpha}$

$$\tilde{S}_{nc}(\omega) = \begin{vmatrix} \tilde{S}_{11} & \tilde{S}_{12} \\ \tilde{S}_{21} & \tilde{S}_{22} \end{vmatrix} \qquad (53)$$

for

$$\left.\begin{aligned} \tilde{S}_{11}(\omega) &= \\ \tilde{S}_{12}(\omega) &= \\ \tilde{S}_{21}(\omega) &= \\ \tilde{S}_{22}(\omega) &= \end{aligned}\right\} \quad \text{Independent solution follows}$$

Thus:

$$\tilde{S}_{11}(\omega)=T_c\,\frac{\sigma_o\sigma_d\tau^2}{8}\left\{\sum_{R=-\infty}^{\infty}\left(\frac{\sin(\frac{2\pi R}{T}-\omega_1)\frac{\tau}{2}}{(\frac{2\pi R}{T}-\omega_1)\ \frac{\tau}{2}} + \frac{\sin(\frac{2\pi R}{T}+\omega_1)\frac{\tau}{2}}{(\frac{2\pi R}{T}-\omega_1)\ \frac{\tau}{2}}\right)^2\right. \Bigg[$$

$$\frac{4}{1+T_c^2(\omega-\frac{2\pi R}{T})^2} + \cos 4\Theta_{RV}\sum_{n=o}^{\infty}(-1)^n\frac{\phi_o^{2n}}{2^{2n-1}(n!)^2}\sum_{i=o}^{n}\binom{2n}{i}\left(\frac{1}{1+T_c^2[(\omega-\frac{2\pi R}{T})+(n-i)\omega_\alpha]^2}\right. +$$

$$+ \frac{1}{1+T_c^2[(\omega-\frac{2\pi R}{T})-(n-i)\omega_\alpha]^2}\Bigg) + \sum_{n=o}^{\infty}(-1)^n \frac{\phi_o^{2n}}{2^{2n-1}(n!)^2} \sum_i \binom{2n}{i}(-1)^i$$

$$\left(\frac{1}{1+T_c^2[(\omega-\frac{2\pi R}{T})+(n-i)\omega_\alpha]^2} + \frac{1}{1+T_c^2[(\omega-\frac{2\pi R}{T})-(n-i)\omega_\alpha]^2}\right) - 8\cos 2\Theta_{RV}$$

$$\sum_{n=o}^{\infty}(-1)^n \frac{\phi_o^{2n}}{2^{2n}(n!)^2}\left(\frac{1}{1+T_c(\omega-\frac{2\pi R}{T})^2}\right] + \sum_{R=-\infty}^{\infty}$$

$$\left(\frac{\sin(\frac{2\pi R}{T}-\omega_2)\frac{\tau}{2}}{(\frac{2\pi R}{T}-\omega_2)\frac{\tau}{2}} + \frac{\sin(\frac{2\pi R}{T}+\omega_2)\frac{\tau}{2}}{(\frac{2\pi R}{T}+\omega_2)\frac{\tau}{2}}\right)\left[\sum_{n=o}^{\infty}\frac{\psi_o^{2r}}{2^{2n-1}(n!)^2}\sum_{n=o}^{n}\binom{2n}{i}(-1)^8\right.$$

$$\left(\frac{1}{1+T_c^2[(\omega-\frac{2\pi R}{T})+(n-i)\omega_\alpha]^2} + \frac{1}{1+T_c^2[(\omega-\frac{2\pi R}{T})-(n-i)\omega_\alpha]^2}\right) - \cos 4\Theta_{RV}$$

$$\sum_{n=o}^{\infty}(-1)^n \frac{\phi_o^{2n}}{2^{n-1}(n!)^2}\cdot\sum_{i=o}^{n}\binom{2n}{i}\left(\frac{1}{1+T_c^2[(\omega-\frac{2\pi R}{T})+(n-i)\omega_\alpha]^2}\right. +$$

$$\left.\left.\frac{1}{1+T_c^2[(\omega-\frac{2\pi R}{T})-(n-i)\omega_\alpha]^2}\right)\right] +$$

$$+2\sum_{R=-\infty}^{\infty}\left(\frac{\sin\left(\frac{2\pi R}{T}-\omega_1\right)\frac{\tau}{2}}{\left(\frac{2\pi R}{T}-\omega_1\right)\frac{\tau}{2}}+\frac{\sin\left(\frac{2\pi R}{T}+\omega_1\right)\frac{\tau}{2}}{\left(\frac{2\pi R}{T}+\omega_1\right)\frac{\tau}{2}}\right)\left(\frac{\sin\left(\frac{2\pi R}{T}-\omega_2\right)\frac{\tau}{2}}{\left(\frac{2\pi R}{T}-\omega_2\right)\frac{\tau}{2}}+\frac{\sin\left(\frac{2\pi R}{T}+\omega_2\right)\frac{\tau}{2}}{\left(\frac{2\pi R}{T}+\omega_2\right)\frac{\tau}{2}}\right).$$

$$\cdot\left[4\sin 2\Theta_{RV}\sum_{n=o}^{\infty}(-1)^n\frac{\phi_o^{2n}}{2^n(n!)^2}\left(\frac{1}{1+T_c^2\left(\omega-\frac{2\pi R}{T}\right)^2}\right)-\sin 4\Theta_{RV}\sum_{n=o}^{\infty}(-1)^n\right.$$

$$\left.\frac{\phi_o^{2n}}{2^{2n-1}(n!)^2}\sum_{i=o}^{n}\binom{2n}{i}\left(\frac{1}{1+T_c^2\left[\left(\omega-\frac{2\pi R}{T}\right)(n-i)\omega_\alpha\right]^2}+\frac{1}{1+T_c^2\left[\left(\omega-\frac{2\pi R}{T}\right)-(n-i)\omega_\alpha\right]^2}\right)\right]\Bigg\}$$

$$\tilde{S}_{12}(\omega)=\frac{T_c\sigma_o\sigma_d\tau^2}{8}\left\{\sum_{R=-\infty}^{\infty}\left(\frac{\sin\left(\frac{2\pi R}{T}-\omega_1\right)\frac{\tau}{2}}{\left(\frac{2\pi R}{T}-\omega_1\right)\frac{\tau}{2}}+\frac{\sin\left(\frac{2\pi R}{T}+\omega_1\right)\frac{\tau}{2}}{\left(\frac{2\pi R}{T}+\omega_1\right)\frac{\tau}{2}}\right)^2\right.\left[4\sin 2\Theta_{RV}\right.$$

$$\sum_{n=o}^{\infty}(-1)^n\frac{\phi_o^{2n}}{2^{2n}(n!)^2}\cdot\left(\frac{1}{1+T_c^2\left(\omega-\frac{2\pi R}{T}\right)^2}\right)-\sin 4\Theta_{RV}\sum_{i=o}^{n}\binom{2n}{i}$$

$$\left.\left(\frac{1}{1+T_c^2\left[\left(\omega-\frac{2\pi R}{T}\right)+(n-i)\omega_\alpha\right]^2}+\frac{1}{1+T_c^2\left[\left(\omega-\frac{2\pi R}{T}\right)-(n-i)\omega_\alpha\right]^2}\right)\right]+\sum_{R=-\infty}^{\infty}$$

$$\left(\frac{\sin\left(\frac{2\pi R}{T}-\omega_1\right)\frac{\tau}{2}}{\left(\frac{2\pi R}{T}-\omega_1\right)\frac{\tau}{2}}+\frac{\sin\left(\frac{2\pi R}{T}+\omega_1\right)\frac{\tau}{2}}{\left(\frac{2\pi R}{T}+\omega_1\right)\frac{\tau}{2}}\right)\left(\frac{\sin\left(\frac{2\pi R}{T}-\omega_2\right)\frac{\tau}{2}}{\left(\frac{2\pi R}{T}-\omega_2\right)\frac{\tau}{2}}+\frac{\sin\left(\frac{2\pi R}{T}+\omega_2\right)\frac{\tau}{2}}{\left(\frac{2\pi R}{T}+\omega_2\right)\frac{\tau}{2}}\right)$$

$$\left[\frac{4}{1+T_c^2\left(\omega-\frac{2\pi R}{T}\right)^2}-2\cos 4\Theta_{RV}\sum_{n=o}^{\infty}(-1)^n\frac{\phi_o^{2n}}{2^{2n-1}(n!)^2}\sum_{i=o}^{n}\binom{2n}{i}\right.$$

$$\left.\left(\frac{1}{1+T_c^2\left[\left(\omega-\frac{2\pi R}{T}\right)+(n-i)\omega_\alpha\right]^2}+\frac{1}{1+T_c^2\left[\left(\omega-\frac{2\pi R}{T}\right)-(n-i)\omega_\alpha\right]^2}\right)\right]+\sum_{R=-\infty}^{\infty}$$

$$\left(\frac{\sin\left(\frac{2\pi R}{T}-\omega_2\right)\frac{\tau}{2}}{\left(\frac{2\pi R}{T}-\omega_2\right)\frac{\tau}{2}}+\frac{\sin\left(\frac{2\pi R}{T}+\omega_2\right)\frac{\tau}{2}}{\left(\frac{2\pi R}{T}+\omega_2\right)\frac{\tau}{2}}\right)^2\left[4\sin 2\Theta_{RV}\sum_{n=o}^{\infty}(-1)^n\frac{\phi_o^{2n}}{2^{2n}(n!)^2}\right.$$

$$\left(\frac{1}{1+T_c^2\left(\omega-\frac{2\pi R}{T}\right)^2}\right)+\sin 4\Theta_{RV}\sum_{n=o}^{\infty}(-1)^n\frac{\phi_o^{2n}}{2^{2n-1}(n!)^2}\sum_{i=o}^{\infty}\binom{2n}{i}$$

$$\left.\left(\frac{1}{1+T_c^2\left[\left(\omega-\frac{2\pi R}{T}\right)+(n-i)\omega_\alpha\right]^2}+\frac{1}{1+T_c^2\left[\left(\omega-\frac{2\pi R}{T}\right)-(n-i)\omega_\alpha\right]^2}\right)\right]\Bigg\}$$

$$\tilde{S}_{21}(\omega) = \frac{T_c\sigma_o\sigma_d\tau^2}{8}\left\{\sum_{R=-\infty}^{\infty}\left(\frac{\sin(\frac{2\pi R}{T}-\omega_1)\frac{\tau}{2}}{(\frac{2\pi R}{T}-\omega_1)\frac{\tau}{2}}+\frac{\sin(\frac{2\pi R}{T}+\omega_1)\frac{\tau}{2}}{(\frac{2\pi R}{T}+\omega_1)\frac{\tau}{2}}\right)^2\right[4\sin 2\Theta_{RV}$$

$$\sum_{n=o}^{\infty}(-1)^n \cdot \frac{\phi_o^{2n}}{2^{2n}(n!)^2}\left(\frac{1}{1+T_c^2(\omega-\frac{2\pi R}{T})^2}\right) - \sin 4\Theta_{RV}\sum_{n=o}^{\infty}(-1)^n\frac{\phi_o^{2n}}{2^{n-1}(n!)^2}$$

$$\left.\sum_{i=o}^{n}\binom{2n}{i}\left(\frac{1}{1+T_c^2[(\omega-\frac{2\pi R}{T})+(n-i)\omega_\alpha]^2}+\frac{1}{1+T_c^2[(\omega-\frac{2\pi R}{T})-(n-i)\omega_\alpha]^2}\right)\right]$$

$$\sum_{R=-\infty}^{\infty}\left(\frac{\sin(\frac{2\pi R}{T}-\omega_2)\frac{\tau}{2}}{(\frac{2\pi R}{T}-\omega_2)\frac{\tau}{2}}+\frac{\sin(\frac{2\pi R}{T}+\omega_2)\frac{\tau}{2}}{(\frac{2\pi R}{T}+\omega_2)\frac{\tau}{2}}\right)\left[4\sin 2\Theta_{RV}\right.$$

$$\sum_{n=o}^{\infty}(-1)^n\frac{\phi_o^{2n}}{2^{2n}(n!)^2}\left(\frac{1}{1+T_c^2(\omega-\frac{2\pi R}{T})^2}\right) + \sin 4\Theta_{RV}\sum_{n=o}^{\infty}(-1)\frac{\phi_o^{2n}}{2^{2n-1}(n!)^2}$$

$$\left.\sum_{i=o}^{\infty}\binom{2n}{i}\left(\frac{1}{1+T_c^2[(\omega-\frac{2\pi R}{T})+(n-i)\omega_\alpha]^2}+\frac{1}{1+T_c^2[(\omega-\frac{2\pi R}{T})-(n-i)\omega_\alpha]^2}\right)\right] +$$

$$\sum_{R=-\infty}^{\infty}\left(\frac{\sin(\frac{2\pi R}{T}-\omega_1)\frac{\tau}{2}}{(\frac{2\pi R}{T}-\omega_1)\frac{\tau}{2}}+\frac{\sin(\frac{2\pi R}{T}+\omega_1)\frac{\tau}{2}}{(\frac{2\pi R}{T}+\omega_1)\frac{\tau}{2}}\right)\left(\frac{\sin(\frac{2\pi R}{T}-\omega_2)\frac{\tau}{2}}{(\frac{2\pi R}{T}-\omega_2)\frac{\tau}{2}}+\frac{\sin(\frac{2\pi R}{T}+\omega_2)\frac{\tau}{2}}{(\frac{2\pi R}{T}+\omega_2)\frac{\tau}{2}}\right)$$

$$\left[\frac{4}{1+T_c^2(\omega-\frac{2\pi R}{T})^2} - 2\cos 4\Theta_{RV} \sum_{n=o}^{\infty}(-1)^n \frac{\phi_o}{2^{2n-1}(n!)^2} \sum_{i=o}^{\infty}\binom{2n}{i}\right.$$

$$\left.\left(\frac{1}{1+T_c^2[(\omega-\frac{2\pi R}{T})+(n-i)\omega_\alpha]^2} + \frac{1}{1+T_c^2[(\omega-\frac{2\pi R}{T})-(n-i)\omega_\alpha]^2}\right)\right]\Bigg\}$$

$$\tilde{S}_{22}(\omega) = \frac{T_c\sigma_o\sigma_c\tau^2}{8}\left\{\sum_{R=-\infty}^{\infty}\left(\frac{\sin(\frac{2\pi R}{T}-\omega_1)\frac{\tau}{2}}{(\frac{2\pi R}{T}-\omega_1)\frac{\tau}{2}} + \frac{\sin(\frac{2\pi R}{T}+\omega_1)\frac{\tau}{2}}{(\frac{2\pi R}{T}+\omega_1)\frac{\tau}{2}}\right)^2\right.$$

$$\left[\sum_{n=o}^{\infty}\frac{\phi_o^{2n}}{2^{2n-1}(n!)^2}\sum_{i-o}^{n}\binom{2n}{i}(-1)^i\left(\frac{1}{1+T_c^2[(\omega-\frac{2\pi R}{T})+(n-i)\omega_\alpha]^2}\right.\right. +$$

$$\left.\frac{1}{1+T_c^2[(\omega-\frac{2\pi R}{T})-(n-i)\omega_\alpha]^2}\right) - \cos 4\Theta_{RV}\cdot\sum_{n=o}^{\infty}(-1)^n\frac{\phi_o^{2n}}{2^{2n-1}(n!)^2}\sum_{i=o}^{n}\binom{2n}{i}$$

$$\left.\left(\frac{1}{1+T_c^2[(\omega-\frac{2\pi R}{T})+(n-i)\omega_\alpha]^2} + \frac{1}{1+T_c^2[(\omega-\frac{2\pi R}{T})-(n-i)\omega_\alpha]^2}\right)\right] + \sum_{R=-\infty}^{\infty}$$

$$\left(\frac{\sin(\frac{2\pi R}{T}-\omega_1)\frac{\tau}{2}}{(\frac{2\pi R}{T}-\omega_1)\frac{\tau}{2}} + \frac{\sin(\frac{2\pi R}{T}+\omega_1)\frac{\tau}{2}}{(\frac{2\pi R}{T}+\omega_1)\frac{\tau}{2}}\right)\left(\frac{\sin(\frac{2\pi R}{T}-\omega_2)\frac{\tau}{2}}{(\frac{2\pi R}{T}-\omega_2)\frac{\tau}{2}} + \frac{\sin(\frac{2\pi R}{T}+\omega_2)\frac{\tau}{2}}{(\frac{2\pi R}{T}+\omega_2)\frac{\tau}{2}}\right)$$

$$\left[4\sin 2\Theta_{RV} \sum_{n=o}^{\infty}(-1)^n \frac{\phi_o^{2n}}{2^{2n}(n!)^2}\left(\frac{1}{1+T_c^2(\omega-\frac{2\pi R}{T})^2}\right)+2\sin 4\Theta_{RV}\right.$$

$$\sum_{n=o}^{\infty}(-1)^n \frac{\phi_o^{2n}}{2^{2n-1}(n!)^2} \sum_{i=o}^{n}\binom{2n}{i}\left(\frac{1}{1+T_c^2[(\omega-\frac{2\pi R}{T})+(n-i)\omega_\alpha]^2}+\right.$$

$$\left.\left.\frac{1}{1+T_c^2[(\omega-\frac{2\pi R}{T})-(n-i)\omega_\alpha]^2}\right)\right] + \sum_{R=-\infty}^{\infty}\left(\frac{\sin(\frac{2\pi R}{T}-\omega_2)\frac{\tau}{2}}{(\frac{2\pi R}{T}-\omega_2)\frac{\tau}{2}} +\right.$$

$$\left.\frac{\sin(\frac{2\pi R}{T}+\omega_2)\frac{\tau}{2}}{(\frac{2\pi R}{T}+\omega_2)\frac{\tau}{2}}\right)^2 \left[\frac{1}{1+T_c^2(\omega-\frac{2\pi R}{T})^2} + \sum_{n=o}^{\infty}\frac{\phi_o^{2n}}{2^{2n-1}(n!)^2}\sum_{i=o}^{n}\binom{2n}{i}(-1)^i\right.$$

$$\left(\frac{1}{1+T_c^2[(\omega-\frac{2\pi R}{T})+(n-i)\omega_\alpha]^2} + \frac{1}{1+T_c^2[(\omega-\frac{2\pi R}{T})-(n-i)\omega_\alpha]^2}\right)+$$

$$\cos 4\Theta_{RV} \sum_{n=o}^{\infty} (-1)^n \frac{\phi_o^{2n}}{2^{2n-1}(n!)^2} \sum_{i=o}^{\infty} \binom{2n}{i} \left(\frac{1}{1+T_c^2[(\omega - \frac{2\pi R}{T}) + (n-i)\omega_\alpha]^2} + \right.$$

$$\left. \frac{1}{1+T_c^2[(\omega - \frac{2\pi R}{T}) - (n-i)\omega_\alpha]^2} \right) + 8\cos 2\Theta_{RV} \sum_{n=o}^{\infty} (-1)^n \frac{\phi_o^{2n}}{2^{2n}(n!)^2}$$

$$\left. \left(\frac{1}{1+T_c^2(\omega - \frac{2\pi R}{T})^2} \right) \quad \right] \Bigg\}$$

V. CONCLUSIONS

It has been the intent of this work to provide a unified analysis of clutter suppression through the radar polarization process.

The models used for $\tilde{\mathbf{f}}(t)$ and $\tilde{\mathbf{b}}(t, \lambda)$ were based on the premise that

a.) The optimal low pass equivalent transmit waveform was of the type commonly used and b.) the scattering matrix was assumed to be a vector function describing the physical phenomena pertaining to a slow fluctuating point target (with zero mean complex Gaussian random elements) as seen from the radar.

The choices of the aforementioned mathematical models have not been proven either correct nor incorrect, simply because the implementation of the final equations was not completed due to lack of sufficient time.

As it has been shown, the partial solutions attained reflect a very high degree of mathematical complexities and it is the author's opinion that there might not be any easier method of solution.

Most likely only few terms of the long equations are necessary and important for the final solutions; however without this knowledge, complete solutions are necessary.

The indicated complexities should not be a deterrent as per the model used and the methodology followed. The final implementation of the solutions could, very well, determine the feasibility of the approach followed.

SUGGESTIONS:

Additional choice for $K_\alpha(\tau)$ and $\tilde{H}(t, \lambda)$ are listed below. They should be tested and compared with respect to the method used in this work.

i.e. $K_\alpha(\tau) = \sigma_0 e^{-\frac{\tau^2}{2T_c{}^2}}$

$$\text{or}\quad K_\alpha(\tau) = \begin{cases} \sigma_o \cos 2\pi\, \tau/T_c; & -\frac{T_c}{4} < t < \frac{T_c}{4} \\ o\ ; \text{ elsewhere.} \end{cases}$$

$$\tilde{H}_{VV} = \sqrt{.9}\ \lambda \cos^2 [\phi(t)]$$

$$\tilde{H}_{HH} = \sqrt{.9}\ \lambda \sin^2 [\phi(t)]$$

$$\tilde{H}_{HV} = \tilde{H}_{VH} = \sqrt{.9}\ \lambda \sin [\phi(t)] \cos [\phi(t)]$$

$$\text{for}\quad \phi(t) = \frac{\phi_o}{2} \sin \omega_\alpha t$$

Another possible way of physically determining the $\tilde{\mathbf{H}}$ matrix, would be to use photography in monitoring the free-falling chaff. This visual aid could, as well, give a real life representation of the phenomenon, from which to derive the scattering matrix.

V. REFERENCES:

[1] Van Trees, H. L., "Detection, Estimation and Modulation Theory", Part 3, Wiley, New York, 1971.

[2] Vannicola, Vincent, "Radar Polarization Processing for Clutter Suppression", RADC/OI - 1978 Report.

[3] Poelman, A. J., "Cross Correlation of Orthogonally Polarized Backscatter", IEEE AES-12, No. 6, pp 674 - 682.

[4] Varshanchuk, M. L. and Kobak, V. O., "Cross Correlation of Orthogonally Polarized Components of Electromagnetic Field, Scattered by an Extended Object", Radio Eng. Electron Phys., Vol 16, pp 201 - 205, February 1971.

[5] Deschamps, G., "Geometrical Representation of the Polarization of a Plane Electromagnetic Wave", Proc. IRE Vol 39 pp 543, May 1951.

[6] IRE Standards on Radio Aids to Navigation: "Definition Terms", 1954; Proc. IRE, Vol 43, pp 194, Feb 1955.

[7] Morse, P. M. and Feshbach, H.; "Methods of Theoretical Physics", Vol 2 New York, McGraw Hill 1953, pp 1886 - 1887.

ACKNOWLEDGEMENT

The author wishes to thank Messrs. V. C. Vannicola, C. Silfer and Mrs. P. Kelley from RADC/OCTS; Mr. J. Huss from RADC/XP and Mr. F. O'Brien from Auburn University for their professional help and encouragement in the course of this investigation.

1978 USAF-ASEE SUMMER FACULTY RESEARCH PROGRAM
sponsored by
THE AIR FORCE OFFICE OF SCIENTIFIC RESEARCH
conducted by
AUBURN UNIVERSITY AND OHIO STATE UNIVERSITY

PARTICIPANT'S FINAL REPORT

MEASUREMENT OF PHOTODISSOCIATION CROSS SECTIONS OF WATER CLUSTER IONS

Prepared by:	Timothy F. Thomas, PhD.
Academic Rank:	Associate Professor
Department and University:	Department of Chemistry Univ. of Missouri-Kansas City Kansas City, MO 64110
Assignment:	Hanscom AFB, MA 01731 Air Force Geophysics Lab. Aeronomy Division Atmospheric Structure Branch
Research Colleague:	John F. Paulson, PhD.

Date:	August 25, 1978
Contract No.:	F44620-75-C-0031

MEASUREMENT OF PHOTODISSOCIATION CROSS SECTIONS
OF WATER CLUSTER IONS

by

Timothy F. Thomas

ABSTRACT

Photodissociation cross sections have been measured for $H_3O^+\cdot(H_2O)_n$, n=1 and 2, and it has been concluded that these species are photochemically stable for wavelengths $\lambda \geq 264.9$ nm. Measurements on the photodissociation of $OH^-\cdot H_2O$ led to the same conclusion for $\lambda \geq 513.4$ nm, but some unexplained results were obtained when the quadrupole mass spectrometer used to analyze the photo-fragments was biased to exclude OH^-.

LIST OF TABLES

INTRODUCTION AND OBJECTIVES

The initial objective was to measure the photodissociation cross sections of hydrated oxonium ions, $H_3O^+ \cdot (H_2O)_n$, whose importance in the lower ionosphere is well established (Ref.1 and 2). Previous attempts to obtain these cross sections in other laboratories, using discrete wavelengths between 377.1 nm and 676.4 nm, had been unsuccessful (Ref. 3-5). It was therefore intended to use the ion photodissociation apparatus at AFGL, which has a unique capability for measuring absolute cross sections in the UV with a tunable laser (Ref. 6), to look for photodissociation of $H_3O^+ \cdot (H_2O)_n$ at shorter wavelengths.

After completion of the experiments on the above positive cluster ions, it was decided to attempt to measure photodissociation cross sections for a negative cluster ion, $OH^- \cdot H_2O$. This ion is presumed to exist in the D-region of the ionosphere because of the known importance of OH^- in the chemistry of this region, but its detection by rocketborne mass spectrometers has been obscured by the presence of Cl^- ions (Ref. 7). Given that the known threshhold for the reaction

$$OH^- \cdot H_2O + h\nu \rightarrow OH + H_2O + e^- \qquad (1)$$

lies at ~ 420 nm (Ref. 8) and that the absorption spectrum (electronic transition) for OH^- begins at 679 nm (Ref. 9), it was reasoned that the photochemical process

$$OH^- \cdot H_2O + h\nu \rightarrow OH^- + H_2O \qquad (2)$$

should be observable between 420 and 679 nm. Process (2) becomes energetically possible for wavelengths shorter than 1,100 nm.

RESULTS

A. Photodissociation of $H_3O^+ \cdot (H_2O)_n$

Table 1 shows a sample of the results obtained while attempting to maximize the primary ion current for the various positive cluster ions in water vapor using a simple electron impact ion source. For the data shown in this table the electron beam was positioned ~ 2 mm behind the ion extraction hole. In later experiments, including those reported in Table 2, this distance was increased to 8 mm in an attempt to increase the current of cluster ions. Several experiments were made using a N_2 carrier gas bubbled through a reservoir of liquid H_2O, also in hopes of increasing the ion currents of the larger cluster ions, but this technique showed no advantage over directly evaporating the liquid water through a controlled leak.

TABLE 1

MASS SPECTRA OF H_2O VERSUS PRESSURE

Ion Currents in Nano-Amps

Ion	P_{H_2O} (μ) = 2.4*	15	52	75	99
H_2O^+	0.039	0.021	0.015	0.015	~0.02
H_3O^+	0.020	0.16	1.24	1.83	4.10
H_5O^+	--	--	0.032	0.14	0.69
$H_7O_3^+$	--	--	--	0.005	0.036

Conditions: Filament Current = 8.0A
Electron Energy = 80 V
Repeller = 0 V

* e^- beam ~ 2 mm back from exit hole, then moved to 8 mm back before 2nd run in Table 1.

Table 2 shows the results of several cross section measurements for photodissociation of $H_3O^+ . (H_2O)_n$, n=1 and 2. Combined with measurements made by T. L. Rose at AFGL shortly before this participant's arrival, these results led to the conclusion that $H_3O^+ . (H_2O)_n$, n=1 and 2, are photochemically stable for wavelengths $\geq$ 264.9 nm.

B. Photodissociation of $OH^- \cdot H_2O$

In order to detect negative ions, it was necessary to reconstruct the mounting of the electron multiplier so that its anode could be floated as high as + 4500V above ground. Problems with this mounting and subsequent arcing which adversely effected several electronic components, consumed too much time to permit completion of this part of the project. Tables 3 and 4 show the results which were obtained.

TABLE 2

PHOTODISSOCIATION CROSS SECTIONS FOR $H_3O^+ \cdot (H_2O)_n$

n	λ(nm)	P_{H_2O} (μ)	$10^9 \times i_p$ (A)	$10^{19} \times \sigma$ (cm^2)
1	264.9	∿90.	2.8	$\leq$ 1.9
1	266.9	44.	1.15	8.0 $\pm$ 6.5
1	266.9	55.	0.25	2.4 $\pm$ 6.1
2	266.9	68.*	0.58	1.2 $\pm$ 8.9
1	528.5	52.*	0.40	-0.3 $\pm$ 0.7

i_p = Primary ion current

P_{H_2O} = Pressure of H_2O in ion source

σ = Photodissociation cross section for production of H_3O^+

* Includes small contribution from N_2 carrier gas.

In Table 3 is a negative ion mass spectrum obtained from pure water vapor with the same ion source as for Tables 1 and 2, except that a piece of copper-beryllium alloy was added as a target for the electron beam (to generate secondary electrons), and the appropriate voltages on the mass spectrometer were reversed.

Table 4 lists the photodissociation cross sections measured for $OH^- \cdot H_2O$. As discussed below, only the first five entries are thought to be reliable. Thus it appears that, contrary to initial expectation, $OH^- \cdot H_2O$ is photochemically stable for wavelengths $\geq$ 513.4 nm. This may be because photodetachment of electrons occurs at longer wavelengths than previously believed (i.e., λ > 420 nm), or because the absorption spectrum of $OH^- \cdot H_2O$ is blue-shifted by more than 160 nm from that of OH^-, or possibly because the first electronically excited state of $OH^- \cdot H_2O$ is stable with respect to dissociation.

TABLE 3

NEGATIVE ION MASS SPECTRUM OF H_2O

Ion	$10^9 x\ i_p$ (A)
O^-	0.04
OH^-	0.41
$H_3O_2^-$	0.14
NO_2^- (?)	0.017
$H_5O_3^-$	0.051
NO_3^- (?)	0.017
$H_7O_4^-$	0.006

Conditions: $P_{H_2O} = 50\ \mu$

Electron Energy = 150 V

Repeller = 21.V

Filament Emission = 1.0×10^{-3}A

The last five experiments shown in Table 4 were done with a bias voltage on the rods of the quadrupole mass spectrometer (used to mass-analyze the photo-fragments) set sufficiently negative to deflect all ionized photoproducts from passing through to the detector*. The source of the excess ion (or electron) counts which led to the apparently non-zero cross sections in the last five entries is at present unknown. The possibility has been considered that an electric field penetrates into the ion-laser beam interaction region, so that photoproduct ions are produced from lower energy ions (lower than 289 eV), which are then accelerated, but this fails to explain why the cross sections (at the same

---

* The photofragments have $\sim\frac{17}{35}$ of the primary ion energy along the flight axis, on the average, or $\sim$140 eV. Setting the bias voltage to <-140 V (for negative ions) will therefore send the photofragment ions away from the detector.

TABLE 4

PHOTODISSOCIATION CROSS SECTIONS FOR $OH^{-} \cdot H_2O$

λ (nm)	P_{H_2O} (μ)	10^{10} x i_p (A)	V_p (V)	Pole Bias (V)	10^{19} x σ (cm^2)
650.2	52.	0.92	200.0	0	3.2 $\pm$ 2.5
650.2	63.	0.68	200.0	0	0.05 $\pm$ 0.19
635.1	61.	1.54	200.0	0	0.53 $\pm$ 0.78
528.6	65.	1.87	200.0	0	-0.26 $\pm$ 0.74
513.4	60.	1.47	200.0	0	-0.50 $\pm$ 1.20
548.1	65.	3.82	289.8	-191.6	5.1 $\pm$ 0.8
528.5	67.	2.44	289.8	-191.6	7.1 $\pm$ 1.9
528.6	64.	2.60	289.8	-191.6	6.5 $\pm$ 1.9
513.2	62.	4.37	289.8	-191.6	9.0 $\pm$ 1.2
503.6	64.	3.30	289.8	-191.6	6.0 $\pm$ 0.9

σ = cross section for formation of OH^{-}

V_P = Primary ion energy

Pole Bias = DC voltage on quadrupole rods

Conditons:

Repeller = -30V

Electron Energy = 150 V

Electron Multiplier: 1st Dynode = + 900 V

Anode = + 4500 V

Ion Deflector (oppostie 1st Dynode) = -400V.

wavelengths) are zero when the Pole Bias is set to zero. Another possibility, detection of fast neutrals formed by photodetachment, encounters the problem of explaining how the flight path of these neutrals can be bent to hit the off-axis electron multiplier.

Clearly more work can and should be done on the photodissociation of $OH^- \cdot H_2O$ with the present apparatus. The ion is a possible source of dominant atmospheric negative ions by fast ion-molecule reactions, and it is important to determine whether the photodissociation channel competes efficiently with these ion-molecule reactions.

REFERENCES

1. M.J.McEwan and L.F. Phillips, Chemistry of the Atmosphere, Wiley (1975), pp.174-181.

2. C.F. Sechrist, Jr., "The Ionospheric D Region", pp.102-116 in The Upper Atmosphere and Magnetosphere, National Academy of Science (1977).

3. W.R. Henderson and A.L. Schmeltekopf, J. Chem. Phys., 57, 4502 (1972).

4. R.A. Beyer and J.A. Vanderhoff, J. Chem. Phys., 65, 2313(1976); J.A. Vanderhoff, Tech. Rep. ARBRL-TR-02070(1978).

5. R.R. Burke and R.P. Wayne, Int. J. Mass Spectrom. Ion Phys., 25, 199(1977).

6. T.F. Thomas, F. Dale, and J.F. Paulson, J. Chem. Phys., 67,793(1977).

7. Ref. No. (1), pp. 181-188.

8. S. Golub and B. Steiner, J. Chem. Phys., 49, 5191(1968).

9. H. Hotop, T.A. Patterson, and W.C. Lineberger, J. Chem. Phys.,60, 1806(1974).

1978 USAF-ASEE SUMMER FACULTY RESEARCH PROGRAM
sponsored by
THE AIR FORCE OFFICE SCIENTIFIC RESEARCH
conducted by
AUBURN UNIVERSITY AND OHIO STATE UNIVERSITY

PARTICIPANT'S FINAL REPORT

A QUANTITATIVE APPROACH TO AGGREGATION IN THE MODELING OF TACTICAL COMMAND AND CONTROL SYSTEMS

Prepared by: Henry D'Angelo, Ph.D.

Academic Rank: Professor

Department and University: Mathematical Sciences
Memphis State University
Memphis, Tennessee 38152

Assignment: Hanscom AFB
Electronic Systems Division
Deputy for Development Plans

USAF Research Colleague: Donald B. Brick, Ph.D.

Date: August 25, 1978

Contract No.: F44620-75-C-0031

ABSTRACT

The application of modeling and simulation methods in the design and operation of tactical command, control, and communication systems (i.e., tactical C^3 systems) has been of little value, largely due to the enormous complexity of the problems involved in relation to the limitations of the present state-of-the-art in modeling and simulation. Tactical C^3 systems belong to the class of systems which are large scale, have system components for which fundamental system relationships are not well known, and which contain subsystems representing intelligent competing factions. There has been essentially no success in the application of modeling and simulation methods to other systems in this category and, as a result, there is little pertinent experience to draw on in addressing the tactical C^3 problems.

The basic problems in trying to model large-scale, poorly understood, competitive systems fall rather naturally into two categories:

(1) The need for reliable models for those poorly understood system components (e.g., man-machine interface, human interactions, jammed communication systems, etc.).

(2) The need for aggregation methods which lead to models useful for system design and the development of winning operational strategies. It is especially important that the aggregation be such that model limitations are difficult to identify from observations of the system outputs (i.e., the model outputs should be insensitive to excluded system dynamics).

This research, dealing with the aggregation process, addresses the latter category of problems.

An approach is proposed for the design of aggregated models which is based on the concept of structural sensitivity (i.e., the sensitivity of system variables to the cutting of a connecting link). Specifically, the dependency of important system variables to be preserved in the aggregated model on other system variables is represented by connecting links to a proposed aggregated model from another system generating these other variables. The proposed aggregation process is based on varying design parameters to minimize the sensitivity of the important system variables, which appear as outputs of the proposed agggregated model, to the cutting of the connecting links. Promising directions for continued research in this area are outlined.

ACKNOWLEDGMENTS

I am grateful to the Air Force Office of Scientific Research, the American Society for Engineering Education, and Auburn University for the opportunity afforded to me this summer. Special thanks are due Mr. Fred O'Brien, Program Director, who somehow manages to maintain his enthusiasm and dedication to the program in the face of a Herculean traveling schedule and an endless stream of difficult domestic and logistic problems.

One might expect to find researchers who are facing impending deadlines, disruptions due to vacationing staff, etc., somewhat terse, at the very least, in dealing with a "ten-weeker" who is not even slightly familiar with their problems. The fact that this was not generally the case is a credit to the generosity of the members of the ESD/XR group and the MITRE Corp. I am especially indebted to Capt. B. A. Eggers, R. A. Games, D. E. Howes, Major C. T. Jaglinski, K. R. Johnson, J. E. Kriegel, Capt. D. E. Kawamura, Lt.Colonel J. R. Garey, Capt. K. Voges, and R. P. Witt each of whom, at some point during my ten-week tenure, took time from busy schedules to either explain the fundamental of tactical systems, listen to and comment on my proposed research, provide me with key references, or in some other way help get me over a difficult hurdle. Dr. R. E. Lovell, who was also in the USAF-ASSEE Summer Faculty Research Program, was particularly helpful. Having already been here for three weeks at the time I arrived, he spared me much of the start-up trauma and immediately provided me with a valuable set of references.

I have especially valued my association with Dr. Donald B. Brick, Technical Director, who was my ESD/XR research colleague for the summer. He has been extremely helpful in solving problems at every level of detail, from arranging for office space to criticising my research effort. He has demonstrated that rare understanding of the stuff that research is made of and works efficiently to establish the necessary conditions.

I am most appreciative of the level of professionalism demonstrated by the secretarial staff here. Special thanks to Mrs. Bea Murphy and Mrs. Rose Burns, for the typing of this report, and to Mrs. Joyce Glavin, who typed my Mid-Point Progress Report.

INTRODUCTION

This research is addressed to the problems of applying modeling and simulation methods to the design and operation of tactical command, control, and communication systems (i.e., tactical C^3 systems). Tactical C^3 systems belong to that class of systems which are large scale, have system components for which the fundamental relations are not well known, and which contain subsystems representing intelligent competing factions. It seems safe to say that this class of systems represents the most difficult challenge for modeling and simulation. It is noteworthy that although there have been numerous modeling and simulation efforts in this area, this writer knows of no successful effort that has been subjected to the scrutiny of a careful validation.

It should be no surprise that large-scale, poorly-understood, competitive systems provide the modelors and simulators with their most difficult problem. Most significant is that any model used as a basis for a computer simulation must be highly aggregated. The process of aggregation involves the representation of large complex subsystems by small simple models for the purpose of either (1) reducing the size of the overall model to the point that computer simulation is possible or (2) characterizing poorly understood subsystems with simple relationships (e.g., simple statistical models, empirical table lookups, etc.) which are based on limited observations and educated speculations. The immutable weakness of such aggregated models when used for designing winning systems and winning strategies, are twofold:

1. Limiting the size of the model reduces both the number of observations that can be processed and the range of controls that are possible. Thus, the use of the model for either prediction or control is necessarily limited.

2. Most importantly, perhaps, an intelligent opponent can identify the model's limitations from observations of system responses and, consequently, take actions that are virtually invisible in the simulation and, thus, for which no counteraction is possible.

Clearly, if a simulation is to be used to design and operate tactical C^3 systems, the model on which such simulations are based must be kept secret. However, it may not be a simple matter to keep the model's limitations a secret during a battle. Strategic responses in a few confrontations could easily reveal important model deficiencies. In essence, the enemy would begin to identify the model used as the battle progresses. Thus, if an aggregated model is to be used for such a simulation, then special care must be taken in the design of such an aggregated model. It seems prudent that:

1. Necessary precautions be taken to assure that the enemy's understanding of fundamental relations characterizing important system

components be no better than our own.

2. The aggregation process used in reducing model size be such that the enemy's ability to identify the model during the course of battle be minimized.

Item 1 requires that basic research continue in trying to determine fundamental relations of important system components (e.g., human behavior in man/machine interfaces, communication systems under adverse conditions, etc.). Item 2 requires that the process of aggregation be studied with special attention being given to the competitive aspects of the problem. This research deals with the latter. In particular, this research addresses the problem of designing aggregated models whose outputs are the least sensitive to the dynamic modes of the real system that are excluded in the model.

OBJECTIVES

The objectives of this research effort are: (1) To develop measures of effectiveness for aggregated models based on the sensitivities of important system variables to variations in system structure; (2) To determine how such measures can be used as design parameters in designing aggregated models of large-scale competitive systems, such as tactical C^3 systems - the validity of such models will depend on the usefulness of the model in system design and in operations design; (3) To define promising directions of research likely to yield useful results with respect to difficult aggregation problems typical of those encountered in trying to model tactical C^3 systems.

BACKGROUND

There are growing convictions, as evidenced by increasing levels of effort, [1 through 15] that modeling and simulation should play a more important role in the decision making processes associated with tactical C^3 systems. Although there seems to be no agreement on what the exact role of modeling and simulation should be in tactical C^3, the rationale behind the increased effort in this area seems clear. Modeling and simulation have played an important role in other areas, particularly in the space program, in the design and evaluation of complex weaponry and communication systems, and in the design of complex logistical operations, and it seems reasonable to try to transfer some of this highly developed technology to the area of tactical C^3. An important question, of course, is whether or not the areas in which modeling and simulation have been successful have enough in common with tactical C^3 systems so that a reasonable payoff can be expected by a simple technology transfer. In particular, one must consider the possibility that the problems in designing and operating tactical C^3 systems are so different and so poorly understood that there is considerable fundamental research to be done before modeling and simulation will play a major role in tactical C^3. It is the opinion of this writer that the problems in analyzing

and designing tactical C^3 systems belong to a class of complex problems which will not yield to the present state-of-the-art in modeling and simulation. Needless to say, modeling and simulation can be valuable in analyzing and designing various subsystems of tactical C^3 systems. But, capturing the essence of an entire tactical C^3 system in a computer simulation, sufficient for generating actual commands and control, is quite another matter.

To obtain perspective on the magnitude of the problem, consider categorizing all systems in terms of (1) size, (2) whether or not all the fundamental relations of system components are known, and (3) whether or not the system includes intelligent competing factions. For the sake of simplifying this discussion the three criteria are dichotomized and Table 1, illustrates the resulting eight categories, giving some examples of systems in each category.

The application of modeling and simulation has proved advantageous in studying systems in all four noncompetitive categories (but, certainly, not for all systems in these categories). In the first two categories, the modeling efforts are girded by scientific laws and time-tested empirical results which provide the fundamental relations for all system components. The continually increasing data-processing capabilities of digital computers coupled with progress in the development of efficient computational algorithms continues to increase the size of systems that can be simulated. The use of statistics has proved useful in inferring average behavior in certain situations where the dynamics of elemental system components are not well understood but where there are sufficient constraints limiting both the responses possible and the number of interactions possible between system components. Thus, for example, although it is not possible to model the action of each individual entering an airport terminal, a simulation based on a rather simple queuing model can provide valuable information which could be used to optimize many airport terminal operations. Such an approach provides the basis for the server queuing languages such as GPSS. Of course, such a model would be useless in trying to develop a strategy to defend the terminal from an intelligent powerful conspiracy intent on destroying the terminal. (How would one now model the terminal? . . . The behavior of the passengers? . . . The behavior of the flight attendants? . . . etc.) In addition, methods of aggregation have been developed for certain large scale systems (particularly some linear systems with special dynamics) which allow low dimensional models to be used to represent large scale systems. Reference 16 provides an excellent survey and bibliography on the state-of-the-art of aggregation for control purposes.

In each of the competitive categories, one might consider two subcategories based on whether the state of each opponent is known by the others. Clearly, most difficult is the case in which an opponent's state is not known completely. However, where the fundamental relations are known, modeling and simulation can play a useful role since one can determine what the outcomes will be for a variety of opponent strategies

	SYSTEM SIZE	FUNDAMENTAL RELATIONS	COMPETITIVE (INTELLIGENT OPPONENTS)	EXAMPLES
1)	Small	Known	No	Electric circuits, digital logic, gear trains, motors, etc.
2)	Large	Known	No	Power systems, aircraft, communication networks, etc.
3)	Small	Not well Known	No	A human performing a simple manual task (response times, queuing through a serving line, etc.), etc.
4)	Large	Not well Known	No	Ecological systems (animal population, disease, etc.), queuing systems, etc.
5)	Small	Known	Yes	Tic-tac-toe, scissor-paper-rock, etc.
6)	Large	Known	Yes	Chess, bridge, wargames, etc.
7)	Small	Not well Known	Yes	Two-person sales interaction, tennis, duels, etc.
8)	Large	Not well Known	Yes	War, societal systems, economic systems, business, etc.

TABLE 1 Categorization of Systems

and states. Yet, in the case of large-dimensional systems (e.g., chess and bridge), exhaustive methods for developing winning strategies are not feasible and heuristic methods from the area of artificial intelligence play an important role.

Little will be said about the small competitive systems in which the fundamental relations are not known. In fact, a strong argument may be made that there are no small scale systems for which fundamental relations are not known or, at least, cannot easily be found. It seems that if a system really is of low dimension that a moderate effort would result in a system model. Perhaps all these systems are really large-scale systems.

The final competitive category, in which the fundamental relations characterizing system components are not well known, represents an area in which the application of modeling and simulation methods has had very little success. Unfortunately, tactical C^3 systems fall into this category. The existence of an intelligent opponent when trying to determine controls in a large-scale system for which the fundamental relations are not well known is indeed a serious problem. Whether or not the use of modeling and simulation methods will help solve the decision making problems associated with tactical C^3, or compound them, is not clear.

Perhaps the most serious problem in trying to apply modeling and simulation methods to aid in the decision making processes of tactical C^3 stems from the fact that aggregation is necessary in order to make a modeling and simulation effort feasible. In such applications, aggregation is used for two reasons. The first is due to system size; the model would simply be too large for computer simulation if every detail of the actual system was modeled. As a result, certain components of the system that could be well modeled, if model size were of no concern, are grossly simplified. The second reason for aggregation is the result of an incomplete understanding of the system being modeled either due to the lack of fundamental relations for certain processes (e.g., human encounters, etc.) or due to the intentional withholding of important information by an enemy. In either case, the process of aggregation results in some dynamic modes of the real system not being present in the model and in some dynamic modes of the model not adequately representing the dynamic modes of the real system. If such an aggregated model is used to generate commands and controls for a real tactical C^3 system, the possibility exists for an enemy to probe the system for dynamic modes neither included nor well represented in the model and to then use this information to his advantage. Such probes need be neither costly nor complex and could be based on observing responses to specific sorties.

By far the most common criticism of tactical command and control models and simulations concerns the lack of detail included in some subsystem or other. An example of such criticism, typical of much of the criticism, is the following criticism of TAC [14]:

> Limitations in the basic TAC Controller program have recently surfaced . . . "recent simulation runs made for ESD/MITRE show that the FACPs are operated well beyond their true operational capacity and provide an unrealistic mode of operation". Also, it is not possible to access certain kinds of data related to the sensors in the model . . . Finally, TAC Controller (like the previous models considered) ignores the question of identification. Attrition of friendly forces because of mistaken identity or imperfect information is not explicitly modeled.

The typical response to such criticism is the design of the next-generation model containing much greater detail, usually to the point that the newer model bears little or no structural resemblance to the earlier models. For example, Bonder [12], in describing VECTOR-2, an improvement over VECTOR-1, says:

> As you will see in a moment, in order to incorporate the command and control, intelligence and communication processes, VECTOR-2 turned out to be a totally new structure (as compared to VECTOR-1) in the manner in which we had to consider the battlefield geometry, forced employments and locations, the command hierarchy, and the timing of the various combat and combat related process events.

But, inevitibly, the new model falls far short of reality. In the case of VECTOR-2, Bonder continues [12]:

> Before describing some of the model content, I should hasten to add that the model (VECTOR-2) still does not include explicitly a number of relevant phenomena, including non-integral feedback situations, tactical nuclear warfare, and explicit representation of electronic warfare (although elements of this can be implicitly played). It does not include some elements of command and control specified by General Welch and Mr. Robinson at this conference, but which are to be included in the eventual development of the Combined Arms Simulation Model (CASM).

Needless to say, VECTOR-3 is now in the works in spite of the fact that according to Bonder [12]:

> We have not performed a real verification in the scientific sense. We haven't collected war data to do this. . . All I am saying is that the analytic models were compared to models that the military seems to think are realistic. Both models could be wrong.

What is most hypnotic in this process of going from one generation of models to the next in response to specific criticisms is that the

newer models always appear to be more realistic than the preceding models when compared to the preceding models. Unfortunately, the only meaningful validation of a model possible is by comparison to data taken from the real system, not by comparing it to an earlier model known to be inadequate.

Clearly, a strong case can be made for fundamental research for (1) scientific and engineering studies to determine fundamental relations characterizing components of tactical C^3 systems that are now not well known, (2) modeling and simulation research to develop methods of aggregation for developing models for simulations that can be used for generating controls that are insensitive to excluded dynamic modes. This research deals with the latter.

PROBLEM STATEMENT

The general aggregation problem is stated here for the case that the system of interest is well modeled by a set of ordinary differential equations. All the results can be trivially extended to discrete-time systems which are modeled by difference equations. However, the extension of these results to the important class of systems which are best modeled by discrete-event models is not trivial, particularly with respect to the computation of sensitivities within dynamic systems, and additional research is called for here.

Consider that the system to be studied is well modeled by a set of ordinary differential equations given in canonical state-variable form:

$$\frac{dx}{dt} = f_x(x,u), \quad x(t_0) = x_0, \quad t \geq t_0 \qquad (1)$$

where:

$$x = \begin{bmatrix} x_1 \\ \vdots \\ x_n \end{bmatrix}, \quad u = \begin{bmatrix} u_1 \\ \vdots \\ u_m \end{bmatrix}, \quad f_x = \begin{bmatrix} f_{x1} \\ \vdots \\ f_{xn} \end{bmatrix}$$

For the case that n is very large, one is seldom interested in observing all the state variables. In such cases, one observes only a small subset of the state variables or, more generally, a small number of functions of the state variables: i.e.,

$$q = g(x)$$

where

$$q = \begin{bmatrix} q_1 \\ \vdots \\ q_p \end{bmatrix}, \quad g = \begin{bmatrix} g_1 \\ \vdots \\ g_p \end{bmatrix}$$

and $p < n$. The function g is called the aggregation function. The problem of aggregation is that of trying to find a simpler model to generate the observed variables q than that provided by equations (1) and (2). Ideally, one seeks an aggregated model characterized by function f_q such that

$$\frac{dq}{dt} = f_q(q,u), \quad q(t_o) = g(x_o), \quad t \geq t_o \qquad (3)$$

where

$$fq = \begin{bmatrix} f_{q1} \\ \vdots \\ f_{qp} \end{bmatrix}$$

In general there exists no f_q such that an aggregated model can generate the observed variables of a disaggregated model (If the state x is observable through output q, then q cannot, in general, be generated by a system of dimension less than n). In special cases where an f_q can be found such that equation (3) is valid, the aggregated model is said to be dynamically exact to the disaggregated model with respect to q. However, dynamic exactness is so rare in practical situations that, practically, the problem of aggregation is that of finding a function f_q that can be used in generating an approximation q_a to q:

$$\frac{dq_a}{dt} = f_q(q_a,u), \quad q_a(to) = g(x_o), \quad t \geq t_o \qquad (4)$$

where

$$q_a = \begin{bmatrix} q_{a1} \\ \vdots \\ q_{ap} \end{bmatrix}$$

Often, the variables of interest are so few in number compared to the dimension of the disaggragated model (e.g., one may be interested in only the average of all the state variables in a complex system having, say, 50,000 state variables) that there is little hope of finding any f_q to generate a reasonable approximation to q. In such cases, it is necessary to increase the dimension of the aggregated model. Toward

this end the aggregation function is redefined:

$$q = \begin{bmatrix} q_c \\ q_v \end{bmatrix} = \begin{bmatrix} g_c(x) \\ g_v(x) \end{bmatrix}$$

where

$$q_c = \begin{bmatrix} q_{c1} \\ \vdots \\ q_{cr} \end{bmatrix} = \begin{bmatrix} g_{c1}(x) \\ \vdots \\ g_{cr}(x) \end{bmatrix}, \quad q_v = \begin{bmatrix} q_{v,r+1} \\ \vdots \\ q_{vp} \end{bmatrix} = \begin{bmatrix} g_{v,r+1}(x) \\ \vdots \\ g_{vp}(x) \end{bmatrix}$$

where q_c represents the variables of interest and q_v represents the additional variables to be included in the aggregated model to increase model dimension for purposes of improving the approximation. Thus, function g_c is a fixed function defining the variables of interest and function g_v is a function to be selected in the most advantageous manner in designing the aggregated model.

In trading dynamic exactness for model simplicity by accepting an approximation to q, a difficult problem arises. Namely, one must have a basis for comparing alternate approximations. Clearly, the effectiveness of an approximation is closely tied to the use that the aggregated model is to be put to. Thus, the criteria that might be used in evaluating aggregated models to be used for estimation and prediction could be significantly different from the criteria used when the models are to be used for determining controls. The development of pertinent criteria for evaluating aggregated models is an essential part of the aggregation problem.

AN APPROACH TO THE AGGREGATION PROBLEM: STRUCTURAL SENSITIVITY

1. Structural Sensitivity

The approach taken to the aggregation problem is based on system structure. Specifically, system models are represented by graphs such as link-node structures 11', system diagrams [17], or signal-glow graphs [18, 19] in which certain points on the graphs represent system variables and an influence of one variable on another is denoted by the existence of a path from that variable to the other. Fundamental to this approach is the premise that a proposed aggregated model can be imbedded within a larger system defined by the disaggregated system (i.e., the function f_x) and the aggregation function (i.e., the functions g_c and g_v). Importantly, in order that the proposed aggregated, model exactly generate the variables of interest q_c, it is necessary that additional variables, say x_Δ, which are functions of the state variables of the disaggregated model, be provided as special inputs to the aggregated model. These relations between the larger-system variables x_Δ, and the proposed aggregated system variables q_c and q_v represent connections in the system graph. Perfect aggregation is achieved when the q_c generated by the aggregated model is totally insensitive to the existence of these connections.

With such insensitivity, all connections from the larger system can be literally cut and the aggregated model can be removed from the larger system. This sensitivity of a system's variables to the cutting of connecting links is called structural sensitivity. By introducing a gain parameter in such connecting links it is possible to relate structural sensitivities to the well-defined parameter sensitivities (e.g., a link gain equal to 1 implies the connection exists and a link gain equal to 0 implies the connection is broken). The following example illustrates the proposed approach to aggregation.

Consider a continuous autonomous system that is well modeled by

$$\frac{dx}{dt} = f_x(x)$$

(x is an n vector). We would like to design an aggregated model of this system and we demand that the aggregated model generate a specified set of outputs q_c defined by a fixed aggregation function:

$$q_c = g_c(x)$$

(q_c is an r vector). However, although we wish to design an r-th order aggregated model in which q_c is the state, we are willing to increase the dimension of the aggregated model by adding variables

q_v to the state in the hope that the inclusion of important dynamic modes of the original system in the aggregated model will lead to a better approximation of q_c. The variables q_v are selected by the designer as a function of the state variables:

$$q_v = g_v(x)$$

(q_v is a p vector). Thus, here we seek an aggregated model of the form:

$$\frac{dq_c}{dt} = f_{qc}(q_c, q_v)$$

$$\frac{dq_v}{dt} = f_{qv}(q_c, q_v)$$

With proper care in selecting the aggregation functions g_c and g_v so as to avoid algebraic dependencies among the elements of q_c and q_v, one can think of q_c and q_v as being a set of r+p state variables in a new state description. This would then leave n-p-r state variables to be selected to complete the new state description. Denote the new state vector by $\hat{x}$, we have

$$\hat{x} = \begin{bmatrix} q_c \\ q_v \\ x_\Delta \end{bmatrix}$$

where x_Δ is an n-p-r vector that is augmented to q_c and q_v to complete the state description. x_Δ is not unique and can be obtained by an appropriate transformation from the original state description.

$$x_\Delta = g_\Delta(x)$$

Thus, the transformation from x to $\hat{x}$ is given by

$$\hat{x} = \begin{bmatrix} g_c(x) \\ g_v(x) \\ g_\Delta(x) \end{bmatrix} = g_t(x)$$

where g_t is a transformation function and as such has an inverse: i.e.

$$x = g_t^{-1}(\hat{x})$$

Differentiating $\hat{x}$ with respect to time gives

$$\frac{d\hat{x}}{dt} = \begin{bmatrix} \nabla_x(g_c(x)) \\ \nabla_x(g_v(x)) \\ \nabla_x(g_\Delta(x)) \end{bmatrix} \frac{dx}{dt}$$

where $\nabla_x(g_c(x))$ is an r+n matrix such that each row of $\nabla_x(g_c(x))$ is the gradient, in the x space, of the corresponding element of $g_c(x)$. Thus, for example, the i-th row of $\nabla_x(g_c(x))$ is

$$\nabla_x(g_{ci}(x)) = \begin{bmatrix} \frac{\partial g_c}{\partial x_1} & \frac{\partial g_c}{\partial x_2} & \cdots & \frac{\partial g_c}{\partial x_n} \end{bmatrix}$$

Similarly, $\nabla_x(g_v(x))$ is a pxn matrix and $\nabla_x(g_\Delta(x))$ is an (n-p-r)xn matrix. Since $\frac{dx}{dt} = f_x(x)$, we may write

$$\frac{d\hat{x}}{dt} = \begin{bmatrix} \nabla_x(g_c(x)) \\ \nabla_x(g_v(x)) \\ \nabla_x(g_\Delta(x)) \end{bmatrix} f_x(x)$$

And since $\hat{x} = g_t^{-1}(x)$, we obtain a set of transformed state equations for the original system:

$$\frac{d\hat{x}}{dt} = \begin{bmatrix} \nabla_x(g_c(g_t^{-1}(\hat{x}))) \\ \nabla_x(g_v(g_t^{-1}(\hat{x}))) \\ \nabla_x(g_\Delta(g_t^{-1}(\hat{x}))) \end{bmatrix} f_x(g_t^{-1}(\hat{x}))$$

or, equivalently

$$\frac{dq_c}{dt} = f_{qc}(q_c, q_v, x_\Delta)$$

$$\frac{dq_v}{dt} = f_{qv}(q_c, q_v, x_\Delta) \qquad (5)$$

$$\frac{dx_\Delta}{dt} = f_{x\Delta}(q_c, q_v, x_\Delta)$$

where

$$f_{qc}(q_c,q_v,x_\Delta) = \nabla_x(g_c(g_t^{-1}(\hat{x})))f_x(g_t^{-1}(\hat{x}))$$

$$f_{qv}(q_c,q_v,x_\Delta) = \nabla_x(g_v(g_t^{-1}(\hat{x})))f_x(g_t^{-1}(\hat{x}))$$

$$f_{x\Delta}(q_c,q_v,x_\Delta) = \nabla_x(g_\Delta(g_t^{-1}(\hat{x})))f_x(g_t^{-1}(\hat{x}))$$

Figure 1 shows the system diagram for this transformed system. Clearly, if g_v and g_t can be selected so that q_c is completely independent of x_Δ, then perfect aggregation is achieved. This independence is equivalent to being able to cut the connection marked with an "X" without affecting q_c. Note that perfect aggregation is achieved if $f_{qc}(q_c,q_v,q_\Delta)$ is insensitive to x_Δ . However, in terms of designing an aggregated model, this condition may be much too strong. For example, suppose the system's operations is such that $\frac{dx_\Delta}{dt} \cong 0$ (i.e., $f_{x\Delta}(q_c,q_v,x_\Delta) \cong 0$) and $f_{x\Delta}$ is such that $f_{x\Delta}(q_c,q_v,x_\Delta) = 0$ can be solved for x_Δ in terms of q_c and q_v. In this case although $f_{qv}(q_c,q_v x_\Delta)$ is a function of x_Δ , the additional relation relating x_Δ to q_c and q_v makes perfect aggregation possible.

In situations where no functions g_v and g_t can be found that desensitize q_c to cutting the connections bringing x_Δ to the f_{qc} and f_{qv} blocks, an approximation procedure is suggested which is based on introducing a cutting parameter α. Figure 2 shows the system diagram of equations (5) with such a cutting parameter: $\alpha = 1$ gives the original system; $\alpha = 0$ cuts the connections. In this system, one may use the sensitivity of q_v to the cutting parameter α as an indicator of the effectiveness of aggregation and proceed to look for the functions g_v and g_t that minimize this sensitivity. It should be noted that the sensitivity of q_c to α not only depends on the aggregation function g_v but also on the set of state variables selected for x_Δ : i.e., on the selection function g_t.

The approach to the computation of the structural sensitivities is straightforward. The outputs q_c are computed with $\alpha = 1$. For large systems, this computation could strain the capacity of the computer being used and, perhaps, prove to be impractical in certain cases. In such situations where the limits of the computer are being tested, it is essential that efficient computational algorithms be used [19,20]. By setting $\alpha = 0$, the smaller, proposed aggregated system is separated from the larger system and the outputs of this smaller system, q_{ca}, are computed. The structural sensitivities are simply the differences:

$$\frac{\Delta q_c}{\Delta \alpha} = q_{ca} - q_c$$

2. Linear Systems

Although it is quite unreasonable to expect that any tactical C^3 system could be realistically represented by a linear time-invariant model, it is nevertheless useful to look at the aggregation problem for this special case. Importantly, many large subsystems of tactical C^3 systems are well modeled by linear differential equations and some progress toward obtaining useful aggregated models can be made by aggregating individual subsystems separately. Further, some of the ideas set forth here are rather simply illustrated using linear systems as examples. However, it must be noted that the assumption of linearity gives rise to significant simplifications that do not exist for any other class of systems.

Consider the case that the system of interest is well modeled by the set of linear differential equations, written in matrix form

$$\frac{dx}{dt} = Ax \quad (= f_x(x))$$

where x is an n vector and A is an nxn matrix of constants with the element in the i-th row and the j-th column represented by a_{ij}. The variables of interest, which are to be outputs of the aggregated model, are linear combinations of the original set of state variables:

$$q_c = G_c x \quad (= g_c(x))$$

where q_c is an r vector (r<n) and G_c is an rxn matrix. Variables q_c are to be state variables of the aggregated model. Additional state variables q_v, where q_v is a p vector (p<n-r), may be allowed in the aggregated model to improve accuracy:

$$q_v = G_v x \quad (= g_v(x))$$

where G_v is a pxn matrix. If q_c and q_v are considered to be state variables in a transformed coordinate system, an additional n-p-r state variables must be selected, also as linear combinations of the original state variables, to complete the transformed state description:

$$x_\Delta = G_\Delta x \quad (= g_\Delta(x))$$

where x_Δ is an n-p-r vector and G_Δ is an (n-p-r)xn matrix. Thus, representing the new state description with the n vector $\hat{x}$, we have

$$\hat{x} = \begin{bmatrix} G_c \\ G_v \\ G_\Delta \end{bmatrix} x = Gx \quad (= g_t(x))$$

where G is an nxn nonsingular transformation matrix appropriately constructed from submatrices G_c, G_v, and G_Δ. Differentiating the transformation equation $\hat{x}$=Gx with respect to t gives

$$\frac{d\hat{x}}{dt} = GAG^{-1}x = G_{qv\Delta}x$$

where

$$G_{qv\Delta} = GAG^{-1}$$

This can be written in expanded form as

$$\frac{dq_c}{dt} = G_{qq}q_c + G_{qv}q_v + G_{q\Delta}x_\Delta \quad (= f_{qc}(q_c, q_v, x_\Delta))$$

$$\frac{dq_v}{dt} = G_{vq}q_c + G_{vv}q_v + G_{v\Delta}x_\Delta \quad (= f_{qv}(q_c, q_v, x_\Delta)) \qquad (6)$$

$$\frac{dx_\Delta}{dt} = G_{\Delta q}q_c + G_{\Delta v}q_v + G_{\Delta\Delta}x_\Delta \quad (= f_{x\Delta}(q_c, q_v, x_\Delta))$$

where the matrix coefficients of q_c, q_v, x_Δ are the apprpriate partitions of $G_{qv\Delta}$. Figure 3 shows the system diagram corresponding to equations (6) with the cutting parameter α included. The objective, of course, is to find the transformation submatrices G_v and G_Δ that minimize the sensitivity of q_c to the cutting parameter α.

To illustrate the process consider the following simple numerical example. The system of interest is well modeled by

$$\begin{bmatrix} \frac{dx_1}{dt} \\ \frac{dx_2}{dt} \end{bmatrix} = \begin{bmatrix} -1 & 0 \\ 0 & -10 \end{bmatrix} \begin{bmatrix} x_1 \\ x_2 \end{bmatrix}, \quad 0 \le t \le 1, \quad \begin{bmatrix} x_1(0) \\ x_2(0) \end{bmatrix} = \begin{bmatrix} 1 \\ 1 \end{bmatrix}$$

The variable of interest is

$$q_c = [\,0.1 \quad 1\,] \begin{bmatrix} x_1 \\ x_2 \end{bmatrix}$$

We wish to model this system as a first-order linear time-invariant system: i.e., we seek a constant g_{qq} such that

$$\frac{dq_{ca}}{dt} = g_{qq}q_{ca}$$

where q_{ca} is a "good" approximation to q_c on the time interval [0,1]. Note, in this case we allow no additional state variables q_v in the aggregated model.

Paralleling the preceeding development we have

$$A = \begin{bmatrix} -1 & 0 \\ 0 & -10 \end{bmatrix}, \quad G = \begin{bmatrix} G_c \\ G_\Delta \end{bmatrix} = \begin{bmatrix} 0.1 & 1 \\ g_{\Delta 1} & g_{\Delta 2} \end{bmatrix}$$

and, thus,

$$GAG^{-1} = \begin{bmatrix} g_{qq} & g_{q\Delta} \\ g_{\Delta q} & g_{\Delta\Delta} \end{bmatrix}$$

where

$$g_{qq} = \frac{10g_{\Delta 1} - 0.1g_{\Delta 2}}{0.1g_{\Delta 2} - g_{\Delta 1}}, \quad g_{q\Delta} = \frac{-0.9}{0.1g_{\Delta 2} - g_{\Delta 1}}$$

$$g_{\Delta q} = \frac{9g_{\Delta 1}g_{\Delta 2}}{0.1g_{\Delta 2} - g_{\Delta 1}}, \quad g_{\Delta\Delta} = \frac{g_{\Delta 1} - g_{\Delta 2}}{0.1g_{\Delta 2} - g_{\Delta 1}}$$

and

$$\begin{bmatrix} \frac{dq_c}{dt} \\ \frac{dx}{dt} \end{bmatrix} = \begin{bmatrix} g_{qq} & g_{q\Delta} \\ g_{\Delta q} & g_{\Delta\Delta} \end{bmatrix} \begin{bmatrix} q_c \\ x_\Delta \end{bmatrix}, \quad 0 \le t \le 1, \quad \begin{bmatrix} q_c(0) \\ x_\Delta(0) \end{bmatrix} = GAG^{-1} \begin{bmatrix} x_1(0) \\ x_2(0) \end{bmatrix}$$

Perfect aggregation (i.e., dynamic exactness) is achieved when $G_\Delta = [g_{\Delta 1}\ g_{\Delta 2}]$ is selected so that

$$\frac{\Delta q_c}{\Delta \alpha} = 0, \quad 0 \le t \le 1$$

However, since dynamic exactness is not possible in this case, as in most, the problem is to select $G_\Delta = [g_{\Delta 1}\ g_{\Delta 2}]$ such that some figure of merit derived from the sensitivity $\Delta q_c/\Delta\alpha$ is minimized. There are many possibilities for defining a figure of merit. Some examples are:

$$M_1 = \left|\frac{\Delta q_c}{\Delta\alpha}(1)\right|$$

$$M_2 = \int_0^1 \left(\frac{\Delta q_c}{\Delta\alpha}(\tau)\right)^2 w(\tau)\ d\tau$$

$$M_3 = \int_0^1 \left|\frac{\Delta q_c}{\Delta\alpha}(\tau)\right| w(\tau)\ d\tau$$

$$M_4 = \int_0^1 \left|\frac{\Delta q_c}{\Delta\alpha}(\tau)\cdot\frac{\alpha}{q_c}\right| w(\tau)\ d\tau$$

where figure of merit M_1 stresses the importance of the final value of q_c, M_2 and M_3 consider the accuracy of q_c to be important over the entire time interval (the weighing function w allows the emphasis to vary over the time interval), and M_4 is in terms a normalized sensitivity for situations in which one is concerned with percent errors. Clearly, the figure of merit to be used in any instance depends on the system being modeled. For this example, figure of merit M_4 was arbitrarily chosen.

A simple BASIC program was written to determine the value of $G_\Delta = [g_{\Delta 1}\ g_{\Delta 2}]$ that minimizes M_4. It was found that the values $g_{\Delta 1} = -0.1256$ and $g_{\Delta 2} = 0.8744$ result in $[M_4]_{min} = 0.6275$. Thus,

$$g_{qq} = \frac{10 g_{\Delta 1} - 0.1 g_{\Delta 2}}{0.1 g_{\Delta 2} - g_{\Delta 1}} = -6.306$$

Therefore, the aggregated model is

$$\frac{dq_{ca}}{dt} = -6.306 q_{ca},\quad 0 \le t \le 1,\quad q_c(0) = 0.1x_1(0) + x_2(0)$$

For purposes of comparison, other values are given:

$G_\Delta = 1 \quad 0.1$ results in $M_4 = 0.785$ and $g_{qq} = -10.09$

$G_\Delta = 0.5 \quad 0.5$ results in $M_4 = 0.825$ and $g_{qq} = -11.0$

The interpretation of the results in this simple example is rather straightforward. By defining the variable to be observed as $q_c = 0.1x_1 + x_2$, we have in effect specified an interest in variable x_2 that is 10 times greater than our interest in x_1. Since we wish to desensitize q_c to $x_\Delta = g_{\Delta 1}x_1 + g_{\Delta 2}x_2$, $g_{\Delta 1}$ and $g_{\Delta 2}$ must be selected so that x_Δ contains more of x_1 than x_2. However, since the relative magnitudes of x_1 and x_2 are neither constant nor known, it is not obvious how $g_{\Delta 1}$ and $g_{\Delta 2}$ should be selected. It would seem natural to try $g_{\Delta 1} = 1$ and $g_{\Delta 2} = 0.1$ and, in fact, this does result in a reasonable approximation. However,

this choice results in an excessive suppression of x_1 which, due to its relatively large magnitude, contributes to q_c to a greater degree than is indicated by the definition of q_c.

It is important to note that minimizing the figure of merit in this example did not involve a two-parameter search. The sensitivity is determined only by the ratio $g_{\Delta 2}/g_{\Delta 1}$. It appears that the sensitivity $\Delta q_c/\Delta\alpha$ is a function only of the eigenvalues of the transformation matrix G. Thus, row operations on the submatrix of G, G_{Δ}, that eliminates variables appear to be legitimate. In this example we could just have well used $G_{\Delta} = \begin{matrix} 1 & r \end{matrix}$, where $r = g_{\Delta 2}/g_{\Delta 1}$, instead of $G_{\Delta} = \begin{matrix} g_{\Delta 1} & g_{\Delta 2} \end{matrix}$.

CONCLUSIONS AND RECOMMENDATIONS

Structural sensitivities appear to lead to a useful measure of effectiveness for aggregated models and thus appear to provide the basis for a quantitative approach to the design of aggregated models. Especially important, insofar as competitive systems is concerned, is that by using structural sensitivities in the design of an aggregated model, attention must be given to all excluded dynamic modes; it is simply not suffcient that the variables of interest appear to be reasonably approximated. In minimizing structural sensitivities it is virtually not possible to accidently overlook important system dynamics in the aggregated model.

Although the reasearch conducted thus far is promising, it is the result of little more than one month's effort by this writer and is, in fact, truly preliminary. Some important questions have been raised which point to promising directions for future research. For example:

1. In designing aggregated models of large-scale systems, a minimization must be carried out with respect to a large parameter space. Such minimizations can be difficult, especially when there are many local minima to contend with. Attention should be given to trying to reduce the dimension of the parameter space by using the least number of parameters possible in defining the transformation functions g_v and g_{Δ}. In addition, a study should be made to determine which minimization algorithms (e.g., the Powell-Flectcher algorithms, etc.) are most suitable in this application.

2. By actually cutting the connecting links, the variables x_{Δ} being fed to the proposed aggregated model are actually set to zero. This is of no concern when dynamic exactness can be achieved. However, when the aggregated model can only generate an approximation to the variables of interest, one should consider the possibility of introducing bias inputs to the aggregated model at the points where the links have been cut.

3. Frequently, one may wish to constrain the form of the aggregaged model, even at the cost of having a deteriorated aggregated model or one of higher dimension. For example, one may require that the aggregated model be linear and time-invariant so as to permit analytic studies of the model instead of, or in addition to, simulation studies. Methods for introducing this model constraint into the setting of structural sensitivities should be studied. This possibility was briefly considered and the simple ploy of replacing the first of equations (5) by the following equation seems promising:

$$\frac{dq_c}{dt} = f_q(q_c,q_v) + [f_{qc}(q_c,q_v,x_\Delta) - f_q(q_c,q_v)]$$

where function f_q characterizes the constrained aggregated model. However, further study is necessary to determine how variations in the constrained model parameters affect the dynamics of the sensitivity function.

4. Considerable effort should be directed toward developing rationales for various forms of figures of merits derived from structural sensitivities. Many possibilities come to mind, including integral forms (with and without weighing functions) and those based on final values, and the implications of each ought to be examined, particularly with respect to the relationship of the effectiveness of the aggregated model to the magnitude of the figure of merit.

5. Since the computations of sensitivities are so much simpler for static systems than for dynamic systems, the possibility of designing aggregated models by examining only the right-hand side of the canonical state equations should be carefully investigated.

6. Linear time-invariant systems should be studied as an important special case. Certainly, many important real systems are modeled as linear time-invariant systems. However, the fact that linear time-invariant systems yield to analysis can be quite helpful in developing valuable insights into the implications of structural sensitivities.

7. A system can be defined such that the sensitivities $\Delta q_c/\Delta\alpha$ appear as the system outputs. Using this system, the problem of aggregation can be cast as a control problem in which the sensitivities can be considered to be error signals to be driven to zero. Such an approach to the aggregation problem should be studied. It seems likely that certain aspects of control theory will prove useful here.

8. The proposed approach to aggregation should be studied with respect to the zero-state response of systems to classical test inputs (e.g., unit steps, sinusoids, etc.). It is clear that the aggregated models depend on the system's initial state. Yet, in many systems it is unlikely that certain system state variables will ever assume

significant values because of the large attenuations between the input adn the storage devices associated with those state variables. In such cases, determining acceptable aggregated models might be simplest by dealing only with zero-state input-output responses. For the linear case, this is equivalent to looking for aggregated transfer functions.

9. A study should be made on the controllability of systems using controls derived from aggregated models. It seems that such a study makes sense only if a weaker definition of controllability is used so as to take into account the extraordinary controls generally necessary before the neglected dynamics modes can significantly affect the outputs. Particular attention should be given to the role of the extra state variables q_v which are included in the aggregated model only for accuracy. It may be desirable to include some additional state variables for purposes of controllability. For competitive systems, it is especially important to determine the effect that an opponent can have on controllability and to try to design an aggregated model so as to minimize this effect.

10. A study should be made to extend the results to discrete-event systems.

11. Finally, the proposed approach to aggregation should be used to model a real system.

REFERENCES

1. D. B. Wortman, et al., "New Developments in SAINT: The SAINT III Simulation Program", AMR-TR-75-117, Aerospace Medical Research Laboratory, Wright-Patterson AFB, June 1976.

2. C. C. Joyce, D. D. Penrod, "Combat Effectiveness Analysis Technique for Battlefield Systems Architecture Project", MTR Draft, The MITRE Corp., December 1976.

3. R. A. Games and R. P. Witt, "Simplified Tactical Air C^3 Simulation (STACS)", A MITRE Corp. Working Paper, July 1978.

4. L. B. Anderson, et al., "IDA Ground-Air Model I (IDAGAM I)", Institute for Defense Analysis, Arlington, VA., Report R-199, 1974.

5. A. F. Karr, "On the Lulejan - I Combat Model", Institute for Defense Analysis, Arlington, Va., Report P-1182, 1976.

6. P. E. Louer, et al., "Conceptual Design for the Army in the Field Alternative Force Evaluation - CONAF Evaluation Model IV - Part I - Model Description", Report OAD-CR-60, General Research Corp., September 1974.

7. K. Harris, L. H. Wegner, "TACTICAL Airpower in NATO Contingencies: A Joint Air-Battle/Ground Battle Model (TALLY/TOTEM)", R-1194-PR, The Rand Corp., May 1974.

8. F. S. Preston, R. C. Baxter, "TACEM (Tactical Air Campaign Effectiveness Model) - Naval Campaign Model - Final Report", Vol 1, Norden Report 2068-R-0001, Norden Division, United Technologies Corp., June 1976.

9. C. B. Valrand, "Air Defense System Performance and Operational Cost Analysis Model (PERCAM)", DAAH01-75-C-0084, TRW Systems Group, December 1974.

10. "TAC Controller User's Manual", Westinghouse Defense and Electronic Systems Center, Baltimore, October 1976.

11. E. D. Howes, B. L. Renninger, "Preliminary Notes on a C^3I Evaluation Model", A MITRE Corp. Memorandum - Memo No. D53-M-142, April 1978.

12. S. Bonder, "A Summary Description of the Vector-2 Theatre Level Campaign Model", Proceedings of Workshop on Decision Information for Tactical Command and Control, R. M. Thrall and Associates, Publisher, Houston, Texas, September 1976.

13. "Combined Arms Simulation Model (CASM)", General Research Corp., Quarterly Review, Contract NR-F33615-17-C-0400, 9 November 1977.

14. R. A. Games, "A Survey of Tactical Command and Control Models", A MITRE Corp. Working Paper (WP-21483), October 1977.

15. K. R. Johnson, "Comments on TAC Controller and CASM Simulations", A MITRE Corp. Working Paper (WP-21142), January 1977.

16. N. R. Sandell, et al., "Survey of Decentralized Control Methods for Large-Scale Systems", IEEE Transactions on Automatic Control, Vol. AC-23, No. 2, April 1978, pp108-128.

17. H. D'Angelo, T. G. Windeknecht, "A System Graph and Canonical State Equations", Proceedings Sixth Annual Southeastern Symposium on System Theory, Baton Rouge, 1974.

18. S. I. Mason, "Feedback Theory - Some Properties of Signal Flow Graphs", Proceedings Institute of Radio Engineers, Vol. 41, September 1953, pp 1144-1156.

19. A. Y. Lee, "Signal Flow Graphs - Computer-Aided System Analysis and Sensitivity Calculations", IEEE Transactions on Circuits and Systems, Vol. CAS-21, No. 2, March 1974, pp 209-216.

20. T. G. Windeknecht, A. Y. Lee, H. D'Angelo, "An Approach to the Computer-Aided Analysis of Signal-Flow Graphs without the Use of Iterative Methods or Matrix Inversions", Proceedings International Contenance on Cybernetics and Society, 1976.

FIGURES

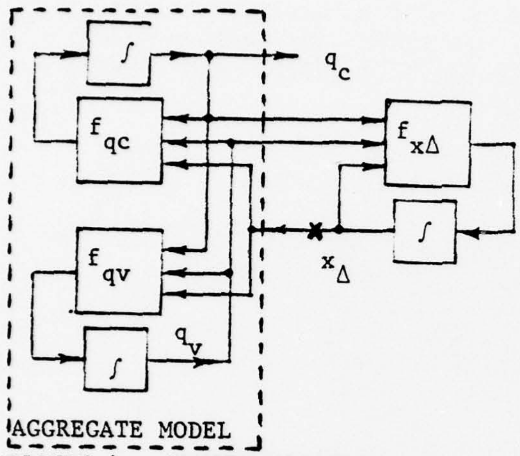

FIGURE 1. SYSTEM DIAGRAM FOR EQUATIONS 5

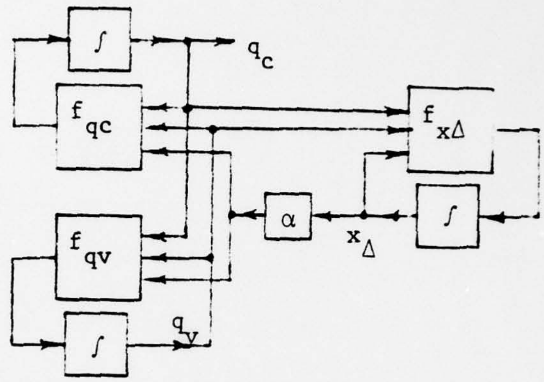

FIGURE 2. INTRODUCTION OF CUTTING PARAMETER

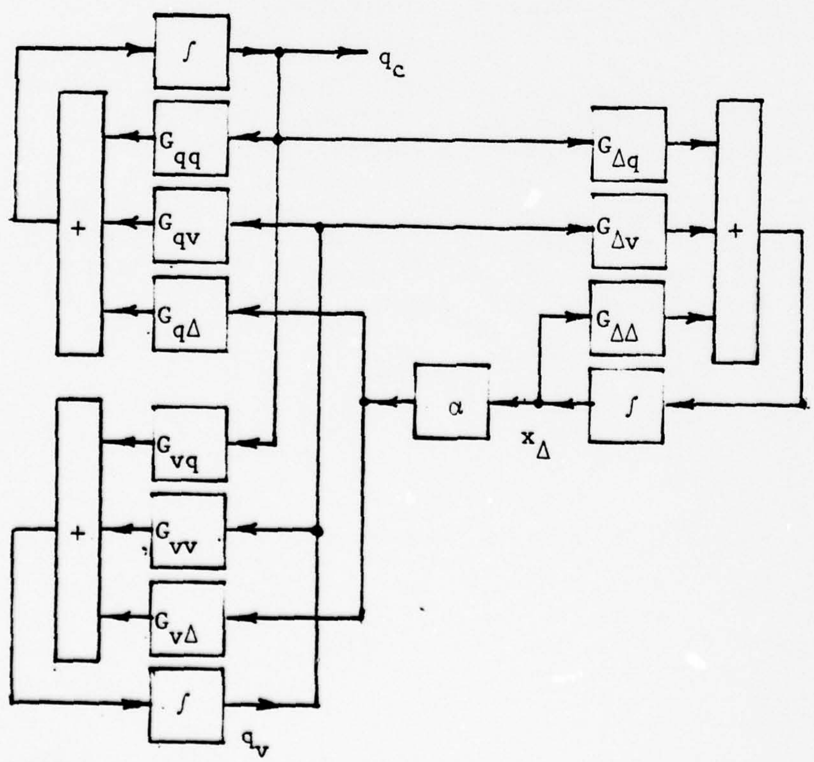

FIGURE 3. LINEAR SYSTEM: SYSTEM DIAGRAM FOR EQUATIONS 6

1978 USAF-ASEE SUMMER FACULTY RESEARCH PROGRAM
sponsored by
THE AIR FORCE OFFICE OF SCIENTIFIC RESEARCH
conducted by
AUBURN UNIVERSITY AND OHIO STATE UNIVERSITY

PARTICIPANT'S FINAL REPORT

SPECIALIZED SIMULATION CONCEPTS FOR COMMAND-CONTROL-COMMUNICATIONS-INTELLIGENCE (C^3I) SYSTEMS

Prepared by:	Robert E. Lovell, Ph.D.
Academic Rank:	Associate Professor
Department and University:	Faculty of Industrial and Management Systems Engineering, Arizona State University
Assignment:	Hanscom AFB Electronic Systems Division Deputy for Development Plans
USAF Research Colleague:	Donald B. Brick, Ph.D.

Date:	August 4, 1978
Contract No.:	F44620-75-C-0031

SPECIALIZED SIMULATION CONCEPTS FOR
COMMAND-CONTROL-COMMUNICATIONS-INTELLIGENCE (C^3I)
SYSTEMS

by

Robert E. Lovell

ABSTRACT

From the spectrum of simulation models and techniques that have potential applicability to development of the next generation of C^3I systems for the Tactical Air Force, the multicomponent extension of Lanchester's equations was selected for detailed investigation. These are from a class of models which are termed here "overview" models and have important attributes for combat simulations.

Multicomponent Lanchester equations are cast into the standard state variable form for linear differential equations with autonomous behavior $\dot{x} = Fx$, which has the solution $\dot{x} = e^{Ft}x(t_o)$. However, it is shown that a small block (RB) of the F^2 matrix, containing no more than ¼ of the elements of the original, contains the key to both computation and the structural properties of the engagement. The incidence matrices from the submatrices R, B and RB are used to generate connection graphs which make the engagement under study visible. The properties of RB in terms of the various engagement properties -- such as inaction, attacks without defender response, indirect engagements, engagement trees, direct engagements and loop engagements -- are presented and illustrated with example. Mathematically these give rise to various properties associated with non-negative matrix theory such as transient blocks, primitive blocks, cyclic blocks, and certain decompositions into independent engagements.

Directions are suggested for additional research both in the mathematical analysis of attrition relationships, and in computer aided studies of higher level attrition relationships that do not lend themsleves to closed form mathematical treatment.

ACKNOWLEDGMENT

This summer has been personally very rewarding. An opportunity to spend ten weeks exploring an unfamiliar field in order to identify and pursue a research topic without the press of other duties must happen only a few times in a career. I would like to express my appreciation to the Air Force Office of Scientific Research and the American Society for Engineering Education for making all this possible through its contract F44620-75-C-0031 with Auburn University.

This report represents the distillation of some of the activities I was able to pursue and some of the mash that has been generated from which future distillates may come. In the ten weeks it has been possible to identify many more avenues of research activity than it has been possible to pursue. Many of these will be included in proposals for further work at Arizona State University.

The first few weeks were a blur of briefings, personal discussions and review of technical papers on the unfamiliar topic of C^3I. Major C. Jaglinski, USAF, ESD/XRT, and Messrs. Richard Witt and Richard Games of the MITRE Corporation were extremely helpful during this period. When enough had been learned to penetrate more deeply, Messrs. John Kreigel and Kent R. Johnson of MITRE were able to add their help in my searches for information and in setting some directions for my investigations.

I have particularly enjoyed working with Dr. Henry D'Angelo of Memphis State University -- also a member of the USAF-ASEE Summer Faculty Research Program. We were able to use each other as sounding boards for many ideas, and he provided valuable critiques of the report.

Dr. Donald B. Brick, Technical Director, ESD/XR research colleague for this summer's activity, and Mr. Fred O'Brien, Program Director, Auburn University were extremely helpful throughout.

Particular thanks also to Mrs. Bea Murphy and Mrs. Rose Burns for producing this final report on a very tight schedule.

NOMENCLATURE

b or $b(t)$	a time variable m-vector (or column matrix) containing as elements the size of the components (or elements) making up the blue force.
r or $r(t)$	a time variable n-vector (or column matrix) containing as elements the size of the components (or elements) making up the red force.
m	the number of components of the blue force ($m \leq n$).
n	the number of components of the red force ($n \geq m$).
B	a non-negative $n \times m$ matrix of constants representing the capacity of components of the blue force to cause attrition of the appropriate red component.
B_{ij}	the ij element of the B matrix representing the capacity of blue component j (b_j) to cause attrition of the red component i (r_i).
R	a non-negative $m \times n$ matrix on constants representing the capacity of components of the red force to cause attrition of the appropriate blue component.
R_{ij}	the ij element of the R matrix representing the capacity of red component j (r_j) to cause attrition of the blue component i (b_i).
x	$\left[\begin{array}{c} b \\ \hline r \end{array}\right]$. A vector (column matrix) that can be partitioned into two column matrices with b as the upper block and r as the lower block. The state vector of the combat model.
0	represents the scalar zero, or a matrix of zeros. Subscripts represent the order or dimension of zero matrix. The subscripts are sometimes implied.
I	the identity matrix. A subscript gives the order, but it is sometimes implied.
F	$\left[\begin{array}{c\|c} 0_m & -R \\ \hline -B & 0_n \end{array}\right]$ The matrix of system coefficients which can be partitioned as shown.
$\dot{x}$	dx/dt. It is represented here for the most part by $\dot{x} = Fx$ -- the canonical form for linear state variable differential equations with autonomous behavior.
Φ	e^{Ft}. The state transition matrix. With subscripts it represents blocks of the partitioned state transition matrix.
t	the time variable.
t_o	the starting time; time zero.

INTRODUCTION

The military services have become very concerned with improving the overall effectiveness of their decision-making and decision-execution processes. Command, control, communications, and intelligence are important ingredients in such processes and the integration of such processes into a single concept is now denoted C^3I.

The development of C^3I systems -- integrated hardware and software with well conceived man-system interfaces -- is now receiving high priority, and the Electronic Systems Division, Air Force Systems Command, is concerned with the next generation systems for the Tactical Air Force. Any ideas of potential consequence for such systems are being examined critically by a number of analysts. One area where such interest lies is in the use of simulation -- and its subset, emulation -- in a variety of ways. As one working with simulation in the academic world this 10-week period has been an excellent opportunity to obtain a real sense of needs in this important field. This summer's activity has led to the following:

1. an excellent indoctrination in the needs of the Air Force for C^3I systems;

2. an examination of many simulation models that have been used or are presently in development;

3. a better understanding of the areas where the Air Force presently has hope of using simulation successfully; and

4. a preliminary analysis of where simulation might prove successful and helpful, and conversely where it seems to have little likelihood of success.

All of this has resulted in an unparalleled opportunity to look at important aspects of C^3I in some detail, and to see what individual expectations are for simulation in support of it. Special attention was given to one aspect of C^3I simulation -- that concerned with overview models of combat attrition

OBJECTIVE

Simulation is under consideration for several C^3I applications. Broadly speaking these applications fall into two groupings: one, the use of simulation for support in the design and test of new C^3I systems, and two, the embedding of simulations in some of the C^3I system hardware/software for a variety of real-time operational and training needs. In both cases, however, simulations of actual air and ground combat seem to be needed.

Much work has been done on combat simulations and specialized models have been constructed at many levels of detail. For example, the PERCAM Model (Volrand 1974) simulates a micro air defense environment by looking at the dynamics of ground based radar (pulsing, scanning, sensitivity of threshholds), the associated ground-to-air missile dynamics and warhead capabilities, and the geometry of the intruding aircraft. All of this is done on a probabilistic basis to determine expected outcome of a small encounter.

On a much larger scale extremely simple models of large engagements involving forces of many components and many types of weapons in large scale conflicts have also been used extensively. Such models are referred to here as "overview" models, since, in their simplicity, they do not include the dynamics of the individual encounters. Such models may provide useful long range planning information, but the lack of detail makes it impossible to see the little things that can often make the big difference in actual warfare.

To bridge this gap many Department of Defense agencies are supporting development of large models which can simulate large scale warfare but with a level of detail approaching that of the models of individual weapons. ESD and MITRE have been following the development of such models to see what implications they may have for C^3I. Games (1977a) and Johnson (1977a) have analyzed many of these models. Games in particular provided extensive references to many of these models. Whatever the success of these might be, it seems clear that their complexity will limit their usefulness largely to studies. The ability to exercise them in an operating environment seems limited.

Accordingly it seems that the parallel development of overview models, which can make use of information generated at the detailed level innovative and useful ways, is indicated.

The change to expand the horizon and sensitivities of such overview models led to the present study of attrition relationships for overview models.

ATTRITION RELATIONSHIPS

As discussed earlier, simulation models which exercise the dynamics of interactions between weapons of different types are difficult to embed in models of large engagements. The combinatorial problems often make the models too large and the computation time too long for present computers. Further, the problem of design of input scenarios for the friendly and response rules for the enemy could make exercising the model under a variety of options prohibitive.

However, if overview models are to prove useful, it is necessary to embed in them the results of detailed studies of individual weapon effectiveness against different types of target. The development of such attrition relationships, however, need not be delayed until detailed evaluations of weapon effectiveness are made. Whether detailed weapon effectiveness information has been developed in actual combat, in war games, in equipment test at proving grounds, by simulation, or from the judgment of those individuals with the requisite expertise, such information may be expected to lead to functional attrition relationships and schemes for selecting parameters for particular applications.

At the same time it is necessary to examine the classes of overview models which may be useful in the higher levels of C^3I, while making effective use of information developed in the detailed studies. Accordingly, some promising structures for overview models are discussed in this section.

Lanchester's Relationships

In any studies of overview models of warfare the starting point is often the work of F. W. Lanchester (1916). His relationships have been the basis of many recent modelling efforts and it is important to review them here.

Lanchester, in a collection of papers, Mathematics in Warfare, proposed three pairs of simple simultaneous linear differential equations to represent three different perceptions of the nature of warfare. His analyses centered on relative measure of strength of forces rather than on the time oriented dynamics of the engagements. Accordingly he suppressed the time variable. His results are summarized briefly below.

1. Ancient Warfare - The Linear Law. In the case of weapon against weapon in a target poor environment massing of forces produced no particular advantage. The describing differential equations are $\dot{b} = -R$, and $\dot{r} = -B$. The solution with time suppressed is $Bb - Rr =$ constant. Here force effectiveness is proportional to force sizes and a plot of b versus r produces a straight line. If the constant is not zero one of the forces will be extinguished in a finite time.

2. Modern Warfare - The Square Law. Lanchester describes the typical modern warfare situation, one of aimed fire in a target rich environment, by the following relationships: $\dot{b} = -Pr$, and $r = Bb$. The solution with time suppressed is $Bb^2 - Rr^2 =$ constant. A plot of r versus b produces a hyperbola. Here massing of forces gives a distinct advantage -- the square law advantage -- since the effectiveness of each force is proportional to the square of its size. Again if the constant is not zero, one of the forces will be extinguished in finite time.

3. Area Fire - Another linear relationship. Lanchester describes a third form of warfare in which area fire ("firing into the brown") replaces aimed fire. In this situation combat effectiveness is treated as proportional to the size of the enemy force present and the describing differential equation are $\dot{b} = RBr$, and $\dot{r} = BRb$. The solution with time suppressed is identical to the first case. Again, the effectiveness of each force is proportional to its size. The timewise behavior, however, differs from the first; no force is extinguished in a finite time.

Lanchester examined the validity of these relationships in the context of historical engagements. He also looked briefly into mixed situation in which one force is using aimed fire, and the other is using area fire.

Lanchester-like Attrition Relationships

Lanchester concepts have been extended in several directions. Games (1977a), looked at the aimed fire cases where the red and blue forces are represented by multiple components rather than aggregated amounts. Games & Witt (1978) created a simulation model (Simplified Tactical Air C^3 Simulation, or STACS) in which they exercised several concepts of engagements, disengagements, mobility and allocation of force components. This model takes the form $\dot{x} - Fx$, where F is the matrix of coefficients of the perceived linear interactions.

Johnson (1978a) with Edwin Key examined multi-component models of the $\dot{x} = Fx$ form, and succeeded in extracting "constants of the engagement" for some specialized cases.

Johnson (1977b) also looked at one-versus-one situations of the form $\dot{b} = -Rr^ib^j$, and $\dot{r} = -Br^kb^p$, where the exponents i, j, k, and p can be selected to accommodate a modeller's perception of force interrelationships. By selection of exponents from the set $\{0, 1\}$ any of Lanchester's three original formulations can be reproduced. For these forms Johnson derived a generalized formula for computation of the "constant of the engagement". Fain (1977) and Willard (1962) examined many historical engagements using a subset of these relationships in attempts to impute values of some of the exponents -- and to examine their credibility.

Everett (1977) formulated some extensions of Lanchester models in order to explore the effects of firing accuracy, resolution of targets, delayed intelligence information, and motion of targets on force effectiveness.

Durstine (1963) and Latchaw (1972) examined cases where forces were replenished at constant rates. Latchaw also included losses of effectiveness of forces due to illness, accident, desertion, etc. Both of these studies were extensions of Lanchester's Modern Warfare format.

It can be seen that there has been a sustained interest in the Lanchester-based relationships.

Multi-component Lanchester Linear Systems

Analytically tractable Lanchester-like cases arise from those multi-component cases that can be represented in the canonical form for linear state variable differential equations with autonomous behavior ($\dot{x} = Fx$). Although there are limitations in such formulations, we can learn from a number of special cases. Using the definitions provided in the Nomenclature section we proceed:

Richard Games (1977a) has shown that

$$F^0 = \left[\begin{array}{c:c} I_m & 0 \\ \hdashline 0 & I_n \end{array}\right], \quad F^1 = \left[\begin{array}{c:c} 0 & -R \\ \hdashline -B & 0 \end{array}\right], \quad F^2 = \left[\begin{array}{c:c} RB & 0 \\ \hdashline 0 & BR \end{array}\right],$$

$$F^3 = \left[\begin{array}{c:c} 0 & -RRB \\ \hdashline -BRB & 0 \end{array}\right], \quad F^4 = \left[\begin{array}{c:c} (RB)^2 & 0 \\ \hdashline 0 & (BR)^2 \end{array}\right], \text{ and, in general}$$

$$F^n \begin{cases} \left[\begin{array}{c:c} (RB)^{n/2} & 0_{mxn} \\ \hdashline 0_{nxm} & (BR)^{n/2} \end{array}\right] & \text{for } n \geq 0 \text{ and even,} \\ \left[\begin{array}{c:c} 0_m & -(RB)^{(n-1)/2}R \\ \hdashline -(BR)^{(n-1)/2}B & 0_n \end{array}\right] & \text{for } n \geq 1 \text{ and odd.} \end{cases}$$

Note that $(RB)^0 = I_m$ and $(BR)^0 = I_n$.

The solution is of the form $x(t) = e^{Ft}x(t_o)$, with $e^{Ft} = \sum_{n=0}^{\infty}(Ft)^n/n!$

Defining

$$e^{Ft} = \Phi(t) = \left[\begin{array}{c:c} \Phi_{11} & \Phi_{12} \\ \hdashline \Phi_{21} & \Phi_{22} \end{array}\right] \quad \text{we note that}$$

$$b(t) = \Phi_{11}(t)b(t_o) + \Phi_{12}(t)r(t_o), \text{ and}$$

$$r(t) = \Phi_{21}(t)b(t_o) + \Phi_{22}(t)r(t_o).$$

The Φ_{ij} can be expressed in terms of sums of a potentially infinite number of terms made up from the powers of either RB or BR. Since RB is, in general, of lower order than BR (since $m \leq n$) it is useful to recast the Φ_{ij} in terms of sums related to RB. (Note that if e^{Ft} is to be approximated by truncated power series, no more than m^2 elemental approximate sums are required. All elements of e^{Ft} are linear combinations of these sums.) Proceeding, the Φ_{ij} can be found using the powers of F previously given:

$$\Phi_{11} = I_m + (RB)t^2/2! + (RB)^2t^4/4! + (RB)^3t^6/6! + \ldots$$

$$\Phi_{12} = -Rt - (RB)Rt^3/3! - (RB)^2Rt^5/5! - \ldots$$

$$\Phi_{21} = -Bt - (BR)Bt^3/3! - (BR)^2Bt^5/5! - \ldots$$

$$\Phi_{22} = I_n + (BR)t^2/2! + (BR)^2t^4/4! + (RB)^3t^6/6! + \ldots$$

The $(BR)^k$ are now reformulated in terms of powers of RB as $(BR)^k = B(RB)^{k-1}R$. Note, however, it is not possible in general to use $(RB)^{-1}$ since there is no assurance that RB is full rank. (Further, BR can never be of full rank when m<n.) Working first with Φ_{12} and Φ_{21}:

$$\Phi_{12} = -(I_mt + (RB)t^3/3! + (RB)^2\ t^5/5! \ldots)R$$

$$\Phi_{21} = -B(I_mt + (RB)t^3/3! + (RB)^2t^5/5! \ldots)$$

Note that the parenthetical expressions are the same in each case and will be denoted Sum_1. Similarly,

$$\Phi_{11} = I_m + (I_mt^2/2! + (RB)t^4/4! + (RB)^2t^6/6! + \ldots)RB, \text{ and}$$

$$\Phi_{22} = I_n + B(I_mt^2/2! + (RB)t^4/4! + (RB)^2t^6/6! + \ldots)R.$$

Again the two parenthetical expressions are the same and will be denoted Sum_2.

Thus,

$$\left[\begin{array}{c} b \\ \hline r \end{array}\right] = \left[\begin{array}{c|c} I_m + (Sum_2)RB & -(Sum_1)R \\ \hline -B(Sum_1) & I_n + B(Sum_2)R \end{array}\right] \left[\begin{array}{c} b(t_o) \\ \hline r(t_o) \end{array}\right]$$

Note that the time variable appears only in the summations.

Sum_1 and Sum_2 are easily comouted using the following process:

	Working Term $(m \times m)$		Accumulation of Sum_1 $(m \times m)$	Accumulation of Sum_2 $(m \times m)$
Start	$I_m t$	=	$I_m t$	
x	$t/2$	=		$I_m t^2/2!$
x	$RBt/3$	=	$(RB)t^3/3!$	
x	$t/4$	=		$(RB)t^4/4!$
x	$RBt/5$	=	$(RB)^2t^5/5!$	
x	$t/6$	=		$(RB)^2t^6/6!$
		etc.		

Towards Physical Interpretation of Multi-component Lanchester Systems.

Observing that RB is a square non-negative matrix it is useful to examine some general properties of such matrices (Senata 1973).

A non-negative matrix T is a matrix in which all elements are non-negative and is denoted by $T \geq 0$. Similarly, a positive matrix T is one in which all elements all elements are greater than zero and is denoted $T > 0$. A square non-negative matrix is called primitive if there exists a positive integer k such that T^k is a positive matrix. Clearly such a T raised to any power higher than k would also be positive.

An incidence matrix $\tilde{T}$ corresponding to a given non-negative matrix T replaces all the positive entries of T by ones. $\tilde{T}$ is primitive if and only if T is primitive. All of the properties of connectivity between indices of T can be examined by treating the incidence matrix T as a graph of paths between indices. Matrices that are not primitive can be rearranged by a permutation of indices into a canonical form (a lower triangular block form) making it easier to recognize the submatrices that exhibit cyclic or transient behavior. Cyclic behavior is indicated when a specific matrix element periodically assumes a zero value as T (≥ 0) is raised to increasingly high powers. For example, in any sort of a complex engagement the -F matric is cyclic since zero blocks appear alternately in the diagonal and off diagonal positions. Transient behavior is indicated when the value of a specific matrix element in T^k reaches zero and remains so for all T^j, $j>k$. An example will be given later for the transient case where $(RB)^k = 0$ for some $k>1$. In this particular case all elements exhibit transient behavior.

Note in particular that it is possible for the ranks of T and $\tilde{T}$ to be different. For example:

$$T = \begin{bmatrix} 4 & 3 \\ 1 & 2 \end{bmatrix} \text{ (rank 2), whereas } \tilde{T} = \begin{bmatrix} 1 & 1 \\ 1 & 1 \end{bmatrix} \text{ (rank 1)}$$

Hence rank does not determine the connectivity between indices (and, therefore, does not reflect the engagement relationships between components of forces). Rank is simply an accident of the numbers that are selected as attrition coefficients.

Games (2977a) examined the properties of the F matrix in terms of diagonalability of RB and BR, and the ranks of R, B, RB and BR, to establish the circumstances that give rise to the occurrences of finite powers of t in the elements of e^{Ft}. However, he attached no physical interpretation to these results. Also Edwin Key and Kent Richard Johnson (Johnson 1978a) looked at "constants of the engagement" and decomposition of state vectors (subject to rank B = m) but they deferred examining the physical significance.

Using non-negative matrix concepts we are able to attach physical significance to some special cases and speculate about the physical significance of others. Since the behavior of the RB matrix pervades all subsequent discussion it will be convenient to first give its physical interpretation. Accordingly, $\widetilde{RB}_{ij} = 1$ means that blue component j (b_j) is attacking one or more red components that are themselves directly attacking blue component i (b_i). When $\widetilde{RB}_{ij} = 0$, b_j may or may not be engaging other components, and b_i may be receiving attrition from some red component, but the relationship of these encounters is not of the type described for $RB_{ij} = 1$.

It was shown that the behavior of the elements of e^{Ft} could be determined from the various integer powers of RB. Note, however, this formulation is valid only as long as x remains non-negative.* At any point in time when an element of the b or r vector tends to go below zero, the coefficients of both the R and B matrices must be adjusted to show no further attrition to that element.

In a large simulation involving many components over an extended period of time, it may be expected that the matrix F will be reformulated many times to accommodate destruction or withdrawal of components. Generally, in a computer model it is not desirable to adjust the matrix and state vectors sizes, and renumber components each time a unit is entered into or

*As a practical matter the behavior might not be well described by constant coefficients when the component size is reduced to near zero. As Lanchester points out in his original work, such situations are not well described by this model. To the extent that wipe-out is threatened the Lanchester model becomes more and more questionable.

removed from the engagement. Within a constant matrix size it is important to reflect such circumstances by changing entries in the R and B matrices as well as in the state vector. A unit may become "uninvolved" in the engagement by changing all coefficients in the R and B matrices associated with that unit to zero -- no changes required in its state vector.

We not examine the various types of physical engagement in the context of their R and B representations.

Case I. The Constant Case. (No engagements)

For the condition R = 0 and B = 0, RB = 0, $e^{Ft} = I_{m+n}$, and $b(t_o)$ and $r(t_o)$ remain constant. There is no interaction, no attrition: nothing is taking place. Such a situation represents peace -- although perhaps a short one, since this situation could arise during periods of maneuvering, reinforcement, etc. in preparation for engagements or as a deterrent to engagements. So while this situation may occur over intervals of the time scale of a large dynamic simulation model (as well as in actual war) we can conclude this case by a representative graph showing nodes with no branches.

Blue force	Red force
b_1	r_1
b_2	r_2
	r_3

Case II. The Linear Cases. (No counter response to attacks)

The linear cases arise when both RB and BR are equal to zero. Either R or B, but not both, may be equal to zero. When $R \neq 0$ and $B \neq 0$ the state transition matrix becomes

$$e^{Ft} = \left[\begin{array}{c|c} I_m & -Bt \\ \hline -Rt & I_n \end{array}\right].$$

The two identity blocks pick up the initial conditions for all components. The elements of the B matrix that are not zero cause linear time reduction of the corresponding red elements. Similarly, the elements of the R matrix that are not zero cause linear time reduction of the corresponding blue elements.

A specific dxample of a 2-component blue force in the field with

a 3-component red force will show this type of relationship. Here, the attack is shown by an arrow from the attacking component to the one under attack.

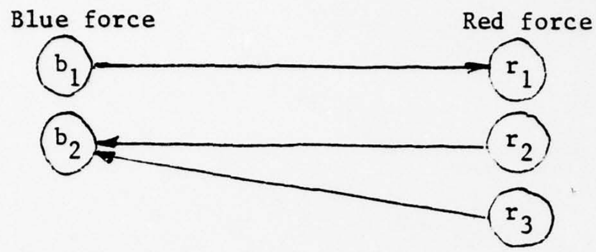

Here $\tilde{B} = \begin{bmatrix} 1 & 0 & 0 \\ 0 & 0 & 0 \end{bmatrix}^T$ and $\tilde{R} = \begin{bmatrix} 0 & 0 & 0 \\ 0 & 1 & 1 \end{bmatrix}$. RB = 0 and BR = 0.

The engagment here represents components under attack "holding their peace" either literally or due to their inability to respond to the enemy in general, or the attacking element(s) in particular. Such situations could easily arise in situations where units have no effective fighting power, but are present in the war theatre for other reasons, such as intelligence or logistic activities.

<u>Case III. The Quadratic Cases. (Indirect Engagements)</u>

Moving up the scale in combat complexity as evidenced by the increasing complexity of the RB matrix, simple quadratic cases arise when one or the other (but not both) RB and BR are equal to zero. Note that when RB = 0, $\text{Sum}_1 = I_m t$ and $\text{Sum}_2 = I_m t^2/2$. Accordingly the state transition matrix becomes

$$e^{Ft} = \Phi = \left[\begin{array}{c|c} I_m & -Rt \\ \hline -Bt & I_n + BRt^2/2 \end{array}\right]$$

(When instead, BR = 0 the quadratic term appears in the first diagonal blocks are unchanged although $\text{Sum}_1 = I_m t + (RB)t^3/3!$. The pre-multiplication of this sum by B, and the post-multiplication by R remove the cubic terms.)

Staying with the 2-versus-3 situations to generate examples, the RB = 0 quadratic case is shown here.

In this example $\tilde{B} = \begin{bmatrix} 1 & 0 & 0 \\ 0 & 0 & 0 \end{bmatrix}^T$ and $\tilde{R} = \begin{bmatrix} 0 & 1 & 0 \\ 0 & 0 & 0 \end{bmatrix}$. Here RB = 0, but BR has a single non-zero element in the 1,2-position equal to $B_{11}R_{12}$. The resulting state equations are

$$b_1 = b_1(t_o) - R_{12}r_2(t_o)t$$

$$b_2 = b_2(t_o)$$

$$r_1 = r_1(t_o) - B_{11}\left[b_1\ (t_o) - R_{12}r_2(t_o)t/2\right]t$$

$$r_2 = r_2(t_o)$$

$$r_3 = r_3(t_o)$$

Reviewing these results, we see that the attrition of the blue-1 component is proceeding linearly with time under attack of the constant red-2 component. The attrition of the red-1 component would proceed linearly with time but for the secondary effect of red-2's concurrent action against blue-1. Note that while red-2 is involved in the action it is receiving no attrition. Neither blue-2 nor red-3 are involved. It should be clear from the graph why the quadratic cases were identified as indirect engagements.

Case IV. Higher Order Polynomial Cases. (Also Indirect)

The above three cases are illustrative of situations in which the calculations of Sum_1 and Sum_2 involve the summation of finite numbers of terms. Clearly in any situation where $(RB)^k = 0$ for some positive integer k, it will be zero for all higher powers as well. The following example illustrates that if the graph of the incidence matrix - F has no loops (or cycles) that $F^k = 0$ for some k. Accordingly, all the elements of the state transition matrix will be polynomials of finite degree.

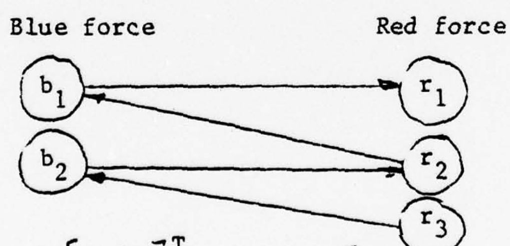

In this case $\tilde{B} = \begin{bmatrix} 1 & 0 & 0 \\ 0 & 1 & 0 \end{bmatrix}^T$ and $\tilde{R} = \begin{bmatrix} 0 & 1 & 0 \\ 0 & 0 & 1 \end{bmatrix}$. Here

$\widetilde{RB} = \begin{bmatrix} 0 & 1 \\ 0 & 0 \end{bmatrix}$, but $\widetilde{(RB)^2} = 0$.

Case V. Infinite Series of Matrices (Direct Engagement)

When loops appear in the connection diagram the idea of full engagement is encountered. The existence of a loop can be confirmed by observing that there is no integer k such that $(RB)^k = 0$.

In the case of no loops Sum_1 and Sum_2 could be represented by finite sums. However, the presence of loops in the connection diagram creates a situation in which the matrix power series for Sum_1 and Sum_2 do not terminate.* The case of concern here -- the direct engagement case -- is one which a block of the RB matrix can be identified as primitive. The cyclic blocks make up the next case. To clarify this two examples are given.

Simple Direct Engagement

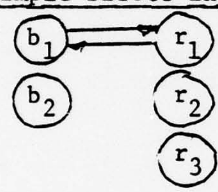

$$\tilde{B} = \begin{bmatrix}1 & 0 & 0\\ 0 & 0 & 0\end{bmatrix}^T, \quad \tilde{R} = \begin{bmatrix}1 & 0 & 0\\ 0 & 0 & 0\end{bmatrix}$$

$\widetilde{RB} = \begin{bmatrix}1 & 0\\ 0 & 0\end{bmatrix} = \widetilde{(RB)}^k$ for all $k > 0$. If $\widetilde{RB}$ is treated as a partitioned matrix $\left[\begin{array}{c|c}1 & 0\\ \hline 0 & 0\end{array}\right]$ it can be seen that block 1,1 is primitive. (The 0 blocks occur because the uninvolved components were retained in the model.)

Extensive Involvement

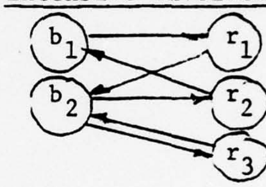

$$\tilde{B} = \begin{bmatrix}1 & 0 & 0\\ 0 & 1 & 1\end{bmatrix}^T, \quad \tilde{R} = \begin{bmatrix}0 & 1 & 0\\ 1 & 0 & 1\end{bmatrix}$$

$$\widetilde{RB} = \begin{bmatrix}0 & 1\\ 1 & 1\end{bmatrix}, \quad \widetilde{(RB)}^2 = \begin{bmatrix}1 & 1\\ 1 & 1\end{bmatrix}.$$

Here RB is primitive. All elements of the state transition matrix are made up of infinite series in t.

From the examples given, it would appear that the existence of direct confrontations -- such as b_1 versus r_1 in the first example and b_2 versus r_3 in the second example -- causes primitive blocks to appear. (The existence of primitive blocks, however, does not imply direct confrontation.) Cyclic cases also produce series for Sum_1 and Sum_2 that do not terminate. These do not have direct confrontations. The next case should clarify this point.

*There may be elements in Sum_1 and Sum_2 that are made up of terminating series. Such elements simply indicate that the corresponding force components are not "fully involved". That is, they are not part of a loop. Our interest here is focused on the components that are fully involved.

Case VI. Infinite Series of Matrices (Circular Interaction)

The fact that there is no k which causes $(RB)^k$ to disappear does not guarantee the presence of primitive blocks. Engagements with only cyclic blocks do occur. Let us examine the following connection diagram:

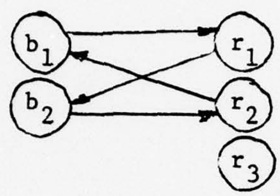

$$\tilde{B} = \begin{bmatrix} 1 & 0 & 0 \\ 0 & 1 & 1 \end{bmatrix}^T, \quad \tilde{R} = \begin{bmatrix} 0 & 1 & 0 \\ 1 & 0 & 0 \end{bmatrix}, \quad \widetilde{RB} = \begin{bmatrix} 0 & 1 \\ 1 & 0 \end{bmatrix}, \quad \widetilde{(RB)}^2 = \begin{bmatrix} 1 & 0 \\ 0 & 1 \end{bmatrix}, \quad \widetilde{(RB)}^3 = \widetilde{RB}, \text{ etc.}$$

Here RB has a cyclic behavior of period 2. Although Sum_1 and Sum_2 are still non-terminating series, alternate power terms (since the period is 2) will be missing.

Note that the connections here are the same as those in the second example of Case V, except that here r_3 is not involved in the engagement. Thus, it is seen that the inclusion of r_3 in the engagement in the manner specified in Case V changes the RB matrix from cyclic to primitive.

The technique for creating examples of engagements containing periods greater than two can easily be visualized.

Summarizing Cases V and VI we note that it is only when RB has primitive or cyclic blocks that the defined sums (Sum_1 and Sum_2) will be non-terminating. This condition implies loops in the connection diagram.

Case VII. One-versus-many. A special case with closed form solution.

As development of overview models proceeds many special features will have to be considered. Some of these may be optimum allocation, mobility, the timing of reallocation decisions, time varying coefficients, and reinforcement policy. For these deliberations it may be useful to have an analytic solution of the most general Lanchester model that lends itself to such treatment. This appears to be the one-versus-many case for which the closed form solutions are given:

For m = 1 (the blue force has only one component), and by defining a scalar constant $c = +(RB)^{\frac{1}{2}}$ the state transition matrix takes on the form:

$$
e^{Ft} = \begin{cases} \left[\begin{array}{c|c} 1 & -Rt \\ \hline -Bt & I_n + BRt^2/2 \end{array}\right] & \text{if } c = 0, \text{ and} \\[2ex] \left[\begin{array}{c|c} \cosh(ct) & -(1/c)\sinh(ct)R \\ \hline -(1/c)\sinh(ct)B & I_n = (1/c^2)\left[\cosh(ct)-1\right] BR \end{array}\right] & \text{otherwise.} \end{cases}
$$

Case Z. Combinations of Engagements.

As one might expect in larger systems, mixtures of all of the preceeding cases can occur. When it is possible to decompose the F matrix and state vectors into separate encounters these subsidiary engagements become visible. An alternate method of making the separate engagements visible is to rearrange the -F matrix into the canonical (lower triangular block form). All closed primitive and cyclic blocks would then appear in the diagonal blocks, and the contributions of elements not fully engaged would appear in the lower trianglaur part of the matrix.

Note that not all types of engagements have been examined. We have not considered connections that may be described as trees leading into loops, loops within loops, connected loops, trees leading out from loops, and other exotic non-decomposible combinations. Although physical interpretation of such cases is obvious from the connection graphs, the detailed influence of these connections on the state transition matrix is not obvious and further study is called for: But, no matter. Whatever behavior obtains, the RB matrix is the key to finding all of the elements of e^{FT}.

At the very least, this approach to analyzing the exponential matrix in power series form is developing insight into fundamental relationships. In any actual simulation, approximate solutions of $\dot{x} = Fx$ would most likely be found by numerical integration using a variable time step. Upon the occurance of certain state conditions -- e.g., the impending attrition of a component to a negative value -- the F matrix would have to be adjusted before the integration

could continue. The Fortran-based combined simulation method GASP IV developed by Pritsker (1974) is well suited to such investigations. It is capable of treating all of the continuous and discrete behaviors the various models might take on. Further, extensions to studies of non-linear, parametric, and probabilistic attrition relationships could be easily accommodated by simple programming changes.

CONCLUSIONS AND RECOMMENDATIONS

The results of this study of the expanded Lanchester model show that there is still much to learned by mathematical inquiry into attrition relationships. In this particular case it was shown for the multi-component model that a small incidence submatrix (derived from RB) of the overall system matrix (F) held the key to perceptions of the interactions.

Much work remains to be done in the development and examination of force relationships for inclusion in overview models for C^3I. In the past such force relationships have been based on Lanchester's pioneering work. His equations can be extended to deal with such issues as reinforcement, fratricide, and time-varying force effectivenesses. Future overview models, however, will require much more. They will need to treat optimum movement of forces, time lost in such movements, changes in effectiveness of forces as well as their size, measured responses in place of all-out conflict, behavior during quiet periods, optimum allocation of forces, reallocation of forces during engagements, etc.

Such requirements extend well beyond the mathematically tractable cases such as the one treated in this report. It may be necessary to break completely out of the Lanchester pattern. Computer studies will have to produce the insights previously provided by analysis. So in some sense the computer will be instrumental in developing the theory of simulation modelling for C^3I. Proposals for work of this nature will be forthcoming.

REFERENCES

Durstine, R. M. (1963), A Lanchester Model Incorporating the Introduction of Reinforcements (Project 850), MITRE Corporation Working Paper W-5791, Bedford, Massachusetts, February 1, 1963.

Everett, Robert R. (1977), Lanchester and C^3, Draft Final Report of the Air Force Command, Control and Communications Technology Panel, Air Force Studies Board, October 1977.

Fain, Janice Bloom (1977), The Lanchester Equations and Historical Warfare: An Analysis of Sixty Wold War II Land Engagements., History, Number and War, Spring 1977.

Games, Richard A. (1977a), A Survey of Tactical Command & Control Models, MITRE Corporation Working Paper WP-21483, Bedford, Massachusetts, October 1977.

Games, Richard A. (1977b), The Solution of the Multicomponent Lanchester Equations using the Matrix Exponential, MITRE Corporation Working Paper 21482, Bedford, Massachusetts, November 1977.

Games, Richard A., and Richard P. Witt (1978), Simplified Tactical Air C^3 Simulation (STACS), the MITRE Corporation, Bedford, Massachusetts, Working Paper in preparation.

Johnson, Kent Richard (1977a), Comments on TAC Controller and CASM Simulations, MITRE Corporation Working Paper WP-21142, Bedford Massachusetts, January, 1977.

Johnson, Kent Richard (1977b), Thoughts on C^3I Implications of the Lanchester Equations, MITRE Corporation Memorandum D53-M-337, Bedford, Massachusetts, May 3, 1977.

Johnson, Kent Richard (1978a), Solutions of the Lanchester Equations, MITRE Corporation Working Paper WP-21660, Bedford, Massachusetts, February, 1978.

Johnson, Kent Richard (1978b), Lanchester Representation of Engagements, MITRE Corporation Memorandum D54-M-347, March 31, 1978.

Lanchester, F. W. (1916), Mathematics in Warfare, <u>The World of Mathematics</u>, edited by J. R. Newman, Simon and Schuster, Vol. 4, pp 2138-2157, 1956.

Latchaw, John H., Capt., USAF (1972), A Lanchester Model for Air Battles, Air Force Institute of Technology - Thesis, February 1972.

Pritsker, A. Alan B. (1974), The GASP IV Simulation Language, Wiley, New York.

Seneta, E. (1973), Non-Negative Matrices: An Introduction to Theory and Applications, John Wiley & Sons, New York.

Valrand, Carlos (1974), Air Defense System Performance and Operational Cost Analysis Model (PERCAM), TRW Systems Group, Huntsville, Alabama, December 1974.

Willard, D. (1962), Lanchester as a Force on History: An Analysis of Land Battles of the Years 1618-1905, RAC-TD-74, Research Analysis Corporation.

1978 USAF-ASEE SUMMER FACULTY RESEARCH PROGRAM

SPONSORED BY

THE AIR FORCE OFFICE OF SCIENTIFIC RESEARCH

CONDUCTED BY

AUBURN UNIVERSITY

OVERLAPPED SUB-ARRAY TECHNIQUES FOR USE IN A SPACE RADAR

PREPARED BY: PAUL R. CARON, PH.D.
ACADEMIC RANK: PROFESSOR
DEPARTMENT AND UNIVERSITY: DEPARTMENT OF ELECTRICAL ENGINEERING, SOUTHEASTERN MASSACHUSETTS UNIVERSITY

ASSIGNMENT: HANSCOM AIR FORCE BASE
LABORATORY: RADC
DIVISION: ELECTROMAGNETIC SCIENCES
BRANCH: ANTENNAS AND R-F COMPONENTS

USAF RESEARCH COLLEAGUE: ROBERT MAILLOUX, PH.D.
DATE: JULY 28, 1978
CONTRACT NUMBER: F44620-75-C-0031

ABSTRACT

In applications of phased array antennas for limited scan, sub-array schemes prove to be useful in reducing costs and space. This report is an investigation of two such techniques, namely the space fed lens and a constrained feed system.

Radiation patterns for a space-fed flat lens are presented and it is shown that this system compares favorably in performance with the spherical lens, the latter being more difficult and expensive to construct in a space environment. Results on the effects of surface perturbations in the lens are presented along with an embryonic concept for phase correcting at the feed for these perturbations.

A synthesis technique is presented for constrained sub-array feed systems. It is based on Fourier techniques and leads to approximate implementation by Butler Matrices. The performance of this technique is quite good with the exception of efficiency and techniques to improve the latter need to be investigated.

ACKNOWLEDGEMENTS

The author wishes to express his deepest appreciation to Dr. Robert Mailloux for his suggestions, interest, encouragement and consultations throughout the course of this work.

The financial support provided by the USAF and ASEE Summer Faculty Research Program administered by Auburn University and the facilities provided by the Antennas Branch of RADC at Hanscom Field are acknowledged.

The author also wishes to acknowledge the administrative efforts of Mr. J. Fred O'Brien, Director of this program.

All of the above contributed to a professionally rewarding experience.

LIST OF FIGURES

I. INTRODUCTION

Many military and civilian applications of phased array antennas require less than full sector scan. Two general classes of sub-array systems are used for this purpose are[1]: (1) an array near the focal point of a lens or reflector and (2) a constrained feed system which suppresses grating lobes.

The first part of this report will present some results pertaining to one-dimensional lens systems. Computer programs have been written to give results on a spherical lens system; this system was previously studied by Borgiotti[2]. Results are also presented for a flat lens system. Antenna radiation patterns are displayed for both systems as a function of scan angle. The effects of mechanical deformation of the flat lens surface are detailed along with a possible approach to correcting for these deformations by the feed system.

The second part of this report concentrates on the synthesis of a constrained sub-array system. The synthesis is based on the circuits of Dufort[3]. However, modified expressions for the radiation pattern are obtained and a Fourier Synthesis Method is utilized leading to the required circuit transfer functions being well approximated by Butler Matrices.

II. OBJECTIVES

One of the objectives of this research was to obtain data on a flat-lens system and to compare this with the spherical-lens data. In particular, tolerance effects and corrections for thses effects were looked into. Also design techniques for constrained sub-array systems were developed.

III. THE LENS PROBLEM

Figure 1 shows the lens system analyzed by Borgiotti[2]. A Butler Matrix is used to form multiple beams which are directed at the lens. The source is "phase-focused" to the center of the lens which, in turn, is focused at the center of the source. Computer programs were written to give results on this system as well as the flat lens system. In contrast to Borgiotti[2], a discrete antenna approach is used. Results are shown in Figures (2) - (6) and differ little from the cited reference. Figures (2) and (3) show the radiation pattern obtained when just one of the two outer and inner beams are driven, respectively. Figures (4), (5) and (6) give radiation patterns at three different scan angles. The plots shown use sixteen antennas in the source, 100 antennas in the lens and in both cases the element seperation in $\lambda/2$. The inputs to the Butler Matrix have a Taylor amplitude distribution. The computer programs have been written in modular form, i.e., as a system of subprograms to enhance their flexibility. For example, the program which gives the transfer function of the Butler Matrix can be used with any order Butler and switches allow one to set a progressive phase or take inputs from the main program or write out the output quantities, etc. Also, switches in the program allow radiation patterns to be obtained as DB or magnitude as a function of angle in radians or degrees or as a function of the since of the angle and over any range of these variables. To obtain results on either lens system one simply links the requisite programs. Most of the work has been done on a time-sharing computer system giving fast "turn-around" of results. One of the disadvantages of the system is apparent in the radiation patterns, namely that details of the side-lobes are not recognizable. This is not a problem in the interactive mode since any portion of the patterns may be inspected but, from the standpoint of displaying the results in a limited length report, the plots leave something to be desired.

Results for the flat-lens system of Figure (7) are given in Figures (8) - (12) for conditions similar to the spherical lens. In this case the focal length is increased to minimize spatial phase distortion. This is accompanied by an increase in the element spacing of the source antenna to

$$d = 1.45 \ (\lambda/2)$$

The inner eight beams of the Butler matrix are used and there are 107 antennas in the lens. Figures (8) and (9) show the radiation patterns of two individual beams and Figures (10), (11) and (12) are patterns for three progressive phases with Taylor amplitude distributions. Clearly, the results are similar to the spherical lens.

One of the possible difficulties with the space radar array involves mechanical deformations in the flat lens surface. To investigate this effect the computer programs were modified so that either sine or cosine surface deformations of arbitrary amplitude could be investigated. Figures (13) and (14) show radiation patterns for peak-to-peak deformations (cosine) of 0.1λ with a period of twice the lens length and 20 times the lens length, respectively. Similar results for peak-to-peak deformation of λ are shown in Figures (15) and (16). However, in this latter case a mechanical period of 20 results in an unusable pattern. Results are thus shown for a period of 2 in Figure (16).

One of the possible advantages of the space-fed lens concept involves the possible correction for such deformations at the feed. This concept was investigated in only a preliminary way. Assume that the sub-array functions, F_n, at the output of the lens are known. If surface deformations, y_n, at each element are assumed perpendicular to the lens face then the radiation pattern is

$$P(u) = \sum_n^1 F_n \, e^{jn\frac{u}{M} + j\,k\,y_n \cos\theta}$$

where

$$u = k\,D\,\sin\theta$$
$$D = Md$$
$$d \sim \text{element spacing}$$

Using notations similar to Dufort[3] we define

$F_n \sim$ output to each antenna from a given sub-array input with all sub-array driven and with no surface deformations.

$$F_{no} = \sum_\ell^1 F_{n - M\ell}\, Z_{\ell o}$$

where

$$Z_{\ell o} = |Z_{\ell o}| e^{-j\ell u_o}$$

thus

$$P_o(u) = \sum_n \sum_\ell f_{n - M\ell}\, Z_{\ell o}\, e^{j\,n\frac{u}{M}}$$

$$= \sum_\ell |Z_{\ell o}| e^{j\ell(u - u_o)} \sum_p F_p \, e^{jp\,\frac{u}{M}}$$

where the second factor is clearly the individual sub-array pattern. If with surface deformations we let

$$Z_\ell = Z_{\ell o}\, e^{j\alpha_\ell}$$

So that α_ℓ can be set to compensate for these deformations then a similar development yields

$$P(u) = \sum_n \sum_\ell f_{n - m\ell}\, e^{j(\frac{n}{M} - \ell)u} e^{j\ell(u - u_o)}\, |Z_{\ell o}|\, e^{j\alpha_\ell}\, e^{jky_n \cos\theta}$$

$$= \sum_p^1 f_p\, e^{j\frac{P}{M}u} \sum_\ell^1 |Z_{\ell o}| e^{j\alpha_\ell}\, e^{j\ell(u - u_o)}\, e^{jky_{P + M\ell}\cos\theta}$$

If, we expand the last term as follows:

$$e^{jky_n \cos\theta_o} = \sum_q^1 a_q f^*_{n - Mq}$$

where θ_o is the direction of the main beam

$$P(u_o) = \sum^1 |Z_{\ell o}| c^{j\alpha_\ell} \sum_q^1 a_q \sum_p^1 f_p f^*_{p - M(q - \ell)} e^{j\frac{P}{M}u_o}$$

and we wish to choose $\alpha\ell$ so that

$$P(u_o) = P_o(u_o)$$

the case $u_o = 0$ with orthogonal f_n is particularly simple since

$$\sum_p^1 f_p f^*_{p - M(q - \ell)} = \partial_{q\ell}$$

which leads to

$$\alpha_\ell = -k Y_\ell \cos\theta_o$$

which is intuitively satisfying and somewhat obvious.

Clearly much work must be done before the above has significance. In the future the following will be investigated.

1. Obtain more data on the effects of surface deformations on radiation patterns and try to relate the deformation quantities to antenna performance indicators such as gain, beamwidth, sidelobe levels, etc.
2. Using the above as a guide develop expressions for phase correction of deformations in the space fed lens - i.e. account for the effects of deformations in the source-to-lens path as well as in the radiation from the lens.

3. Investigate the functional implications of the expansion of $\exp(j\, k\, y_n \cos\theta)$ in terms of sub-array functions.
4. In the above we have tried to minimize variations in the main beam. Clearly one might also work to keep the effects on sidelobes low at some degradation in the main beam.
5. Once a suitable phase correction scheme is developed, the existing computer programs can be used to obtain radiation pattern with deformations and with and without phase corrections.

IV. CONSTRAINED SUB-ARRAY SYNTHESIS

We wish to consider the class of circuits of Dufort[3] as shown in Figure 17. Two types of circuits labeled A and B are utilized. As shown in the Figure Z represents the sub-array inputs, g represents the M outputs of the B circuits, h represents these outputs as rearranged to be the inputs to the A circuits and t represents the outputs of the A circuits. If, we consider an infinite array so that ℓ takes on all integer values and $o \leq n \leq M - 1$,

$$g_{h + M\ell} = B_n Z_\ell$$

$$h_{n + M\ell} = g_{n + (\ell - n)M}$$

$$t_{n + M\ell} = \sum_{q = 0}^{M - 1} A_{n,q} h_{q + M\ell}$$

$$= \sum_{q = 0}^{M - 1} A_{n,q} g_{q + (\ell - q)M}$$

$$= \sum_{q = 0}^{M - 1} A_{n,q} B_q Z_{\ell - q}$$

Hence the radiation pattern is

$$P(u) = \sum_{\ell} \sum_{n = 0}^{M - 1} t_{n + M\ell} e^{j(n + M\ell) \frac{u}{M}}$$

where

$$u = k D \sin\theta, D = Md, k = 2\Pi/\lambda$$

and d is the element spacing (we will use $d = \lambda/2$). Thus

$$P(u) = \sum_{\ell} \sum_{n=0}^{M-1} \sum_{q=0}^{M-1} A_{n,q} B_q \sum Z_{\ell - q} e^{j \ell u}$$

in the summation over ℓ let $\ell - q = p$

$$P(u) = \sum_{n=0}^{M-1} e^{jn\frac{u}{M}} \sum_{q=0}^{M-1} A_{n,q} B_q e^{jqu} \sum_{p} Z_p e^{jpu}$$

and if we let

$$Z_p = a_p e^{-jpu_o}$$

representing normal progressive phasing of the sub-arrays, then we may write

$$P(u) = G(u) H(u)$$

where H(u) represents the array factor

$$H(u) = \sum_{p} a_p e^{jp(u - u_o)}$$

and G(u) is the "element factor" or sub-array pattern

$$G(u) = \sum_{n=0}^{M-1} e^{jn\frac{u}{M}} \sum_{n=0}^{M-1} A_{n,q} B_q e^{jqu}$$

and it is this function which we will synthesize. Let

$$W = e^{j\frac{u}{M}}$$

$$G(W) = \sum_{q=0}^{M-1} B_q W^{qM} \sum_{n=0}^{M-1} 1 A_{n,q} W^n$$

where we have interchanged the order of summations. This is a polynomial of order $M^2 - 1$ in the variable W.

We synthesize the function G(W) using a Fourier expansion. We will consider the case M = 4 and get the best RMS fit to the function shown in Figure 18.

This gives the Fourier coefficients

$$a_n = \frac{2}{n\pi} \sin(\frac{n\pi}{4})$$

where n takes on half-integer values from $-\infty$ to $+\infty$.

The polynominal G(W) is

$$G(W) = B_o \{A_{0,0} + A_{1,0} W + A_{2,0} W^2 + A_{3,0} W^3\} + B_1 W^4 \{A_{0,1} + A_{1,1} W + A_{2,1} W^2 + A_{3,1} W^3\} + B_2 W^8 \{A_{0,2} + A_{1,2} W + A_{2,2} W^2 + A_{3,2} W^3\} + B_3 W^{12} \{A_{0,3} + A_{1,3} W + A_{2,3} W^2 + A_{3,3} W^3\}$$

Thus, we require

$$B_1 A_{3,1} = B_2 A_{0,2} = \frac{2}{\pi} \sin(\frac{\pi}{8})$$

$$B_1 A_{2,1} = B_2 A_{1,2} = \frac{2}{3\pi} \sin(\frac{3\pi}{8})$$

$$B_1 A_{1,1} = B_2 A_{2,2} = \frac{2}{5\pi} \sin(\frac{5\pi}{8})$$

$$B_1 A_{0,1} = B_2 A_{3,2} = \frac{2}{7\pi} \sin(\frac{7\pi}{8})$$

$$B_0 A_{3,0} = B_3 A_{0,3} = \frac{2}{9\pi} \sin(\frac{9\pi}{8})$$

$$B_0 A_{2,0} = B_3 A_{1,3} = \frac{2}{11\pi} \sin(\frac{11\pi}{8})$$

$$B_0 A_{1,0} = B_3 A_{2,3} = \frac{2}{13\pi} \sin(\frac{13\pi}{8})$$

$$B_0 A_{0,0} = B_3 A_{3,3} = \frac{2}{15\pi} \sin(\frac{15\pi}{8})$$

It does not appear to be possible to synthesize these networks in a lossless way. Combining these various outputs for the broadside case shows that the illumination efficiency will be good if appropriate circuits can be constructed.

Let us assume that the B network is a simple power divider

$$B_0 = B_1 = B_2 = 1/\sqrt{4} = \tfrac{1}{2}$$

The A network can be represented as a matrix

$$\{A\} = \begin{bmatrix} \frac{4}{15\pi}\sin\left(\frac{15\pi}{8}\right) & \frac{4}{7\pi}\sin\left(\frac{7\pi}{8}\right) & -\frac{4}{\pi}\sin\left(-\frac{\pi}{8}\right) & \frac{4}{9\pi}\sin\left(\frac{9\pi}{8}\right) \\ \frac{4}{13\pi}\sin\left(\frac{13\pi}{8}\right) & \frac{4}{5\pi}\sin\left(\frac{5\pi}{8}\right) & \frac{4}{3\pi}\sin\left(\frac{3\pi}{8}\right) & \frac{4}{11\pi}\sin\left(\frac{11\pi}{8}\right) \\ \frac{4}{11\pi}\sin\left(\frac{11\pi}{8}\right) & \frac{4}{3\pi}\sin\left(\frac{3\pi}{8}\right) & \frac{4}{3\pi}\sin\left(\frac{5\pi}{8}\right) & \frac{4}{13\pi}\sin\left(\frac{13\pi}{8}\right) \\ -\frac{4}{9\pi}\sin\left(-\frac{9\pi}{8}\right) & -\frac{4}{\pi}\sin\left(-\frac{\pi}{8}\right) & \frac{4}{7\pi}\sin\left(\frac{7\pi}{8}\right) & \frac{4}{15\pi}\sin\left(\frac{15\pi}{8}\right) \end{bmatrix}$$

$$= \begin{bmatrix} -.0325 & .0696 & .4872 & -.0541 \\ -.0905 & .2353 & .3921 & -.1069 \\ -.1069 & .3921 & .2353 & -.0905 \\ -.0541 & .4872 & .0696 & -.0325 \end{bmatrix}$$

Inspection of the first form or the very method itself suggests that the transfer function is a Fourier Transform Device. Consequently, it seems reasonable that synthesis be tried using Butler Matrices or Rotman Lenses. One circuit which gives an excellent approximation to the required A circuit is shown in Figure 19.

The inputs are to a fourth order Butler which feeds the "inner beams" of a sixteenth order Butler and the outputs are taken from the inner terminals of the latter. Using the notation shown on the left of Figure 19,

$$E_\ell^1 = \frac{1}{\sqrt{M}} \sum_{P = -\frac{M-1}{2}}^{\frac{M-1}{2}} e^{j\ell p\frac{2\pi}{M}} E_p^0$$

where M = 4 and ℓ assumes the values of -3/2, -1/2, 1/2, 3/2. Also,

$$E_P^2 = \frac{1}{M} \sum_{\ell = -\frac{M-1}{2}}^{\frac{M-1}{2}} e^{jp\ell \frac{2\pi}{M^2}} E_\ell^1$$

where M = 4 and q also assumes the values -3/2, -1/2, 1/2, 3/2. Thus

$$E_q^2 = \frac{1}{M^{3/2}} \sum_{\ell = -\frac{M-1}{2}}^{\frac{M-1}{2}} \sum_{P = -\frac{M-1}{2}}^{\frac{M-1}{2}} e^{j\ell\left(\frac{P}{M} + \frac{q}{M^2}\right) 2\pi} E_p^o$$

if we assume only one input is driven by a unity wave we may describe the transfer function

$$C_{q,p} = \frac{1}{M^{3/2}} \sum_{\ell = -\frac{M-1}{2}}^{\frac{M-1}{2}} e^{j\ell\left(\frac{P}{N} + \frac{q}{M^2}\right) 2\pi}$$

$$= \frac{1}{M^{3/2}} \quad \frac{\sin\{(P + \frac{1}{M} q)\pi\}}{\sin\{(P + \frac{1}{M} q) \frac{\pi}{M}\}}$$

and for M = 4,

$$C_{q,p} = \frac{1}{8} \frac{\sin\{(P + q/4)\pi\}}{\sin\{(P + q/4)\pi\}}$$

Care is needed in associating this transfer function with the required A circuit since in C the indices take on values -3/2, -1/3, 1/2, 3/2 and in the A circuit the corresponding indices are 0, 1, 2, 3.

The matrix which represent the A circuit as synthesized using Butler Matrices is shown below. Clearly, the agreement with the required {A} is good.

$$
\{A\} = \underset{\text{Butler Synthesized}}{} \begin{bmatrix} -.048 & .075 & .488 & -.062 \\ -.121 & .245 & .398 & -.131 \\ -.131 & .398 & .245 & -.121 \\ -.062 & .488 & .075 & -.048 \end{bmatrix}
$$

The output phase variations that obtains from this type of circuit are shown in Figures 20 - 22 for M = 2, 4, and 8. The verticle bars indicate the extent of adjacent element-to-element phasing, clearly the "phase interpolation" is quite good until one reaches near the scan limit. Figure 23 shows the radiation pattern from a system formed of 25 of these modules with M = 4 (i.e., total of 100 antennas) for input phasing of 0^o, 80^o, 160^o. The main beam is positioned as expected and the grating lobe (at $0 = -30^o$ for broadside case) which moves toward the field of view grows as scan angle is increased. The grating lobe which moves away from the field of view virtually disappears.

One of the major difficulties of the technique is that the sixteenth order Butler must have twelve of its outputs terminated and this results in substantial loss. Figures 24 - 26 show the efficiency of this type system as a function of scan for M = 2, 4, 8.

Future work on this technique will be along the following lines:

1. Use the circuit as synthesized and obtain radiation patterns of various size arrays as a function of scan angle.
2. Search for ways of eliminating the losses associated with the above technique. First attempts will focus on rearranging the way in which the A and B circuits are interconnected and the possible use of the unused inputs and outputs in the higher order Butler.

V. CONCLUSIONS AND RECOMMENDATION

It has been shown that the flat lens system operates in a fashion similar to the spherical lens system with little degradation in performance. It offers the advantage of constructional simplicity. Methods of compensating for positive mechanical deformations have been investigated and it is recommended that research along these lines be persued.

A design technique for constrained feed systems for sub-arrays has been introduced and results on a system which implements this scheme using Butler Matrices have been presented. While this scheme has promise, the efficiency is the primary difficulty and it is recommended that techniques to improve the efficiency be investigated.

VI. REFERENCES

1. Mailloux, R. J., Trends in Array Antenna Research, RADC-TR-77-195, June, 1977.

2. Borgiotti, G. V. (1977), An Antenna for Limited Scan in One Plane: Design Criteria and Numerical Simulation, IEEE Trans. AP-25, (No.2), 232 - 243.

3. Dufort, E. C. (1978), Constrained Feeds for Limited Scan Arrays, IEEE Trans. AP-26, (No. 3), 407 - 413.

4. Collin, R. and Zucker, F., Antenna Theory, Part 1, Chapter 7, McGraw-Hill, 1969.

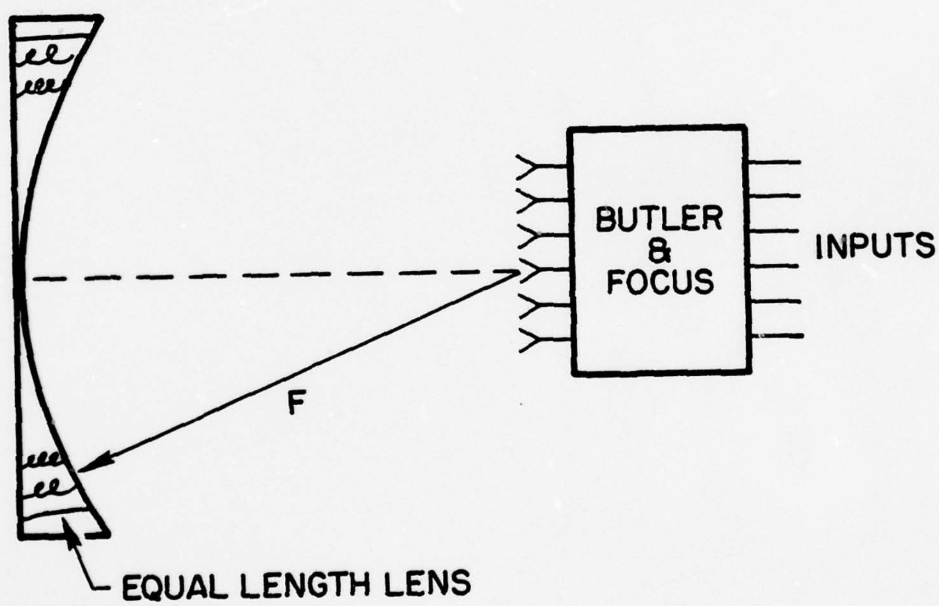

FIG. 1 - THE SPHERICAL LENS CONFIGURATION

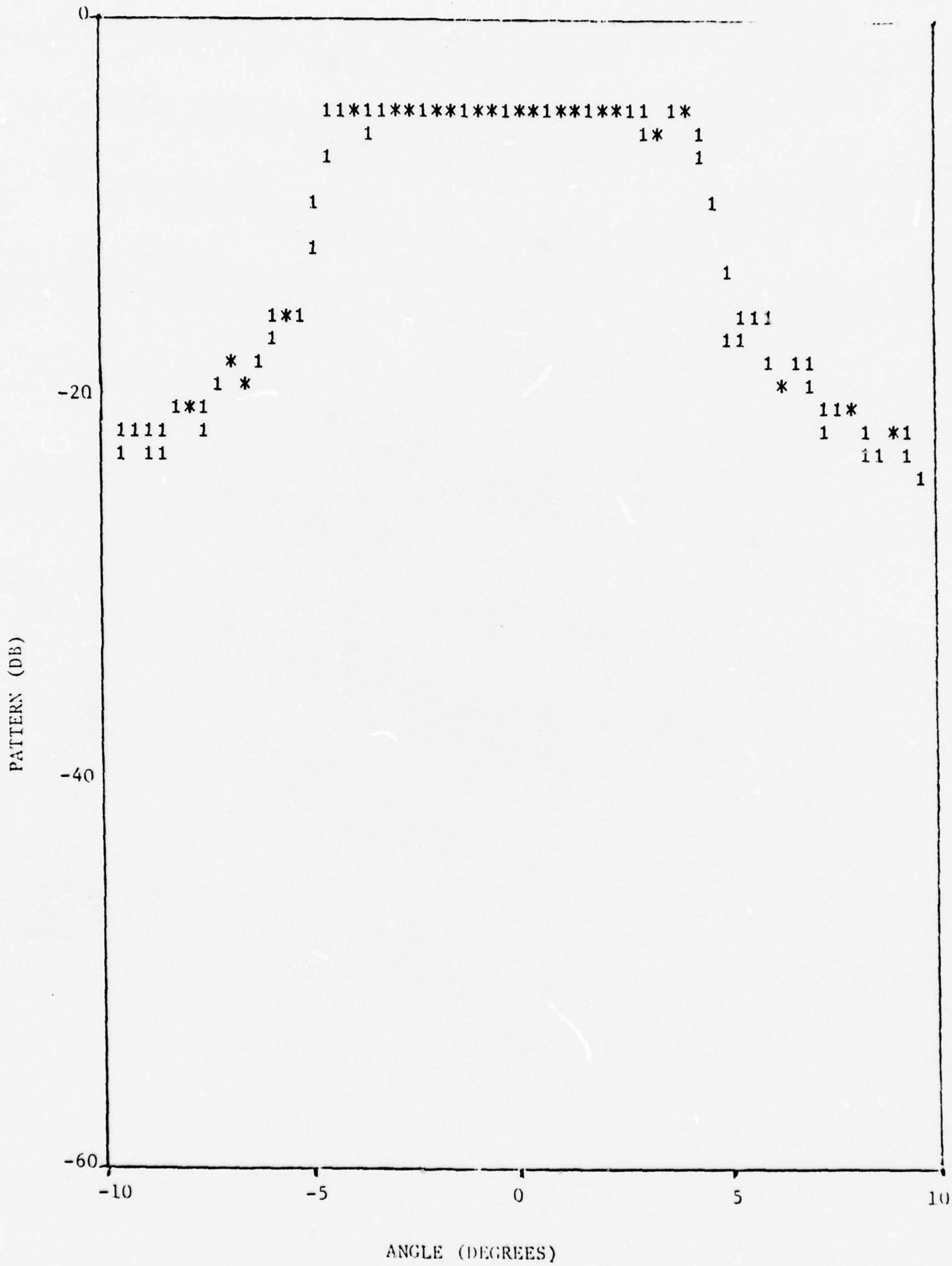

FIG. 2 - RADIATION PATTERN FROM SPHERICAL LENS WHEN ONLY THE LEFT, OUTERMOST BEAM IS DRIVEN

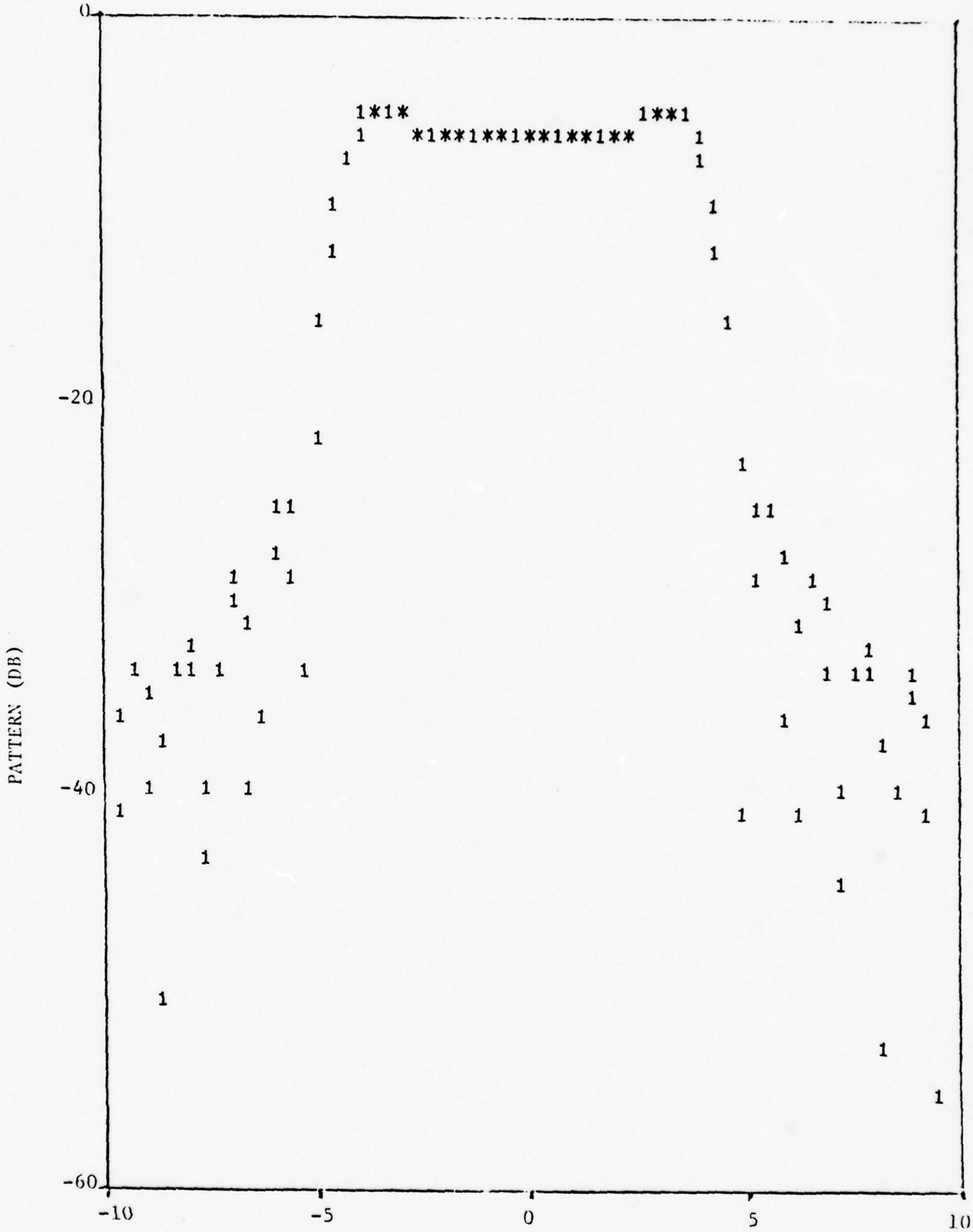

FIG. 3 - RADIATION PATTERN FROM SPHERICAL LENS WHEN ONLY THE LEFT, INNERMOST BEAM IS DRIVEN

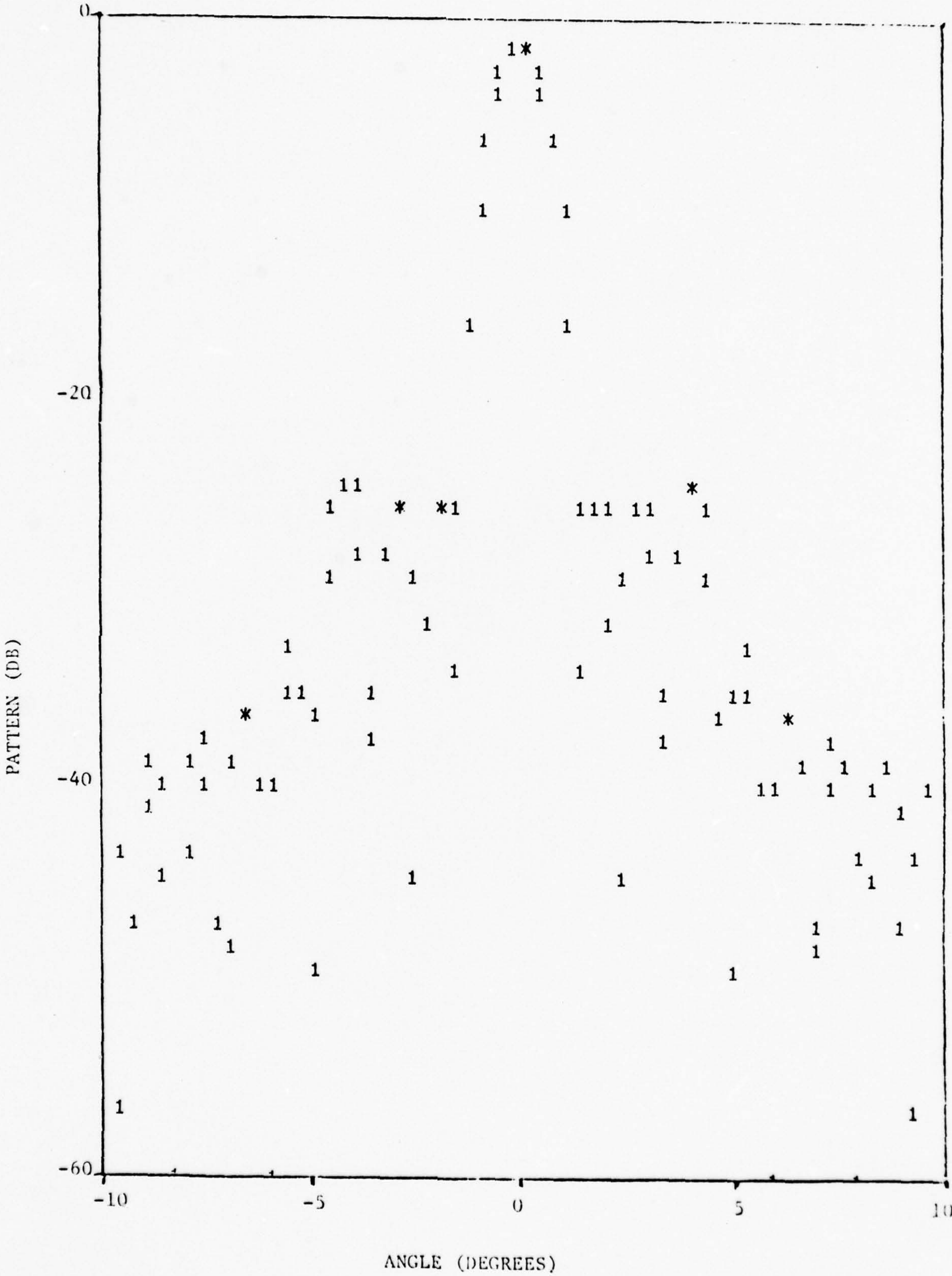

FIG. 4 - RADIATION PATTERN FROM SPHERICAL LENS FOR PROGRESSIVE PHASE = 0°

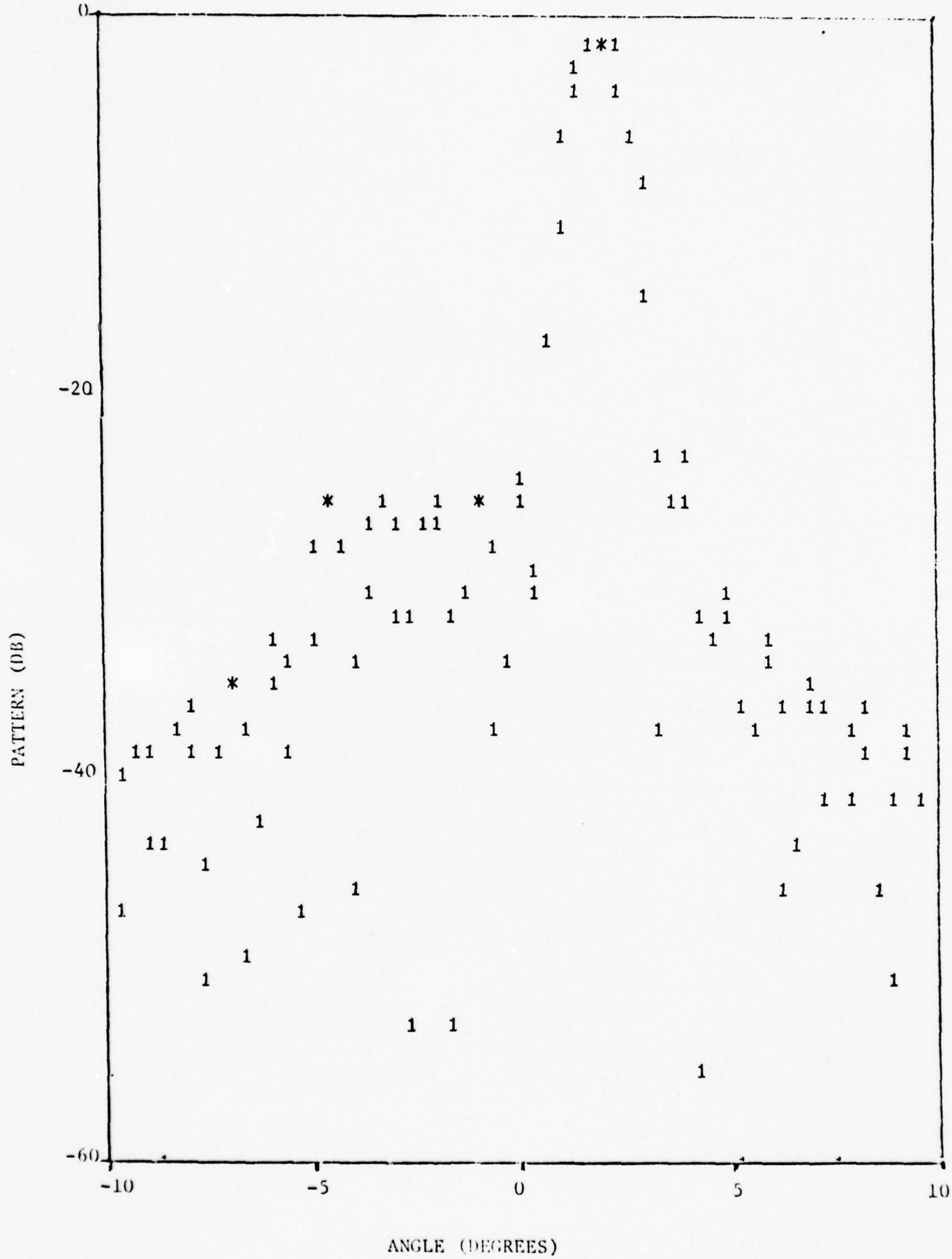

FIG. 5 - RADIATION PATTERN FROM SPHERICAL LENS FOR PROGRESSIVE PHASE = 80°

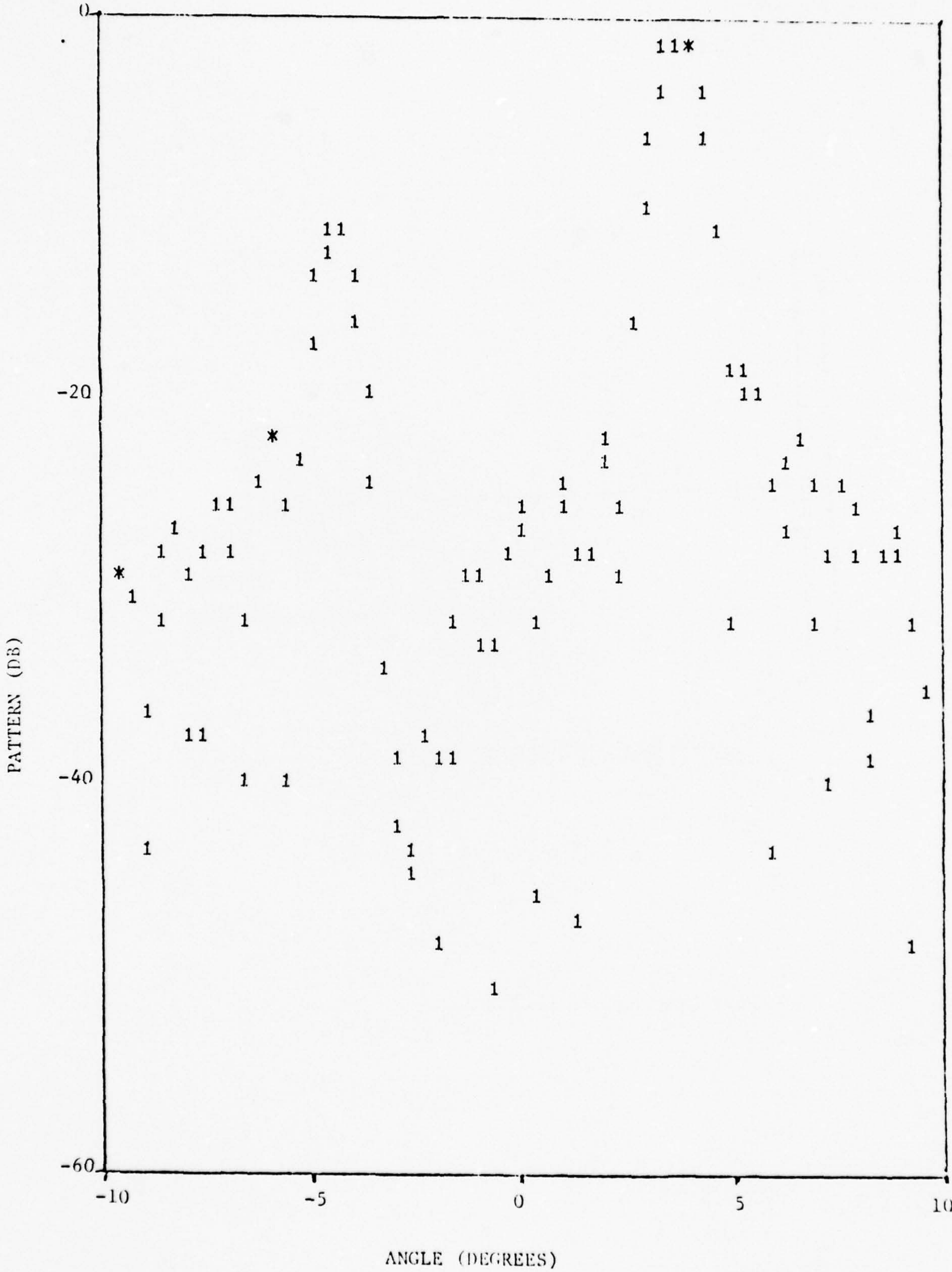

FIG. 6 - RADIATION PATTERN FROM SPHERICAL LENS FOR PROGRESSIVE PHASE = 160°

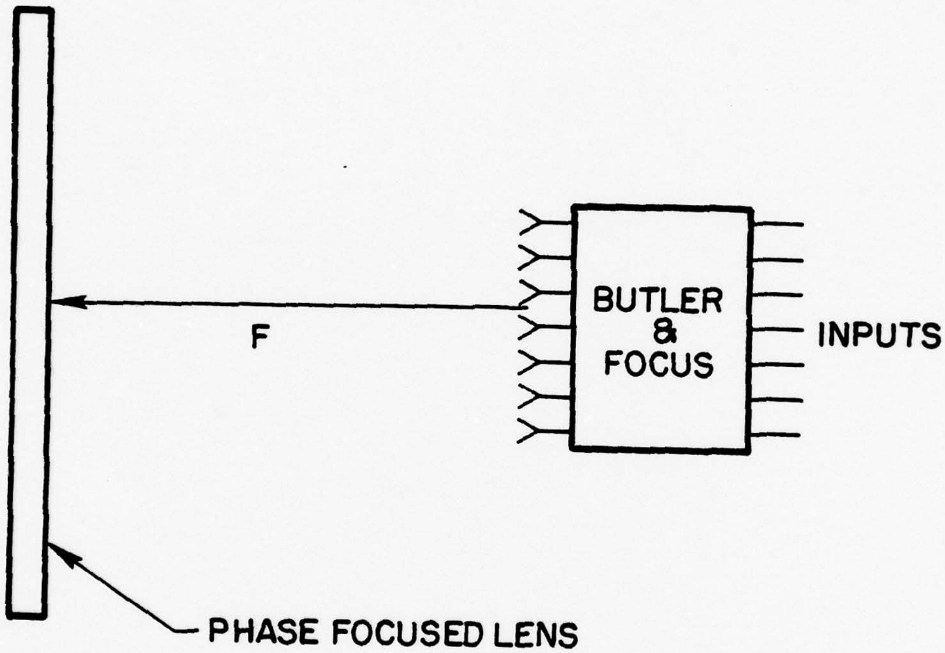

FIG. 7 - THE FLAT LENS CONFIGURATION

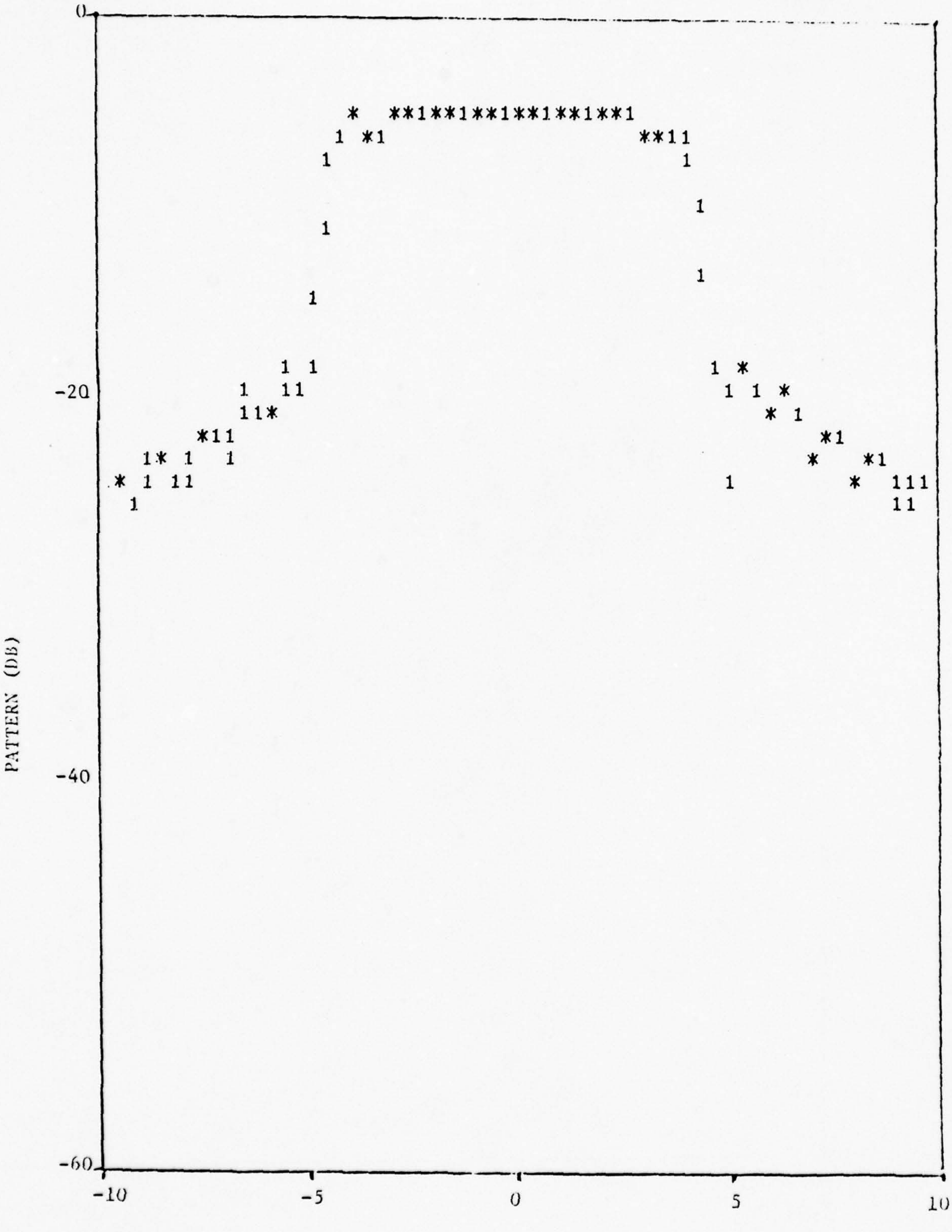

FIG. 8 - RADIATION PATTERN FROM FLAT LENS WHEN ONLY THE LEFT, OUTERMOST BEAM IS DRIVEN

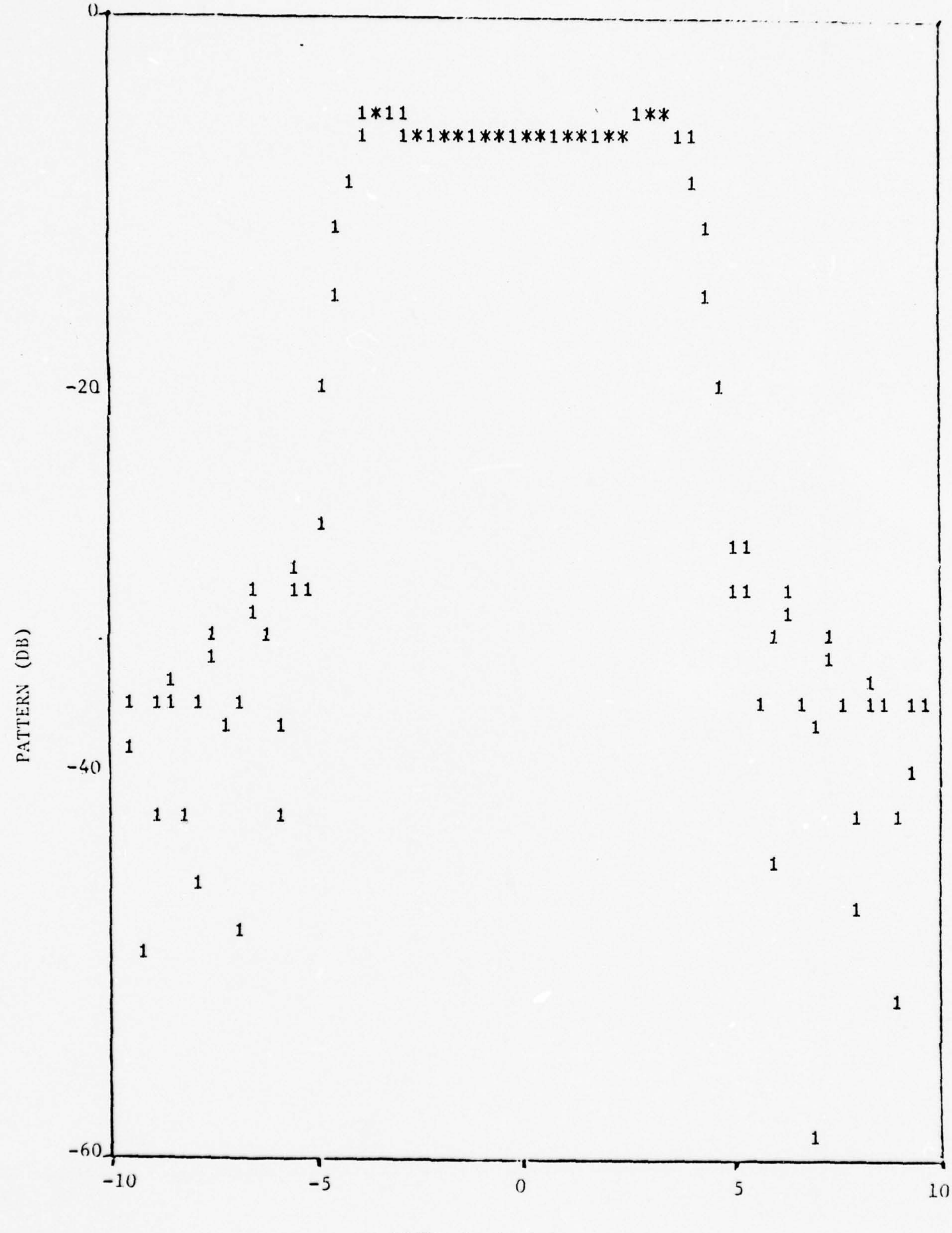

FIG. 9 - RADIATION PATTERN FROM FLAT LENS WHEN ONLY THE LEFT, INNERMOST BEAM IS DRIVEN

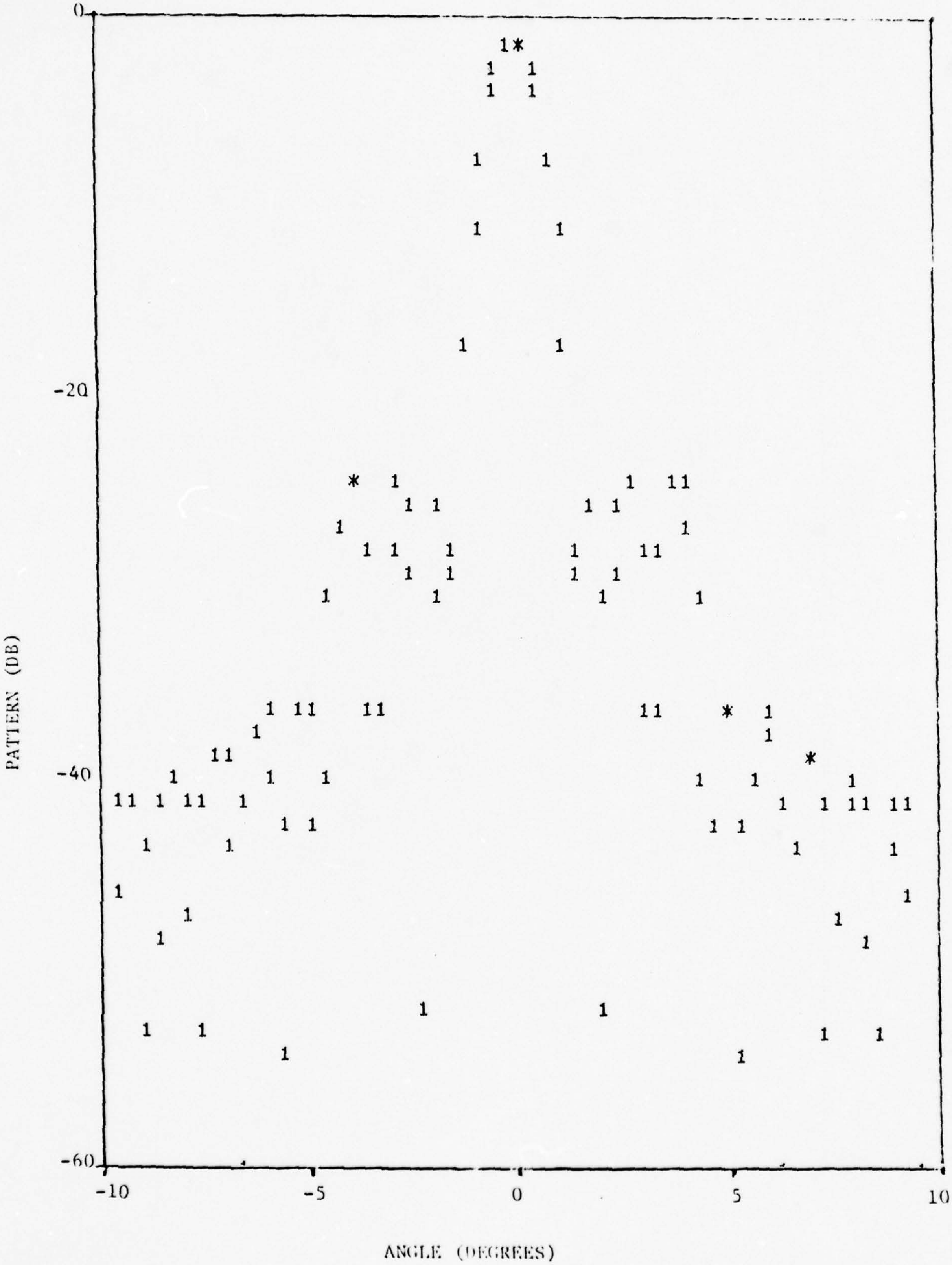

FIG. 10 - RADIATION PATTERN FROM FLAT LENS FOR PROGRESSIVE PHASE = 0°

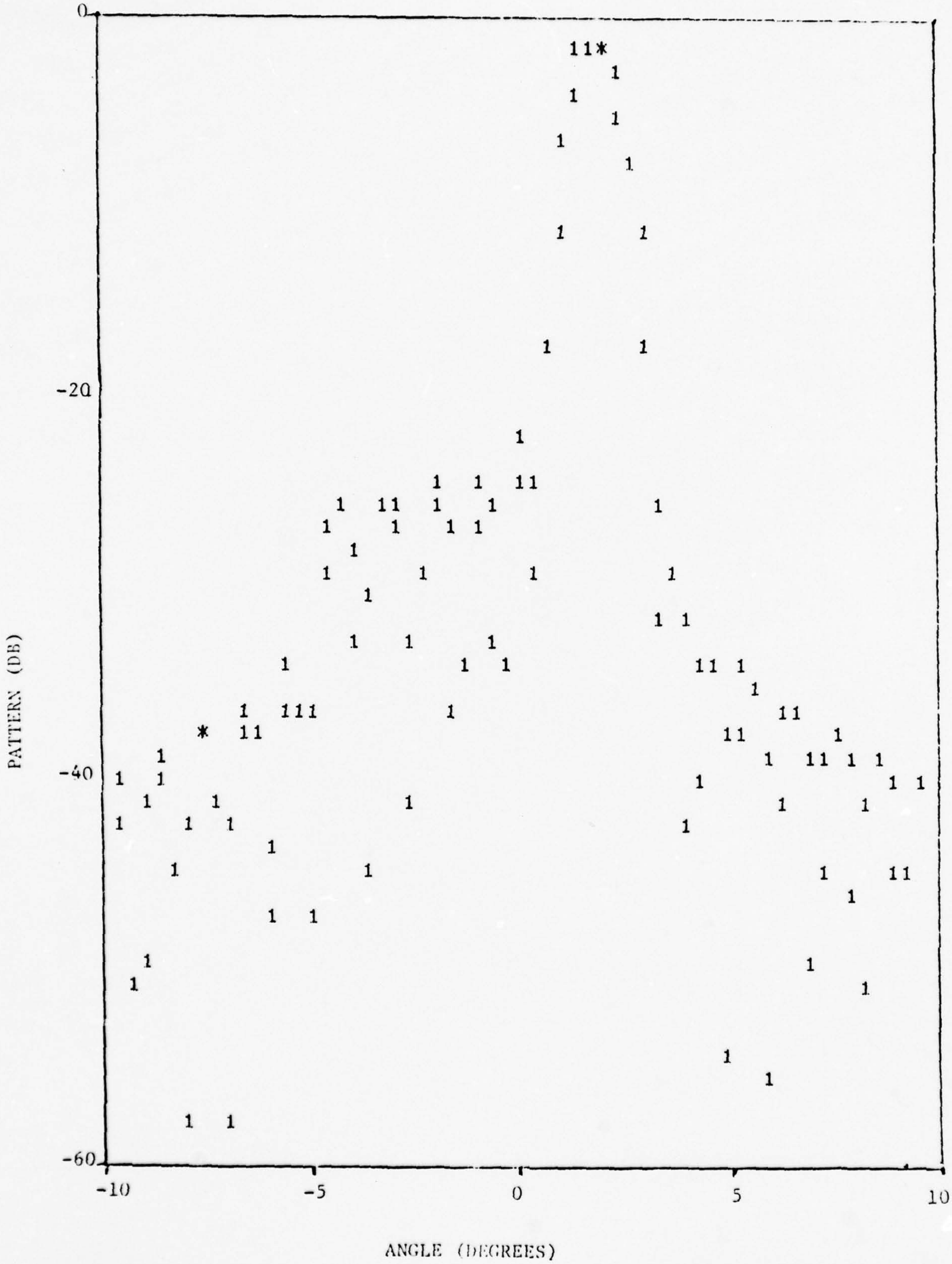

FIG. 11 - RADIATION PATTERN FROM FLAT LENS FOR PROGRESSIVE PHASE = 80°

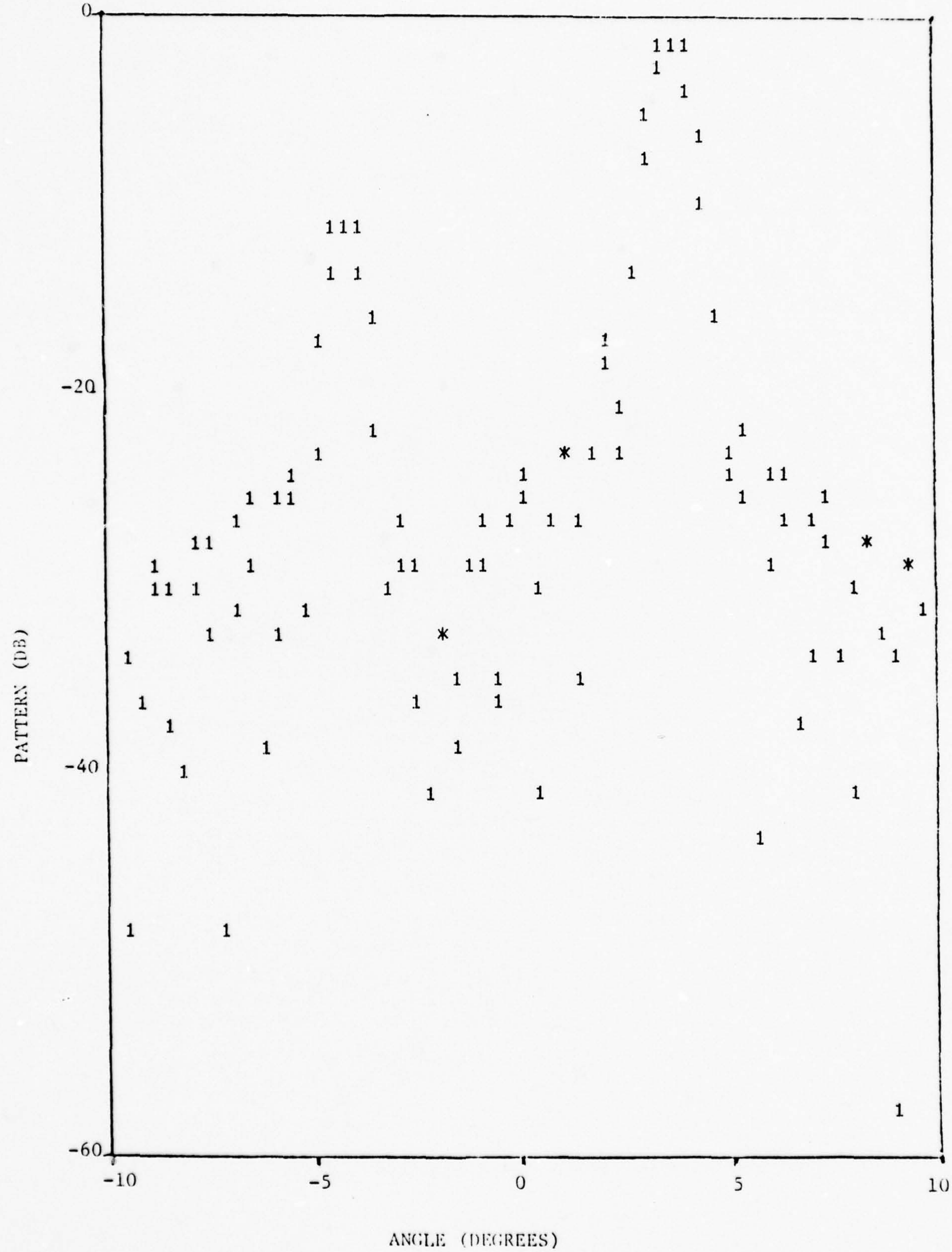

FIG. 12 - RADIATION PATTERN FROM FLAT LENS FOR PROGRESSIVE PHASE = 160°

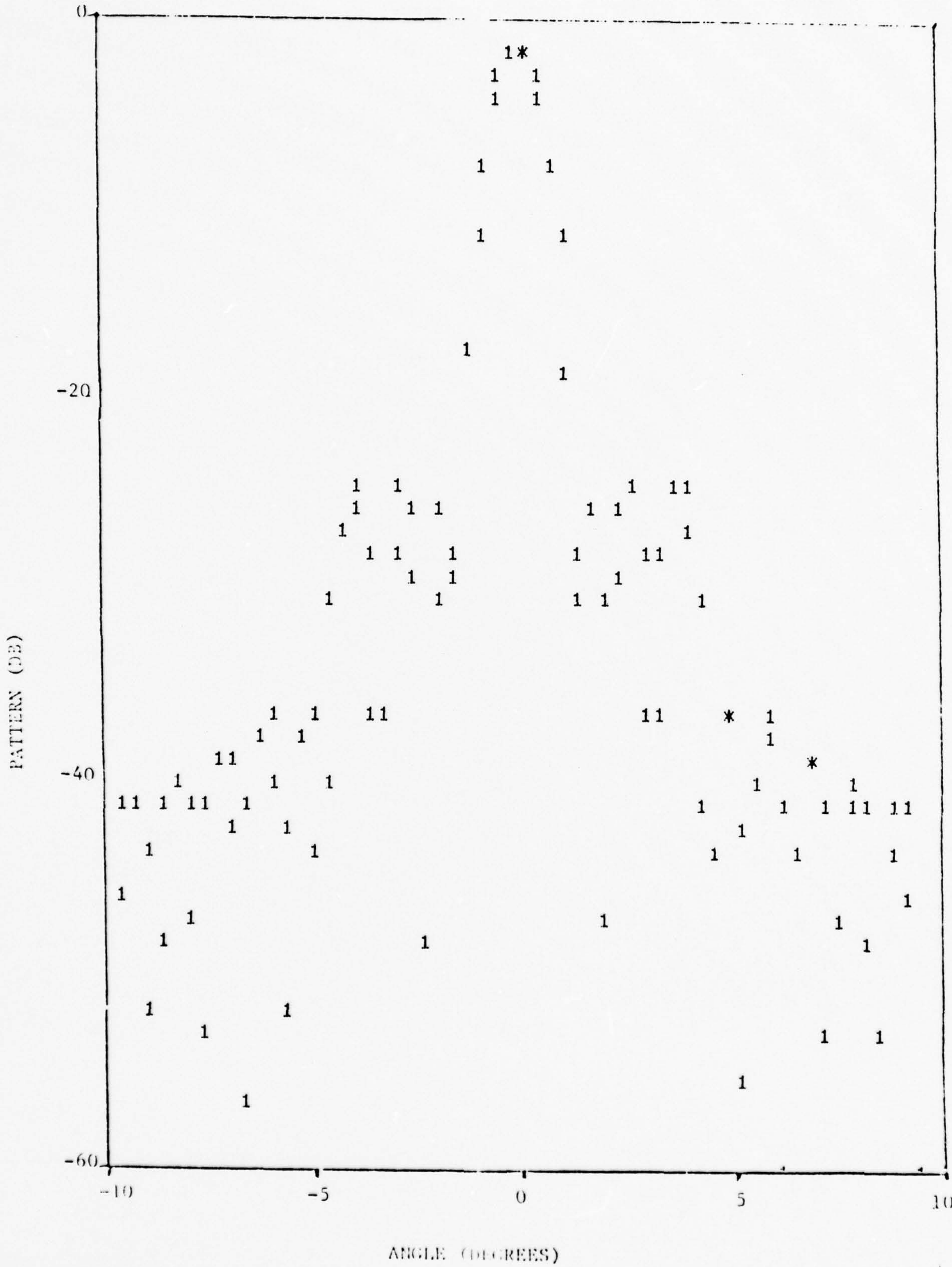

FIG. 13 - RADIATION PATTERN OF FLAT LENS WITH PROGRESSIVE PHASE = 0° AND WITH PEAK-TO-PEAK MECHANICAL DEFORMATION OF 0.1λ WITH PERIOD OF TWICE ARRAY LENGTH (COSINE DEFORMATION).

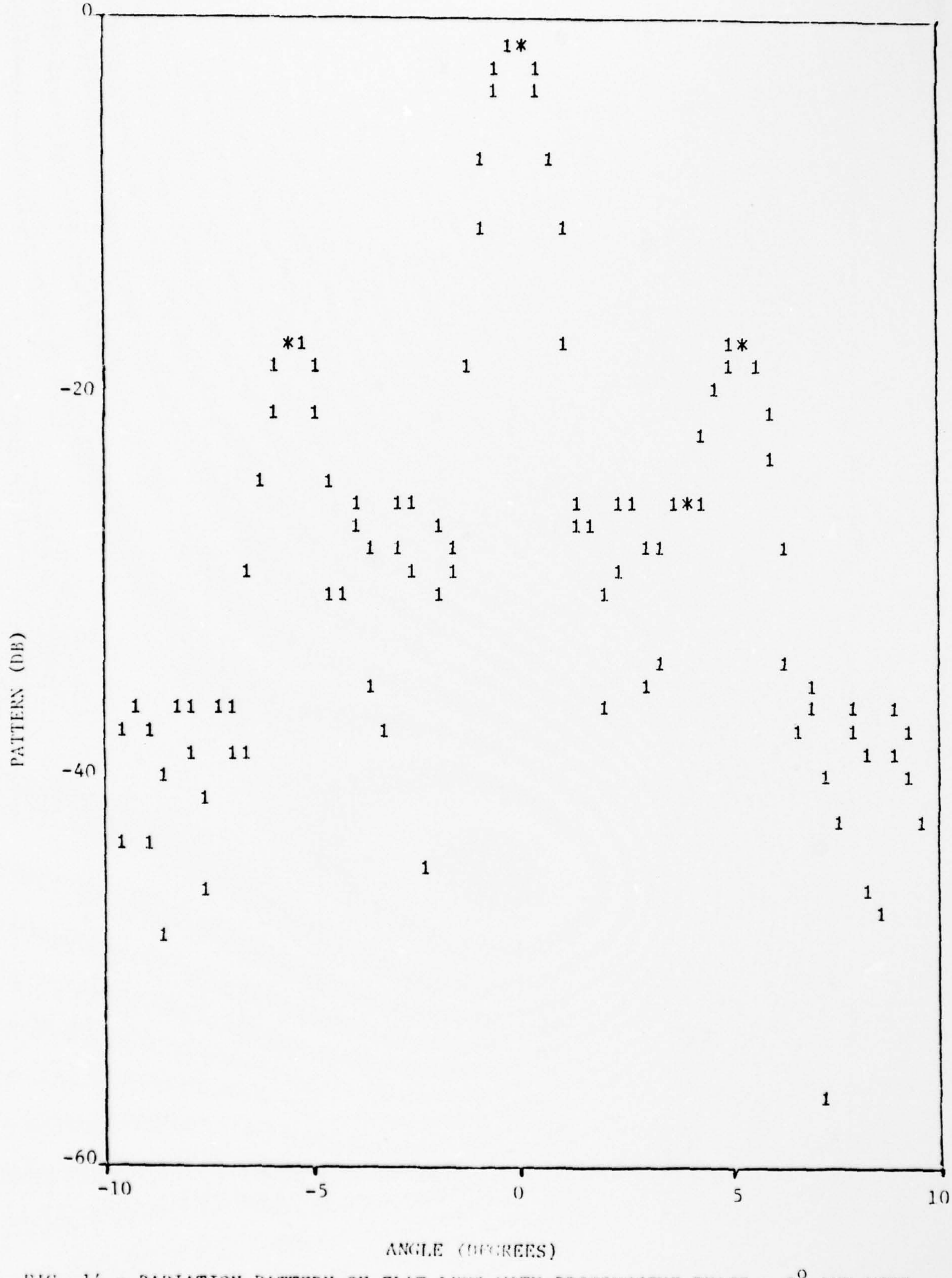

FIG. 14 - RADIATION PATTERN OF FLAT LENS WITH PROGRESSIVE PHASE = 0° AND WITH PEAK-TO-PEAK MECHANICAL DEFORMATION OF 0.1λ WITH PERIOD OF 20 TIMES ARRAY LENGTH (COSINE DEFORMATION).

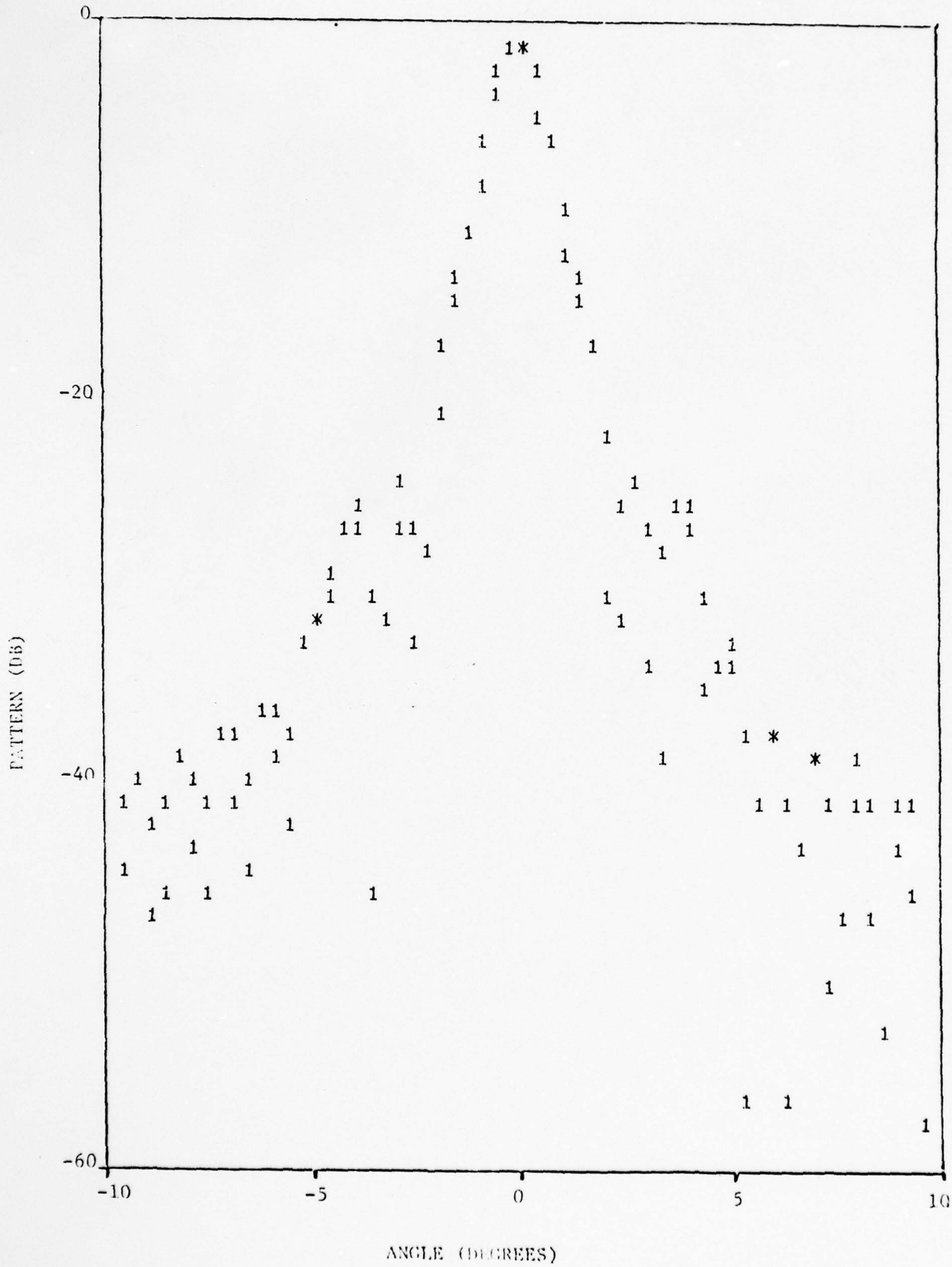

FIG. 15 - RADIATION PATTERN OF FLAT LENS WITH PROGRESSIVE PHASE = 0° AND WITH PEAK-TO-PEAK MECHANICAL DEFORMATION OF 0.5λ WITH PERIOD OF TWICE ARRAY LENGTH (COSINE DEFORMATION).

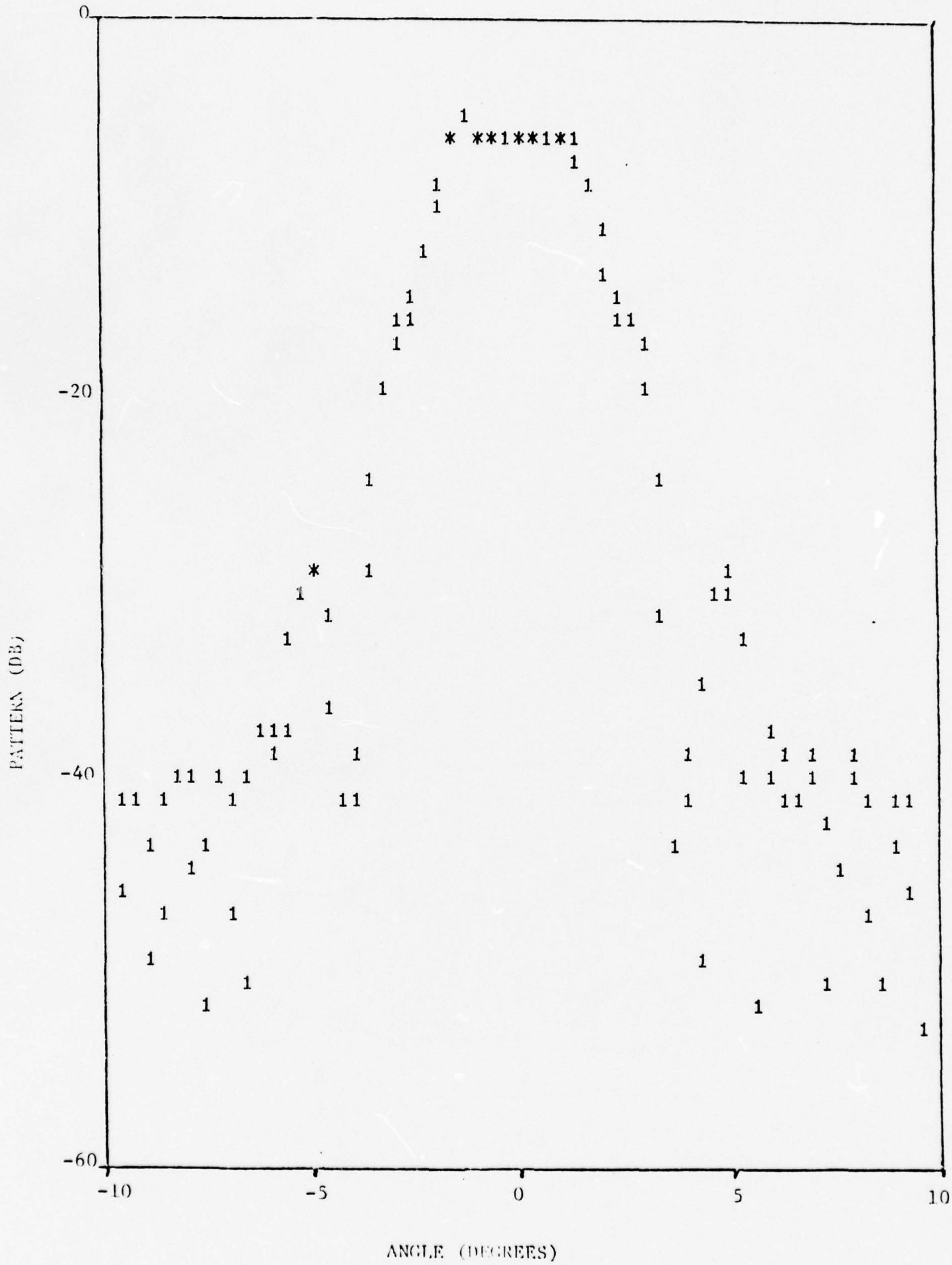

FIG. 16 - RADIATION PATTERN OF FLAT LENS WITH PROGRESSIVE PHASE = 0° AND WITH PEAK-TO-PEAK MECHANICAL DEFORMATION OF 0.5λ WITH PERIOD OF 4 TIMES ARRAY LENGTH (COSINE DEFORMATION)

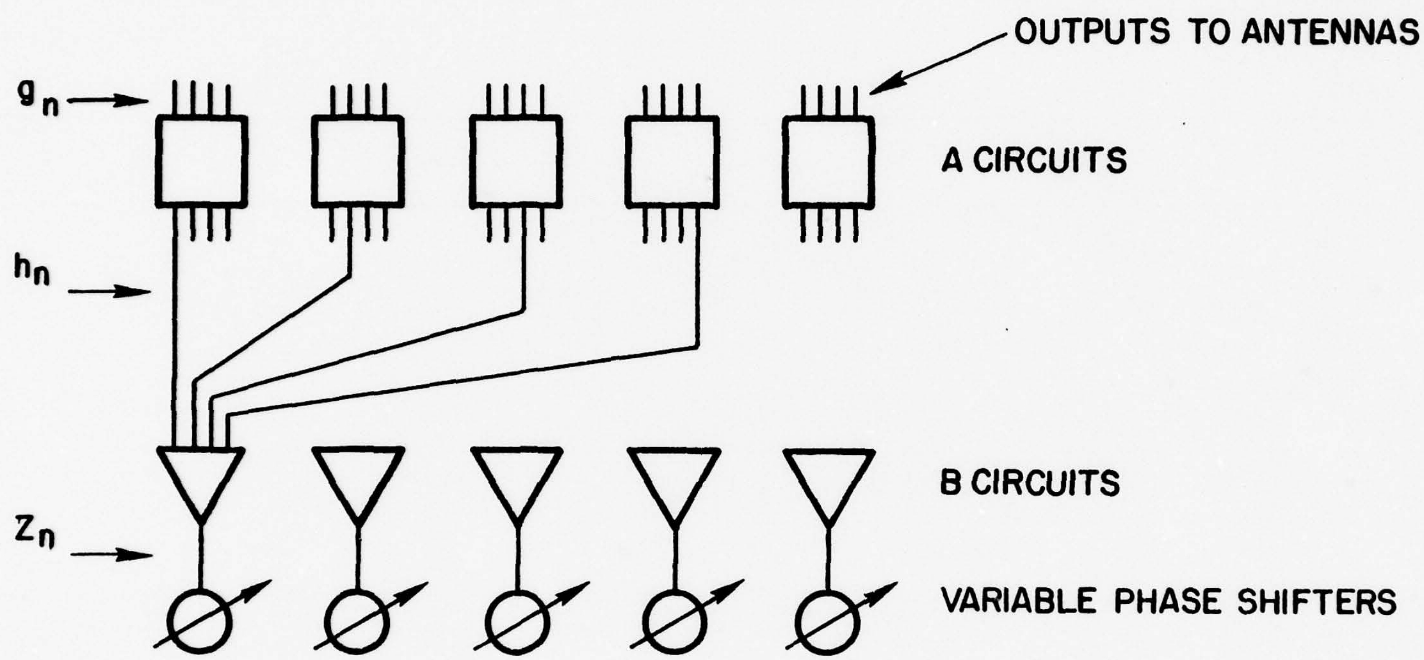

FIG. 17 - SUB-ARRAY CIRCUITS

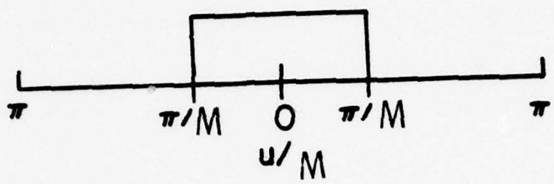

FIG. 18 - OPTIMUM SUB-ARRAY PATTERN TO ELIMINATE GRATING LOBES AND GIVE IDEAL PERFORMANCE WITHIN FIELD OF VIEW

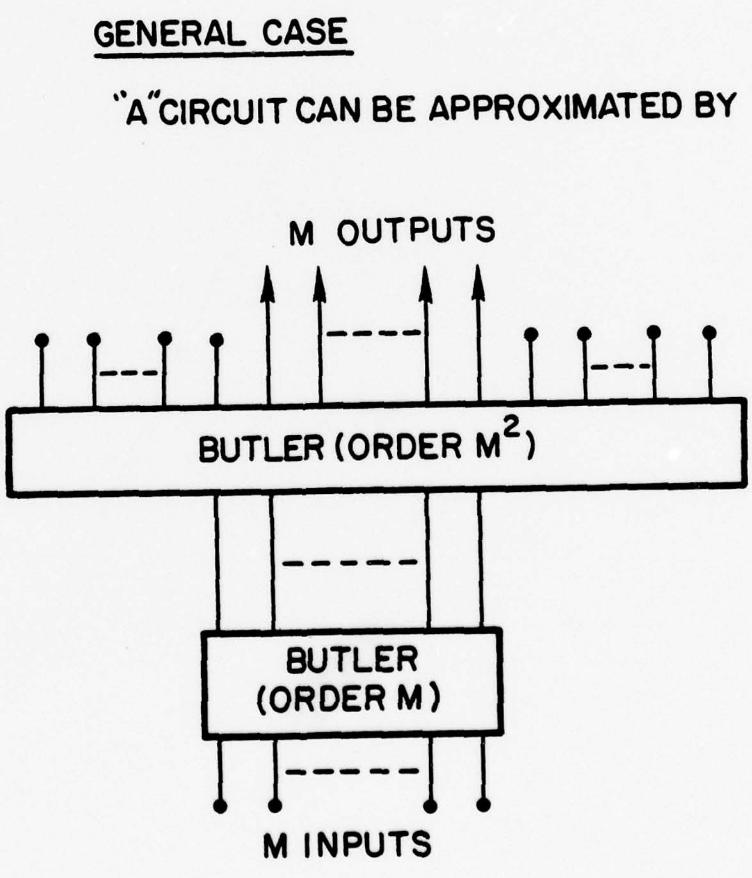

FIG. 19 - TECHNIQUE TO IMPLEMENT THE "A" CIRCUIT BASED ON FOURIER SYNTHESIS OF ELEMENT PATTERN FOR THE CASE M = 4

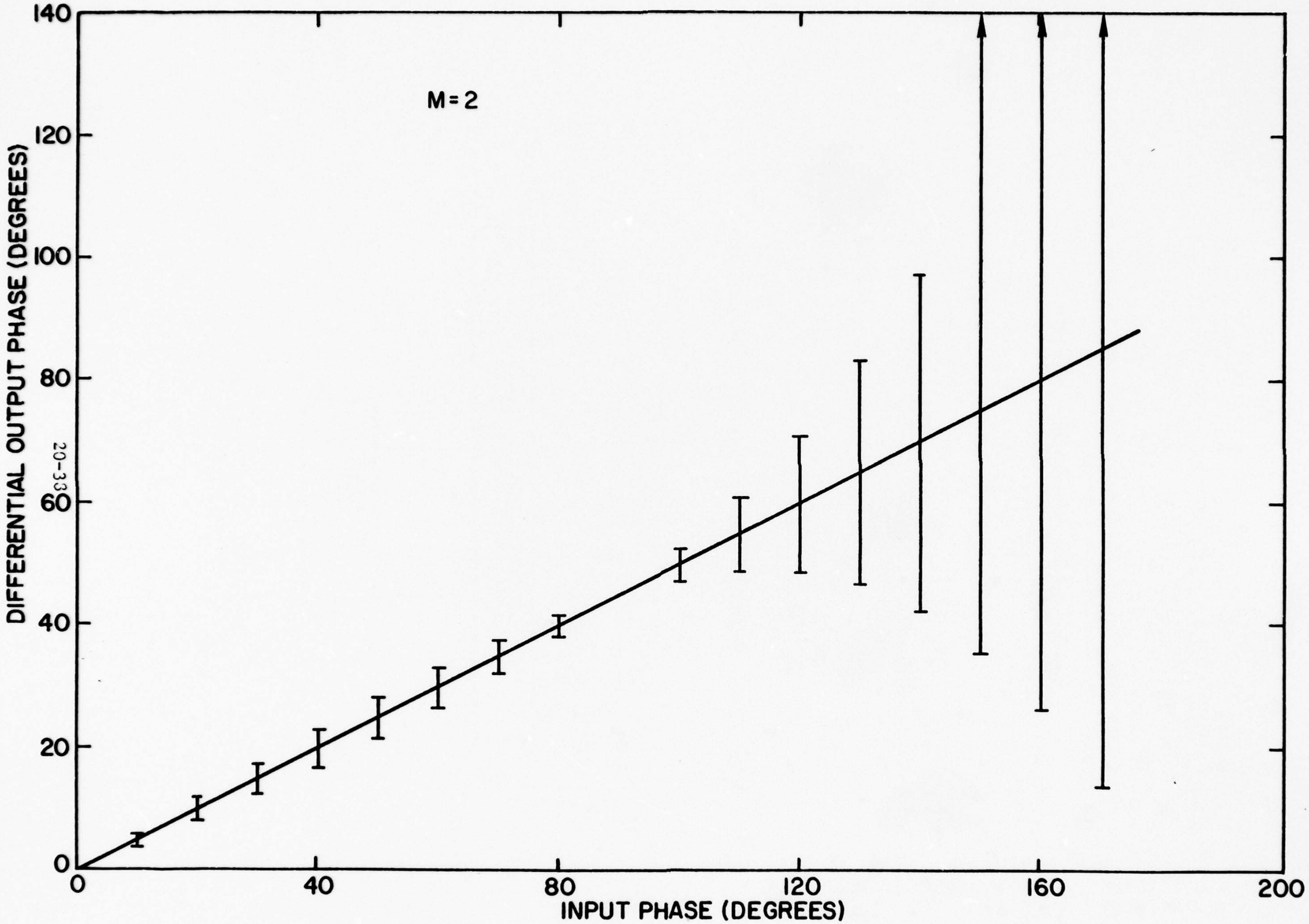

FIG. 20 - OUTPUT PHASE VARIATIONS AS A FUNCTION OF INPUT PROGRESSIVE PHASE FOR THE CASE M = 2

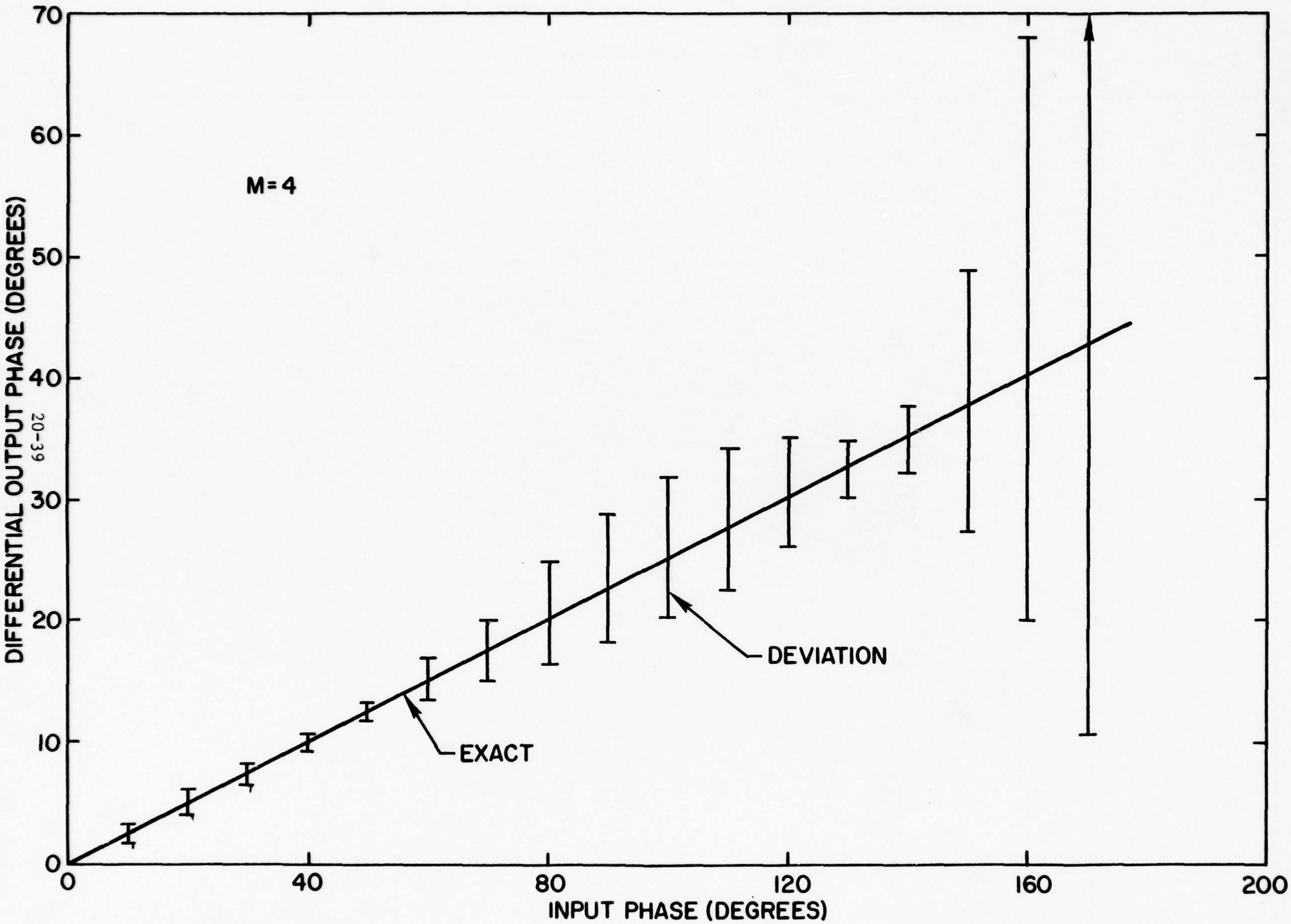

20-39

FIG. 21 - OUTPUT PHASE VARIATIONS AS A FUNCTION OF INPUT PROGRESSIVE PHASE FOR THE CASE M = 4

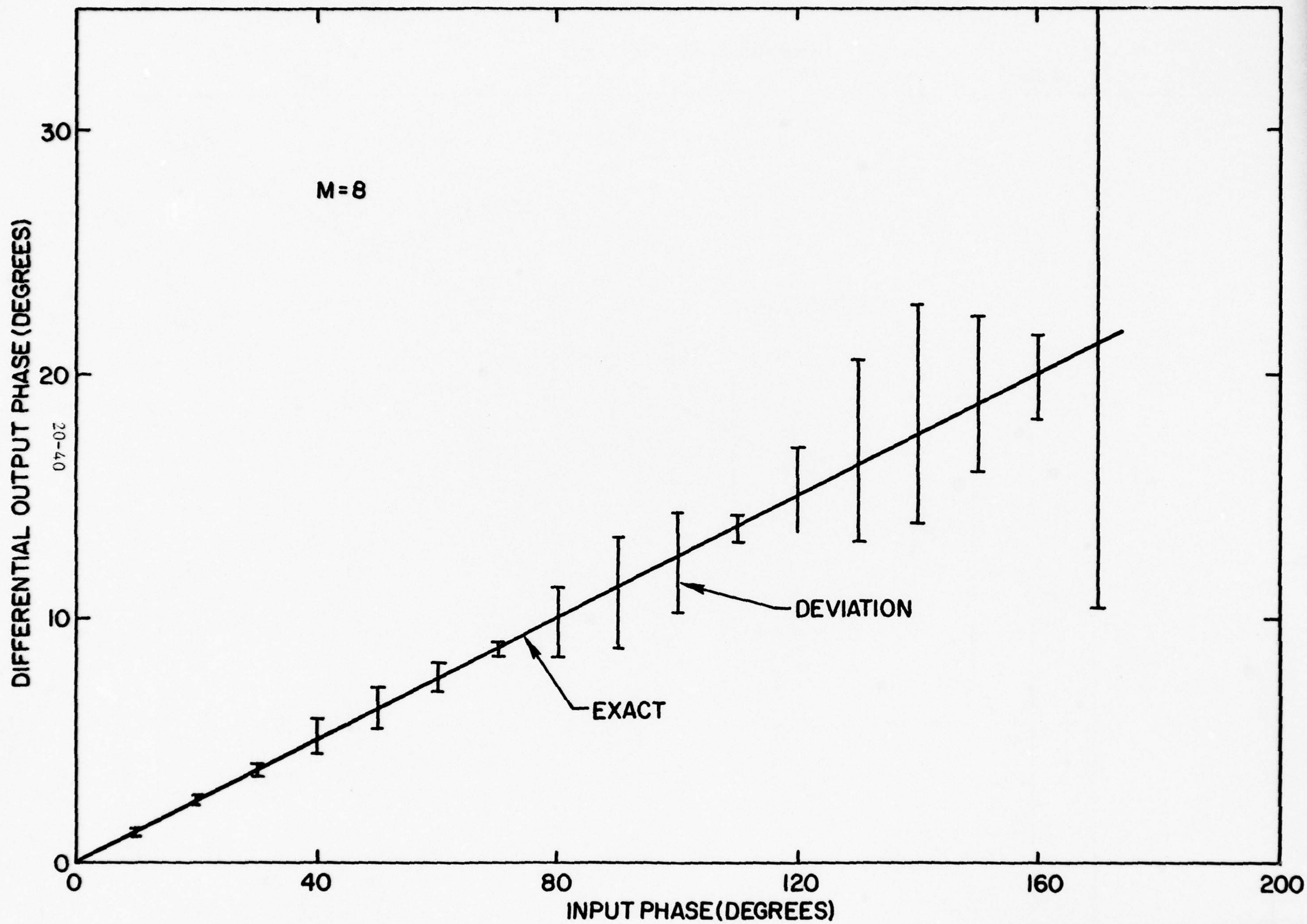

FIG. 22 - OUTPUT PHASE VARIATIONS AS A FUNCTION OF INPUT PROGRESSIVE PHASE FOR THE CASE M = 8

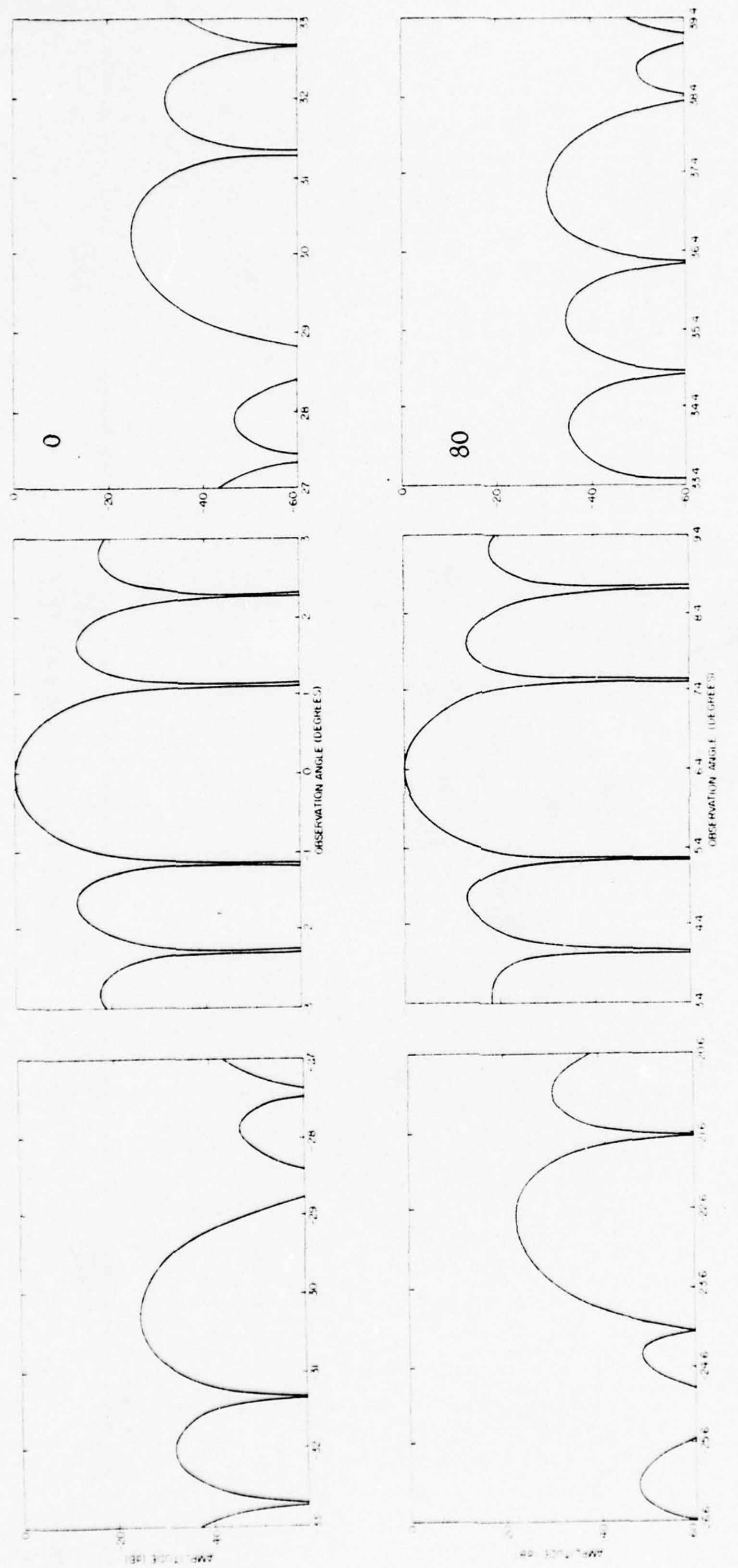

FIG. 23 - RADIATION PATTERNS FOR INPUT PROGRESSIVE PHASES OF 0^o, 80^o, 160^o FOR 25 MODULES WITH M = 4

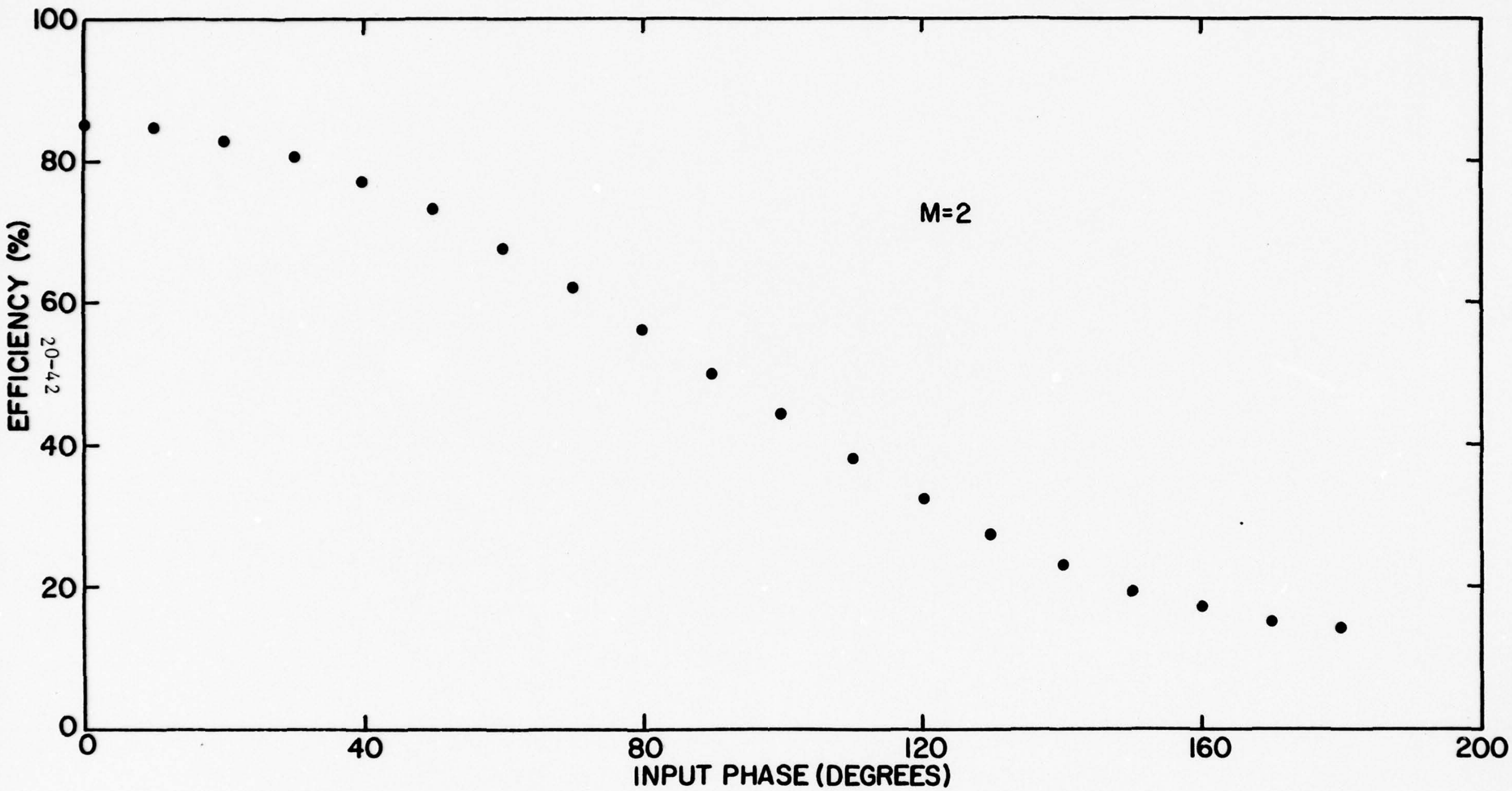

FIG. 24 - EFFICIENCY AS A FUNCTION OF SCAN FOR M = 2

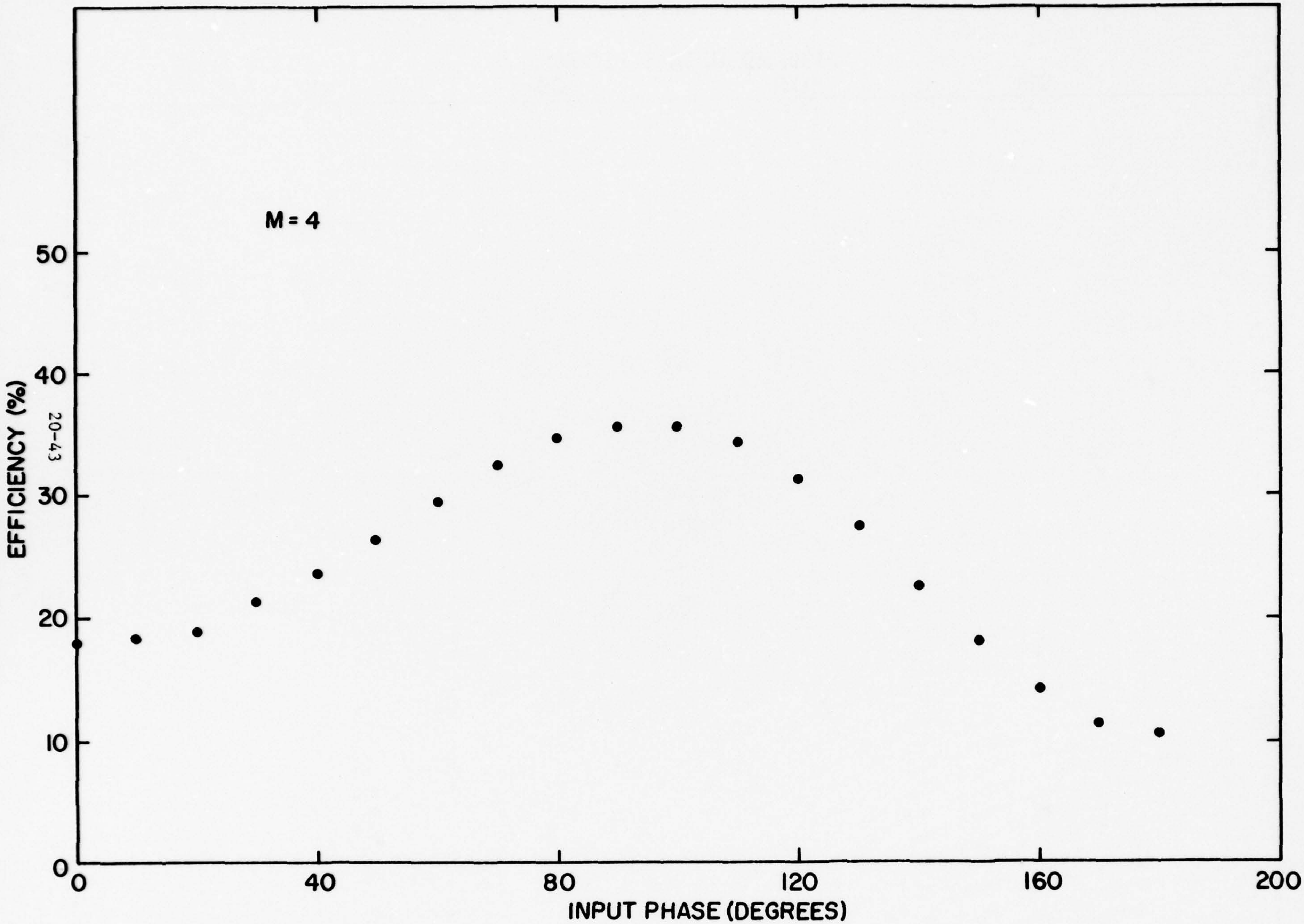

FIG. 25 - EFFICIENCY AS A FUNCTION OF SCAN FOR M = 4

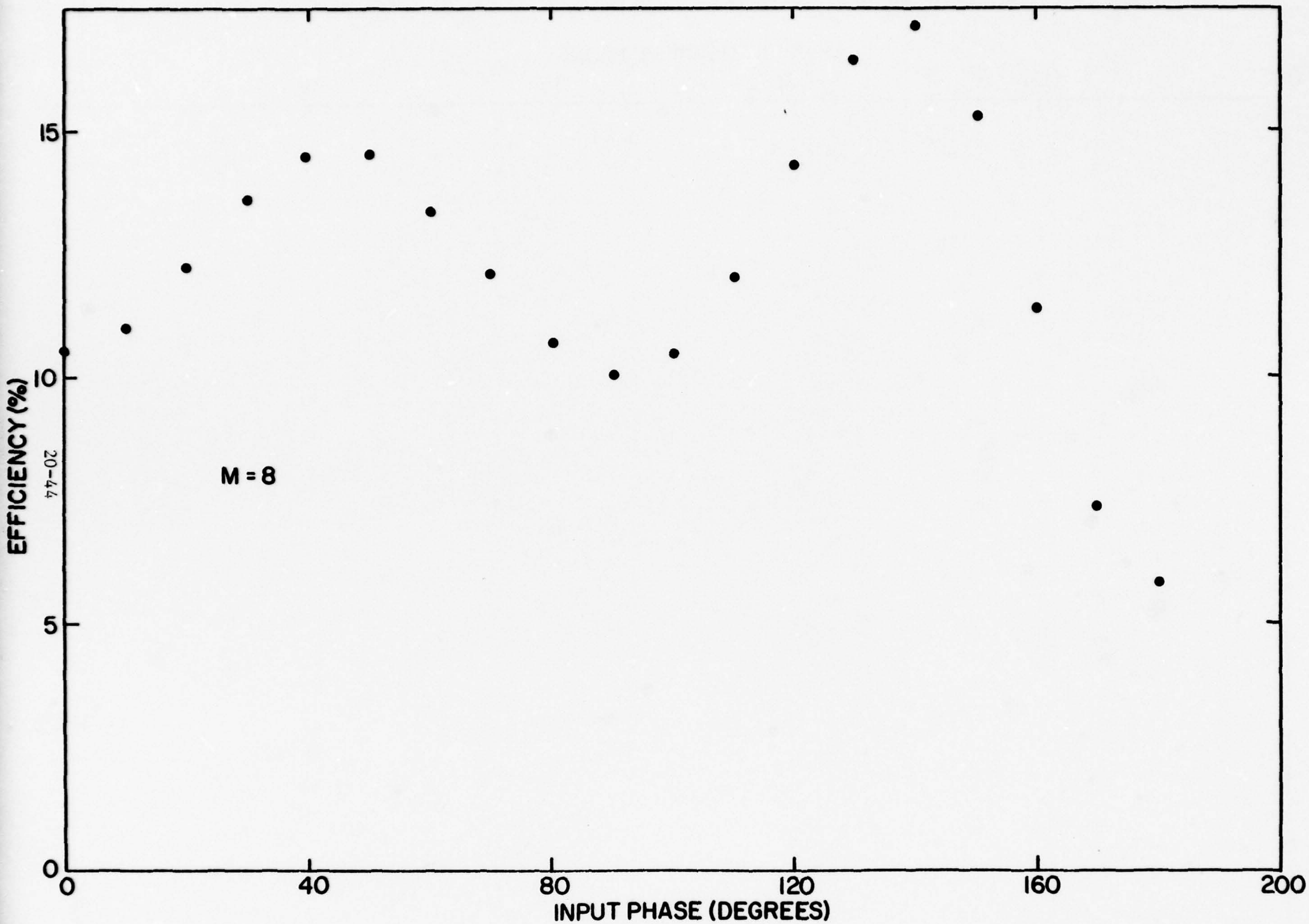

FIG. 26 - EFFICIENCY AS A FUNCTION OF SCAN FOR M = 8

1978 USAF-ASEE SUMMER FACULTY RESEARCH PROGRAM

sponsored by

THE AIR FORCE OFFICE OF SCIENTIFIC RESEARCH

conducted by

AUBURN UNIVERSITY AND OHIO STATE UNIVERSITY

PARTICIPANT'S FINAL REPORT

Design of an Imaging System to Conduct Human Thermal Signature Analysis with a 256 Element Schottky Barrier IRCCD Detector

Prepared by:	Richard Dobrin, Ph.D.
Academic Rank:	Professor
Department and University	Department of Physics Sarah Lawrence College Bronxville, New York

Assignment:	
(Air Force Base) (Laboratory) (Division) (Branch)	Hanscom AFB Rome Air Development Center Solid State Sciences Electronic Device Technology
USAF Research Colleague:	Lyn Skolnik, Ph.D.
Date:	August 18, 1978
Contract No.:	F44620-75-C-0031

DESIGN OF AN IMAGING SYSTEM TO CONDUCT HUMAN THERMAL SIGNATURE ANALYSIS WITH A 256 ELEMENT SCHOTTKY BARRIER IRCCD DETECTOR

by
Richard Dobrin Ph.D.

ABSTRACT

A 256 element Pt_xSi IRCCD detector is under development by Rome Air Development Center ES branch for future use by the DOD Base and Installation Security System Program Office (BISSPO) at Hanscom AFB. This detector will be used to generate a passive thermal "fence" line which will provide early warning against intrusion by unauthorized personnel or vehicles. Target recognition and false alarm analysis requires that infrared human signature data be obtained. As a USAF/ASEE summer faculty research program project, a synchronous mirror scanning and electronic imaging system was designed to obtain these human thermal signatures against various ambient backgrounds. The system, which has been tested under simulated operational conditions, will produce high resolution two-dimensional infrared images in grey scale, topological view, and black and white or pseudcolor video. Data can be obtained from this system on magentic tape for computer analysis of thermal signatures, and image enhancement of the visual display.

ACKNOWLEDGEMENTS

The author would like to express his gratitude to the Air Force Office of Scientifice Research, Air Force Systems Command and the American Society for Engineering Education for making this summer research possible. A special thanks is due to my research colleague, Dr. Lyn Skolnik, and to Mr. Fred O'Brien who administered the summer program. I would also like to thank Mr. Richard Taylor, Dr. Freeman Shepherd, Jr., Dr. William Ewing, Mr. Robert Phipps, Mr. Jerry Friedman, Dr. Andrew Yang, Mr. Ben Capone, Mr. Sven Roosild, and Ms. Jeanne Cullen for the help and assistance I recieved from them while working on this research project.

INTRODUCTION

A 256 element Pt_xSi IRCCD detector is under development by Rome Air Development Center ES branch for future use by the DOD Base and Installation Security System Program Office (BISSPO) at Hanscom AFB.[1-3] This sensor will be used to generate a passive thermal "fence" line which will provide early warning against intrusion by unauthorized personnel or vehicles. Target recognition and false alarm analysis requires that infrared human signature data be obtained.

This report documents the effort involved in the design and testing of a synchronous mirror scanning and electronic imaging system for the 256 element IRCCD staring array to obtain Schottky human infrared images in grey scale, topological view, and black and white or pseudocolor video. Data can be obtained from this system on magentic tape for computer analysis of thermal sigratures, and image enhancement of the visual display.[4]

THEORY OF DETECTION

Schottky diodes are formed by evaporation of Pt onto a p-type silicon substrate and reacting the metal at temperatures varying from 200^o - 650^{o}C to form a platinum silicide (Pt_xS) layer.[1] A barrier potential is set up between the Pt_xS layer and the p-Si of approx. 0.27 eV which is roughly equal to the energy difference between the work function of the metal and the electron affinity of the semiconductor.[5] The formation of the Pt_xS layer avoids the defects which would be formed from simple evaporation of the metal, particularly the presence of trapped surface contaminents and patches of surface oxide.

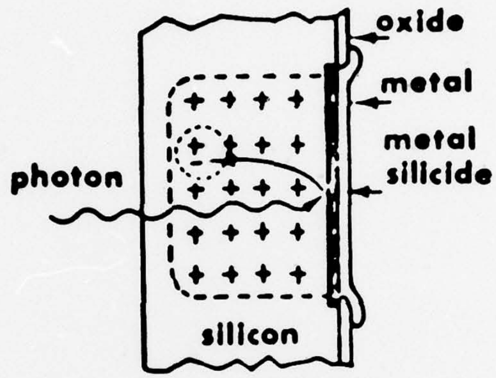

1a

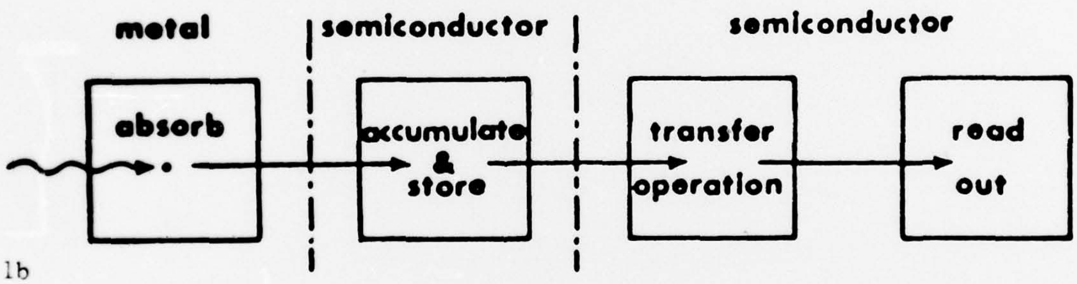

1b

Figure 1a the operation of the Pt_xSi Schottky diode.

Figure 1b Storage and transfer operations of the IRCCD,(from reference 7).

Figure 1a shows the operation of the Pt_xSi Schottky diode. The diode array is illuminated through the silicon substrate. Wavelengths shorter than 1.1 micrometers are absorbed in the substrate. Longer wavelengths are absorbed in the Schottky electrodes, giving rise to the internal photoemission of majority carriers from the metal to the silicon substrate. The photoyield Y, for Schottky emission is given by:

$$Y = \frac{C_1 \, (h\nu - \psi_{ms})^2}{h\nu} \qquad \frac{\text{(electrons)}}{\text{(photon)}} \qquad (1)$$

where: ψ_{ms} is the barrier height

h is Plancks constant

ν is the photon frequency

C_1 is a factor determined by the geometrical, optical, and transport properties of the substrate layer. 6-8

Figure 1b shows both the storage and transfer operations. After the 30 ms. intergration time, charge is transferred from the diodes to the CCD shift registers and read out.

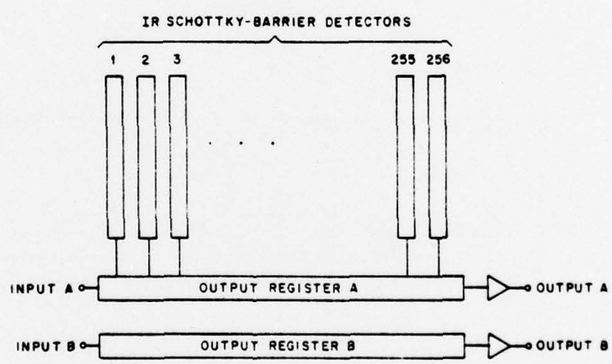

Figure 2. The block diagram of the 256 element IRCCD (from reference 9).

A block diagram of the device is shown in Figure 2. The individual detectors are 8,0 mils, 0.9 mils wide, and are 1.6 mils on center. The array of Schottky barrier detectors is read out by output register A. Output register B has common clock electrodes with output register A. The output registers have been designed with identical input and output circuits. The dual output register construction is used for elimination of clock pickup by subtraction of the signal in register B from the signal in register A.[9 10]

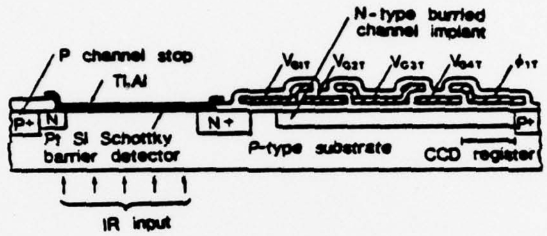

Figure 3. A schematic drawing of the IRCCD showing the detector, the four transfer gates, and the CCD registers (from reference 9).

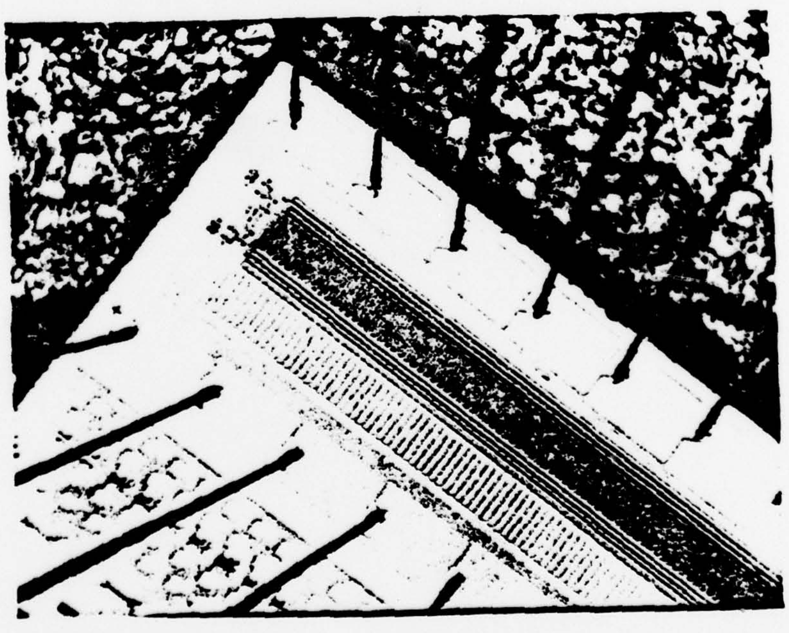

Figure 4. A photomicrograph of the 256 element IRCCD (frome reference 9).

The charge accumulated in the Schottky diodes is transferred to the output register. The charge transfer takes place in an n-type buried channel implant. Figure 3 is a schematic of the elements and transfer gates. Figure 4 shows an enlarged view of the device.[1]

The detector must be cooled for operation. For temperatures above 103°K, dark current causes the loss of the infrared signal. For temperatures below 40°K, carriers are frozen out in the CCD registers resulting in increased noise.[1,12] Consequently, the detector is kept at 80°K in an expander cooled by a helium refrigerator. An anti-reflecting germanium coated window with a passband of 2-5 microns is located at the front of the expander. A sapphire with dielectric coating cold filter restricts the incoming radiation to the detector to the region between 3.4 - 4.2 microns. The incoming infrared radiation is focused on the detector by an f1.2 optical system. Charge is accumulated and stored for the length of the staring time, which for this experiment is 30 ms.

SYSTEM DESIGN

The existing IRCCD experimental set up is shown in Figure 5. The image of a bar target illuminated by a black body source is displayed on the oscilloscope screen. Also shown are the infrared optics, the helium expander, and the CCD driver circuits. Figure 6 shows the response of a typical portion of the array to a 500°K black body source, 50% neutral density filtered.

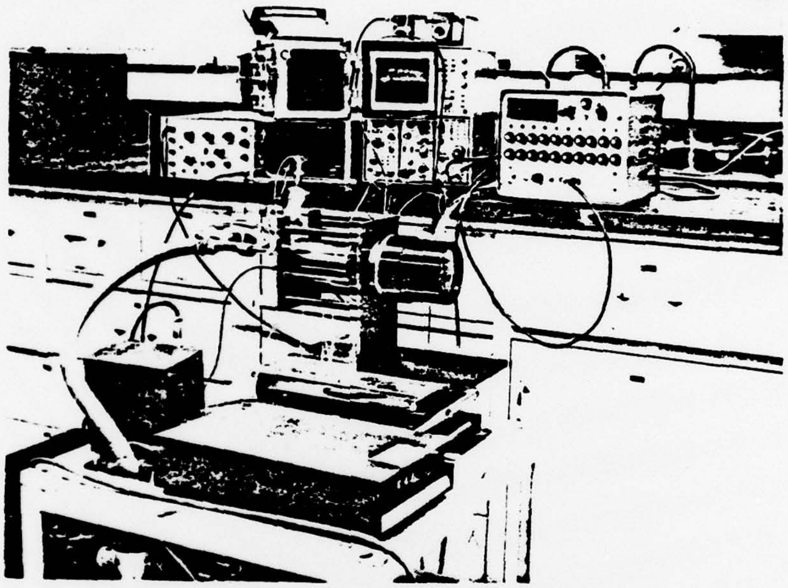

Figure 5. Experimental set up, showing IR optics, helium expander, and CCD driver circuits (from reference 1).

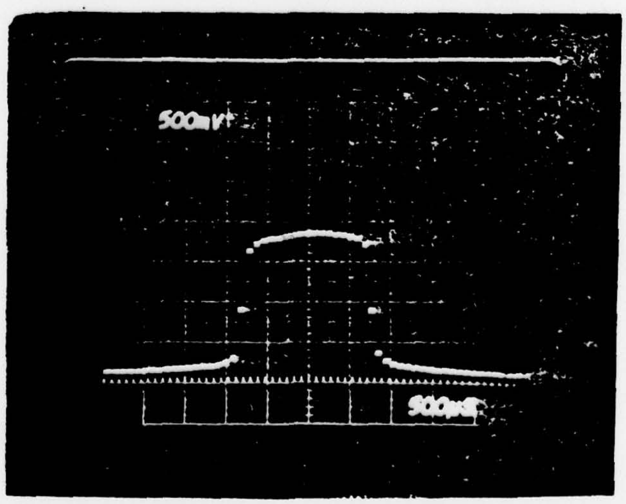

Figure 6. Response of a typical portion of the IRCCD to a 500°K source (50% neutral density filtered, from reference 1).

The system designed to produce a two dimensional infrared scan using the 256 element IRCCD is shown in block diagram form in Figure 7. The detector is operated with a 30 ms. signal intergration time. A mirror scans the field of view for a period of 6 seconds to produce a 200 scan line display on a Tektronix model 7633 storage oscilloscope.

To minimize dark current the sensor is kept at $80^{\circ}K$ by an Air Products and Chemicals, Inc. Model CS-1003 Displex Cryogenic Detector Cooler expander which is cooled by a helium refrigeration system. An ion pump is used to evacuate the expander. The infrared signal from a human subject is reflected onto the array through f1.2 IR optics by a 101 X 82 mm. aluminum coated mirror whose motor drive is controlled by an electrical ramp signal of 6 seconds duration, which is simulataneously applied to the vertical amplifier of the oscilloscope. The input of the sensor is also connected to the vertical input of the oscilloscope and the horizontal sweep is initiated by a sync pulse from the waveform generator which occurs simultaneously with the transfer of charge to the readout register of the sensor. This mode of operation will give a topological display of the sensor output on the oscilloscope screen.

The ramp generation system consists of a 0-5V ramp voltage source, which programs a Kepco model CK-18-3 power supply to provide the current required (0-1 amperes) by the mirror motor drive. The voltages required for the operation of the Schottky barrier detector and the CCD readout are provided by the waveform generator.

The output of register B is subtracted from the output in register A in the model 7A-13 preamplifier of the oscilloscope. The resultant signal (A-B) is amplified and applied to the Z axis modulation terminal of the oscilloscope.

Two modes of image storage operation are available, both triggered by the end of the ramp signal. Mode one erases the stored image of the previous mirror scan and records the image from the subsequent mirror sweep until the original erase cycle is initiated manually.

The Z axis (grey scale) modulated image can be scanned with a Sony Model AVC-3200 television camera, and the video image colorized by a Spatial Data Systems pseudocolor generator. A large scale format (12' X 16') topological view of the television image can be simultaneously displayed using an Interpretation System VP-8 image analyzer.

Figure 7. **BLOCK DIAGRAM OF SCANNING AND DISPLAY SYSTEM**

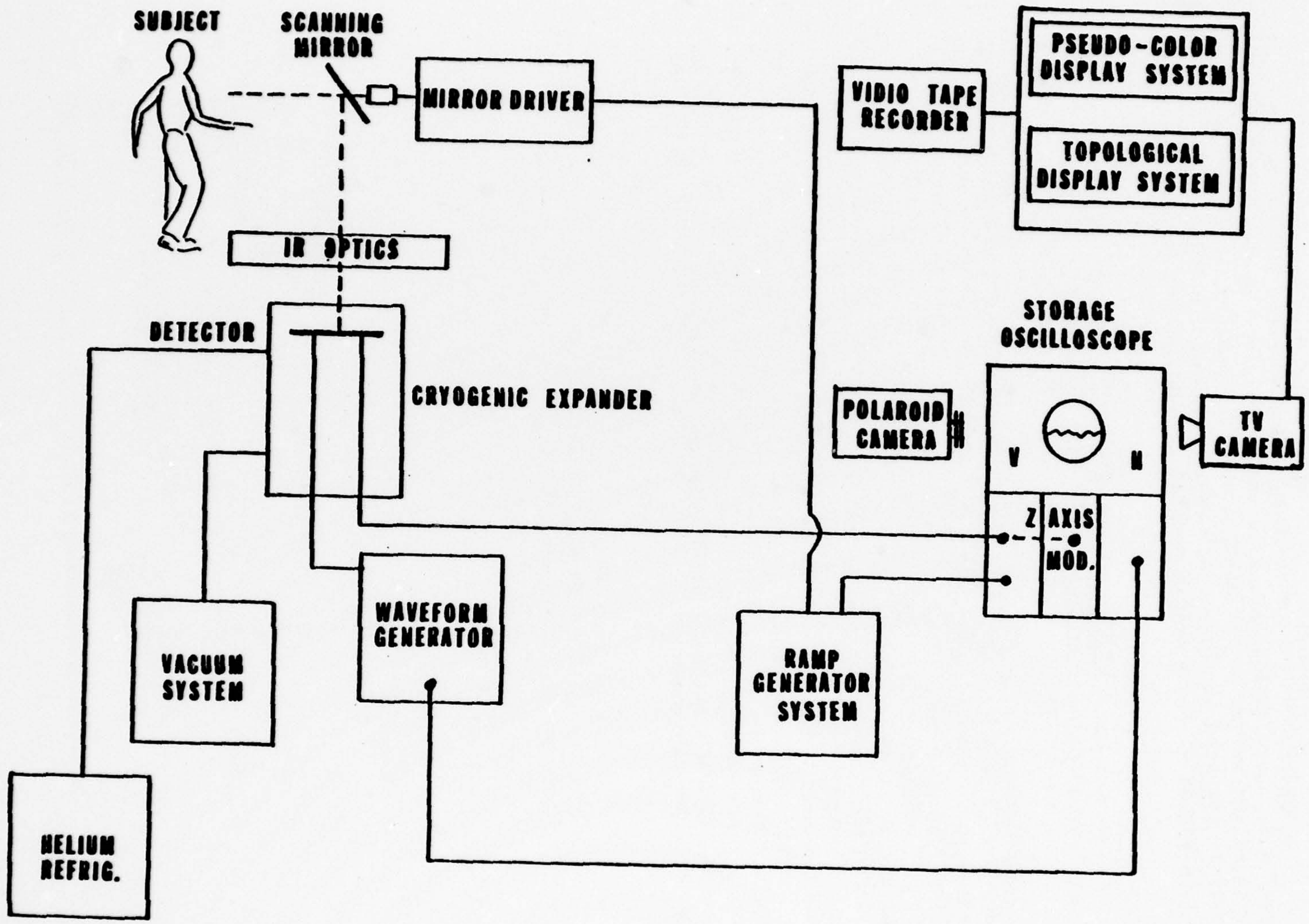

EXPERIMENTAL RESULTS

The synchronous mirror scanning and electronic imaging system was tested under simulated conditions. Problems arose with the helium refrigerator, which required its return to the manufacturer for repairs. However, the detector could be operated in the visible region without requiring cooling, and a simulated series of tests were conducted to evaluate the systems operational capabilities.

TESTING OF THE OPERATION OF THE SYNCHRONOUS MIRROR SCANNER, AND OSCILLOSCOPE TOPOLOGICAL AND GREY SCALE DISPLAY MODES

In place of using a human subject an an infrared source, a 6.35 mm. circular aperature illuminated by a Spectra Physics model 132 He-Ne laser was used as a test object. The scanning mirror reflected the well collimated circular image of the test aperature directly onto the IRCCD which had the 3.4 to 4.2 micrometer infrared passband filter removed. (No-IR Optics or helium expander present). This system is shown in Figure 8. The 0.6328 micrometer line from the laser produces electron-hole pairs in the depletion region of the CCD. The electrons are collected in the wells formed by the gating electrodes of the individual diode channels. and read out in CCD register B. Figure 9 shows the readout from the individual diode channels. Figure 10 shows a topological view of the circular aperature formed by mirror scanning the laser light passing through the aperture. Precision alignments will be made in the optical system to be used for infrared signature analysis and the deviations from symmetry as in this photograph will not be present.

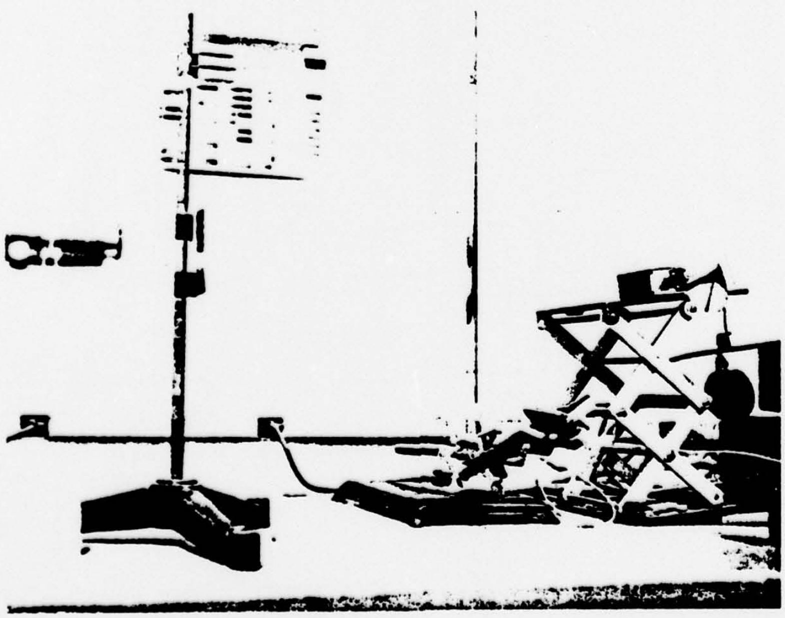

Figure 8. Equipment set up for the simulation experiment. Shown left to right are: The laser beam expander, circular aperature plate (on ring stand), the detector and collimator (in claw clamp), and mirror and scanning motor.

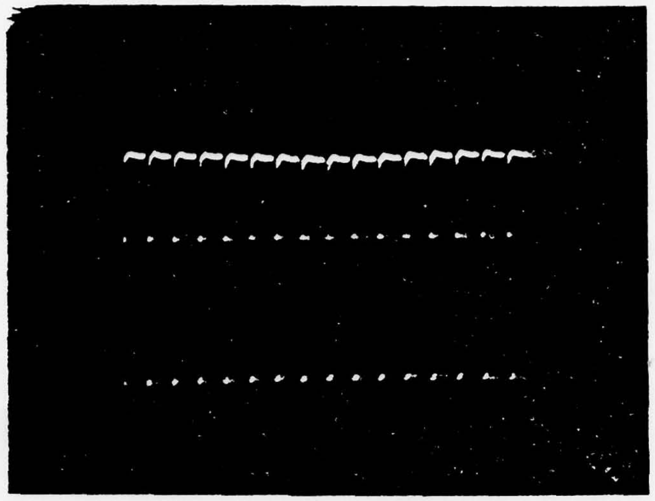

Figure 9. Readouts from the individual diode channels of the 256 element IRCCD.

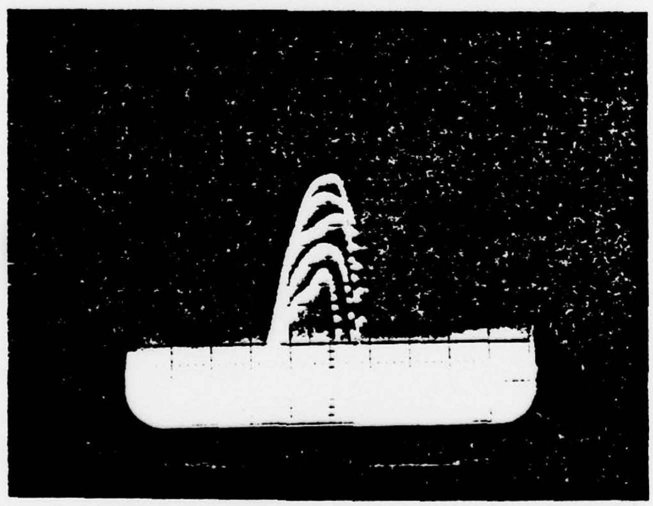

Figure 10. Topological view of a 6.35 mm aperature illuminated by a He-Ne laser.

Proper operation of Z axis modulation (grey scale) imaging was checked by varying the intensity of visible light on the diode array. It was found that modulation of the light intensity caused visible variations in the image of the diode outputs on the oscilloscope screen, verifying that the system was functioning correctly.

TESTING OF THE VIDEO PSEUDO-COLOR AND TOPOLOGICAL DISPLAY MODES

In order to test out the video and topological display portions of this system, images formed by a 25 X 50 element IRCCD square array were used. This array, which is shown in Figure 11 is presently in operation at Rome Air Development Center, Electronic Device Technology Branch.

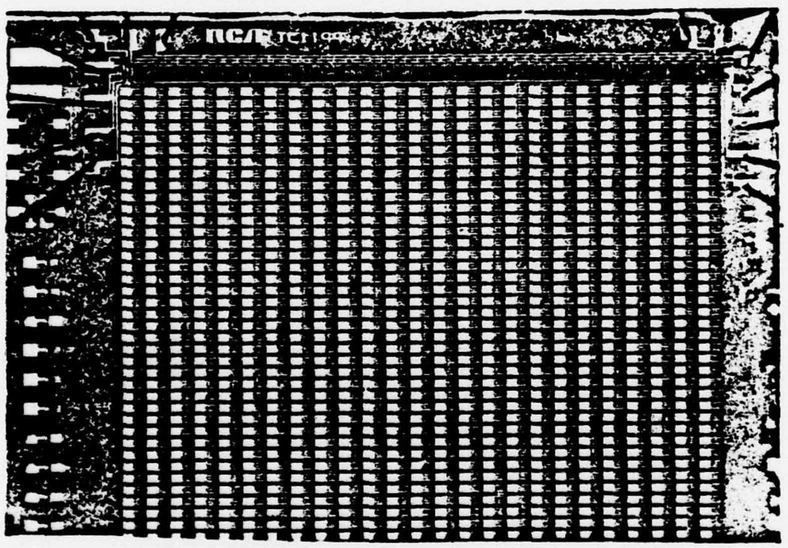

Figure 11. Photomicrograph of the 25 X 50 element IRCCD square array (from reference 1).

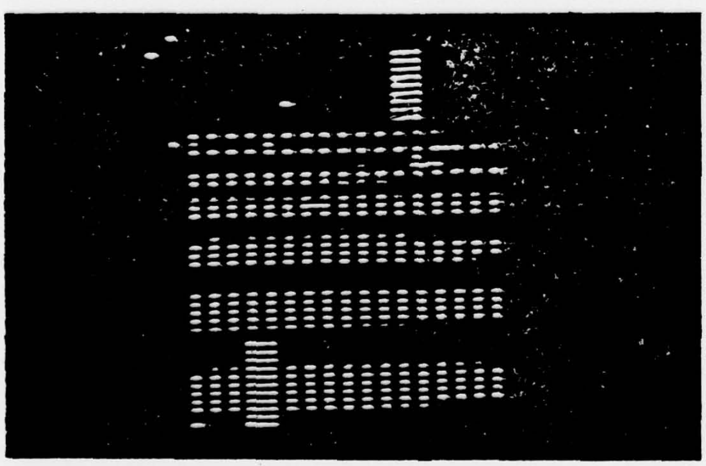

Figure 12. Image of a bar target recorded by the 25 X 50 element IRCCD array.

Figure 12 is the image of a 27°C bar target illuminated by a 31.4°C black body source. To test the pseudocolor and topological display modes, the bar target was imaged by was the television camera and simultaneously displayed in pseudo-color on a Conrac Model 5111-19 video monitor, and in topological view on a Hewlett Packard 1310A video display unit. The topological view is shown in Figure 13, and a black and white photograph of the colorized display in Figure 14. It was not possible to reproduce a color photograph in this manuscript, which would indicate the ability of the pseudo-color format to highlight and differentiate image detail.

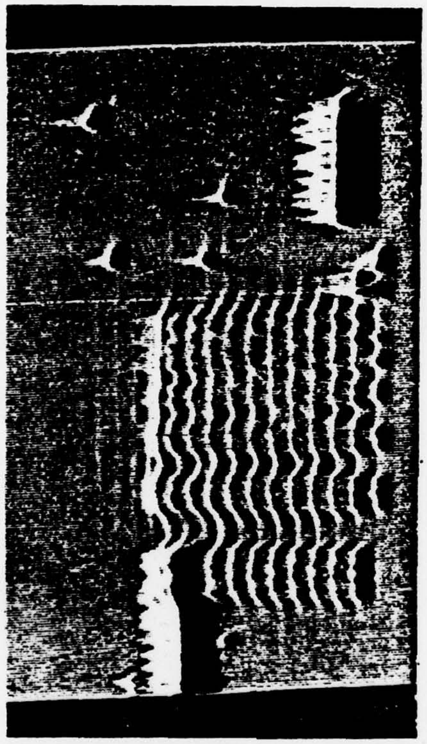

Figure 13. Topological view of the bar target recorded by the 25 X 50 IRCCD element array.

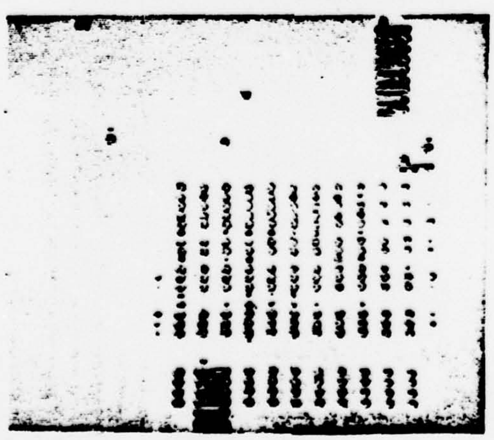

Figure 14. Colorized image of the bar target recorded by the 25 X 50 element IRCCD array (in black and white).

The several forms of topological image profiling offered by the image analyzer, and the latitude of color assignments made available by the pseudo-color generator will give a high degree of flexibility in the analysis of thermal signatures.

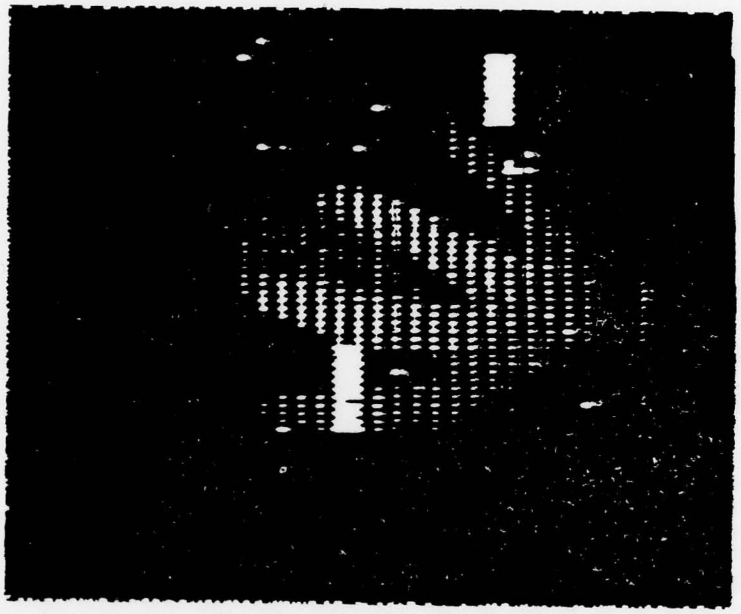

Figure 15. View of a human hand recorded by the 25 X 50 element IRCCD array.

Figure 15 shows the image of a human hand recorded by the 25 X 50 element IRCCDsquare array. Human images recorded by synchronous mirror scanning of the 256 element linear IRCCD array would be similar in appearance, but in far more detail owing to the greater number of recording elements.

CONCLUSION

The system designed to obtain human thermal signatures by synchronous mirror scanning of the 256 element Schottky barrier linear array has been tested using visible light illumination of the silicon substrate, and seen to function according to design. Photographs have been obtained of a laser illuminated test object, and oscilloscope topological and grey scale display modes have been found to function correctly. In addition, colorized and topological view photographs have been obtained of a bar pattern recorded by the 25 X 50 element staring array, thus demonstrating the feasibility of using this type of display format with the mirror scanned array.

It is recommended that a detailed analysis of infrared thermal signatures be made using the system discussed above. Data would be obtained at Hanscom AFB, Rome Air Development Center, Electronics Device Technology Branch. Modifications should be made in the present video system to eliminate the television camera and record the image directly, to insure optimum image quality. Special emphasis should be placed on computer analysis of the thermal signal information and enhancement of the visual image.

A 256 X 256 element Schottky barrier detector array is presently in the planning stage. I recommend that the thermal signature studies be extended to the 256 X 342 element array when it becomes operational.

In parallel with the analysis of thermal signatures, I recommend that the results of these studies be applied to medical thermography. Present medical thermographic systems employ a single mechanically scanned detector which produces an image of relatively poor spatial resolution. The IRCCD detector system will provide higher spatial and temperature resolution than existing thermographic systems. The presentation of this high resolution visual display in topological view, as well as grey scale and colorized formats should greatly enhance the capability for detailed diagnosis from the thermographic image. In addition, computer analysis of the image should be used to obtain additional diagnostic information, as well as for enhancement of the visual display. These applications of the IRCCD system in medical diagnosis should realize a new generation of medical thermographic scanners capable of producing highly detailed physical diagnostic examinations.

REFERENCES

1. L. Skolnik, R. Taylor, B. Capone, F. Shepherd, S. Roosild, W. Kosonocky, "A Platinum Silicide Schottky Barrier IRCCD for Base Security Surveillance." Proc. of the Infrared Information Symposium (IRIS) USAFA, Colorado Springs, Colorado, May 1978.

2. E. Kohn, "A Charge Coupled Infrared Imaging Array with Schottky Barrier Detectors," IEEE J. Solid State Physics, SC-11, 139 (1976).

3. E. Kohn, W. Kosonocky, F. Shallcross, "Charge-Coupled Scanned IR Imaging Sensors," Report from RCA Laboratories, Princeton, New Jersey, for Rome Air Development Center, Griffiss AFB, New York, 1977.

4. A. Oppenheim and R. Schafer, Digital Signal Processing, Prentice Hall, New Jersey, 1975.

5. S. M. Sze, Physics of Semiconductor Devices, John Wiley and Sons, New York, 1969.

6. V. E. Vickers, "Model of Schottky Barrier Hot-Electron-Mode Photodetection," Applied Optics, 10, 2190 (1971).

7. R. D. Shepherd, Jr. et al, "Silicon Schottky Barrier Monolithic IRTV Focal Planes," Advances in Electronics and Electron Physics, 40B, 981 (1975).

8. R. Taylor, F. Shepherd, S. Roosild, A. Yang, and E. Kohn, "Schottky IRCCD's," IRIS Detector Specialty Group Meeting, AF Academy CO, March 1977.

9. "256-Element Schottky Barrier IR-CCD Sensor," Report from RCA Laboratories for Rome Air Development Center, Griffiss AFB, New York, 1977.

10. C. Sequin, and M. Tompsett, Charge Transfer Devices, Academic Press, New York, 1975.

11. D. Barbe, "Imaging Using Charge Coupled Devices," Proc. of the IEEE, 63, 38 (1975).

12. F. D. Shepherd, Jr., R. W. Taylor, S. A. Roosild, L. H. Skolnik, B. L. Cochrun, and E. S. Kohn, "Ambient Thermal Response of Monolithic Schottky IRCCD'S." Proc. of IRIS Thermal Specialty Group, El Toro, CA 1977.

13. W. Kosonocky, E. Kohn, F. Shallcross, "Optimization Study of IR-CCD Array," Report from R. C. A. Laboratories, Princeton, N. J. for Rome Air Development Center, Griffiss AFB, New York, 1978.